DINOSAURS AND TIME: CHRONOSTRATIGRAPHIC FRAMEWORKS AND THEIR UTILITY IN ANALYSIS OF DINOSAUR PALEOBIOLOGY

by

Denver Warwick Fowler

A dissertation submitted in partial fulfillment
of the requirements for the degree

of

Doctor of Philosophy

in

Earth Sciences

MONTANA STATE UNIVERSITY
Bozeman, Montana

April 2016

©COPYRIGHT

by

Denver Warwick Fowler

2016

All Rights Reserved

ACKNOWLEDGEMENTS

This has been a long journey, with so many people to thank for helping me along the way. My wife, Elizabeth Freedman Fowler, has been a rock throughout it all. I will be forever grateful to my supervisor, Jack Horner, for taking me on in the first place. My family, especially mum, Jackie, and dad, Warwick, have always supported me and taken me on many fossil hunting holidays. Bob Sullivan, for being there when everything went wrong. Mick Green and Keith Simmonds, who both taught me so much. Barbara and Geoff Phillips, for getting me that chicken shed! My field crews, especially Jack Wilson and Danny Anduza who have been so supportive in these final days. MOR staff, especially the paleo lab team, Bob, Carrie, Jamie and the Paleoldladies. My fellow MOR grad students, Alida Bailleul, John Scannella, Katie Tremaine, Cary Woodruff, Holly Woodward, and Badmaa Zorigt. My committee members Dave Varricchio, Dave Bowen, and Dave Eberth. Hell Creek ranchers, especially the Holen, Isaacs, Taylor and Twitchell families, along with the BLM and US Fish and Wildlife, and everyone at APR. Other people who helped me include Mike Benton, Ray Butler, Josh Fry, David Gillette, Joe Hartman, Spencer Lucas, Paul Renne and his team, Remmert Schouten, Scott Taylor, and Greg Wilson. Funding was kindly provided to MOR by Ameya Preserve, Nathan Myhrvold, Damaris Waggoner, David Sands, and the Smithsonian; and to myself by Keith Anderson and the APR, the Welles Fund (UCMP), the Jurassic Foundation, Jackson School of Geosciences (SVP), MSU Dept. Cell Biology and Neuroscience, and MSU College of Letters and Science. Thanks to members of the DDLP.

TABLE OF CONTENTS

1. INTRODUCTION TO DISSERTATION 1

References Cited 7

2. A TERRESTRIAL SEQUENCE STRATIGRAPHIC INTERPRETATION OF THE HELL CREEK FORMATION OF NORTHERN MONTANA 8

Contribution of Authors and Co-Authors 8
Manuscript Information Page 9
Abstract 10
Introduction 11
Geological Setting 14
Stratigraphy and Age 17
Biostratigraphy 17
Chemostratigraphy 18
Lithostratigraphy 18
Well Log Analysis 20
Magnetostratigraphy 20
Chronostratigraphy 22
Age of the Upper and Lower Contacts, and Duration 23
Marine Influence and Sequence Stratigraphic Analysis 24
Methods 26
Stratigraphic Abbreviations 26
Orders of Cyclicity 27
Terrestrial Sequence Stratigraphy 27
Results 33
Lithofacies and Generalized Section (Figure 2.3) 33
Bearpaw Shale (Kbp) 33
Fox Hills Sandstone (Kfh) 34
Colgate Sandstone (Kfhc) 35
Colgate Tidal Flats (Kcp) 37
?Battle Formation (Kba) 38
Hell Creek Basal Sand (Khc-bs) 39
Lower Hell Creek Formation Fines (Khc-lf) 40
Jen Rex Sand (Khc-jrs) 41
Middle Hell Creek Formation Fines (Khc-mf) 42
Apex Sand (Khc-as) 43
Upper Hell Creek Formation Fines Part 1 (Khc-uf1) 44
10 Meter Sand (Khc-10ms) 44
Upper Hell Creek Formation Fines Part 2 (Khc-uf2) 45

TABLE OF CONTENTS - CONTINUED

Fort Union Formation (PgF) 45
Study Localities and Measured Sections 46
Drainage of Crooked Creek, North of Winnett, MT 46
Cole Creek, Near Hell Creek Marina, North of Jordan, MT 47
Hell Creek, Near the Marina Road (FWS-105), North of Jordan, MT 47
"Best Butte" and "Hike Cliff" 48
Manaige Spring and "Battle Butte" 49
East Ried Coulee, Flag Butte (New Type Section) 50
Sand Creek, Sheep Mountain, Carter County MT 55
East Gilbert Creek and Penick Coulee 56
Gilbert Creek 58
Lost Creek (Ducky Tail) 58
Cottonwood Creek (Brownie Butte; Lon's Trike) 59
Short Creek (Tom's Old Duck) 60
Lone Tree Creek (Sandy Chicken and The Doldrums) 60
Bug Creek – Russell Basin, McCone County MT 61
Magnetostratigraphic Corrections 62
Depositional Sequences and Systems Tracts 64
Bearpaw Shale – Fox Hills Sandstone Depositional Sequence (Kbp, Kfh) 65
Colgate and ?Battle Depositional Sequence (SB1, Kfhc, Kcp, Kba) 66
Lower Hell Creek Formation Depositional Sequence (SB2, Khc-bs, Khc-lf) 69
Middle Hell Creek Formation Depositional Sequence (SB3, Khc-jrs, Khc-mf) 72
Upper Hell Creek Formation Depositional Sequence Parts 1 and 2 75
Discussion 78
Stratigraphy 78
Time Duration of Depositional Cycles 81
Autocyclic or Allocyclic Processes 82
Regional Correlation and Biostratigraphy 87
Paleontology 89
Further Work 92
Conclusions 93
Acknowledgements 95
References Cited 130

TABLE OF CONTENTS - CONTINUED

3. A NEW CORRELATION OF THE CRETACEOUS FORMATIONS OF THE WESTERN INTERIOR OF THE UNITED STATES, I: SANTONIAN-MAASTRICHTIAN FORMATIONS AND DINOSAUR BIOSTRATIGRAPHY 146

Contribution of Authors and Co-Authors 146
Manuscript Information Page 147
Abstract 148
Introduction 148
1. It is Difficult to Find the Reasoning Behind Some Correlations 150
2. Lacunae are Not Depicted 151
3. Radiometric Dates May be Incorrect or Incomparable 152
Methods 153
Abbreviations Used 153
Display Format – Excel Sheets 153
Electronic Supplementary File 1 153
Electronic Supplementary File 2 154
Stratigraphic Chart (Electronic Supplementary File 1) 156
Definitions: Stage and Substages, Magnetostratigraphy, and Ammonite Biostratigraphy 156
Positioning of Geological Units and Dinosaur Taxa 157
Sequence Stratigraphy and Lithostratigraphy 158
Limitation of Scope and Future Versions 158
Institutional Abbreviations 159
Taxa Display Format – Phylogenies and Lineages 159
Magnetostratigraphy 160
Radiometric Dating 161
U-Pb and K-Ar 161
$^{40}Ar/^{39}Ar$ 163
Standards (Neutron Fluence Monitor) 163
Decay Constants 166
Recalibration and Current Standards 166
Choice of Mineral 167
Reporting of Uncertainty / Error 168
Agreement of $^{40}Ar/^{39}Ar$ Dates with U-Pb Dates 169
Other General Comments 169
Results 170
Notes on Recalibrations by Other Authors 170
Various Analyses Published by J. D. Obradovich (~1990 Until at Least 2002) 170
Kuiper et al. (2008) 172

TABLE OF CONTENTS - CONTINUED

Schmitz (2012)....173
Roberts et al. (2013)....173
Discussion....176
Geology....176
Judith River Formation – Subdivision Required....176
Age of the Aguja Formation, Texas....177
Age of the Javelina Formation, Texas....178
Thinking about Taxa as Lineages....179
The Trouble with "Turnover"....180
North-South Biogeography and Extreme Faunal Endemism....181
Biostratigraphy....182
Conclusions....184
Acknowledgements....184
References Cited....186

4. TRANSITIONAL EVOLUTIONARY FORMS AND STRATIGRAPHIC TRENDS IN CHASMOSAURINE CERATOPSID DINOSAURS....195

Contribution of Authors and Co-Authors....195
Manuscript Information Page....196
Abstract....197
Keywords....197
Introduction....197
Institutional Abbreviations....203
Anatomical Abbreviations....204
Geological Setting....204
Fruitland – Kirtland Formational Boundary....205
Kirtland Formation, Internal Stratigraphy....206
Age....207
Map and Stratigraphic Positioning of San Juan Basin Fossils....208
Stratigraphic Terminology....210
Materials and Methods....210
Interbasinal Correlation....210
Fossil Materials and Accepted Taxonomy....211
Phylogenetic Analysis....213
Morphometric Analysis....214
Angle Measurements....215
Results....216
Systematic Paleontology....216
Pentaceratops sternbergii (Osborn, 1923)....216
Type Specimen....216

TABLE OF CONTENTS - CONTINUED

Referred Specimens 216
Locality and Stratigraphy....217
Diagnosis 217
Comment....218
Aff. *Pentaceratops* n. sp. 220
Referred Specimens 220
Locality and Stratigraphy....220
Diagnosis 220
Comment....221
Navajoceratops sullivani gen. et sp. nov.. 222
Etymology....222
Holotype....222
Locality and Stratigraphy....222
Diagnosis 223
Description of *Navajoceratops sullivani*. 223
Parietal 223
Squamosal....225
Jugal / Epijugal or Episquamosal....226
Terminocavus sealeyi gen. et sp. nov.. 226
Etymology....226
Holotype....227
Locality and Stratigraphy....227
Comment....228
Diagnosis 228
Description of *Terminocavus sealeyi*....229
Parietal 229
Right Squamosal....232
Jugal / Epijugal 233
Chasmosaurine sp. “Taxon C”....233
Material....233
Locality and Stratigraphy....233
Comment....234
Diagnosis 234
Description of Chasmosaurine sp. “Taxon C”....234
Parietal 234
Epijugal....235
Ontogenetic Assessment....236
Size....236
Cranial Fusion....237
Frill Epiossifications....238
Frill Surface Texture....240
Squamosal Elongation 241

TABLE OF CONTENTS - CONTINUED

Geometric Morphometric Analysis 242
Phylogenetic Analysis....244
Discussion....247
Comparisons and Discussion of Morphological Characters....247
Median Embayment of the Parietal Posterior Bar 248
Epiparietal Number, Shape, Size, and Orientation 249
Anteroposterior Thickness of the Posterior Bar Lateral Rami 252
Characters of the Median Bar and Parietal Fenestrae....252
Implications of Findings 255
Phylogeny: Anagenetic Stacks of Stratigraphically Segregated "Species"....255
Phylogeny: a Deep-Split Chasmosaurinae....257
Latitudinal Biogeography and Vicariance 260
The Role of Heterochrony in Evolution of the Frill and Effects on Phylogenetic Analysis 263
Development of the Median Embayment 264
Development of Parietal Fenestrae....265
Origin of *Arrhinoceratops* and the Triceratopsini: a Second Speciation? 267
Conclusions....268
Acknowledgements....270
References Cited....293

5. A STRATIGRAPHIC SURVEY OF *TRICERATOPS* LOCALITIES IN THE HELL CREEK FORMATION, NORTHEASTERN MONTANA (2006-2010)....306

Contribution of Authors and Co-Authors....306
Manuscript Information Page 307
Abstract....308
Introduction....308
Institutional Abbreviations 311
Materials and Methods....312
Triceratops localities 313
UCMP Locality V88001 (High Ceratopsian): UCMP Specimen 137263....313
UCMP Locality V83224 (Dave's Nose): UCMP Specimen 128561....314
UCMP Locality V88081 (Russell Basin *Triceratops*) UCMP Specimen 136092 315
UCMP Locality V75046 (Ruben's *Triceratops*): UCMP

TABLE OF CONTENTS - CONTINUED

Specimen 113697 316
MOR Locality HC-135 (MORT): MOR Specimen 004 317
MOR Locality HC-425 (Afternoon Delight): MOR Specimen 2569 317
MOR Locality HC-531 (Lauren's Trike): MOR Specimen 2938 318
MOR Locality HC-520 (Joe's Half Day Trike): MOR Specimen 2923 318
MOR Locality HC-702 (JD Trike12): MOR Specimen 3056 and MOR Locality HC-541 (JD Trike14): MOR Specimen 2950 319
MOR Locality HC-426 (Mark's Scavenged Trike: MOR Specimen 2570 and MOR Locality HC-639 (Anky Breaky Heart): MOR Specimen 3011 320
MOR Locality HC-430 (Quittin' Time): MOR Specimens 2574 and 2702 321
MOR Locality HC-521 (Lon's Trike): MOR Specimen 2924 321
MOR Locality HC-571 (Seth's Trike): MOR Specimen 2979 and MOR Locality HC-543 (TriSarahTops): MOR Specimen 2980 322
MOR Locality HC-544 (DFJuvieTrike3): MOR Specimen 2951 and MOR Locality HC-627 (Situ But Sad): MOR Specimen 2999 322
MOR Locality HC-565 (Supernasal): MOR Specimen 2972 and MOR Locality HC-628 (Ashes Trike): MOR Specimen 3000 323
MOR Locality HC-573 (Three Amigos): MOR Specimen 2982 And MOR Locality HC-576 (Six O'Clock Trike): MOR Specimen 2985 324
MOR Locality HC-532 (Ducky Tail): MOR Specimen 6648 325
MOR Locality HC-638 (Golden Goose): MOR Specimen 3010 326
MOR Locality HC-668 (Yoshi's Trike): MOR Specimen 3027 and MOR Locality HC-682 (Cliffhanger): MOR Specimen 3045 326
MOR Locality HC-716 (Little Horny Devil): MOR Specimen 3064 327
Discussion and Conclusions 327
Acknowledgements 329
References Cited 347

6. EVOLUTIONARY TRENDS IN *TRICERATOPS* FROM THE HELL CREEK FORMATION, MONTANA 352

Contribution of Authors and Co-Authors 352
Manuscript Information Page 353
Abstract 354

TABLE OF CONTENTS - CONTINUED

Significance Statement 354
Introduction....355
Results....356
L3 *Triceratops* 357
M3 *Triceratops* 357
U3 *Triceratops* 358
Shifts in Morphology over Time 359
Cladistic and Stratocladistic Analyses....361
Discussion....363
Evolutionary Patterns....363
A Biogeographic Signal? 365
Anagenesis and Cladogenesis....365
Conclusions....367
Materials and Methods....368
Acknowledgements....370
References Cited 376

7. REANALYSIS OF "*RAPTOREX KRIEGSTEINI*": A JUVENILE TYRANNOSAURID DINOSAUR FROM MONGOLIA 381

Contribution of Authors and Co-Authors 381
Manuscript Information Page 382
Abstract....383
Key Words 383
Introduction....384
Materials and Methods....386
Results and Discussion 387
Stratigraphy....387
Ontogeny....390
Osteological Indications of Maturity 392
Histology....394
Taxonomy 398
Conclusions....400
Acknowledgements....401
References Cited 404

8. SPECIATION OF LATE CRETACEOUS DINOSAURS OF THE WESTERN INTERIOR: INITIATED BY TRANSGRESSION/ CLIMATE-INDUCED ALLOPATRY, AND COMPLETED BY REINFORCEMENT-DRIVEN ANAGENESIS 412

Abstract....412

TABLE OF CONTENTS - CONTINUED

Introduction....413
Bizarre Structures....416
Reinforcement....424
Example....425
The Hypothesis Regarding Dinosaurs of the Western Interior....429
Methods....430
Testing the Evolution of Prezygotic Barriers in the Extant and Fossil Record....430
1. Phylogeny....431
2. Morphology....431
3. Geography....431
4. Stratigraphy....432
5. Ontogeny....432
Results....432
1. Phylogeny....432
2. Morphology....433
3. Geography....433
4. Stratigraphy....435
5. Ontogeny....436
Other Potential Causes of the Same Patterns....436
Discussion....438
Geographic Barriers....438
Allopatry and Endemism....440
Significance of These Concepts for Dinosaur Paleontology....444
Impact of These Concepts on Speciation Studies....446
Conservation and Environment....447
References Cited....449

9. CONCLUSION....456

APPENDICES....459

APPENDIX A: Supplementary Information for Chapter 2....460
APPENDIX B: Supplementary Information for Chapter 3....503
APPENDIX C: Supplementary Information 1 for Chapter 4: Review of Fossil Materials and Figures....546
APPENDIX D: Supplementary Information 2 for Chapter 4: Phylogenetic Analysis....640
APPENDIX E: Supplementary Information 3 for Chapter 4: Justification for Genera....670

TABLE OF CONTENTS - CONTINUED

APPENDIX F: Supplementary Information for Chapter 5 as Published in the Geological Society of America Special Paper 503 674
APPENDIX G: Supplementary Information for Chapter 6 as Published in the Proceedings of the National Academy of Sciences 679

REFERENCES CITED 732

LIST OF TABLES

Table Page

4.1 List of specimens discussed in this study 271

LIST OF FIGURES

Figure Page

2.1 Map showing outcrop of Pierre (Bearpaw) Shale, Fox Hills Sandstone, Hell Creek, Lance, and Fort Union Formations in the Williston and Powder River Basins 96

2.2 Location of principal study localities discussed in text, south Ft. Peck Lake area near Jordan (Garfield County), Montana 97

2.3 Generalized section of the Bearpaw Shale (partial), Fox Hills Sandstone, Colgate Sandstone, Battle, Hell Creek, and Fort Union (partial) formations illustrating sequence boundaries (SB) and sequence tracts 98

2.4 Exposure of the Bearpaw Shale through Jen Rex Sand 99

2.5 Exposure of the Fox Hills Sandstone (Kfh) through Hell Creek Formation Basal Sand (Khc-bs) 100

2.6 Exposures of the lower part of the type section 101

2.7 Sequence boundary 2 separates the Colgate Sandstone from the overlying Basal Sand of the Hell Creek Formation 101

2.8 Coaly layers are relatively rare in the Colgate Sandstone 102

2.9 Close-up photograph of the contact between the upper pale unit, and lower tan unit of the Colgate Sandstone 103

2.10 Variable contact of the Hell Creek Basal Sand with underlying Colgate depositional sequence and Fox Hills Sandstone at Ekalaka, Carter County Montana 104

2.11 Overbank fines and isolated fluvial channels of the lower Hell Creek depositional sequence (Khc-lf; ~15 m thickness) overlain by cliff-forming amalgamated channel complex of the Jen Rex Sandstone (Khc-jrs), basal unit of the middle Hell Creek depositional sequence 105

LIST OF FIGURES – CONTINUED

Figure Page

2.12 Middle and Upper depositional sequences of the Hell Creek Formation at the new type section (Hartman et al., 2014) 105

2.13 Exposure of the lower to middle Hell Creek Formation, middle of Penick Coulee. 106

2.14 Exposure of the lower to middle Hell Creek Formation, north side of Penick Coulee 107

2.15 Measured sections taken in Penick Coulee and East Gilbert Creek, exposing the complete Hell Creek Formation 108

2.16 Exposure of lower contact of the Apex Sand in Lost Creek 109

2.17 Measured sections taken in Lost Creek, exposing the uppermost 60 m of the Hell Creek Formation 110

2.18 Sequence boundary 4 (SB4) separates the middle and upper depositional sequences 111

2.19 Exposure of the upper Hell Creek depositional sequence 112

2.20 Upper 15 m of the Hell Creek Formation on western side of Short Creek 113

2.21 The 10 Meter Sand is variably ~3-4 m thick and laterally extensive in the Lone Tree Creek Area 113

2.22 Upper 13 m of the Hell Creek Formation on eastern side of Short Creek 114

2.23 Outcrop of the 10 Meter Sand that forms short steep cliffs 114

2.24 At Russell Basin, only the upper 20 m of the Hell Creek Formation is exposed 115

LIST OF FIGURES – CONTINUED

Figure Page

2.25 Measured section taken in Cole Creek, exposing the uppermost 10 m of the Bearpaw Shale through lowermost 30 m of the Hell Creek Formation 116

2.26 Exposure of the lower contacts of the Hell Creek Formation and underlying units exposed at "Best Butte" 117

2.27 Exposure of the lower contacts of the Hell Creek Formation and underlying units exposed at "Battle Butte" which records a stratigraphic succession intermediate between Manaige Spring (~1 km SSW; Figure 2.5) and Best Butte (~3 km NE; Figure 2.26) 118

2.28 Basal contacts of the Hell Creek Formation at the new type section, East Ried Coulee 119

2.29 Possible Inclined Heterolithic Strata exposed as part of large channels in the Hell Creek Formation Basal Sand at East Ried Coulee (the new type section; Hartman et al., 2014) 120

2.30 Channel scour filled with conglomerate (A; highlighted in B) exposed in the Hell Creek Basal Sand (Khc-bs) at East Ried Coulee (the new type section; Hartman et al., 2014) 121

2.31 Measured sections taken at Sand Creek, near Sheep Mountain, 55 km SE of Ekalaka, Carter County Montana 122

2.32 Measured section taken at Brownie Butte, exposing the uppermost 17 m of the Hell Creek Formation 123

2.33 Measured sections taken in Short Creek, exposing the uppermost 31 m of the Hell Creek Formation 124

2.34 Exposure of the Null Coal at Lone Tree Creek 125

2.35 Suggested revision of Hell Creek Formation magnetostratigraphy of the Manaige Spring locality 126

LIST OF FIGURES – CONTINUED

Figure Page

2.36 Suggested magnetostratigraphic revision of the new type section of the Hell Creek Formation 127

2.37 Exposure of the Null Coal at Lost Creek 128

2.38 Exposure of the Null Coal at East Gilbert Creek 129

4.1 Hypothesis of chasmosaurine relationships from Lehman (1998) 273

4.2 Alternative hypotheses of chasmosaurine phylogeny 274

4.3 Geological map of the southeast San Juan Basin showing localities of radiometric dates and important fossil specimens mentioned in the text 275

4.4 Historical stratigraphic terminology of the Fruitland and Kirtland Formations 276

4.5 Generalized stratigraphic column of the Fruitland and Kirtland Formations with radiometric dates and fossil occurrences 277

4.6 Morphological landmarks used in morphometric analysis of chasmosaurine parietals 278

4.7 *Navajoceratops sullivani* holotype SMP VP-1500 parietal exposed before collection 279

4.8 *Navajoceratops sullivani* holotype SMP VP-1500 parietal exposed before collection 280

4.9 *Navajoceratops sullivani* holotype SMP VP-1500 parietal 281

4.10 *Navajoceratops sullivani* holotype SMP VP-1500 isolated frill episossification 282

4.11 *Navajoceratops sullivani* holotype SMP VP-1500 squamosal fragments 282

LIST OF FIGURES – CONTINUED

Figure Page

4.12 *Navajoceratops sullivani* holotype SMP VP-1500 jugal 283

4.13 *Terminocavus sealeyi* holotype NMMNH P-27468 parietal 283

4.14 *Terminocavus sealeyi* holotype NMMNH P-27468 right squamosal....284

4.15 *Terminocavus sealeyi* holotype NMMNH P-27468 left jugal 285

4.16 Chasmosaurinae sp. "Taxon C" NMMNH P-33906 parietal median bar....286

4.17 Parietal relative sizes among specimens of *Pentaceratops* and related chasmosaurines 287

4.18 Morphometric analysis of chasmosaurine posterior parietals....288

4.19 Strict consensus tree showing all taxa (MPT = 6; L = 319; CI = 0.72; RI = 0.79)....289

4.20 Reanalysis 1, strict consensus tree (MPT = 6; L = 310; CI = 0.72; RI = 0.79)....290

4.21 Strict consensus tree showing all taxa (MPT = 28; L = 308; CI = 0.72; RI = 0.79)....291

4.22 Stratigraphic positions of chasmosaurine taxa....292

5.1 Collection areas for specimens of *Triceratops* discussed in the text, south Fort Peck Lake in Garfield and McCone Counties, Montana 331

5.2 Relative positions of *Triceratops* localities discussed in the text superimposed on a generalized section....332

5.3 The Russell Basin *Triceratops* (University of California Museum of Paleontology [UCMP] 136092), photographed while still under preparation at the UCMP 333

LIST OF FIGURES – CONTINUED

Figure Page

5.4 Relocating the Russell Basin *Triceratops* quarry (University of California Museum of Paleontology [UCMP] locality V88081) 334

5.5 Ruben's *Triceratops* (University of California Museum of Paleontology [UCMP] locality V75046) 335

5.6 Museum of the Rockies (MOR) *Triceratops* (MORT; MOR 004), jacketed and awaiting collection in 1981 336

5.7 Correlation of measured sections and Museum of the Rockies (MOR) *Triceratops* localities, ~4.5 km across the Short Creek area (Garfield County, Fig. 5.1, locality 6) from northwest to southeast....337

5.8 Joe's Half Day Trike (Museum of the Rockies [MOR] locality HC-520) 338

5.9 Fowler discovers JDTrike12 (Museum of the Rockies [MOR] specimen 3056) eroding from a gray mudstone stratigraphically high in the upper unit of the Hell Creek Formation....339

5.10 JDTrike14 (Museum of the Rockies [MOR] locality HC-541) 340

5.11 Correlation of measured sections and Museum of the Rockies (MOR) *Triceratops* localities ~2.5 km across Lost Creek Bay area (Garfield County, Fig. 5.1, locality 5) from north to south 341

5.12 Museum of the Rockies (MOR) locality HC-571 plotted on measured section, Brownie Butte (Garfield County; Fig. 5.1, locality1)....342

5.13 Seth's Trike (Museum of the Rockies [MOR] locality HC-571) 343

5.14 DFJuvieTrike3 (Museum of the Rockies [MOR] locality HC-544) 344

LIST OF FIGURES – CONTINUED

Figure Page

5.15 Correlation of measured sections and Museum of the Rockies (MOR) *Triceratops* localities across ~6.5 km of the Pennick Coulee area (Garfield County, Fig. 5.1, locality 3) from northwest to southeast....345

5.16 Yoshi's Trike (Museum of the Rockies [MOR] locality HC-668) 346

6.1 Stratigraphic placement of HCF *Triceratops* reveals trends in cranial morphology including elongation of the epinasal and change in morphology of the rostrum 372

6.2 Stratigraphic variation in cranial morphology 373

6.3 Results of cladistic analysis of HCF *Triceratops* 374

6.4 Potential patterns of HCF *Triceratops* evolution....375

7.1 Comparison of the LH PV18 fish centrum (D) to an ellimmichthyiform centrum (A-C) (Horseshoeichthyes) from the Dinosaur Park Formation (Campanian) of Alberta 402

7.2 Osteohistological features of LH PV18 and a near adult *Tyrannosaurus rex* for comparison....403

ABSTRACT

Stratigraphy is the study of the position of rock strata, in order to determine their age. Dinosaur fossils have been recovered from North America for over 150 years, yet the stratigraphy of the localities from which they were collected has rarely been analysed at high resolution, either due to lack of original locality data, or that precise correlation between depositional basins was not technologically possible. This dissertation analyses what effect the introduction of high-resolution chronostratigraphic data has on our understanding of dinosaur paleobiology. Terrestrial sequence stratigraphy was used in combination with previously published data in order to subdivide the uppermost Cretaceous Hell Creek Formation of Montana into lower, middle, and upper units, shown to be consistent across the formation type area. Similar stratigraphic data was gathered for each of the Late Cretaceous dinosaur-bearing formations of the North American Western Interior, which was combined with nearly 200 radiometric dates (newly recalibrated here) to plot a comprehensive high-resolution correlation chart. The stratigraphic occurrence of dinosaur taxa was consequently plotted upon this chart. Similarly, the new Hell Creek Formation stratigraphic framework was used to plot the stratigraphic occurrence of *Triceratops* fossils. From this it can be seen that many dinosaur groups form stacks of stratigraphically separated species, a pattern indicative of linear, non-branching evolution (anagenesis). A similar pattern is observed for two new taxa of chasmosaurine ceratopsid (horned) dinosaurs from New Mexico, which form morphologic and stratigraphic intermediates between the slightly older taxon, *Pentaceratops*, and the younger *Anchiceratops*. Phylogenetic and geometric morphometric analysis supports the hypothesis that the posterior embayment of the parietal deepens and closes in on itself over ~ 2 million years from *Pentaceratops* through the new taxa, to *Anchiceratops*, and suggests a deep split within Chasmosaurinae that occurs before the Middle Campanian. These findings imply that dinosaur evolution in the Late Cretaceous Western Interior was characterized mostly by anagenesis, punctuated by occasional speciation events, perhaps triggered by high sealevel creating a north / south geographic barrier. The evolutionary process of reinforcement is discussed as a possible mechanism for the development of cranial display organs, linked to speciation.

CHAPTER ONE

INTRODUCTION TO DISSERTATION

Studies of dinosaur evolution and paleobiology have long benefited from the excellent fossil record of the Campanian and Maastrichtian of the North American Western Interior. Not only has this area been prolifically collected for over 100 years, but it also includes the K-Pg boundary, at which non-avian dinosaurs and other important members of the biota went extinct. This has naturally attracted extra attention from researchers, making this interval and its dinosaurs probably the most intensively studied in the world. However, despite this outpouring of research, the context within which dinosaur evolution is studied is clouded by poor resolution at a number of scales.

A robust taxonomy is a necessary underpinning for biological research. In the ~170 years since the definition of Dinosauria (Owen, 1842), 527 dinosaur genera have been described (as of 2006; Wang and Dodson, 2006). As fossils, dinosaur taxa are defined on morphology alone: thus, morphological variation both within and among fossil species is vitally important to both define and interpret. If we wish to study dinosaur paleobiology and evolution, we must identify and attempt to understand sources of morphological variation, rather than simply describing observed variation with little thought to its origin or its effect on studies that depend on our devised taxonomy.

Two factors that strongly affect morphology, but which are often neglected in dinosaur studies, are ontogeny and stratigraphy. However, the usefulness of understanding ontogeny is severely hampered if high-resolution stratigraphic data does

not accompany the specimens. Ontogenetic sequences are best assembled from single bonebeds, thereby minimizing the potential effects of differing stratigraphy, geography, or taphonomic history. Still, most dinosaur taxa are not known from bonebeds, such that ontogenetic sequences must be constructed from specimens collected from different localities (e.g. Horner and Goodwin, 2006). This strategy is not a major problem if good stratigraphic data is available for the specimens; however, most historically collected dinosaur remains lack detailed stratigraphic data, meaning that we are often unsure how far apart stratigraphically (and therefore in time) specimens may have been, even within a single formation. This is important as it is becoming increasingly clear that even relatively short periods of time (manifested as short stratigraphic distances; especially across sequence boundaries) may yield morphologic changes considered significant enough to warrant description as a new taxon, or at least recognizable morphotype (e.g. Horner et al. 1992 contrasted with Sampson, 1995). Subtle changes in the timing of heterochronic shifts through development cannot be demonstrated unless the stratigraphic relationship of the specimens is known.

The importance of stratigraphy to paleobiological interpretation is the main subject of this dissertation, essentially building on concepts put forth by Horner et al. (1992), taking the overarching themes of how much of the dinosaur fossil record is dominated by unbranching anagenetic change, and what might be the causes of morphologic change and / or speciation? These themes are investigated with a stratigraphic approach, by breaking down formations into constituent depositional sequences in order to understand better the passage of time, and how much of that time is

represented by fossils. Each part of this synthesis looks at a different aspect of what happens when we have high resolution stratigraphic frameworks.

For Chapter Two, I created an internal stratigraphic subdivision for the Hell Creek Formation in the area immediately south of Fort Peck Lake, Montana, through use of the burgeoning field of terrestrial sequence stratigraphy. This provides a preliminary sequence stratigraphic model that can then be tested and correlated regionally by outcrop analysis, possibly combined with subsurface well logs and magnetostratigraphic data. This analysis also presents new informal definitions for the lower, middle, and upper depositional sequences of the Hell Creek Formation. This is of utility in discussion of the formation, and the placement of fossils in section. Important changes are proposed for interpretation of the new type section, and minor corrections are suggested for previous magnetostratigraphic interpretations.

Chapter Three is a comprehensive stratigraphic correlation chart comprising the major terrestrial geological formations of the North American Western Interior. The chart is plotted based on extensive review of the pertinent stratigraphic literature on each formation, and on nearly two hundred ^{40}Ar / ^{39}Ar radiometric dates, correctly recalibrated here for the first time. This new work represents the most precise and comprehensive correlation currently available for terrestrial geological formations of the North American Western Interior. This is used in combination with locality data for individual dinosaur specimens to plot the stratigraphic ranges for dinosaur taxa. This replotting of dinosaur taxa is discussed with regards to current hypotheses of dinosaur biogeography and evolution.

Chapter Four describes two new taxa of chasmosaurine ceratopsid from the Kirtland Formation, New Mexico, which form stratigraphic and morphologic intermediates between *Pentaceratops* and *Anchiceratops*. Geometric morphometric analysis supports the hypothesis that the posterior embayment of the parietal deepens and closes in on itself over ~ 2 million years from *Pentaceratops* through the new taxa, to *Anchiceratops*. Phylogenetic analysis recovers the new taxa as successive stem taxa leading to *Anchiceratops* and more derived chasmosaurines, and suggests a deep split within Chasmosaurinae that occurs before the Middle Campanian. This is supportive of true speciation (branching) by vicariance occurring relatively basally within Chasmosaurinae, followed by more prolonged periods of anagenetic (unbranching) evolution. Recent hypotheses of extreme faunal endemism are not supported; however, it appears likely that continental-scale latitudinal faunal variation occurred in the Campanian. The new specimens document incipient paedomorphic trends that come to characterize more derived chasmosaurines in the Maastrichtian, such as *Triceratops*

Chapter Five is a gazetteer of Hell Creek Formation *Triceratops* localities used in Chapter Six. Notably, each locality record gives a detailed justification for its stratigraphic position, in association with more typical details of the specimen, and other geographic and contextual information. Too often this kind of detailed data is not available for even recently collected specimens, something personally encountered during research for Chapter Six.

Chapter Six plots the stratigraphic position of over 50 skulls of the horned dinosaur *Triceratops* within the Upper Cretaceous Hell Creek Formation (HCF) of

Montana, showing that the two recognized morphospecies, *T. horridus* and *T. prorsus*, are stratigraphically separated; *T. prorsus* is only recovered from the upper third of the formation, *T. horridus* is found lower in the formation, with transitional morphologies in the middle unit of the formation. This finding is consistent with the evolution of *Triceratops* being characterized by anagenesis. These findings underscore the critical role of stratigraphic data in deciphering evolutionary patterns in Dinosauria.

Chapter Seven presents a rebuttal of the stratigraphic and ontogenetic data recently presented for a small tyrannosaurid dinosaur specimen designated the holotype of a new taxon: *Raptorex kreigsteini*. We suggest that an associated fish centrum was misidentified by the original authors, and show that other stratigraphic evidence originally provided is uninformative and cannot be used to infer that the *Raptorex* specimen derived from the Lower Cretaceous of China. Using histological and osteological analysis, we show that there is no reason to believe that the holotype of *Raptorex* has reached subadult or young adult ontogenetic status. Further, it is revealed that the specimen was originally sold as a juvenile *Tarbosaurus* from Mongolia: a diagnosis consistent with its morphology and the results of our independent analysis.

Chapter Eight is an essay which investigates the possibility that the selective process of reinforcement may be the best explanation for the opposite morphological trends seen in the display organs of some dinosaur sister lineages. This requires recognition that Western Interior dinosaurs were largely characterized by anagenetic lineages only occasionally punctuated by true speciation events; the perspective extolled in this dissertation. Although difficult to demonstrate in extinct taxa, reinforcement has

the potential to reconcile current debate over whether dinosaur cranial display structures functioned for species recognition or sexual selection. This chapter proposes a synthesis whereby the interplay of transgression cyclicity with speciation explains patterns of diversity, mode of evolution, and morphologic variation in dinosaurs of the Late Cretaceous Western Interior.

References Cited

Horner, J. R., and M. B. Goodwin. 2006. Major cranial changes during Triceratops ontogeny. Proceedings of the Royal Society B: Biological Sciences 273:2757–2761.

Horner, J. R., D. J. Varricchio, and M. B. Goodwin. 1992. Marine transgressions and the evolution of Cretaceous dinosaurs. Nature 358:59–61.

Owen, R. 1842. Report on British Fossil Reptiles. Part II. Reports of the British Association for the Advancement of Science 11:60-204.

Sampson, S. D. 1995. Two new horned dinosaurs from the upper Cretaceous Two Medicine Formation of Montana; with a phylogenetic analysis of the Centrosaurinae (Ornithischia: Ceratopsidae). Journal of Vertebrate Paleontology 15:743–760.

Wang, S. C., and P. Dodson. 2006. Estimating the diversity of dinosaurs. Proceedings of the National Academy of Sciences 103:13601–13605.

CHAPTER TWO

A TERRESTRIAL SEQUENCE STRATIGRAPHIC INTERPRETATION OF THE HELL CREEK FORMATION OF NORTHERN MONTANA

Contribution of Authors and Co-Authors

Manuscript in Chapter 2

Author: Denver W. Fowler

Contributions: Conceived and designed the study, performed experiments, analyzed data, and wrote the manuscript.

Co-authors: none

Manuscript Information Page

Denver W. Fowler
Status of Manuscript:
_x_Prepared for submission to a peer-reviewed journal
___Officially submitted to a peer-reviewed journal
___Accepted by a peer-reviewed journal
___Published in a peer-reviewed journal

Abstract

The Upper Maastrichtian fluvial Hell Creek Formation of the Fort Peck Lake area, Montana (and regional equivalents) is notable for its vertebrate fossils and for the K-Pg mass extinction at or near its upper contact. Despite intense study, internal stratigraphy of the Hell Creek Formation is still poorly constrained, limited by problems with lithostratigraphic methodology, discontinuous outcrop, lateral discontinuity of facies, weakly constrained biostratigraphy, lack of radiometric dates, and magnetostratigraphic data of limited use. This has hindered our ability to study this important interval. By use of terrestrial sequence stratigraphic methods, this analysis has subdivided the Montanan Hell Creek Fm into four depositional sequences. These reflect 4th order cycles of accommodation and sediment supply superimposed over hypothesized 3rd order base-level rise of an incipient transgression of the Cannonball Seaway. Sequence boundaries are defined by four, laterally continuous disconformities formed by pauses in the creation of accommodation space. The disconformities are overlain by amalgamated channel complexes, or less commonly, correlative interfluve paleosols. Cyclicity in the Montanan sections may be correlative with similar 4^{th} order cyclicity and marine influence recorded in North and South Dakota, Alberta, and Saskatchewan. Magnetostratigraphy and new biostratigraphic data support correlation of the upper Montanan sequence with the North Dakotan Cantapeta tongue (and overlying fines) and Canadian Scollard and Frenchman Fms. This work also proposes important revisions to the recently proposed type section, particularly concerning complexity of the Hell Creek Formation basal contact.

Introduction

Laramide synorogenic fluviatile sediments of the Hell Creek Formation (and regional correlates) were deposited on a coastal plain bordering the Western Interior Seaway during the Maastrichtian stage of the latest Cretaceous (Hartman and Kirkland, 2002). The Hell Creek Formation is among the few geological units worldwide that record terrestrial depositional environments at the close of the Cretaceous period. It is famous for the Cretaceous - Paleogene mass extinction which occurs at or near the upper contact with the overlying Fort Union Formation, and for its vertebrate fossils, especially dinosaurs.

Paleontology remains an enduring subject of research in the Hell Creek Formation. Indeed, it was paleontological interest that first prompted Barnum Brown to investigate the badlands north of the town of Jordan, in what is now Garfield County, Montana, seeking grand exhibits for the halls of the American Museum of Natural History, New York (AMNH). Aside from collecting fine specimens of fossil vertebrates, Brown recorded the first details of the local geology. In his 1907 account of the AMNH expedition, Brown recognized the "Hell Creek beds" as distinct from the overlying unit, partly based on the absence of significant lignites in the Hell Creek, compared to their abundance in the basal part of what we now recognize as the Fort Union Formation (then referred to separately as the "lignite beds"). Brown also recognized the disconformable nature of the basal contact of the Hell Creek with the underlying Fox Hills Formation (1907; 1914), and was the first to note the prominent Hell Creek Basal Sand, and its variable thickness. Since Brown never formalized the Hell Creek beds as a distinct

formation, nor designated a type section, researchers persisted with referring to the Montana exposures as “Lance Formation” for a further 45 years (e.g. Gilmore, 1946). The Hell Creek was not designated a formation in its own right until 1952 in Cobban and Reeside’s grand correlation of Late Cretaceous strata of the Western Interior (although see Colbert and Bump, 1947, p. 94, who refer to the “Hell Creek Formation” of South Dakota). However, Cobban and Reeside (1952) also did not designate a type section, and despite recent renewed interest in the formation, this problem remained until 2014 when a lectostratotype was described by Hartman et al.

In the history of Hell Creek studies, stratigraphic analysis has often lagged behind other areas of investigation such as paleontology or sedimentology. Exceptions include important research into the uppermost Hell Creek Formation and the contact with the overlying Fort Union Formation (Archibald, 1982; Archibald et al., 1982; Dingus, 1983; 1984; Fastovsky and Dott, 1986; Smit et al., 1987; Lofgren, 1995; Turner, 2010). Otherwise, problems with lithostratigraphic methodology, discontinuous outcrop, lateral discontinuity of facies, weakly constrained biostratigraphy, lack of radiometric dates (although see Sprain et al., 2015), and magnetostratigraphic data of limited use have hindered our ability to study this important interval. For example, without internal marker beds within the Hell Creek Formation, it can be difficult to judge stratigraphic position if the upper and lower formational contacts are not observable locally, as is often the case. While this can sometimes be overcome by long traverses to areas where one of these contacts might be exposed, this is time consuming, and not always ideal as the particular horizon in which you are interested may be difficult to track. As a result, precise

stratigraphic placement of fossil specimens has been neglected, limiting our understanding of biotic change within the formation. Only relatively recently is this beginning to be unraveled (Flight, 2004; Wilson, 2005, 2014; Wilson et al., 2014; Scannella and Fowler, 2014; Scannella et al., 2014).

With renewed interest in the formation and its fauna through the pioneering work of the Clemens lab (UC Berkeley, California), and later the Hell Creek Project (a multi-institutional collaboration between the Museum of the Rockies, Montana State University; University of California Museum of Paleontology, UC Berkeley; and the University of North Dakota) the time is ripe for a reanalysis of Hell Creek stratigraphy. In conjunction with the step forward provided by the designation of a new type section (Hartman et al., 2014), this analysis looks to help structure the next phase of paleontological investigation by providing an internal stratigraphic subdivision for the Hell Creek Formation in the area south of Fort Peck Lake, through use of the burgeoning field of terrestrial sequence stratigraphy. This provides a preliminary sequence stratigraphic model that can then be tested and correlated regionally by outcrop analysis combined with subsurface well logs and magnetostratigraphic data. This analysis also presents new informal definitions for the lower, middle, and upper depositional sequences of the Hell Creek Formation (previously categorized as the lower, middle, and upper thirds; Horner et al., 2011; Scannella et al., 2014). This is of utility in discussion of the formation, and the placement of fossils in section (Scannella and Fowler, 2014; Scannella et al., 2014). Important changes are proposed for interpretation of the new type section and some of the other stratigraphic designations of Hartman et al. (2014); mainly

related to the highly variable nature of the basal contact of the Hell Creek Formation (and some underlying units. Finally, some minor corrections are suggested for previous magnetostratigraphic interpretations of Lerbekmo (2009) and LeCain et al. (2014).

Geological Setting

In the area of study around the town of Jordan, Garfield County, Montana, extensive outcrops of the Hell Creek Formation can be observed, including the upper and lower contacts (Figure 2.1).

The geological succession begins with the Bearpaw Shale (Stanton and Hatcher, 1905; equivalent to the Pierre Shale of North and South Dakota), a dark grey clay shale recording marine to offshore deposition. In its uppermost parts, the Bearpaw Shale coarsens upwards, and is gradationally supplanted by the Fox Hills Formation.

The Fox Hills Formation (Meek and Hayden, 1862) is an upward-coarsening sandstone, typically weathering to a conspicuous tan to yellow-orange color, and representing lower through upper shoreface environments deposited as the Fox Hills delta prograded north and west, out into the Bearpaw seaway (Jensen and Varnes, 1964; Waage, 1968; Lillegraven and Ostresh, 1990; Cobban et al., 1994; Flight, 2004). In Montana, the Fox Hills Formation is undivided other than that in places, the top of the Fox Hills Formation is represented by the Colgate Member (Calvert, 1912; hereafter referred to as the Colgate Sandstone; Thom and Dobbin, 1924), a fine-grained typically pale green-grey sandstone, occasionally outcropping as striking white cliffs when strongly weathered. It should be noted that the Colgate Sandstone was included within the original definition of the Hell Creek Formation Basal Sandstone by Brown (1907).

Historically, the Colgate Sandstone has been hypothesized to have been deposited in a variety of environments including fluvial, back-barrier beach, lagoonal, tidal, and shallow marine (Waage, 1968; Feldman, 1972; Butler, 1980; Wheeler, 1983; Daly, 1984). More recent work has characterized the Colgate Sandstone as representing a broad incised valley fill deposited under initially fluvial, and later estuarine conditions (Flight 2004; Behringer 2008).

Inclusion of the Colgate Sandstone within the Fox Hills Formation (e.g. Thom and Dobbin, 1924) becomes a problem during stratigraphic discussion, as there is no convenient or established term with which to refer to the lower, non-Colgate Sandstone part of the Fox Hills Formation (unlike in other states; see Waage, 1968; Fowler, Chapter 3), and there is evidence that the Colgate Sandstone represents both a different depositional environment and is possibly much younger in age (Collier and Knechtel, 1939; Waage, 1968; Flight, 2004; Behringer, 2008). Collier and Knechtel (1939) define a Lower Mbr of the Fox Hills Formation, but their lithological descriptions of this and the overlying Colgate Mbr do not match with my personal experience, nor the descriptions of Thom and Dobbin (1924), Waage (1968), or Flight (2004), in that their Colgate Sandstone is described as "light brown", whereas the defining characteristic of the Colgate Sandstone is that it is conspicuously white, or greyish-white (see refs above). In which case, my solution here is simply to treat the Colgate Sandstone as separate from the Fox Hills Formation.

The overlying Hell Creek Formation (Cobban and Reeside, 1952) consists of interbedded sandstones and mudstones, which are for the most part fluvial in origin,

although there is some indication of possible marine or tidal influence in basal beds (Tamm, 1994; Flight, 2004) and limited horizons throughout the formation in North Dakota (Murphy et al., 2002; Hoganson and Murphy, 2002). The Hell Creek is overlain by fluvial sandstones and mudstones of the Paleogene Fort Union Formation, which exhibits a series of well developed coals that are especially conspicuous at and immediately above the formational contact (Archibald, 1982; Archibald et al., 1982; Fastovsky and Dott, 1986; Fastovsky, 1987; Swisher et al., 1993).

The Upper Maastrichtian sediments of the Hell Creek Formation were deposited into the Williston and Powder River Basins of the Western Interior (Figure 2.1). The Powder River Basin is a Laramide basin, created by lithospheric flexure resulting from Laramide orogenic thrusting, and extends from east-central Wyoming to south eastern Montana (Lawton, 2008; Miall et al., 2008). The Williston Basin is an intracratonic basin active since the Cambrian, which extends across southern Alberta, Saskatchewan, Montana, North Dakota, and South Dakota, (Lawton, 2008; Miall et al., 2008). In contrast to the largely interconnected basins of the Sevier orogeny, Laramide uplifts divided depositional basins to the point where many became isolated (especially intermontane basins) and consequently might have had wildly different histories of tectonic uplift and subsidence (Lawton, 2008). However, Belt et al. (1997: page 2) noted that for the Laramide synorogenic sediments of the Northern Rockies at least, the Powder River and Williston Basins might be the only post-Bearpaw Shale examples that "share widely inter-related basinal patterns and also presumably unconformities." In which case,

sediments of the Williston and Powder River Basins represent an ideal starting point from which to construct a regional sequence stratigraphic framework for the latest Cretaceous.

Sedimentology of the Montana Hell Creek Formation has been intensively studied. Early work focused on describing broad sedimentological patterns and the nature of formational contacts (Brown, 1907; 1914; Calvert, 1912; Jensen and Varnes, 1964). Later, pioneering work of the Clemens Lab and others (e.g. Butler, 1980, Archibald, 1982) critically analysed sediments throughout the formation and laid the foundation for more detailed sedimentological descriptions and facies analysis (e.g. Fastovsky, 1986; Fastovsky and Dott, 1986; Murphy, 1986; Fastovsky and McSweeney, 1987; Fastovsky, 1987; Zaleha, 1988; Fastovsky et al., 1989; Tamm, 1993; Shoup, 2001; Flight, 2004; Hartman et al., 2014). The results of these studies have led to Hell Creek Formation paleoenvironments being relatively well understood, although their stratigraphic significance and distribution has attracted less attention.

Stratigraphy and Age

Biostratigraphy. Biostratigraphic subdivision of the Hell Creek has had some success. Johnson and Hickey (1990) subdivided the Hell Creek Formation of southwestern North Dakota into three megafloral zones, later correlating these partially with magnetostratigraphic data (Johnson, 2002). Palynostratigraphic analysis has mostly concentrated on the 20 or so meters either side of the K-Pg boundary (e.g. Bercovici et al., 2012), although some analyses have documented change through the entire formation (or equivalent; e.g. Braman and Sweet, 1999; 2012; Nichols, 2002; Koppelhus and Braman, 2010). Wilson (2005) noted variation in mammalian faunal dynamics through

the Hell Creek Formation, and related this to environmental changes. Scannella et al. (2014) showed that different species of the dinosaur *Triceratops* occur at different stratigraphic levels of the Hell Creek Formation, partly correlatable to magnetostratigraphy. Other biostratigraphic studies (Archibald, 1982; Archibald et al., 1982; Dingus, 1983; 1984; Fastovsky and Dott, 1986; Lofgren, 1995) have concentrated on variation at the K-Pg boundary, and as such do not address the formation as a whole.

Chemostratigraphy. Chemostratigraphic analyses have mostly concerned the uppermost 20 meters or so (e.g. Arens and Jahren, 2002). However, some analyses have addressed the entire formation, documenting a negative carbon isotope excursion at the K-Pg boundary, with six negative carbon isotope excursions, and four tentative positive carbon isotope excursions within the Hell Creek Formation itself (Arens et al. 2014).

Lithostratigraphy. Lithostratigraphic subdivision of the Hell Creek Formation into individual members has proven challenging due to lateral discontinuity of distinctive facies over any more than a few km. However, Frye (1967, 1969) described and named a number of lithostratigraphic members for outcrop in North Dakota, although most workers have since considered Frye's members unrecognizable in the field (e.g. Johnson, 1989; Murphy et al., 2002; although see Butler, 1980).

Internal divisions of the Montanan Hell Creek Formation include recognition of the Basal Sandstone by Brown (1907; who included in the Hell Creek Basal Sandstone a unit which would later be considered the Colgate Sandstone; Thom and Dobbin, 1924), informal definitions for upper and lower divisions offered in various unpublished

graduate theses (Flight, 2004; Wilson, 2004), and definition of the new type section (Hartman et al., 2014). Flight (2004) took a lithostratigraphic approach (very similar to Brown's original definitions in 1907), defining the lower Hell Creek Formation as comprising the various mudstones, siltstones and organic rich horizons that typically overlie the Fox Hills Formation (~2 m), combined with the overlying Hell Creek Formation basal sand (0-12 m). Flight's upper Hell Creek (typically ~75-80 m) comprises everything above the upper contact of the Basal Sand to the upper formational contact with the overlying Fort Union Formation. Wilson (2004) takes a more utilitarian approach, referring to the lower 47.2 m (155 ft) as "the lower part of the Hell Creek Formation" and the upper 45.7 m (150 ft) as "the upper part of the Hell Creek Formation".

The most recent attempt to standardize Hell Creek Formation lithostratigraphy was conducted by Hartman et al. (2014), who defined a lectostratotype (hereafter referred to as the "type section") at Flag Butte, near Hell Creek itself. This new type section comprises ~110 m thickness of exposure, of which 84.2 m was determined to represent the full thickness of the Hell Creek Formation. Hartman et al. (2014) publish informal names for the major sand units (Basal Sandstone, JenRex sandstone, Apex sandstone, Ten Meter Sandstone) which have been used by members of the Hell Creek Project for over a decade. However, my analysis suggests that Hartman et al. (2014) probably misinterpret the basal contact of the Hell Creek Formation at the type section and elsewhere (see Results).

A lithostratigraphic unit of use (at least locally) is the Ø or "Null" coal (so named because it occurs below the z coal); a lignite that occurs within the Hell Creek Formation, ~30 m below the upper contact (Lofgren, 1995; Sprain et al., 2014). The Null coal is well documented in the Bug Creek area (Lofgren, 1995), but thins to the west (pers. obs.), and is probably absent at the type section. Thickness and lateral continuity of the Null coal east of Bug Creek is undocumented. Although relatively laterally restricted, the Null coal is very important as it bears two ashes which have been recently dated by Sprain et al. (2014; see chronostratigraphy, below). Location of new exposures of the Null Coal has been one of the results of the current project.

Well Log Analysis. Connor (1992) used spontaneous potential (SP) and resistivity geophysical logs to document regional thickness variation of the Hell Creek and Lance Formations in northeastern Wyoming and southeastern Montana. The sampled area did not reach as far north as the type area around Jordan, but did include wells ~140 km southwest, near Roundup, and ~ 80 km south of Glendive in eastern Montana. Due to limitations with the SP and resistivity logs, Connor (1992) could not differentiate the Fox Hills Formation from the Hell Creek / Lance, nor did he mark any specific horizons or subunits within the Hell Creek or Lance Formations.

Magnetostratigraphy. The lowermost two thirds of the Hell Creek Formation is of normal polarity, assigned to C30n (68.196 to 66.398 Ma; Ogg 2012; Swisher et al.,1993; Lerbekmo, 2009; LeCain et al., 2014). However, as sandstone bodies are not amenable to paleomagnetic analysis, then the polarity of the Basal Sand cannot be tested, although it

can be inferred to fall within C30n as the underlying Colgate Sandstone is also of normal polarity, and considered to lie within C30n (Lerbekmo, 2009).

The uppermost Hell Creek Formation (10-20 m in Montana; Archibald et al., 1982; Swisher et al. 1993; Lerbekmo, 2009; LeCain et al., 2014) is of reversed polarity, assigned to chron C29r, and corroborated in North Dakota sections (up to 24 m below the K-Pg boundary; Hicks et al., 2002; Lund et al., 2002) and Canadian equivalents (Lerbekmo, 1999; 2009; Lerbekmo and Coulter, 1985)..The boundary between C30n and C29r is typically plotted as occurring within a thick sandstone unit (correlating with the Apex sandstone, but not explicitly identified as such; Hartman et al., 2014; LeCain et al., 2014). However, as this sandstone cannot be magnetostratigraphically sampled, then it is convention to place the boundary half way between sampled horizons below and above the sandstone (hence plotting within the sandstone itself). Given that the basal scour at the base of the sandstone may represent a considerable hiatus, then it is at least possible that the C29r-C30n boundary occurs at this horizon rather than within the sandstone itself.

Within C29r, a short, normal polarity subchron has been detected at the K-Pg boundary, at the top of the Hell Creek equivalent Frenchman Fm (Sakatchewan, Canada; Lerbekmo, 1999; corroborated in time with at least two cores from the Atlantic Ocean; Lerbekmo et al., 1996). A similarly placed normal subchron was detected 15-20m below the K-Pg boundary in the Scollard Fm, Red Deer River, Alberta (Lerbekmo and Coulter, 1985). A normal subchron has not yet been detected within C29r in US sections.

Some corrections have been made to magenetostratigraphic zones defined by Lerbekmo (2009) and LeCain et al. (2014), based on ammonite biostratigraphy and revision to the new type section (see Results section).

Chronostratigraphy. Constraining an age for the Hell Creek Formation has proven problematic due to sparse chronostratigraphic markers within the unit. Despite bentonite clays (derived from volcanic ash; although see Fastovsky and Bercovici, 2015) being prevalent throughout the Hell Creek Formation, they have not yielded any radiometric dates (Murphy et al., 2002), although research is ongoing (K. Johnson, pers. comm., 2009; P. Renne, pers. comm., 2011). Although recent publications (e.g. Fastovsky and Bercovici, 2015) have lamented a lack of radiometric dates from within the Hell Creek Formation, in actuality the first radiometric date was published (to little fanfare) in 2014 by Sprain et al.; they had retrieved an Ar / Ar date of 66.298 +/- 0.051 Ma for an ash within the Null coal, ~30 m below the K-Pg boundary (incorrectly shown as ~50 m in the figure of Sprain et al., 2014; pers. obs.; Sprain pers. comm.). The same analysis sampled a number of horizons within the z-coal complex (at the K-Pg boundary, technically the basalmost unit of the overlying Fort Union Formation), recovering a range of dates from 65.962 - 66.035 Ma; note that all the dates in Sprain et al. (2014) use the standard and decay constant pairing of Renne et al. (2011), which produces slightly older dates than the more commonly used pairing of Kuiper et al. (2008), and Min et al. (2000). The Null coal date is important for two reasons; firstly, it shows that the upper ~30m of the Hell Creek Formation was deposited in the last 0.263 - 0.336 Ma of the Cretaceous (which corresponds to the final two depositional cycles identified here; see later). Secondly, it

occurs within sediments magnetostratigraphically dated as C30n, but only 5-10 m or so below the first sediments which belong to C29r (extrapolation from LeCain et al., 2014), and thus may be of use in constraining the age of the C30n - C29r boundary.

Age of the Upper and Lower Contacts, and Duration. In Montana, age of the upper formational contact is roughly coincident with the K-Pg boundary, and is therefore ~66.0 Ma (Kuiper et al., 2008; Gradstein et al. 2012). As stated above, the boundary is coincident with a complex of coals in the lowermost Fort Union Formation, which have been recently dated as between 65.962 - 66.035 Ma (Sprain et al., 2014).

Age determination of the basal contact has been more difficult to place precisely, but can be roughly constrained based on magnetostratigraphy. Lerbekmo (2009) demonstrated that along the Hell Creek Marina Road (Fish and Wildlife Service Road 105), the Fox Hills Formation is of reversed polarity immediately below the contact with the Colgate Sandstone (similarly observed in the Canadian equivalent Whitemud Formation; Lerbekmo, 1985). Lerbekmo assigns this reversed polarity zone to C30r (68.196 to 68.369 Ma; Ogg, 2012). This would be consistent with biostratigraphic analysis of ammonites from the Fox Hills Formation of North Dakota (Landman and Waage, 1993; Landman et al., 2004). If these magnetostratigraphic zone designations are correct, then the base of the Hell Creek can therefore be constrained to no older than ~68.0 Ma. However, there is evidence that the Fox Hills Formation in Montana is older than in North Dakota, suggesting that revision of this designation is required (see magnetostratigraphy section of Results).

Regardless, if the underlying Colgate Sandstone is indeed C30n (Lerbekmo, 2009) then the base of the Hell Creek Formation can be no older than the base of C30n (68.196 Ma; Ogg 2012). Duration of the Hell Creek Formation can therefore be constrained as no more than ~2 million years (basal contact no older than ~68.2 Ma, upper contact 66.0Ma), and likely substantially less. This is consistent with estimates by Wilson (2004; 2005; 2014) of ~1.8 million years. Hicks et al. (2002) calculated an age estimate of 66.71 to 66.87 Ma (compared to an older date for the K-Pg boundary of 66.5 Ma) for the base of the North Dakota Hell Creek Formation by extrapolating sedimentation rates from the upper part of the succession, giving a total duration of ~1.36 million years. Lund et al. (2002) estimated the duration of the Hell Creek as ~2.5 million years.

Marine Influence and Sequence Stratigraphic Analysis. With lithostratigraphic recognition of marine influence in the Hell Creek Formation of North Dakota (Breien Member and Cantapeta Tongue; Seager et al., 1942; Laird and Mitchell, 1942; Frye, 1967; 1969; Butler, 1980; Murphy et al., 2002), supported by floral and faunal data from the formation as a whole (Kennedy et al., 1998; Hartman and Kirkland, 2002; Johnson, 2002; Longrich et al., 2011; Moore et al., 2014), it has been realized that unlike in many paleogeographical reconstructions (Lillegraven and Ostresh, 1990), the Western Interior Seaway may not have fully retreated from the Northern US in the latest Maastrichtian (Johnson et al., 2002; Boyd and Lillegraven, 2011). In 2002, Johnson and colleagues proposed that Hell Creek sediments were not in fact, deposited during the final regression of the Western interior Seaway (as had been the generally accepted view; e.g. Lillegraven

and Ostresh, 1990; Archibald, 2011). Rather, the Hell Creek and overlying Fort Union Formations were deposited under transgressive conditions during early inception of the Cannonball transgression. This non-traditional interpretation is more consistent with current sequence stratigraphic depositional models, since transgressive conditions (through base-level rise) are one stratigraphic control which can create the necessary accommodation required for sediment deposition and preservation. Indeed, there has never been any strong evidence supporting the view that the seaway fully retreated (see the excellent review in Boyd and Lillegraven, 2011).

Traditional lithostratigraphic methods correlate packages of similar lithologies into formations, or members. However, in fluvial depositional systems, facies are generally laterally consistent only over a few kilometers at best, making detailed correlations and interpretations difficult. In contrast, sequence stratigraphic methods recognize and correlate cycles of sedimentation, utilizing key surfaces and stratal stacking patterns. Thus, application of sequence stratigraphic methodology to the Hell Creek Formation has the potential to subdivide and correlate within the formation beyond the limitations of traditional lithostratigraphic techniques. Following the work of Johnson et al. (2002), Flight (2004) provided the first sequence stratigraphic interpretation of the Bearpaw Shale through to the lower third of the Hell Creek Formation in the area surrounding Ft. Peck Reservoir, Montana. Behringer (2008) elaborated upon Flight's (2004) interpretation of the Colgate Sandstone as an incised valley filled with estuarine deposits, adding further detail.

This study follows the work of Flight (2004), to develop a sequence stratigraphic framework to establish correlations and the pattern of cyclic sedimentation for the complete Hell Creek Formation in the Fort Peck area. This is a necessary preliminary step that can then be tested further afield by analysis of subsurface logs in order to construct a regional sequence stratigraphic interpretation for the latest Cretaceous. This paper also includes regional correlates in the analysis that greatly enhance the ability to interpret sequence boundaries observed in outcrop. This broader focus helps explain small differences between this interpretation and that of Flight (2004).

Methods

This study is based on field observations and 27 measured sections detailed during fieldwork in the summers of 2007-2011 mostly in the area immediately south of Ft. Peck Reservoir, north of Jordan, eastern Montana (Figures 2.1, 2.2). This data is augmented by sections recorded near Ekalaka, southeast Montana, and field observations of outcrop exposed in Makoshika State Park, Glendive, eastern Montana. Sections were measured using a Brunton compass and a 1.5m Jacob's Staff.

Stratigraphic Abbreviations

In stratigraphic order, oldest first; see results for definitions and descriptions. Kbp, Bearpaw Shale; Kfh, Fox Hills Sandstone; Kfhc, Colgate Sandstone; Kcp, Colgate tidal flats; Kba, possible Battle Formation; Khc-bs, Hell Creek Formation Basal Sand; Khc-lf, Hell Creek Formation lower fines; Khc-jrs, Hell Creek Formation Jen Rex Sandstone; Khc-mf, Hell Creek Formation middle fines; Khc-as, Hell Creek Formation

Apex Sandstone; Khc-uf1, Hell Creek Formation upper fines unit 1; Khc-10ms, Hell Creek Formation 10 Meter Sandstone, Khc-uf2, Hell Creek Formation upper fines unit 2; PgF, Fort Union Formation.

Orders of Cyclicity

Depositional cycles are commonly referred to as representing different orders of magnitude based on their wavelengths (duration), although there are sometimes inconsistencies with how this is reported. Here I follow the definitions given in Miall (2010), where a first-order cycle is 200 - 400 m.y.; a second-order cycle, 10 - 100 m.y.; third- to fifth-order cycles are 0.01 - 10 m.y.; and fourth- to fifth order cycles are 0.01 to 2 m.y. (overlaps are as given by Miall, 2010). It is worth noting that Miall (2010) cautions that such terminology is no longer recommended; however, they are used here as they are convenient and prevalent in the literature.

Terrestrial Sequence Stratigraphy

Sequence stratigraphic analysis relies upon interpretation of sedimentological responses to cycles of accommodation and sediment supply that are subject to a number of primary allogenic and autogenic controls, including eustasy, climate, basin subsidence, and source area tectonism. Strata are arranged into depositional sequences originally defined as “a relatively conformable succession of genetically related strata bounded by unconformities or their correlative conformities” (Mitchum et al., 1977: p. 53). A revised definition is offered by Catuneanu et al. (2009a: p. 19) as “a succession of strata deposited during a full cycle of change in accommodation or sediment supply”. This

removes the need for a depositional sequence to specifically be bound by unconformities, and intentionally excludes reference to the controversial term “base-level” (Catuneanu et al., 2009b).

Cyclic patterns of deposition have long been recognized in terrestrial sediments, but their study through sequence stratigraphic methods is relatively new. Since the foundational work of Vail and colleagues (1977), the principal focus of sequence stratigraphic study has been on depositional systems influenced by relative changes in sea level. Terrestrial sequence stratigraphy has been studied to a much lesser degree. Nevertheless, a series of interpretations have been presented utilizing cycles of accommodation and sediment supply to explain variation in channel stacking patterns of multistory amalgamated channel sandstones, and isolated channels within floodplain dominated mudstone successions (Posamentier and Vail, 1988; Miall, 1991; Legaretta et al., 1993; Schumm, 1993; Wright and Marriot, 1993; Shanley and McCabe, 1993; 1994; Aitken and Flint, 1994; Kamola and Van Wagoner, 1995; McCarthy and Plint, 1998; Marriot, 1999; Posamentier and Allen, 1999; summarized in Catuneanu, 2006, leading to the most recent revision and standardization by Catuneanu et al., 2009a). Other recent work has emphasized the importance of both the frequency and maturity of paleosols (Bown and Kraus, 1987; Kraus, 1987; 1999; 2002; Cleveland et al., 2007) and trace fossils (Buatois and Mangano, 2004) in interpreting cyclic patterns of deposition. However, controversy exists as to the appropriate application of sequence stratigraphic methods and terminology to terrestrial depositional cycles.

In terrestrial systems, it is conventional to consider that the influence of eustatic sealevel decreases upstream, however, it has become a recent point of discussion as to just how far upstream this influence can extend. Catuneanu (2008) represents a typical viewpoint that sealevel might influence deposition in low-relief systems up to about 250 km inland from the shoreline, although significantly less in fluvial systems where barriers might exist. However, in the extremely low-relief Amazon River Basin, Quaternary sealevel change has been shown to have affected valley incision and sedimentation up to 1500 km inland (Irion et al., 2009). Another study on the Amazon River Basin documented tidal effects on sedimentation occurring over 1000 km inland (Kosuth et al., 2009).

Due to difficulty directly linking sealevel change with terrestrial depositional cycles, then a systems tract or depositional sequence terminology that is linked to sealevel and shoreline trajectories (e.g. Falling Stage, Lowstand, Transgressive, and Highstand Systems Tracts; FSST, LST, TST, HST, respectively) may not be strictly applicable to inland terrestrial deposits without demonstrating regional correlation to paralic and marine sediments. Further, the cause of cyclicity in terrestrial sedimentation probably more strongly reflects a balance of allogenic and autogenic factors (including eustasy, climate, basin subsidence and source area tectonism), rather than only sea-level. Consequentially, recent work on terrestrial sequence stratigraphic models have steered away from traditional sea-level linked nomenclature and instead use alternative terms of High- and Low-Accommodation Systems Tracts (HAST and LAST, respectively;

Schumm, 1993; Tandon and Gibling, 1994; Shanley and McCabe, 1994; Holbrook, 1996; Legarreta and Uliana, 1998; Miall, 2002; Catuneanu, 2006; Catuneanu et al., 2009a).

Cycles of sedimentation in terrestrial deposits tend to follow a pattern of stacked sequences consisting of a sequence boundary, overlain by a LAST, and subsequent HAST. Sequence boundaries are created by periods of zero or negative accommodation (i.e. loss), represented by non-deposition or erosion, hence a surface of subaerial unconformity or disconformity (Type 1 sequence boundaries; Posamentier and Allen, 1988; Catuneanu et al., 1999). These can take the form of erosive scours (sometimes with significant incision forming incised valleys, or alternatively forming a regional flattened "peneplanation surface") or correlative development of mature interfluve paleosols (Wright and Marriot, 1993; Kraus, 1999, 2002; Miall, 2013). Alternatively (perhaps more terminologically than conceptually), recent work has suggested that sequence boundaries may instead follow a compounded "cut and cover" formational mechanism where rivers quickly erode then deposit channel facies, without a prolonged nor laterally extensive subaerial exposure (Holbrook, 2001; Strong and Paola, 2008; Holbrook, 2010; Gibling et al., 2011; Holbrook and Bhattacharya, 2012; Miall, 2013). Under this model, repeated "cut and cover" events amalgamate laterally to produce amalgamated channel deposits (either sheet-like or confined within a valley) basically identical to that under previous models with the conceptual difference that the underlying sequence boundary surface of erosion may be more strongly diachronous (Gibling et al., 2011). Regardless, sequence boundaries are usually placed at the base of the LAST, representing a period of low accommodation where floodplain aggradation rates were slow. Thus LAST is typically

characterized by, laterally extensive amalgamated channel complexes, and / or incised valley-fills. In HAST, accommodation is created and filled rapidly, leading to thick successions of aggrading overbank fines with only weakly developed paleosols on the floodplain, and isolated rather than amalgamated channels. The terrestrial equivalent of a marine maximum flooding surface (i.e. maximum basinal subsidence) may be represented by extensive coal seams and / or lacustrine sediments (Catuneanu and Sweet, 1999). During later HAST deposition, as the rate of accommodation diminishes, floodplain aggradation decreases and more strongly developed soils may form, including a more mature paleosol at the top of the HAST (Kraus, 1987, 1999, 2002). However preservation may be limited because of potential erosion of the subsequent sequence boundary, or that aggradation rates of the following LAST are so low that sediment reworking by channel combing is intense.

There is an increasing amount of literature that utilizes terrestrial sequence stratigraphic methods to identify cyclic depositional sequences in ancient fluvial systems (e.g. Aitken and Flint, 1994; Kamola and Van Wagoner, 1995; Eberth et al., 2001; Plint et al., 2001; Zerfass et al., 2003, Catuneanu et al., 2006; Cleveland et al., 2007; Roca and Nadon, 2007). Examples from retroarc foreland basins (Laramide and Sevier synorogenic systems) of the Upper Cretaceous of the Western Interior of the United States include the Campanian Two Medicine Formation, Montana (Rogers, 1994;1995;1998; Shelton, 2007); Maastrichtian upper Bearpaw through basal Hell Creek Formation, Montana (Flight, 2004; Behringer, 2008); Campanian to Paleocene strata of the Bighorn Basin, Wyoming (Mitchell, 2002); the Maastrichtian Ferris Formation, Wyoming, (Wroblewski,

2006); Cenomanian Dakota Sandstone, Utah (Antia and Fielding, 2011), Campanian to Paleocene Mesaverde Group, Utah (Olsen et al., 1995), and Maastrichtian Javelina Formation, Texas (Atchley et al., 2004). Of particular interest are cyclic depositional models that have been developed over the past 20 years in Alberta, as these relate to depositional systems very similar to the Hell Creek Formation. Here, depositional sequences and sequence boundaries of distal floodplain and marine intertonguing sediments of the Belly River Group (Eberth, 1990; 1996; 2005; Eberth and Hamblin, 1993; Eberth and Brinkman, 1994) and Edmonton Group (Catuneanu et al., 1999; Straight and Eberth, 2002; Chen et al., 2005) have been correlated with the contemporaneous inland Wapiti Formation (Fanti and Catuneanu, 2010). This provides an ideal case study of what can be achieved by developing an initial model from outcrop in a relatively restricted area, through expansion using subsurface data, eventually leading to a regional model, including units that are entirely terrestrial with no marine tongues.

In terms of applying a sequence stratigraphic model, the Montanan Hell Creek Formation presents a slightly unusual case for two reasons. Firstly, in the Fort Peck area, the underlying Bearpaw Shale, Fox Hills Sandstone, Colgate Sandstone (in part), and lowermost part of the Hell Creek Formation Basal Sand are either marine in origin, or exhibit marine influence. Secondly, Hell Creek Formation sediments can be linked to marine transgression in North Dakota (Johnson, 2002; Murphy et al., 2002; Hoganson and Murphy, 2002). Hence it is possible to employ marine-related sequence stratigraphic terminology in at least the lower parts of the succession, up to the Basal Sand. Thus, this

analysis uses traditional nomenclature for the marine influenced units, and terrestrial nomenclature for units that cannot as yet be linked to marine units.

Here I use the terms offered by Hartman et al. (2014) for sandstone units found at consistent stratigraphic positions within the Hell Creek Formation, correlated to either the upper or lower contact. The “Basal Sandstone” is typically present at the base of the Hell Creek Formation (Brown, 1907; although see discussion). The “Jen Rex Sandstone” occurs ~15 m above the top of the Basal Sandstone. The “Apex Sandstone” and “10 Meter Sandstone” occur ~25-30 m and ~10 m (respectively) below the contact with the Fort Union Formation (Hartman et al., 2014).

Results

Lithofacies and Generalized Section (Figure 2.3)

Lithofacies descriptions mostly follow those of Flight (2004). Detailed descriptions can be found in Appendix A. As Flight (2004) is the most detailed treatment of Hell Creek lithofacies in the type area, and of a sequence stratigraphic framework, it was desirable to stay as close to Flight's definitions as possible in order to facilitate cross comparison between measured sections and interpretation.

With a few exceptions, most of the described features can be seen in the area of the new type section (Flag Butte; Hartman et al., 2014; see below).

Bearpaw Shale (Kbp). The Bearpaw Shale is the basalmost formation considered in this study; as such only the uppermost 10-20 m have been observed in outcrop. The Bearpaw Shale consists of a generally coarsening upwards sequence, predominantly shale

(massive to laminated mudstone, Mml) with occasional interbedded silty sandstone (horizontally stratified silty sandstone, Sh; massive silty sandstone, Sm). Shales are typically mid-dark grey, fissile, massive to laminated, weather a dark grey color with occasional iron staining, and form low rounded hills. Beds of pale grey to tan, fine grained silty sandstone, up to 1 m thick, become increasingly common in the upper 5-10 m of the formation, where they are interbedded with shale. Silty sandstones are massive, planar bedded or occasionally hummocky-cross-stratified, weather a pale grey color, and form steeper slopes than the underlying shale. The Bearpaw sandstones eventually grade into the overlying Fox Hills Sandstone.

Fox Hills Sandstone (Kfh). The Fox Hills Sandstone is a complex unit that generally coarsens upwards and exhibits a sheet-like geometry with considerable variation in thickness. Lithologies are typically fine-grained sandstones (hummocky cross-stratified, Shcs; trough cross-bedded, St; ripple cross laminated, Sr; low angle planar bedded, Sl; and massively bedded, Sm) with less common interbedded mudstone (Mm). The Fox Hills Sandstone is conspicuous in outcrop by its yellow-orange coloration (Figures 2.4-2.6); generally distinct from the more pale grey sandstones and silty sandstones of the underlying Bearpaw Shale, or overlying Colgate Sandstone and Hell Creek Formation (although the latter are often tan colored). The gradational transition from the Bearpaw Shale to Fox Hills Sandstone has led to variable lithostratigraphic definitions of the position of the contact (e.g. Landman and Waage, 1993; Landman and Cobban, 2003). For consistency, here the basalmost bed of the Fox Hills Sandstone follows Flight (2004) as being either the first amalgamated hummocky cross-stratified

sandstone (in contrast to the isolated units of the Bearpaw Shale), first massive sandstone, or first trough cross-stratified sandstone. Typically the Fox Hills Sandstone is 4-6 m thick, but can reach up to 15 m thick locally (Flight, 2004). Massive bedding and hummocky cross stratification is more common near the base of the formation, with trough cross bedding and ripple cross lamination more common higher up. Grain size is lower to upper fine (Jensen and Varnes, 1964). *Thalassinoides* and *Planolites* burrows are recorded in trough cross-stratified sands by Flight (2004). Large carbonate-concretions are common throughout (Jensen and Varnes, 1964), but especially in the upper part of the unit, which is typically capped by prominent bench-forming cemented sandstones.

Colgate Sandstone (Kfhc). The Colgate Sandstone is most easily distinguished from the underlying Fox Hills Sandstone by its grey to white weathering color, and greenish-grey fresh surfaces (Figure 2.7; Calvert, 1912; Thom and Dobbin, 1924; Murphy et al., 2002, although see below). Where present, the Colgate Sandstone rests on an erosive scour (Se) that is typically shallow (0-2 m), but sometimes incises up to 25 m into the Fox Hills Sandstone, or even into the underlying Bearpaw Shale (Flight, 2004; Behringer, 2008). A coarse grained basal lag was recorded by Wheeler (1983) although this is rarely encountered (Flight, 2004; Behringer, 2008). Otherwise, the Colgate Sandstone is a micaceous, clay-rich fine-grained sandstone, with occasional thin interbedded mudstones (Mm), and rare, laterally restricted coals (C2; Figure 2.8). Bedding is typically planar (Sh) or massive (Sm), although trough cross stratification (St) is visible in particularly thick sections. Total thickness of the Colgate Sandstone varies,

and is typically 2-5 m, but up to 15m in geographically restricted areas (see below; Flight, 2004).

The Colgate sandstone is not typically laterally extensive and exhibits mostly restricted channelized geometry (Flight, 2004; Behringer, 2008). Although the degree of cementation may vary, concretions are notably absent from the Colgate Sandstone, unlike the underlying Fox Hills Sandstone and overlying Basal Sand of the Hell Creek Formation (which may aid in distinguishing the Colgate Sandstone from these units; although note that Waage, 1968, suggests calcareous concretions are present in Colgate Sandstone exposures of South Dakota, none were observed by myself in Montana). *Skolithos* burrows are recorded in massive and planar-bedded sandstones by Flight (2004).

Although the bold white weathered color is considered characteristic of the Colgate Sandstone (Calvert, 1912; Thom and Dobbin, 1924; Waage, 1968; Murphy et al., 2002; Flight, 2004; Behringer, 2008), this is variable geographically, and not commonly seen in the Hell Creek type area (Jensen and Varnes, 1964), although it is conspicuous at the northern edge of "Best Butte" (see section description or the Marina Road exposures). The Colgate Sandstone more typically exhibits conspicuous dual color banding (Figures 2.5, 2.7, 2.8), with a lower pale tan unit, and a less colorful but brighter pale grey upper unit. The upper unit exhibits more thin interbedded mudstones than the lower unit, and it is the upper unit that sometimes weathers to a bold white color (Figure 2.7). In a fresh surface, the contact between the two beds is marked by a thin (~1-2 mm) iron-rich horizon, while the initial 2-3 cm above the contact are notably gleyed (Figure 2.9). The

Colgate Sandstone fines rapidly in the upper 1-2 meters into a grey siltstone (Fsm), and is almost always overlain by an organic-rich horizon (C1). These two lithofacies are included here within the Colgate Sandstone, mainly due to the transitional contact of Sm with Fsm making separation difficult. Previous authors (e.g. Dobbin and Reeside, 1929; Flight, 2004; Behringer, 2008) have included these units as the basalmost facies of the Hell Creek Formation, but again, the transitional nature of Sm to Fsm makes this undesirable. However, to be consistent with original descriptions, and to aid in sequence stratigraphic interpretation, the term Colgate Sandstone is used here to refer only to the sandy part of the unit. The overlying silt and organic-rich horizon are referred to as the Colgate Tidal Flats (Kcp; see below).

Colgate Tidal Flats (Kcp). This unit has previously been (and is currently technically) assigned to the lowermost Hell Creek Formation (Erickson, 1992; Murphy et al., 2002; Flight, 2004); however, this is problematic as it is part of the underlying Colgate depositional sequence (see discussion), so it is treated separately here. The Colgate tidal flats is a thin (typically <2 m) unit with a sheet-like geometry that is more commonly present in outcrop than the Colgate Sandstone itself. It either overlies the Colgate Sandstone (Figures 2.4, 2.5) or lies directly on the Fox Hills Sandstone (Figure 2.10), and consists of two beds: a lower pale grey muddy siltstone typically ~0.5-1 m thick (although sometimes up to 2m) that is capped by a prominent organic rich siltstone to sandy siltstone ~1 to 50 cm in thickness (Figures 2.4, 2.5, 2.10). The depositional environment has been interpreted as a paleosol (Erickson, 1992), and by Flight (2004) as tidal flats deposited during the HST of the Colgate depositional sequence. This unit is

overlain by the basal sand (or equivalent) of the Hell Creek Formation, or very rarely by a series of lithofacies here tentatively assigned to the Battle Formation.

?Battle Formation (Kba). An unusual set of lithofacies up to 10 m in thickness occurs between the underlying Colgate Sandstone (C1), and erosively overlying Basal Sand of the Hell Creek Formation (Figure 2.5; Se, followed by Sm, Shcs, or St). The set of lithofacies comprise a basal pale colored siltstone (seatearth, Fr), an organic rich silt or sandstone (C), and mauve or green-grey banded mudstone (Fml).

These lithofacies were assigned (in part) to Fml of the lower Hell Creek Formation by Flight (2004). However, here I very tentatively refer them to the Battle Formation (otherwise only recorded in southern Alberta and Saskatchewan). This referral is based on lithological similarity to description of the Battle Formation given by Irish (1970), and the occurrence of palynomorphs that have correlated with the Battle Formation in Alberta and Saskatchewan (Lerbekmo, 2009).

These facies show similarity to the organic rich C1 facies as defined above as the uppermost facies of the underlying Colgate Sandstone. However, I chose to include C1 within the Colgate Sandstone (rather than the Battle Formation) as C1 is encountered overlying Fsm of the Colgate Formation in sections where neither the sandstone facies of the Colgate Sandstone, nor the Battle Formation facies are present. In the future it might be desirable to remove both Fsm and C1 from the Colgate Sandstone and place them within the Battle Formation, although definition of the boundary between these units is not clear, and I am unable to find good photographs; for example, it is not clear if the

basal bed of the Battle Formation is one of the organic-rich horizons, or the underlying pale siltstone (Irish, 1970; Eberth and Braman, 2012).

It is necessary to separate these possible Battle Formation facies mainly due to the confusion that their inclusion in either the Colgate or Hell Creek formations might cause concerning the age of these units and their contacts. I also consider that the basal unit of the Hell Creek Formation should be maintained as the Basal Sandstone as originally defined by Brown (1907), and consistent with current understanding of depositional cyclicity.

I have only encountered these probable Battle Formation facies in the area around Hell Creek itself, most easily observable at Manaige Spring (Figure 2.5), but also in the cliffs visible on both sides of the usually flooded tributary of Hell Creek itself ("Battle Butte"). Combined thickness of the Battle Formation lithofacies is 10 m at Manaige Spring, but thins northwards such that it is only ~ 5 m thick at Battle Butte (~ 1 km north of Manaige Spring), and absent at "Best Butte" (~3 km NE of Manaige Spring). I suspect that this represents considerable northwards thinning and hence consider the Battle Formation as lenticular in geometry.

These facies descriptions are only preliminary as a more detailed investigation of these specific beds has not been conducted.

Hell Creek Basal Sand (Khc-bs). The Hell Creek Basal Sand is an amalgamated channel complex of variable thickness that is usually present as the basalmost bed of the Hell Creek Formation. Normally the contact with the underlying Colgate units is non-erosive (Figures 2.4, 2.5, 2.10), but is occasionally marked by an erosive scour (Se; up to

5m depth; Figure 2.10). However, scouring is relatively rare and very localized in nature, perhaps explaining how it was not observed by Flight (2004), although it was mentioned by Brown (1907; 1914) and Jensen and Varnes (1964), who suggested incisions up to 10 m are known. Geometry of the Basal Sand is sheet-like, and although laterally continuous over many kilometers, thickness varies (Brown, 1907), being up to 15 m, but typically 5 m or less (recorded as 5.8m in the new type section; Hartman et al., 2014). The Basal Sand varies in color from mid-pale grey through to tan or brown. In contrast to the fine grain size of the underlying Colgate Sandstone, the Basal Sand is typically medium to coarse grained at its base, fining upwards, and exhibits a "peppered" appearance which can help distinguish it from Colgate or Fox Hills Sandstones (Jensen and Varnes, 1964). Bedding consists of inclined heterolithic strata (Sihs; especially near the base; Figure 2.7), trough cross-bedded sandstone (St; more common), massively bedded sandstone (Sm), ripple cross-laminated sandstones (Sr), and occasional interbedded siltstones and mudstones (Fml). Conglomerate channel lags are occasionally observed within the lower 2-3 m, and comprise weathered bone and mudstone clasts typically <2cm in diameter, but occasionally up to 10cm. Concretions are frequent and sometimes large, on the scale of meters. Where present, the upper 1-2 m of the Basal Sand fine upward rapidly and are overlain by a package of fine grained sediments and isolated channels: the lower Hell Creek Formation fines.

Lower Hell Creek Formation Fines (Khc-lf). The lower Hell Creek Formation fines are a variable package of typical overbank fluvial sediments consisting of mudstones (Fml), organic-rich mudstones (C), crevasse splay sandstones, siltstones

(Fml), and isolated channel facies (St, Sr, Sm; Figures 2.4-2.6, 2.10-2.14). Mudstones are variegated, banded, often bentonitic, and typically "somber" (Brown, 1907) low-chroma shades of grey, brown, purple, or green. Organic-rich shales are common, red-brown in color, laminated, and friable. Infrequent channel sandstones are isolated and typically more fine grained than the amalgamated channels of the Basal and Jen Rex Sands that bracket Khc-lf. Individual beds are typically lenticular in geometry and rarely traceable over any more than a kilometer. Repeated packages of a basal fine crevasse splay sandstone or siltstone that fines upwards through a massive mudstone, and finally an organic rich shale, are common and interpreted as stacked paleosol successions (Kraus, 1987). Thickness of the Lower Hell Creek Formation fines is variable, in part due to the varying incision depth of the overlying Jen Rex Sand. Typically, the Lower Fines are ~15 m thick (19.2 m in the new type section; Hartman et al., 2014), although this can be as little as 2-3 m (Flight, 2004).

Jen Rex Sand (Khc-jrs). The Jen Rex Sand is an amalgamated channel complex that typically occurs ~15 m above the top of the Basal Sand, immediately overlying the overbank fines and isolated channels of the lower Hell Creek Formation (Khc-lf). This contact is highly variable, and as a consequence the thickness of the Jen Rex Sand is similarly variable. The contact is usually marked by an erosive scour, with depth variation highly localized, typically from 0-5 m, but up to 15 m (Flight, 2004). Geometry of the Jen Rex Sand is sometimes channelized in lower parts, but is otherwise sheet-like and can be laterally continuous over several kilometers. Thickness varies, and is usually 5-6 m (where present) but is often much thicker, up to 12 m (11.9 m in the new type

section; Hartman et al., 2014; Figures 2.6, 2.11-2.14), giving it the greatest maximum thickness of the Hell Creek Formation amalgamated channel complexes. The Jen Rex Sand is typically tan or brown colored, often with prominent orange, concreted horizons (Figures 2.4, 2.5, 2.11-2.14). Typically, the basal erosive scour is overlain by a medium to coarse-grained sandstone, or occasionally coarse conglomerate lenses comprised of mudstone pebbles up to 15 cm in diameter. Some localities have a rich bone lag at the base of the unit, immediately overlying the erosive scour. Indeed, the Jen Rex Sand is named after *Tyrannosaurus rex* bones found by Jennifer Flight in the basal lag. Sand is typically medium grained at the base of the unit, fining upwards, and exhibits a "peppered" appearance similar to the Basal Sand. Bedding consists of trough cross-bedded, planar bedded, and massive sandstones. In its uppermost ~2 m the Jen Rex Sand fines into a siltstone and is overlain by fine grained sediments and isolated channels of the middle Hell Creek Formation fines.

Middle Hell Creek Formation Fines (Khc-mf). Immediately overlying the Jen Rex Sand is a ~20-30 m package of fine-grained overbank facies. Facies descriptions are the same as the lower Hell Creek Formation fines (see above). Typically, the Middle Fines are thickest of the fine-grained units, being typically ~30 m thickness (25.3 m in the new type section; Hartman et al., 2014), but can be up to 35 m (e.g. Penick Coulee, Figure 2.15; Lost Creek, Figures 2.16, 2.17). In some localities (e.g. Bug Creek; Lost Creek, Figure 2.16; East Gilbert Creek, Figure 2.18), the top of the middle fines is marked by an unusually thick organic-rich unit; this takes the form of either an organic rich mudstone with root traces, or a coal. This is the Null Coal (or equivalent organic-rich shale), and is

the only coal present within the Hell Creek Formation of Montana. The Null Coal contains two ash horizons, which have been dated by Sprain et al. (2015; see above). The Null Coal is up to 1 m thick in western McCone County (e.g. Bug Creek; Lofgren, 1995), but thins slightly to the west, being ~50 cm in eastern Garfield County (East Gilbert Creek), where it may be either fully replaced by an organic shale, or only the lower half is organic shale, maintaining an upper ~25 cm of coal.

Apex Sand (Khc-as). The Apex Sand is an amalgamated channel complex that typically occurs ~26-30 m below the contact between the Hell Creek Formation and overlying Fort Union Formation (Figures 2.6, 2.12, 2.16, 2.18, 2.19). It immediately overlies the Middle Hell Creek Formation fines (Khc-mf). Although this contact is erosive, it does not exhibit any significant relief. Geometry of the Apex Sand is sheet-like and laterally continuous over several kilometers. Thickness is typically 4-6 m (6 m in the new type section; Hartman et al., 2014). The Apex Sand is typically tan or brown colored, with occasional concreted horizons. The Apex Sand commonly yields large quantities of both macrovertebrate and microvertebrate fossil material. Often this is disarticulated and abraded, although partly articulated unabraded material is known (Scannella and Fowler, 2014). Grain size is typically medium at the base of the unit, quickly fining upwards. Sand exhibits a “peppered” appearance similar to the Basal Sand. Bedding consists of trough cross-bedded, planar bedded, and massive sandstones. In its uppermost ~1-2 m the Apex Sand fines into a siltstone and is overlain by fine grained sediments and isolated channels of the upper Hell Creek Formation fines part 1.

Upper Hell Creek Formation Fines Part 1 (Khc-uf1). Immediately overlying the Apex Sand is a ~10-15 m package of fine-grained overbank facies (Figures 2.12, 2.18-2.21). Facies descriptions are the same as the lower Hell Creek Formation fines (see above). In areas where the 10 Meter Sand is not present, Khc-uf1 and Khc-uf2 are continuous. Rarely, a thick organic rich mudstone is present at the very top of Khc-uf1, immediately underlying the 10 Meter Sand.

10 Meter Sand (Khc-10ms). The 10 Meter Sand is an amalgamated channel complex (Figures 2.19-2.24) that derives its name from its typical occurrence ~10 m below the contact between the Hell Creek Formation and overlying Fort Union Formation. It immediately overlies the overbank fines and isolated channels of the upper Hell Creek Formation (Khc-uf1). This contact is erosive, but rarely exhibits any significant relief (although it does incise down ~10 m into the Apex Sand at the southern end of East Gilbert Creek; see below). Geometry of the 10 Meter Sand is sheet-like and often laterally continuous over several kilometers. The 10 Meter Sand is usually less thick than the other amalgamated channel complexes, typically being 4-5 m or less in thickness (4 m in the new type section; Hartman et al., 2014). It is typically tan or brown color, with occasional concreted horizons. The 10 Meter Sand is a good source of fossil macro and microvertebrate material, sometimes partly articulated and relatively unabraded. Grain size is typically medium to upper fine at the base of the unit, quickly fining upwards. Sand exhibits a “peppered” appearance similar to the Basal Sand. Bedding consists of trough cross-bedded, planar bedded, and massive sandstones. In its

uppermost ~2 m the 10 Meter Sand fines into a siltstone and is overlain by fine grained sediments and isolated channels of the upper Hell Creek Formation fines part 2.

Upper Hell Creek Formation Fines Part 2 (Khc-uf2). Immediately overlying the 10 Meter Sand is a ~5-8 m package of fine-grained overbank facies (Figures 2.19-2.24). Facies descriptions are the same as the lower Hell Creek Formation Fines (see above). The uppermost bed of Khc-uf2 is typically a thin grey leached mudstone or siltstone that is immediately overlain by a thin (<20cm) coal, the first bed of the Fort Union Formation.

Fort Union Formation (PgF). As this study concentrates on the Hell Creek Formation, only the lowermost parts of the Fort Union Formation that are adjacent to the contact will be considered. The overlying Tullock member of the Fort Union Formation represents a conspicuous change in facies, exhibiting numerous coals, with mudstones, siltstones, and sandstones that are a much deeper yellow color than the somber beds of the Hell Creek Formation (Figures 2.18-2.24). The first coal marks the formational contact with the underlying Hell Creek Formation. This is usually very thin (<20cm) and laterally inconsistent. This thin coal is not always immediately obvious in section; however, the coals usually ~1-2 m above it (the Z-coal complex) have thicknesses up to 1.4 m (more typically ~ 50cm) and are thus more prominent in outcrop, but can laterally inconsistent (Turner, 2010), sometimes splitting into upper and lower Z-coals, and being referred to by a number of different names (HFZ, MCZ, Z, IrZ; Sprain et al., 2015). Other than coals, basal facies of the Fort Union Formation are quite variable. The thicker coals may be absent, and instead may be replaced by a banded “variegated” siltstone facies

(Archibald, 1982; Fastovsky, 1987), or yellow channel sandstones (some of which incise deeply into the Hell Creek Formation; e.g. Lofgren, 1995).

Study Localities and Measured Sections

The following sections are described in stratigraphic order, geographically roughly west to east. Emphasis is placed on well-exposed outcrop, and unusual features. All localities are in Garfield County, Montana, unless otherwise stated (Figures 2.1, 2.2). Named horizons of the Hell Creek Formation (e.g. Jen Rex Sand, Apex Sand) are correlated based on similar distances from the basal and / or upper formational contact (ie. a consistent datum).

Drainage of Crooked Creek, North of Winnett, MT. The Colgate Sandstone is well exposed and easily accessible ~46 km north of the small town of Winnett (Petroleum County, ~120 km west of Jordan; Figure 2.1). This area was surveyed by Flight (2004) and was the principal study area for Behringer (2008). At Crooked Creek (Figures 2.7-2.9; 47°24'13" N, 108°14'35" W; NAD27CONUS; a slightly more easily accessible section is observable only 200m from the road at 47°24’24” N 108°13’14” W, NAD27CONUS) the Colgate Sandstone is unusually thick for the Ft. Peck area (up to 12 m, compared to more typical 2-5 m). The erosive contact with the underlying Fox Hills Sandstone is sharp, and of variable incision depth. Elsewhere in this general area, the Colgate Sandstone incises completely through the Fox Hills Sandstone, and into the Bearpaw Shale (Flight, 2004; Behringer, 2008). The Colgate Sandstone exhibits the same 2-tone coloration as seen in other sections, but differs in the thicknesses of each

individual unit. The lower tan-grey unit is 4m thick and is overlain by 8m of the pale grey unit, which weathers into the distinctive bold white characteristic of the Colgate Sandstone (Figures 2.7, 2.8). The Colgate tidal flats are not obviously visible here. Instead the Colgate Sandstone is overlain by the Hell Creek Formation Basal Sand (~4 m thick).

Cole Creek, Near Hell Creek Marina, North of Jordan, MT. The steep cliffs of Cole Creek (47°38'26" N, 106°55'25" W; NAD27CONUS; Figure 2.25) expose the Bearpaw Shale through to Jen Rex Sandstone of the Hell Creek Formation. The Colgate Sandstone is absent, but the Colgate tidal flats are present. Here the lower grey siltstone of the Colgate tidal flats is relatively thick (2 m), and is in turn overlain by a thin (20 cm) organic-rich mudstone. There is no obvious deep erosional scour at the base of the overlying Hell Creek Basal Sand, although it is thick here (12 m), and is subsequently overlain by 8 m of overbank fines. These are overlain by the resistant Jen Rex Sandstone that forms a steep 8 m cliff that caps the section (the complete Jen Rex Sand may be thicker). Here, the base of the Jen Rex Sand contains a bone lag from which some relatively large dinosaur bones have been collected. Nearby, 0.5 km southwest (47°38'12" N, 106°55'40" W; NAD27CONUS) the Jen Rex Sand incises deeply into the underlying strata (at least 10 m), and similarly exhibits an unusually coarse conglomerate at its base, comprising angular mudstone clasts 10-15 cm across.

Hell Creek, Near the Marina Road (FWS-105), North of Jordan, MT. The transition from the Bearpaw through to the Hell Creek Formation is particularly well

exposed at Hell Creek itself, with easily accessible near-continuous outcrop along the Hell Creek Marina Road (FWS-105). Here I illustrate and briefly describe four sections (referred to as "Hike Cliff", "Best Butte", "Battle Butte", and "Manaige Spring") which change from a typical or normal section in the north at Best Butte (and the Hell Creek State Park), to an atypical (but commonly described) section south at Manaige Spring. Interpretation of these well-exposed sections differs significantly between authors (Flight, 2004; Lerbekmo, 2009; Hartman et al., 2014), with important implications, not the least that a small part of the Battle Formation (a unit otherwise recorded only in Canada) may be exposed in this area (Lerbekmo, 2009).

"Best Butte" and "Hike Cliff". Two sections immediately adjacent to each other record comparable stratigraphy, considered here as "typical" for the Hell Creek Formation in this area; "Hike Cliff" (Figure 2.4; 47°36’5” N, 106°55’14” W, NAD27CONUS) and "Best Butte" (Figure 2.26; 47°35’36” N, 106°54’50” W, NAD27CONUS; section #10 in Flight, 2004). In both buttes the pale grey transitional facies of the Bearpaw Shale grade into the conspicuous yellow sands of the Fox Hills Sandstone, which form a gradual slope. The Fox Hills Sandstone is abruptly overlain by a relatively thin (~4 m) cliff-forming sandstone, conspicuously more pale in color than the Fox Hills Sandstone, lacking in concretions, and capped by a thin grey siltstone and prominent purple mudstone. This is consistent with the appearance and stratigraphic position of the Colgate Sandstone and Colgate tidal flats (respectively) in the Manaige Spring section (Figure 2.5). At Best Butte and Hike Butte however, the Colgate tidal flats are directly overlain by a cliff-forming amalgamated channel sandstone, identified here as

the Hell Creek Basal Sand. Concretions in the Basal Sand can be seen clearly in the lower ~4-5 m, but are absent from the upper ~6 m (the Basal Sand thickens northwards so that in the cliffs immediately west of the Hell Creek Marina it achieves considerable thickness of ~12 m or more, and inclined heterolithic strata are clearly visible in the upper 3-4 m). The Basal Sand is overlain by typical banded mudstones of the Lower Hell Creek Formation fines, although these vary in thickness between Hike Cliff and Best Butte. At Hike Cliff, the lower fines are ~10-15 m thick with the section is capped by the Jen Rex Sandstone (Figure 2.4). At Best Butte the lower fines are only ~4 m thick and are then capped by a sand unit which probably is an isolated channel sand (Figure 2.26).

It is important to note that Best Butte was figured by Hartman et al. (2014) in their Supplementary Information (Supplementary Figure DR85), who offer a different interpretation of the stratigraphy. They suggest that the white sandstone here identified as the Colgate Sandstone is in fact the Hell Creek Basal Sand, with the overlying major sand unit (which I identify here as the Basal Sand) referred to the Jen Rex Sand. Here I consider the stratigraphic referrals of Hartman et al. (2014) to be incorrect. Error rests upon the misidentification of the Colgate Sandstone; this is perhaps due to the fact that the photograph of Best Butte used by Hartman et al. (2014; Supplemeentry Figure DR85) does not include the smaller butte seen on the left of my own Figure 2.26). This smaller butte clearly exhibits the characteristic striking white weathering of the Colgate Sandstone.

Manaige Spring and "Battle Butte". At the point where the Marina Road crosses Hell Creek itself (Manaige Spring; 47°34’15” N, 106°57’0” W; NAD27CONUS; Figure

2.5), the transition from the Bearpaw Shale to Hell Creek Formation is atypical and has been interpreted differently between authors (Lerbekmo, 2009; Hartman et al., 2014), most notably in the identification of a white-colored sandstone near the base of the exposure. Observation of sections further north along the Marina Road (Hike Butte and Best Butte) allows correlation with the Manaige Spring section, and confirmation of the identity of the white-colored sandstone as the Colgate Sandstone.

At Manaige Spring, the Bearpaw Shale grades into the Fox Hills over ~10 m (seen in the side of the valley on the western side of the road). The Fox Hills Sandstone is overlain by an 8m thick pale-colored sandstone, which weathers into a distinctive rilled pattern, strikingly different from the blocky weathering of the Fox Hills Sandstone. This pale sandstone is visibly divided into two bands of color, with the upper band a more pale shade of grey. This sand unit was identified as the Colgate Sandstone by Lerbekmo (2009), with whom I agree here. However, Hartman et al. (2014; Appendix A) disagree with Lerbekmo (2009; and the current analysis), identifying this pale sandstone instead as the Basal Sand of the Hell Creek Formation, citing (p.54) that the "white coating (alkaline deposits) is not present laterally (yellowish gray Hell Creek sandstone beds)". However, this is in error as a Colgate Sandstone identification is corroborated by the same horizon visible at Best Butte (see above; Figure 2.26) where it exhibits the striking white weathering pattern characteristic of the Colgate Sandstone.

The upper band of the Colgate Sandstone fines upwards into the Colgate tidal flats: a 50 cm grey siltstone capped by a 50 cm purple-brown organic rich muddy siltstone. Above the Colgate tidal flats is an unusual package of facies not encountered

anywhere outside of this local area (see also Battle Butte and Eastside Overlook, below). Instead of the basal sandstone there is a conspicuous leached siltstone (30 cm thick), overlain by a 30 cm thick dark organic rich siltstone. The siltstone is a deep red-brown to black color with much organic debris, including twigs and rootlets. This horizon is similarly present, but as a medium grained sandstone ~1.5km east near the mouth of Jordan Coulee (pers. obs.; Shoup, 2001). Above the organic tidal flats are ~10 m of mauve, purple, and grey-green mudstones. These beds are here tentatively referred to the Battle Formation, consistent with their stratigraphic position (e.g. Eberth and Braman, 2012), lithofacies (Irish, 1970; see Appendix A), and preliminary palynostratigraphic analysis (Lerbekmo, 2009). The possible Battle Formation is overlain by the Basal Sand of the Hell Creek Formation (~9 m thick), which forms the uppermost unit of this section.

"Battle Butte" (47°34’43” N, 106°56’39” W; NAD27CONUS; Figure 2.27) is another butte exposed at the roadside ~1 km NNE of Manaige Spring, and records a stratigraphic succession intermediate between Manaige Spring and Best Butte (located ~3 km NE). The lowermost visible unit is the transitional facies (grey silty sandstone) between the Bearpaw Shale and Fox Hills Formation, forming a gradual slope at the base of the butte. These are overlain by the orange sandstone of the uppermost Fox Hills Formation (~20 m in total relief). Overlying the Fox Hills Formation is a pale colored cliff forming sandstone capped by an organic rich horizon. This is interpreted here to be the Colgate Sandstone and tidal flats, but was interpreted by Hartman et al. (2014; Supplementary Figure DR84) as the Basal Sand of the Hell Creek Formation (this is considered an error here; see above). Overlying the Colgate tidal flats is a thin exposure

of the possible Battle Formation, which is ~3 m thick on the western edge of the butte (left side of Figure 2.27B), but is absent at the small butte closest to the road (right side of Figure 2.27B), having been completely removed by incision of the overlying Basal Sand of the Hell Creek Formation. Hence this locality records the removal of the possible Battle Formation facies, to leave the direct contact of the Hell Creek Formation Basal Sand upon the Colgate Sandstone (and / or tidal flats) that is observed to the north (e.g. Best Butte; see above). The overlying Hell Creek Basal Sand is ~6 m thick and exhibits some inclined heterolithic strata, fining upwards in to a package of 5-6 m of mudstones of the Hell Creek Lower Fines, which complete the top of the butte.

East Ried Coulee, Flag Butte (New Type Section). The new type section for the Hell Creek Fm is located at Flag Butte, near East Ried Coulee (47°33'34" N, 106°52'52" W, NAD27CONUS), ~5 km east of the Marina Road (FWS-105), and is described in detail by Hartman et al. (2014). However, based on personal observation of the type section, I consider that the definition of the basal contact of the Hell Creek Formation given by Hartman et al. (2014) may be misinterpreted. However, it should also be noted that the stratigraphic relationships immediately below the basal contact of the Hell Creek Formation Basal Sand are very complex and easy to misinterpret, and as such assertions given here are tentative pending testing by other analytical methods.

The deep ravine at East Ried Coulee exposes the Bearpaw Shale at its base with continuous exposure through to the top of nearby Flag Butte (~ 1 km SE; 47°33'22" N, 106°52'8" W, NAD27CONUS), which is capped by the lowermost 10 m of the Fort Union Formation (Hartman et al., 2014). The steep walls of East Ried Coulee are mostly

composed of ~20 m of tan to orange colored medium to coarse-grained sandstone (Figure 2.6). However, the base of these cliffs expose horizontally stratified or massively bedded grey silty sandstone, here attributed to the transitional beds of the Bearpaw Shale (Figure 2.28). Identity of the silty sandstones as the transitional beds of the Bearpaw Shale is supported by magnetostratigraphic analysis (LeCain et al., 2014; Lerbekmo, 2009; see later discussion).

These basalmost beds of the succession are not figured in the sections measured by Hartman et al. (2014), yet may prove critical to its interpretation. The overlying tan to orange colored sandstones are referred to the Fox Hills Sandstone by Hartman et al. (2014), and this would seem to be consistent with their stratigraphic position. However, the base of these tan-orange sandstones is erosive and has an abrupt contact with the underlying silty sandstones of the Bearpaw Shale: an erosive relationship between the Fox Hills Formation and Bearpaw Shale has not been observed elsewhere, nor noted by other workers. Furthermore, the tan-orange sandstone exhibits large scale trough cross-bedding, medium to coarse sand grain size, fining upwards successions both within individual beds and overall though the unit, possible inclined heterolithic strata (Figure 2.29), internal scour surfaces at the bases distinct channels sometimes infilled with conglomerate (Figure 2.30; Hartman et al., 2014, supplementary figures DR36-37; Rogers, pers. comm. 2014), and has a "peppered" texture (Jensen and Varnes, 1924), none of which are observed in the Fox Hills Formation, but are characteristic of the Basal Sand of the Hell Creek Formation. I therefore tentatively suggest that this unit is not referable to the Fox Hills Formation, and instead represents the Hell Creek Formation

Basal Sand which is unusually thick at this location as it has incised down through the Colgate Sandstone (if originally present) and Fox Hills Formation into the transitional beds of the Bearpaw Shale. In their supplementary materials, Hartman et al. (2014) document that this view was shared by A. G. Leonard's contribution to Hell Creek stratigraphy. Leonard (1906; who visited East Ried Coulee with Barnum Brown) stated that "The basal sandstone of the Laramie [Hell Creek] is finely exposed in the gorge at the headwaters of the East Fork of Hell Creek [Ried Coulee] where it has the exceptional thickness of 150(?) feet [45.7 m]". Thus it would appear from this account that Leonard (1906) agreed that the thick sandstone present in Ried Coulee is the Basal Sand of the Hell Creek, and not (mostly) the Fox Hills Sandstone (ie. sensu Hartman et al., 2014). This referral is also supported by preliminary palynostratigraphic analysis, where palynomorphs extracted from the tan-orange sand unit show affinity with those of the Hell Creek Formation (Braman, pers. comm. 2012).

The Basal Sand of the Hell Creek Formation fines upwards in the upper 5 m and changes from tan-orange color into a pale sandstone overlain by a thick organic rich mudstone (Figure 2.6). This is unusual for the Basal Sand, but a stratigraphic relationship is observed at the northern edge of Penick Coulee (Figures 2.13, 2.14), where an organic shale immediately overlies the top of the Basal Sand.

Regardless of the identity of the basal units, further overlying subunits of the Hell Creek Formation (beginning with the Lower Hell Creek Formation Fines) are typical in occurrence and thickness (Jen Rex Sand is 19.2 m above the top of the pale sandstone; Apex Sand is 25.3 m above the top of the Jen Rex Sand, 10 Meter Sand is ~9 m below

the Hell Creek - Fort Union formational contact; Figures 2.11, 2.12). In conclusion then, the new type section can be considered to exhibit an unusual basal contact of the Hell Creek Formation, but is otherwise typical for the unit as a whole.

Sand Creek, Sheep Mountain, Carter County MT. A small area of outcrop in Sand Creek (55 km southeast of Ekalaka, Carter County, Montana; 45°30'8"N, 104°8'0"W, NAD27CONUS) records the transition from the Fox Hills Sandstone through the lower 30 m of the Hell Creek Formation (Figures 2.10, 2.31), and is lithostratigraphically comparable to sections in the Ft. Peck area, 300 km northwest. The section begins with the uppermost 3 m of the Fox Hills Sandstone, which is typically yellow in color and in its upper 1 m exhibits prominent orange-concreted sandstone lenses, with ripple cross-lamination. The Colgate Sandstone is absent here, instead, the Fox Hills Sandstone is irregularly overlain by the Colgate tidal flats (Figure 2.10) consisting of a 50-60 cm thick grey silt, overlain by 20-30 cm of purple-brown organic-rich silty mudstone. This is overlain by the 10 m thick Basal Sandstone of the Hell Creek Formation, but it is the variable nature of this contact that is of particular interest. Typically, the Basal Sand lies disconformably on top of the organic rich horizon of the Colgate tidal flats. However, in places (Figure 2.10B) the Basal Sand has eroded down ~3 m through the Colgate, and into the Fox Hills Sandstone. With the limited outcrop and time spent in this area, it was not possible to trace the contact further, but it illustrates the occasionally incising nature of the Hell Creek Basal Sand. 13-17 m of overbank fines overlie the Basal Sand, followed by the Jen Rex Sand that caps the succession in this small area.

East Gilbert Creek and Penick Coulee. Excellent badland exposures at the headwaters of East Gilbert Creek (47°41’13” N, 106°31’44” W; NAD27CONUS) north into Penick Coulee (47°43’51” N, 106°30’23” W; NAD27CONUS) represent one of the few localities where a complete section from the Bearpaw Shale to Fort Union Fm can be observed in easily accessible BLM-administered land (Figure 2.15). On the southern edge of East Gilbert Creek, and immediately north of the Haxby Road (47°39’6” N, 106°30’59” W; NAD27CONUS), a 3.5-mile SW-NE trending cliff exposes the upper 10-20m of the Hell Creek Formation and upper contact with the Fort Union Formation. At the Isaac’s Ranch the cliff turns north and the exposure deepens into the wash, exposing the Fox Hills sandstone and uppermost Bearpaw Shale. The East Gilbert Creek section is typical in the presence of the Basal Sandstone, Jen Rex Sandstone, Apex Sandstone, and 10-Meter Sandstone in their expected positions. Of interest is an especially thick (30 cm) organic-rich mudstone that occurs immediately below the Apex Sand (Figure 2.18; 47°41'32" N, 106°30'47" W, NAD27CONUS); this is in the same stratigraphic position as the Null Coal, but does not contain any ash horizons. To the south east 1.5 km there is an exposure of the Null Coal (47°40'48" N, 106°30'16" W, NAD27CONUS) which contains both upper and lower ashes. At this locality the upper ash is contained within a coal, but the lower ash is within a red organic rich shale (by comparison, both ashes are within coals in Bug Creek ~25 km to the east; Lofgren, 1995; Sprain et al., 2015). This suggests that coal swamp conditions spread westwards (landward) between the deposition of the lower and upper ashes. Also of interest is that the southern part of East Gilbert Creek is one of the few localities where the 10 Meter Sand can be observed with any incision

depth. At the same locality as the above Null Coal (47°40'48" N, 106°30'16" W, NAD27CONUS) the 10 Meter Sand incises ~ 10 m into the top of the Apex Sand, to create a combined sandstone thickness of ~18 m.

In contrast, if the continuous outcrop is followed north into Penick Coulee the section becomes atypical in a number of respects. In north Penick Coulee, the Basal Sandstone (8 m thick) is extensively exposed forming a prominent bench (Figures 2.13, 2.14), and contains unusually large quantities of silicified wood. The Basal Sand is overlain by an organic rich red mudstone, and a conspicuous popcorn-weathering dark gray-green bentonite (Figures 2.13, 2.14; this has been sampled for radiometric analysis). The bentonite is 1.5 m thick at the northern extent of Penick Coulee, but thins southwards and was not observed in East Gilbert Creek. In northwest Penick Coulee (Figure 2.14, section 1; 47°43'50"N, 106°30'01"W NAD27CONUS) the Jen Rex Sand is typical and prominent, 15 m above the top of the Basal Sand, but it thins rapidly and is not traceable 0.5 km east (Figure 2.15, section 2, 3). However, it is again present ~ 1km south, in the middle of the coulee (Figure 2.13). Similarly, the Apex Sand is atypically thin or absent in northern to middle parts of Penick Coulee, although in southern Penick Coulee it is present. Also, in Penick Coulee the Z-coal and K-Pg boundary have sometimes been removed by channeling that incises down from the Paleocene (Figure 2.15, section 3; similar to incised channels in Bug Creek, Carter County, ~50km East; Smit et al., 1987; Lofgren, 1995; see later). As in Bug Creek, the Penick Coulee channels exhibit reworked coal at their base; however, they only incise ~10 m below the Hell Creek-Fort Union Formational contact (compared to ~35-40 m at Bug Creek). Consequently, since the

upper contact cannot be determined, the complete thickness of the section in Penick Coulee is not precisely known.

Gilbert Creek. Gilbert Creek is an extensive area of badlands that exposes the upper 50-60 m of the Hell Creek Formation (although exposures probably reach lower in section than this on Charles M. Russell Reserve land), and upper contact with the Fort Union Formation. Only the uppermost part of the Hell Creek was surveyed as part of this analysis, although prospecting for vertebrate fossils was conducted deep into Gilbert Creek (preliminary surveying of BLM land in 2010). Gilbert Creek exposures are continuous with East Gilbert Creek, but the connecting area of outcrop has yet to be investigated. The 10 Meter Sand and Apex Sand are present in Gilbert Creek, and have yielded some important vertebrate fossils (Scannella and Fowler, 2014).

Lost Creek (Ducky Tail). Extensive outcrop in Lost Creek (Figures 2.16, 2.17, 2.19; 47°40’10”N, 106°19’13”W, NAD27CONUS) exposes the upper ~50m of the Hell Creek Formation through to the lower ~10m of the Fort Union Formation (over a traverse of ~2 km). Outcrop is often of moderate to high relief and continuous, giving excellent exposure of the contacts of the Apex Sand, 10 Meter Sand, and Fort Union Formation. The base of Lost Creek exposes the lowermost Middle Hell Creek Formation Fines, with no obvious outcrop of the Jen Rex Sand, although isolated channels are present in some sections (Figure 2.16). The Middle Hell Creek Fines are at least 35 m thick here, and are overlain by the Apex Sand (4-8 m thick). The Apex Sandstone is laterally extensive over the entire local area: 3-4 km^2, and in most sections (e.g. Figures 2.16, 2.17) is underlain

by a prominent and well developed organic-rich mudstone and / or coal horizon, here correlated to the Null Coal (Lofgren, 1995; Sprain et al., 2015). The Hell Creek Upper Fines Part 1 are ~13 m thick and overlain by the 10 Meter Sand (up to 6 m thick; Figure 2.19). There is only limited outcrop of the 10 Meter Sand, as most of the exposures are stratigraphically lower in section, such that the 10 Meter Sand tends to be exposed only at the tops of small buttes. Despite limited outcrop, the 10 Meter Sand is quite fossiliferous in this area, yielding associated and partly articulated dinosaur remains. Neither the Apex Sand nor 10 Meter Sand shows any significant erosional relief at their bases.

Cottonwood Creek (Brownie Butte; Lon's Trike). A limited area of study in Cottonwood Creek (~1 km northwest of Brownie Butte; 47°31’58” N 107°1’17” W, NAD27CONUS; Figure 2.32) exposes the Apex Sand through to the Fort Union Formation. Approximately 2 km north of the study area, Cottonwood Creek feeds into Hell Creek, and exposures here record the complete thickness of the Hell Creek Formation. Brownie Butte itself has been subject to a number of studies, mainly focusing on various aspects of the K-Pg boundary (Bohor et al., 1984; Fastovsky, 1987; Fastovsky et al., 1989; Sweet et al, 1999). The Apex Sand is ~4-5 m thick here and has a claystone pebble conglomerate at its base, interpreted as a channel lag. Locally this unit contains well-preserved macrovertebrate fossils mixed in with the pebble clasts (Scannella and Fowler, 2014). Limited exposure of the Apex Sand limits assessment of its continuity; however, Fastovsky (1987) documented that the 10 Meter Sandstone pinches out at Brownie Butte itself, but thickens northwards to 5.7m in Cottonwood Creek. Also notable that at the old Trumbo ranch area (Hell Creek; 47°33’26” N, 107°0’50” W,

NAD27CONUS) the Basal Sand is unusually thick, forming steep cliffs over 10 m high (also noted for this area by Brown, 1907).

Short Creek (Tom's Old Duck). The area of Short Creek has good exposures of the upper 30 m of the Hell Creek and Fort Union formational contact (Figures 2.20, 2.22, 2.33). The deepest part of the wash exposes the upper 3-4 m of the Middle Hell Creek Fines, which are overlain by the laterally extensive Apex Sand (5 m thick). The contact is erosive but shows no significant relief. In most areas where it is exposed, the Apex Sand has a fossil-rich lag at its base, mostly containing isolated abraded bones and teeth, but occasionally associated material. This is overlain by ~12 m of overbank fines, followed by the 10 Meter Sand. The 10 Meter Sand is continually exposed over 6 km, but thickness varies considerably from a 10 m thick cliff-forming sand in the eastern side of Short Creek (47°35'49" N, 106°17'54" W NAD27CONUS; Figure 2.22; Figure 2.33, section 3), 4 m thick close to Twitchell Point (47°34'58" N, 106°15'43" W, NAD27CONUS; Figure 2.28, section 6) to as little as 2 m on the western side of Short Creek (47°35'35" N, 106°18'24" W, NAD27CONUS; Figure 2.20; Figure 2.33, section 2). Thickness of the overlying fines thus varies from 12 m down to as little as 5 m. Coals immediately above the Z-coal are especially prominent in the south of this area (47°33'51" N, 106°16'46" W, NAD27CONUS), reaching up to 1.4 m thick and conspicuous from great distance.

Lone Tree Creek (Sandy Chicken and The Doldrums). The uppermost 35 m of the Hell Creek Formation, and Fort Union formational contact are observable in extensive

outcrops at the eastern edge of Lone Tree Creek. The uppermost 15 m of the Hell Creek Formation, and Fort Union formational contact are observable in extensive outcrops on the southeastern side of Lone Tree Creek (47°36'17" N, 106°21'28" W, NAD27CONUS; Figure 2.21). The 10 Meter Sand is 3-4 m thick here, and present across an area of at least 2 km^2. Exposure is continuous southeast to connect with the headwaters of Short Creek; hence the 10 Meter Sand can be traced continuously for 7-8 km in this area, although thickness varies.

Although most of the Lone Tree Creek area only exposes the uppermost 20 m of the Hell Creek Formation (mainly above the Apex Sand), a small ravine on the northeast side provides one of the best known exposures of the Null Coal (47°37'33" N, 106°21'9" W, NAD27CONUS; Figure 2.34). Here the Null Coal horizon is 60 cm thick, with the upper half represented by coal, and the lower half an organic-rich red mudstone. Both upper and lower ash horizons are present.

Bug Creek – Russell Basin, McCone County MT. Badlands in the area around Bug Creek (47°41'10"N, 106°12'57"W, NAD27CONUS) have been historically important in studies of the fauna across the K-Pg boundary (Archibald, 1982; Smit et al., 1987; Lofgren, 1995). This area exposes the upper ~50 m of the Hell Creek Formation, and the contact with the Fort Union Formation. The Hell Creek - Fort Union formational contact here is atypical in that in many places (especially within 1 km south of Lonnies Bench; 47°41'34" N, 106°13'26" W, NAD27CONUS) large channels incise from the Paleocene deep into the Hell Creek Formation. Near an important *Triceratops* locality (UCMP locality V75046; Ruben's Trike; UCMP specimen 113697), channeling incises

~30m into the Hell Creek Formation. These channels are known to rework Paleocene and Cretaceous fossils into a single deposit (Lofgren, 1995). Bug Creek is also important as the first locality where the Null Coal was recorded (Lofgren, 1995). At the same locality as above (47°41'10"N, 106°12'57"W, NAD27CONUS), the Null Coal is present as a 1 m thick coal (unlike further west in Garfiled County where it is typically at least partly represented by organich-rich mudstone). Both ash horizons are present in the Bug Creek exposure of the Null Coal, and this is one of the localities sampled by Sprain et al. (2015) for radiometric dating.

At Russell Basin (47°40'38" N, 106°11'13" W, NAD27CONUS; ~2.5 km southeast of Lonnie's Bench area), only the upper 20 m of the Hell Creek formation are observed (Figure 2.24). This is the location for another important *Triceratops* specimen (UCMP locality V88081; Russell Basin Trike; UCMP specimen 136092). Here the 10 Meter Sand is 4 m thick and contains numerous large concretions. It is overlain by 4-5 m of the Hell Creek Upper Fines Part 2, followed by the Z-coal and numerous coals and banded mudstones of the Fort Union Formation.

Magnetostratigraphic Corrections

Here I suggest alterations to the magnetostratigraphic interpretations of Lerbekmo (2009) and LeCain et al. (2014), based on ammonite biostratigraphy, and reinterpretation of the basal contacts of the new type section (Hartman et al., 2014).

Ammonite biostratigraphy suggests that the identity of magnetochrons in the Fox Hills Formation by Lerbekmo (2009) and LeCain et al., (2014) need to be altered from C30r and C31n to C31r. The basal contact of the Colgate Sandstone with the underlying

Fox Hills Formation records a change from reversed to normal polarity, shown by Lerbekmo (2009) as representing the boundary between C30n and C30r (68.369 Ma; Ogg and Hinnov, 2012; Figure 2.35). However, ammonite biostratigraphy of the underlying Bearpaw and Fox Hills Formation suggests that the non-Colgate part of the Fox Hills Formation is probably no younger than the *Baculites clinolobatus* zone (70.44 - 69.91 Ma; Ogg and Hinnov, 2012), and possibly slightly older (Gill and Cobban, 1973; Lillegraven and Ostresh, 1990; Cobban, 1994). This precludes an identity of C30r (68.369 - 68.196 Ma) or C31n (69.269 - 68.369 Ma) for the reversed zone that occurs in the Fox Hills Formation immediately underlying the Colgate Sandstone (Lerbekmo, 2009). Given that a hiatus probably exists at the base of the Colgate Sandstone (Lawton, 2002; Flight, 2004; Behringer, 2008; Lerbekmo, 2009), then it seems likely that the zones of reversed polarity within the Fox Hills Formation actually correspond to subzones within C31r (71.449 - 69.269 Ma; all dates Ogg and Hinnov, 2012; Figure 2.35).

Minor alterations are also required to the magnetostratigraphic analysis of the new type section (LeCain et al., 2014), located ~5km east of the Manaige Spring section studied by Lerbekmo (2009). The major sand unit which forms the steep cliffs of East Ried Coulee (type section; Figures 2.28, 2.29, 2.30) was considered to be the Fox Hills Formation (Hartman et al., 2014), but is here tentatively reidentified as the Basal Sand of the Hell Creek Formation (see above). This atypically deep incision of the Basal Sand cuts entirely through the Fox Hills Formation (Shcs, St, Sm, Sr) into the pale grey silty sandstones (Sh, Sm) transitional between the Bearpaw and Fox Hills Formations (Figure 2.28). LeCain et al. (2014) recorded this pale grey silty sandstone as normal polarity, and

attributed it to C30n (Figure 2.36A), the same chron as the majority of the Hell Creek Formation and the Colgate Sandstone (Figure 2.35). Even if the revision to the major sand unit given here is rejected, the normal polarity zone within the pale grey silty sandstone should not be considered as C30n because the host unit is not correlative with the Colgate Sandstone, the base of which marks the base of C30n (Lerbekmo, 2009). Any normal polarity zone below the stratigraphic position of the Colgate Sandstone is probably attributable to 31r (Lerbekmo, 2009, identified these as 31n, but see correction, above), and this is indicated in the revised version of LeCain et al. (2014)'s figure (Figure 2.36B). It should probably also be noted here that although LeCain et al. (2014) follow Hartman et al. (2014) in lithostratigraphic designations for the new type section, in their correlation chart (their Figure 7) they follow the original designations of Lerbekmo (2009; miscited by LeCain et al., as 2008) for the Manaige Spring section; ie. they do not follow Hartman et al. (2014; appendices therein) in their revision of the Manaige Spring section whereupon they state that the unit which Lerbekmo (2009) identified as the Colgate Sandstone, is actually the Basal Sandstone of the Hell Creek Formation. This has no serious implications if the revised correlations presented here are followed.

Depositional Sequences and Systems Tracts

LAST in the Hell Creek Formation record periods of low accommodation and are represented by amalgamated channel sandstone complexes. HAST record periods of high accommodation, represented by strata typical of overbank fines (mudrocks) containing isolated channel sandstones. Sequence boundaries are identifiable as disconformities at the bases of amalgamated channel complexes, representing periods of erosion or non-

deposition. Regional extent, thickness, and the multi-storey nature of deposits distinguishes incised valley fill and amalgamated channel sandstone complex features from smaller scale, single-storey localized erosion, and channel-fill sandstone units associated with normal, autocyclic fluvial processes. Cliff-forming amalgamated channel sandstones are conspicuous, and consistent in their stratigraphic position and sedimentology, being at their base typically more coarsely grained than preceding deposits, and trough cross-stratified. In the absence of amalgamated channel complexes, periods of low accommodation space creation should be represented by mature interfluve paleosol horizons, although in outcrop these are difficult to observe. Potential correlative Maximum Flooding Surfaces may be represented in concentration of lacustrine organic-rich horizons within HAST, but these are difficult to define in the current work. For the most part, defined depositional sequences represent 4^{th} order cyclicity, such that facies juxtapositions are not as severe as across sequence boundaries of 3^{rd} order or less. 4^{th} order sequence boundaries have been described for the Upper Maastrichtian Whitemud and Battle Formations of Alberta by Catuneanu and Sweet (1999).

Sequences and boundaries have been plotted on a generalized section (Figure 2.3). These initially follow Flight (2004), but differ with respect to the upper part of the Colgate depositional sequence, the lower Hell Creek depositional sequence, and in the completion of the upper part of the succession.

Bearpaw Shale – Fox Hills Sandstone

Depositional Sequence (Kbp, Kfh). The Bearpaw Shale – Fox Hills Sandstone contact is gradational (e.g. Figure 2.4) and records shallowing conditions from fully

marine mudstones, through offshore transition silty sandstones, to shoreface sandstones of the Fox Hills Formation (excluding the Colgate Sandstone). No significant disconformity has been detected through this succession. Here I follow Flight (2004) in recognizing the Bearpaw Shale through Fox Hills Sandstone as the latter stages of HST, and early LST where stillstand sea-level causes a forced regression as the Fox Hills delta progrades out into the Bearpaw seaway. Flight (2004) notes that westward downstepping of parasequences indicates a forced regression, supporting the interpretation of early LST.

Colgate and ?Battle Depositional Sequence (SB1, Kfhc, Kcp, Kba). This analysis mostly follows Flight (2004) in definition and interpretation of the Colgate depositional sequence, which comprises sequence boundary 1, the overlying Colgate Sandstone, the Colgate tidal flats, and the possible Battle Formation. Deposits of the Colgate sequence record a broad incised valley fill deposited under initially fluvial, and later estuarine conditions, followed by tidal flats and terrestrial mudstones (Flight 2004; Behringer 2008).

Sequence boundary 1 occurs at the basal contact of the Colgate Sandstone, and is typically marked by an erosive scour. Flight (2004) and Behringer (2008) suggest the erosive scour represents a broad incised valley formed by fall in accommodation (in this case, linked to sea-level fall). Evidence in support of this diagnosis includes depth (up to 25 m); lateral continuity of the erosive scour; a non-Waltheran facies shift from marine Bearpaw Shale to estuarine deposits of the Colgate Sandstone, and onlap of the Colgate Sandstone to incised valley walls (Flight, 2004; Behringer, 2008). Flight interprets the

overlying Colgate Sandstone as representing the TST, with the successively overlying Basal Sand of the Hell Creek Formation representing HST (with which I only partially agree; see below). Expected late lowstand fluvial backfill deposits were not observed by the author, nor by Flight (2004) although Flight does cite Wheeler (1983) as having identified coarse-grained fluvial facies directly above the erosional scour. Early TST deposits of the Colgate Sandstone are estuarine, reflecting increasing marine influence due to rising base-level (Flight, 2004; Behringer, 2008), although in some sections, only the upper part of the Colgate sandstone is estuarine (Behringer, 2008). Sequence boundary 1 is regionally extensive with good examples of the contact at the Marina Road (Figures 2.4, 2.5), Crooked Creek (~120 km west; Figures 2.7, 2.8), and Sheep Mountain, Ekalaka (~300 km southeast; Figures 2.10, 2.26).

The Colgate tidal flats are almost always present above the Colgate Sandstone, or in place of it, immediately beneath the Basal Sand, or rarely, the possible Battle Formation (e.g. Manaige Spring section; Figure 2.5). Areas where the Colgate tidal flats are absent typically correlate with incision of the Basal Sand, potentially removing any of the organic-rich facies (and sometimes, the rest of the Colgate, or equivalent, along with it; e.g. North Penick Coulee section; Figures 2.14, 2.15; Sheep Mountain section, Ekalaka; Figure 2.10, 2.26).

The depositional environment of the Colgate tidal flats was interpreted by Flight (2004; who included it as the basalmost unit of the Hell Creek Formation) as tidal flats deposited during late TST of the Colgate depositional sequence. The tidal flats represent a maximum flooding surface, which was subsequently drained through base-level fall.

This analysis agrees with Flight (2004) that the Colgate Sandstone represents the TST, but differs slightly in interpreting the overlying mudstones of the possible Battle Formation as a remnant of HST of the Colgate Sequence.

In one locality (Manaige Spring, and local area within ~ 2 km; Figures 2.5, 2.27) the Colgate tidal flats are overlain by a second bed of tidal flats (~1 m), and ~10 m of mudstones, here tentatively referred to the Battle Formation. The lack of any erosive contact between the Battle beds and underlying Colgate beds suggest that this represents a continuation of the Colgate depositional sequence, probably the HST. However, Catuneanu and Sweet (1999) propose an unconformity exists between the (Colgate-equivalent) Whitemud and Battle Formations in southern Alberta and Saskatchewan, based on palynological differences (Binda et al. 1991; Nambudiri and Binda 1991). This would suggest that the Battle Formation (if correctly identified) might represent an additional sequence sandwiched between the Colgate depositional sequence, and the Lower Hell Creek depositional sequence. Whether this is also true of the Manaige Spring section requires detailed palynological analysis, although initial results (see Lerbekmo, 2009) suggest that the possible Battle Formation facies present at this locality has palynomorphs comparable to the Battle Formation of Alberta.

In summary, this analysis considers the Colgate Sandstone represents the TST, with the Colgate tidal flats a MFS and possible Battle Formation as HST, followed by LAST of the Basal Sand (see next).

Lower Hell Creek Formation

Depositional Sequence (SB2, Khc-bs, Khc-lf). The Lower Hell Creek Formation depositional sequence comprises sequence boundary 2 (SB2), the overlying Basal Sand (LAST), and Khc-lf (HAST). These have a combined thickness of 15-26 m (~26 m in the new type section; Hartman et al., 2014; variability is mostly dependent on the presence or absence of the Basal Sand).

In a departure from the work of Flight (2004), this analysis places the second sequence boundary at the base of the Basal Sand. This contact is erosive (Figures 2.4, 2.5), and is occasionally marked by a moderately deep erosive scour (up to 5m depth; Figures 2.5, 2.6) which may incise through the underlying units as deep as the Bearpaw Shale, though more typically it might only incise as deep as the Fox Hills Sandstone. This scour is rarely observed in the field and may be localized in nature, perhaps explaining how it was not observed by Flight (2004), although it was mentioned by Brown (1907; 1914), Bauer (1924), Jensen and Varnes (1964), and Lerbekmo (2009), who suggested incisions up to 10 m are known. Lerbekmo suggested that significant fall in sealevel may have occurred after deposition of the Colgate Sandstone (Colgate depositional sequence), leading to significant leaching of the Colgate Sandstone. Immediately overlying Sequence Boundary 2 is the Hell Creek Formation basal sand: an amalgamated channel complex that forms the basalmost bed of the lower depositional sequence. The presence of inclined heterolithic strata in lower parts of the basal sand is typically attributed to lateral migration of tidally influenced point bars (Thomas et al., 1987). However, recent work has suggested that in some cases IHS may instead represent deposition in an entirely terrestrial setting (Eberth, 2005). Flight (2004) interprets IHS in the Basal Sand

as indicative of estuarine influence, and this is followed here. The sharp contact of sequence boundary 2 typically juxtaposes fine-grained tidal flat (Colgate tidal flats) or estuarine (Colgate Sandstone) deposits with medium grained alluvial and estuarine sandstones of the Basal Sand. This constitutes a basinward shift in facies (*sensu* Shanley and McCabe, 1994), consistent with a type 1 sequence boundary, but not a non-Waltheran facies shift. However, in localities (e.g. Sheep Mountain, Figures 2.10, 2.26; and probably the new type section; Figure 2.11) where the Basal Sand directly overlies the Fox Hills Sandstone (shallow marine) or Bearpaw Shale (marine), facies juxtapositions are non-Waltheran. Sequence boundary 2 and the basal sand are regionally extensive with good outcrop visible at East Ried Coulee (Figure 2.11; the new type section; Hartman et al., 2014), the Marina Road (Figures 2.4, 2.5), Penick Coulee (Figure 2.13), and East Gilbert Creek (all within ~40 km in a region south of Fort Peck Reservoir), but also as far away as Crooked Creek (~120 km west; Figures 2.7, 2.8), and Sheep Mountain, Ekalaka (~175 km southeast; Figures 2.10, 2.26).

Sequence boundary 2 is interpreted as having formed during a period of negative accommodation, potentially representing base-level fall. Significant base-level fall at sequence boundary 2 is corroborated by Lerbekmo (2009) where he suggests that significant eustatic sea-level fall at this time caused leaching of the Whitemud Formation (the Canadian equivalent to the Colgate sequence; Fraser et al., 1935). Further, the Colgate tidal flats, and possibly the Battle Formation, exposed along the Marina Road (FWS-105; Figure 2.5) is indicative of a stable land surface that might be expected at the top of a transgressive sequence (e.g. Kraus, 1987; 1999; 2002; see above). The overlying

Basal Sand is interpreted as having been deposited during a period of low accommodation space (LAST; Figure 2.3). The Basal Sand is discriminated from normal channel cut and fill by a combination of features: its occasional deep incision; multi-storey vertically amalgamated stacks of channels; and the lateral amalgamation of many channels such that the Basal Sand can be traced laterally over many kilometers. This represents the last time that Hell Creek Formation terrestrial deposition can be correlated with sea-level. From hereon, depositional sequence components are referred to as low or high accommodation settings.

Overlying the Basal Sand are approximately 15 m of typical floodplain deposits and isolated channel deposits (Khc-lf) that comprise the remainder of the lower Hell Creek depositional sequence. The transition from Khc-bs to Khc-lf records a landward shift in facies, a sharp decrease in the ratio of sand to mud, and a change in channel stacking patterns from multi-story amalgamated channels (Khc-bs) to smaller isolated channels within thick deposits of overbank fines. This represents a shift from low-accommodation to high-accommodation conditions, hence Khc-lf represents a HAST. Good exposures of Khc-lf can be seen at East Ried Coulee (Figure 2.12; the new type section; Hartman et al., 2014), the Marina Road (Figures 2.4, 2.5), Cole Creek (Figure 2.25), East Gilbert Creek, Penick Coulee (Figures 2.13, 2.15; all within ~40 km in a region south of Fort Peck Reservoir), and as far away as Crooked Creek (~120 km west; Figures 2.7, 2.8), and Sheep Mountain, Ekalaka (~175 km southeast; Figures 2.10, 2.26). Khc-lf is overlain by sequence boundary 3 (SB3) and the Jen Rex Sand of the Middle Hell Creek depositional sequence.

Middle Hell Creek Formation

Depositional Sequence (SB3, Khc-jrs, Khc-mf). The Middle Hell Creek Formation depositional sequence comprises sequence boundary 3, the overlying Jen Rex Sand (LAST), and Khc-mf (HAST), with a combined thickness of 25-40 m (~37 m in the new type section; Hartman et al., 2014), which is typically thicker than either the lower or upper sequences. The middle Hell Creek Formation can be the most problematic sequence to identify in the field, since it lacks the obvious formational contacts that are present for the lower and upper sequences. Nevertheless, the prominent Jen Rex Sand is almost always present at the base of this sequence, and usually either the lower or upper formational contact can be observed within a few kilometers, permitting correlation.

Sequence boundary 3 typically occurs at the base of the Jen Rex Sand, approximately 15 m above the top of the Basal Sand (18 m above the upper surface of the Hell Creek Formation Basal Sand in the new type section; Hartman et al., 2014), and is marked by an erosive scour of variable relief (0-5 m, this analysis; up to 5 m, new type section, Hartman et al., 2014; up to 15 m, Flight, 2004). Sequence boundary 3 juxtaposes different channel stacking patterns from overbank fines and thin isolated channels sands of Khc-lf to multi-story amalgamated channels of the Jen Rex Sand. This constitutes a basinward shift in facies (*sensu* Shanley and McCabe, 1994), consistent with a type 1 sequence boundary, but not a non-Waltheran facies shift. However, Flight (2004) notes localities where amalgamated fluvial deposits of the Jen Rex Sand (my usage) erosively overlie estuarine strata of the Colgate Sandstone. This still does not constitute a non-Waltheran facies shift, but represents a more significant basinward shift in facies than typical for the Jen Rex Sand and other Hell Creek Formation amalgamated channel

deposits. Occasional deep channel incision into the underlying Khc-lf (and especially into the Colgate depositional sequence; Flight, 2004), and a basinward shift of facies supports the interpretation that sequence boundary 3 formed during a period of falling accommodation. Furthermore, across sequence boundary 3, the ratio of sand to mud increases from Khc-lf to the Jen Rex Sand, representing a shift from a high-accommodation to low-accommodation depositional setting (hence the Jen Rex Sand is interpreted as a LAST). Sequence boundary 3 and the Jen Rex Sand are regionally extensive with good examples of the contact and amalgamated channel complex at East Ried Coulee (Figures 2.11, 2.12; the new type section; Hartman et al., 2014), Cole Creek (Figure 2.25), the Marina Road (Figures 2.4, 2.5), Penick Coulee (Figures 2.13-2.15), and East Gilbert Creek (all within ~40 km in a region south of Fort Peck Reservoir), but also as far as Sheep Mountain, Ekalaka (~175 km southeast; Figures 2.10, 2.26).

Overlying the Jen Rex Sand is a package of approximately 20-30 m of typical floodplain deposits and isolated channels: the Middle Hell Creek Formation Fines. The transition from Khc-jrs to Khc-mf records a landward shift in facies, a sharp decrease in the ratio of sand to mud, and a change in channel stacking patterns from multi-story amalgamated channels (Khc-jrs) to smaller isolated channels within thick deposits of overbank fines. This represents a shift from low-accommodation to high-accommodation conditions, hence Khc-mf represents a HAST. Khc-mf is overlain by sequence boundary 4 and the Apex Sand of the Upper Hell Creek depositional sequence. The Null coal (Lofgren, 1995; Sprain et al., 2015) is a thin (<50 cm) lignite that occurs in the uppermost part of Khc-mf, typically 0-5 m below the base of the Apex Sand. It is well developed in

Bug Creek, being ~50 cm thick, but thins slightly to the east, and is gradually replaced by an organic-rich shale (e.g. Lost Creek; Figure 2.16; East Gilbert Creek; Figure 2.18). In some localities the Null Coal (or equivalent) is the uppermost bed of Khc-mf being directly overlain by the Apex Sand (e.g. Lost Creek, Figure 2.16; the northern part of East Gilbert Creek; Figure 2.18). However, in other localities (e.g. Lost Creek, Figure 2.37; southern part of East Gilbert Creek Figure 2.38; Lone Tree Creek, Figure 2.34) the Null Coal is overlain by up to 5 m of typical Hell Creek Formation mudstones, which are then erosively overlain by the Apex Sand. The Null Coal (or equivalent organic-rich mudstone) represents a period of widespread swampy conditions present at the end of the HAST of the Khc-mf. This might be considered as representing a maximum flooding surface if it could be linked to sealevel, but at least represents the period of maximum accommodation during the HAST. The overlying mudstones (where present) represent the lattermost part of the HAST when accommodation space creation is waning, and might be considered HST if it could be linked to sealevel. Removal of these uppermost mudstones by the incision or lateral cut-and-fill amalgamation of the overlying Apex Sand (Khc-as) is consistent with interpretation of an overlying sequence boundary (SB4?), and subsequent LAST of the Khc-as.

Good exposures of Khc-mf can be seen at East Ried Coulee (Figure 2.12; the new type section; Hartman et al., 2014), the Marina Road (Figures 2.4, 2.5), East Gilbert Creek (Figure 2.18), Penick Coulee (Figures 2.13, 2.15), and Lost Creek (Figures 2.16, 2.19; all within ~40 km in a region south of Fort Peck Reservoir).

Upper Hell Creek Formation

Depositional Sequence Parts 1 and 2. The Upper Hell Creek depositional sequence is divided into two parts, based on the identification of sequence boundary 5 at the base of the 10 Meter Sand (Khc-10ms). Part 1 comprises sequence boundary 4, the overlying Apex Sand (LAST; Khc-as), and Khc-uf1 (HAST), with a combined thickness of ~15-20 m (~15 m in the new type section; Hartman et al., 2014). Part 2 comprises sequence boundary 5, the overlying 10 Meter Sand (LAST; Khc-10ms), and Khc-uf2 (HAST), with a combined thickness of ~9-12 m (~10 m in the new type section; Hartman et al., 2014). The complete thickness of the Upper Hell Creek depositional sequence (i.e. parts 1 and 2 combined) is ~26-30 m (27 m in the new type section; Hartman et al., 2014).

Part1: (SB4, Khc-as, Khc-uf1). Sequence boundary 4 occurs at the base of the Apex Sand, approximately 26 m below the contact with the overlying Fort Union Formation (~63 m above the lower contact of the Basal Sand in the new Hell Creek Formation type section; Hartman et al., 2014). It is marked by an erosive scour, along which no significant relief typically occurs, but up to 5 m has been observed by the author (East Gilbert Creek; see above), and is overlain by the amalgamated channel complex of the Apex Sand. Sequence boundary 4 juxtaposes different channel stacking patterns from overbank fines and thin isolated channels sands of Khc-mf to multi-story amalgamated channels of the Apex Sand. This constitutes a basinward shift in facies (*sensu* Shanley and McCabe, 1994), consistent with a type 1 sequence boundary, but not a non-Waltheran facies shift. Lack of any significant incision at the sequence boundary suggests that it was formed during a period of accommodation stillstand. Across

sequence boundary 3, the ratio of sand to mud increases from Khc-mf to the Apex Sand, representing a shift from a high-accommodation to low-accommodation depositional setting. Sequence boundary 4 and the overlying Apex Sand are regionally extensive, supporting recognition as a sequence boundary and LAST respectively. Good examples of the sequence boundary and Apex Sand are visible at East Ried Coulee (Figure 2.12; the new type section; Hartman et al., 2014), Cottonwood Creek, Bug Creek, Short Creek (Figure 2.28) and Lost Creek (Figures 2.16, 2.19), Penick Coulee (Figure 2.15), and East Gilbert Creek (Figure 2.18); all within ~40 km in a region south of Fort Peck Reservoir. The sequence boundary is overlain by sediments of the upper Hell Creek depositional sequence.

Overlying the Apex Sand is a package of approximately 10 m of typical floodplain deposits and isolated channels comprising Khc-uf1. The transition from the Apex Sand to Khc-uf1 records a landward shift in facies, a sharp decrease in the ratio of sand to mud, and a change in channel stacking patterns from multi-story amalgamated channels (Khc-as) to smaller isolated channels within thick deposits of overbank fines (Khc-uf1). This represents a shift from low-accommodation to high-accommodation conditions, hence Khc-uf1 represents a HAST. Khc-uf1 is overlain by tentative sequence boundary 5 and the 10 Meter Sand.

Part2: (SB5, Khc-10ms, Khc-uf2). A fifth sequence boundary is present approximately 10m below the contact with the Fort Union Formation, slightly more than halfway through the Upper Hell Creek depositional sequence (~79 m above the bottom of the Basal Sand in the new type section; Hartman et al., 2014). The tentative sequence

boundary is normally overlain by the amalgamated channel complex informally named the 10-Meter Sand (Hartman et al., 2014). Although the base of the 10 Meter Sand is erosive, significant relief is rarely observed, although at one locality the 10 Meter Sand is observed to incise ~10 m into the top of the Apex Sand (see East Gilbert Creek, above). Further, although the 10 Meter Sand is typically present, its thickness varies considerably (no more than 4 m usually), and is often much thinner, more fine grained, and less prominent in outcrop than other amalgamated channel units that occur lower in section. Typical lack of incision at sequence boundary 5 may indicate that it was formed during accommodation stillstand, although highly localized incision suggests accommodation fall. Clustering of channel belts at this stratigraphic horizon is indicative of either low accommodation, a period of slowed accommodation space creation, or a period of normal accommodation, but high sedimentation rate (as has been suggested for the basal sands of the Dinosaur Park formation, Alberta; Eberth and Brinkman, 1994; Eberth, 2005). For the purposes of this analysis, the 10 Meter Sand is identified as a LAST.

Overlying the 10 Meter Sand (where present) is a package of approximately 4-10 m of typical floodplain deposits and isolated channels comprising Khc-uf2. The transition from the 10 Meter Sand to Khc-uf2 records a landward shift in facies, a decrease in the ratio of sand to mud, and a change in channel stacking patterns from multi-story amalgamated channels (Khc-10ms) to smaller isolated channels within deposits of overbank fines (Khc-uf2). This represents a shift from medium/low-accommodation to high-accommodation conditions, hence Khc-uf2 represents a HAST. Khc-uf2 is overlain by the Fort Union Formation and as such is the last unit considered in this study.

Discussion

Stratigraphy

The Hell Creek Formation of Montana comprises four disconformity bound depositional sequences, and conforms well to terrestrial sequence stratigraphic models. The described sequence boundaries are consistent across ~50 km in the area studied south of Fort Peck (Figures 2.1, 2.2), and lower sequence boundaries are similarly observed in sections ~120 km west at Crooked Creek (north of Winnett, MT; Flight, 2004; Figure 2.7), ~175 km east at Makoshika State Park (Glendive, MT; Butler, 1980; Hartman et al. 2014), and ~300km southeast at Sand Creek (Sheep Mountain, near Ekalaka; Figures 2.10, 2.31). Lateral extent of the described features differentiates them from isolated channels or autocyclic processes.

The amalgamated channels that lie immediately above sequence boundaries are conspicuous in outcrop, and almost always present, making useful marker beds for ascertaining stratigraphic position. Moreover, their resistance to erosion means that they commonly form valley floors or the tops of buttes, strongly affecting outcrop patterns. The Fox Hills Sandstone and Bearpaw Shale are less resistant to erosion, facilitating modern channel incision, and giving way to deep valleys and steeper landscapes. This can make outcrop of the Lower Hell Creek depositional sequence difficult or slow to traverse, which may partially explain why the Lower Hell Creek is less well prospected for fossils than Middle or Upper depositional sequences (a reason why the Hell Creek Project initially specifically targeted the Lower part for collecting). It is fortunate that individual depositional sequences of the Hell Creek Formation are rarely thicker than

~30m, since the typical relief of any given outcrop of the Hell Creek Formation usually exceeds 30m. Therefore at least one sequence boundary or formational contact should be visible locally.

The varying classification of geologic units at the lower contact of the Hell Creek Formation highlights problems in reconciling traditional lithostratigraphy (a purely descriptive method) with sequence stratigraphy (a more interpretative method). Inclusion of the uppermost part of the Colgate depositional sequence (pale grey silt capped by an organic rich horizon: the Colgate tidal flats, and possible Battle Formation) into the Hell Creek Formation (Erickson, 1992; Murphy et al., 2002; Flight, 2004) results in a confusing classification, as they do not belong to the same depositional sequence and the basalmost bed of the Hell Creek Formation would therefore no longer be the basal sand (as suggested by its name, and as was the original intention of Brown, 1907). Flight's designation is understandable in that these tidal flat deposits are lithologically unlike the underlying Colgate Sandstone (or the Fox Hills Formation, of which the Colgate Sandstone is a member), but they are also equally distinct from the basal sand of the Hell Creek Formation which can almost always be found immediately overlying them. The tidal flat deposits have some resemblance to fluvial silts and organic-rich facies of the Hell Creek Formation (Fastovsky, 1987), but this is largely superficial since tidal flat facies are not found above the Hell Creek basal sand (i.e. within the Hell Creek Formation). Considering the stratigraphic distinction and dissimilar depositional environment, it is probably desirable to designate the entire Colgate depositional sequence as a separate formation. In southern Alberta and Saskatchewan, Canada, the

Colgate depositional sequence is separated into its own formation: the Whitemud Formation (Irish, 1960; Catuneanu and Sweet, 1999; Lerbekmo, 2009). While redefinition of the Colgate is beyond the scope of this paper, further work involving regional correlation will probably render this nomenclatural change necessary.

Previous informal divisions of the Hell Creek into upper and lower units (Brown, 1907; Flight 2004; Wilson, 2004) do not agree with the definitions given here, and none is ideal. Flight (2004) takes a lithostratigraphic approach, defining the lower Hell Creek as consisting of the uppermost part of the Colgate depositional sequence (as explained in the paragraph above) and the Hell Creek Basal Sand. In terrestrial lithostratigraphy it is commonplace for the top of a sandstone unit to be picked out as a member or formational contact, so from this perspective Flight's definition is not unusual, but it is difficult to see how it is a useful classification since the majority of the formation remains undivided. The more utilitarian approach: basing division simply on a given measurement (such as Wilson, 2004), while convenient in a relatively small geographic area, is unlikely to be consistent over any great distance since formational thickness varies. Moreover, since sequence boundaries represent periods of non-deposition, time is not evenly distributed throughout the formation. Consequently, divisions of even thickness will likely not pertain to equivalent amounts of time. This is especially important in studies of faunal change. The Lower, Middle, and Upper depositional sequences as presented here, are probably the most useful stratigraphic divisions since they depend upon lithological criteria observable in the field, and correlate with the passage of time more directly, although how much time is represented by each sequence has yet to be determined.

Time Duration of Depositional Cycles. With few chronostratigraphic indicators within the geological succession, it is difficult to ascertain how much time might be represented by disconformities at sequence boundaries, and by the depositional sequences themselves. Belt et al. (1997) argued for a fairly substantial (~2 m.y.) regional unconformity between the Fox Hills Sandstone and Hell Creek Formation, placing the top of the Fox Hills Sandstone at about 70 Ma. While this interpretation remains controversial (Murphy et al., 2002), a regional unconformity would be a reasonable hypothesis for the interconnected Williston and Powder River Basins, and a hiatus of some length is suggested by the disconformable erosive basal contacts of the Colgate Sandstone (up to 25 m relief; Behringer, 2008) and Hell Creek Formation (at least 5m relief), and also ammonite biostratigraphy (Gill and Cobban, 1973; Lillegraven and Ostresh, 1990; Cobban, 1994; see magnetostratigraphic corrections, above). However, if the magnetostratigraphic work of Lerbekmo (2009) is correct in assigning the top of the Fox Hills sandstone as C30r (top of C30r = 67.696 Ma; Ogg and Smith, 2004), this would suggest a much shorter hiatus, probably much less than 1 m.y., although again, ammonite biostratigraphy suggests that Lerbekmo (2009) is in error.

Magnetostratigraphy similarly provides some of the only available constraints in determining depositional sequence duration within the Hell Creek Formation itself. The upper depositional sequence typically comprises the uppermost 26 -30 m of the Hell Creek Formation, of which the upper 10-20 m is of reversed polarity, pertaining to C29r (Archibald et al., 1982; Lerbekmo, 1999; LeCain et al., 2014). The base of C29r is placed at 66.398 Ma (Ogg, 2012), which combined with a K-Pg placement of 66.0 Ma (roughly

in the middle of C29r; Ogg and Hinnov, 2012), brings the duration of Hell Creek Formation part of C29r to 0.398 m.y. (comparable to ~333 k.y. suggested for the Cretaceous part of C29r by D'Hondt et al., 1996). Using this estimate, the upper third of the Hell Creek Formation (cycles 3 and 4) represents approximately 0.4 m.y. of deposition, plus some time accounted for at the hiatus (sequence boundary). By comparison Sprain et al. (2015) dated an ash in the Null Coal, located 0-5 m below the base of the Apex sandstone, recovering a date 0.263 - 0.336 Ma older than the Irz coal (K-Pg boundary; the precise dates recovered use a different standard and decay constant than). Based on this radiometric date, the upper third of the Hell Creek (cycles 3 and 4) probably represents less than 300 k.y. in duration. If it is assumed that the lower ~60 m of the Hell Creek Formation was deposited at approximately the same rate (by thickness), then the entire formation may have been deposited in approximately 0.9 Ma. This very rough figure is comparable to the estimated duration of ~1.36 m.y. published by Hicks et al. (2002), but less comparable to the maximum of 2.1 m.y. (based on magnetostratigraphy; Wilson, 2004, 2005; Lerbekmo, 2009; LeCain et al., 2014). A cycle wavelength of ~0.3 m.y. places the Hell Creek Formation depositional sequences as representative of 4th order cyclicity (0.1-1 m.y.; Miall, 2010). These are superimposed over the top of 3rd order cyclicity (1-10 m.y.; Miall, 2010), in the same fashion as illustrated by Barrell (1917).

Autocyclic or Allocyclic Processes. The question remains as to the relative influence of autocyclic (autogenic) or allocyclic (allogenic) processes on patterns of deposition; were Belt et al. (1997) correct in suggesting that internal stratigraphic

divisions (4^{th} order, as shown here) may be related to basin-wide patterns of base-level change, and hence be correlatable further afield than the immediate Ft. Peck area? Deep scouring observed at the base of the Colgate Sandstone, Hell Creek Basal Sand and Jen Rex Sand (sequence boundaries 1, 2 and 3, respectively), is indicative of significant fall in accommodation. Decrease in intensity of accommodation fall at sequence boundaries 4 and 5 is consistent with interpretation of 4^{th} order cyclicity superimposed on overall 3^{rd} order base-level rise (Barrell, 1917). However, 3^{rd} and 4^{th} order cyclicity are often attributed to different forcing mechanisms (Mitchum and Vail, 1977; Catuneanu, 2006).

Factors that dictate cycles of deposition are complex, often cryptic, and the subject of much recent literature. Terrestrial deposits in other parts of the Western Interior similarly exhibit 3^{rd} and 4^{th} order depositional sequences thought to record cycles of base-level (including eustasy), basinal flexure, sediment supply, and climate (Eberth, 1990; 1996; 2005; Eberth and Hamblin, 1993; Eberth and Brinkman, 1994; Bhattacharya and Posamentier, 1994; Rogers, 1994;1995;1998; Olsen et al., 1995; Catuneanu and Sweet, 1999; Catuneanu et al., 1999; Chen and Bergman, 1999; Straight and Eberth, 2002; Mitchell, 2002; Atchley et al., 2004; Chen et al., 2005; Wroblewski, 2006; Shelton, 2007; Cleveland et al. 2007; Fanti and Catuneanu, 2010; Antia and Fielding, 2011). Working under an assumption that the Hell Creek Formation was deposited under incipient transgression of the Cannonball Seaway (Johnson et al., 2002), it is tempting to attribute cyclic deposition within the formation to pulses of transgression and regression, as would be expected in such conditions, and is suggested by the presence of marine influenced units within the Hell Creek Formation of North Dakota (Hoganson and

Murphy, 2002), and the presence of marine dinoflagellates in the uppermost Hell Creek of Montana (Moore et al., 2014). This would seem reasonable for sediment packages that exhibit marine influence (e.g. Bearpaw-Fox Hills, Colgate and Lower Hell Creek depositional sequences), but might not be considered likely for sequences which were deposited during a period when the shoreline was many hundreds of kilometers to the east, although recent evidence suggests that sealevel and even tides may influence sedimentation 1000-1500 km inland from the shoreline in very low relief systems (Irion et al., 2009; Kosuth et al., 2009). Plint et al. (2001) suggest that sea-level change may be manifested as tabular units over large distances (basin-wide) whereas tectonically controlled depositional cycles may exhibit more wedge-shaped geometries. This is difficult to assess without a broader regional subsurface correlation of depositional sequences. Apparent changes in sea-level may represent eustatic events (as suggested for the leaching of the Colgate Sandstone / Whitemud Formation; Lerbekmo, 2009), although neither the Haq et al. (1987) nor Miller et al. (2004) sea-level curves are at high enough resolution to see 4th order fluctuations. Nevertheless, the presence of polar ice caps in the latest Cretaceous is suggested by Miller et al. (2004), and even Miall (2013) suggests that glacioeustasy must be considered for high frequency accommodation fluctuations in the Campanian and Maastrichtian.

Alternatively, apparent sea-level changes may reflect a depositional system response to localized basin subsidence, where sediment supply is not high enough to fill accommodation created by subsidence. Differential basinal flexure may also result in varying patterns of subsidence and uplift in different areas within the same basin (e.g.

Dinosaur Park Formation, Alberta; Eberth and Hamblin, 1993; Eberth, 2005; Hanna Basin, Wyoming; Wroblewski, 2006). Similarly, movement of the foreland basin hingeline was suggested as a potential cause of 4th order cyclicity in the Horseshoe Canyon through Scollard Formations of Alberta, Saskatchewan (Catuneanu and Sweet, 1999), units that are contemporaneous (in part) with the Montanan Hell Creek Formation, and only 200-300 km northwest. Although Catuneanu and Sweet (1999) focus on Canadian Maastrichtian formations, they also infer that 4th order cyclicity in the Hell Creek Formation of north-central Montana might be caused by cycles of basin flexure and hingeline migration, which might therefore account for broad patterns of accommodation space change observed in this analysis. However, I find it difficult to imagine hingeline migration occurring over cycle wavelengths as little as 150,000 years or less, as observed in the upper Hell Creek Formation, and consider eustasy a more likely forcing factor for 4th order cyclicity, with tectonics perhaps possible for the overall 3rd order cyclcity seen over the full duration of Hell Creek time (1-2 m.y.). Testing of this hypothesis awaits analysis of subsurface data.

Elsewhere, periods of transgression are indicated in the Hell Creek Formation by nearshore marine tongues observed in North Dakota (Breien Member and Cantapeta tongue; Hoganson and Murphy, 2002) and coal units in the middle of the Hell Creek Formation in South Dakota (Firesteel coal; Searight, 1931), both of which are bound above and below by non-marine strata. While accurate correlation of the Firesteel coal, and Breien and Cantapeta tongues to Montanan sections awaits more detailed regional sequence stratigraphic analysis, it is possible that these nearshore marine units and coals

represent maximum flooding surfaces correlative with sequences identified here in Montana. Similarly, during periods of high accommodation (HAST), large-scale storage of sediment in terrestrial settings is likely to have resulted in sediment starvation basinward of the floodplain (and thus, potentially transgression). However, lack of significant landward movement of the shoreline (compared to previous Late Cretaceous transgressions of the WIS) suggests that sediment supply was high enough to be able to keep up with substantial accommodation space creation. Conversely, during periods of low accommodation (LAST) or static / lessening accommodation (formation of sequence boundaries), lack of accommodation space would have caused sediment bypass of the floodplain, with deposition occurring more basinward, probably in the form of a progradational delta. During periods of static accommodation (e.g. sequence boundaries 4 and 5) this would take the form of a normal regression, whereas during periods of falling accommodation (e.g. sequence boundaries 1, 2, and 3), this should be a forced regression. In which case, upper parts of the Fox Hills Sandstone in eastern North Dakota may in part serve as correlative conformities to the disconformities (sequence boundaries) of the Hell Creek Formation, rather than being coevally deposited with floodplain sediments. However, testing of this hypothesis awaits further work.

It has been proposed relatively recently that apparent cyclicity in alluvial sequences (as documented here) might form from entirely autogenic processes (Wang et al., 2011; Hajek et al., 2010, 2012). Experimental models and some observational studies (Hajek et al., 2010; 2012) propose that after avulsion, channels self-organize to preferentially occupy slight topographic "low spots" which, once filled with channel

deposits, consequently undergo further avulsion to other topographic lows. This "avulsion clustering" forms clusters of closely-spaced channel-belts separated by extensive intervals of overbank deposits which it is proposed might appear similar or identical to amalgamated channel complexes produced by changes in accommodation, or other allogenic forcing factors. It is not yet clear how to discriminate between amalgamated channels formed by "avulsion clustering" compared to allogenic forcing factors. However, one test would be to consider the lateral extent of proposed sequence boundaries or cycle bases, where avulsion clustering should not exhibit lateral continuity over a great distance, especially outside of a given drainage basin. By contrast, allogenic forcing factors should impose sequence boundaries or cycle bases across entire regions, regardless of drainage basins. It is also suggested that avulsion clustering may operate at shorter timescales than the 3rd and 4th order cycle wavelengths suggested here. The lateral extent of the cycles identified here, and cycle wavelengths observed suggest self-organization is not responsible for cycles within the Hell Creek Formation. However, this area of research remains in development and so this interpretation may change pending further research.

Regional Correlation and Biostratigraphy

Although this analysis is principally concerned with creating a framework for the Hell Creek Formation of the Fort Peck area, Montana, some regional correlations are possible, and can be stratigraphically informative. In the northern reaches of the Williston Basin, in Alberta, Canada, the Lower Scollard Formation is the equivalent unit (in part) to the Hell Creek Formation, with most workers placing the base of the Scollard

approximately halfway through the C30n magnetozone (Eberth pers. comm. 2006; Lerbekmo and Braman, 2002). The Scollard Formation lies disconformably upon the Battle Formation, a shaly unit 8.1m thick (Russell, 1983), from which a radiometric date of 66.97 Ma has been extracted (placing it about halfway through C30n; Hicks et al., 2003; Lerbekmo, 2009; Fowler, Chapter 3). If the Scollard Formation is found to be equivalent to the upper or upper and middle Hell Creek depositional sequences (as is consistent with its magnetostratigraphic record), then the radiometric date for the underlying Battle Formation may provide an additional maximum age constraint for these depositional sequences.

Further east in Saskatchewan, Canada, the (partial) Scollard-equivalent Frenchman Fm has an erosive contact with the Battle Fm, and can be shown to be younger at its base than the Scollard (Lerbekmo, 1999; Lerbekmo and Braman, 2002).The base of the Frenchman Formation occupies the uppermost C30n magnetozone, with the remainder residing in C29r (Lerbekmo and Braman, 2002; Lerbekmo, 1999). Therefore the Frenchman Formation is equivalent to the upper Hell Creek depositional sequence only. This is important as new research (Scannella et al., 2014) has shown that the ceratopsid dinosaur *Triceratops prorsus* only occurs in the upper depositional sequence, with different *Triceratops* morphospecies occurring lower in the formation (including *T. horridus*). Subsequently, Scannella and Fowler made the prediction that only *T. prorsus* should be found in the Frenchman Formation, which at the time of writing is true of all diagnostic published specimens.

If it can be demonstrated that *Triceratops* morphology changes consistently through time, without overlap of species, then the use of *Triceratops* as a biostratigraphic zonal fossil should be reconsidered. All vertebrate taxa are potentially biostratigraphically informative, and in the case of ceratopsid dinosaurs, potentially at a much higher resolution than mammals (Fowler, 2006). *Triceratops* was used as a zonal fossil by Cobban and Reeside (1952), and with species-level biostratigraphic separation (Scannella et al., 2014), it could potentially provide a means to correlate across upper Maastrichtian deposits of the Western Interior, including those outside of the Williston and Powder River Basins.

Paleontology

An understanding of sequence stratigraphy can assist in other aspects of paleontological research. Non-material time at sequence boundaries can account for seemingly instantaneous changes in morphology (faunal turnover). For example, it is of little surprise that we often see the greatest morphologic differences in *Triceratops* when comparing specimens from either side of a sequence boundary (Scannella and Fowler, 2009; Scannella et al., 2014), than within a sequence itself. Similarly it is important to register the stratigraphic position of a fossil locality relative to one, or preferably more datum points. Ideally a datum would be a radiometrically dated horizon, such as the Null Coal at the top of the middle depositional sequence, or the Z-coal at the K-Pg boundary (Sprain et al., 2015). However, it is more typical to measure the stratigraphic position of a fossil locality relative to the base, or top of a formation. In the specific example of the Hell Creek Formation, given that incision of the Basal Sand can vary by 10 m or more,

then it would be best to measure locality stratigraphic positions relative to both the bottom of the Basal Sand (which is contentious) and the top of the Basal Sand (which is much less contentious). Indeed this method is advised for localities relative to other amalgamated channel horizons as they all exhibit variable incision depths, albeit to different degrees.

The effects of terrestrial sequence stratigraphy on paleoecological interpretation have been broached before by Flight (2004), but also by Lofgren (1995) in his solution to "the Bug Creek problem". Here, base-level fall in the Paleogene incised a deep valley (at least 30 m) into the Hell Creek Formation, resampling and mixing microvertebrate faunas of the Paleogene and Cretaceous. The Bug Creek problem represents an extreme example, but it should be understood that fossil samples collected from other incised valley fills and amalgamated channel complexes may still be subject to fairly strong time averaging, and there are limitations that this may impose on paleontological interpretation.

In another example, a recent paper by Lyson and Longrich (2010) studied dinosaur taxon-facies associations in the Hell Creek Formation. They noted that *Triceratops* comprises a larger proportion of the fauna collected from mudstones, whereas ornithopod remains are more common in sandstones. This is consistent with my own field observations and the results of Horner et al., (2011). Lyson and Longrich literally interpret this taxon-facies association as floodplain "spatial niche partitioning": proposing that ornithopods lived close to river channels while ceratopsids preferred to live farther away from rivers. An understanding of terrestrial sequence stratigraphy can

help better interpret such facies-taxon associations as taxon preferences for differing basin drainage regimes and possibly proximity to the shoreline (the same pattern might also be explained by taxon-specific taphonomic preservation bias; Fowler et al., 2003; D. Evans, pers. comm., 2011). The amalgamated channel complexes that form Hell Creek Formation sequence boundaries are the primary source of vertebrate material from sandstones. These represent deposition during periods of low-accommodation when the floodplain would have been better drained and the shoreline was likely to have been regressing or stable. By comparison, the mudstones that overlie the amalgamated channels were deposited in a high-accommodation setting, which may typically be associated with a rise in the position of the groundwater table, resulting in more poorly drained conditions (Wright and Marriot, 1993; Shanley and McCabe, 1994; Currie, 1997; see above discussion) during periods when the floodplain was closer to the shoreline. It has already been noted by Brinkman et al. (1998) that ceratopsids were more abundant in coastal areas: their apparent abundance in mudstones of the Hell Creek Formation supports this view. Thus, it is more likely that the variation in abundance of ornithopods and ceratopsids between facies is a result of ceratopsids preferring more coastal, swampy environments, and hadrosaurs having a preference for more well-drained, inland habitat.

Finally, sequence stratigraphic interpretation may have implications for mass extinction at the K-Pg boundary. Patterns of extinction and diversity change approaching and across the K-Pg may indeed reflect gradual or abrupt extinction (Archibald, 2011), but they may also reflect changing patterns of accommodation and depositional environment. In addition to the high-low accommodation bias mentioned above, coaly

units of the basal Fort Union Formation represent periods of maximum accommodation (potentially, maximum flooding surfaces). Coaly units that occur at the K-Pg boundary itself may not be conducive towards preservation of vertebrate material, perhaps providing an explanation for the paucity of specimens recovered from the upper 3 m of the Hell Creek Formation. Further, recent studies of Hell Creek dinosaurs have demonstrated a new understanding that morphologies once thought to be different species actually represent ontogenetic variation within single species (Carr, 1999; Horner and Goodwin, 2006; Scannella and Horner, 2010). This has had the result of drastically reducing the number of dinosaur taxa present immediately before the K-Pg extinction event. A higher resolution stratigraphic framework for these final throes of the Cretaceous will give greater ability to test rates of extinction and faunal change through to the K-Pg extinction.

Further Work

It remains to be tested whether or not the proposed depositional cycles extend beyond the 100 km or so represented. Although gamma ray well log analysis might be expected to be useful in identifying laterally extensive amalgamated channel sandstones (SP and resistivity logs were not of sufficient resolution in the analysis of Connor, 1992), regional variation in unit thickness may make correlation difficult to justify. The best available test would be magnetostratigraphic analysis of the C29r zone boundary through to the K-Pg boundary, an interval, which contains the two uppermost cycles identified here (Khc-as to Khc-uf1, Khc-10ms to Khc-uf2). If these two proposed cycles are regional in extent, then we would expect to see the C30n-C29r boundary occurring within

or at the base of a LAST, with a second LAST shortly before the K-Pg boundary, as in the Hell Creek type area.

Conclusions

The Hell Creek Formation of the Fort Peck area, Montana can be subdivided into four depositional sequences, each consisting of an erosional scour, amalgamated channel complex, and overlying overbank fines with isolated channels. Each sequence (including non-material time) is approximately 0.3 - 0.5 m.y. in duration, representing 4^{th} order cyclicity superimposed over a 3^{rd} order transgression. Subdivision of the Hell Creek Formation into separate sequences gives a more precise framework than is provided by lithostratigraphy, and a more powerful base within which to frame further research.

It is clear from this analysis, and prior research, that the Hell Creek Formation and adjacent units were deposited under fairly complex cycles of accommodation and sediment supply, at multiple scales. Slight differences between this work and previous (Flight, 2004; Behringer, 2008) and current (Hartman et al., 2014) analyses (especially with regard to the identification of sand units from the Fox Hills Sandstone through Basal Sand of the Hell Creek formation) illustrate that Hell Creek cyclic deposition is only starting to be understood. At this current stage, cyclicity within the Hell Creek cannot be definitively linked to sealevel. However the presence of marine influence within the Hell Creek of Eastern Montana, North Dakota, and South Dakota suggests that such correlations may be possible in the future. More in-depth analysis may elucidate further subtle changes, and consequently redefinition of the various sequences described in this

preliminary account may be required. However, recognition of depositional sequences in geographically restricted outcrop is a necessary first stage in development of a regional sequence stratigraphic model. Further work should utilize extensive subsurface well-log and outcrop data from across the Williston and Powder River Basins, which will be integrated with this analysis.

It should probably be noted that opposition is building towards accommodation-based models of terrestrial sequence stratigraphy (Strong and Paola, 2008; chapter 6 in Miall, 2013). Whether or not the accommodation paradigm will remain valid is unclear in the long term. Debate mostly concerns the causative nature of sequence boundaries; whether they truly represent variation in accommodation, or whether simple changes in climate (etc) may cause non-erosional sequence boundaries; a major criticism leveled at accommodation-based models seems to stem from a perceived necessity for sequence boundaries to be represented by incision and subaerial erosion surfaces (chapter 6 in Miall, 2013). Much of the debate seems more concerned with terminology, where even the word "sequence" is considered by some to be only appropriate for cyclicity attributable to sealevel change, which is itself synonymized with baselevel by some workers. Even the word "accommodation" is entrenched in terminology used for categorizing depositional cycles in terrestrial settings (LAST, HAST; Catuneanu et al. 2009a), despite this cyclicity not being necessarily tied to a single forcing mechanism. However, there is no widely accepted alternative terminology; "transgressive/regressive systems tracts" (e.g. Miall, 2013) are arguably worse, being forcibly attached to recognition of shoreline movement that may not be demonstrable for most units.

Regardless of the debate, the purpose of this current work is to recognize cyclicity in the Hell Creek Formation: whatever the cause may be. I hope that this study will make a worthy and lasting contribution in offering alternative interpretations for key study sections (such as Manaige Spring, and the new type section), and more simply as a source of observations and record of localities at which particular stratigraphic contacts of interest can be observed. Moving forward in understanding of Hell Creek Formation stratigraphy does not require consensus on terminology, but it does require replicability; the opportunity for future researchers to revisit important localities and assess the differing interpretations. I further hope that this study helps emphasize the effect of stratigraphy on paleobiological interpretation (my principal interest here), particularly regarding the uneven distribution of time within a formation, and the influence of cyclicity on fossil preservation and ecology.

Acknowledgements

For assistance in measuring sections, thanks to John Scannella, Sarah Keenan, Leigha King, Thomas Rendle, Bobby Ebelhar, Rebecca Cook, John Wilson, Danny Anduza, and Laura Wilson. Thanks extended to Jack Horner, David Bowen, David Varricchio, David Eberth, Liz Freedman Fowler, Warwick and Jackie Fowler, Mark Goodwin, Joe Hartman, Ray Butler, Arthur Bogan, Greg Wilson, Dean Pearson, John Hoganson, Kirk Johnson, MOR preparators and staff, MOR field crews, various land owners, especially the Holen, Isaac, Taylor and Twitchell families, Bob Sullivan, Spencer Lucas, and everyone at the Digital Library Project. Fieldwork was funded by the

Smithsonian Institute and Nathan Myrhvold. Funding for the Museum of the Rockies graduate student fund was provided by Damaris Waggoner and David Sands.

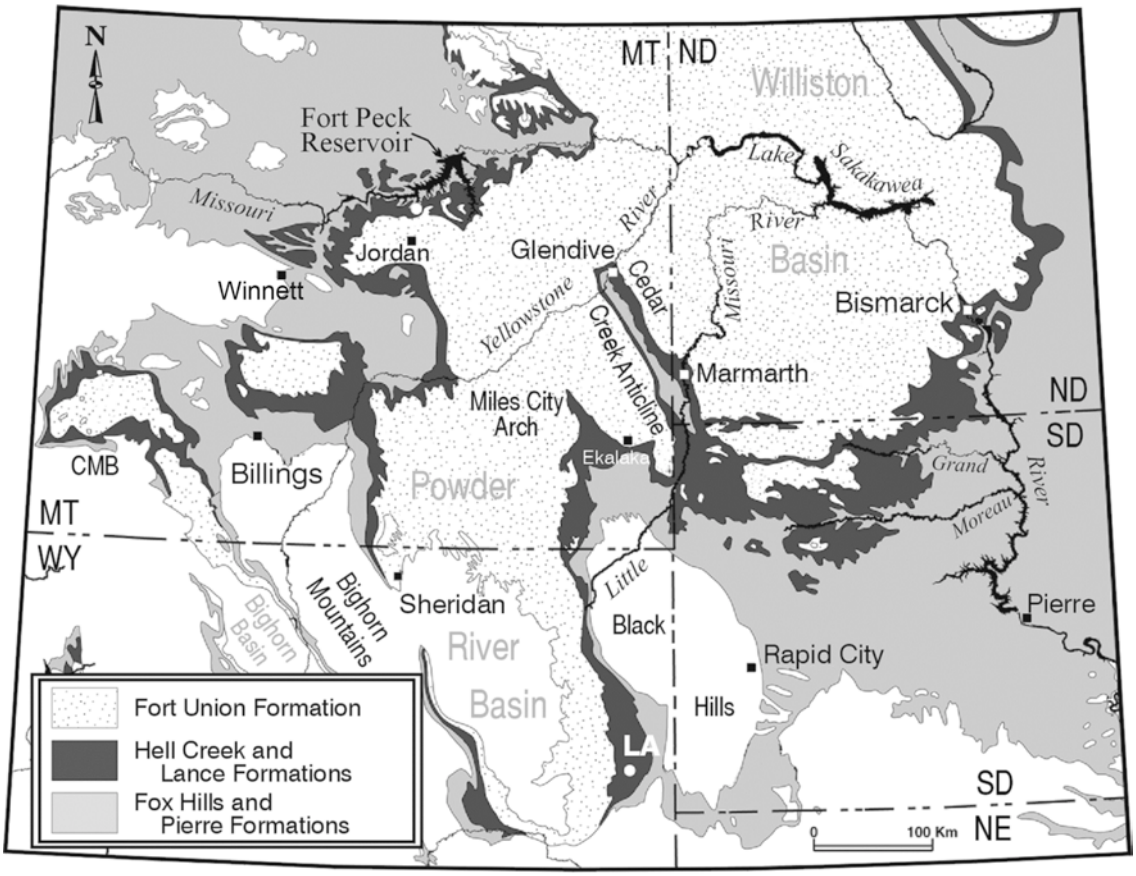

Figure 2.1. Map showing outcrop of Pierre (Bearpaw) Shale, Fox Hills Sandstone, Hell Creek, Lance, and Fort Union Formations in the Williston and Powder River Basins. Outcrop studied for this investigation was located around the towns of Jordan, Winnett, Glendive, and Ekalaka, Montana. Modified from Hartman (2002).

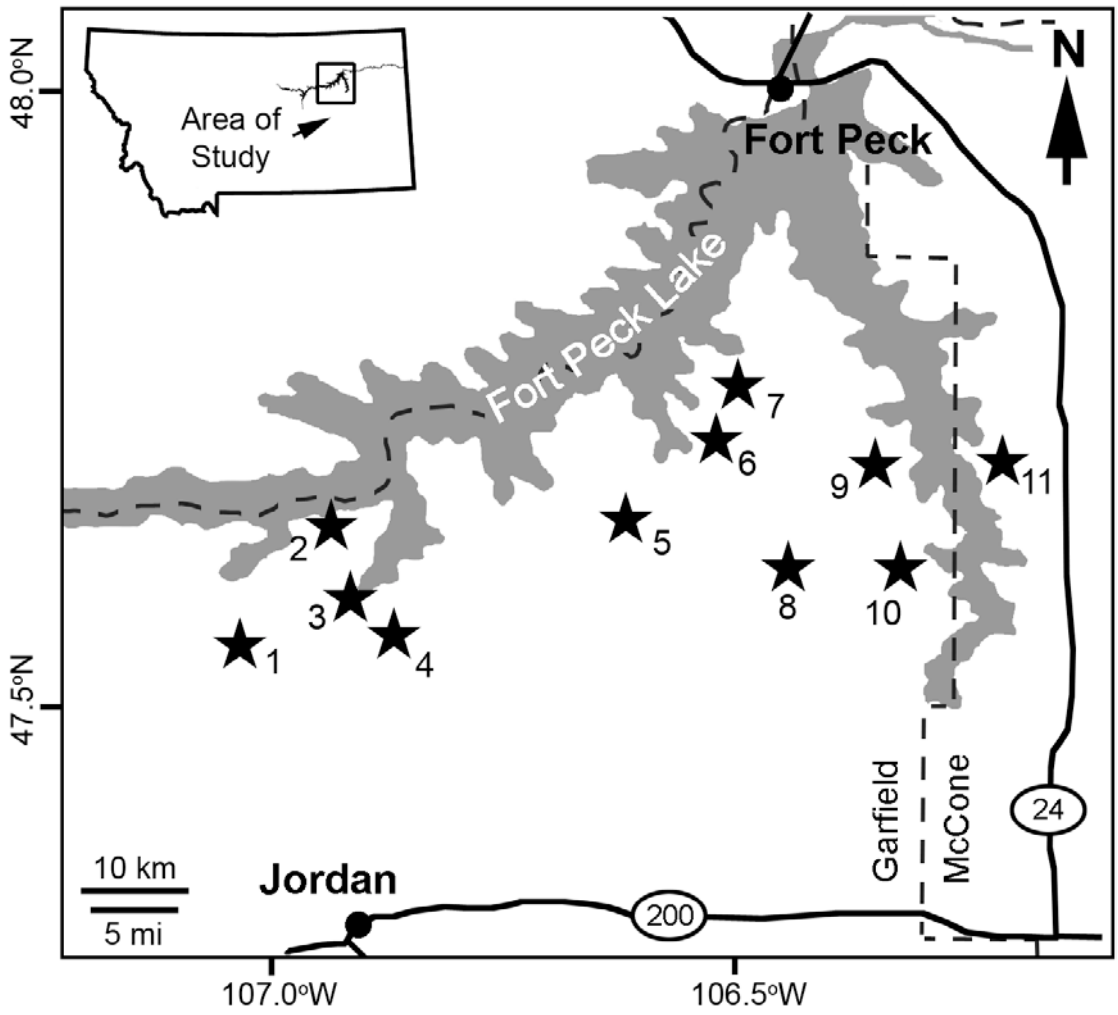

Figure 2.2. Location of principal study localities discussed in text, south Ft. Peck Lake area near Jordan (Garfield County), Montana. 1: Cottonwood Creek (including Brownie Butte). 2: Cole Creek. 3: Marina Road intersection with Hell Creek (Manaige Spring). 4: Ried Creek (including Flag Butte; new type section; Hartman et al., 2014). 5: Gilbert Creek. 6: East Gilbert Creek. 7: Penick Coulee. 8: Lone Tree Creek. 9: Lost Creek. 10: Short Creek. 11: Bug Creek (McCone County).

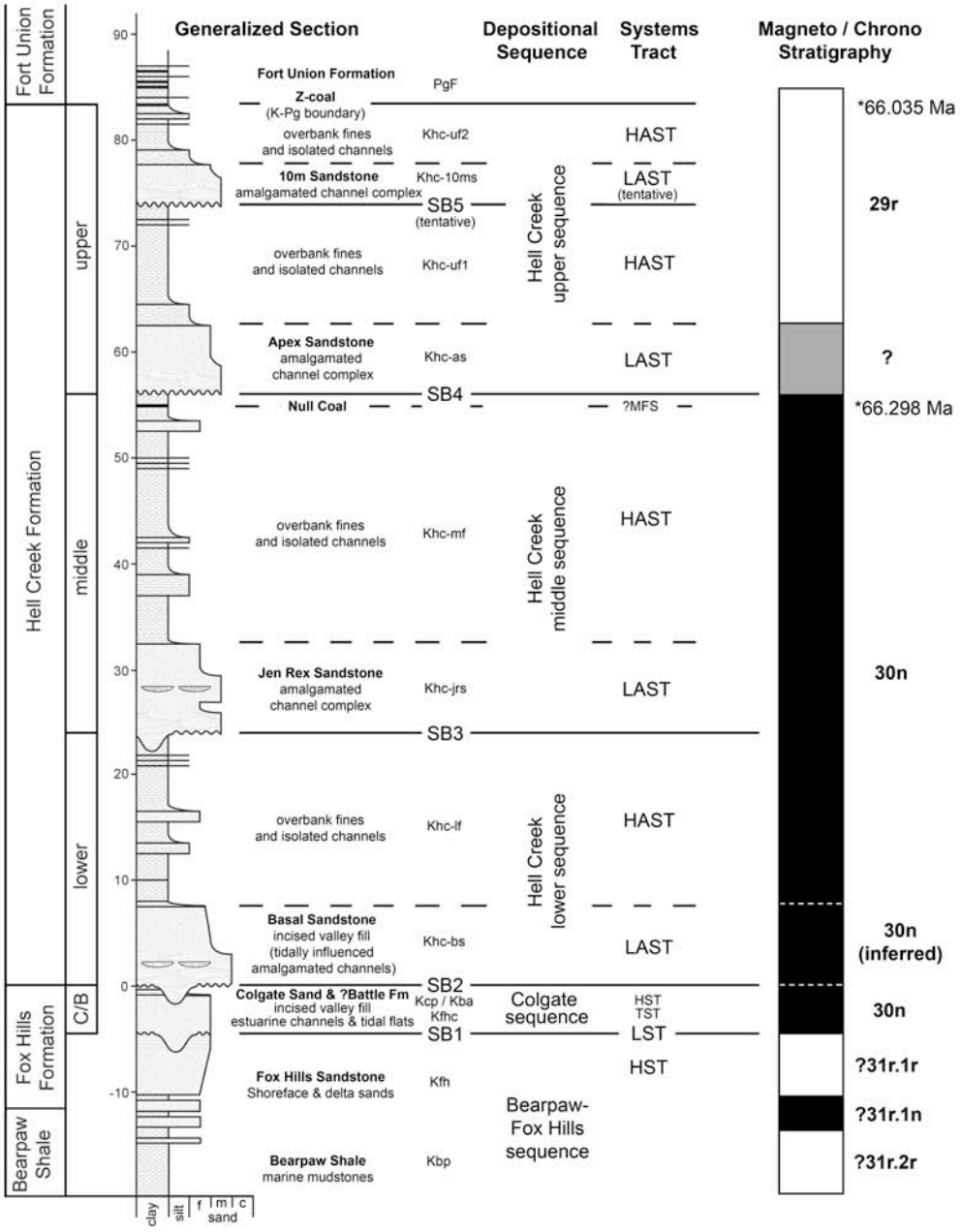

Figure 2.3. Generalized section of the Bearpaw Shale (partial), Fox Hills Sandstone, Colgate Sandstone, Battle, Hell Creek, and Fort Union (partial) formations illustrating sequence boundaries (SB) and sequence tracts (LST: lowstand systems tract; TST: transgressive systems tract; HST: highstand systems tract; LAST: Low Accommodation Systems Tract; HAST: High Accommodation Systems Tract; MFS: Maximum Flooding Surface). The Hell Creek Formation is informally divided into lower, middle, and upper depositional sequences based on the presence of sequence boundaries and amalgamated channel complexes. Magnetostratigraphic column adapted from Lerbekmo (2009; see main text for alterations); Ar / Ar radiometric dates from Sprain et al., (2015).

Figure 2.4. Exposure of the Bearpaw Shale through Jen Rex Sand. The bottom of the photograph shows the grey Bearpaw shales (Kbp) gradually overlain by the pale yellow Fox Hills Sandstone (Kfh). Sequence boundary 1 separates Lfh from the pale-colored Colgate Sandstone (Kfhc) that forms a small cliff, and is overlain by the thin grey silt and conspicuous purple organic-rich mudstone of the Colgate tidal flats (Kcp). Here, sequence boundary 2 is not erosive, and separates Kcp from the overlying Hell Creek Basal Sand (Khc-bs, basal unit of the lower Hell Creek depositional sequence), which exhibits concretions in its lower third. Sequence boundary 3 is not cleanly exposed here, but the basal unit of the middle Hell Creek depositional sequence, the Jen Rex Sand, forms the resistant band at the top of the cliff. Photograph taken facing southwest ~1 km west of Hell Creek Marina Road (FWS-105), ~35km north of Jordan, MT. 47°36’5” N, 106°55’13” W, (NAD27CONUS).

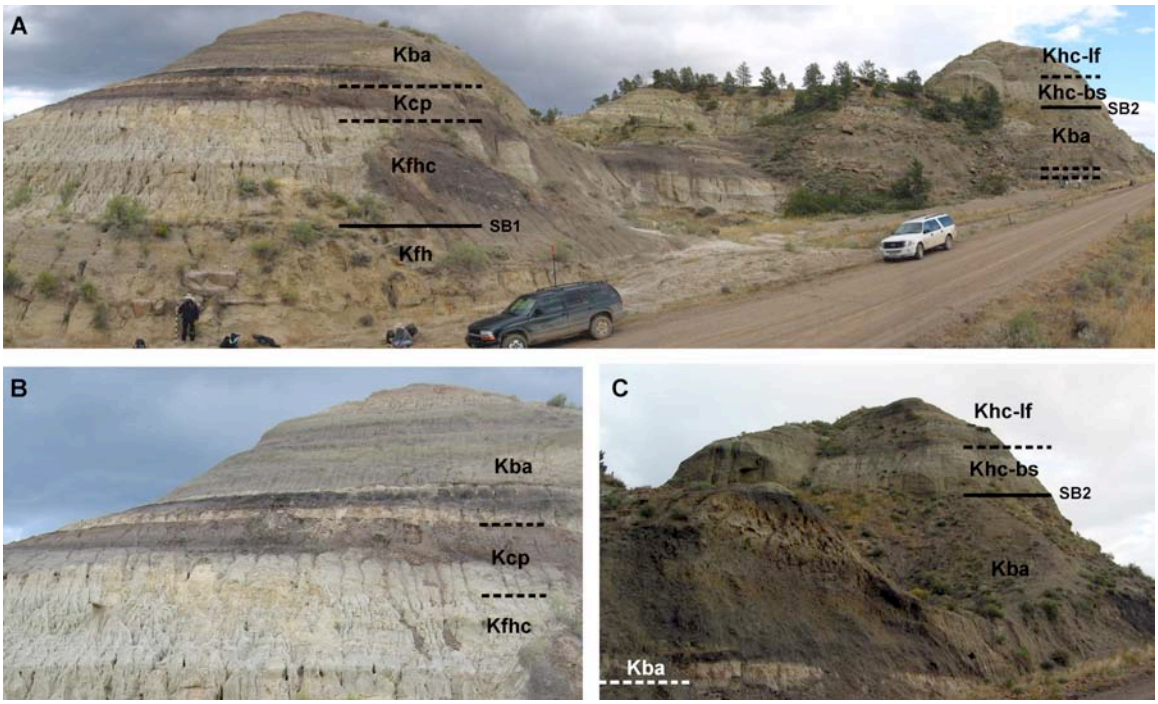

Figure 2.5. (A) Exposure of the Fox Hills Sandstone (Kfh) through Hell Creek Formation Basal Sand (Khc-bs). This locality is unusual in that the Colgate tidal flats (Kcp) are overlain by additional tidal flat facies and mauve colored mudstones of the Battle Formation (Kba), itself overlain by the Basal Sand (Khc-bs) of the Hell Creek Formation. Note that the white sandstone here referred to the Colgate Sandstone (Kfhc) was referred to Khc-bs by Hartman et al. (2014). Identity of this unit as the COlgate Sandstone is confirmed by the distinctive white weathered surfaces visible at nearby locality "Best Butte" (Figure 2.26) (B) Detail of SB2. (C) Detail of SB3. Photo taken at facing east at Manaige Spring, Marina Road (FWS-105) just before crossing Hell Creek, ~30 km north of Jordan, MT (47°34’15” N, 106°57’0” W; NAD27CONUS). Scalebar = 1.5 m.

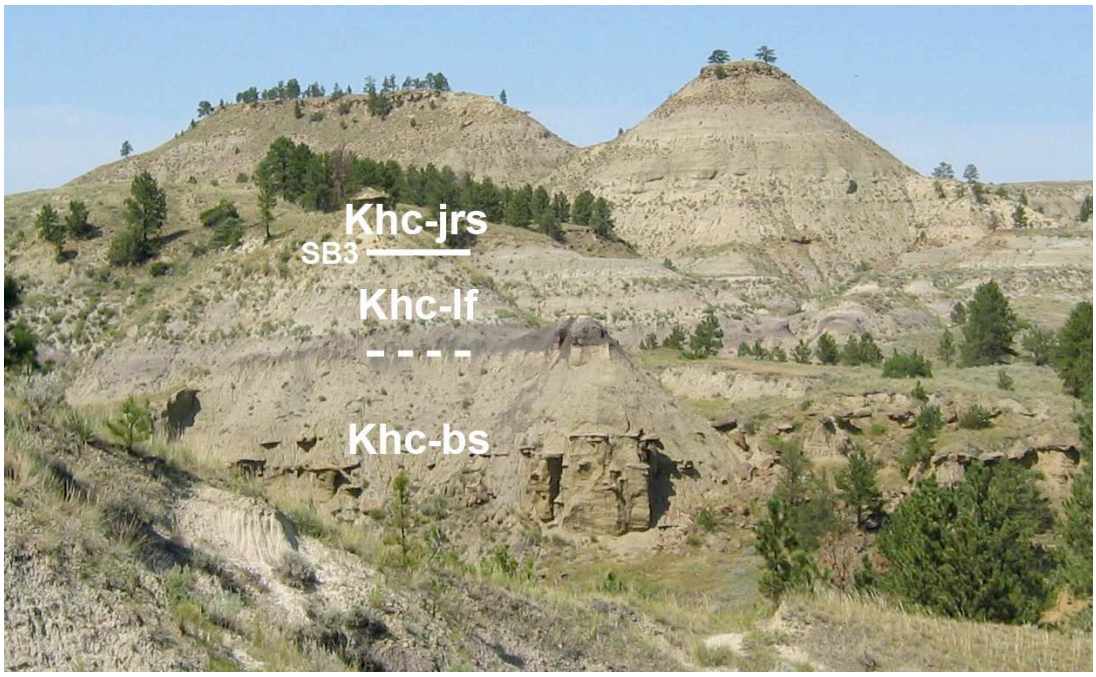

Figure 2.6: Exposures of the lower part of the type section. Overlying the Basal Sand of the Hell Creek Formation (Khc-bs) is an organic-rich mudstone, reminiscent of the organic-rich mudstone which overlies the Basal Sand in Penick Coulee. The Apex Sand caps the buttes in the background. Photo taken facing north at East Ried Coulee, North of Jordan, Garfield Co. MT, 47° 33’48” N, 106°52’40” W (NAD27CONUS).

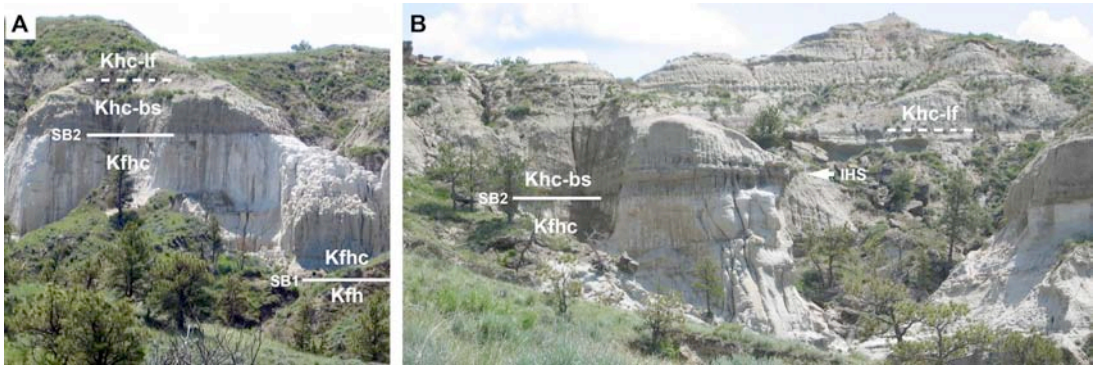

Figure 2.7. Sequence boundary 2 separates the Colgate Sandstone from the overlying Basal Sand of the Hell Creek Formation. Here the Colgate Sandstone is divided into a pale brown lower unit, and an upper unit that is more pale grey, and weathers to a brilliant white. Sequence boundary 1 is just visible at the bottom of photograph A, separating the Colgate sandstone from the underlying Fox Hills Sandstone. Photos taken facing south at Crooked Creek, near Winnett, Garfield Co. MT, 47°24'13" N, 108°14'35" W; (NAD27CONUS).

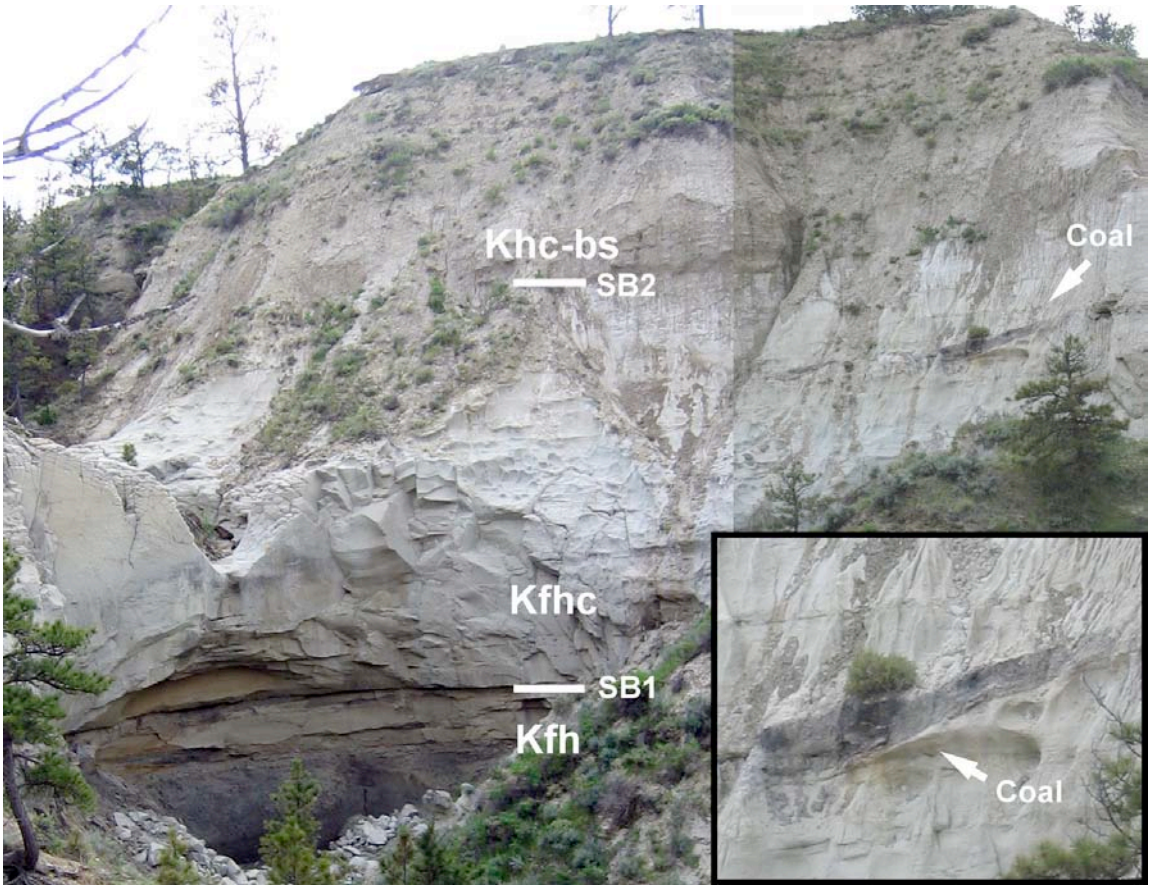

Figure 2.8. Coaly layers are relatively rare in the Colgate Sandstone. This thin coal (inset) is preserved in a channel fill in the upper part of the Colgate Sandstone. Other similar laterally restricted coals were present in this area. Photo taken at Crooked Creek, near Winnett, Garfield Co. MT, 47°24'13" N, 108°14'35" W; (NAD27CONUS).

Figure 2.9. Close-up photograph of the contact between the upper pale unit, and lower tan unit of the Colgate Sandstone. Note the thin (1mm) iron-rich oxidation zone at the contact, and overlying 2 cm grey gleyed zone in the upper unit. Hammer head length: 17 cm. Photo taken at Crooked Creek, near Winnett, Garfield Co. MT, 47°24'13"N, 108°14'35"W; (NAD27CONUS).

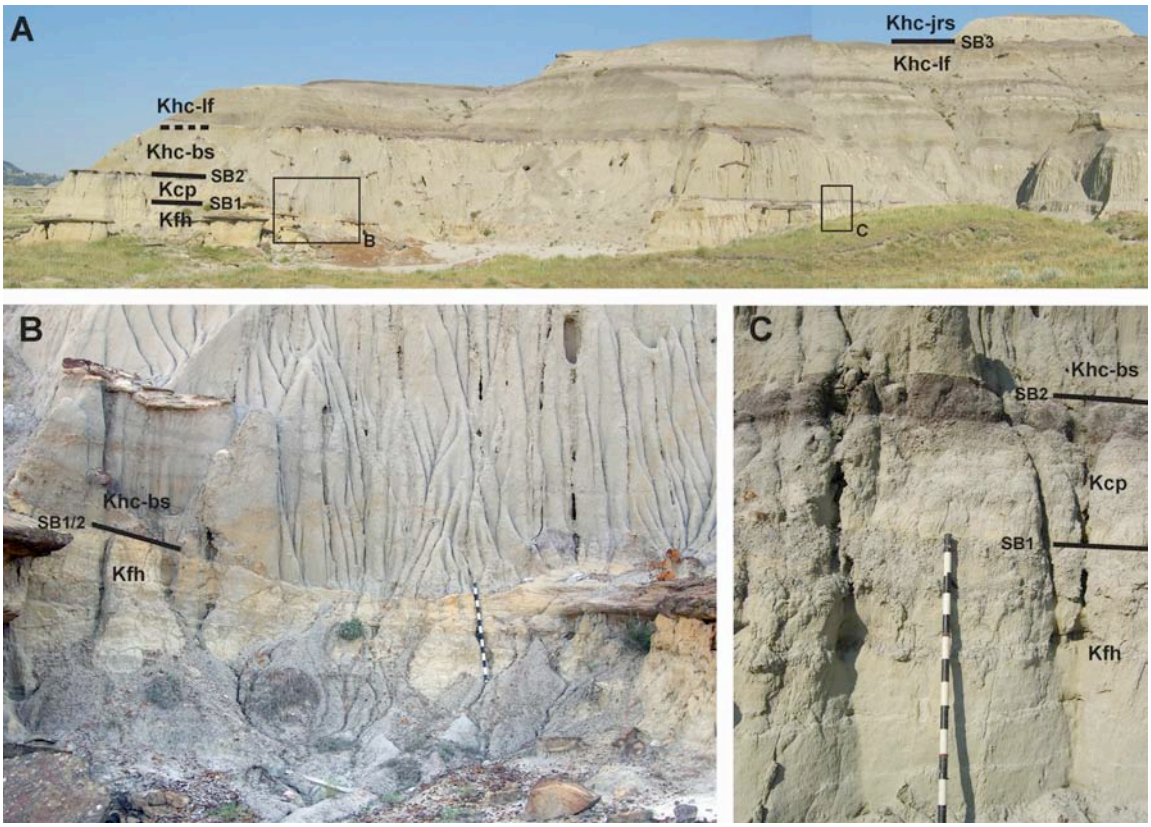

Figure 2.10. (A) Variable contact of the Hell Creek Basal Sand with underlying Colgate depositional sequence and Fox Hills Sandstone at Ekalaka, Carter County. (B) The erosive scour at the base of the Hell Creek Basal Sand has incised down ~5 m through the Colgate tidal flats, into the top of the Fox Hills Sandstone. Consequentially sequence boundaries 1 and 2 are combined into a single surface. Scalebar = 1.5 m. (C) Typical non-erosive contact (SB2) of the Hell Creek Basal Sand overlying Colgate tidal flats. Divisions on scalebar = 10 cm. Photos correspond to Figure 2.26, section 1. Photos taken facing north, at Sand Creek, near Sheep Mountain, 55 km SE of Ekalaka, Carter Co., MT (45°30’8” N, 104°8’0” W, NAD27CONUS).

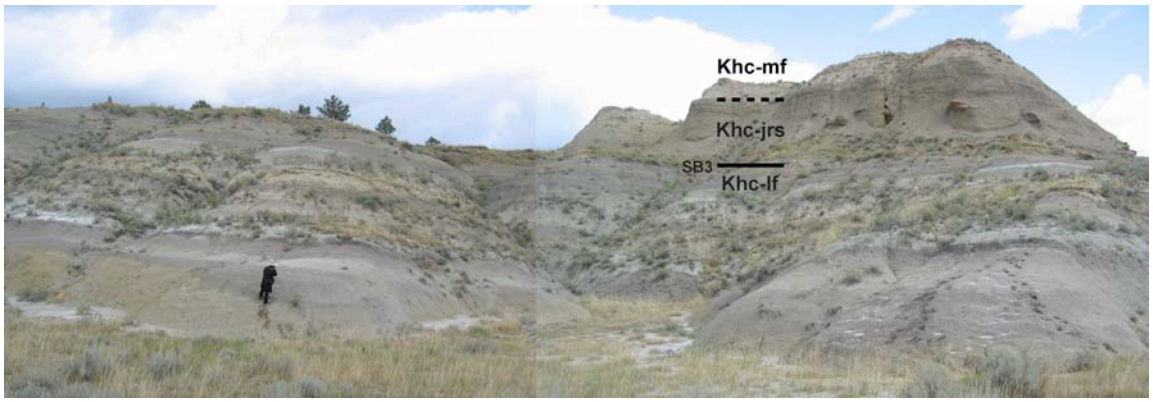

Figure 2.11. Overbank fines and isolated fluvial channels of the lower Hell Creek depositional sequence (Khc-lf; ~15 m thickness) overlain by cliff-forming amalgamated channel complex of the Jen Rex Sandstone (Khc-jrs), basal unit of the middle Hell Creek depositional sequence. Photo taken near the new type section (Hartman et al., 2014), Flag Butte, North of Jordan, Garfield Co. MT, 47° 33'34" N, 106°52'24" W, (NAD27CONUS). Scalebar = 1.5 m.

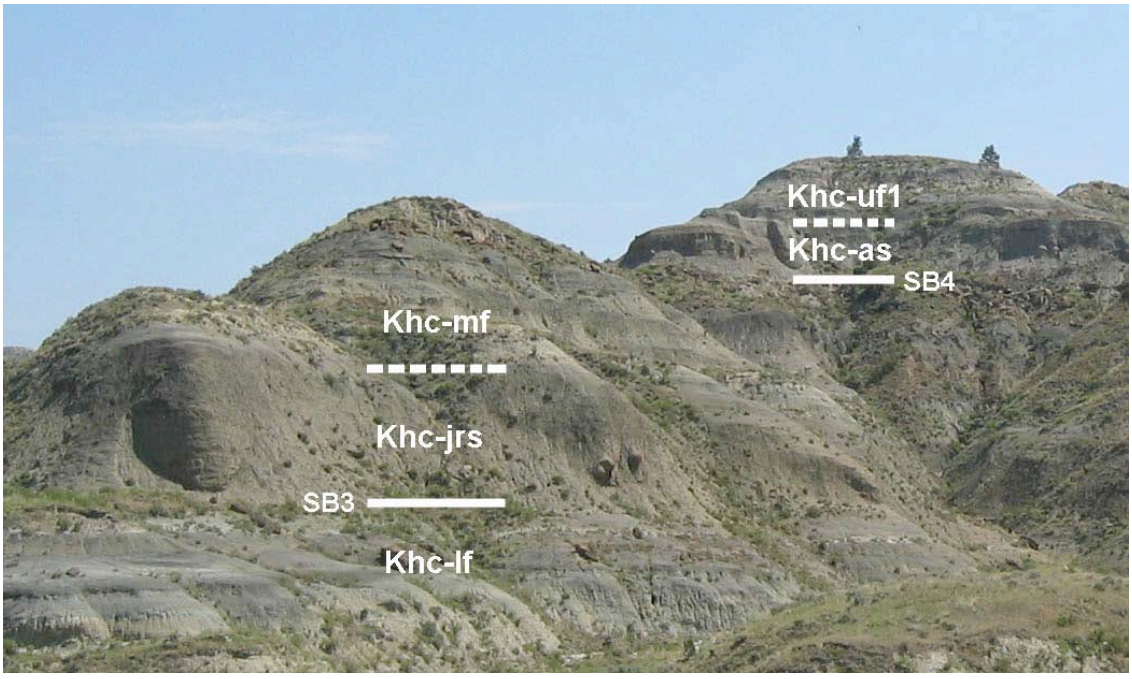

Figure 2.12. Middle and Upper depositional sequences of the Hell Creek Formation at the new type section (Hartman et al., 2014). Here the Jen Rex (Khc-jrs) and Apex (khc-as) Sands form small cliffs. The K-Pg boundary is not visible, but it present at the top of the butte. Photo taken at Flag Butte, North of Jordan, Garfield Co. MT, 47° 33'33"" N, 106°52'20" W, (NAD27CONUS).

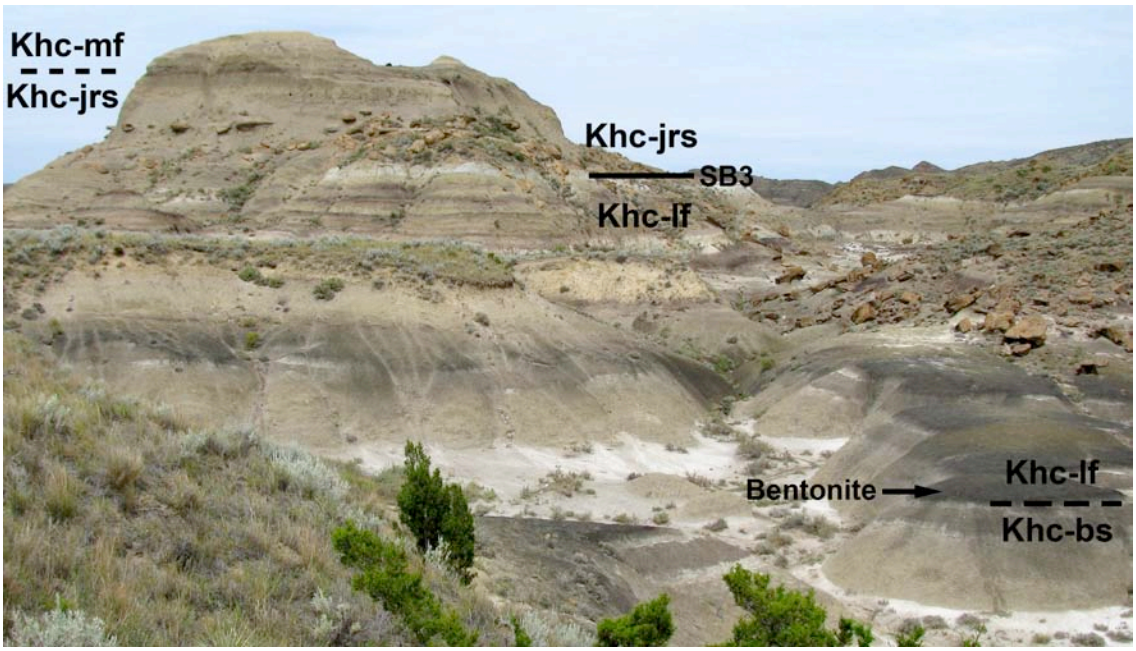

Figure 2.13. Exposure of the lower to middle Hell Creek Formation, middle of Penick Coulee. In Penick Coulee, a prominent bentonite overlies the basal sand, although this is not present 3.5 km south in East Gilbert Creek. The Jen Rex Sand is ~6 m thick at this locality, but in Penick Coulee its presence and thickness varies over <1 km. Photo taken facing northeast at Penick Coulee, near Isaac ranch, northeast of Jordan, MT, 47°43’50” N, 106°30’01” W (NAD27CONUS).

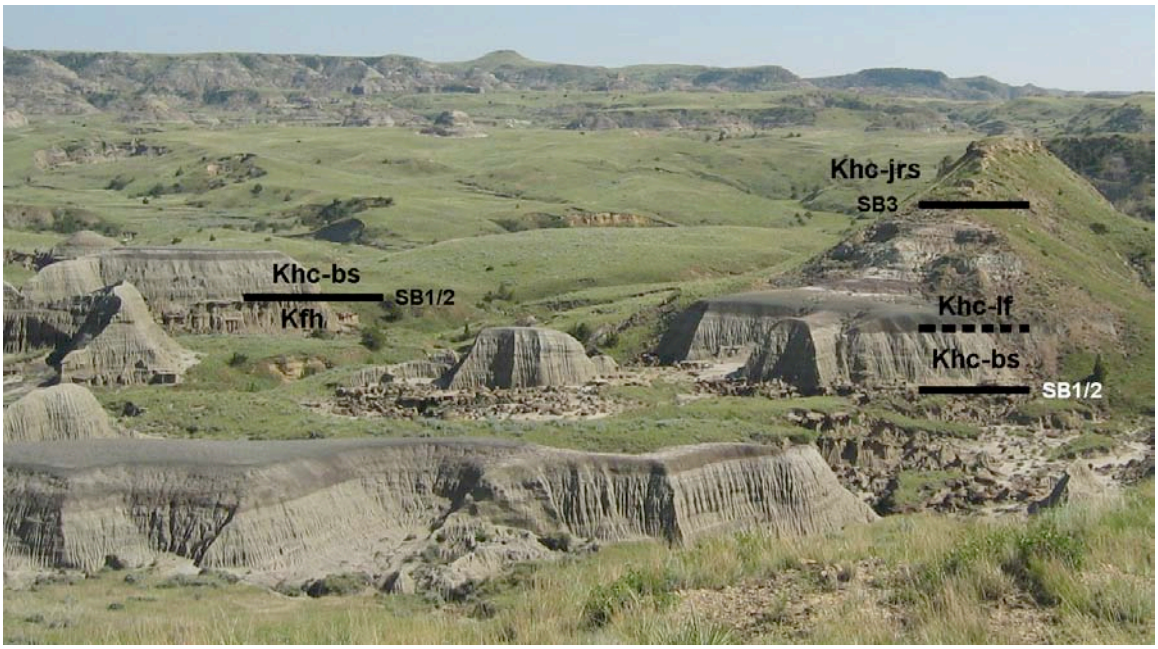

Figure 2.14. Exposure of the lower to middle Hell Creek Formation, north side of Penick Coulee. In Penick Coulee, a prominent dark grey bentonite overlies the basal sand, although this is not present 3 km south in East Gilbert Creek. An organic-rich mudstone is variably present here at the top of the Basal Sand, but pinches out to the north (Figure 2.13). The Jen Rex Sand is thick here (<7 m) with many beds of conglomerate near the base. Hill on right of photo corresponds to Figure 2.15, section 1. Photograph taken facing south at Penick Coulee, near Isaac ranch, northeast of Jordan, MT, 47°44'09"N, 106°31'06" W (NAD27CONUS).

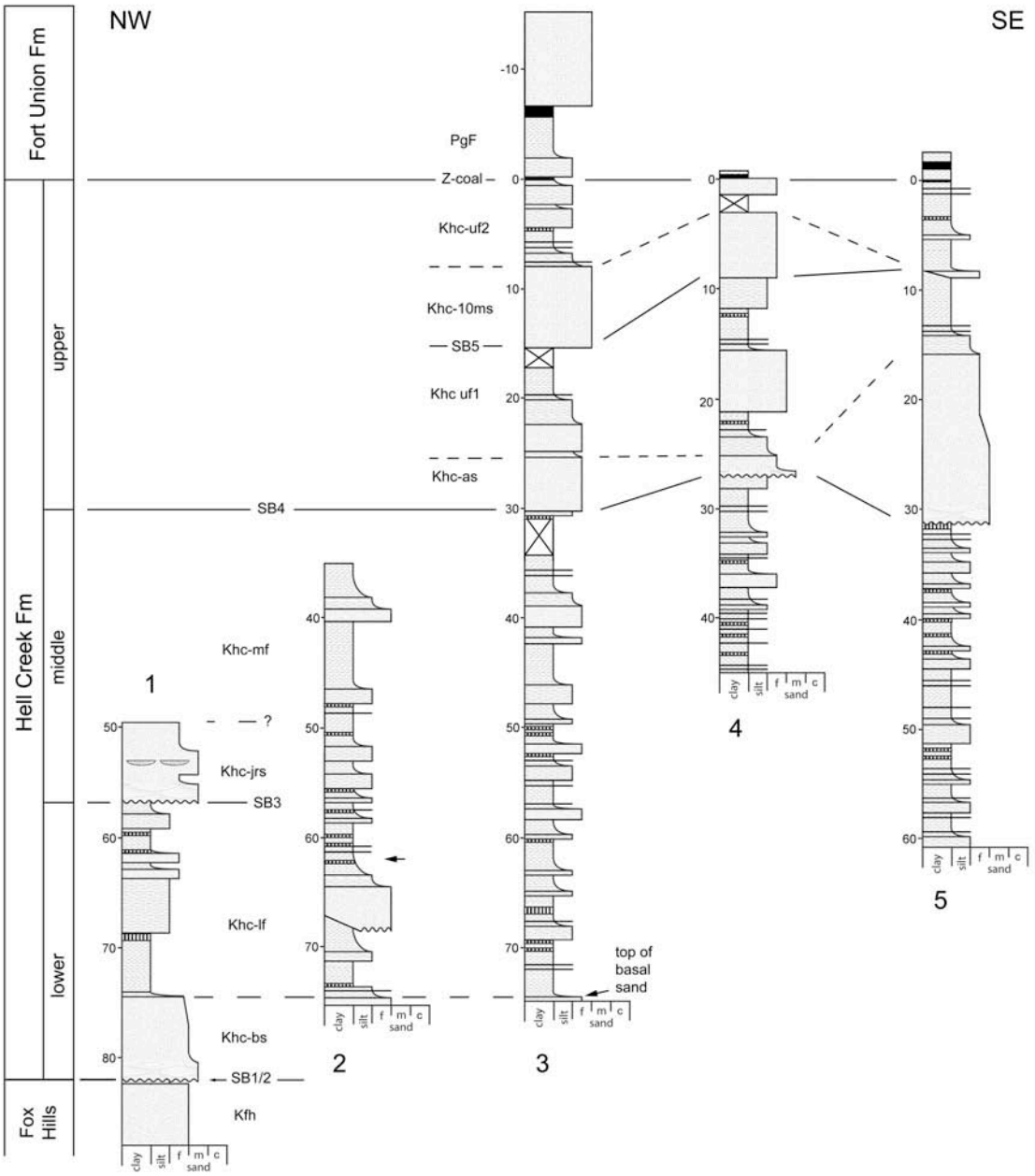

Figure 2.15. Measured sections taken in Penick Coulee and East Gilbert Creek, exposing the complete Hell Creek Formation. (1) North Penick Coulee, 1st section (Figure 2.14); 47°44'09" N, 106°31'06" W. (2) North Penick Coulee, 2nd section; 47°44'29" N, 106°30'35" W. (3) Mid Penick Coulee; 47°44'18"N, 106°29'58"W. (4) South Penick Coulee; 47°42'45" N, 106°30'23" W. (5) Mid East Gilbert Creek (Figure 2.18); 47°41'32" N, 106°30'47" W. All coordinates NAD27CONUS. Vertically striped horizons indicate organic-rich shale / mudstone.

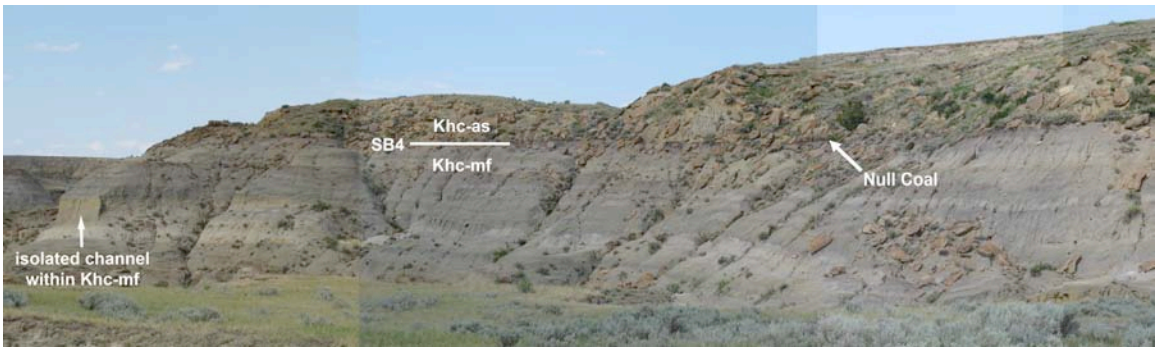

Figure 2.16. Exposure of lower contact of the Apex Sand in Lost Creek. Amalgamated channels of the Apex Sand are laterally extensive in this area, and can be traced for 2-3 km, forming a resistant cap of small buttes. This is in contrast with isolated channels (pictured) within Khc-mf, that are only ~100 m in lateral extent. In many parts of Lost Creek, the Apex Sand is directly underlain by the Null Coal in the uppermost Khc-mf (purple-brown layer in photo). Photo taken facing east at Lost Creek, near Jordan MT, 47°40'03" N, 106°20'16" W (NAD27CONUS).

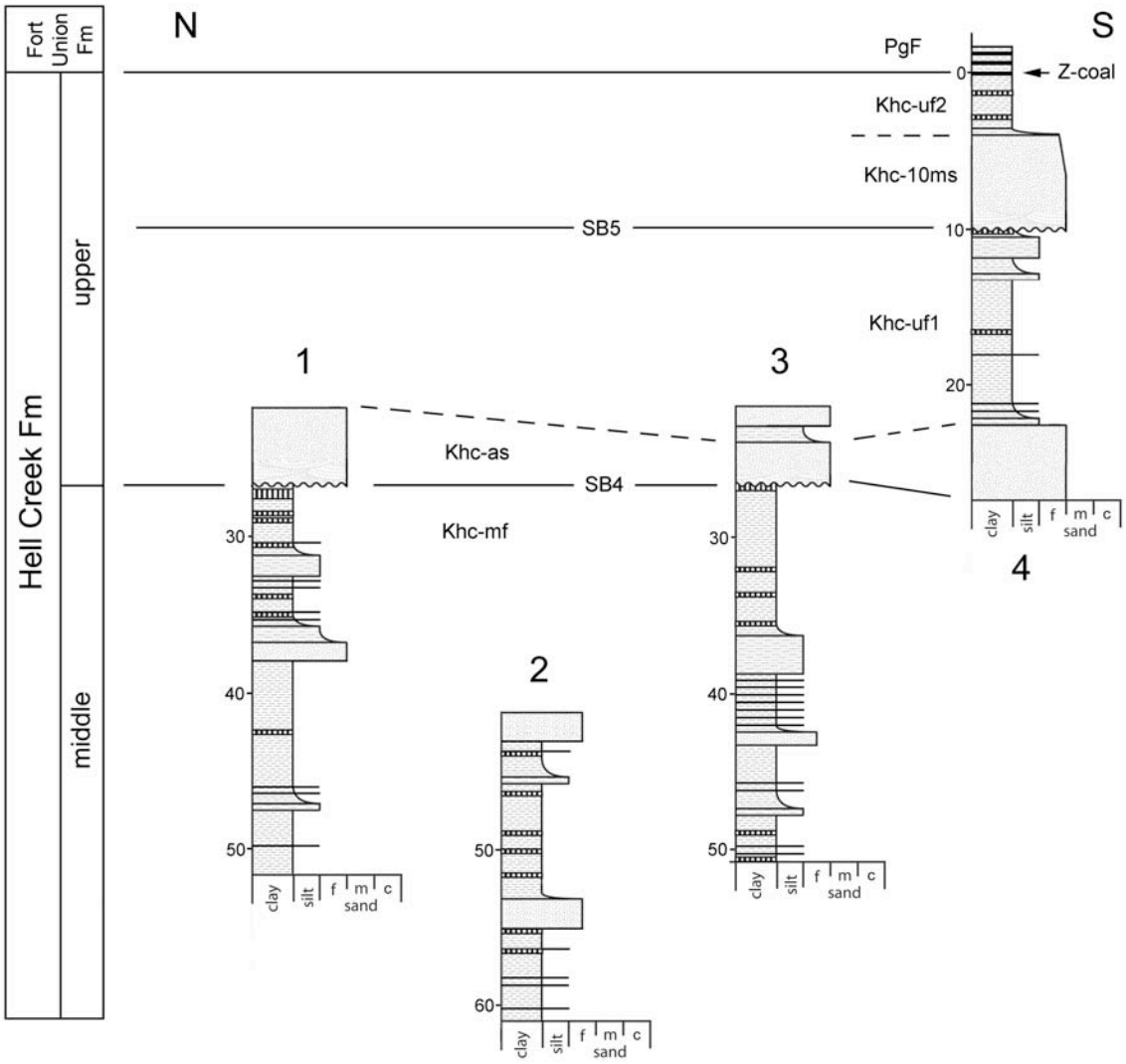

Figure 2.17. Measured sections taken in Lost Creek, exposing the uppermost 60 m of the Hell Creek Formation. (1) Northwest Lost Creek; 47°40'30" N, 106°20'07" W. (2) North Lost Creek; 47°40'32" N, 106°19'19" W. (3) South Lost Creek (Figure 2.16); 47°40'03" N, 106°20'16" W. (4) Southeast Lost Creek (Figure 2.19); 47o39'36"N, 106o19'54"W. All coordinates NAD27CONUS. Vertically striped horizons indicate organic-rich shale / mudstone.

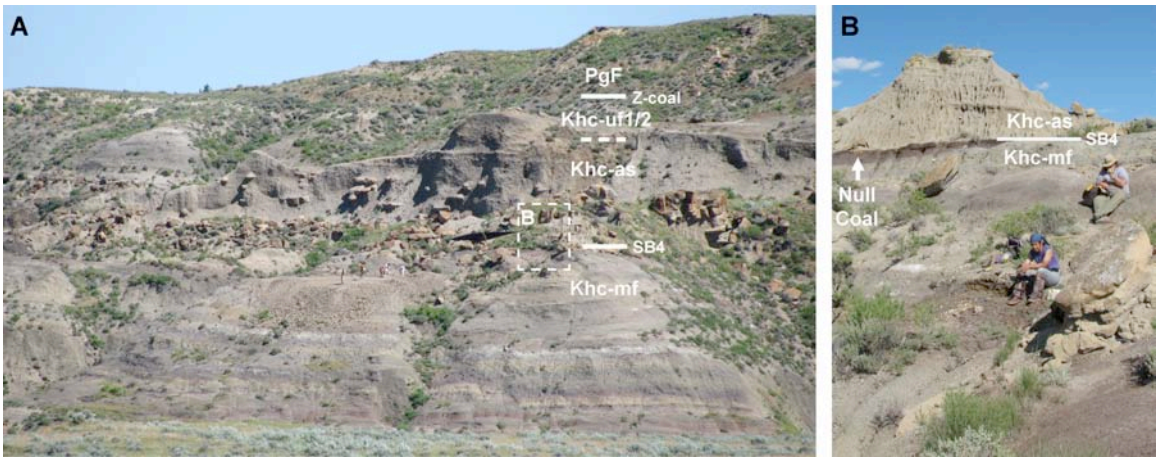

Figure 2.18. Sequence boundary 4 (SB4) separates the middle and upper depositional sequences. Here the lowermost unit of the upper depositional sequence, the Apex Sand (Khc-as), is ~14 m thick and overlies overbank fines of the Middle Hell Creek Formation (Khc-mf). The uppermost unit of the middle fines is an organic-rich mudstone (correlated with the Null Coal) directly underlying the Apex Sand (visible in photo B, and inset in A). The 10 Meter Sand is not present in this section, but is present 2 km north in Penick Coulee, and 1 km south along the southern border of East Gilbert Creek. The Z-coal is barely visible in this photograph, but is present between the pale silt and below the conspicuous color change to the yellow-orange sediments of the Fort Union Formation (PgF). Photographs A and B taken at East Gilbert Creek, near Isaac ranch, North of Jordan, Garfield Co. MT. Photo A taken facing northeast at 47°41’2” N, 106o30’58” W (NAD27CONUS). Photo B taken facing east at, 47°41'32" N, 106°30'47" W (NAD27CONUS). Photo A corresponds to Figure 2.15, section 5.

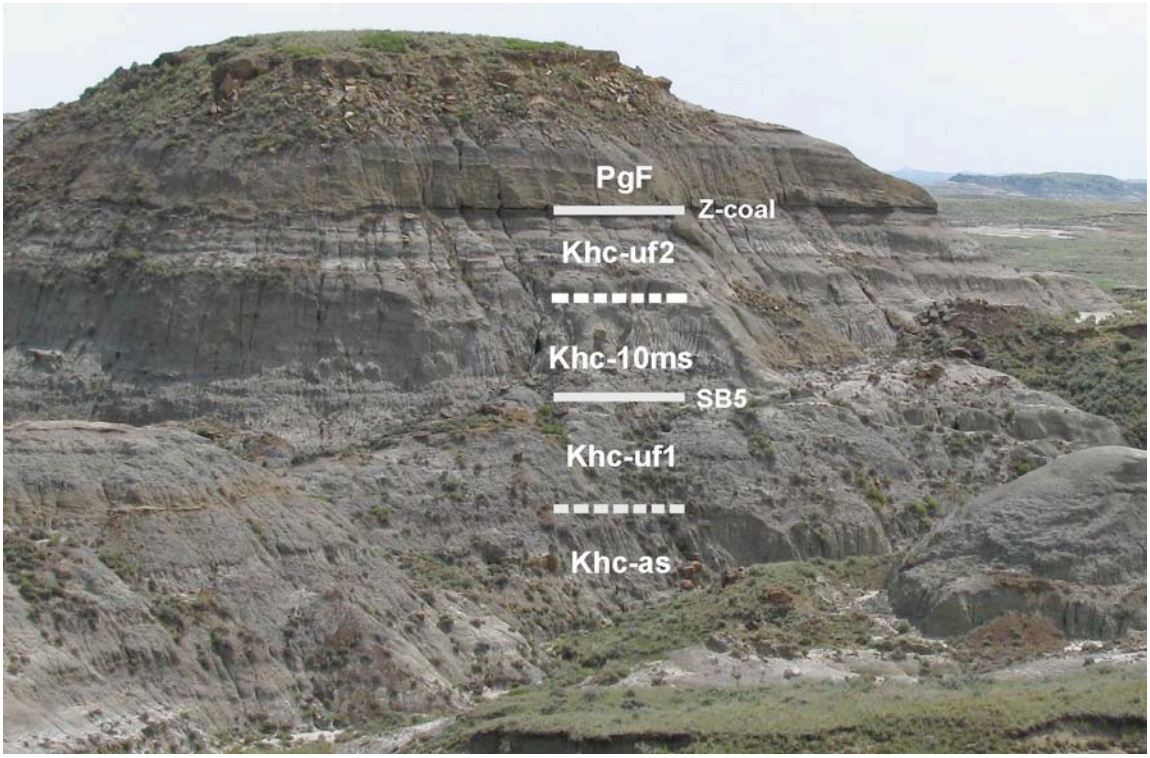

Figure 2.19. Exposure of the upper Hell Creek depositional sequence. The Apex Sand (Khc-as) can be seen at the base of the butte, with the 10 Meter Sand (Khc-10ms) forming a small cliff approximately half way up (above SB5). A bone lag is present at the base of Khc-10ms in parts of this area. Photo taken facing east at Lost Creek, near the Taylor Ranch, North of Jordan, Garfield Co. MT, 47°39'35" N, 106°19'59" W (NAD27CONUS).

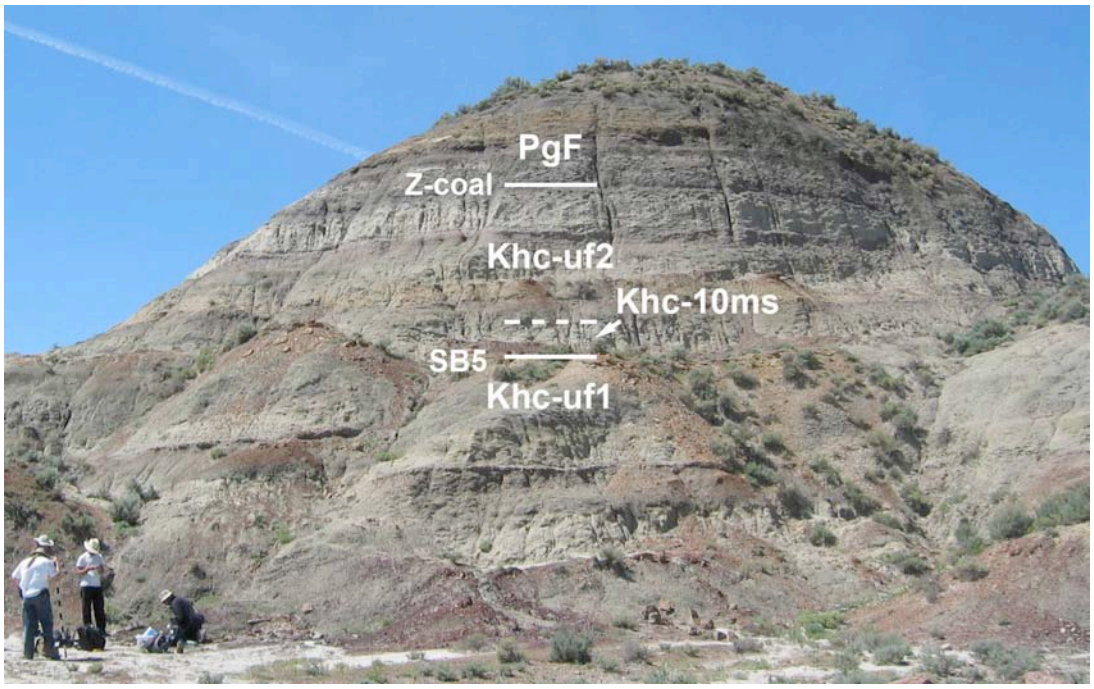

Figure 2.20. Upper 15 m of the Hell Creek Formation on western side of Short Creek. The 10 Meter Sand is only 2 m thick, compared to 10 m thick 1 km northeast (Figure 2.22). Photo corresponds to Figure 2.28, section 2. Photograph taken facing west at Short Creek, 47°35'35" N, 106°18'24" W (NAD27CONUS).

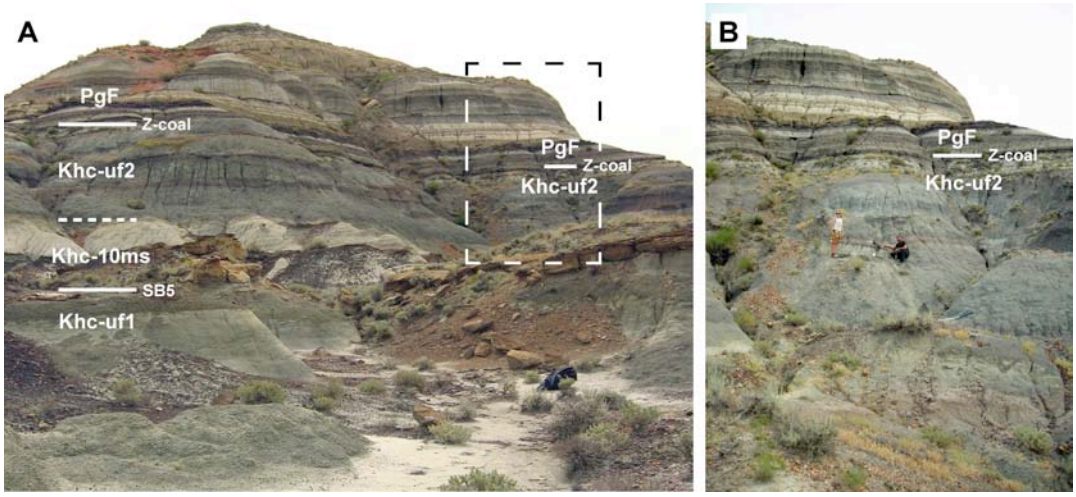

Figure 2.21. The 10 Meter Sand is variably ~3-4 m thick and laterally extensive in the Lone Tree Creek Area. Exposures in this area are continuous with those at Short Creek, allowing the10 Meter Sand to be traced over ~8 km. Photo taken facing southeast at Lone Tree Creek, near Jordan MT, 47°36'05" N, 106°21'22" W (NAD27CONUS).

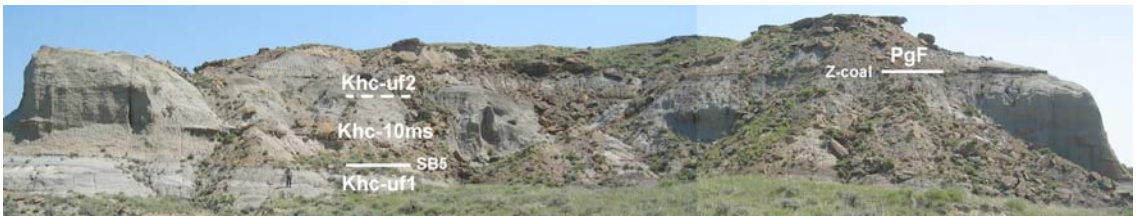

Figure 2.22. Upper 13 m of the Hell Creek Formation on eastern side of Short Creek. The 10 Meter Sand is up to 10 m thick, but thins to <1 m in western Short Creek (Figure 2.28 section 2; Figure 2.20). Photo corresponds to Figure 2.28, section 3. Photograph taken facing east at Short Creek, 47°35'46" N, 106°18'04" W (NAD27CONUS). Scale = 1.5 m.

Figure 2.23. Outcrop of the 10 Meter Sand that forms short steep cliffs. Here the 10 m Sand had a number of dinosaur bones preserved in its basal lag. Photo taken facing northeast at "Albie's site", Lone Tree Creek, near Taylor Ranch, north of Jordan, Garfield Co. MT, 47°38'03" N, 106°22'49" W (NAD27CONUS).

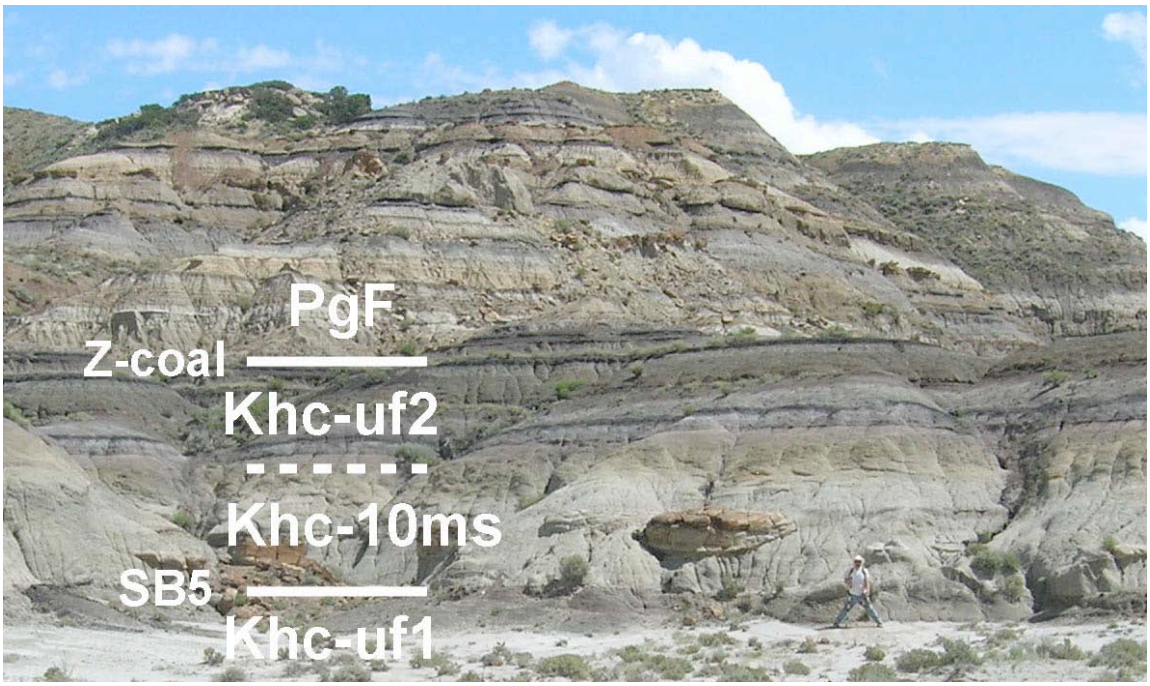

Figure 2.24. At Russell Basin, only the upper 20 m of the Hell Creek formation is exposed. Here the 10 Meter Sand is 4 m thick and is overlain by 4-5 m of the Hell Creek Upper Fines part 2, followed by the Z-coal. Photo taken facing east at Russell Basin, near Bug Creek, McCone Co., 47°40’38” N, 106°11’13” W, (NAD27CONUS). Scalebar = 1.5 m.

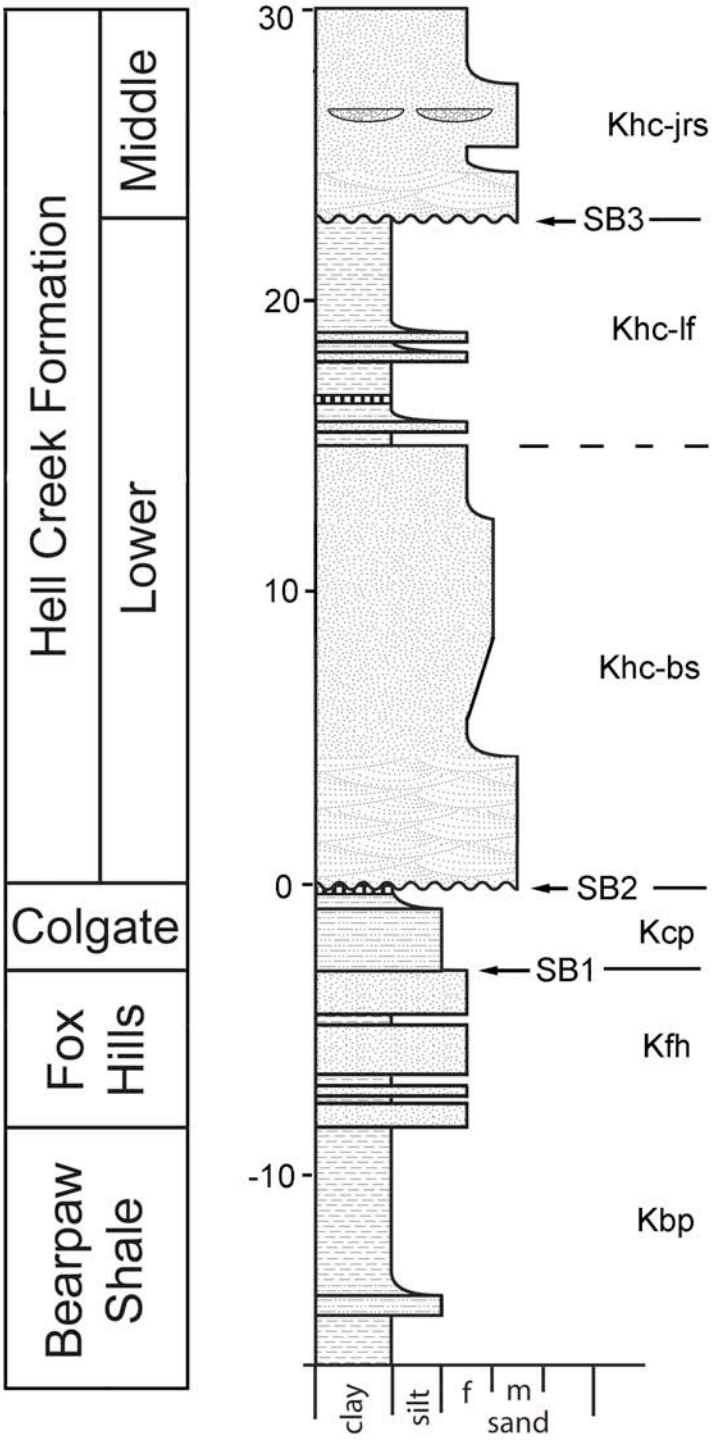

Figure 2.25. Measured section taken in Cole Creek, exposing the uppermost 10 m of the Bearpaw Shale through lowermost 30 m of the Hell Creek Formation. Section taken at 47°38'26" N, 106°55'25" W, NAD27CONUS. Vertically striped horizons indicate organic-rich shale / mudstone.

Figure 2.26. Exposure of the lower contacts of the Hell Creek Formation and underlying units exposed at "Best Butte". The left side of this exposure clearly shows the conspicuous bleached white weathering surface of the Colgate Sandstone (Kfhc). The Colgate Sandstone is overlain by the purple mudstone of the Colgate tidal flats (Kcp), then the Basal Sand of the Hel Creek Formation (Khc-bs), which exhibits inclined Heterolithic Strata in the upper 2-5 m. This exposure is important as it confirms the identity of the Colgate Sandstone in this area (which was interpreted as the Basal Sandstone of the Hell Creek by Hartman et al., 2014). This butte also shows no exposure of the possible Battle Formation, present between Kcp and Khc-bs at other localities 3-5 miles southwest of this outcrop (Figures 2.5, 2.27). Here the Battle Formation was either never deposited, or has been eroded away by the overlying erosive sour of the Hell Creek Basal Sand. Photo taken facing north at “Best Butte”, Hell Creek marina road, north of Jordan, Garfield Co. MT, 47°35’36” N, 106°54’50” W (NAD27CONUS).

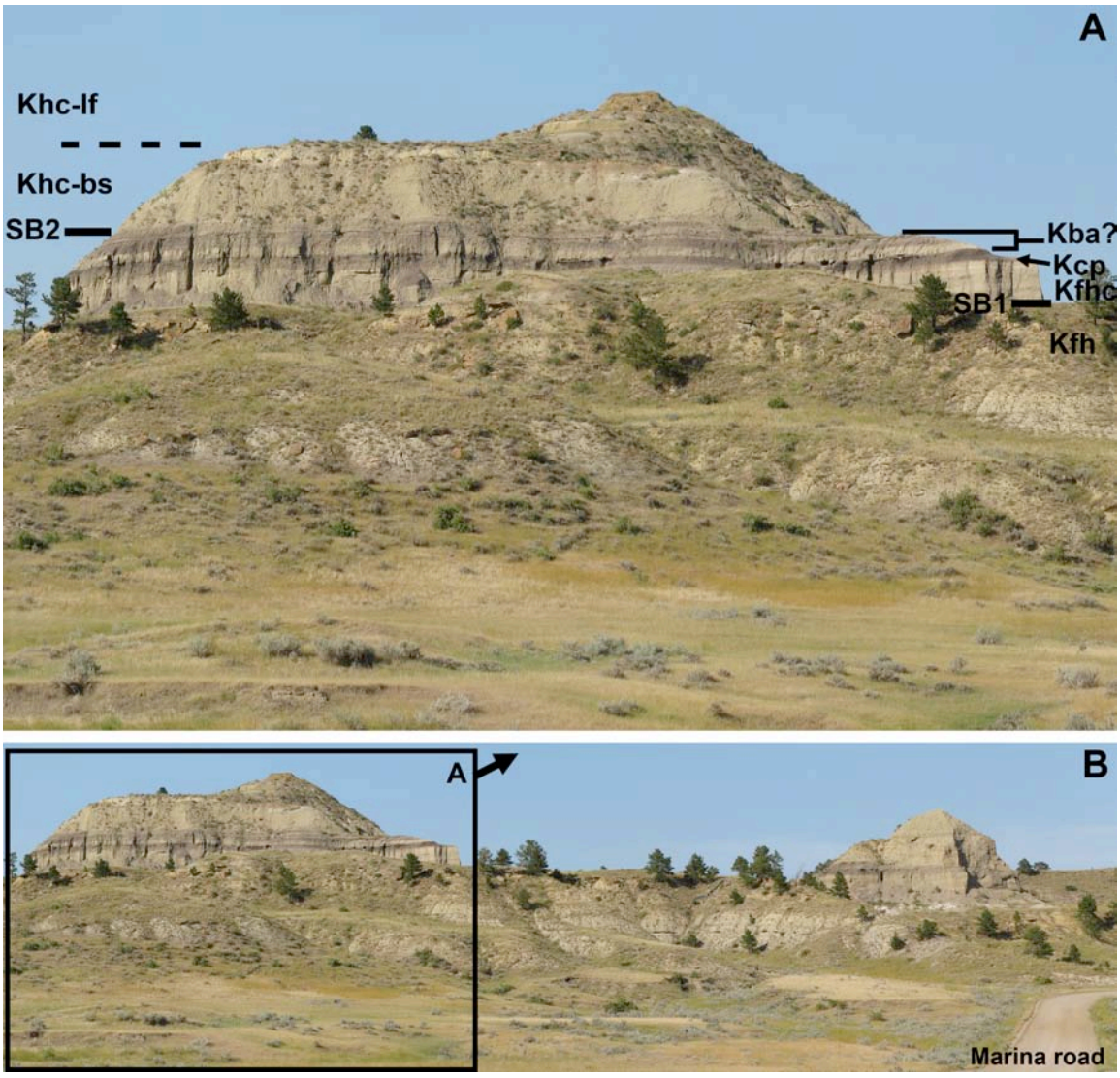

Figure 2.27. (A) Exposure of the lower contacts of the Hell Creek Formation and underlying units exposed at "Battle Butte" which records a stratigraphic succession intermediate between Manaige Spring (~1 km SSW; Figure 2.5) and Best Butte (~3 km NE; Figure 2.26). The Battle Formation (Kba) exposed at Battle butte is thinner (~3 m) than that observed at Manaige Spring (~ 10 m). (B) The left side of the main butte (A) exposes ~3 m of Kba, but on the smaller butte on the right side of (B), Kba is mostly eroded away by incision from the erosional scour at the base of Khc-bs. Hence this locality records the removal of the possible Battle Formation facies, to leave the direct contact of the Hell Creek Formation Basal Sand upon the Colgate Sandstone (and / or tidal flats) that is observed to the north (e.g. Best Butte; see above) Photo taken facing north at “Battle Butte”, Hell Creek marina road, north of Jordan, Garfield Co. MT, 47°34’43” N, 106°56’39” W; (NAD27CONUS).

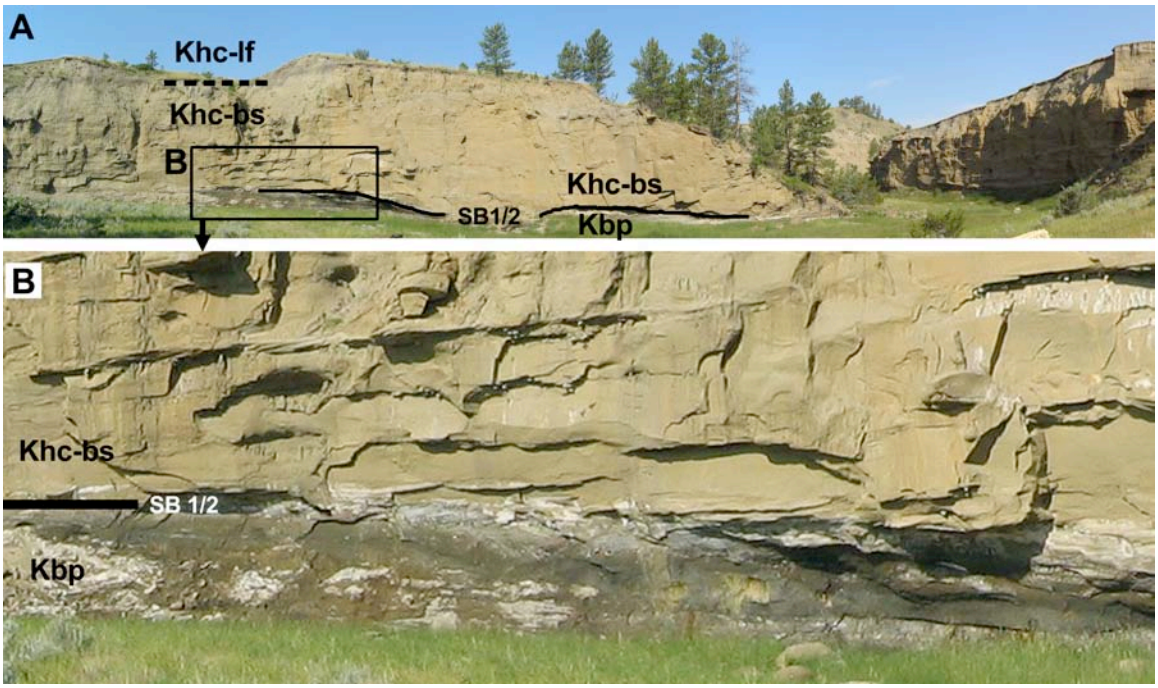

Figure 2.28. Basal contacts of the Hell Creek Formation at the new type section, East Ried Coulee. This locality is important as it exposes the grey silty sandstone transitional beds between the Bearpaw Shale (Kbp) and Fox Hills Formation. The tan-orange sandstone erosively overlying Kbp was identified as the Fox Hills Formation by Hartman et al. (2014), but is here identified as an unusally deeply incising Hell Creek Basal Sand (Khc-bs), measuring up to ~20 m thick, and capped by an organic mudstone of the Hell Creek lower fines (Khc-lf). Photo taken facing west at East Ried Coulee, near Hell Creek marina road, north of Jordan, Garfield Co. MT, 47°33’34” N, 106°52’52” W, (NAD27CONUS).

Figure 2.29. Possible Inclined Heterolithic Strata exposed as part of large channels in the Hell Creek Formation Basal Sand at East Ried Coulee (the new type section; Hartman et al., 2014). Photo taken facing north at East Ried Coulee, near Hell Creek marina road, north of Jordan, Garfield Co. MT, 47°33’42” N, 106°52’54” W, (NAD27CONUS).

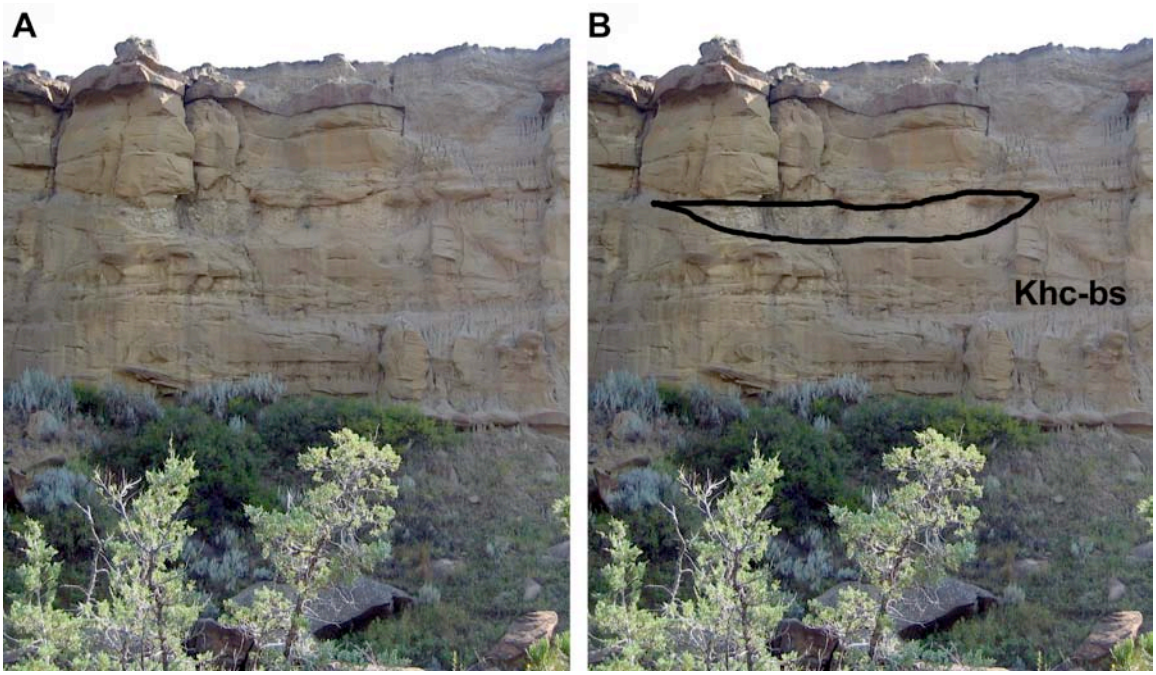

Figure 2.30. Channel scour filled with conglomerate (A; highlighted in B) exposed in the Hell Creek Basal Sand (Khc-bs) at East Ried Coulee (the new type section; Hartman et al., 2014). Presence of large channels within the tan-orange sandstone makes an identification of this unit as the Fox Hills Formation unlikely, and here it is referred to Khc-bs. Photo taken facing northeast at East Ried Coulee, near Hell Creek marina road, north of Jordan, Garfield Co. MT, 47°33’42” N, 106°52’54” W, (NAD27CONUS).

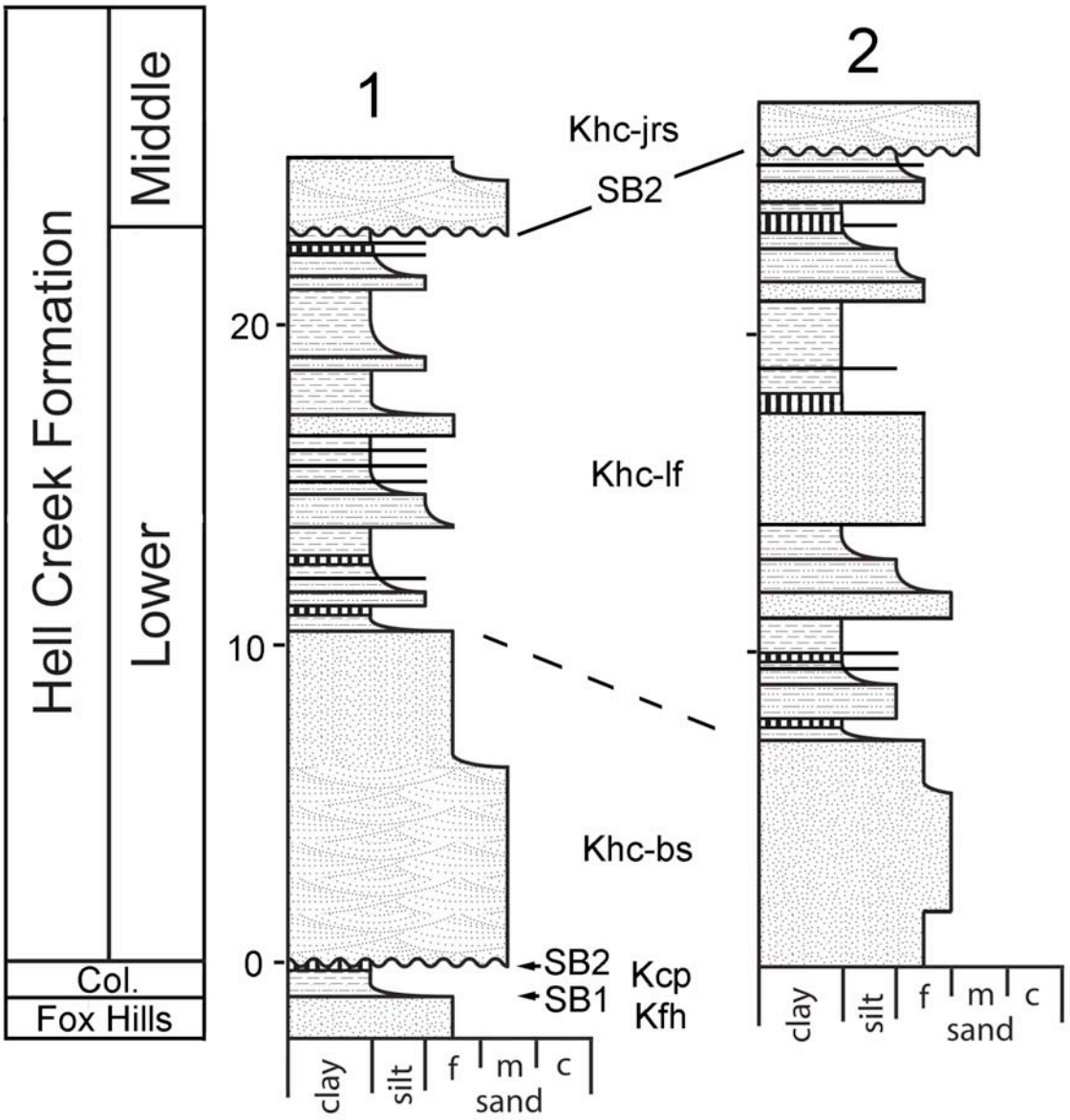

Figure 2.31. Measured sections taken at Sand Creek, near Sheep Mountain, 55 km SE of Ekalaka, Carter Co. MT. (1) Campsite section, south Sand Creek (Figure 2.10); 45°30’8” N, 104°8’0” W. (2) Northwest Sand Creek, 45°30’12” N, 104°8’43” W. All coordinates NAD27CONUS. Vertically striped horizons indicate organic-rich shale / mudstone.

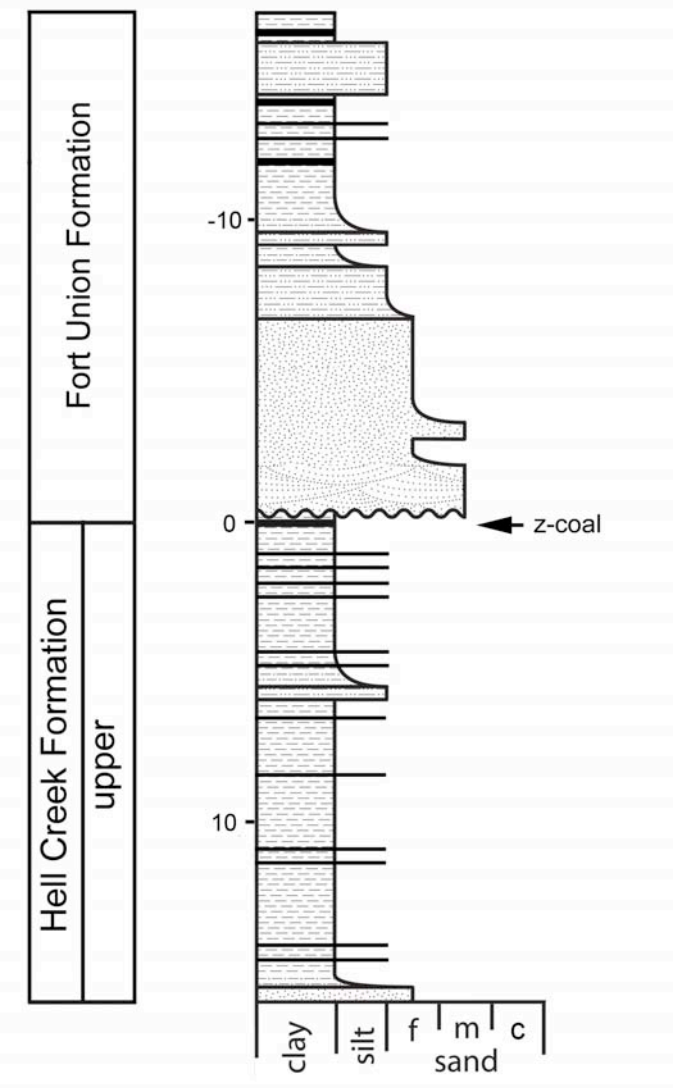

Figure 2.32. Measured section taken at Brownie Butte, exposing the uppermost 17 m of the Hell Creek Formation. Section taken at 47°31’58” N 107°1’17” W, NAD27CONUS.

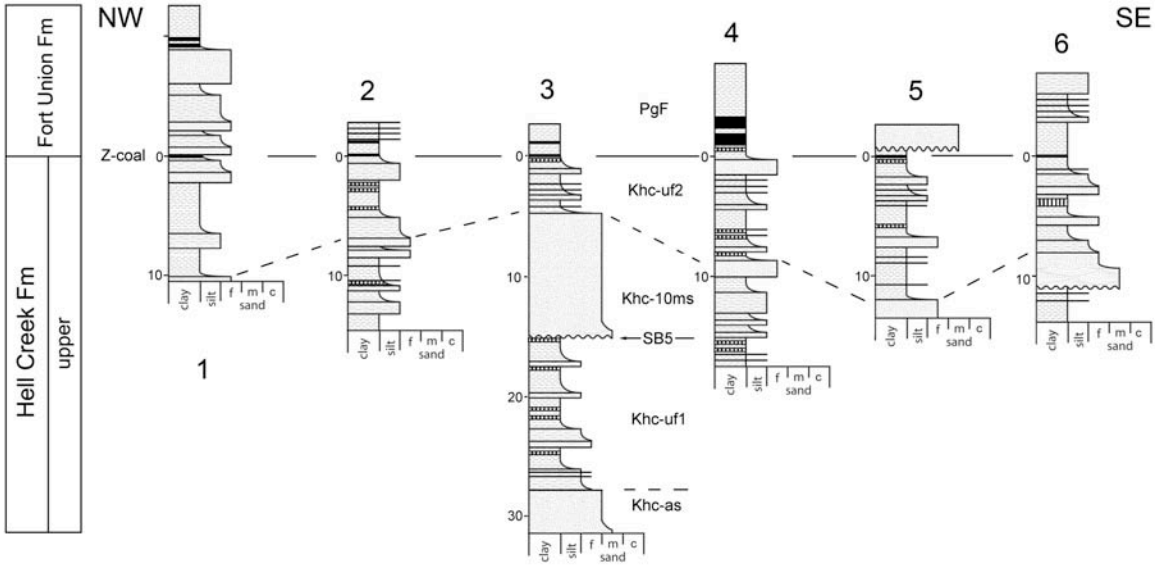

Figure 2.33. Measured sections taken in Short Creek, exposing the uppermost 31 m of the Hell Creek Formation. (1) North Short Creek, near Joe's Trike and Lauren's Trike localities; 47°36'20" N, 106°18'47" W. (2) West Short Creek, near Ashes Trike locality, (Figure 2.20); 47°35'35" N, 106°18'24" W. (3) Mid East Short Creek (Figure 2.22); 47°35'46" N, 106°18'04" W. (4) South Short Creek, near Snap Creek Camp; 47°35'00" N, 106°17'49" W. (5) East Short Creek, near to Situ but Sad Trike locality; 47°34'51" N, 106°16'50" W. (6) East Short Creek, close to Ft. Peck Lake, near to Tom's Old Duck locality; 47°34'58" N, 106°15'43" W. Fossil localities noted in Scannella and Fowler (2014). All coordinates NAD27CONUS. Vertically striped horizons indicate organic-rich shale / mudstone.

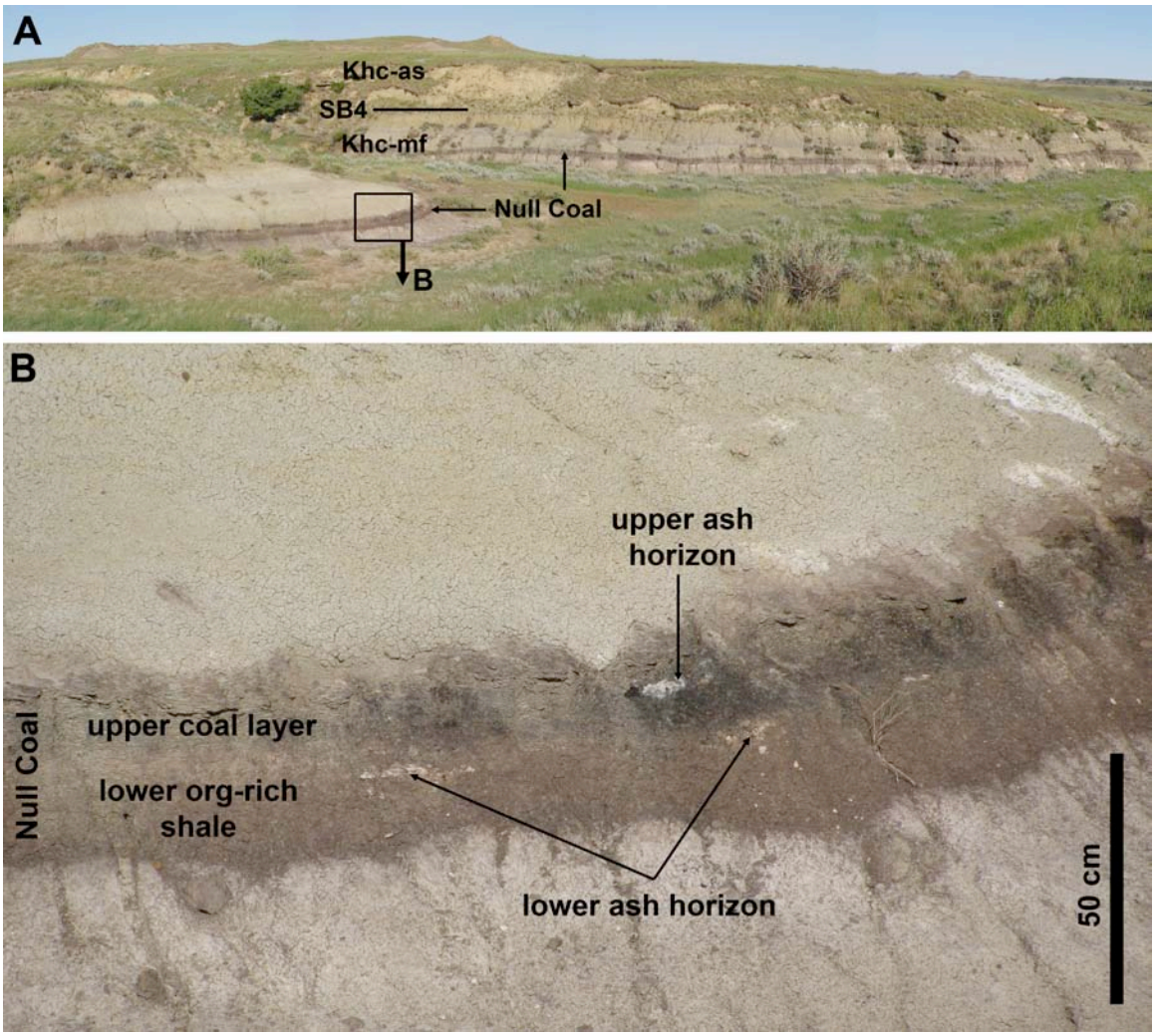

Figure 2.34. Exposure of the Null Coal at Lone Tree Creek. Both upper and lower ashes are visible within the Null Coal at this locality. Here the Null Coal comprises an upper true coal and a lower organic-rich shale, both of which contain ash horizons. This is unlike further east at Bug Creek (McCone County), where the entire Null Coal is true coal. This locality is one of the most extensive easily-acessible exposures known of the Null Coal in Garfield County and contains abundant ash horizons for radiometric sampling. Photo taken facing east at Lone Tree Creek, near the old Taylor Ranch, northeast of Jordan, Garfield Co. MT, 47°37'33" N, 106°21'9" W (NAD27CONUS).

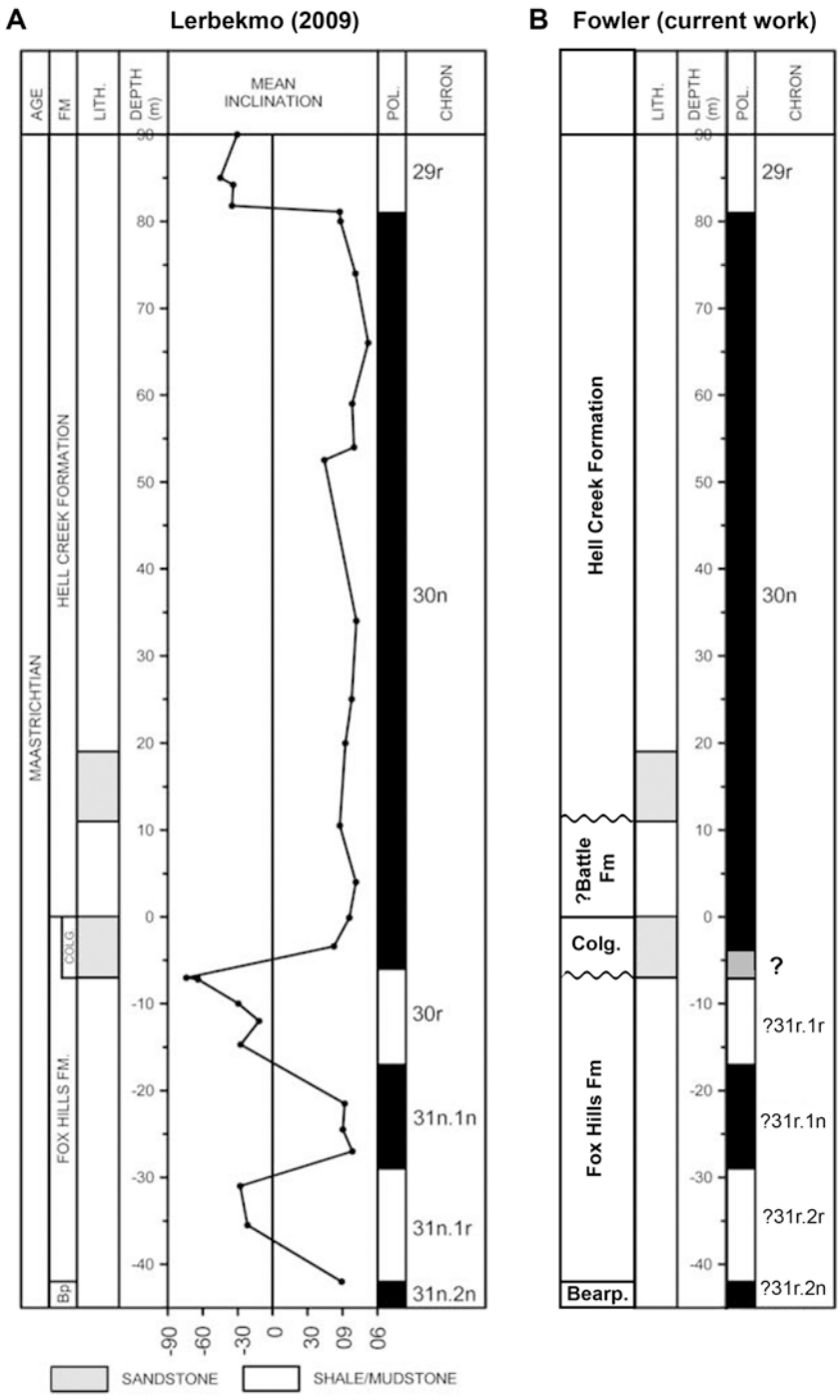

Figure 2.35. Suggested revision of Hell Creek Formation magnetostratigraphy of the Manaige Spring locality. Ammonite biostratigraphy of the Fox Hills and Bearpaw Formations of Eastern Montana suggests that the original identity of C30r and C31n by Lerbekmo (2009, A), should be revised to the older C31r (B). See main text for discussion. Adapted from Lerbekmo (2009).

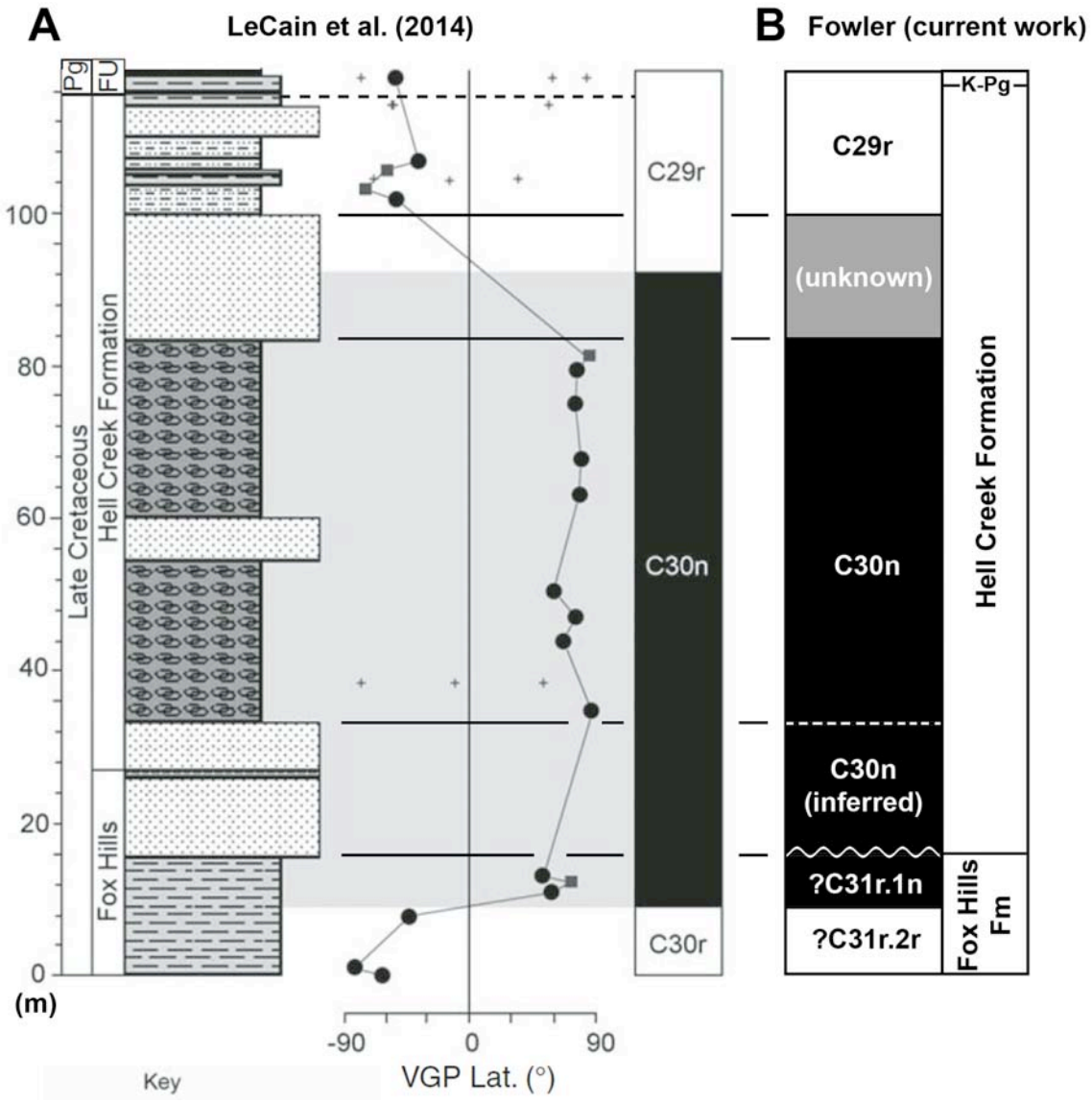

Figure 2.36. Suggested magnetostratigraphic revision of the new type section of the Hell Creek Formation. The original interpretation by LeCain et al. (2014, A) shows a normal polarity zone within the silty facies of the Fox Hills Formation interpreted as continuation of C30n. This is revised in (B) to illustrate the reinterpretation of the thick channelized sand unit as the Basal Sand of the Hell Creek Formation, and revisions to the interpretations of Lerbekmo (2009; see Figure 2.35). Regardless of the reinterpretation offered here, the normal polarity zone present within the silty facies of the Fox Hills Formation should not be interpreted as a continuation of C30n. Adapted from LeCain et al. (2014).

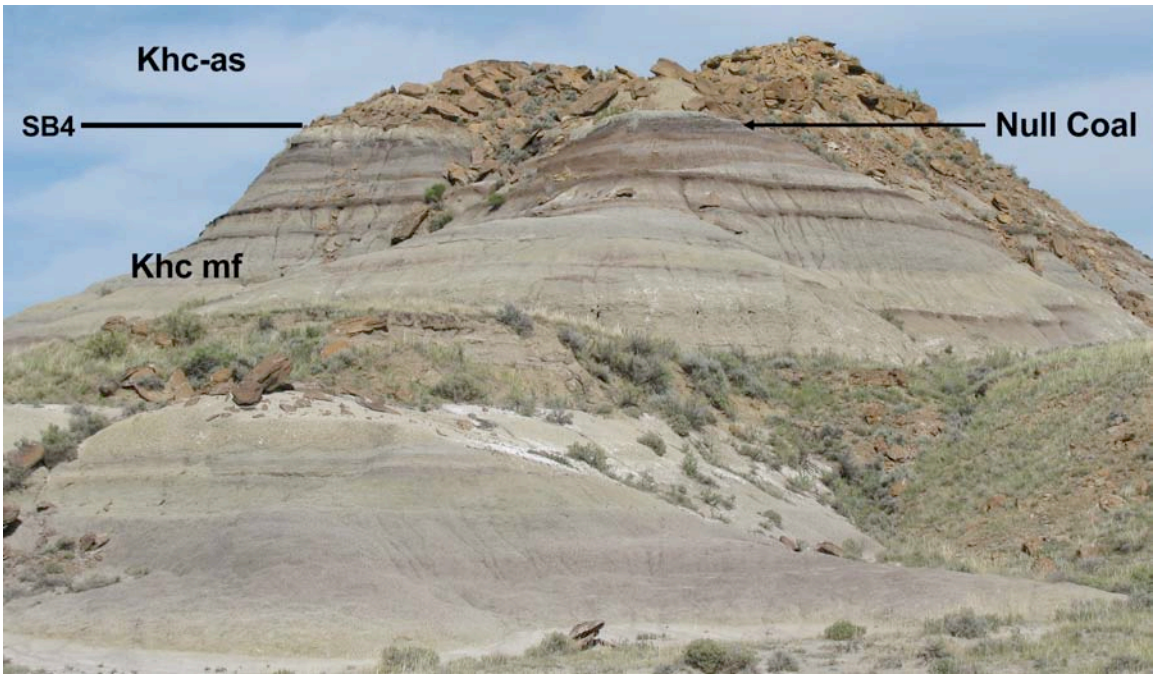

Figure 2.37. Exposure of the Null Coal at Lost Creek. Here the Null Coal comprises an upper true coal and a lower organic-rich shale. Prominent ash horizons are present. Photo taken facing east at Lost Creek, near the old Taylor Ranch, northeast of Jordan, Garfield Co. MT, 47°40'28" N, 106°20'10" W (NAD27CONUS).

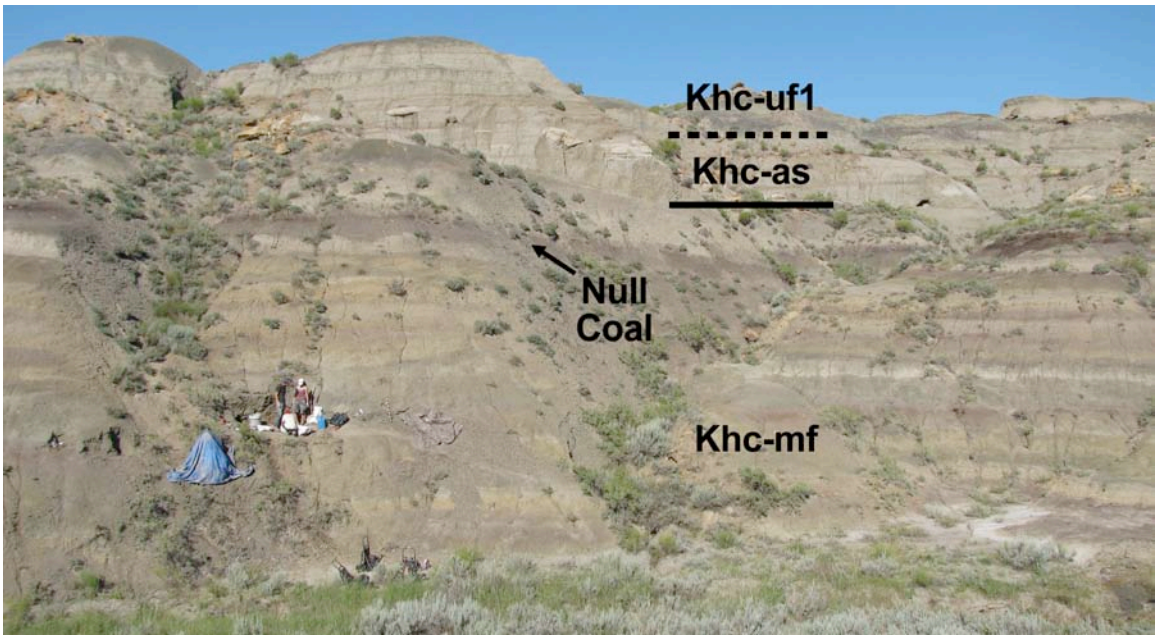

Figure 2.38. Exposure of the Null Coal at East Gilbert Creek. Here the Null Coal comprises an upper true coal and a lower organic-rich shale, although in this area the true coal facies is extremely patchy. Ash horizons are present, but very thin and not as easily sapled as other localities. At this locality there are ~ 5 m of mudstone above the Null Coal before the occurrence of the Apex Sand (Khc-as) of the upper Hell Creek Formation. Photo taken facing east at southern edge of East Gilbert Creek, near the old Isaacs' Ranch, Haxby Road, northeast of Jordan, Garfield Co. MT, 47°40'48" N, 106°30'16"W (NAD27CONUS).

References Cited

Aitken, J. F., and S. S. Flint. 1994. High-frequency sequences and the nature of incised-valley fills in fluvial systems of the Breathitt Group (Pennsylvanian), Appalachian foreland basin, eastern Kentucky. 353–368.

Antia, J., and C. R. Fielding. 2011. Sequence stratigraphy of a condensed low-accommodation succession: Lower Upper Cretaceous Dakota Sandstone, Henry Mountains, southeastern Utah. AAPG Bulletin 95:413–447.

Archibald, J. D. 1982. A study of Mammalia and geology across the Cretaceous-Tertiary boundary in Garfield County, Montana. University of California Publications in the Geological Sciences 122:1–286.

Archibald, J. D. 2011. Extinction and Radiation: How the Fall of Dinosaurs Led to the Rise of Mammals, 1st ed. The Johns Hopkins University Press, 120 pp.

Archibald, J. D., R. F. Butler, E. H. Lindsay, W. A. Clemens, and L. Dingus. 1982. Upper Cretaceous–Paleocene biostratigraphy and magnetostratigraphy, Hell Creek and Tullock Formations, northeastern Montana. Geology 10:153–159.

Arens, N. C., and A. H. Jahren. 2002. Chemostratigraphic correlation of four fossil-bearing sections in southwestern North Dakota. Geological Society of America Special Papers 361:75–93.

Arens, N. C., A. H. Jahren, and D. C. Kendrick. 2014. Carbon isotope stratigraphy and correlation of plant megafossil localities in the Hell Creek Formation of eastern Montana, USA. Geological Society of America Special Papers 503:149–171.

Atchley, S. C., L. C. Nordt, and S. I. Dworkin. 2004. Eustatic Control on Alluvial Sequence Stratigraphy: A Possible Example from the Cretaceous-Tertiary Transition of the Tornillo Basin, Big Bend National Park, West Texas, U.S.A. Journal of Sedimentary Research 74:391–404.

Barrell, J. 1917. Rhythms and the measurements of geologic time. Bulletin of the Geological Society of America 28:745–904.

Behringer, D. H. 2008. Geometry, genesis and sequence stratigraphic framework of the Colgate Sandstone Member of the Fox Hills, Garfield County, MT. M.S., Montana State University, Bozeman, Montana, 134 pp.

Belt, E. S., J. F. Hicks, and D. A. Murphy. 1997. A pre-Lancian regional unconformity and its relationship to Hell Creek paleogeography in south-eastern Montana. Rocky Mountain Geology 31:1–26.

Bercovici, A., V. Vajda, D. Pearson, U. Villanueva-Amadoz, and D. Kline. 2012. Palynostratigraphy of John's Nose, a new Cretaceous–Paleogene boundary section in southwestern North Dakota, USA. Palynology 36:36–47.

Bertog, J. 2011. Stratigraphy of the Lower Pierre Shale (Campanian): Implications for the Tectonic and Eustatic Controls on Facies Distributions. Journal of Geological Research 2010.

Binda, P. L., E. V. Nambudiri, S. K. Srivastava, M. Schmitz, A. Longinelli, and P. Iacumin. 1991. Stratigraphy, paleontology, and aspects of diagenesis of the Whitemud Formation (Maastrichtian) of Alberta and Saskatchewan. AAPG Sixth International Williston Basic Symposium October 7, 8, and 9, 1991:179-192.

Bird, P. 1988. Formation of the Rocky Mountains, Western United States: A Continuum Computer Model. Science 239:1501–1507.

Bown, T. M., and M. J. Kraus. 1987. Integration of channel and floodplain suites; I, Developmental sequence and lateral relations of alluvial Paleosols. Journal of Sedimentary Research 57:587–601.

Boyd, D. W., and J. A. Lillegraven. 2011. Persistence of the Western Interior Seaway Historical background and significance of ichnogenus Rhizocorallium in Paleocene strata, south-central Wyoming. Rocky Mountain Geology 46:43–69.

Braman, D. R., and A. R. Sweet. 1999. Terrestrial palynomorph biostratigraphy of the Cypress Hills, Wood Mountain, and Turtle Mountain areas (Upper Cretaceous-Paleocene) of western Canada. Canadian Journal of Earth Sciences 36:725–741.

Braman, D. R., and A. R. Sweet. 2012. Biostratigraphically useful Late Cretaceous–Paleocene terrestrial palynomorphs from the Canadian Western Interior sedimentary basin. Palynology 36:8–35.

Brown, B. 1907. The Hell Creek beds of the Upper Cretaceous of Montana: their relation to contiguous deposits, with faunal and floral lists, and a discussion of their correlation. Bulletin of the American Museum of Natural History 823–845.

Brown, R. W. 1948. The Cretaceous-Eocene boundary in Montana and North Dakota. Washington Academy of Sciences Proceedings 28:421–422.

Brown, R. W. 1962. Paleocene Flora of the Rocky Mountains and Great Plains. United State Geological Survey Professional Paper 375. 119 pp.

Buatois, L. A., and M. G. Mángano. 2004. Animal-substrate interactions in freshwater environments: applications of ichnology in facies and sequence stratigraphic analysis of fluvio-lacustrine successions. Geological Society, London, Special Publications 228:311–333.

Burgess, P. M. 2008. Phanerozoic evolution of the sedimentary cover of the North American craton. Sedimentary Basins of the World 5:31–63.

Butler, R. D. 1980. Stratigraphy, sedimentology, and depositional environments of the Hell Creek Formation (Late Cretaceous) and adjacent strata, Glendive area, Montana. Ph.D, University of North Dakota, Grand Forks, North Dakota, 398 pp.

Calvert, W. R., C. F. Bowen, F. A. Herald, J. H. Hance, E. Stebinger, and A. L. Beekly. 1912. Geology of Certain Lignite Fields in Eastern Montana. United States Geological Survey Bulletin 471-D:187-358.

Catuneanu, O. 2006. Principles of Sequence Stratigraphy. Elsevier Science, Amsterdam, 375 pp.

Catuneanu, O., and A. R. Sweet. 1999. Maastrichtian-Paleocene foreland-basin stratigraphies, western Canada: a reciprocal sequence architecture. Canadian Journal of Earth Sciences 36:685–703.

Catuneanu, O., M. A. Khalifa, and H. A. Wanas. 2006. Sequence stratigraphy of the Lower Cenomanian Bahariya Formation, Bahariya Oasis, Western Desert, Egypt. Sedimentary Geology 190:121–137.

Catuneanu, O., V. Abreu, J. P. Bhattacharya, M. D. Blum, R. W. Dalrymple, P. G. Eriksson, C. R. Fielding, W. L. Fisher, W. E. Galloway, M. R. Gibling, K. A. Giles, J. M. Holbrook, R. Jordan, C. G. S. C. Kendall, B. Macurda, O. J. Martinsen, A. D. Miall, J. E. Neal, D. Nummedal, L. Pomar, H. W. Posamentier, B. R. Pratt, J. F. Sarg, K. W. Shanley, R. J. Steel, A. Strasser, M. E. Tucker, and C. Winker. 2009. Towards the standardization of sequence stratigraphy. Earth-Science Reviews 92:1–33.

Chen, D., C. W. Langenberg, and A. P. Beaton. 2005. Horseshoe Canyon-Bearpaw Transition and Correlation of Associated Coal Zones across the Alberta Plains. Alberta Energy and Utilities Board: Alberta Geological Survey, Edmonton, Alberta, 22 pp.

Cifelli, R. L., J. J. Eberle, D. L. Lofgren, J. A. Lillegraven, and W. A. Clemens. 2004. Mammalian biochronology of the latest Cretaceous; pp. 21–42 in M. O. Woodburne (ed.), Late Cretaceous and Cenozoic Mammals of North America. Columbia University Press, New York.

Clemens, W. A. 1963. Fossil mammals of the type Lance Formation Wyoming Part I: Introduction and Multituberculata. University of California Publications in the Geological Sciences 48:1–105.

Clemens, W. A., and J. D. Archibald. 1980. Evolution of terrestrial faunas during the Cretaceous-Tertiary transition. Société Géologique de France, Mémoires 139:67–74.

Cleveland, D. M., S. C. Atchley, and L. C. Nordt. 2007. Continental Sequence Stratigraphy of the Upper Triassic (Norian–Rhaetian) Chinle Strata, Northern New Mexico, U.S.A.: Allocyclic and Autocyclic Origins of Paleosol-Bearing Alluvial Successions. Journal of Sedimentary Research 77:909–924.

Cobban, W. A., and J. B. Reeside. 1952. Correlation of the Cretaceous formations of the Western Interior of the United States. Geological Society of America Bulletin 63:1011–1044.

Cobban, W. A., E. A. Merewether, T. D. Fouch, and J. D. Obradovich. 1994. Some Cretaceous shorelines in the western interior of the United States. In Caputo, M. V., Peterson, J. A., and Frenczyk, K. J., eds., Mesozoic Systems of the Rocky Mountain Region, USA: Rocky Mountain Section, Society of Economic Paleontologists and Mineralogists, Society for Sedimentary Geology:393-414.

Collier, A. J., and M. M. Knechtel. 1939. Coal resources of McCone County, Montana. U.S. Geological Survey Bulletin 905:1–80.

Coney, P. J., and S. J. Reynolds. 1977. Cordilleran Benioff zones. Nature 270:403–406.

Connor, C. W. 1992. The Lance Formation; Petrography and Stratigraphy, Powder River Basin and Nearby Basins, Wyoming and Montana. United States Geological Survey Bulletin 1917-I:17 pp.

Cross, W. 1909. The Laramie Formation and the Shoshone Group. Washington Academy of Sciences, Proceedings 11:27–45.

DeCelles, P. G. 2004. Late Jurassic to Eocene evolution of the Cordilleran thrust belt and foreland basin system, western U.S.A. American Journal of Science 304:105–168.

DeCelles, P. G., and K. A. Giles. 1996. Foreland basin systems. Basin Research 8:105–123.

Denson, N. M. 1950. The Lignite Deposits of the Cheyenne River and Standing Rock Indian Reservations, Corson, Dewey, and Ziebach Counties, South Dakota and Sioux County, North Dakota. U.S. Geological Survey Circular 78:1–22.

Dickinson, W. R., and W. S. Snyder. 1978. Plate tectonics of the Laramide orogeny. Geological Society of America Memoir 151:355–366.

Dickinson, W. R., M. A. Klute, M. J. Hayes, S. U. Janecke, E. R. Lundin, M. A. McKittrick, and M. D. Olivares. 1988. Paleogeographic and paleotectonic setting of Laramide sedimentary basins in the central Rocky Mountain region. Geological Society of America Bulletin 100:1023–1039.

Eberth, D. A. 1990. Stratigraphy and sedimentology of vertebrate microfossil sites in the uppermost Judith River Formation (Campanian), Dinosaur Provincial Park, Alberta, Canada. Palaeogeography, Palaeoclimatology, Palaeoecology 78:1–36.

Eberth, D. A. 1996. Origin and significance of mud-filled incised valleys (Upper Cretaceous) in southern Alberta, Canada. Sedimentology 43:459–477.

Eberth, D. A. 2010. A revised regional stratigraphy and stratigraphic architecture for the Horseshoe Canyon Formation: outcrop and subsurface. Field Trip 14, May 17–18, 2010.

Eberth, D. A., and A. P. Hamblin. 1993. Tectonic, stratigraphic, and sedimentologic significance of a regional discontinuity in the upper Judith River Group (Belly River wedge) of southern Alberta, Saskatchewan, and northern Montana. Canadian Journal of Earth Sciences 30:174–200.

Eberth, D. A., and D. R. Braman. 2012. A revised stratigraphy and depositional history for the Horseshoe Canyon Formation (Upper Cretaceous), southern Alberta plains. Canadian Journal of Earth Sciences 49:1053–1086.

Eberth, D. A., D. Brinkman, and S. M. Kwasniowski. 1994. Sequence Stratigraphy, Depositional Environments and Paleoecology of the Judith River Group (Upper Cretaceous), Southern Alberta. Society of Petroleum Geologists Field guide PR-3, Calgary, Alberta, 69 pp.

Eberth, D. A., D. B. Brinkman, P.-J. Chen, F.-T. Yuan, S.-Z. Wu, G. Li, and X.-S. Cheng. 2001. Sequence stratigraphy, paleoclimate patterns, and vertebrate fossil preservation in Jurassic–Cretaceous strata of the Junggar Basin, Xinjiang

Autonomous Region, People's Republic of China. Canadian Journal of Earth Sciences 38:1627–1644.

English, J. M., and S. T. Johnston. 2004. The Laramide Orogeny: What Were the Driving Forces? International Geology Review 46:833–838.

Evans, D. C., C. A. Forster, and R. R. Reisz. 2005. The type specimen of Tetragonosaurus erectofrons (Ornithischia: Hadrosauridae) and the identification of juvenile Lambeosaurines; pp. 349–366 in P. J. Currie and E. B. Koppelhus (eds.), Dinosaur Provincial Park: A Spectacular Ancient Ecosystem Revealed. Indianapolis, Indiana University Press, Bloomington, Indianapolis.

Fanti, F., and O. Catuneanu. 2010. Fluvial Sequence Stratigraphy: The Wapiti Formation, West-Central Alberta, Canada. Journal of Sedimentary Research 80:320–338.

Fastovsky, D. E. 1987. Paleoenvironments of Vertebrate-Bearing Strata during the Cretaceous-Paleogene Transition, Eastern Montana and Western North Dakota. PALAIOS 2:282.

Fastovsky, D. E., and K. McSweeney. 1987. Paleosols spanning the Cretaceous-Paleogene transition, eastern Montana and western North Dakota. Geological Society of America Bulletin 99:66–77.

Fastovsky, D. E., and P. M. Sheehan. 2005. The Extinction of the Dinosaurs in North America. GSA Today 15(3):4-10.

Fastovsky, D. E., and A. Bercovici. 2015. The Hell Creek Formation and its contribution to the Cretaceous–Paleogene extinction: A short primer. Cretaceous Research 57:368-390.

Flight, J. N. 2004. Sequence stratigraphic analysis of the Fox Hills and Hell Creek Fms (Maastrichtian), Eastern Montana and its relationship to dinosaur paleontology. MS, Montana State University, Bozeman, Montana, 164 pp.

Fraser, F. J., F. H. McLearn, L. S. Russell, P. S. Warren, and R. T. D. Wickenden. 1935. Geology of Southern Saskatchewan. Geological Survey of Canada Memoir 176:137 pp.

Frye, C. I. 1967. The Hell Creek Formation in North Dakota. Ph.D, University of North Dakota, Grand Forks, North Dakota, 411 pp.

Frye, C. I. 1969. Stratigraphy of the Hell Creek Formation in North Dakota. North Dakota Geological Survey Bulletin 54:1–65.

Gibling, M. R., C. R. Fielding, and R. Sinha. 2011. Alluvial valleys and alluvial sequences: towards a geomorphic assessment. From River to Rock Record: The Preservation of Fluvial Sediments and Their Subsequent Interpretation. SK Davidson, S. Leleu, and CP North (eds.). Society for Sedimentary Geology, Special Publication 97:423–447.

Gillespie, J. M., and J. E. Fox. 1991. Tectonically Influenced Sedimentation in the Lance Formation, Eastern Wind River Basin, Wyoming. The Mountain Geologist 28:53–66.

Gilmore, C. W. 1946. A new carnivorous dinosaur from the Lance Formation of Montana. Smithsonian Miscellaneous Collections 106:1–19.

Hajek, E. A., P. L. Heller, and B. A. Sheets. 2010. Significance of channel-belt clustering in alluvial basins. Geology 38:535–538.

Hajek, E. A., P. L. Heller, and E. L. Schur. 2012. Field test of autogenic control on alluvial stratigraphy (Ferris Formation, Upper Cretaceous–Paleogene, Wyoming). Geological Society of America Bulletin 124:1898–1912.

Hares, C. J. 1928. Geology and lignite resources of the Marmarth field, southwestern North Dakota. U.S. Geological Survey Bulletin 775:1–110.

Hartman, J. H., and J. I. Kirkland. 2002. Brackish and marine mollusks of the Hell Creek Formation of North Dakota: Evidence for a persisting Cretaceous seaway. Geological Society of America Special Papers 361:271–296.

Hartman, J. H., R. D. Butler, M. W. Weiler, and K. K. Schumaker. 2014. Context, naming, and formal designation of the Cretaceous Hell Creek Formation lectostratotype, Garfield County, Montana. Geological Society of America Special Papers 503:89–121.

Hatcher, J. B. 1893. The Ceratops Beds of Converse County, Wyoming. American Journal of Science 45:135–144.

Hicks, J. F., K. R. Johnson, J. D. Obradovich, L. Tauxe, and D. Clark. 2002. Magnetostratigraphy and geochronology of the Hell Creek and basal Fort Union Formations of southwestern North Dakota and a recalibration of the age of the Cretaceous-Tertiary boundary. Geological Society of America Special Papers 361:35–55.

Hoganson, J. W., and E. C. Murphy. 2002. Marine Breien Member (Maastrichtian) of the Hell Creek Formation in North Dakota: Stratigraphy, vertebrate fossil record, and age. Geological Society of America Special Papers 361:247–269.

Holbrook, J. M. 1996. Complex fluvial response to low gradients at maximum regression; a genetic link between smooth sequence-boundary morphology and architecture of overlying sheet sandstone. Journal of Sedimentary Research 66:713–722.

Holbrook, J. M. 2010. Valleys that never were: time surfaces versus stratigraphic surfaces—discussion. Journal of Sedimentary Research 80:2–3.

Holbrook, J. M., and J. P. Bhattacharya. 2012. Reappraisal of the sequence boundary in time and space: Case and considerations for an SU (subaerial unconformity) that is not a sediment bypass surface, a time barrier, or an unconformity. Earth-Science Reviews 113:271–302.

Irion, G., J. Müller, J. O. Morais, G. Keim, J. N. de Mello, and W. J. Junk. 2009. The impact of Quaternary sea level changes on the evolution of the Amazonian lowland. Hydrological Processes 23:3168–3172.

Irish, E. J. W. 1970. The Edmonton Group of South-Central Alberta. Bulletin of Canadian Petroleum Geology 18:125–155.

Jensen, F. S., and H. D. Varnes. 1964. Geology of the Fort Peck Area, Garfield, McCone and Valley Counties, Montana. USGS Professional Paper 414-F, 49 pp.

Johnson, K. R. 1989. A high resolution megafloral biostratigraphy spanning the Cretaceous-Tertiary boundary in the Northern Great Plains. Ph.D, Yale University, New Haven, Connecticut, 581 pp.

Johnson, K. R. 2002. Megaflora of the Hell Creek and lower Fort Union Formations in the western Dakotas: Vegetational response to climate change, the Cretaceous-Tertiary boundary event, and rapid marine transgression. Geological Society of America Special Papers 361:329–391.

Johnson, K. R., and L. J. Hickey. 1990. Megafloral change across the Cretaceous/Tertiary boundary in the northern Great Plains and Rocky Mountains, U.S.A. Geological Society of America Special Papers 247:433–444.

Johnson, K. R., D. J. Nichols, and J. H. Hartman. 2002. Hell Creek Formation: A 2001 synthesis. Geological Society of America Special Papers 361:503–510.

Jordan, T. E. 1995. Retroarc Foreland and Related Basins; pp. 331–362 in C. J. Busby and R. V. Ingersoll (eds.), Tectonics of Sedimentary Basins. Blackwell, London.

Kamola, D. L., and J. C. Van Wagoner. 1995. Stratigraphy and Facies Architecture of Parasequences with Examples from the Spring Canyon Member, Blackhawk

Formation, Utah. American Association of Petroleum Geologists, Memoir 64:27–54.

Kennedy, W. J., N. H. Landman, W. K. Christensen, W. A. Cobban, and J. M. Hancock. 1998. Marine connections in North America during the late Maastrichtian: palaeogeographic and palaeobiogeographic significance ofJeletzkytes nebrascensisZone cephalopod fauna from the Elk Butte Member of the Pierre Shale, SE South Dakota and NE Nebraska. Cretaceous Research 19:745–775.

Koppelhus, E. B., and D. R. Braman. 2010. Upper Cretaceous palynostratigraphy of the Dry Island area. Canadian Journal of Earth Sciences 47:1145–1158.

Kosuth, P., J. Callède, A. Laraque, N. Filizola, J. L. Guyot, P. Seyler, J. M. Fritsch, and V. Guimarães. 2009. Sea-tide effects on flows in the lower reaches of the Amazon River. Hydrological Processes 23:3141.

Kraus, M. J. 1987. Integration of channel and floodplain suites; II, Vertical relations of alluvial Paleosols. Journal of Sedimentary Research 57:602–612.

Kraus, M. J. 1999. Paleosols in clastic sedimentary rocks: their geologic applications. Earth-Science Reviews 47:41–70.

Kraus, M. J. 2002. Basin-Scale Changes in Floodplain Paleosols: Implications for Interpreting Alluvial Architecture. Journal of Sedimentary Research 72:500–509.

Kuiper, K. F., A. Deino, F. J. Hilgen, W. Krijgsman, P. R. Renne, and J. R. Wijbrans. 2008. Synchronizing Rock Clocks of Earth History. Science 320:500–504.

Laird, W. M., and R. H. Mitchell. 1942. Geology of the southern part of Morton County, North Dakota. North Dakota Geological Survey Bulletin 14:1–42.

Landman, N. H., and K. M. Waagé. 1993. Scaphitid ammonites of the Upper Cretaceous (Maastrichtian) Fox Hills Formation in South Dakota and Wyoming. Bulletin of the American Museum of Natural History 215:1–257.

Landman, N. H., R. O. Johnson, and L. E. Edwards. 2004. Cephalopods from the Cretaceous/Tertiary boundary interval on the Atlantic Coastal Plain, with a description of the highest ammonite zones in North America. Part 2. Northeastern Monmouth County, New Jersey. Bulletin of the American Museum of Natural History 1–107.

Lawton, T. F. 2008. Chapter 12 Laramide Sedimentary Basins; pp. 429–450 in Andrew D. Miall (ed.), Sedimentary Basins of the World. vol. Volume 5. Elsevier.

Legarreta, L., and M. A. Uliana. 1998. Anatomy of hinterland depositional sequences: Upper Cretaceous fluvial strata, Neuquen basin, west-central Argentina; pp. 83–92 in K. W. Shanley and P. McCabe (eds.), Relative role of eustasy, climate and tectonism in continental rocks. SEPM Special Publication vol. 59.

Legarreta, L., M. A. Uliana, C. A. Larotonda, and G. R. Meconi. 1993. Approaches to nonmarine sequence stratigraphy – theoretical models and examples from Argentine basins. Proceedings of Institut Francais Du Petrole, Conference on Exploration and Production: Subsurface Reservoir Characterization from Surface Observations, April 12-17, 1992 125–143.

Lerbekmo, J. F. 1985. Magnetostratigraphic and Biostratigraphic Correlations of Maastrichtian to Early Paleocene Strata Between South-Central Alberta and Southwestern Saskatchewan. Bulletin of Canadian Petroleum Geology 33:213–226.

Lerbekmo, J. F. 1987. Magnetostratigraphic Restrictions on the Age of the Frenchman Formation and the Magnitude of the Sub-Frenchman Disconformity in Southwest Saskatchewan. Bulletin of Canadian Petroleum Geology 35:454–459.

Lerbekmo, J. F. 1999. Magnetostratigraphy of the Canadian Continental Drilling Program Cretaceous-Tertiary (KT) Boundary Project core holes, western Canada. Canadian Journal of Earth Sciences 36:705–715.

Lerbekmo, J. F. 2009. Glacioeustatic sea level fall marking the base of supercycle TA-1 at 66.5 Ma recorded by the kaolinization of the Whitemud Formation and the Colgate Member of the Fox Hills Formation. Marine and Petroleum Geology 26:1299–1303.

Lerbekmo, J. F., and K. C. Coulter. 1985. Late Cretaceous to early Tertiary magnetostratigraphy of a continental sequence: Red Deer Valley, Alberta, Canada. Canadian Journal of Earth Sciences 22:567–583.

Lerbekmo, J. F., A. R. Sweet, and M. J. Duke. 1996. A normal polarity subchron that embraces the K/T boundary: A measure of sedimentary continuity across the boundary and synchroneity of boundary events. Geological Society of America Special Papers 307:465–476.

Lillegraven, J. A., and L. M. Ostresh. 1990. Late Cretaceous (earliest Campanian/Maastrichtian) evolution of western shorelines of the North American Western Interior Seaway in relation to known mammalian faunas. Geological Society of America Special Papers 243:1–30.

Livaccari, R. F., K. Burke, and A. M. C. Şengör. 1981. Was the Laramide orogeny related to subduction of an oceanic plateau? Nature 289:276–278.

Longrich, N. R., T. Tokaryk, and D. J. Field. 2011. Mass extinction of birds at the Cretaceous–Paleogene (K–Pg) boundary. Proceedings of the National Academy of Sciences 108:15253–15257.

Love, J. D., and A. C. Christiansen. 1985. Geologic map of Wyoming.

Lund, S. P., J. H. Hartman, and S. K. Banerjee. 2002. Magnetostratigraphy of interfingering upper Cretaceous–Paleocene marine and continental strata of the Williston Basin, North Dakota and Montana. Geological Society of America Special Papers 361:57–74.

Marriott, S. B. 1999. The use of Models in the Interpretation of the Effects of Base-Level Change on Alluvial Architecture; pp. 269–281 in N. D. Smith and J. Rogers (eds.), Fluvial Sedimentology VI. Blackwell Publishing Ltd.

Marsh, O. C. 1889. Notice of gigantic horned Dinosauria from the Cretaceous. American Journal of Science 38:173–175.

McCarthy, P. J., and A. G. Plint. 1998. Recognition of interfluve sequence boundaries: Integrating paleopedology and sequence stratigraphy. Geology 26:387–390.

Miall, A. 2010. The Geology of Stratigraphic Sequences. Springer Science & Business Media, 522 pp.

Miall, A. D. 1991. Stratigraphic Sequences and Their Chronostratigraphic Correlation. Journal of Sedimentary Petrology 61:497-505.

Miall, A. D. 2002. Architecture and sequence stratigraphy of Pleistocene fluvial systems in the Malay Basin, based on seismic time-slice analysis. American Association of Petroleum Geologists Bulletin 86:1201–1206.

Miall, A. D., O. Catuneanu, B. K. Vakarelov, and R. Post. 2008. Chapter 9 The Western Interior Basin; pp. 329–362 in Andrew D. Miall (ed.), Sedimentary Basins of the World Volume 5. Elsevier.

Min, K., R. Mundil, P. R. Renne, and K. R. Ludwig. 2000. A test for systematic errors in 40 Ar/39 Ar geochronology through comparison with U/Pb analysis of a 1.1-Ga rhyolite. Geochimica et Cosmochimica Acta 64:73–98.

Mitchell, J. H. 2002. Sedimentary record of Late Cretaceous through Paleocene evolution of the Bighorn Basin, Wyoming. M.S., University of Montana, Missoula. 107 pp.

Mitchum Jr., R. M., and J. C. Van Wagoner. 1991. High-frequency sequences and their stacking patterns: sequence-stratigraphic evidence of high-frequency eustatic cycles. Sedimentary Geology 70:131–160.

Mitchum Jr, R. M., P. R. Vail, and S. Thompson III. 1977. Seismic Stratigraphy and Global Changes of Sea Level: Part 2. The Depositional Sequence as a Basic Unit for Stratigraphic Analysis: Section 2. Application of Seismic Reflection Configuration to Stratigraphic Interpretation. Seismic Stratigraphy - Applications to hydrocarbon exploration. American Association of Petroleum Geologists, Tulsa, Oklahoma.165:53–62.

Molina, E., L. Alegret, I. Arenillas, J. A. Arz, N. Gallala, J. Hardenbol, K. von Salis, E. Steurbaut, N. Vandenberghe, and D. Zaghbib-Turki. 2006. The Global Boundary Stratotype Section and Point for the base of the Danian Stage (Paleocene, Paleogene," Tertiary", Cenozoic) at El Kef, Tunisia-Original definition and revision. Episodes 29:263–273.

Moore, J. R., G. P. Wilson, M. Sharma, H. R. Hallock, D. R. Braman, and P. R. Renne. 2014. Assessing the relationships of the Hell Creek–Fort Union contact, Cretaceous-Paleogene boundary, and Chicxulub impact ejecta horizon at the Hell Creek Formation lectostratotype, Montana, USA. Geological Society of America Special Papers 503:123–135.

Murphy, D. A. 1986. Sedimentation of the upper Hell Creek Formation (Upper Cretaceous), Carter County, Montana. M.S., San Diego State University, San Diego, California, 104 pp.

Murphy, E. C., J. W. Hoganson, and K. R. Johnson. 2002. Lithostratigraphy of the Hell Creek Formation in North Dakota. Geological Society of America Special Papers 361:9–34.

Nambudiri, E. M. V., and P. L. Binda. 1991. Paleobotany, palynology and depositional environment of the Maastrichtian Whitemud Formation in Alberta and Saskatchewan, Canada. Cretaceous Research 12:579–596.

Nichols, D. J. 2002. Palynology and palynostratigraphy of the Hell Creek Formation in North Dakota: A microfossil record of plants at the end of Cretaceous time. Geol. Soc. Am. Spec. Pap 361:393–456.

Ogg, J. G. 2012. Geomagnetic Polarity Time Scale; pp. 85–113 in F. M. Gradstein, J. G. Ogg, M. D. Schmitz, and G. M. Ogg (eds.), The Geologic Time Scale 2012. Elsevier, Amsterdam.

Ogg, J. G., and A. G. Smith. 2004. The geomagnetic polarity time scale; pp. 63–86 in F. M. Gradstein, J. G. Ogg, and A. G. Smith (eds.), A Geologic Time Scale. Cambridge University Press, Cambridge, UK.

Ogg, J. G., and L. A. Hinnov. 2012. Cretaceous; pp. 793–853 in F. M. Gradstein, J. G. Ogg, M. D. Schmitz, and G. M. Ogg (eds.), The Geologic Time Scale 2012. Elsevier, Amsterdam.

Olsen, T., R. Steel, K. Hogseth, T. Skar, and S. L. Roe. 1995. Sequential architecture in a fluvial succession; sequence stratigraphy in the Upper Cretaceous Mesaverde Group, Prince Canyon, Utah. Journal of Sedimentary Research 65:265–280.

Peale, A. C. 1909. On the application of the term Laramie. American Journal of Science 45–58.

Plint, A. G., P. J. McCarthy, and U. F. Faccini. 2001. Nonmarine sequence stratigraphy: Updip expression of sequence boundaries and systems tracts in a high-resolution framework, Cenomanian Dunvegan Formation, Alberta foreland basin, Canada. AAPG Bulletin 85:1967–2001.

Posamentier, H. W., and P. R. Vail. 1988. Eustatic controls on clastic deposition II—sequence and systems tract models. SEPM Special Publication 42:125–154.

Posamentier, H. W., and G. P. Allen. 1999. Siliciclastic Sequence Stratigraphy: Concepts and Applications. SEPM (Society for Sedimentary Geology), 210 pp.

Raynolds, R. G., and K. R. Johnson. 2003. Synopsis of the stratigraphy and paleontology of the uppermost Cretaceous and lower Tertiary strata in the Denver Basin, Colorado. Rocky Mountain Geology 38:171–181.

Renne, P. R., G. Balco, K. R. Ludwig, R. Mundil, and K. Min. 2011. Response to the comment by WH Schwarz et al. on “Joint determination of 40 K decay constants and 40 Ar□/40 K for the Fish Canyon sanidine standard, and improved accuracy for 40 Ar/39 Ar geochronology” by PR Renne et al.(2010). Geochimica et Cosmochimica Acta 75:5097–5100.

Roca, X., and G. C. Nadon. 2007. Tectonic Control on the Sequence Stratigraphy of Nonmarine Retroarc Foreland Basin Fills: Insights from the Upper Jurassic of Central Utah, U.S.A. Journal of Sedimentary Research 77:239–255.

Rogers, R. R. 1994. Nature and origin of through-going discontinuities in nonmarine foreland basin strata, Upper Cretaceous, Montana: Implications for sequence analysis. Geology 22:1119–1122.

Rogers, R. R. 1995. Sequence stratigraphy and vertebrate taphonomy of the Upper Cretaceous Two Medicine and Judith River Formations, Montana. Ph.D, University of Chicago, Chicago, Illinois, 400 pp.

Rogers, R. R. 1998. Sequence analysis of the Upper Cretaceous Two Medicine and Judith River formations, Montana; nonmarine response to the Claggett and Bearpaw marine cycles. Journal of Sedimentary Research 68:615–631.

Scannella, J. B., D. W. Fowler, M. B. Goodwin, and J. R. Horner. 2014. Evolutionary trends in Triceratops from the Hell Creek Formation, Montana. Proceedings of the National Academy of Sciences 111:10245–10250.

Schumm, S. A. 1993. River response to baselevel change: implications for sequence stratigraphy. Journal of Geology 279–294.

Seager, O. A., W. N. Ballard, D. L. Blackstone, W. A. Cobban, and G. R. Downs. 1942. Discussion; Stratigraphy of North Dakota. AAPG Bulletin 26:1414–1423.

Shanley, K. W., and P. J. McCabe. 1994. Perspectives on the Sequence Stratigraphy of Continental Strata. AAPG Bulletin 78:544–568.

Shanley, K. W., and P. J. McCabe. 2009. Alluvial Architecture in a Sequence Stratigraphic Framework: A Case History from the Upper Cretaceous of Southern Utah, USA; pp. 21–55 in S. S. Flint and I. D. Bryant (eds.), The Geological Modelling of Hydrocarbon Reservoirs and Outcrop Analogues. Blackwell Publishing Ltd.

Shelton, J. A. 2007. Application of sequence stratigraphy to the nonmarine Upper Cretaceous Two Medicine Formation, Willow Creek anticline, northwestern Montana. M.S., Montana State University, Bozeman, Montana, 238 pp.

Sprain, C. J., P. R. Renne, G. P. Wilson, and W. A. Clemens. 2015. High-resolution chronostratigraphy of the terrestrial Cretaceous-Paleogene transition and recovery interval in the Hell Creek region, Montana. Geological Society of America Bulletin 127:393–409.

Stanton, T. W. 1909. The age and stratigraphic relations of the “Ceratops beds” of Wyoming and Montana. Proceedings of the Washington Academy of Sciences 11:239–293.

Stanton, T. W. 1910. Fox Hills sandstone and Lance Formation (“ Ceratops beds”) in South Dakota, North Dakota, and eastern Wyoming. American Journal of Science 172–188.

Stanton, T. W. 1914. Boundary between Cretaceous and Tertiary in North America as indicated by stratigraphy and invertebrate faunas. Geological Society of America Bulletin 25:341–354.

Straight, W. H., and D. A. Eberth. 2002. Testing the Utility of Vertebrate Remains in Recognizing Patterns in Fluvial Deposits: An Example from the Lower Horseshoe Canyon Formation, Alberta. PALAIOS 17:472–490.

Strong, N., and C. Paola. 2008. Valleys that never were: time surfaces versus stratigraphic surfaces. Journal of Sedimentary Research 78:579–593.

Tamm, V. 1993. Depositional environments of the Lower Hell Creek Formation (Maastrichtian), Eastern Montana. M.S., University of Rhode Island, Kingston, 122 pp.

Tandon, S. K., and M. R. Gibling. 1994. Calcrete and coal in late Carboniferous cyclothems of Nova Scotia, Canada: Climate and sea-level changes linked. Geology 22:755–758.

Thom, W. T., and C. E. Dobbin. 1924. Stratigraphy of Cretaceous-Eocene transition beds in eastern Montana and the Dakotas. Geological Society of America Bulletin 35:481–505.

Thomas, R. G., D. G. Smith, J. M. Wood, J. Visser, E. A. Calverley-Range, and E. H. Koster. 1987. Inclined heterolithic stratification—terminology, description, interpretation and significance. Sedimentary Geology 53:123–179.

Vail, P. R., R. M. Mitchum Jr., and S. Thompson. 1977. Seismic stratigraphy and global changes of sea level, part 3: relative changes of sea level from coastal onlap; pp. 63–81 in Seismic Stratigraphy - Applications to hydrocarbon exploration. American Association of Petroleum Geologists, Tulsa, Oklahoma.

Veatch, A. C. 1907. Origin and definition of the geologic term Laramie. American Journal of Science 4:18–22.

Waagé, K. M. 1968. The Type Fox Hills Formation, Cretaceous (Maestrichtian), South Dakota. Peabody Museum of Natural History, Yale University, 175 pp.

Waagé, K. M. 1975. Deciphering the basic sedimentary structure of the Cretaceous System in the Western Interior. Geological Association of Canada, Special Paper 13:55–81.

Wang, Y., K. M. Straub, and E. A. Hajek. 2011. Scale-dependent compensational stacking: An estimate of autogenic time scales in channelized sedimentary deposits. Geology 39:811–814.

Wheeler, K. L. 1983. Maestrichtian shoreline sedimentation in northeastern Montana. University of Iowa, 310 pp.

Willmarth, M. G. 1938. Lexicon of geologic names of the United States (including Alaska). Part 1, A-L. US Geological Survey Bulletin 896: 1244 pp.

Wilson, G. P. 2004. A quantitative assessment of mammalian change leading up to and across the Cretaceous-Tertiary boundary in northeastern Montana. Ph.D, University of California, Berkeley, Berkeley, 432 pp.

Wilson, G. P. 2005. Mammalian Faunal Dynamics During the Last 1.8 Million Years of the Cretaceous in Garfield County, Montana. Journal of Mammalian Evolution 12:53–76.

Wilson, G. P. 2014. Mammalian extinction, survival, and recovery dynamics across the Cretaceous-Paleogene boundary in northeastern Montana, USA. Geological Society of America Special Papers 503:365–392.

Wright, V. P., and S. B. Marriott. 1993. The sequence stratigraphy of fluvial depositional systems: the role of floodplain sediment storage. Sedimentary Geology 86:203–210.

Wroblewski, A. F.-J. 2006. Relative influences of tectonism, climate, and sea level on valley incision and sedimentary fill: new insights from Upper Cretaceous and Paleocene examples. SEPM Special Publication 85:309–326.

Zerfass, H., E. L. Lavina, C. L. Schultz, A. J. V. Garcia, U. F. Faccini, and F. Chemale Jr. 2003. Sequence stratigraphy of continental Triassic strata of southernmost Brazil: a contribution to Southwestern Gondwana palaeogeography and palaeoclimate. Sedimentary Geology 161:85–105.

CHAPTER THREE

A NEW CORRELATION OF THE CRETACEOUS FORMATIONS OF THE WESTERN INTERIOR OF THE UNITED STATES, I: SANTONIAN-MAASTRICHTIAN FORMATIONS AND DINOSAUR BIOSTRATIGRAPHY

Contribution of Authors and Co-Authors

Manuscript in Chapter 3

Author: Denver W. Fowler

Contributions: Conceived and designed the study, performed experiments, analyzed data, and wrote the manuscript.

Co-authors: none

Manuscript Information Page

Denver W. Fowler
Status of Manuscript:
_x_Prepared for submission to a peer-reviewed journal
___Officially submitted to a peer-reviewed journal
___Accepted by a peer-reviewed journal
___Published in a peer-reviewed journal

Abstract

A comprehensive high-resolution stratigraphic chart is presented for terrestrial Late Cretaceous units of North America, combining published chronostratigraphic, lithostratigraphic, and biostratigraphic data. For the first time, nearly two hundred ^{40}Ar / ^{39}Ar radiometric dates are recalibrated to both current standard and decay constant pairings, correcting errors in previous recalibrations. Revisions to the stratigraphic placement of most units are slight, but important changes are made to the proposed correlations of the Aguja and Javelina Formations, Texas.

The stratigraphic ranges of selected dinosaur clades are plotted on the chronostratigraphic framework, forming stacks of short-duration species which do not overlap stratigraphically. This is the expected pattern produced by an anagenetic mode of evolution, suggesting that true branching (speciation) events were rare and may have geographic significance. Purported north-south provinciality of dinosaurs is shown to be mostly an artifact of stratigraphic miscorrelation. Rapid stepwise acquisition of display characters in many dinosaur clades, in particular chasmosaurine ceratopsids, suggests that they may represent the highest resolution biostratigraphic markers to be used where radiometric dates are not available.

Introduction

In 1952, Cobban and Reeside published a grand correlation of Cretaceous rocks of the Western Interior of central and southern North America, including both marine and terrestrial units, and biostratigraphic ranges for a variety of invertebrates and vertebrates.

Such interbasinal correlation diagrams are useful for making stratigraphic comparisons between units and similar style diagrams have become commonplace in the geological literature, albeit few with such broad geographical scope. The interbasinal correlation chart of Cobban and Reeside (1952) was important in its day, but it has been rendered obsolete by the advent of advanced chronostratigraphic methods which offer current workers much greater precision and accuracy in placing stratigraphic boundaries. However, most recently published correlations are fairly local in scale, aligning units within the same or adjacent basins, and thus limiting applicability. An exception was presented by Krystinik and DeJarnett (1995) that was specifically intended to show sequence stratigraphic correlations (and lack of correlations) between Western Interior units. This work incorporated sea-level curves and radiometric dates, yet is now largely outdated with inaccuracies in many of the depicted unit ages and especially unit durations. Another analysis (Miall et al., 2008) was similarly broad in geographic scope, but also similarly lacking in detail (although this was not their main intent).

Interbasinal correlation charts are not just of use to geologists; more frequently than ever, paleontologists are using high-resolution chronostratigraphic data to formulate and test evolutionary hypotheses. A simple example is that of "time-calibrated phylogenies", where the stratigraphic positions of individual taxa are superimposed on phylogenetic trees. These are becoming much more prominent in the dinosaur literature (e.g. Sampson et al., 2010; Evans et al., 2013), and are used to deduce the timing of important phylogenetic branching events, infer ghost ranges, and potentially to calculate rates of evolution. A more nuanced application that is especially important to my research

is assessing whether two sister taxa are contemporaneous (thereby inferring a genuine speciation event), or whether they form a succession of stratigraphically separated morphologies (supportive of anagenesis; e.g. Horner et al, 1992; Scannella et al., 2014). The value of such analyses is inherently dependent upon the accuracy of the plotted taxa, which in turn depend upon the accuracy of the stratigraphic correlations of the formations from which their fossils were recovered, and herein lies the problem. Precise dating of geological formations is especially critical for determining anagenesis or cladogenesis in dinosaurs, but when specimens are very similar in age, a difference of only a few hundred thousand years is often enough to completely reverse paleobiological interpretation.

The Late Cretaceous deposits of the North American Western Interior represent the best, if not only, opportunity to make a high-resolution chronostratigraphic framework within which to study dinosaur evolution. This is due to the serendipitous combination of large areas of outcrop, interfingering marine units with biostratigraphically informative fossils, a consistent scattering of radiometric dates due to synorogenic volcanic activity, not to mention the vast literature detailing over a century's worth of research. However, despite the large amount of data available, many published correlations suffer from inaccuracies that inevitably strongly affect paleobiological interpretations:

1. It is Difficult to Find the Reasoning Behind Some Correlations

In paleontological papers especially, correlation charts are typically presented as a series of geological columns, and rarely contain clear or detailed justifications for the

stratigraphic positions of the depicted horizons. Usually a few citations are given for stratigraphic position, and radiometric dates may be marked (also including citations), but important details may be lacking. This can create many problems, including circular citation of incorrect or unknown stratigraphic data (e.g. the age of the '*Alamosaurus* fauna'; e.g. Lehman 2001; see trends paper) or unknowingly mismatching old outdated stratigraphic data with new interpretations or calibrations (e.g. the changing correlations and calibrations of radiometric dates from the Kaiparowits Formation Utah; Roberts et al., 2005; 2013; Sampson et al., 2010; Zanno et al., 2011). Admittedly, justifying every horizon in a stratigraphic column is an arduous task, but without detailed work like this, precise stratigraphic placement of taxa can be either impossible or done incorrectly.

2. Lacunae are Not Depicted

Geological columns often do not emphasize the lacunae that exist within formations. For example, a historical problem in terrestrial lithostratigraphy is that laterally consistent resistant sandstones are often used as uppermost units for formational contacts; e.g. the Capping Sandstone Member, Wahweap Formation, Utah (Eaton, 1991). This is a problem as amalgamated channel sandstones typically form the basalmost unit of depositional sequences; it happens that the uppermost unit of the Wahweap Formation (Capping Sandstone) is actually the basal amalgamated channel complex of the overlying sequence that comprises the Kaiparowits Formation (Lawton et al., 2003). Hence, the Wahweap and Kaiparowits Formations can appear to represent a more conformable succession than what is in reality, and the correctly cited durations for each of the

formations are misinformative. For this and other reasons, members and the lacunae between them should be plotted on correlation charts and explained where possible.

3. Radiometric Dates May be Incorrect or Incomparable

Many currently cited radiometric dates are not properly comparable as from the early 1980's through to the current day, radiometric analyses have used a variety of standards, decay constants, or different methods. There is also an emerging issue that analyses performed in different laboratories produce slightly different results, and this is being investigated internally by those labs (Renne, pers. comm.).

Here I present a comprehensive stratigraphic correlation chart comprising the major terrestrial geological formations of the North American Western Interior (Electronic Supplementary File 1). The chart is plotted based on extensive review of the pertinent stratigraphic literature on each formation, and on the recalibration of nearly 200 ^{40}Ar / ^{39}Ar radiometric dates. Recalibrated radiometric dates are presented both on the chart itself, and as a separate excel sheet (Electronic Supplementary File 2), and are recalibrated to both currently accepted ^{40}Ar / ^{39}Ar standards (Kuiper et al., 2008, combined with Min et al., 2000; and Renne et al., 2011). The recalibrations correct errors (some minor, some major) in previous works (Kuiper et al., 2008; Schmitz, 2012; Roberts et al., 2013). This new work represents the most precise and comprehensive correlation currently available for terrestrial geological formations of the North American Western Interior. This is used in combination with locality data for individual dinosaur specimens to plot the stratigraphic ranges for dinosaur taxa (currently restricted to

Neoceratopsia, Sauropoda, and Hadrosauridae). This replotting of dinosaur taxa is discussed with regards to current hypotheses of dinosaur biogeography and evolution.

Methods

Abbreviations Used

Gp, Group; Fm, Formation; Mbr, Member. Ma, millions of years ago; Ka thousands of years ago; m.y. million years; k.y. thousands of years; c.z., coal zone; FCT, Fish Canyon Tuff; TCR, Taylor Creek Rhyolite.

Display Format – Excel Sheets

The recalibration sheet and stratigraphic correlation chart are offered as two separate Microsoft Excel files (Electronic Supplementary Files 1 and 2). They are kept separate for ease of cross referencing. References cited in these Microsoft Excel files are listed in Appendix B.

Electronic Supplementary File 1. The stratigraphic chart is arranged as an excel spreadsheet (Electronic Supplementary File 1), and is intended to be used directly in this format as it offers a number of advantages over a graphic embedded within a PDF or printed page. The grid of cells naturally permit precise plotting of stratigraphic boundaries, with each vertical cell height representing 0.1 m.y.. Most usefully, each cell, (or group of cells) can be tagged with a pop-up note that is activated by simply hovering the mouse cursor over any cell with a red triangle in the upper right corner. These pop-up notes comprise the bulk of the results of this study, providing the information that

supports each depicted stratigraphic position or boundary of the geologic unit or taxon, along with introductory text. For ideal formatting, the reader is advised to view the chart in native resolution, at 22% zoom level.

Some disadvantages of the excel format include the limited range of line styles and orientations, such that (for example) it is not possible to represent unconformities by a wavy line, and cell borders necessarily are straight. Due to the need to keep font size small (to increase available space), taxon names are not produced in italics as it makes them much less readable. The reader is advised that under some levels of zoom, a note box might not be fully readable; if so, right click and select edit note, then either read the note in place, or resize the note box such that all the text is visible.

References used in the construction of the chart are available as a separate document (Appendix B).

Electronic Supplementary File 2. The recalibration sheet (Electronic Supplementary File 2) is also made available in the form of an excel sheet. This is due to its large size, but also enjoys the benefit of the pop-up notes, providing additional information on radiometric dates and the original publications. Maintaining the recalibrations as an excel sheet also permits the retention of the active formulae used to calculate the new dates.

The recalibration sheet is adapted from the EARTHTIME excel recalculation sheet provided by Noah McLean at the earthtime.org website. This is the same source as for the recalibrations performed by Roberts et al. (2013), cited as: http://www.earth-time.org/ar-ar.html, by those authors. Unfortunately, the earthtime.org website is

currently listed as "under construction", and so I have not been able to relocate the original download location.

The original recalibration formulae were duplicated into Electronic Supplementary File 2 such that this is a "live" document which independently recalculates dates based on the input data on each line of the sheet. I have also adapted the source lines for each recalculation such that all the original input data (standards, decay constant, etc.) are visible for each recalculation. This way the sheet shows all the "working" for all of the 200 recalculations, and each can be properly independently assessed (by comparison, the original sheet provided by McLean and EARTHTIME only had space for a few recalculations at a time). This is a direct response to the lack of such data provided in previous recalculation publications (e.g. Roberts et al., 2013), requiring therefore that the reader must replicate the result for themselves in order to check that the recalibration was performed correctly (see results section for discussion of errors encountered in previous recalibrations).

There is a problem with the recalculation of error in the original formulae present in the McLean EARTHTIME sheet. This has the result that for some recalibrations, the excel sheet will only produce a "!VALUE" statement for the recalibrated uncertainty/error (caused by the formula attempting to divide by zero). As a result, the uncertainty/error for many recalibrations cannot be computed (an additional problem is the lack of J-value data in most analyses). To overcome this, for analyses where the new error cannot be directly computed, I have multiplied the original error by the % change output factor; error values calculated by this method are shown in red (normally

calculated error values are shown in black). Comparison to normally calculated error values show that this method produces comparable results such that the new stated error values are not notably different from what would be calculated if J-values (etc) were known.

There are two tabs of recalibrations. The first, labeled "Kuiper et al 2008", recalibrates all the dates to the Kuiper et al. (2008) FCT standard, coupled with the Min et al. (2000) decay constant. Dates from this fist tab are plotted on the stratigraphic chart (Electronic Supplementary File 1). The second tab, labeled "Renne et al 2011", recalibrates all dates to the standard and decay constant pairing of Renne et al. (2011). This second set of recalibrations is provided for comparison. Both tables of recalibrations have the same formatting for ease of comparison.

Stratigraphic Chart (Electronic Supplementary File 1)

Construction of the chart is complex and depends upon many different stratigraphic methods. Here I explain the underlying definitions which provide the base framework for the chart, and highlight some of the issues surrounding its construction.

Definitions: Stage and Substages, Magnetostratigraphy, and Ammonite Biostratigraphy

Here I follow The Geological Time Scale 2012 (GTS2012; Gradstein et al., 2012) for definitions of stage and substage boundaries (Ogg and Hinnov, 2012), magnetostratigraphic boundaries (Ogg, 2012), and ammonite biostratigraphy (Ogg and Hinnov, 2012). Although more recent revisions of these definitions are available, GTS2012 integrates all these defined units with

chronostratigraphic dates which use the $^{40}Ar/^{39}Ar$ standard and decay constant pairing of Kuiper et al. (2008) and Min et al. (2000), which are used here. A second magnetostratigraphic column is also offered containing some revised chron boundaries and includes many of the very short duration cryptochrons that have not yet been officially recognised, but are often named in magnetostratigraphic analyses (e.g. Lerbekmo and Braman, 2002). Individual definitions and discussion (where appropriate) can be found in the popup notes in the respective parts of the chart.

In some places I have been forced to provide a compromise in stratigraphic placement, generally where a magnetostratigraphic assertion does not match, say, the ammonite zonation (e.g. age of the Dorothy bentonite in the Drumheller Member, Horseshoe Canyon Formation, Alberta). In such cases, text boxes provide explanation of the problem, and references.

Positioning of Geological Units and Dinosaur Taxa. The stratigraphic ranges of geological units and fossil taxa are plotted as a solid bordered white cell with the lower and upper borders representing the upper and lower contacts of the geological unit, or first and last documented taxon occurrences (respectively). If stratigraphic position is not sufficiently documented, the possible or likely stratigraphic range is illustrated as a block arrow. A combination of a solid cell and block arrow may be used if a taxon comprises some specimens for which stratigraphic position is precisely known (depicted by the solid cell) and some specimens for which stratigraphic position is unknown (block arrows). Periods of non-material time (lacunae) are represented by blank spaces. A graded block

arrow is used for units which may continue for a long period time below the period of interest (typically used for thick marine shales).

Sequence Stratigraphy and Lithostratigraphy. Some features of typical lithostratigraphic units are not possible to properly depict on the stratigraphic chart format. In the Western Interior, many terrestrial packages form clastic wedges thinning basinwardly. I have attempted to represent this in the chart where possible, although for the most part depicted stratigraphic sections are based on single well-sampled sections, cores, or geographic areas, and so the wedge-shaped overall geometry might not be visible.

Limitation of Scope and Future Versions. There are some limitations of scope for this initial version of the correlation chart. Stratigraphic age is currently mostly limited to units of Santonian age (86.3 Ma) up to the K-Pg boundary (66.0 Ma). There are a few exceptions (e.g. Moreno Hill Fm, NM; Straight Cliffs Fm, UT) which are included because they have yielded important specimens, or provide stratigraphic context for overlying units.

Geological units featured in the correlation chart are currently limited to those for which dinosaurian material has been collected, or which provide contextual information for surrounding units (e.g. intertonguing marine units with biostratigraphically informative fauna; overlying or underlying units with chronostratigraphic marker beds).

Dinosaurian fossils are limited to Neoceratopsia, Sauropoda, and Hadrosauridae as these are the most abundant and biostratigraphically informative taxa.

Future versions of the chart are intended to extend stratigraphic range down to the Jurassic-Cretaceous boundary. Plans for the first expansion concern inclusion of more Late Cretaceous formations from North America and similarly aged deposits in Asia. Initial work on expanding faunal coverage has already begun concerning the addition of all remaining dinosaur taxa (including birds), crocodilians, and mammals, with the intent of eventually incorporating all useful taxa if possible (coauthors will be sought for this).

Institutional Abbreviations. A list of institutional abbreviations used in the correlation chart are provided in a separate tab of the excel sheet (Electronic Supplementary File 1) labeled "repository codes".

Taxa Display Format – Phylogenies and Lineages. It is not the intention of this project to make significant comment on phylogenies *per se*. However, precise stratigraphic placement of taxa permits testing of speciation hypotheses (see discussion) and so the arrangement of taxa on the chart should reflect up-to-date phylogenies. In this current version, this only affects Ceratopsidae and Hadrosauridae. For ceratopsids, the general arrangement follows the chasmosaurine phylogeny from Fowler (in prep / Chapter 4), and for centrosaurines I follow the phylogeny of Evans and Ryan (2015). For hadrosaurids, the general arrangement of hadrosaurines follows Freedman Fowler and Horner (2015), and lambeosaurines follows Evans and Reisz (2007). An important difference with the arrangement of taxa in the strat chart is that unless they are contemporaneous, taxa are arranged as lineages of stratigraphically separated "species".

Magnetostratigraphy. In magnetostratigraphic analysis, if two stratigraphically adjacent sample points yield opposite polarities (i.e. they are recognisable as different chrons), then it is convention to draw the chron boundary stratigraphically halfway between the two points. However an issue arises when these lower and upper sample points are separated by a sandstone from which it is difficult or impossible to extract a magnetostratigraphic signal. In terrestrial floodplain deposition (typical of the units studied in this work), the bases of depositional sequences are characterized by a surface of non-deposition or erosion, overlain by a low accommodation systems tract, typically comprising an amalgamated channel sandstone. The combination of the depositional hiatus at the base of the sandstone, and the sandstone itself, means that there may be a considerable time gap (up to millions of years) between the last sampled horizon immediately below the sandstone, and the first sampled horizon immediately above the sandstone. If opposite polarities are recorded for the two sampled horizons either side of the unsampled sandstone, then the chron boundary would be drawn halfway, within the sandstone, whereas it is more likely to occur at the base of the sandstone, as this is where the hiatus occurs. This can have the effect of making a unit appear older or younger than it really is. For example, the mudstone immediately beneath the Apex sandstone (basal unit of the upper Hell Creek Formation, Montana; Hartman et al., 2014) is of normal polarity, assigned to C30n, whereas the mudstone immediately above the Apex Sandstone is of reversed polarity (assigned to C29r; LeCain et al., 2014). The C30n-C29r boundary is therefore drawn within the Apex Sandstone, whereas it is more likely that it occurs at the hiatus at the base of the sandstone. A more significant case arises with the

contact between the Laramie Formation and overlying D1 sequence in central Colorado: here, because of the halfway convention, the uppermost part of the Laramie is drawn as being within the lowermost C31r zone (Hicks et al., 2003), whereas in reality, all magnetostratigraphic samples from the Laramie are normal, and it is probably entirely C31n. These are just two examples, and more are highlighted as notes in the chart. So long as the reader is careful and remains cautious of this issue, then mistaken correlation and / or artificial age extension can be avoided.

Radiometric Dating. This analysis reports nearly 200 radiometric dates, most of which are ^{40}Ar / ^{39}Ar dates which have been recalibrated to the standard and decay constant pairing of Kuiper et al. (2008), and Min et al. (2000). It is not my intention to provide a thorough review of all radiometric dating methods (see Villeneuve, 2004), nor is this my personal research specialisation. However, given the large number of ^{40}Ar / ^{39}Ar dates used here, and given discrepancies in past recalibrations, I give a cursory overview to the method. This text is also included (and expanded) in the chart itself (Electronic Supplementary File 1).

U-Pb and K-Ar. Most radiometric dates reported for Upper Cretaceous units use either U-Pb, K-Ar, or ^{40}Ar / ^{39}Ar dating methods. U-Pb and K-Ar are primary dating methods, which directly determine the age of a sample and do not require recalibration (unless decay constants change, which is rare); whereas relative or secondary methods (such as ^{40}Ar / ^{39}Ar dating) require use of a monitor mineral of known or presumed age

("standard"). It is the recent changes to the recognized age of these standards which has been the cause of changing ^{40}Ar / ^{39}Ar dates.

U-Pb dating actually analyses two decay series (^{235}U decay to ^{207}Pb, and ^{238}U decay to ^{206}Pb), such that there are two independent measures of age, the overlap of which is the concordant age of the sample (Villeneuve, 2004). Recent improvements in analytical techniques (High-Resolution–Secondary Ion Mass Spectrometry: SHRIMP) have brought greater precision and accuracy to U-Pb dating and it remains one of the best methodologies currently available (Villeneuve, 2004). The decay constant for U-Pb analysis is well established (Steiger and Jaeger, 1977), and known to better than 0.07% (Villeneuve, 2004). It is noted however (Villeneuve, 2004) that uncertainty in the U-Pb decay constant is not typically included in cited final ages; this is not an issue when comparing among U-Pb dates, but should be properly included when comparing (say) U-Pb to ^{40}Ar / ^{39}Ar dates.

K-Ar dating is an older method of radiometric dating that was commonplace up until the end of the 1980's when it was essentially replaced by the more precise and accurate ^{40}Ar / ^{39}Ar method (Villeneuve, 2004). K-Ar had a number of benefits, including a large number of possible datable minerals, due to the common abundance of potassium, but among its many drawbacks was a relative lack of precision, largely due to the requirement to run two separate analyses per sample for K and ^{40}Ar. As such, analytical precision was never better than 0.5%, and with the development of new technologies K-Ar dating was quickly replaced by ^{40}Ar / ^{39}Ar in the early 1990's (Villeneuve, 2004). Even so, some K-Ar dates are still the only dates available for a given unit, and so are

included in the chart. K-Ar dates typically have error in the region of 1-2 m.y for Upper Cretaceous units, so are useful indicators as to a general age range for a unit, but not for precise correlation.

^{40}Ar / ^{39}Ar. Detailed reviews of ^{40}Ar / ^{39}Ar dating have been published elsewhere (e.g. McDougall & Harrison, 1999). Notes given here are for the purpose of aiding the reader in understanding the recalculation of radiometric dates reported in this work, how ^{40}Ar / ^{39}Ar dates are affected by changing standards and decay constants, and comparability of radiometric dates recovered by different methods (e.g. ^{40}Ar / ^{39}Ar vs U-Pb).

Standards (Neutron Fluence Monitor). As ^{40}Ar / ^{39}Ar dating is a relative dating method, every unknown sample needs to be analysed alongside a sample of known age: a standard. Primary standards are minerals from specific rock samples that have been directly dated by 40K / 40Ar dating or another method; whereas secondary standards are based on ^{40}Ar / ^{39}Ar intercalibration with a primary standard (Renne et al., 1998). The following list includes (but is not limited to) some of the more popular standards that have been used historically (see McDougall & Harrison, 1999, for a more complete list):

MMhb-1 McClure Mountain hornblende, primary standard: ~420 Ma

GA-1550 Biotite, monazite, NSW, Australia, primary standard: ~98 Ma

TCR Taylor Creek Rhyolite (or sanidine, TCs), secondary standard: ~28 Ma

FCT Fish Canyon Tuff (or sandine, FCs), secondary standard: ~28 Ma

ACR Alder Creek Rhyolite (or sanidine, ACs), secondary or tertiary standard: ~1 Ma

Standards are chosen depending on availability, and should be of comparable age to the unknown sample (Renne et al., 1998). Hence, for Late Cretaceous deposits, usually the secondary standards TCR or FCT have been used, typically themselves being calibrated against a primary standard (historically, the MMhb-1 is commonly used, although this depends on the preference of the particular laboratory). Many historically popular standards are no longer used as repeated calibration studies have found the original sample to give inconsistent dates; for example, Baksi et al. (1996) found the widely used MMhb-1 primary standard to be inhomogenous, making its use as a standard no longer tenable. Further, intercalibration studies have continually honed and refined the ages of standards (especially the more widely used secondary standards), with the result that radiometric dates published years apart are typically not precisely comparable without recalibration.

For ^{40}Ar / ^{39}Ar analysis, a significant problem concerns the changing age of the Fish Canyon Tuff (FCT: the relative standard used for most ^{40}Ar / ^{39}Ar analyses of Cretaceous rocks), and to a lesser extent, the associated decay constants ($\lambda\beta$: β- decay of 40K to 40Ca; and $\lambda\varepsilon$: electron capture or β+ of 40K to 40Ar; which combined are referred to as λT or $\lambda total$; Beckinsale and Gale, 1969).

Cebula et al. (1986) first proposed an age of 27.79 Ma for the Fish Canyon Tuff. This was quickly refined to 27.84 Ma by Samson and Alexander (1987), which remained the standard used by ^{40}Ar / ^{39}Ar analyses published up to the mid 1990's (e.g. Rogers et

al., 1993). Renne et al. (1994) revised the FCT to 27.95 Ma (although this new figure was not commonly used at the time). The next major update was that of Renne et al. (1998) whereupon the FCT was revised to 28.02 Ma, which was widely accepted up to 2008 when Kuiper et al. published the current standard of 28.201 Ma, which also brought ^{40}Ar / ^{39}Ar dates into line with U-Pb dates, unifying these two major chronostratigraphic dating systems. Two further revisions have been offered by Renne et al. in 2010 and 2011, of 28.305 Ma, and 28.294 Ma (respectively). Rivera et al. (2011), Meyers et al. (2012), Singer et al. (2012), and Sageman et al. (2014) all found independent support for Kuiper et al. (2008)'s 28.201 Ma age for the Fish Canyon Sanidine (and therefore rejected Renne et al.'s (2010) further revised 28.3 Ma standard as too old). These three analyses also used three methods (^{40}Ar / ^{39}Ar, U-Pb, cyclostratigraphy) to reach consensus, confirming alignment of U-Pb and ^{40}Ar / ^{39}Ar dates.

When applied to Late Cretaceous units, a ~0.2 m.y. difference between the age of two different standards corresponds to ~0.4 - 0.5 m.y. difference in the ^{40}Ar / ^{39}Ar age of the analysed sample, and this is exacerbated if the standards used were further apart. For example, using the 27.84 standard of Samson and Alexander (1987), Rogers et al., 1993 published an ^{40}Ar / ^{39}Ar date of 74.076 Ma for a bentonite at the top of the Two Medicine Formation, MT. This becomes 75.038 Ma if using the current Kuiper et al. (2008) standard, and 75.271 Ma under the less commonly used Renne et al. (2011) standard. This difference of 1.28 m.y. between 1987 and 2008 standards highlights why it is important to know which standards were used for an analysis, especially since only a few hundred thousand years make critical differences in paleobiological interpretation.

Decay Constants. The ^{40}Ar / ^{39}Ar method depends upon the β- decay of ^{40}K to ^{40}Ca ($\lambda\beta$), and electron capture or β+ of ^{40}K to ^{40}Ar ($\lambda\varepsilon$), which combined are referred to as λT or $\lambda total$ (Beckinsale & Gale, 1969). The value of the decay constant λT (and its components) have historically been subject to fewer changes than the standards listed above, but have come under increased scrutiny since the late 1990's. It is also notable that different values of λT have been used historically by geochronologists compared to physicists and chemists (further details and a history of decay constant values can be found in the corresponding note within the chart).

Recalibration and Current Standards. In order to compare ^{40}Ar / ^{39}Ar dates, it is essential to ensure that the same standards and decay constants were used in their calculation, which may require recalibration. If the standards used are different, for example, if an old analysis used the TCR standard, and a more recent one used the FCT, then it will be necessary to find what the equivalent FCT value was to the TCR used in the original analysis. This is usually achieved by referencing either the original publication of the standard, or the relevant published intercalibration analysis (e.g. Renne et al. 1994). It is critical to understand that recalculation cannot simply be performed by entering the original standard used (e.g. TCR = 28.32 Ma) into the equation provided on the recalculation sheet from McLean and EARTHTIME (or the adapted spreadsheet used here); the equivalent FCT value is what is entered as the formula only uses FCT. This might seem obvious, but this error was the cause of numerous miscalculations in Roberts et al. (2013; see later).

The decay constant absolute value has only a small effect on the absolute age of a sample, but decay constants contribute a greater amount to the error of a radiometric date. There are two currently prominently used pairings of standard and decay constant: Kuiper et al. (2008) combined an FCT standard age of 28.201 +/-0.023 Ma, with the decay constant of Min et al. (2000), $\lambda T = 5.463 +/- 0.214$ E-10/y. Renne et al. (2011) use an FCT standard age of 28.294 +/- 0.036 Ma, with a λT of 5.5305 E-10/y. This work is calibrated to the Kuiper et al. (2008) standard, paired with the Min et al. (2000) decay constant. This is not a judgment on the reliability of one method over another; rather it is out of convenience, since the various ammonite biozones and magnetochrons detailed in The Geological Time Scale 2012 (Gradstein et al., 2012; upon which this chart is based) use the Kuiper et al. (2008) FCT standard, and Min et al. (2000) decay constant.

Choice of Mineral. Direct comparisons between ^{40}Ar / ^{39}Ar dates require not only the same standard and decay constant pairing, but also that the subject mineral is the same. Although it is theoretically possible that a date obtained from biotite crystals might be comparable with one from sanidine, in practice the difference in closure temperature (the temperature at which the mineral no longer loses any products of radioactive decay; Villeneuve, 2004) and other factors such as recoil effects (Obradovich, 1993) mean that (for example) biotite dates are typically ~0.3% older than sanidine dates (e.g. see Rogers et al., 1993). The current "gold standard" mineral for ^{40}Ar / ^{39}Ar dating is sanidine, and most modern analyses use this mineral exclusively (where possible), however plagioclase and biotite dates are quite common in literature from the 1990's. I recalibrate these non-sanidine dates, and they are comparable to each other (ie. biotite dates can be directly

compared with other biotite dates), but caution is advised when comparing non-sanidine dates with those of sanidine (although this is sometimes unavoidable).

Reporting of Uncertainty / Error. Reporting of error associated with ^{40}Ar / ^{39}Ar derived ages is not standardized and varies in the inclusiveness of sources of error, the statistical method used to calculate error, the type of error, and in the amount of analytical information provided.

Sources of error in ^{40}Ar / ^{39}Ar analyses include analytical error (e.g. J-value), uncertainty in the standard used (e.g. age of the Fish Canyon sanidine, FCs is 28.201 +/- 0.23 Ma at 1σ; Kuiper et al., 2008), uncertainty in the decay constant (e.g. λ_T of 5.463 +/- 0.214 E-10/y; Min et al., 2000), and geological processes that may lead to post-crystallization alteration of isotope ratios (Villeneuve, 2004). Most older publications do not explicitly state what is included in the reported error, but newer studies (e.g. Sprain et al., 2014) report both analytical and systematic error.

The statistical method used to report error is not standardized, and is typically given in one of three forms; some authors report 1 or 2 standard deviations (σ); Standard Error is also commonly reported (especially for population means); finally, some authors report 95% confidence intervals for the population mean, which is roughly equivalent to 2σ (=95.45% confidence interval).

It is common for published radiometric dates to lack associated details of the analysis, by either the date being given as a pers. comm., or simply the omission of analytical details. Consequently, it is sometimes unclear as to whether (for example) a

stated error of +/- 0.15 Ma refers to 1σ, 2σ, Standard Error, or whether it includes analytical and systematic error.

As such, it is not possible to make the error consistent between each recalibration (although the effects are relatively minor). Where possible, I have reported recalibrated error to 1σ analytical error, but generally I have simply taken the original reported error and processed it through the recalibration spreadsheet, noting wherever possible all possible details and any issues that may arise. Direct comparison of error between dates (both recalibrated and unrecalibrated) should therefore be approached with caution.

Agreement of ^{40}Ar / ^{39}Ar Dates with U-Pb Dates. ^{40}Ar / ^{39}Ar dates have historically tended to be younger than U-Pb dates by about 1% (Schoene et al., 2006), equating to ~750 ky difference in a 75 m.y. old sample. Possible explanations include longer zircon magma residence times prior to an eruption (Villeneuve, 2004), error in the potassium-40 decay constant (Schmitz & Bowring, 2001), or interlaboratory bias and geological complexities (Kuiper et al., 2008). Recent revisions of standards and decay constants for ^{40}Ar / ^{39}Ar dating have closed the gap to within ~0.3% (Kuiper et al., 2008; Renne et al., 2011). This led Kuiper et al. (2008) to suggest that ^{40}Ar / ^{39}Ar dating has improved "absolute uncertainty from ~2.5% to 0.25%"

Other General Comments. The number of decimal places for reported dates and error are left in their original published form where possible.

In previous publications, a large number of radiometric dates are reported as pers. comm. or featured only in abstracts. Such references typically lack any analytical data

and so original standards etc must be assumed based on the year in which the analysis was (likely) conducted, and any details of the typical standards used by the scientist and laboratory which carried out the analysis (if known; see individual notes for details of sleuthing).

Results

An early version of this chart was presented by Fowler (2006). This prior version was not finalized, contained taxonomic misplots, and was based on unrecalibrated radiometric dates and stratigraphic boundary definitions from the previous version of A Geologic Time Scale (Gradstein et al., 2004; as opposed to Gradstein et al., 2012). As such, the previous data presented in Fowler (2006) should be disregarded and replaced by this new version.

The results of this study are presented as separate Microsoft Excel files: the stratigraphic chart (Electronic Supplementary File 1), and the recalibration sheet (Electronic Supplementary File 2). These documents contain detailed information in the various pop up notes, most of which is not repeated here.

Notes on Recalibrations by Other Authors

Various Analyses Published by J. D. Obradovich (~1990 Until at Least 2002). Recalibration of radiometric dates from analyses by J. D. Obradovich (USGS, Colorado) conducted in the 1990's (and possibly early 2000's) requires special caution due to the particular methodology of Obradovich during this time, which differs slightly from what might be expected. Obradovich

typically uses the TCR as the standard for his analysis, but the equivalent age of the FCT (required for recalibration) is not typical. Indication of this is noted by Hicks et al. (2002, p.43) who state:

> "The TCR (Duffield & Dalrymple, 1990) has been used exclusively since 1990 by one of us (Obradovich) with an assigned age of 28.32 Ma normalized to an age of 520.4 Ma for MMhb-1 (Samson & Alexander, 1987). This age differs from that of 27.92 Ma assigned by Sarna-Wojcicki and Pringle (1992). The choice of 28.32 Ma was entirely pragmatic because this monitor age provided the best comparison with ages delivered by Obradovich and Cobban (1975). In an intercalibration study [...] Renne et al. (1998) obtained ages of 28.34 Ma for TCR and 28.02 Ma for FCT when calibrated against GA1550 biotite as their primary standard with an age of 98.79 Ma. This value of 28.02 agrees quite well with [..] 28.03 Ma obtained through calibration based on the astronomical time scale (Renne et al., 1994). On the basis of unpublished data, one of us (Obradovich) obtained an age of 28.03 Ma for the FCT [...] of W, McIntosh (Geoscience Dept. NM Institute Mining * Technology, Socorro), calibrated against an age of 28.32 Ma for TCR."

However, Obradovich-published analyses from this time do not exclusively use the TCR at 28.32 Ma, as Izzett and Obradovich (1994) state that they use FCT sanidine at 27.55 Ma, and TCR sanidine at 27.92 Ma, both relative to MMhb-1 at 513.9 Ma (in conjunction with λT = 5.543 E-10/y). They note that the 513.9 Ma age of MMhb-1 differs from the then standardized age of 520.4 Ma (Samson & Alexander, 1987) as the former age was calibrated in the lab where their current samples were analysed (Lanphere et al., 1990; Dalrymple et al., 1993).

This creates a problem when recalibrating ^{40}Ar / ^{39}Ar ages that used TCR as the fluence monitor (standard). The "official" TCR age of 27.92 Ma has a corresponding FCT age of 27.84 Ma (Samson & Alexander, 1987; Renne et al., 1998). However, since most analyses by Obradovich use TCR at 28.32 Ma, then the question remains as to what

number to use for the equivalent FCT when performing recalibrations. Renne et al. (1998) provide an intercalibration factor for FCT : TCR of 1 : 1.00112 +/- 0.0010, which simply calculated is FCT = 28.32 / 1.100112 = 28.006 Ma. This agrees well with the calculated FCT equivalent of 28.03 Ma (Hicks et al., 2002; above; Obradovich, 2002) and a value of 28.02 Ma of Renne et al. (1998). In the Geological Time Scale 2012 (Gradstein et al., 2012), Schmitz (2012) recalibrates dates from Obradovich (1993), and Hicks et al. (1995, 1999) using a legacy FCT age of 28.00 Ma (not stated, but retrocalculated by DF). Sageman et al. (2014; cited as Siewert et al., in press, by Schmitz, 2012) recalibrate Obradovich's older dates using a legacy FCT age of 28.02 Ma (thereby agreeing with Renne et al., 1998).

In this analysis, when recalibrating an ^{40}Ar / ^{39}Ar date that was calculated by Obradovich using a TCR = 28.32, I use an FCT value of 28.03, as this is the equivalent FCT explicitly stated by Obradovich (2002). This is a very close value to 28.02 (Renne et al., 1998; where the TCR equivalent is 28.34 +/- 0.16 Ma; 1σ, ignoring decay error) so confusion between the two should be avoided, although the difference between ages calculated using 28.03 or 28.02 Ma standards would correspond to only 0.02 to 0.04 m.y. for ages in the Late Cretaceous (100.5 - 66 Ma; Ogg & Hinnov, 2012)

Kuiper et al. (2008). In their presentation of the new standard and decay constant pairing for the FCT, Kuiper et al. (2008) recalibrate some radiometric dates which are of general interest. One of these dates (the K-Pg boundary dates of Swisher et al., 1993) is used in my current stratigraphic chart, but I found that my own recalibration (66.06 Ma) did not agree with that presented by Kuiper et al. (2008; 65.99 Ma). Through

retrocalculation, I determined that Kuiper et al. (2008) had not accounted for the fact that Swisher et al. (1993) had used the Steiger and Jaeger (1977) decay constant; Kuiper et al. (2008) had only accounted for change in the standards used (thereby assuming that Swisher et al., 1993, had used the decay constant of Min et al., 2000, which was clearly impossible). The difference between the two dates is only 0.07 Ma, but I feel that it is worth highlighting in case this discrepancy is of greater significance to other works.

Schmitz (2012). As mentioned above, recalibrations of Obradovich dates (Obradovich, 1993; Hicks et al., 1995; 1999) that use the 28.32 TCR standard are recalibrated using an FCT equivalent of 28.00 by Schmitz (2012). Schmitz's recalibrated dates form the basis of the spline fits (etc.) of the Geological Time Scale (Gradstein et al., 2012), and so any slight changes might be important. The correct date to use for the FCT equivalent would be either 28.03 Ma (used by me; see above note), or 28.02 Ma (based on Renne et al., 1994).

Roberts et al. (2013). Roberts et al. (2013) present a table of recalibrated radiometric dates from a selection of important dinosaur-bearing formations of the North American Western Interior. Unfortunately, 11 out of 18 dates are incorrectly recalibrated, with different kinds of errors in different recalibrations, producing dates that are incorrect by up to a million years.

Roberts et al. (2013) recalibrate the dates for the Judith River Formation (originally published by Goodwin and Deino, 1989), however they input an incorrect original (legacy) FCT standard of 28.02 Ma (i.e. from Renne et al., 1998, published after

the original 1989 analysis). For the recalibration to be correct, the legacy standard must be the value of FCT that was equivalent to the MMhb-1 at 420.4 Ma, which is FCT = 27.84 Ma (Samson & Alexander, 1987; see Renne et al., 1998). As it stands, the Roberts et al. (2013) recalibrations for the Judith River Formation are incorrect by nearly half a million years. For example, the sample 84MG8-3-4 was originally published as 78.2 Ma (Goodwin and Deino, 1989). Roberts et al. (2013) recalibrate it as 78.71 Ma, whereas the correct recalibration (see Electronic Supplementary Files 1 and 2) is 79.22 Ma, a difference of half a million years, which can have serious implications for correlation.

It is likely that the same error is made for the Bearpaw, Dinosaur Park, and Oldman Formations as Roberts et al. (2013) also use the Renne et al. (1998) FCT date of 28.02 as their legacy FCT for dates originally published by Eberth and Hamblin (1993) and Eberth and Deino (1992); i.e. before the 1998 paper was published.

When recalibrating ^{40}Ar / ^{39}Ar dates for the Fruitland and Kirtland Formations, New Mexico (originally published by Fassett & Steiner, 1997), Roberts et al. (2013) input the incorrect original (legacy) decay constant (λ) and standard, producing recalibrated dates that are incorrect by nearly a million years (see below). First, the legacy λ used by Roberts et al. (2013) is 4.962E-10/y, which was presumably copied from the bottom of the chart on p. 243 of Fassett & Steiner (1997), where it is clearly referred to as the value of $\lambda\beta$ (ie. the probability of β- decay of 40K to 40Ca), and which is printed below the value $\lambda\varepsilon$ (0.581 E-10/y; probability of electron capture or β+ of 40Kto 40Ar). In this case, the correct λ value to use for recalibration is 5.543 E-10/y (Steiger & Jaeger, 1977), which is the total (λT) of $\lambda\beta$ plus $\lambda\varepsilon$. Second, Roberts et al.

(2013) correctly state that the legacy standard used by Fassett & Steiner (1997) for fluence monitoring was the TCR at 28.32 Ma; however Roberts et al. (2013) then use this number directly for their recalibration to the new FCT standard (28.201; Kuiper et al., 2008). This is incorrect as recalculation must use the same standard mineral (e.g. FCT) for both legacy and recalibrated dates. For the recalculation to be correct, the legacy standard must therefore be the value of FCT that was equivalent to the TCR at 28.32 at the time of the 1997 analysis, which is either FCT = 27.84 Ma or ~28.03 (see Electronic Supplementary File 1), both of which produce recalibrated ages ~1 million years older than the dates presented by Roberts et al. (2013). This miscalibration is all the more surprising as the newly recalibrated dates of Roberts et al. (2013) are actually younger than the original dates, which should have been obviously incorrect as the standards for ^{40}Ar / ^{39}Ar dating have been getting progressively older, and so all recalibrations should produce older dates.

The recalibrated dates of Roberts et al. (2013) were replicated (therefore confirmed) by rerunning the legacy values through the recalibration spreadsheet provided by the Earth-Time institute.

Roberts et al. (2013) correctly recalibrated only seven out of eighteen ^{40}Ar / ^{39}Ar dates, notably five from the Kaiparowits Formation, Utah, and two from the Two Medicine Formation, Montana. All other dates published in their recalibration chart are incorrect and should be discarded.

Discussion

Here I discuss some of the implications of this stratigraphic reassessment. It is beyond the scope of this chapter to summarize everything in the stratigraphic chart, so here I will highlight some of the important changes which might affect geological or paleontological interpretation.

Geology

Judith River Formation – Subdivision Required. The currently undivided Judith River Formation of Montana should probably be upgraded to group status, and subdivided into many constituent formations (or alternatively, merely subdivided into members). This is the case in Canada, where the equivalent unit is the Belly River Group, which is subdivided into the Foremost, Oldman, and Dinosaur Park Formations (Eberth and Hamblin, 1993; Eberth, 2005). The currently undivided status of the Judith River Formation in Montana makes it awkward to discuss lateral equivalents, as there is not an easy terminology that can be used: typically we refer to units as "the Foremost equivalent in Montana" or such, but this is impractical. Furthermore, lack of subdivision causes the base of the Judith River Formation to be strongly diachronous, being ~ 80 Ma in the area around Rudyard (base of the Foremost Formation equivalent), but perhaps as young as 77.5 Ma 200km to the east near Malta (base of the upper Oldman Formation equivalent). This is not the "true" diachronaeity which occurs at the base of (say) a prograding deltaic deposit (e.g. the Fox Hills Formation), but rather it is mostly an artifact of the lack of subdivision. Formal subdivision of the Judith River Formation is beyond the scope of this

work. However, here I informally refer to the lower-Oldman equivalent of the Judith River Formation as the "Rudyard beds", and the upper Oldman Formation equivalent as the "Malta beds" in reference to the geographic locations where these particular parts of section are well exposed. It is a long term goal to formalize these names.

Age of the Aguja Formation, Texas. The Aguja Formation of southwest Texas is typically considered as an Upper Campanian or even Maastrichtian aged unit (e.g. Longrich et al., 2010; Sankey, 2010). This is based on low resolution magnetostratigraphy (Sankey and Gose, 2001), misinterpretation of the formational mechanism for phreatomagmatic volcanism (Longrich et al., 2010), and chemostratigraphic correlation (Nordt et al., 2003). However, detailed review of more reliable published stratigraphic evidence is not supportive of this view. Ammonite remains from the marine tongue which separates the Lower and Upper Shale Members indicate that the Lower Shale Member can be no younger than the Early Campanian *Baculites mclearni* zone (Rowe et al., 1992; Lehman and Tomlinson, 2004). A recently published radiometric date of 69.0 Ma recovered from the overlying Javelina Formation, ~60 m above the formational contact (Lehman et al., 2006) demonstrates that the Upper Shale Member of the Aguja Formation cannot be any younger than this (e.g. *contra* Sankey et al., 2010). Furthermore, the Upper Shale Member of the Aguja Formation contains phreatomagmatic volcanic deposits dated at 76.9 +/- 1.2 Ma (Befus et al., 2008) and 72.6 +/- 1.5 Ma (Breyer et al., 2007), which must have been emplaced after deposition of the Upper Shale Member itself, meaning that it cannot be any younger than 76.9 Ma +/- 1.2 Ma, and is probably much older based on the absence of any obvious

lengthy hiatus separating the Upper Shale Member from the underlying Lower Campanian units. Thus it is likely that the Upper Shale Member is probably Middle Campanian, as shown in the stratigraphic chart (Electronic Supplementary File 1; see included notes for a more detailed account of the evidence). This revision of the age of the Aguja Formation is important as dinosaur taxa from the Upper Shale Member probably represent early, more basal forms of their respective clades (e.g. chasmosaurines), giving key insight into the morphological changes and timing of lineage splitting events (speciation, or true cladogenesis), rather than merely being regional endemic species (e.g. as per the hypothesis of Sampson et al., 2010).

Age of the Javelina Formation, Texas. The Javelina Formation (and basal part of the overlying Black Peaks Formation, sensu Lehman and Coulson, 2002) of southwest Texas has often been considered as Upper Maastrichtian, even uppermost Maastrichtian (e.g. Lawson, 1976; Lehman and Coulson, 2002; Atchley et al., 2004), and is based on comparison of the Javelina Formation dinosaur fauna with that of the Hell Creek and Lance Formations (Lawson, 1976; Lehman, 2001). From this perspective then, it was perhaps surprising when Lehman et al. (2006) published a U-Pb date of 69.0 +/- 0.9 Ma for the middle of the Javelina Formation. This date plots firmly in the lowermost part of the Late Maastrichtian (69.1 - 66.0 Ma; Ogg and Hinnov, 2012). The Javelina Fm is often considered to represent continuous deposition up to and through the K-Pg boundary (e.g. Atchley et al., 2004). If this were the case, then it would mean that the ~90m of deposits overlying the 69 Ma datum (Lehman et al., 2006) represented the 3 m.y. leading up to the K-Pg boundary, and that the ~60 m below might represent 2 m.y. (if average rates of

deposition were assumed). This would seem to be an unusually long period of time for such a thin unit, although not impossible. Alternatively, considerable hiatuses (up to 2 m.y.) are suggested to occur within the Javelina Fm (Nordt et al., 2003). This would be consistent with the findings of Fowler (Chapter 4) which proposes that the recently named ceratopsid dinosaur *Bravoceratops* (collected from the basalmost part of the Javelina Fm; Wick and Lehman, 2013), is probably Upper Campanian in age, similar to the Fruitland and Kirtland Formations of New Mexico. This is of great importance to regional correlation and warrants further consideration.

Thinking about Taxa as Lineages

One of the striking results of the accurate replotting of both geological formations and dinosaur taxa is that dinosaur taxa often from stacked columns of short-duration species which do not overlap stratigraphically. This is the expected pattern produced by anagenesis, the evolutionary mode whereupon lineages or populations transform morphologically through time without branching into multiple contemporaneous species (cladogenesis; also technically, speciation; sensu Cook, 1906). This is an important finding as it suggests that most of the morphological change which we observe through time is probably not related to the multiplication of species. If cladogenesis was the most important driver of morphological change, then we would expect to see stratigraphic overlap between different morphologies. Although this does occur, it is much more rare than stratigraphically successive replacement. In itself this is very interesting as it reduces the likely number of genuine lineage splitting events to maybe only three within the best studied group, chasmosaurine ceratopsids. Further support for this interpretation is that

many stratigraphically intermediate forms are also intermediate in morphology; this is best shown in chasmosaurine ceratopsids of the Upper Maastrichtian Hell Creek Formation (*Triceratops*; Scannella et al., 2014), but also in the *Pentaceratops* lineage chasmosaurines of the Middle to Upper Campanian (Fowler, Chapter 4), and probably *Chasmosaurus* in the Dinosaur Park Formation, Alberta (Fowler, Chapter 4).

The Trouble with "Turnover". Stratigraphic successions of non-overlapping species have previously been referred to as "turnover". Among many examples, Mallon et al. (2012) refer to the rapid succession of different dinosaur species within Dinosaur Provincial Park as turnover; Gates et al. (2013) suggest that a change from *Gryposaurus notablis* in the lower Kaiparowits Formation, Utah, to *G. monumentensis* in the middle Kaiparowits Formation is an example of "intergeneric [sic] faunal turnover" (presumably the authors mean intrageneric). However, if these records are indicative of anagenesis (i.e. non-branching evolution of one form into an another) then they technically cannot be "turnover" by definition. In one of the few publications that attempt a definition of "turnover", Vrba (1985) defines “lineage turnover” as: “includes speciation, extinction and migration, all of which change the composition of species in particular areas.” (p. 229).

Therefore, “turnover” appears to refer to a point where one species disappears from the fossil record, and is replaced by another; apparently implying stasis followed by turnover. The notable exclusion of anagenesis (or any synonym) from this list suggests that it should therefore not be considered as part of turnover events (Vrba, 1985, includes a definition for "phyletic evolution", a synonym of anagenesis, within the same paper, so

she is not using "speciation" in the general sense to mean any change in morphology). Expanding and clarifying upon the concepts and definitions presented in Vrba (1985), Vrba (1993) specifically notes (her Fig. 1) that she considers the phyletic evolution (anagenesis) of one form into another as representing neither species extinction (of the ancestor) nor origination (of the descendant).

This may seem pedantic, but turnover is an important concept used to explain (for example) the replacement of a native species by non-native immigrants, or the classic example of a "turnover pulse", where many turnover events occur to multiple lineages simultaneously, indicating a major immigration event. If turnover is merely used as a synonym of anagenesis, then explanatory power of the term is lost. Anagenesis is not turnover, and researchers need to stop using the term incorrectly. Admittedly, this discussion is only a short and simple treatment of a complex subject; a more detailed account is in preparation.

North-South Biogeography
and Extreme Faunal Endemism. Anagenesis also provides explanatory power challenging the hypothesis of extreme faunal endemism proposed for the Campanian Western Interior. It has been proposed that during the Campanian, the Western Interior of North America was divided into basin-scale faunal provinces, each with a unique fauna (Sampson et al., 2010). This is based primarily on the description of new genera and species of dinosaur collected from the Kaiparowits Formation, Utah (e.g. Gates and Sampson, 2007; Sampson et al., 2010; 2013), and the perception that the Kaiparowits Formation was deposited contemporaneously with other dinosaur-bearing deposits (e.g.

the Dinosaur Park Formation, Alberta; Fruitland and Kirtland Formations, New Mexico). However, recalibration here of critical radiometric dates shows that only the lower part of the Kaiparowits Formation stratigraphically overlaps with the fossiliferous portion of the Dinosaur Park Formation (see Electronic Supplementary File 1). This is important as the lower Kaiparowits Formation does not yield the taxa purportedly endemic to southern Utah, and fragmentary specimens suggest that taxa are shared between the upper part of the Dinosaur Park and lower Kaiparowits Formations (Gates et al., 2013; Fowler, Chapter 4). Here I consider it more likely that differences between dinosaur species found in the Dinosaur Park Formation, and middle Kaiparowits Formation are an artifact of sampling different stratigraphic levels (likely, though not necessarily an anagenetic lineage), rather than biogeographic segregation; at the least the anagenetic hypothesis remains unfalsified. Similarly, differences between the middle Kaiparowits taxa, and those of the Fruitland and Kirtland Formations, New Mexico, are also more parsimoniously explained by the slight difference in age of the units, with the Fruitland and Kirtland being slightly younger than the middle Kaiparowits Formation. Moreover, the recent identification of purportedly southern *Pentaceratops*-lineage chasmosaurines within the Dinosaur Park Fm, Alberta (Longrich, 2014; Fowler, Chapter 4), demonstrates that this lineage was able to move between northern and southern regions in the middle Campanian, further falsifying the extreme faunal endemism hypothesis.

Biostratigraphy. Cobban and Reeside (1952) used the ceratopsid dinosaur *Triceratops* as an index taxon of the latest Maastrichtian. Similarly, dinosaurs were part of the original Land Vertebrate Ages (LVA; Aquilian; Judithian; Edmontonian; Lancian)

described by Russell (1964) before revision into North American Land Mammal Ages (NALMA; Russell, 1975; Lillegraven & McKenna 1986; Cifelli et al., 2004). More recently, dinosaurs have been used to stratigraphically correlate Maastrichtian units of the Southwestern United States (Lawson, 1976; Lehman 1987, 2001) and were utilized by Sullivan and Lucas (2003, 2006) in their definition of the "Kirtlandian": an additional LVA roughly equivalent to the early part of the Bearpaw Shale and positioned in the gap between the Judithian and Edmontonian identified by Russell (1964; 1975).

The demonstration here that individual dinosaur species form stratigraphically stacked sequences of non-overlapping taxa should make them ideal for use as biostratigraphic indicators. It is probably not an exaggeration to claim that the single most biostratigraphically indicative skeletal element that can be found in the Late Cretaceous of North America is the midline portion of the posterior parietal border from an adult chasmosaurine ceratopsid dinosaur (Fowler, Chapter 4). The use of dinosaurs as biostratigraphic indicators might be seen as controversial, since generally dinosaur taxa are known from relatively few specimens and are arguably less abundant than mammals. However, if current hypotheses of rapid evolution are correct (e.g. Horner et al., 1992; Holmes et al., 2001; Scannella et al., 2014; Fowler, Chapter 4), then at least some clades of dinosaurs would seem ideal for biostratigraphic correlation. If we are able to understand the stratigraphic distribution and ontogenetic variation of dinosaurs well enough, then conceivably they may represent the most biostratigraphically informative taxa that we have for terrestrial sediments, potentially at resolutions of ~200Ka (or less; see Electronic Supplementary File 1; Mallon et al., 2012), superior to the resolution

available using mammals or palynomorphs, the other primary options in terrestrial biostratigraphy.

Conclusions

It is critical that paleontologists understand the value of precise stratigraphic placement of specimens. Horner et al. (1992) demonstrated that a better understanding of the mode of evolution in dinosaurs can be achieved with careful stratigraphic analysis. However, all too often in descriptions of new specimens, stratigraphic and geologic data are ignored, or only poorly described. The value of such data in testing paleobiological hypotheses is incomparable.

Similarly, it is clear that care needs to be taken when recalibrating radiometric dates. Although it is time consuming to intensively search older publications for analytical data, a better approximation for the original standards can be found with careful reading and some knowledge of past procedures. Misinformation in the form of mistakenly recalibrated dates could potentially be a source of significant error in the literature.

Future versions of this biostratigraphic chart will include additional stratigraphic units and taxa.

Acknowledgements

Grateful thanks extended to my committee: Jack Horner, David Bowen, David Varricchio, and David Eberth, as well as Liz Freedman Fowler, Warwick and Jackie Fowler, Mark Goodwin, Joe Hartman, Ray Butler, Arthur Bogan, Greg Wilson, Dean

Pearson, John Hoganson, Kirk Johnson, MOR preparators and staff, Bob Sullivan, Spencer Lucas, and everyone at the Digital Library Project. Funding for the Museum of the Rockies graduate student fund was provided by Damaris Waggoner and David Sands. Additional funding was provided by the Welles Fund (UCMP), the Jurassic Foundation, Jackson School of Geosciences (SVP), MSU Dept. Cell Biology and Neuroscience, and MSU College of Letters and Science.

References Cited

Atchley, S. C., L. C. Nordt, and S. I. Dworkin. 2004. Eustatic Control on Alluvial Sequence Stratigraphy: A Possible Example from the Cretaceous-Tertiary Transition of the Tornillo Basin, Big Bend National Park, West Texas, U.S.A. Journal of Sedimentary Research 74:391–404.

Baksi, A. K., D. A. Archibald, and E. Farrar. 1996. Intercalibration of 40Ar39Ar dating standards. Chemical Geology 129:307–324.

Beckinsale, R. D., and N. H. Gale. 1969. A reappraisal of the decay constants and branching ratio of 40K. Earth and Planetary Science Letters 6:289–294.

Befus, K. S., R. E. Hanson, T. M. Lehman, and W. R. Griffin. 2008. Cretaceous basaltic phreatomagmatic volcanism in west Texas: maar complex at Pena Mountain, Big Bend National park. Journal of Volcanology and Geothermal Research 173:245–264.

Breyer, J. A., A. B. Busbey III, R. E. Hanson, K. E. Befus, W. R. Griffin, U. S. Hargrove, and S. C. Bergman. 2007. Evidence for Late Cretaceous Volcanism in Trans□Pecos Texas. The Journal of Geology 115:243–251.

Cebula, G. T., M. J. Kunk, H. H. Mehnert, C. W. Naeser, J. D. Obradovich, and J. F. Sutter. 1986. The Fish Canyon Tuff, a potential standard for the 40Ar-39Ar and fission-track dating methods. Terra Cognita 6:139–140.

Cifelli, R. L., J. J. Eberle, D. L. Lofgren, J. A. Lillegraven, and W. A. Clemens. 2004. Mammalian biochronology of the latest Cretaceous; pp. 21–42 in M. O. Woodburne (ed.), Late Cretaceous and Cenozoic Mammals of North America. Columbia University Press, New York.

Cobban, W. A., and J. B. Reeside. 1952. Correlation of the Cretaceous formations of the Western Interior of the United States. Geological Society of America Bulletin 63:1011–1044.

Cook, O. F. 1906. Factors of species-formation. Science 23:506–507.

Duffield, W. A., and G. B. Dalrymple. 1990. The Taylor Creek Rhyolite of New Mexico: a rapidly emplaced field of lava domes and flows. Bulletin of Volcanology 52:475–487.

Eaton, J. G. 1991. Biostratigraphic framework for the Upper Cretaceous rocks of the Kaiparowits Plateau, southern Utah. Geological Society of America Special Papers 260:47–64.

Eberth, D. A., and A. P. Hamblin. 1993. Tectonic, stratigraphic, and sedimentologic significance of a regional discontinuity in the upper Judith River Group (Belly River wedge) of southern Alberta, Saskatchewan, and northern Montana. Canadian Journal of Earth Sciences 30:174–200.

Evans, D. C., and R. R. Reisz. 2007. Anatomy and relationships of Lambeosaurus magnicristatus, a crested hadrosaurid dinosaur (Ornithischia) from the Dinosaur Park Formation, Alberta. Journal of Vertebrate Paleontology 27:373–393.

Evans, D. C., and M. J. Ryan. 2015. Cranial Anatomy of Wendiceratops pinhornensis gen. et sp. nov., a Centrosaurine Ceratopsid (Dinosauria: Ornithischia) from the Oldman Formation (Campanian), Alberta, Canada, and the Evolution of Ceratopsid Nasal Ornamentation. PLOS ONE 10:e0130007.

Evans, D. C., R. K. Schott, D. W. Larson, C. M. Brown, and M. J. Ryan. 2013. The oldest North American pachycephalosaurid and the hidden diversity of small-bodied ornithischian dinosaurs. Nature Communications 4:1828.

Fowler, D. 2006. Terrestrial Late Cretaceous stratigraphy of North America and the utility of ceratopsids in biostratigraphy. Society of Vertebrate Paleontology Annual Meeting 26:63A.

Freedman Fowler, E. A., and J. R. Horner. 2015. A New Brachylophosaurin Hadrosaur (Dinosauria: Ornithischia) with an Intermediate Nasal Crest from the Campanian Judith River Formation of Northcentral Montana. PLOS ONE 10:e0141304.

Gates, T. A., and S. D. Sampson. 2007. A new species of Gryposaurus (Dinosauria: Hadrosauridae) from the late Campanian Kaiparowits Formation, southern Utah, USA. Zoological Journal of the Linnean Society 151:351–376.

Gates, T. A., E. K. Lund, C. A. Boyd, D. D. DeBlieux, A. L. Titus, D. C. Evans, M. A. Getty, J. I. Kirkland, J. G. Eaton, A. L. Titus, and others. 2013. Ornithopod dinosaurs from the Grand Staircase-Escalante National Monument region, Utah and their role in paleobiogeographic and macroevolutionary studies. Advances in Late Cretaceous Western Interior Basin Paleontology and Geology; pp. 463–481 in At the top of the Grand Staircase: The Late Cretaceous of southern Utah. Indiana University Press.

Goodwin, M. B., and A. L. Deino. 1989. The first radiometric ages from the Judith River Formation (Upper Cretaceous), Hill County, Montana. Canadian Journal of Earth Sciences 26:1384–1391.

Gradstein, F. M., J. G. Ogg, and A. G. Smith. 2004. A Geologic Time Scale 2004. Cambridge University Press, pp.

Gradstein, F. M., J. G. Ogg, M. Schmitz, and G. Ogg. 2012. The Geologic Time Scale 2012 2-Volume Set, 1st ed. Elsevier, 1176 pp.

Hartman, J. H., R. D. Butler, M. W. Weiler, and K. K. Schumaker. 2014. Context, naming, and formal designation of the Cretaceous Hell Creek Formation lectostratotype, Garfield County, Montana. Geological Society of America Special Papers 503:89–121.

Hicks, J. F., J. D. Obradovich, and L. Tauxe. 1995. A New Calibration Point for the Late Cretaceous Time Scale: The (40)Ar/(39)Ar Isotopic Age of the C33r/C33n Geomagnetic Reversal from the Judith River Formation (Upper Creataceous), Elk Basin, Wyoming, USA. Journal of Geology 103:243–256.

Hicks, J. F., K. R. Johnson, J. D. Obradovich, L. Tauxe, and D. Clark. 2002. Magnetostratigraphy and geochronology of the Hell Creek and basal Fort Union Formations of southwestern North Dakota and a recalibration of the age of the Cretaceous-Tertiary boundary. The Hell Creek Formation and the Cretaceous-Tertiary Boundary in the Northern Great Plains: An Integrated Continental Record of the End of the Cretaceous 35–55.

Hicks, J. F., K. R. Johnson, J. D. Obradovich, D. P. Miggins, and L. Tauxe. 2003. Magnetostratigraphy of upper Cretaceous (Maastrichtian) to lower Eocene strata of the Denver Basin, Colorado. Rocky Mountain Geology 38:1–27.

Hicks, J. F., M. Watabe, D. E. Fastovsky, K. R. Johnson, and D. J. Nichols. 1999. Magnetostratigraphic correlation of Late Cretaceous dinosaur-bearing localities, Nemegt Basin, Gobi Desert, Mongolia. Abstracts with Programs - Geological Society of America 31:234.

Holmes, R. B., C. A. Forster, M. Ryan, and K. M. Shepherd. 2001. A new species of Chasmosaurus (Dinosauria: Ceratopsia) from the Dinosaur Park Formation of southern Alberta. Canadian Journal of Earth Sciences 38:1423–1438.

Horner, J. R., D. J. Varricchio, and M. B. Goodwin. 1992. Marine transgressions and the evolution of Cretaceous dinosaurs. Nature 358:59–61.

Izett, G. A., and J. D. Obradovich. 1994. 40Ar/39Ar age constraints for the Jaramillo Normal Subchron. Journal of Geophysical Research 99:2925–2934.

Krystinik, L. F., and B. B. DeJarnett. 1995. Sequence stratigraphy of foreland basin deposits: Outcrop and subsurface examples from the Cretaceous of North America. American Association of Petroleum Geologists Memoir 64:11–25.

Kuiper, K. F., A. Deino, F. J. Hilgen, W. Krijgsman, P. R. Renne, and J. R. Wijbrans. 2008. Synchronizing Rock Clocks of Earth History. Science 320:500–504.

Lanphere, M. A., G. B. Dalrymple, R. J. Fleck, and M. S. Pringle. 1990. Intercalibration of mineral standards for K-Ar and 40Ar/39Ar age measurements. EOS, Transactions of the American Geophysical Union 71:1–658.

Lawson, D. A. 1976. Tyrannosaurus and Torosaurus, Maastrichtian dinosaurs from Trans-Pecos, Texas. Journal of Paleontology 50:158–164.

Lawton, T. F., S. L. Pollock, and R. A. J. Robinson. 2003. Integrating sandstone petrology and nonmarine sequence stratigraphy: application to the Late Cretaceous fluvial systems of Southwestern Utah, USA. Journal of Sedimentary Research 73:389–406.

LeCain, R., W. C. Clyde, G. P. Wilson, and J. Riedel. 2014. Magnetostratigraphy of the Hell Creek and lower Fort Union Formations in northeastern Montana. Geological Society of America Special Papers 503:137–147.

Lehman, T. M. 1987. Late Maastrichtian paleoenvironments and dinosaur biogeography in the western interior of North America. Palaeogeography, Palaeoclimatology, Palaeoecology 60:189–217.

Lehman, T. M. 2001. Late Cretaceous dinosaur provinciality; pp. 310–328 in D. H. Tanke and K. Carpenter (eds.), Mesozoic Vertebrate Life. Indiana University Press, Bloomington, Indiana.

Lehman, T. M., and A. B. Coulson. 2002. A juvenile specimen of the sauropod dinosaur Alamosaurus sanjuanensis from the Upper Cretaceous of Big Bend National Park, Texas. Journal of Paleontology 76:156–172.

Lehman, T. M., and S. L. Tomlinson. 2004. Terlinguachelys fischbecki, a new genus and species of sea turtle (Chelonioidea: Protostegidae) from the Upper Cretaceous of Texas. Journal of Paleontology 78:1163–1178.

Lehman, T. M., F. W. Mcdowell, and J. N. Connelly. 2006. First isotopic (U-Pb) age for the Late Cretaceous Alamosaurus vertebrate fauna of West Texas, and its significance as a link between two faunal provinces. Journal of Vertebrate Paleontology 26:922–928.

Lerbekmo, J. F., and D. R. Braman. 2002. Magnetostratigraphic and biostratigraphic correlation of late Campanian and Maastrichtian marine and continental strata from the Red Deer Valley to the Cypress Hills, Alberta, Canada. Canadian Journal of Earth Sciences 39:539–557.

Lillegraven, J. A., and M. C. McKenna. 1986. Fossil mammals from the "Mesaverde" Formation (late Cretaceous, Judithian) of the Bighorn and Wind River basins, Wyoming: with definitions of late Cretaceous North American land-mammal "ages". American Museum novitates; no. 2840. American Museum Novitates 2840:1–68.

Longrich, N. R. 2014. The horned dinosaurs Pentaceratops and Kosmoceratops from the upper Campanian of Alberta and implications for dinosaur biogeography. Cretaceous Research 51:292–308.

Longrich, N. R., J. Sankey, and D. Tanke. 2010. Texacephale langstoni, a new genus of pachycephalosaurid (Dinosauria: Ornithischia) from the upper Campanian Aguja Formation, southern Texas, USA. Cretaceous Research 31:274–284.

Mallon, J. C., D. C. Evans, M. J. Ryan, and J. S. Anderson. 2012. Megaherbivorous dinosaur turnover in the Dinosaur Park Formation (upper Campanian) of Alberta, Canada. Palaeogeography, Palaeoclimatology, Palaeoecology 350–352:124–138.

McDougall, I., and T. M. Harrison. 1999. Geochronology and Thermochronology by the 40Ar/39Ar Method, 2nd ed. Oxford University Press, 288 pp.

Meyers, S. R., S. E. Siewert, B. S. Singer, B. B. Sageman, D. J. Condon, J. D. Obradovich, B. R. Jicha, and D. A. Sawyer. 2012. Intercalibration of radioisotopic and astrochronologic time scales for the Cenomanian-Turonian boundary interval, Western Interior Basin, USA. Geology 40:7–10.

Miall, A. D., O. Catuneanu, B. K. Vakarelov, and R. Post. 2008. The Western Interior Basin; pp. 329–362 in Andrew D. Miall (ed.), Sedimentary Basins of the World. vol. 5. Elsevier.

Min, K., R. Mundil, P. R. Renne, and K. R. Ludwig. 2000. A test for systematic errors in 40 Ar/39 Ar geochronology through comparison with U/Pb analysis of a 1.1-Ga rhyolite. Geochimica et Cosmochimica Acta 64:73–98.

Nordt, L., S. Atchley, and S. Dworkin. 2003. Terrestrial evidence for two greenhouse events in the latest Cretaceous. GSA Today 13:4–9.

Obradovich, J. D. 1993. A Cretaceous time scale. Evolution of the Western Interior Basin 39:379–396.

Obradovich, J. D. 2002. Geochronology of Laramide synorogenic strata in the Denver Basin, Colorado. Rocky Mountain Geology 37:165–171.

Obradovich, J. D., and W. A. Cobban. 1975. A Time-Scale For The Late Cretaceous Of The Western Interior Of North America. Geological Association of Canada Special Paper 13:31–54.

Ogg, J. G., and L. A. Hinnov. 2012. Cretaceous; pp. 793–853 in The geologic time scale. vol. 2. Elsevier.

Renne, P. R., R. Mundil, G. Balco, K. Min, and K. R. Ludwig. 2010. Joint determination of 40K decay constants and 40Ar□/40K for the Fish Canyon sanidine standard, and improved accuracy for 40Ar/39Ar geochronology. Geochimica et Cosmochimica Acta 74:5349–5367.

Renne, P. R., G. Balco, K. R. Ludwig, R. Mundil, and K. Min. 2011. Response to the comment by WH Schwarz et al. on "Joint determination of 40 K decay constants and 40 Ar□/40 K for the Fish Canyon sanidine standard, and improved accuracy for 40 Ar/39 Ar geochronology" by PR Renne et al.(2010). Geochimica et Cosmochimica Acta 75:5097–5100.

Renne, P. R., C. C. Swisher, A. L. Deino, D. B. Karner, T. L. Owens, and D. J. DePaolo. 1998. Intercalibration of standards, absolute ages and uncertainties in 40Ar/39Ar dating. Chemical Geology 145:117–152.

Renne, P. R., A. L. Deino, R. C. Walter, B. D. Turrin, C. C. Swisher, T. A. Becker, G. H. Curtis, W. D. Sharp, and A.-R. Jaouni. 1994. Intercalibration of astronomical and radioisotopic time. Geology 22:783–786.

Rivera, T. A., M. Storey, C. Zeeden, F. J. Hilgen, and K. Kuiper. 2011. A refined astronomically calibrated 40 Ar/39 Ar age for Fish Canyon sanidine. Earth and Planetary Science Letters 311:420–426.

Roberts, E. M., A. L. Deino, and M. A. Chan. 2005. 40Ar/39Ar age of the Kaiparowits Formation, southern Utah, and correlation of contemporaneous Campanian strata and vertebrate faunas along the margin of the Western Interior Basin. Cretaceous Research 26:307–318.

Roberts, E. M., S. D. Sampson, A. L. Deino, S. Bowring, and R. Buchwaldt. 2013. The Kaiparowits Formation: a remarkable record of Late Cretaceous terrestrial environments, ecosystems and evolution in Western North America; pp. 85–106 in At the Top of the Grand Staircase: The Late Cretaceous of Southern Utah. Edited

by AL Titus and MA Loewen. Indiana University Press, Bloomington. Indiana University Press.

Rogers, R. R., C. C. Swisher III, and J. R. Horner. 1993. 40Ar/39Ar age and correlation of the nonmarine Two Medicine Formation (Upper Cretaceous), northwestern Montana, USA. Canadian Journal of Earth Sciences 30:1066–1075.

Rowe, T., R. L. Cifelli, T. M. Lehman, and A. Weil. 1992. The Campanian Terlingua local fauna, with a summary of other vertebrates from the Aguja Formation, Trans-Pecos Texas. Journal of Vertebrate Paleontology 12:472–493.

Russell, L. S. 1964. Cretaceous non-marine faunas of northwestern North America. Life Sciences Contributions, Royal Ontario Museum 61:1–21.

Russell, L. S. 1975. Mammalian faunal succession in the Cretaceous System of western North America. Geological Association of Canada Special Paper 13:137–161.

Sageman, B. B., B. S. Singer, S. R. Meyers, S. E. Siewert, I. Walaszczyk, D. J. Condon, B. R. Jicha, J. D. Obradovich, and D. A. Sawyer. 2014. Integrating 40Ar/39Ar, U-Pb, and astronomical clocks in the Cretaceous Niobrara Formation, Western Interior Basin, USA. Geological Society of America Bulletin 126:956–973.

Sampson, S. D., and E. C. Alexander Jr. 1987. Calibration of the interlaboratory 40Ar/39Ar dating standard, MMhb-1. Chemical Geology: Isotope Geoscience Section 66:27–34.

Sampson, S. D., E. K. Lund, M. A. Loewen, A. A. Farke, and K. E. Clayton. 2013. A remarkable short-snouted horned dinosaur from the Late Cretaceous (late Campanian) of southern Laramidia. Proceedings of the Royal Society of London B: Biological Sciences 280:20131186.

Sampson, S. D., M. A. Loewen, A. A. Farke, E. M. Roberts, C. A. Forster, J. A. Smith, and A. L. Titus. 2010. New Horned Dinosaurs from Utah Provide Evidence for Intracontinental Dinosaur Endemism. PLoS ONE 5:e12292.

Sankey, J. T. 2010. Faunal composition and significance of high-diversity, mixed bonebeds containing Agujaceratops mariscalensis and other dinosaurs, Aguja Formation (Upper Cretaceous), Big Bend, Texas. New Perspectives on Horned Dinosaurs. The Royal Tyrrell Museum Ceratopsian Symposium 520–37.

Sarna-Wojcicki, A. M., and M. S. Pringle Jr. 1992. Laser-fusion 40 Ar/39 Ar ages of the Tuff of Taylor Canyon and Bishop Tuff, E. California-W. Nevada. Eos Trans. AGU 73:43.

Scannella, J. B., D. W. Fowler, M. B. Goodwin, and J. R. Horner. 2014. Evolutionary trends in Triceratops from the Hell Creek Formation, Montana. Proceedings of the National Academy of Sciences 111:10245–10250.

Schmitz, M. D. 2012. Radiometric Ages used in GTS2012; pp. 1045–1082 in The Geological Time Scale. Elsevier.

Schmitz, M. D., and S. A. Bowring. 2001. U-Pb zircon and titanite systematics of the Fish Canyon Tuff: an assessment of high-precision U-Pb geochronology and its application to young volcanic rocks. Geochimica et Cosmochimica Acta 65:2571–2587.

Schoene, B., J. L. Crowley, D. J. Condon, M. D. Schmitz, and S. A. Bowring. 2006. Reassessing the uranium decay constants for geochronology using ID-TIMS U–Pb data. Geochimica et Cosmochimica Acta 70:426–445.

Singer, B. S., B. R. Jicha, R. S. Coe, and N. Mochizuki. 2012. An Earthtime Chronology for the Matuyama-Brunhes Geomagnetic Field Reversal. AGU Fall Meeting Abstracts 21.

Sprain, C. J., P. R. Renne, G. P. Wilson, and W. A. Clemens. 2014. High-resolution chronostratigraphy of the terrestrial Cretaceous-Paleogene transition and recovery interval in the Hell Creek region, Montana. Geological Society of America Bulletin 127:393–409.

Steiger, R., and E. Jäger. 1977. Subcommission on geochronology: convention on the use of decay constants in geo-and cosmochronology. Earth and Planetary Science Letters 36:359–362.

Sullivan, R. M., and S. G. Lucas. 2003. The Kirtlandian, a new land-vertebrate “age” for the Late Cretaceous of western North America. New Mexico Geological Society Guidebook 54:369–377.

Sullivan, R. M., and S. G. Lucas. 2006. The Kirtlandian land-vertebrate “age”–faunal composition, temporal position and biostratigraphic correlation in the nonmarine Upper Cretaceous of western North America. New Mexico Museum of Natural History and Science Bulletin 35:7–29.

Villeneuve, M. 2004. Radiogenic Isotope Geochronology; pp. in A Geologic Time Scale 2004. Cambridge University Press.

Vrba, E. S. 1985. Environment and evolution: alternative causes of the temporal distribution of evolutionary events. South African Journal of Science 81:229–236.

Vrba, E. S. 1993. Turnover-pulses, the Red Queen, and related topics. American Journal of Science 293:418–452.

Wick, S. L., and T. M. Lehman. 2013. A new ceratopsian dinosaur from the Javelina Formation (Maastrichtian) of West Texas and implications for chasmosaurine phylogeny. Naturwissenschaften 100:667–682.

Zanno, L. E., D. J. Varricchio, P. M. O'Connor, A. L. Titus, and M. J. Knell. 2011. A new troodontid theropod, Talos sampsoni gen. et sp. nov., from the Upper Cretaceous Western Interior Basin of North America. PLOS ONE 6:e24487.

CHAPTER FOUR

TRANSITIONAL EVOLUTIONARY FORMS AND STRATIGRAPHIC TRENDS IN CHASMOSAURINE CERATOPSID DINOSAURS

Contribution of Authors and Co-Authors

Manuscript in Chapter 4

Author: Denver W. Fowler

Contributions: Conceived and designed the study, performed experiments, analyzed data, and wrote the manuscript.

Co-author: John B. Scannella

Contributions: Analyzed data.

Co-author: John R. Horner

Contributions: Conceived the study, contributed materials and analytical tools.

Manuscript Information Page

Denver W. Fowler, John B. Scannella, John R. Horner
Status of Manuscript:
_x_Prepared for submission to a peer-reviewed journal
___Officially submitted to a peer-reviewed journal
___Accepted by a peer-reviewed journal
___Published in a peer-reviewed journal

Abstract

Three new chasmosaurines from the Kirtland Formation (~75.0 - 73.4 Ma), New Mexico, form morphological and stratigraphic intermediates between *Pentaceratops* (~74.7 - 75Ma, Fruitland Formation, New Mexico) and *Anchiceratops* (~72 - 71Ma, Horseshoe Canyon Formation, Alberta). The new specimens exhibit gradual enclosure of the parietal embayment that characterizes *Pentaceratops*, providing support for the phylogenetic hypothesis that *Pentaceratops* and *Anchiceratops* are closely related. This stepwise change of morphologic characters observed in chasmosaurine taxa that do not overlap stratigraphically is supportive of evolution by anagenesis. Recently published hypotheses that place *Pentaceratops* and *Anchiceratops* into separate clades are not supported. This phylogenetic relationship demonstrates unrestricted movement of large-bodied taxa between hitherto purported northern and southern provinces in the Late Campanian, weakening support for the hypothesis of extreme faunal provincialism in the Late Cretaceous Western Interior.

Keywords

Dinosaur; Cretaceous; *Pentaceratops*; *Anchiceratops*; diversity; anagenesis.

Introduction

Intermediate or “transitional” fossils are an expected product of evolution, and are especially celebrated when they occur within major evolutionary transitions (Anderson and Sues, 2007; Wellnhofer, 2010; Daeschler et al., 2006). However, morphological

intermediates also occur within the 'normal' evolution that comprises the majority of the fossil record giving us key insight into evolutionary mode, tempo, and trends, but also providing ancient examples of how organisms respond to changes in their environment, something of paramount concern to modern biologists (Malmgren et al., 1984; Hull and Norris, 2009; Aze et al., 2011; Pearson and Ezard, 2014; Scannella et al., 2014; Tsai and Fordyce, 2015).

The majority of intermediate fossils are described from the invertebrate fossil record, especially plankton (e.g. Malmgren et al., 1984; Pearson and Ezard, 2014), mainly due to the large sample sizes afforded by their abundance (although it has also been suggested that marine invertebrates might be more susceptible to phyletic gradualism, sensu Eldredge and Gould, 1972, due to a lack of barriers to geneflow; Lohmann and Malmgren, 1983; Hull and Norris, 2009). However, marine invertebrates may not provide an appropriate analogue for the evolution of large-bodied terrestrial vertebrates. Although terrestrial vertebrates have an admittedly poorer fossil record, an understanding of how large-bodied vertebrates respond to sea-level and climate change is an increasingly prevalent concern, and seeking historical examples may shed light on potential future issues surrounding current anthropological effects on global climate and environments.

In dinosaurs, recognition of morphologic intermediates is confounded by a typically sparse fossil record, characterized by taxa that may be widely separated in space and time, and often known only from single specimens. Despite this, in the Upper Cretaceous rocks of North America a combination of increasingly intensive sampling and

newly refined stratigraphy is beginning to fill in gaps in the dinosaur record. This is revealing hitherto unknown morphotaxa that link previously disparate or misunderstood morphologies, and/or define new 'end-members' that extend or emphasize stratigraphic morphological trends (Horner et al., 1992; Sampson, 1995; Holmes et al., 2001; Ryan and Russell, 2005; Wu et al., 2007; Currie et al., 2008; Sullivan and Lucas, 2010; Evans et al., 2011; Scannella and Fowler, 2014; Scannella et al., 2014). Such discoveries are challenging previously held assumptions about the mode and tempo of dinosaur evolution (Horner et al., 1992; Scannella et al., 2014), and providing critical insight into the responses of terrestrial megafauna to changes in climate and sea level (Horner et al., 1992).

Central to this emergent understanding are the Ceratopsidae: a North American (although see Xu et al., 2010) clade of Late Cretaceous ornithischian dinosaurs that exhibit famously elaborate cranial display structures (Hatcher et al., 1907). Differences in size or expression of these various horns, bosses, and parietosquamosal frills are used to diagnose different taxa, with ~63 species historically described within two families (the 'short-frilled' Centrosaurinae and 'long-frilled' Chasmosaurinae; Lambe, 1915), ~25 of which have been erected in the past 10 years. This explosion of new taxa has led some researchers (Sampson and Loewen, 2010; Sampson et al., 2010) to propose that ceratopsids radiated through the Campanian-Maastrichtian, exhibiting extreme faunal endemism where numerous defined species are suggested to have been contemporaneous, but lived in very restricted geographic ranges. However, it is becoming clear that differences in cranial morphology are not always representative of (contemporaneous)

diversity. Cranial morphology has been shown to change significantly through ontogeny (Horner and Goodwin, 2006; Scannella and Horner, 2010), such that many historical taxa are now considered growth stages of previously recognized forms. Furthermore, studies conducted within single depositional basins have shown ceratopsid taxa forming stacked chronospecies that do not overlap in time, demonstrating that cranial morphology evolves rapidly (recognizably in as little as a few hundred thousand years), if not constantly, and supporting the hypothesis that much of what has been perceived as diversity might instead represent intermediate morphospecies within evolving anagenetic lineages (Horner et al., 1992; Holmes et al., 2001; Ryan and Russell, 2005; Mallon et al., 2012; Scannella et al., 2014; Fowler, Chapter 3).

Intermediate Campanian chasmosaurine ceratopsids were predicted by Lehman (1998; adapted in Figure 4.1), who showed successive morphospecies of the Canadian genus *Chasmosaurus* (Dinosaur Park Formation, Alberta; Middle to Upper Campanian) with a progressively shallowing embayment of the posterior margin of the parietosquamosal frill. This was contrasted with an opposite trend seen in *Pentaceratops sternbergii* (Fruitland Formation, New Mexico; Upper Campanian) to *Anchiceratops ornatus* (Horseshoe Canyon Formation, Alberta; Lower Maastrichtian), whereupon the midline embayment deepens and eventually closes (Lehman, 1993; Lehman, 1998; later explicitly illustrated by Fowler, 2010; Fowler et al., 2011; and Wick and Lehman, 2013). This hypothesis matched the stratigraphic occurrence of taxa known at the time, and is supported by new taxa described since 1998 (*Vagaceratops* (*Chasmosaurus*) *irvinensis*; *Kosmoceratops richardsoni*; *Utahceratops gettyi*; and *Bravoceratops polyphemus*;

Holmes et al., 2001; Sampson et al., 2010; Fowler, 2010; Fowler et al., 2011; Wick and Lehman, 2013; although see Appendix C).

However, a recent phylogenetic analysis of chasmosaurines (Sampson et al., 2010) proposed a starkly different relationship (Figure 4.2) where a clade comprising *Vagaceratops* (*Chasmosaurus*) *irvinensis* and *Kosmoceratops richardsoni* instead formed the sister group to a clade composed of *Anchiceratops* and all other Maastrichtian chasmosaurines. This is significant as it implies that the clade [*Vagaceratops* + *Kosmoceratops*] is more closely related to *Anchiceratops* than is *Pentaceratops* (i.e. the opposite to the relationship suggested by Lehman, 1993; 1998; Fowler, 2010; Fowler et al., 2011; Wick and Lehman, 2013). Indeed, the poorly known chasmosaurine *Coahuilaceratops magnacuerna* formed a second successive sister taxon to the [*Vagaceratops* + *Kosmoceratops*] + [*Anchiceratops*] clade, suggesting that *Pentaceratops* is even more distantly related. Equally surprising is that Sampson et al. (2010) recover a *Chasmosaurus* clade [*C. russelli* + *C. belli*] that is separated from [*Vagaceratops* + *Kosmoceratops*] despite *Vagaceratops* (*Chasmosaurus*) *irvinensis* being originally recovered as the most derived member of a *Chasmosaurus* clade by Holmes et al. (2001), and the existence of morphological intermediates between *C. belli* and *V. irvinensis* (e.g. cf. *C. belli* specimen YPM 2016; see later). Subsequent analyses by Mallon et al. (2011; 2014; using an altered version of the data matrix from Sampson et al., 2010) recovered cladograms (Figure 4.2) that appear “upside down”, with the Lower Maastrichtian taxa *Anchiceratops* and *Arrhinoceratops* occurring in a basal polytomy, and some of the stratigraphically oldest taxa forming the most derived clade (Middle to Upper Campanian

[*Chasmosaurus belli* + *Chasmosaurus russelli*]). This configuration would require considerable ghost lineages for many clades, which does not seem likely given the relatively good fossil record of chasmosaurines, and the comparatively smooth morphological and stratigraphic transition presented by Lehman (1993; 1998). Mallon et al. (2014; p.63) acknowledged their unlikely topology, stating that "while the monophyly of the Chasmosaurinae is secure, its basic structure is currently in a state of flux and requires further attention". This can only be resolved by a combination of character reanalysis and the discovery and description of new specimens intermediate in morphology between currently recognized taxa.

Here we describe new chasmosaurine material (including new taxa *Navajoceratops sullivani*, holotype SMP VP-1500; and *Terminocavus sealyi*, holotype NMMNH P-27468) from the Kirtland Formation of New Mexico that forms stratigraphic and morphologic intermediates between *Pentaceratops* and *Anchiceratops*. The new taxa are based on fragmentary specimens, but they include the posterior border of the parietal, the most diagnostic element for Campanian chasmosaurines. Geometric morphometric analysis of new and previously described material supports the hypothesis that the posterior embayment of the parietal deepens and closes in on itself over ~ 2 million years (Lehman, 1993; 1998; Fowler, 2010; Fowler et al., 2011; Wick and Lehman, 2013), and that *Vagaceratops* and *Kosmoceratops* probably represent the most derived and successively youngest members of a *Chasmosaurus* lineage. A phylogenetic reanalysis (using a character matrix revised from Mallon et al., 2014) is less conclusive, but recovers new taxa *Navajoceratops* and *Terminocavus* as successive stem taxa leading to

Anchiceratops and more derived chasmosaurines, and suggests a deep split within Chasmosaurinae that occurs before the Middle Campanian. This is supportive of true speciation by vicariance occurring relatively basally within Chasmosaurinae, followed by more prolonged periods of anagenetic (unbranching) evolution (as previously suggested by Horner et al., 1992, and Scannella et al., 2014). Recent hypotheses of extreme faunal endemism (Sampson et al., 2010) are not supported; however, it appears likely that continental-scale latitudinal faunal variation occurred in the Campanian. The new specimens document incipient paedomorphic trends that come to characterize more derived chasmosaurines in the Maastrichtian, such as *Triceratops*.

Institutional Abbreviations

AMNH, American Museum of Natural History, New York; CMN (was NMC), Canadian Museum of Nature, Ottawa, Ontario; MNA, Museum of Northern Arizona, Flagstaff; NMMNH, New Mexico Museum of Natural History and Science, Albuquerque; OMNH, Oklahoma Museum of Natural History, Norman; PMU, Paleontologiska Museet, Uppsala University, Sweden; SDNHM, San Diego Natural History Museum, California; SMP, State Museum of Pennsylvania, Harrisburg; UKVP, University of Kansas, Lawrence; UMNH, Utah Museum of Natural History, Salt Lake City; UNM, University of New Mexico, Albuquerque; USNM, United States National Museum, Smithsonian Institution, Washington D.C.; UTEP, University of Texas at El Paso.

Anatomical Abbreviations

Ep, epiparietal numbered from 1 to 3 (e.g. ep1) from medial to lateral; es, episquamosal.

Geological Setting

All newly described material was collected from the Upper Campanian Fruitland and Kirtland Formations of San Juan Basin, New Mexico (Figures 4.3-4.5). Campanian sediments of the San Juan Basin record transition from the marine Lewis Shale through the shallow marine Pictured Cliffs Sandstone into the nonmarine Fruitland and Kirtland formations (Bauer, 1916; Hunt et al., 1992; Lucas et al., 2006). The Fruitland Formation rests conformably upon the Pictured Cliffs Sandstone, and comprises 40-90 m of sandstones, occasional mudstones, and extensive thick coals deposited in a coastal plain setting. The overlying Kirtland Formation is ~260-360 m thick, and is less sandy, with only occasional thin coals, being similarly deposited on a coastal plain.

The stated variation in thickness of the Fruitland and Kirtland is in part due to the general thinning of San Juan Basin sediment fill towards the southeast, but also because many different definitions of the Fruitland and Kirtland Formations have been offered since their original description by Bauer (1916; Figure 4.4). Mainly this concerns the definition of the lower formational contact between the Fruitland and Kirtland formations, and the upper contact between the Kirtland and Ojo Alamo formations. The result is a complex and confusing stratigraphic nomenclature, which is further complicated by the fact that geological maps of the San Juan Basin do not all use the

same formational definitions, and commonly vary depending on the scale of the maps used, and when they were produced. However, historical stratigraphic usage must be understood if the stratigraphic positions of historical specimens of cf. *Pentaceratops* are to be determined, as most were collected from a stratigraphic zone considered as either the upper Fruitland Formation, or lowermost Kirtland Formation (Appendix C).

Fruitland – Kirtland Formational Boundary

Three definitions of the boundary between the Fruitland and Kirtland formations are commonly encountered in the literature (Figure 4.4), concerning either the highest economic coal, or a horizon known as the Bisti Bed sandstone. In the original definition, Bauer (1916) described the boundary between the Fruitland and Kirtland formations as transitional, and chose to place the formational boundary at the top of a consistent sandy interval (later named the Bisti Bed sandstone; Hunt and Lucas, 1992; Lucas et al., 2006). This definition was used in Bauer's 1916 geological map of the San Juan Basin, and in the current 250k map of the Shiprock quadrangle that covers most of the San Juan Basin (USGS I-345; O'Sullivan and Beikman, 1963).

Fassett and Hinds (1971) redefined the Fruitland - Kirtland formational boundary as occurring at the top of the uppermost "economic" coal bed, which is ~20-30 m stratigraphically lower than the definition of Bauer (1916). This also effectively restricted the Fruitland Formation to the unfossiliferous coal-zone, which is potentially confusing since most of the historical *Pentaceratops* specimens were cited as having been collected in the Fruitland Formation (see Materials). Fassett and Hinds' (1971) definition was used to produce the currently available 24k USGS geological maps of the area (e.g. O'Sullivan

et al., 1979; Weide et al., 1979) and most later maps (100k and 250k) are dependent on these for data.

The coal-based definition of Fassett and Hinds (1971) was criticized by Hunt and Lucas (1992) because of lateral inconsistency of the coals, and because thin coal horizons in the Kirtland Formation might be misinterpreted to be part of the Fruitland Formation, leading to confusion. Indeed, this error occurred during stratigraphic placement of the radiometric dates recovered by Fassett and Steiner (1997; see later), and has led to major inconsistencies in the mapping of the Fruitland - Kirtland boundary in at least some of the 24k USGS maps (for example, see Burnham Trading Post quadrangle; Scott et al. 1979). Hunt and Lucas (1992) therefore proposed using the base of the Bisti Bed sandstone as the Fruitland - Kirtland formational boundary, which is closer to Bauer's original (1916) meaning. Finally, Hunt and Lucas (2003) subdivided the Fruitland Formation into two members: the Neh-nah-ne-zad Member (13 - 30 m thick), comprising the almost completely unfossiliferous lower portion with economic coals (effectively equivalent to the less inclusive "Fruitland Formation" of Fassett and Hinds, 1971); and the Fossil Forest Member (12 - 25 m thick), comprising the fossiliferous mudstones and sandstones immediately underlying the Kirtland Formation.

Kirtland Formation, Internal Stratigraphy

After redefining the Fruitland - Kirtland Formation contact as occurring at the base of the Bisti Bed, Hunt and Lucas (1992) formalized the members of the Kirtland Formation, renaming the lower shale member, Farmington Sandstone Member, and upper shale member (Bauer, 1916), as the Hunter Wash Member, Farmington Member, and De-

na-zin Member, respectively. It is worth noting that, although all members thin to the southeast, the Farmington Member is especially variable in thickness, being up to ~140 m thick in the northern part of the basin, but pinching out entirely to the southeast at Ahshislepah Wash (Bauer, 1916). This accounts for differences that are sometimes encountered between published measured sections. It is important to note that Hunt and Lucas (1992) also chose to follow Baltz et al. (1966; Figure 4.4) in including the dinosaur-bearing part of the overlying Ojo Alamo Formation (the Maastrichtian Naashoibito Member) as the uppermost member of the Kirtland Formation. This was later rescinded (Sullivan et al., 2005; Lucas et al., 2006; Figure 4.4).

Age

A series of five Ar / Ar radiometric dates for the Fruitland and Kirtland formations were published by Fassett and Steiner (1997). The lithostratigraphic positions of these dated horizons were later revised (Sullivan et al., 2005; Sullivan and Lucas, 2006) such that ashes 2 and 4, previously considered to occur in the Fruitland Formation, were shown to actually occur in the Kirtland Formation (stratigraphic positions of the other ashes were not affected). The radiometric dates of Fassett and Steiner (1997) were recalibrated by Fowler (Chapter 3; Ar / Ar standard and decay constant pairing of Kuiper et al., 2008; and Min et al., 2000; respectively) to show the Fruitland through Kirtland formations were deposited between 76.0 and 73.4 Ma (Figures 4.3, 4.5). Note that these dates were previously recalibrated by Roberts et al. (2013) using incorrect Ar / Ar standards and decay constants, which consequently yielded ages ~1 m.y. too young (see Fowler, Chapter 3, for details).

Magnetostratigraphy of the Fruitland and Kirtland formations has been controversial, although there is now a general consensus. The Fruitland and Kirtland formations are mostly of normal polarity, correlated to the upper part of C33n (79.900 - 74.309 Ma; Ogg, 2012). Stratigraphic placement of the C33n - C32r boundary within the San Juan Basin is slightly variable between workers. Lucas et al. (2009) place the C33n - C32r boundary in the lowermost De-na-zin Member, whereas Fassett (2009) places it in the upper part of the Farmington Member. Regarding the current study, there is little meaningful difference between these interpretations.

Maps and Stratigraphic Positioning of San Juan Basin Fossils

To assess stratigraphic position of San Juan Basin specimens (Figure 4.5), locality data was plotted in Google Earth with geologic and topographic maps superimposed on the aerial photographs (Figure 4.3). The locality coordinates of recalibrated radiometric dates were also plotted (Fassett and Steiner, 1997; Sullivan et al., 2005; Sullivan and Lucas, 2006; recalibrations by Fowler, Chapter 3). No geological maps are available that use the current stratigraphic definitions of the Fruitland and Kirtland formations (Sullivan et al., 2005; Lucas et al., 2006), so the main area of the geologic map (Figure 4.3) is traced from the current 250k map of the Shiprock quadrangle (USGS I-345; O'Sullivan and Beikman, 1963) which uses the definitions of Bauer (1916) and covers most of the Fruitland and Kirtland Formation outcrop in the San Juan Basin. Unfortunately, the southeastern portion of the basin (Ahshislepah, Kimbeto, and Tsosie washes) is not covered by a geological map that uses the Bauer (1916) definitions. This issue concerns

only the Fruitland-Kirtland boundary in Ahshislepah Wash, which contains the type locality (SMP Loc. 281; "Denver's Blowout") of *Navajoceratops sullivani* (Figure 4.3A), and some specimens collected by Charles H. Sternberg in the 1920s. To reconcile this, I plotted a tentative Fruitland-Kirtland boundary (sensu Bauer, 1916) based on aerial photography and the position of a prominent sandstone bluff (SMP Loc. 396; "Bob's bloody bluff") present ~0.7 km west-southwest of SMP Loc. 281, which is considered to represent the Bisti Bed sandstone (Sullivan, 2006).

Specimen locality data was retrieved either from the published literature or from institutional specimen databases. Details specific to the placement of individual specimens can be found in the "Materials" section, and in Appendix C. Some localities were historically only recorded as low-resolution Township / Range data, and these are therefore plotted as squares depicting the area of collection.

Relative stratigraphic position of specimens was inferred from the map by position relative to geological unit boundaries, topography, and trigonometric calculations based on a dip of 1-3° basinwards (northeast; Bauer, 1916). Stratigraphic height of the *Navajoceratops* holotype (SMP VP-1500) locality (SMP loc. 281) was calculated by comparison between the locality and two marker horizons. The uppermost prominent coal of the Fruitland Formation occurs ~1800 m to the southwest, 12.1 m topographically lower (Weide et al., 1979). The top of the Bisti Bed sandstone occurs at "Bob's Bloody Bluff" (SMP loc. 396; Sullivan, 2006) ~700 m west-southwest (equivalent to ~500m parallel to dip) ~3 m topographically higher. Stratigraphic height of the *Terminocavus* holotype (NMMNH P-27468) locality (NMMNH L-3503) was calculated

from difference in elevation between the locality and two radiometrically dated horizons. Ash 2 (75.02 ± 0.13 Ma) occurs 3000 m southwest, and 30 m lower topographically. Ash 4 (74.57 ± 0.62) occurs 2200 m northeast, and 9 m higher topographically (ash dates recalibrated from Fassett and Steiner, 1997, by Fowler, Chapter 3)

Stratigraphic Terminology

Through necessity, colored geological units on the map (Figure 4.3) use formational boundaries defined by Bauer et al. (1916), but otherwise the map and manuscript follow the most recent terminology of Sullivan et al. (2005), and Lucas et al. (2006; see Figures 4.4 and 4.5). Other than the names of the individual members, the only difference between Bauer (1916) and the most recent definitions are that Bauer places the Fruitland - Kirtland boundary at the top of the Bisti Bed sandstone, whereas the current definition places it at the base.

Materials and Methods

Interbasinal Correlation

Interbasinal correlation is necessary to ascertain the relative stratigraphic positions of chasmosaurine taxa that occur in different sedimentary basins across the Western Interior (e.g. *Utahceratops gettyi*, Kaiparowits Formation, Utah; Sampson et al., 2010). Correlating between sedimentary basins is fraught with problems, and depends upon accurate chronostratigraphic and biostratigraphic data being available. Here I use the chronostratigraphic framework laid out by Fowler (Chapter 3), which integrates recalibrated radiometric dates with other chronostratigraphic data (e.g. biostratigraphy,

magnetostratigraphy) derived from The Geologic Time Scale 2012 (Gradstein et al., 2012). All radiometric dates are calibrated to the standard - decay constant pairing of Kuiper et al. (2008) and Min et al. (2000). A similar attempt to use recalibrated radiometric dates to correlate between basins by Roberts et al. (2013) used many incorrect standard - decay constant pairings and their proposed dates and correlations are therefore unusable (see Fowler, Chapter 3).

Fossil Materials and Accepted Taxonomy

In order to make proper comparisons with the new specimens, it is necessary to review the taxonomy, stratigraphy, and morphology of historical and type specimens of *Pentaceratops* and related chasmosaurines. These details are discussed at length in Appendix C for specimens with either diagnostic parietal material, important stratigraphic occurrence, or for specimens that are holotypes. Only a brief summary is provided here. The relevant specimens are listed in Table 4.1.

One of the problems facing any new analysis which includes the taxon *Pentaceratops sternbergii* is that although the holotype (AMNH 6325; Osborn, 1923) is a mostly complete skull, it unfortunately lacks the diagnostic posterior end of the parietal, making it difficult to reliably refer other specimens to the taxon. However, it should be noted that the taxonomic importance of the posterior bar was not strongly emphasized until the current work, and so many specimens have been historically referred to *P. sternbergii* by other researchers (see Appendix C for a list). Therefore, I have neccessarily reviewed whether such taxonomic referrals are appropriate, and consequently revised the referrals of many specimens, while simultaneously attempting

to preserve some semblance of taxonomic stability (especially regarding the original material; see Results, and some discussion in Appendix C). I also take into account that some specimens are currently under study by other workers (J. Fry, S. G. Lucas, H. N. Woodward, pers. comm.), and so new names are not yet erected for some specimens. In summary, I follow Lull (1933) and all subsequent workers in considering AMNH 1624 and AMNH 1625 as specimens of cf. *P. sternbergii*. However, I move referred specimens MNA Pl.1747 and UKVP 16100 into aff. *Pentaceratops* n. sp. along with the new specimen NMMNH P-37880. Partial skull SDMNH 43470 is referred to aff. *Pentaceratops* sp., due to uncertainty concerning the relationship of its stratigraphic position and immature ontogenetic condition to morphology. Many other fragmentary specimens previously referred to *P. sternbergii* (e.g. AMNH 1622) are not considered diagnostic and so are here considered Chasmosaurinae indet.. I follow Lehman (1998, the original description) in considering the large skull and skeleton OMNH 10165 as aff. *Pentaceratops* sp., and not the new taxon *Titanoceratops ouranos* (Longrich, 2011). I show that the autapomorphies used to diagnose the new taxon *Pentaceratops aquilonius* (Longrich, 2014) are invalid, and it should be considered a nomen dubium.

Concerning chasmosaurines other than *Pentaceratops*, I follow Maidment and Barrett (2011) and Mallon et al. (2012) in considering *Mojoceratops perifania* (Dinosaur Park Formation, Alberta; Longrich, 2010) as a junior synonym of *Chasmosaurus russelli*. However the taxonomy of *C. russelli* has its own priority problems (see Appendix C) and as such specimens will be referred to as "*Chasmosaurus russelli*" and specimen numbers given. A revision of the epiparietal numbering system is used for *Vagaceratops*

(*Chasmosaurus*) *irvinensis* (Dinosaur Park Formation, Alberta; Holmes et al., 2001; Sampson et al., 2010) and *Kosmoceratops richardsoni* (Kaiparowits Formation, Utah; Sampson et al., 2010), based on comparison to specimens of *Chasmosaurus*, especially *C. belli* YPM 2016 (Dinosaur Park Formation, Alberta). *Bravoceratops polyphemus* (Javelina Formation, Texas; Wick and Lehman, 2013) is shown to be a *nomen dubium* as the element identified as the posterior end of the parietal median bar is reidentified as the anterior end and is shown to be undiagnostic, although it probably originated from a chasmosaurine less derived than Kirtland Taxon C, NMMNH P-33906 (described below).

Justification for naming the new taxa as monospecific genera (rather than assigning them as new species within *Pentaceratops*) is given in Appendix E.

Lehman (1998) makes the technical suggestion that *Pentaceratops sternbergii* should be spelled as *Pentaceratops sternbergi*. This has not been followed by most subsequent workers (e.g. Dodson et al., 2004), thus here I use the original spelling of Osborn (1923).

Phylogenetic Analysis

Phylogenetic analysis was conducted using an adapted version of the character matrix from Mallon et al. (2014), which itself was adapted from Wick and Lehman (2013), Mallon et al. (2011), and originally, Sampson et al. (2010). The character matrix was edited in Mesquite 3.02 (Maddison and Maddison, 2015). Edits were made to 22 characters, including definitions, character states, and previous codings. Four new characters were added concerning the morphology of the parietal, making a total of 156 characters (see Appendix D for details of changes made and new characters). The taxon

Mojoceratops perifania was recoded where necessary, but ultimately was removed from the matrix as it is a junior synonym of *Chasmosaurus russelli* (Maidment and Barrett, 2011). The two new taxa (*Navajoceratops sullivani* and *Terminocavus sealyi*) were added to the matrix to make a total of 26 taxa. *Leptoceratops gracilis* was selected as the outgroup.

Analyses were rerun to investigate the effects of removing problematic fragmentary taxa. The first reanalysis removed *Bravoceratops polyphemus* and *Agujaceratops mariscalensis*, leaving 24 taxa. The second reanalysis further removed *Coahuilaceratops magnacuerna*, leaving 23 taxa.

The analyses were performed with parsimony using PAUP v. 4.0 b10 for Mac OSX (Swofford, 2002) within a heuristic search of 5,000 replicates using ACCTRAN optimization and tree bisection-reconnection swapping to produce a strict consensus tree, followed by a bootstrap analysis using a heuristic search of 5,000 replicates. Tree figures were prepared using FigTree 1.4.2 (Rambaut, 2014).

Morphometric Analysis

Landmark-based geometric morphometric analysis was used to compare parietal shape among 19 specimens (~9 taxa) of chasmosaurine ceratopsids. The analysis was performed by the software package "Geomorph" (version 2.1.1; Adams and Otárola-Castillo, 2013) within the R language and environment for statistical computing, version 3.1.2 for Mac OSX (http://www.R-project.org/; R_Core_Team, 2014). 16 landmarks were plotted onto each image of a parietal in dorsal view. Images used were a combination of photographs and specimen drawings, most of which were taken directly

from the literature. Landmarks were specifically selected to represent morphological features that are observed to vary between specimens (Figure 4.6). Only the left side of the parietal was analysed. Specimens with well preserved left and right sides were sampled for both sides by plotting the coordinates from the left side, then mirroring the image of the right side so that it appears as a left, and analysing those as a separate dataset.

Although the parietal of *Agujaceratops mariscalensis* (UTEP P.37.7.065, 070, 071) is fragmentary, the reconstruction of Lehman (1989) is included for comparison, although only the left side was analysed since it is only this side that is based on fossil material. Only the right sides of *Kosmoceratops richardsoni* holotype UMNH VP 17000 and "*Chasmosaurus russelli*" referred specimen TMP 1983.25.1 were analysed as the left sides were damaged and missing critical areas. Only the left side of *Chasmosaurus belli* specimen AMNH 5402 was used as the right side is unusually distorted.

Landmarks were digitized within the R program using “digitize2d” (version 2.1.1; Adams and Otárola-Castillo, 2013). Parietals were rotated and scaled using Generalized Procrustes Analysis (using the function “gpagen”) so that shape was the only difference among specimens. Consequent Procrustes coordinates were analyzed in a Principal Components Analysis (function “plotTangentSpace”).

Angle Measurements

The angle formed at the midline of the lateral rami of the posterior bar was reconstructed by drawing lines along the midpoint of the rami on digital photographs in Adobe Photoshop CS2. Midpoint lines were originally plotted by drawing a line

perpendicular to width midpoints on each ramus, but the results were inaccurate (due to distortion, asymmetry, and missing parts of the fossils), so lines were plotted by eye instead. The angle was measured using ImageJ 1.46r (Rasband, 1997-2014). See Appendix C Figures 4.S1 and 4.S5.

Results

Systematic Paleontology

DINOSAURIA Owen, 1842, *sensu* Padian and May 1993.

ORNITHISCHIA Seeley, 1887, *sensu* Sereno 1998.

CERATOPSIA Marsh, 1890, *sensu* Dodson, 1997.

CERATOPSIDAE Marsh, 1888, *sensu* Sereno 1998.

CHASMOSAURINAE Lambe, 1915, *sensu* Dodson et al., 2004.

Pentaceratops sternbergii (Osborn, 1923)

Type Specimen. AMNH 6325 (Osborn, 1923), nearly complete skull, missing the mandible and the posterior half of the parietal and squamosals.

Referred Specimens. AMNH 1624, nearly complete skull, missing mandible and the medial part of the parietal; AMNH 1625, nearly complete frill, missing anterior end of the parietal and right squamosal, and most of the left squamosal. Referred to as cf. *Pentaceratops sternbergii*.

Locality and Stratigraphy. AMNH 6325, 1624, and 1625 were all collected by C. H. Sternberg in 1922 and 1923 from the Fruitland Formation, San Juan Basin, New Mexico (Figures 4.3 and 4.5; see Appendix C for discussion).

Diagnosis. Chasmosaurine ceratopsid characterized by the following combination of characters (modified from Lehman, 1998; and Longrich, 2014): Posterior bar of the parietal M-shaped, with well-developed median embayment. Arches of the M-shape angular, with apex of arch occurring at locus ep2. Anteroposterior thickness of the parietal posterior bar uniform (or nearly so) from medial to lateral. Three large subtriangular epiparietals. Ep1 curved dorsally or anterodorsally and sometimes twisted such that the epiparietal contacts the posterior margin of the frill laterally, and lies atop the frill medially. Parietal median bar with slender ovoid cross section. Frill long and narrow, broader anteriorly than posteriorly. Terminal episquamosal enlarged relative to penultimate episquamosal. Parietal fenestrae subangular in shape. Postobital horns present and relatively slender, curving anteriorly (at least in adults). Epijugal spikelike, more elongate than in other chasmosaurines, curving ventrally. Nasal horn positioned over the naris.

Can be distinguished from *Chasmosaurus* by the following characters: Lateral rami of the parietal posterior bar meet medially at <90°, rather than >90°. Ep1 occurs within the embayment of the parietal posterior bar, rather than at the lateral edges of the embayment. Ep1 typically curved anteriorly and oriented anterolaterally, rather than pointing posteriorly. Ep2 oriented to point posteriorly rather than posterolaterally. Ep2 triangular and symmetrical (or nearly so) rather than asymmetrical. Posteriormost point

of the parietal posterior bar (apex of the curved lateral ramus) occurs at locus ep2 rather than ep1. Maximum point of constriction for the parietal median bar occurs approximately halfway along its length, rather than within the posterior third. Frill broader anteriorly than posteriorly. Nasal horn positioned over the naris rather than 50% or more positioned posterior to the naris. Premaxillary flange restricted to dorsal margin of premaxilla, rather than along entire anterior margin of external naris. Postorbital horns elongate and anteriorly curved (in large individuals assumed to represent adults), rather than abbreviated, resorbed, and/or curved posteriorly (adapted from Forster et al., 1993; Maidment and Barrett, 2011; Longrich, 2014).

Can be distinguished from *Utahceratops gettyi* by the following characters: nasal horn more anterior than *U. gettyi*, being positioned over the naris rather than posterior to the naris. Postorbital horns elongate and anteriorly oriented (in large individuals assumed to represent adults), rather than abbreviated or resorbed and oriented anterolaterally.

Comment. The virtually complete parietosquamosal frill, AMNH 1625 is the most diagnostic of the original referred materials. As AMNH 1624 is missing the central part of the parietal it can only be tentatively referred to the same taxon as AMNH 1625 based on the following shared diagnostic characters (which are not seen in aff, *Pentaceratops* n. sp. specimens; MNA Pl. 1747, UKVP 16100, and NMMNH P-37880; see later): the posteriormost point of the parietal posterior bar is positioned at locus ep2. Ep2 is not positioned within the parietal median embayment. Ep2 is oriented posteriorly. The lateralmost edge of the lateral rami of the parietal posterior bar is slightly expanded in AMNH 1624, more so than in AMNH 1625, but less so than seen in MNA Pl.1747 and

UKVP 16100. The M-shape of the posterior bar is slightly angular in AMNH 1624, more similar to AMNH 1625 than the rounded M-shape in MNA Pl.1747 and UKVP 16100.

Both AMNH 1624 and 1625 were referred to *Pentaceratops sternbergii* without comment by Lull (1933; see Appendix C). From 1933 to 1981, the defined morphology of *P. sternbergii* was based on the combination of these specimens along with the holotype AMNH 6325, thus forming a hypodigm (Simpson, 1940). In 1981 Rowe et al. referred the then newly discovered MNA Pl.1747 and UKVP 16100 to *P. sternbergii*, but implicitly recognized that these new specimens were distinct from the *P. sternbergii* hypodigm. They state (p. 40) that the reconstructed frills of AMNH 6325 and 1624 were "on the basis of [MNA Pl.1747], seen to be incorrect". The frills of AMNH 6325 and 1624 were presumably reconstructed based on the complete frill AMNH 1625 (which Rowe et al. 1981 acknowledge the extistence of, but had not been able to locate, nor observe a photograph). Following this, based on the morphology of the posterior end of the parietal, here I show that MNA Pl.1747 and UKVP 16100 should be referred to a different taxon from AMNH 1624 and 1625.

As the *P. sternbergii* holotype AMNH 6325 lacks the diagnostic posterior bar of the parietal, then we cannot currently know whether the holotype would have been more similar to AMNH 1624 and 1625; MNA Pl.1747 and UKVP 16100; or a different morphology entirely. A possible exception is that the preserved portion of the parietal median bar of AMNH 6325 is narrow and particularly elongate, more so than the median bars of chasmosaurines recovered from the Kirtland Formation (*Navajoceratops*, *Terminocavus*, new taxon C, and "*Pentaceratops fenestratus*"). AMNH 6325, 1625, and

1624, MNA Pl.1747, and UKVP 16100 are all recorded as having been collected in the Fruitland Formation (with no better stratigraphic resolution available for the AMNH specimens; see Appendix C), so that stratigraphy is mostly uninformative regarding their potential separation.

Despite the inadequacy of the holotype AMNH 6325, it is desirable to conserve the name *Pentaceratops*, and *P. sternbergii*. In order to do so I am maintaining the original hypodigm of Lull (1933) and thus referring to specimens AMNH 1624 and 1625 as cf. *P. sternbergii*. For this to be formalized, it would be best to petition the ICZN to transfer the holotype to another specimen, preferably AMNH 1625. Without transfer of the holotype, *Pentaceratops* and *P. sternbergii* should be considered nomen dubia, and a new taxon erected for diagnostic specimen AMNH 1625 and (possibly) 1624.

Aff. *Pentaceratops* n. sp.

Referred Specimens. MNA Pl.1747, complete skull and partial postcranium; UKVP 16100, complete skull; NMMNH P-37880, partial right lateral ramus of parietal posterior bar.

Locality and Stratigraphy. All specimens were collected from the upper part of the Fruitland Formation, San Juan Basin, New Mexico (Figures 4.3 and 4.5; Appendix C).

Diagnosis. Differs from cf. *Pentaceratops sternbergii* (principally, AMNH 1625) by possession of the following characters. Arches of the M-shaped parietal posterior bar

rounded rather than angular. Apices of M-shaped arch more laterally positioned, occurring either between loci ep2 and ep3, or at locus ep3, rather than at locus ep2. Lateral rami of the parietal posterior bar become more anteroposteriorly broad from medial to lateral, rather than being near-uniform thickness. Locus ep2 positioned on the lateralmost edge within the embayment, oriented medioposteriorly. Lateral bars more strongly developed.

Comment. UKVP 16100 and MNA Pl.1747 have historically been referred to *Pentaceratops sternbergii* (e.g. Rowe et al., 1981; Lehman, 1993, 1998; Longrich, 2011; 2014), but are here shown to differ from the historical hypodigm (Lull, 1933; see above). NMMNH P-37880 is described for the first time in Appendix C.

Morphological features known to indicate relative maturity in chasmosaurines (Horner and Goodwin, 2006, 2008) suggest that referred specimens of aff. *Pentaceratops* n. sp. are not fully mature (MNA Pl.1747, subadult or adult; UKVP 16100, subadult; and NMMNH P-37880, subadult; Appendix C). Since AMNH 1625 exhibits features supportive of full adult status (see Appendix C), then this raises the possibility that any morphological differences between cf. *P. sternbergii* and aff. *Pentaceratops* n. sp. are ontogenetic rather than taxonomic. This would possibly be supported by stratigraphic data as AMNH 1625 is thought to have been collected from below the Bisti Bed sandstone, as were MNA Pl. 1747, UKVP 16100, and NMMNH P-37880. However, given the close similarity in size and ontogenetic status of AMNH 1625 and MNA Pl.1747, I prefer to consider their morphological differences as taxonomic, although I

remain open to the ontogenetic hypothesis. Further discovery of mature material with stratigraphic data would help resolve this question.

Navajoceratops sullivani gen. et sp. nov.

Etymology. *Navajoceratops*, 'Navajo horned face', after the Navajo people indigenous to the San Juan Basin; *sullivani*, after Dr. Robert M. Sullivan, leader of the SMP expeditions to the San Juan Basin that recovered the holotype.

Holotype. SMP VP-1500; parietal, squamosal fragments, fused jugal-epijugal, other unidentified cranial fragments. Collected in 2002 by Robert M. Sullivan, Denver W. Fowler, Justin A. Spielmann, and Arjan Boere.

Locality and Stratigraphy. SMP VP-1500 was collected from a medium brown-grey mudstone at SMP locality 281 ("Denver's Blowout"), Ahshislepah Wash, San Juan Basin, New Mexico (Sullivan, 2006; detailed locality data available on request from NMMNH). The locality occurs in the lower part of the Hunter Wash Member of the Kirtland Formation (Figure 4.5), ~ 43 m stratigraphically above the uppermost local coal, and ~ 6 m stratigraphically above the top of a prominent sandstone thought to represent the Bisti Bed (SMP locality 396; "Bob's Bloody Bluff"; Sullivan, 2006). Hence SMP VP-1500 occurs stratigraphically higher than specimens referred to cf. *Pentaceratops sternbergii* and aff. *Pentaceratops* n. sp. which all occur below the Bisti Bed sandstone.

Most elements of SMP VP-1500 were collected as weathered surface material, with the exception of the parietal, which was only partly exposed and required

excavation. The parietal was preserved dorsal-side up with the median bar broken and displaced ~ 10 cm anteriorly (see Figures 4.7 and 4.8), and the distal part of the right ramus of the posterior bar broken and displaced ~ 20 cm posterolaterally.

Bauer (1916) shows the Kirtland Formation as only 830 ft (253 m) thick in the Ahshislepah section (Meyers Creek of Bauer's usage), compared to a thickness of 1031 ft (314 m) at Hunter Wash (see map, Figure 4.3). This does not affect interpretation of stratigraphic relationships in this current work, but should be noted by future researchers who might be working elsewhere in the San Juan Basin, in case specimen stratigraphic positions are cited as the number of metres above or below Kirtland formational contacts.

Diagnosis. Can be distinguished from aff. *Pentaceratops* n. sp. by the following characters: Lateral rami of the parietal posterior bar meet medially at a more acute angle (~60°, rather than 87 or 88°). Median embayment of the parietal posterior bar especially deep, extending anterior to the posteriormost extent of the parietal fenestrae (which consequently overlap anteroposteriorly slightly with ep2).

Description of *Navajoceratops sullivani*

Parietal. The parietal (Figure 4.9) is missing the lateral bars and most of the anterior end, but is otherwise relatively complete. Deep vascular canals are visible across the dorsal and ventral surfaces, and are especially well developed on the ventral surface. The posterior and medial borders of both parietal fenestrae are well preserved; enclosing the parietal fenestrae that are large and subangular. Six epiparietal loci are interpreted to occur on the posterior bar, numbered ep1-3 on each side.

The preserved portion (~60%) of the median bar measures 37.4 cm in length, and tapers anteriorly, measuring 4.1 cm wide at the anteriormost end. The dorsal and ventral surfaces of the median bar are convex, with lateral margins of the median bar tapering to give a lenticular cross section. These tapering lateral edges broaden posteriorly. The dorsal surface bears no prominent medial crest, ridge, or bumps (such features are restricted to the anteriormost third of the median longitudinal bar in other chasmosaurines; e.g. *Anchiceratops*, Brown, 1914, Mallon et al., 2011; "*Torosaurus*" *utahensis*, Gilmore, 1946; "*Torosaurus*" sp., Lawson, 1976; "*Titanoceratops*", Longrich, 2011; *Triceratops*, Hatcher et al., 1907; see discussion in Appendix C on "*Bravoceratops*", Wick and Lehman, 2013). Two fragments found during excavation may represent parts of the anterior end of the median bar (Figure 4.10). The largest fragment bears parallel vascular traces along its length, suggesting it is indeed part of the midline of the anterior end of the parietal.

The median bar and lateral rami of the posterior bar form a Y-shape, with the rami of the posterior bar meeting at an angle of 60°, forming a deep U-shaped median embayment that incises 13.2 cm anterior to the posteriormost extent of the parietal fenestrae. The lateral rami are slightly wavy rather than straight, and form an M-shape with the curved apices of the M occurring between epiparietal loci ep2 and ep3. The lateral rami of the posterior bar vary in anteroposterior thickness, being relatively thick at the contact with the median bar (R: 11.5 cm; L: 12.8 cm), reaching their narrowest point slightly medial of the apex (R: 9.37 cm; L: 9.17 cm), broadening at the apex (R: 20.2 cm; L: 20.0 cm), then narrowing again laterally towards the contact with the squamosal.

There are two raised areas on either side of the anteroventral margin of the posteromedial embayment. During excavation, the lateral rami bore an especially thick concretion in this area, suggesting bone underneath the surface (see Figures 4.7 and 4.8); however, if present, all of this bone was lost during preparation. A very similar raised area is considered as representing ep1 in *Utahceratops* referred specimen UMNH VP 16671 (Sampson et al., 2010). This raised area is also considered as an attachment point of ep1 in aff. *Pentaceratops* n. sp. specimen UKVP 16100 and aff. *P. sternbergii* specimen SDNHM 43470, and is the attachment site for a fused outwardly turned ep1 in specimens MNA Pl.1747, and the left side of AMNH 1625. Therefore I tentatively suggest that these raised areas are the attachment sites for ep1. Both the left and right ep2 are preserved imperceptibly fused to the posterior bar and project posteromedially into the embayment, almost touching medially. Ep2 on both sides is a rounded D-shape, rather than triangular. There is no evidence of ep3, which might be expected to occur at the lateralmost edges of the lateral rami. However, although ep3 is typically reconstructed as occurring in this position in *Pentaceratops sterbergii* (e.g. Lehman, 1998), only AMNH 1624 and 1625 actually preserve an ep3, and in these specimens it abuts or straddles the squamosal-parietal margin (although see notes on MNA Pl.1747 in Appendix C). An isolated D-shaped frill epiossification (Figure 4.10) was recovered adjacent to the parietal during excavation of SMP VP-1500. It is unlike the spindle-shaped or triangular episquamosals, and so may be an unfused ep1or ep3.

Squamosal. SMP VP-1500 includes pieces of at least one squamosal (probably a left), but most of these are too small and fragmentary to impart much morphological

knowledge. The two largest fragments are shown in Figure 4.11. The first fragment (Figure 4.11A, 4.11B) is roughly triangular in shape and preserves part of the lateral margin, which is thicker than the more medial area. Two episquamosals are preserved fused to the lateral margin. Both episquamosals are trapezoidal or D-shaped. The second large fragment (Figure 4.11C, 4.11D) is also triangular, but is narrower than the first fragment and as such might be part of the distal blade of the squamosal. Few features are diagnostic on the second fragment, although a relatively complete straight edge may represent the medial margin where the squamosal articulates with the parietal. Both of the large fragments exhibit the woven, vascularized surface texture typical of ceratopsid skull ornamentation.

Jugal / Epijugal or Episquamosal. A ~10 cm fragment (SMP VP-1813) bearing a pointed epiossification possibly represents the ventral margin of a fully fused right jugal, quadratojugal, and epijugal (Figure 4.12). It was collected as float from the same locality as SMP VP-1500 and possibly pertains to the same individual. The epijugal is relatively stout, but not unusually so, nor is it especially long or pointed ("long" and "hyperlong" were character states of the epijugal for character 50 of Sampson et al., 2010). An alternative identification of this element is a large episquamosal. Regardless, the specimen is not especially diagnostic.

Terminocavus sealeyi gen. et sp. nov.

Etymology. *Terminocavus*, 'closing cavity' after the nearly-closed parietal embayment; *sealeyi* after Paul Sealey who discovered the holotype specimen.

Holotype. NMMNH P-27468; parietal, jugal, epijugal, partial quadratojugal, partial sacrum, vertebral fragments. Collected in 1997 by Paul Sealey.

Locality and Stratigraphy. NMMNH P-27468 was collected from a grey siltstone beneath a white channel sandstone (locality NMMNH L-3503; precise locality data available from NMMNH upon request) in the middle of the Hunter Wash Member, stratigraphically intermediate between ash 2 (75.02 ± 0.13 Ma) and ash 4 (74.57 ± 0.62) (Fowler, Chapter 3). Although in Figure 4.3 NMMNH L-3503 appears to be approximately halfway between these radiometrically dated horizons, it occurs in a topographic high between Hunter Wash and Alamo Wash, placing it stratigraphically closer to ash 4. Trigonometric calculations place the locality at ~83 m stratigraphically above ash 2, and ~48 m stratigraphically below ash 4 (based on a northeast dip of 1°). This agrees quite well with Bauer (1916) who published a thickness of 1031 feet (314 m) for the Hunter Wash Member (then called the Lower Shale Member) at Hunter Wash itself. However, in their description of the ashes, Fassett and Steiner (1997) suggest that the ashes are separated stratigraphically by only ~45 m. This would appear to be an underestimate, based on both Bauer (1916) and on the fact that ash 4 is ~130 ft (40 m) topographically higher than ash 2, and ~5 km NE (basinwards, parallel to 1-3° dip).

It is worth mentioning that the locality is only ~0.6 km SE of another ash (JKR-54) that was dated by Brookins and Rigby (1987). The large margin of error for their K / Ar date of 74.4 ± 2.6 Ma (sanidine) places it within the expected range based on the more precise Ar / Ar recalibrated dates of Fassett and Steiner (1997; recalibrations by

Fowler, Chapter 3). Although the K / Ar date of Brookins and Rigby (1987) is imprecise and not really usable, the JKR-54 horizon would be useful to resample in future San Juan Basin research.

Comment. NMMNH P-27468 has only previously been mentioned in an abstract by Sealey et al. (2005) where it was identified as an aberrant specimen of *Pentaceratops sternbergii*. NMMNH P-27468 is the only diagnostic chasmosaurine specimen from the middle or upper part of the Hunter Wash Member of the Kirtland Formation; other Kirtland Formation chasmosaurine specimens collected by C.H. Sternberg in the 1920s (described by Wiman, 1930; including the holotype of "*Pentaceratops fenestratus*"; see Appendix C) are mostly undiagnostic or fragmentary, and lack detailed locality and stratigraphic data.

Diagnosis. Differs from *Navajoceratops* holotype SMP VP-1500 by the following characters: Posterior bar flattened and plate-like (i.e. not bar-like). Lateral rami of the parietal posterior bar strongly expanded anteroposteriorly both medially and laterally. Maximum anteroposterior thickness of the posterior bar ~35% of the parietal maximum width (compared with <30 % in *Navajoceratops* and ~19-30% in aff. *Pentaceratops* n. sp.). Median embayment of the posterior bar narrower and more notch-like. Parietal fenestrae subrounded rather than subangular.

Description of *Terminocavus sealeyi*

Parietal. The parietal of NMMNH P-27468 (Figure 4.13) is missing ~50% of the anterior end, but is otherwise relatively complete forming a rounded-M or heart-shape reminiscent of later occurring chasmosaurines such as the holotype of "*Torosaurus gladius*" YPM 1831. The parietal is not formed of obvious narrow bars as seen in stratigraphically older chasmosaurines, rather, it is expansive, flat, and more plate-like. The parietal is comparatively thin (typically ~1-2 cm in thickness), although this may reflect post-burial compression. Bone surfaces have a thin concretion of sediment that obscures most fine surface detail, although shallow vascular canals are visible on some areas of the dorsal surface. The ventral surface is mostly either obscured by concreted sediment or damaged, but in some places longitudinal vascular canals can be observed, similar to those in *Navajoceratops* and other chasmosaurines. The posterior and medial borders of both parietal fenestrae are well preserved. However, the posterior, median, and lateral bars are expanded at the expense of the parietal fenestrae, which are thus slightly reduced in size relative to stratigraphically preceding chasmosaurines. The fenestrae are subrounded in shape, comparable to derived chasmosaurines such as *Anchiceratops* and triceratopsins, but unlike the subangular- or angular-shaped fenestrae of stratigraphically older chasmosaurines.

The preserved portion of the median bar measures 31.1 cm in length and tapers anteriorly. The dorsal surface of the midline bar is convex, lacking a medial crest, ridge, or bump. The ventral surface of the median bar is flat to weakly convex. The lateral margins of the median bar taper to give a lenticular cross section. The median bar bears

small flanges that run along both the lateral edges, and are directed laterally into the fenestrae. Although broken anteriorly, the flanges are more laterally extensive than in *Navajoceratops* and other stratigraphically preceding chasmosaurines.

The left and right lateral bars are incomplete and probably represent only ~50% of their original length. The preserved portions are of nearly equal antero-posterior length, and are almost parallel, suggesting the anterior end of the parietal was slightly narrower than the posterior, or at least narrowed in its midline (as in c.f. *Pentaceratops sternbergii* MNA Pl. 1747; Rowe et al., 1981). Both lateral bars are convex dorsally, and flat to weakly convex ventrally. Dorsoventral thickness decreases laterally such that they are moderately lenticular in cross section. The lateral edges, which articulate with the squamosal, are thin and plate-like. Each lateral bar bears a relatively large (diameter ~5mm) blood vessel groove that runs anteroposteriorly to the lateral rami of the posterior bar. However, like other blood vessel traces on this specimen, the grooves are shallow and difficult to trace onto the lateral rami.

The lateral rami of the posterior bar meet medially at an angle of 73°, which is steeper than in stratigraphically preceding chasmosaurines, however, it is awkward to measure as the lateral rami are curved rather than being straight lines (see Appendix C Figure 4.S1 for details of measurement). The lateral rami are anteroposteriorly thicker than those of *Utahceratops*, *Pentaceratops*, and *Navajoceratops*, but less so than in *Anchiceratops*. They vary in anteroposterior thickness from medial to lateral, being at their narrowest medially, at the contact with the median bar (R: 13.2 cm; L: 12.2 cm),

reaching their broadest point at the apex (R: 23.4 cm; L: 23.6 cm), then narrowing again laterally towards the contact with the squamosal.

The median embayment is narrower than in preceding chasmosaurines, forming a notch that is almost enclosed by the first pair of epiparietals. The embayment does not extend anterior to the posteriormost border of the parietal fenestrae. The anterior edge of the embayment is notably thickened, similar to that seen in c.f. *Utahceratops gettyi* specimen UMNH VP-16671 (Sampson et al., 2010). On the left lateral ramus, the thickened border of the embayment is extended continuously in a posterior direction helping form the anteromedial edge of the left ep1 (see below). However, on the right side, the thickened border is discontinuous, forming a small prominent bump below the main part of the ep1. A similar double bump at the ep1 locus is seen on the left side of c.f. *U. gettyi* specimen UMNH VP-16671 where it is labeled as a "dorsal parietal process", with the right side continuous (Sampson et al., 2010).

Five epiparietals are preserved fused to the parietal, with at least one missing, which is therefore probably representative of three pairs of epiparietals (ep1-3) as is typical for chasmosaurines. The medialmost pair of epiparietals is considered to represent locus ep1, and is positioned on the medial margin of the median embayment, as it is in specimens referred to cf. *Pentaceratops sternbergii*, aff. *Pentaceratops* n. sp., and cf. *Utahceratops gettyi*. The left ep1 is triangular, whereas the right ep1 was probably also triangular but is missing the distal tip, instead exhibiting a shallow, possibly pathological trough. This is of interest because if the right ep1 tip was present then the epiparietals are close enough (separated by only ~5 mm) that they would probably have touched

(especially if they bore keratinous sheaths). Ep1 is the only epiparietal that does not lie flat within the plane of the parietal. Both left and right ep1 are deflected slightly dorsally, similar to the ep1 on the right side of cf. *Pentaceratops sternbergii* specimen AMNH 1625 and parietal fragments referred to "*Pentaceratops aquilonius*" (CMN 9814; Longrich, 2014; see Appendix C). Ep2 is preserved on both sides, although it is broken slightly on the right side. Ep2 is triangular and projects posteromedially from the posterior bar, laying flat within the plane of the rest of the parietal. Ep3 is only preserved on the left side where it is fused to the posterior bar. There is an empty space at locus ep3 on the right side. Ep3 is more D-shaped than triangular and projects posteriorly laying flat within the plane of the rest of the parietal. There is no indication of an epiparietal more lateral than the ep3 locus, despite there probably being enough space for an additional epiossification (as seen in some specimens of *Anchiceratops*; Mallon et al., 2011).

Right Squamosal. The preserved right squamosal (Figure 4.14) comprises a nearly complete anterior end (including the narrow processes that articulate with the quadrate and exoccipital), the anteriormost episquamosal, and most of the medial margin of the squamosal blade. Almost the entire lateral margin and the posterior end are not preserved. The medial margin is robust and forms what is termed the squamosal bar. Although incomplete, the squamosal bar is long enough to suggest that the squamosal itself was elongate, as seen in most adult chasmosaurines, rather than short and broad, as seen in young chasmosaurines (Lehman, 1990; Scannella and Horner, 2010); the preserved portion measures 83 cm in length, and the conservative reconstruction (Figure 4.14) is 94

cm. Lateral to the squamosal bar, the squamosal dorsoventrally thins and is broken. The single preserved episquamosal is fused to the anterolateral border and represents the anteriormost episquamosal. It is common in chasmosaurine specimens for the anteriormost episquamosal to be fused to the anterolateral border of the squamosal, suggesting that it is one of the first episquamosals to fuse through ontogeny (Godfrey and Holmes, 1995). The episquamosal is very rugose and not obviously triangular in shape.

Jugal / Epijugal. NMMNH P-27468 also has a fused left jugal, epijugal, and quadratojugal (Figure 4.15). The orbital margin of the jugal is not preserved, and only a little remains of the anterior process. The ventral part of the jugal is tongue shaped, terminating in the indistinguishably fused epijugal. The epijugal is large and robust, but not notably long. Only the ventralmost part of the quadratojugal is preserved, fused to the epijugal. Similar to the parietal, surface texture is partly obscured by sediment, but some shallow vascular grooves are visible.

Chasmosaurinae sp. "Taxon C"

Material NMMNH P-33906; parietal median bar, epijugal, indeterminate skull fragments, vertebral fragments.

Locality and Stratigraphy. NMMNH P-33906 was collected in 2001 by Thomas E. Williamson at NMMNH locality L-4715, from the De-na-zin Member of the Kirtland Formation at South Mesa, San Juan Basin, New Mexico (Figure 4.5; precise locality coordinates are available from NMMNH). Two radiometrically dated ashes (at Hunter

Wash, ~10 km to the northwest) bracket the age of the De-na-zin Member of the Kirtland Formation. Ash H (73.83 +/- 0.18 Ma) occurs less than 5 m above the basal contact of the De-na-zin Member with the underlying Farmington Member (Fassett and Steiner, 1997; Sullivan et al., 2005). Ash J (73.49 +/- 0.25 Ma) occurs 4.9 m below the upper contact of the De-na-zin Member with the overlying Ojo Alamo Sandstone (Fassett and Steiner, 1997; both radiometric dates recalibrated by Fowler, Chapter 3, from Fassett and Steiner, 1997). NMMNH P-33906 therefore occurs between 73.83 Ma and 73.49 Ma.

Comment. Although fragmentary, the previously undescribed specimen NMMNH P-33906 represents one of the few records of chasmosaurines from the De-na-zin Member of the Kirtland Formation, and preserves the median bar of the parietal, which is diagnostic enough to permit comparison to other chasmosaurines.

Diagnosis. Differs from *Utahceratops*, cf. *Pentaceratops sternbergii*, aff. *Pentaceratops* n. sp., *Navajoceratops*, and *Terminocavus* by the following characters: Median bar bears extensive lateral flanges extending into the parietal fenestrae. Flanges are extensive such that the cross section of the median bar is a broad flat lenticular shape, rather than being narrow and strap-like.

Description of Chasmosaurinae sp. "Taxon C"

Parietal. The preserved portion measures 31 cm in length and represents most of the parietal median bar (Figure 4.16). As with many vertebrate fossils from the De-na-zin Member, NMMNH P-33906 has a thin covering of pale-colored concretion, and many

adhered patches of hematite. This obscures fine surface details, although most morphological features can be discerned. The dorsal side is gently curved laterally, but otherwise has no obvious surface features (i.e. it lacks a prominent medial crest, ridge, or bumps). In contrast, the ventral side bears a raised central bar with lateral flanges which extend laterally into the fenestrae. The lateral flanges are much more strongly developed than in *Pentaceratops*, *Navajoceratops*, and *Terminocavus*, but overall the median bar is less broad than in *Anchiceratops* (with the possible exception of referred specimen CMN 8535; Sternberg, 1929; Mallon et al., 2011). The cross section is different at either end of the median bar, which is used to infer orientation. At the inferred anterior end, the cross section is concave-convex, with a shallowly concave ventral side. At the inferred posterior end, the cross section is biconvex and lenticular in shape. In other chasmosaurines the anterior end of the parietal median bar can be slightly concave ventrally (e.g. aff. *Pentaceratops* n. sp., MNA Pl. 1747; Rowe et al., 1981; *Chasmosaurus belli* holotype CMN 491; Hatcher et al., 1907), so I have identified the ventrally concave end as anterior in NMMNH P-33906. The median bar is expanded laterally at both ends; this is typical of chasmosaurine median bars, but is important as it helps constrain the size that the fenestrae would have been. Lateral expansion is more notable at the posterior end, although this is probably due to the anterior end being less complete. At its narrowest point, the median bar is 9 cm wide.

Epijugal. NMMNH P-33906 includes an epijugal, which is fused to the jugal (and probably the quadratojugal). However, the jugal and quadratojugal are almost entirely

missing, with the only remaining parts being small pieces that are fused to the base of the epijugal. The epijugal measures ~10 cm long, and is moderately pointed in shape.

Ontogenetic Assessment

Significant morphologic change through ontogeny can strongly affect the phylogenetic placement of a specimen (Campione et al., 2013). It is therefore important to determine the ontogenetic status of new specimens so that appropriate comparisons can be made. No limb bones are preserved with the new specimens described here, so the age in years of individuals cannot be determined. Ontogenetic change in cranial morphology is not well studied in non-triceratopsin chasmosaurines (although see Lehman, 1990), although it has been intensively studied in the derived chasmosaurine *Triceratops* (Horner and Goodwin, 2006; 2008; Scannella and Horner, 2010; 2011; Farke, 2011; Horner and Lamm, 2011; Longrich and Field, 2012; Maiorino et al., 2013). Based this prior work, a combination of ontogenetically variable cranial features (size, sutural fusion, shape and fusion of epiossifications, frill surface texture, squamosal elongation) are here hypothesized to also be indicative of subadult or adult status in SMP VP-1500, NMMNH P-27468, and NMMNH P-33906.

Size. Size is an unreliable measure of maturity, as individual body size variation has been shown to be considerable in some dinosaurs (Sander and Klein, 2005; Woodward et al., in press). Nevertheless, large size is often used as a rough gauge of maturity (and conversely, small size of immaturity), and this is a reasonable approach when used in combination with other morphological features that are ontogenetically

informative. The holotype parietal of *Navajoceratops*, SMP VP-1500, is of comparable size to other specimens of *Pentaceratops* and related chasmosaurines (Figure 4.17). The holotype parietal of *Terminocavus*, NMMNH P-27468, was described as small in the abstract by Sealey et al. (2005), but it is only slightly smaller than specimens of *Pentaceratops* (Figure 4.17). The squamosal of NMMNH P-27468 has a reconstructed length of 94 cm, which is slightly smaller than MNA Pl.1747 (127 cm, J., Fry pers. comm.), but larger than the juvenile aff. *Pentaceratops* SDMNH 43470 (77 cm; Diem and Archibald, 2005); the only other complete *Pentaceratops* squamosal is AMNH 1624, which is undescribed. The jugal of NMMNH P-27468 is only slightly smaller than *Utahceratops* referred specimen UMNH VP-12198 (Figure 4.15), which is a large and aged individual (fused frill epiossifications that are mediolaterally elongate, spindle-shaped, and blunt; resorbed postorbital horns; fused epijugal; Sampson et al., 2010; pers. obs.). The median bar of NMMNH P-33906 (Taxon C) is much broader than the median bar of any specimen of *Pentaceratops*, *Navajoceratops*, or *Utahceratops* (Figure 4.17). At 10 cm long, the epijugal of NMMNH P-33906 is also of similar size to the epijugal of UMNH VP-12198.

Cranial Fusion. Fusion of cranial sutures is often used as an indicator of maturity, but this is fraught with problems as the timing of suture closure may not be consistent between taxa (for example, the nasals and epinasal fuse relatively early in young subadult specimens of *Triceratops horridus*, whereas the congeneric *T. prorsus* these elements fuse in late subadulthood, to adulthood; Horner and Goodwin, 2006; 2008; Scannella et al., 2014). However, similar to size, degree of cranial fusion can be informative when

used in conjunction with other data. Fusion of the epijugal to the jugal and quadratojugal is observed in all three of the new specimens (albeit based only a tentative identification in SMP VP-1500). In *Triceratops*, fusion of the epijugal to the jugal and quadratojugal occurs relatively late in ontogeny, as a subadult or adult (Horner and Goodwin, 2008). A similar survey has not been conducted for more basal chasmosaurines, although the small-sized purportedly immature aff. *Pentaceratops* specimen SDMNH 43470 (Diem and Archibald, 2005) includes an unfused jugal and quadratojugal, but no epijugal as it was unfused and not recovered with the rest of the skull. Larger specimens of *Pentaceratops* and related taxa exhibit fusion of the epijugal to the jugal (holotype AMNH 6325, AMNH 1625, UKVP 16100; J. Fry, pers. comm.). From this, fusion of the epijugal in NMMNH P-27468 and P-33906 (also, tentatively SMP VP-1500; Figures 4.12, 4.15) is considered supportive of subadult or adult status.

Frill Epiossifications. Shape and fusion of frill epiossifications varies through ontogeny in chasmosaurines. In *Triceratops*, the episquamosals fuse first, followed by the epiparietals (Horner and Goodwin, 2008).

Godfrey and Holmes (1995) suggest that in *Chasmosaurus*, fusion of the episquamosals begins at the anterior end of the squamosal, and proceeds posteriorly through ontogeny. This pattern is similarly observed in *Pentaceratops* and related taxa, notably in aff. *Pentaceratops* n. sp. MNA Pl. 1747 (Rowe et al., 1981) and aff. *P. sternbergii* SDMNH 43470 (Diem and Archibald, 2005) in which only the anterior episquamosals are fused. Fusion of episquamosals in SMP VP-1500 (probably from the middle of the squamosal; Figure 4.11) supports the identification of this specimen as a

subadult or adult. NMMNH P-27468 only preserves the anteriormost fused episquamosal (the rest of the squamosal lateral border is damaged; Figure 4.14), so it is consistent with subadult or adult status, but this cannot be confirmed without additional material or data on the timing of the fusion of the first episquamosal.

The order of epiparietal fusion is not studied in basal chasmosaurines and a specific pattern has not yet been identified for *Triceratops*. However, a survey of specimens referred to *Pentaceratops* (and related taxa) reveals a general pattern where ep1 fuses first, followed by ep2, then ep3 (Figure 4.17). Ep1 is fused in the four largest specimens (cf. *P. sternbergii* AMNH 1625, aff. *Pentaceratops* n. sp. MNA Pl. 1747, UKVP 16100, and cf. *Utahceratops* UMNH VP-16671 and 16784; Figure 4.17), but is unfused in the aff. *P. sternbergii* small specimen SDMNH 43470, and in newly described parietal fragment NMMNH P-37890 (see Appendix C for descriptions). Ep2 is fused in AMNH 1625, MNA Pl. 1747, UMNH VP-16671 and 16784, but not in UKVP 16100. Ep3 is fused in AMNH 1625, UMNH VP VP-16671 and 16784, and possibly MNA Pl. 1747 (see Appendix C), but is unfused in UKVP 16100. The *Navajoceratops* holotype SMP VP-1500 has fused ep1 (probable) and ep2, but ep3 is unfused hence it exhibits a state of fusion between UKVP 16100 and MNA Pl.1747 (or AMNH 1625), and on this basis could be considered subadult. The holotype of *Terminocavus* (NMMNH P-27468) has fused ep1 and ep2 on both sides; ep3 is fused only on the left side, with an open space on the right side at the ep3 locus. On this basis, NMMNH P-27468 should be considered subadult or adult.

Regarding shape, all *Triceratops* frill episossifications develop from being triangular-shaped with pointed apices and short bases in juveniles, to spindle shaped with blunt apices and elongate bases in adults (Horner and Goodwin, 2006, 2008). Similar patterns exist in the episquamosals of more basal chasmosaurines with probable juvenile and immature specimens of *Chasmosaurus*, *Agujaceratops* (Lehman, 1989) and aff. *Pentaceratops* (SDMNH 43470; Diem and Archibald, 2005), exhibiting more short-based, pointed episquamosals. The episquamosals of *Navajoceratops* holotype SMP VP-1500 (Figure 4.11) are spindle shaped, and blunt with elongate bases, consistent with a subadult or adult condition. The *Terminocavus* holotype, NMMNH P-27468, only has the anteriormost episquamosal preserved, which tends to remain triangular and slightly pointed in subadult and adult chasmosaurines, even when more posterior episquamosals develop into spindle shapes. Thus, the triangular shape of the episquamosal of NMMMNH P-27468 is not ontogenetically informative. Note that triceratopsins are slightly unusual among chasmosaurines in that their epiparietals and episquamosals are of similar morphology to each other; whereas in *Anchiceratops* and more basal chasmosaurines, the epiparietals take a greater variety of forms. Most notable is that the epiparietals remain large and triangular through to adulthood in *Utahceratops*, cf. and aff. *Pentaceratops*, *Navajoceratops*, and particularly *Terminocavus* and *Anchiceratops*.

Frill Surface Texture. The texture of the parietosquamosal frill (and many of the facial bones) has been shown to change ontogenetically in both centrosaurine and chasmosaurine ceratopsids (Sampson et al., 1997; Brown et al., 2009; Scannella and Horner, 2010). Adult ceratopsids are characterized by a distinctive frill texture where

indented vascular channels form complex dendritic patterns. This texture gradually develops through ontogeny, with juveniles exhibiting a smooth or "long-grain" bone texture (Sampson et al., 1997; Brown et al., 2009; Scannella and Horner, 2010), which is replaced by a pebbled or pitted texture with shallowly developed vascular traces in young subadults. This is complicated somewhat by recognition that this long-grain texture is associated with rapid growth (Francillon-Vieillot et al., 1990; Sampson et al., 1997) and/or expansion of the frill, as expected in juveniles, but is also seen in some specimens of *Torosaurus* which are reshaping their frills relatively late in ontogeny (Scannella and Horner, 2010). The *Navajoceratops* holotype SMP VP-1500 has well-developed adult frill texture on both the parietal (Figure 4.9) and the squamosal (Figure 4.11). In the *Terminocavus* holotype, NMMNH P-27468, the frill texture on the parietal is partially obscured by a thin layer of sediment covering the surface, but can be seen to be pitted with shallow vascular canals. The same texture is visible on the dorsal surface of the squamosal. This suggests that NMMNH P-27468 is not yet fully mature and may be considered a young subadult. Surface texture is not discernible on Taxon C specimen NMMNH P-33906.

Squamosal Elongation. In juvenile chasmosaurines, the squamosal is anteroposteriorly short, similar to the condition in adult centrosaurine ceratopsids and more basal neoceratopsians (Lehman, 1990; Goodwin et al., 2006; Horner and Goodwin, 2006; Scannella and Horner, 2010). In chasmosaurines, the squamosal elongates through ontogeny, although the timing of the elongation varies phylogenetically (Lehman, 1990; Scannella and Horner, 2010). The derived taxon *Triceratops* has been shown to retain an

anteroposteriorly short squamosal until relatively late in ontogeny (Scannella and Horner, 2010), whereas in *Chasmosaurus* and *Pentaceratops* (albeit based on more limited data) it would appear that elongation occurs at smaller body sizes (inferred to be younger; Lehman, 1990). Although the squamosal of SMP VP-1500 comprises only fragments, one fragment (Figure 4.11C, 4.11D) might represent the more bladed posterior end, which would be supportive of a subadult or adult status. The squamosal of NMMNH P-24768 is incomplete, but enough remains to show that it was relatively elongate, supporting a subadult or adult status.

Geometric Morphometric Analysis

Results of the geometric morphometric Principal Components Analysis (PCA) on chasmosaurine parietals are presented in Figure 4.18. PC 1 (x-axis) accounts for 50.5% of variation, and assesses depth of the median embayment from shallow (negative) to deep (positive), and orientation of ep1 from mediolateral (negative) to anteroposterior (positive); PC 2 (y-axis) accounts for 19.0% of variation and assesses lateral expansion of the ep1 locus, shape of the posterolateral corner of the parietal, and overall anteroposterior length.

Specimens previously assigned to the same taxon largely cluster into groups, with "*Chasmosaurus russelli*", *C. belli*, and *Anchiceratops* specimens all clustering together. Specimens referred to cf. *Pentaceratops* n. sp (MNA Pl.1747 and UKVP 16100) are separated from cf. *P. sternbergii* specimen AMNH 1625, justifying their consideration as different taxa. The new taxa, *Navajoceratops* and *Terminocavus*, plot as intermediate

between these stratigraphically preceding chasmosaurines and the stratigraphically higher *Anchiceratops*.

Two perpendicular morphological trends correlate with the stratigraphic occurrence of taxa and match the lineages proposed by Lehman (1998). From stratigraphically oldest to youngest, "*Chasmosaurus russelli*", *C. belli*, and *Vagaceratops irvinensis* occupy the negative end of the PC 1 axis, and are spread down the PC 2 axis in stratigraphic order, showing little variation along the PC 1 axis. This demonstrates progressive expansion of the ep1 locus, concentrating ep2 and ep3 to the lateralmost corner of the parietal. The trend in *Chasmosaurus* is contrasted by a second group (comprising *Utahceratops*, *Pentaceratops*, *Navajoceratops*, *Terminocavus*, and *Anchiceratops*), which is mostly distributed along the PC 1 axis in stratigraphic order, and shows relatively little variation on PC 2. This group exhibits progressive deepening and eventual closure of the median embayment, an increasingly steep angle of the ep1 locus, and anteroposterior expansion of the posterior bar.

There are some inconsistencies in that *Kosmoceratops* does not plot close to *Vagaceratops* on the PC 1 axis (although it is very close on the PC 2 axis), despite being recovered as sister taxa in most phylogenetic analyses (Sampson et al., 2010; Mallon et al., 2014; and this analysis, see below). Similarly, aff. *Pentaceratops* n. sp. specimen MNA Pl.1747 plots more negatively on the PC 2 axis than other specimens within the *Pentaceratops* grouping (although it is very similarly placed along the PC 1 axis). These issues might be a reflection of potential problems with the input data concerning these two specimens. First, for *Kosmoceratops*, points were plotted on to the dorsal view

provided by Sampson et al. (2010). However, this is not completely perpendicular to the parietal surface. Consultation of photographs of skull casts shows that the parietal posterior bar of *Kosmoceratops* is not as medially embayed as it appears in the image used (this being an artifact of slight arching of the parietal). Hence it is predicted that upon reanalysis of a perpendicular photograph, *Kosmoceratops* might plot more negative along PC 1 (x axis), closer to other members of the *Chasmosaurus* clade. Second, aff. *Pentaceratops* n. sp. MNA Pl.1747 may require revision if the redescription of J. Fry indeed identifies that ep3 is fused to the posterolateral corners of the parietal. This would reduce the anteroposterior offset of the lateralmost margin of the parietal, bringing the morphology of MNA Pl.1747 more similar to UKVP 16100.

Phylogenetic Analysis

Phylogenetic analysis recovers *Navajoceratops sullivani* and *Terminocavus sealyi* as close relatives of both *Pentaceratops* and *Anchiceratops*. The initial analysis was run using the amended matrix of Mallon et al. 2014 (Appendix D), with only *Mojoceratops perifania* excluded because this is considered a junior synonym of *Chasmosaurus russelli* (Maidment and Barrett, 2011; Mallon et al., 2011). This resulted in 6 most parsimonious trees (L = 319 steps; CI = 0.72; RI = 0.79). The strict consensus tree (Figure 4.19) supports a monophyletic Chasmosaurinae, and recovered *Navajoceratops* and *Terminocavus* as successive sister taxa to *Anchiceratops*, *Arrhinoceratops*, and Triceratopsini. However, [*Pentaceratops* + *Utahceratops*] + [*Coahuilaceratops* + *Bravoceratops*] is recovered as sister group to this clade, rather than a direct relationship between *Pentaceratops* and *Navajoceratops*, as would have been predicted based on

parietal morphology. A basal *Chasmosaurus* clade was separated from a [*Vagaceratops* + *Kosmoceratops*] clade by *Agujaceratops*.

Reanalysis 1 additionally excluded *Bravoceratops* because it is a nomen dubium, and *Agujaceratops* because it is coded partly from juvenile material and specimens that may not be referred to the taxon (Appendix C). This yielded 6 most parsimonious trees (L = 310 steps; CI = 0.72; RI = 0.79). The strict consensus tree (Figure 4.20) maintains the relationship of [*Utahceratops* + *Pentaceratops* + *Coahuilaceratops*] as sister group to [*Navajoceratops* + *Terminocavus* + *Anchiceratops* + *Arrhinoceratops* + Triceratopsini]. The most significant result of reanalysis 1 is the unification of a *Chasmosaurus* clade with [*Vagaceratops* + *Kosmoceratops*]. This is similar to the original description of *Vagaceratops* (*Chasmosaurus*) *irvinensis* (Holmes et al., 2001), where the taxon was considered the most derived (and stratigraphically youngest) form of *Chasmosaurus*, a relationship also recovered in the phylogenetic analysis of Longrich (2014).

Reanalysis 2 investigated the effect of excluding *Coahuilaceratops* from the dataset because *Coahuilaceratops* is known from very fragmentary material. This yielded 28 most parsimonious trees (L = 308; CI = 0.72; RI = 0.79). The strict consensus tree (Figure 4.21) maintained the basal *Chasmosaurus* clade, but *Utahceratops*, *Pentaceratops*, *Navajoceratops*, *Terminocavus*, and *Anchiceratops* collapsed into a polytomy.

These analyses support the finding of the morphometric analysis in that the new taxa *Navajoceratops* and *Terminocavus* are morphological intermediates between *Pentaceratops* and *Anchiceratops*, although the absence of a sister group relationship

between *Navajoceratops* and *Pentaceratops* is not supportive of evolution by anagenesis. However, this may be due to the way that *P. sternbergii* is coded in this dataset (see below). The topology of reanalysis 1 and 2 also supports the proposal of Lehman (1998) that a deep split divides the Chasmosaurinae into two lineages (see discussion).

These results match the evolutionary hypotheses based on the stratigraphic positions of taxa, but represent only a first step in the many revisions required of the Sampson et al. (2010) and Mallon et al. (2014) data matrices. Most significant to this study is that in the current matrix, the composite coding of *P. sternbergii* includes specimens that are probably not all referable to the same taxon, e.g. AMNH 6325, 1624, 1625, NMMNH P-50000, and those considered here as aff. *Pentaceratops* n. sp. (MNA Pl.1747 and UKVP 16100). It is therefore required for these specimens to be coded and analysed as at least three separate taxa, but this action awaits the description of the anterior skull elements of these specimens currently being completed by Joshua Fry. A similar recoding is required for *Agujaceratops*; the immature holotype material should not be used for coding the taxon, as its immature status may affect its phylogenetic positioning (e.g. Campione et al., 2013). Instead, referred specimens UTEP P.37.7.065 (isolated parietal) and TMM 43098-1 (near-complete skull, missing the parietal) should be coded separately. The holotype of *Chasmosaurus russelli* (CMN 8800) is in the process of being redescribed (see Campbell et al., 2013), and will likely need to be moved out of *Chasmosaurus* and coded separately from other referred specimens. *Chasmosaurus belli* referred specimen YPM 2016 is also in the process of being redescribed (Campbell et al., 2015), and will need to be coded separately as a

morphologic intermediate between more typical *C. belli* specimens and *Vagaceratops*. Finally, some recently described chasmosaurine taxa (e.g. *Judiceratops*; *Mercuriceratops*; Longrich, 2013; Ryan et al., 2014) have yet to be coded into the matrix of Sampson et al. (2010) / Mallon et al. (2014). *Judiceratops* should be especially informative in phylogenetic analysis as it is one of the oldest known chasmosaurine specimens, having been collected from the lower Oldman-equivalent part of the Judith River Formation north of Rudyard, Montana. However, the material attributed to *Judiceratops* (including the type material) is extremely fragmentary, and forms a composite of four specimens with little overlapping material (Campbell, 2015). *Mercuriceratops* (if it is not pathological) is of aberrant morphology and comprises only two isolated squamosals, so is not likely to improve resolution of Chasmosaurinae.

Discussion

Comparisons and Discussion of Morphological Characters

As the holotype specimens are probable subadults or adults, *Navajoceratops* and *Terminocavus* can be appropriately compared with other taxa that are based on putative adults. *Navajoceratops* and *Terminocavus* form progressive morphological intermediates between the stratigraphically preceding *Pentaceratops* and succeeding *Anchiceratops*. Although limited in available material, Chasmosaurinae sp. "Taxon C" (NMMNH P-33906) exhibits morphology intermediate between the stratigraphically preceding *Terminocavus*, and succeeding *Anchiceratops*. A number of characters of the parietal provide the best means to compare among chasmosaurine taxa.

Median Embayment of the Parietal Posterior Bar. The median embayment of the posterior bar is one of the most important morphological features in distinguishing chasmosaurine taxa. It is defined by the angle at which the lateral rami meet medially, and the proportion of the posterior bar occupied by the embayment.

The angle at which the lateral rami of the posterior bar meet medially (Figures 4.S1 and 4.S5) is comparable in more basal chasmosaurines, but becomes disparate in more derived forms. Within chasmosaurines allied to *Chasmosaurus*, the lateral rami meet at a relatively shallow angle, measuring 87-131° in specimens referred to "*C. russelli*", and shallowing in stratigraphically successive taxa *C. belli* (149-167°) and *Vagaceratops* (177°). In contrast, the lateral rami meet at a relatively steep angle in *Utahceratops* (75°), cf. *Pentaceratops sternbergii* (83°), and aff. *Pentaceratops* n. sp. (87-88°). *Navajoceratops* (60°) and *Terminocavus* (~73°) exhibit angles that are more acute than stratigraphically preceding chasmosaurines, indicating the deepening and enclosing of the median embayment. However, in *Terminocavus* and especially *Anchiceratops*, measurement of the angle of the lateral rami is not straightforward as the lateral rami have become curved and anteroposteriorly expanded.

The median embayment is restricted to the central 30-50% of the posterior bar in stratigraphically older chasmosaurines such as "*Chasmosaurus russelli"*, *Agujaceratops*, *Utahceratops*, and cf. *Pentaceratops sternbergii*. In more derived forms, the apex of the arch formed by each lateral ramus migrates towards the lateral margin, broadening the median embayment. In *C. belli*, *Vagaceratops* and (to an extent) *Kosmoceratops*, this occurs concomitantly with an increase in the angle of the lateral rami such that the

embayment appears weakened or lost. In contrast, in aff. *Pentaceratops* sp., the angle increases, and the embayment appears deeper. In *Navajoceratops* and *Terminocavus* the embayment is again restricted to the central 30-50% of the posterior bar, mainly because anteroposterior expansion of the posterior bar at the ep3 locus gives the lateral rami a more rounded shape. In *Anchiceratops*, the median embayment is effectively completely closed, with only a shallow depression remaining between left and right ep2.

In both *Navajoceratops* and *Terminocavus*, the depth of the embayment and close position of ep1 and ep2 suggest that in life the embayed area might have been completely enclosed by keratin such that an embayment would not be externally visible. This remains speculative, but might be important when formulating hypotheses as to the display function of the frill ornamentation.

Epiparietal Number, Shape, Size, and Orientation. Chasmosaurines typically exhibit three epiparietal loci on each side. Important morphological differences among taxa include shape and size of all epiparietals; position and consequent orientation of ep1 and ep2 relative to the median embayment of the parietal posterior bar; position and orientation of ep3 relative to the posteriormost point of the posterior bar and the articulation with the squamosal.

Of the new specimens, ep1 is only preserved in *Terminocavus* holotype NMMNH P-27468, where its triangular shape is comparable to cf. *Pentaceratops sternbergii*, aff. *Pentaceratops* n. sp., *Anchiceratops*, and some specimens referred to "*Chasmosaurus russelli*", and unlike the laterally expanded ep1 locus in *C. belli*, *Vagaceratops*, and *Kosmoceratops*. In *Terminocavus* ep1 is only slightly deflected dorsally, comparable to

the right side of cf. *P. sternbergii* AMNH 1625, and "*P. aquilonius*" referred specimen CMN 9814 (Longrich, 2014), rather than folded over the posterior bar to point anterolaterally (as in the left side of cf. *P. sternbergii* AMNH 1625, and aff. *Pentaceratops* n. sp.) or laterally (*Anchiceratops*). Given its phylogenetic position, it might be expected for *Terminocavus* to exhibit an anterolaterally oriented ep1 rather than being only slightly deflected dorsally. It is possible that ep1 folds over anteriorly through ontogeny, and that the condition in NMMNH P-27468 is indicative that it is not fully mature; ontogenetic indicators (see above) suggest a status between young subadult to adult for NMMNH P-27468, which leaves open the possibility that the epiparietals might have folded anteriorly if the individual had survived to later greater maturity. However, different ep1 orientations between left and right sides of the putative adult cf. *P. sternbergii*, AMNH 1625, demonstrates that this character is variable, even in an adult.

In *Navajoceratops* and *Terminocavus* locus ep1 occurs within the median embayment, as in *Utahceratops*, cf. *Pentaceratops sternbergii* and aff. *Pentaceratops* n. sp.. This is unlike cf. *Agujaceratops* (UTEP P.37.7.065) and specimens referred to "*Chasmosaurus russelli*" where ep1 occurs at the edge of the embayment. In *C. belli*, *Vagaceratops*, and *Kosmoceratops*, the ep1 locus is expanded laterally and occupies most of the posterior bar (see reinterpretation of *Vagaceratops* and *Kosmoceratops* in Appendix C). In contrast, in *Anchiceratops*, the median embayment is closed such that ep1 effectively occurs at the midline on the dorsal surface of the posterior bar. Orientation of the long axis of ep1 follows the angle of the lateral rami upon which it is mounted. In *Chasmosaurus* it is therefore oriented mostly mediolaterally. In contrast, ep1

is oriented slightly anteroposteriorly in cf. *Pentaceratops sternbergii*, and at an increasingly steep angle from cf. *P. sternbergii* through *Navajoceratops*, *Terminocavus*, and finally *Anchiceratops* in which it is oriented anteroposteriorly such that the tips point laterally.

Ep2 is large and triangular in both *Navajoceratops* and *Terminocavus* holotypes; in *Navajoceratops* the apices are broadly rounded rather than being pointed, whereas in the *Terminocavus* holotype, both ep2 have damaged apices. Large triangular ep2 are seen in most chasmosaurines, although these reach especially large size in *Anchiceratops*. Ep2 is small in some specimens of *C. belli*, and anteriorly inclined in *Vagaceratops*, and *Kosmoceratops*. In the derived *Triceratops* all frill epiossifications are triangular in juveniles, and become broad and flattened in adults (Horner and Goodwin, 2006).

In *Navajoceratops*, ep2 occurs within the median embayment and the pointed tip is medioposteriorly oriented, as in aff. *Pentaceratops* n. sp., and unlike the stratigraphically preceding cf. *P. sternbergii* and *Utahceratops*, where ep2 points posteriorly. In *Terminocavus*, the position and orientation of ep2 is intermediate between *Navajoceratops* and *Anchiceratops*; anteroposterior expansion and increased curvature of the lateral rami causes the constriction of the median embayment such that ep2 is less medially oriented than in *Navajoceratops*, and closer to a posterior orientation.

Locus ep2 is the posteriormost locus in basal chasmosaurines "*Chasmosaurus russelli*", most specimens of *C. belli*, *Kosmoceratops*, *Utahceratops*, and cf. *Pentaceratops sternbergii*. The posteriormost epiparietal locus switches to ep3 in

chasmosaurines more derived than cf. *P. sternbergii* (aff. *Pentaceratops* n. sp, *Navajoceratops*, *Terminocavus*, and *Anchiceratops*).

In chasmosaurines, the apex of locus ep3 points laterally in "*Chasmosaurus russelli*", posterolaterally in *C. belli*; *Vagaceratops*, *Kosmoceratops*, *Utahceratops*, and cf. *Pentaceratops sternbergii*; and posteriorly in aff. *Pentaceratops* n. sp. (inferred from locus), *Navajoceratops* (inferred from locus), *Terminocavus*, and *Anchiceratops*.

Anteroposterior Thickness of the Posterior Bar Lateral Rami. The anteroposterior thickness of the posterior bar is narrow and strap-like in more basal chasmosaurines (*Chasmosaurus*, *Vagaceratops*, *Kosmoceratops*, cf. *Pentaceratops sternbergii*), broadening to become flat and plate like in the most derived forms (*Anchiceratops*, *Arrhinoceratops*, and Triceratopsini). In *Navajoceratops* the posterior bar is anteroposteriorly expanded laterally, being broadest at locus ep3. This is also exhibited by the stratigraphically preceding aff. *Pentaceratops* n. sp., but is unlike cf. *Pentaceratops sternbergii*, *Utahceratops*, *Chasmosaurus*, and *Vagaceratops*, where the posterior bar is strap-like and subequal in anteroposterior thickness along its length. In *Terminocavus* the lateral rami are much more similar to *Anchiceratops* in being strongly anteroposteriorly expanded such that they are plate-like rather than bar-like.

Characters of the Median Bar and Parietal Fenestrae. The parietal median bar exhibits two characters that differ among taxa; the anteroposterior position of the point of maximum constriction, and the development of lateral flanges that invade the parietal fenestrae (with consequent effect on the shape of the cross section).

In referred specimens of "*Chasmosaurus russelli*", *C. belli*, and *Kosmoceratops*, the point of maximum constriction occurs in the posteriormost third of the median bar. In most specimens of *C. belli*, this is immediately at the point of contact with the posterior bar. In *Vagaceratops irvinensis*, the median bar is slightly damaged, but the preserved portion also seems to have the point of maximum constriction in the distal third. In contrast, in cf. *Pentaceratops sternbergii*, aff. *Pentaceratops* n. sp., *Anchiceratops*, *Arrhinoceratops*, and fenestrated specimens of Triceratopsini, the point of maximum constriction occurs approximately at the anteroposterior midpoint of the median bar. The median bar is incomplete in parietals of cf. *Agujaceratops*, *Utahceratops*, *Navajoceratops*, *Terminocavus*, and Chasmosaurinae sp. "taxon C" (NMMNH P-33906), but in these taxa the maximum constriction does not occur adjacent to the posterior bar (ie. as in *Chasmosaurus*), and probably occurs approximately half way along its length.

In basal chasmosaurines *Chasmosaurus*, *Agujaceratops*, *Utahceratops*, cf. *Pentaceratops sternbergii*, aff. *Pentaceratops* n. sp., and *Navajoceratops* the median bar is narrow and strap-like, but develops into a broader structure in *Vagaceratops* (slightly), *Kosmoceratops*, and especially from *Terminocavus* through Chasmosaurinae sp. "taxon C", *Anchiceratops*, *Arrhinoceratops*, and Triceratopsini. Broadening of the median bar is therefore possibly convergent between *Chasmosaurus* and *Anchiceratops* clades. In the taxa basal to *Anchiceratops*, broadening occurs by development of thin lateral flanges that project from the lateral edges of the median bar, generally only easily observable on the ventral side. These are very weakly developed in *Utahceratops* referred specimen UMNH VP-16671, and remain weak to absent in cf. *P. sternbergii* and aff. *Pentaceratops*

n. sp.. In *Navajoceratops* they are slightly more prominent than in stratigraphically preceding taxa, and are similarly further developed in *Terminocavus*. Lateral flanges are much more developed in the stratigraphically younger Chasmosaurinae sp. "taxon C" (NMMNH P-33906; Figure 4.16), where they are conspicuous and approach the level of development seen in some specimens of *Anchiceratops* (e.g. CMN 8535; TMP 1983.001.0001; Mallon et al., 2011). Development of lateral flanges is associated with the reduction in size, and change in shape of the parietal fenestrae.

An obvious character that differentiates basal and derived chasmosaurines is the size and shape of the parietal fenestrae. The fenestrae of derived chasmosaurines (*Kosmoceratops*, *Anchiceratops*, *Arrhinoceratops*, and Triceratopsini) are subrounded to subcircular (although only subangular to subrounded in *Kosmoceratops*), relatively small, and enclosed within the parietal by a broad median bar and wide parietal lateral bars. This is contrasted with the large angular to subangular fenestrae of basal chasmosaurines ("*Chasmosaurus russelli*", *C. belli*, *Vagaceratops irvinensis*, *Utahceratops*, cf. *Pentaceratops sternbergii*, and aff. *Pentaceratops* n. sp, and *Navajoceratops*) which are typically enclosed only by a narrow median bar and thin lateral bars which may not be anteroposteriorly continuous (hence part of the squamosal may form the lateral border of the fenestra). *Terminocavus* is morphologically and stratigraphically intermediate between the two morphotypes, and has subrounded parietal fenestrae. Because Chasmosaurinae sp. "taxon C" is incomplete it is not possible to know the shape of the fenestrae.

The parietal fenestrae of ceratopsian dinosaurs open and expand in size through ontogeny (Dodson and Currie, 1988; Brown et al., 2009; Scannella and Horner, 2010; Fastovsky et al., 2011). As such, it is possible that smaller and more rounded parietal fenestrae in *Terminocavus* holotype NMMNH P-27468 may indicate that the individual was not fully mature, and that the fenestrae would have been larger and perhaps more angular in the final growth stage. Although this is possible, the purportedly juvenile aff. *Pentaceratops* sp. SDMNH 43470 has fenestrae that are relatively larger and more angular (inferrable from the strap-like and straight posterior bar) than in the *Terminocavus* holotype which ontogenetic indicators suggest is a subadult or adult. As such, it is hypothesized that the final size and shape of the fenestrae might not be significantly different from that observed.

Implications of Findings

Although this study demonstrates that most chasmosaurine taxa are still in need of detailed revision, the description of the new taxa provides a good basis from which to investigate the paleobiology of Chasmosaurinae as a group, and the influence of these findings on our understanding of dinosaur evolution in the Late Cretaceous of North America.

Phylogeny: Anagenetic Stacks of Stratigraphically Segregated "Species". In his discussion on the validity of the badly distorted "*Pentaceratops fenestratus*", Mateer (1981; p. 52) suggested that "the presence of two species [of *Pentaceratops*] in the San Juan Basin separated stratigraphically may be real". The new taxa *Navajoceratops* and *Terminocavus*, along

with taxon C (NMMNH P-33906), effectively corroborate this view with better preserved material, expanding it beyond only two taxa, and providing critical morphological links between the stratigraphically preceding form *Pentaceratops* and succeeding *Anchiceratops*.

It is important to recognize that there is little evidence that the naming of these new taxa represents increased diversity in Chasmosaurinae; rather, the new taxa support identification of an unbranching lineage linking *Pentaceratops* and *Anchiceratops*, consistent with the hypothesis of Lehman (1998). The term "diversity" is used broadly in paleontology, typically when referring to multiple named species within a given clade as evidence of diversity. This is often inappropriate; "diversity" should properly only be used to denote two or more contemporaneous species or lineages. In this usage, diversity is therefore evidence of lineage splitting or multiplication, also termed cladogenesis (*sensu* Rensch, 1959) or "speciation" (*sensu* Cook, 1906; Vrba, 1985). The new taxa provide little evidence of lineage splitting, being instead more supportive of an unbranching lineage of stratigraphically separated taxa ("anagenesis"; Rensch, 1959, used here *sensu* Wiley, 1981; syn. "phyletic evolution"; Simpson, 1961) from *Utahceratops* through *Pentaceratops*, *Navajoceratops*, *Terminocavus*, and *Anchiceratops*. The morphometric analysis strongly supports this anagenetic lineage, with each taxon recovered progressively more positive along the PC1 axis (Figure 4.18). The phylogenetic analysis is less supportive of such a long lineage, with [*Utahceratops* + *Pentaceratops*] forming a separate clade to [*Navajoceratops* + *Terminocavus* + *Anchiceratops*]. However, it is expected that this might not be a problem when specimens

of cf. *Pentaceratops sternbergii* (e.g. AMNH 1625), which show strong similarity with *Utahceratops*, are coded separately from aff. *P*. n. sp. (MNA Pl.1747; UKVP 16100). However, this awaits full description of the aff. *P*. n. sp. materials. Since each of the new taxa is stratigraphically separated from preceding and succeeding forms, and stratigraphically preceding forms are recovered as less derived, then we cannot falsify the hypothesis that they are transitional forms within a single unbranching lineage (note that if *Navajoceratops* and *Terminocavus* represent intermediate forms within an anagenetic lineage then it is arguable that they should be considered as a single species, rather than new species or genera; this nomenclatural issue is discussed in Appendix E).

Phylogeny: a Deep-Split Chasmosaurinae. A deep split within a monophyletic Chasmosaurinae is suggested by the morphometric and phylogenetic analyses, supported by stratigraphic data, and consistent with the proposed lineages of Lehman (1998). The split divides Chasmosaurinae into two clades: a *Chasmosaurus* clade ["*C. russelli*" + *C. belli* + *Vagaceratops* + *Kosmoceratops*] and a *Pentaceratops* clade [*Utahceratops* + *Pentaceratops* + *Navajoceratops* + *Terminocavus* + *Anchiceratops* + *Arrhinoceratops* + Triceratopsini]. With the exclusion of [*Arrhinoceratops* + Triceratopsini] (see later discussion) both clades comprise stratigraphically separated taxa that do not overlap (Figure 4.22), with the oldest forms more basal, and younger forms more derived. This is supportive of an initial cladogenesis (speciation) event that created two resultant lineages that subsequently evolved by anagenesis.

The two clades are characterized by a number of divergent, often opposite, morphological trends (expanded from those proposed by Lehman, 1998) observed in

stratigraphically successive taxa within their respective clades. Basal members of both clades exhibit an anteroposteriorly narrow parietal posterior bar bearing a median embayment, and three discrete epiparietals. In the *Chasmosaurus* clade the median embayment shallows as ep1 expands laterally, ep2 and ep3 loci migrate to the posterolateral corners of the parietal, the posterior bar remains anteroposteriorly narrow, and the apices of the curved lateral rami of the posterior bar migrate laterally but remain at ep1 or ep2. This is contrasted with the *Pentaceratops* clade where the median embayment deepens and closes in on itself, ep1 remains medial but rotates its long axis such that it becomes anteroposteriorly oriented, ep2 and ep3 become large and triangular (maintained in adults), and the posterior bar becomes anteroposteriorly broad and plate-like with rounded lateral rami the apex of which occurs at locus ep3. Some morphologic trends are parallel between the clades. The parietal fenestrae of both clades exhibit a trend towards reduction in size, and increase in roundedness, concomitant with laterally expanded median and lateral bars.

The phylogenetic pattern, morphological trends, and stratigraphic occurrence imply divergence from a common ancestral population. The oldest known representative of either clade are specimens referred to "*Chasmosaurus russelli*" from the lower part of the Dinosaur Park Formation (Holmes et al., 2001; Mallon et al., 2012; see Appendix C). This horizon is radiometrically dated as between 77 and 76.3 Ma, corresponding to the uppermost part of the Middle Campanian (Eberth, 2005; 2011; Fowler, Chapter 3). The oldest member of the *Pentaceratops* clade, *Utahceratops*, is slightly younger than this at between ~75.97 Ma to ~75.6 Ma (Roberts et al., 2013; Fowler, Chapter 3). The

cladogenetic split between *Chasmosaurus* and *Pentaceratops* clades must therefore have occurred before 77 Ma.

Collection of new chasmosaurine material from before 77 Ma is thus essential to further our understanding of the timing, rate, and cause of the divergence. Appropriately-aged dinosaur-bearing formations in the Western Interior include the Foremost (~80.2 - 79.4 Ma) and Oldman Formations, Alberta (~79.4 - 77Ma); lower parts of the Judith River (~80 - 77 Ma) and Two Medicine (~81 - 75 Ma) Formations, Montana; Wahweap Formation, Utah (~80 - ~79 Ma), and possibly the Aguja Formation, Texas (Lower to Middle Campanian; Goodwin and Deino, 1989; Rogers et al., 1993; Rogers and Swisher, 1996; Jinnah et al., 2013; Roberts et al., 2013; see Appendix C and Fowler, Chapter 3). Although a good amount of material has been collected from the Aguja Formation (Lehman, 1989; Forster et al., 1993), most is fragmentary, immature, or is missing the critical parietal, making comparisons difficult. However, an isolated middle portion of the parietal posterior bar (UTEP P.37.7.065) is tantalizingly similar to basal members of both *Chasmosaurus* and *Pentaceratops* clades in exhibiting a median embayment restricted to the middle third, however, more complete parietal material is required for further comparisons (also see Appendix C). A range of material has also recently been collected from the Judith River Formation of Montana and lower Oldman of southern Alberta (some published, e.g. the highly fragmentary remains named *Judiceratops tigris*; Longrich, 2013; Campbell, 2015) which has great potential to increase our knowledge of early, and presumably basal, members of these clades.

Latitudinal Biogeography and Vicariance. The deep split within Chasmosaurinae provides support for the hypothesis of latitudinal variation (but critically, not endemism) of North American Campanian dinosaur faunas, implying vicariance in the middle or (more likely) early Campanian which split chasmosaurines into a northern *Chasmosaurus* clade, and a southern *Pentaceratops* clade. Geological and biological evidence demonstrate that geographic isolation of northern and southern populations was not of continuous duration, with northern and southern biomes overlapping or mixing again by the middle Campanian.

In a series of papers, Lehman (1987; 1997, 2001; Lehman et al., 2006) proposed that during the Campanian and Maastrichtian of the North American Western Interior, dinosaur faunas were segregated into northern and southern biogeographic provinces, with the dividing line positioned roughly in central Utah. This hypothesis was criticized and partly falsified as many of the purportedly coeval northern and southern taxa were not contemporaneous and were therefore indicative of stratigraphic rather than geographic segregation (Fowler, 2006; Sullivan and Lucas, 2006). Despite this, an expansion of Lehman's hypothesis was proposed by Sampson et al. (2010), based partly on the description of new chasmosaurine taxa *Kosmoceratops richardsoni* and *Utahceratops gettyi* from the Kaiparowits Formation, Utah. Later, Sampson et al. (2013) rejected previous stratigraphic criticism of the biogeographic hypothesis, suggesting that recalibrated radiometric dates (Roberts et al., 2013) showed that chasmosaurines from the Dinosaur Park Formation, Alberta and Kaiparowits Formation, Utah were indeed contemporaneous, and indicative therefore of intracontinental endemism. However, many

of the radiometric recalibrations of Roberts et al. (2013) are in error, some by as much as a million years (see Fowler, Chapter 3). When properly recalibrated dates are used (Fowler, Chapter 3), the Kaiparowits taxa are shown to be stratigraphically slightly younger than the more basal chasmosaurines from Alberta, with *K. richardsoni* the youngest and most derived member of the *Chasmosaurus* lineage, and *U. gettyi* the oldest and most basal member of the *Pentaceratops* lineage. Thus the contemporaneity required for extreme faunal endemism collapses.

Nevertheless, amidst this criticism, the emphasis on 'lineage-thinking' in the current analysis provides evidence for a subtle form of gradational latitudinal provincialism, but not endemism. Although the *Chasmosaurus* and *Pentaceratops* lineages are not exclusive (ie. endemic) to either north or south (a similar point is raised by both Wick and Lehman, 2013; and Longrich, 2014), it is apparent that the relative abundance of the lineages varies latitudinally in Campanian-aged units (albeit based on a small sample size). Specimens of the *Chasmosaurus* clade are much more abundant in the northern United States and Canada, with the southernmost representative (*Kosmoceratops richardsoni*), represented by two specimens from the Kaiparowits Formation of southern Utah. Specimens of the *Pentaceratops* clade are more common in the southern states of New Mexico and Utah, with only one or two possible representative specimens from southern Alberta (see discussion on *Chasmosaurus russelli* in Appendix C). This biogeographic pattern does not represent endemism as the two lineages overlap geographically during the uppermost part of the middle Campanian in Alberta and Utah. However it is suggestive that latitudinally aligned vicariance might have been the cause

of the speciation event that created the two chasmosaurine lineages. As the oldest member of the *Chasmosaurus* lineage occurs at ~77Ma (see above) then vicariance must have occurred before this time. Similarly, as both lineages are seen to coexist in the uppermost part of the Dinosaur Park Formation (~76 Ma) then any physical barrier must have been passable by this time. The location of the barrier is suggested by the fact that the dividing line between northern and southern provinces appears to lie somewhere between southern Utah and northern Montana.

Sampson et al. (2010; 2013) state that there is currently no evidence for a physical barrier separating northern and southern provinces, but this is not the case. In 1990, Lillegraven and Ostresh (not referenced by Sampson et al., 2010; 2013) produced 33 maps illustrating Late Cretaceous transgression and regression of the western shoreline of the Western Interior Seaway (WIS). The maps were at a very high stratigraphic resolution, documenting almost every ammonite zone from the middle Santonian (*Clioscaphites choteauensis*; 85.23 Ma; Ogg et al., 2012) through to the K-Pg boundary (66 Ma). Most importantly, the maps contrast the paleoshoreline with the modern position of the eastern Sevier thrust front of the Rocky Mountains. Although the position of the thrust front was slightly more western in the Late Cretaceous (and the mountains were not as elevated; DeCelles, 2004), it is a good approximation for the position of the upland or mountainous area which flanked the coastal plain. From these maps it can be readily observed that during the middle Santonian (85 Ma) through to earliest part of the middle Campanian (81 Ma), the shoreline of the WIS intermittently abutted the thrust front of the incipient Rockies from central Utah to southern Alberta. For hundreds of

miles the coastal plain would have been extremely narrow, in some places perhaps as little as 5-10 kilometers, providing very limited habitat. This would be similar to, for example, the modern day Zagros Mountains of Iran which are abutted by the eastern shoreline of the Persian / Arabian Gulf. This bottlenecking of the available coastal plain effectively cut off the north-south dispersal route, latitudinally bisecting the coastal plain habitat of North America into southern and northern areas separated by hundreds of miles. The latitudinal climate gradient might have exacerbated difference in climate between northern and southern regions, although the latitudinal climate gradient was not as strong in the Late Cretaceous as it is today. Lillegraven and Ostresh (1990) show that from the early part of the middle Campanian (~80 Ma) regression of the WIS results in a broader coastal plain, and it is hypothesized here that this may no longer have presented a physiographic boundary, thereby permitting interspersal of chasmosaurine lineages, as evidenced by the presence of *Pentaceratops* lineage taxa in the uppermost Dinosaur Park Formation, ~76 Ma (Longrich, 2014), and later *Anchiceratops* in the Horseshoe Canyon Formation, ~71 Ma (Mallon et al., 2011).

The Role of Heterochrony in Evolution of the Frill and Effects on Phylogenetic Analysis. The process of heterochrony describes changes in the rate and timing of development between stratigraphically successive populations. Most morphological trends recognized in this study are potentially controlled or affected by heterochrony, but inference of this requires knowledge of change through both ontogeny and stratigraphy. Although stratigraphic position is at least roughly known for most species in the current study, few especially young or old individuals of relatively

basal chasmosaurines have been published, such that their ontogenetic change is not well understood. Nevertheless, some possible heterochronic trends can be identified or hypothesized based on the limited available material and comparison to the well-documented growth series of the Late Maastrichtian derived chasmosaurine *Triceratops* (Horner and Goodwin 2006; 2008; Scannella and Horner, 2010). This may have important practical implications for taxonomy and the way specimens are coded for phylogenetic analysis, but also in a broader sense may be informative about some of the unusual features of basal and derived chasmosaurines.

Development of the Median Embayment. The median embayment of the parietal posterior bar successively shallows and broadens through time in the *Chasmosaurus* lineage, and deepens then closes in the *Pentaceratops* lineage. There is some evidence to suggest that similar patterns are observed ontogenetically. In "*Chasmosaurus russelli*", referred adult specimen CMN 2280 has a shallow central embayment with lateral rami at an angle of 131°. The immature referred specimen, AMNH 5656, has an embayment that is less shallow (99°) and is more restricted to the central third of the posterior bar. Adult specimens of the stratigraphically successive *C. belli*, and *Vagaceratops irvinensis* have an even shallower embayment than adult "*C. russelli*" suggesting peramorphosis in the *Chasmosaurus* lineage.

Concerning basal members of the *Pentaceratops* lineage, there are no published juvenile specimens, which preserve the median embayment, that have been recovered from the same strata as the various holotypes (and as such, could be more reliably assigned to a given taxon). Consequently the progressive deepening of the median

embayment (observed stratigraphically and phylogenetically) cannot currently be assessed for an ontogenetic component.

Development of Parietal Fenestrae. In Ceratopsia, the parietal fenestrae open during ontogeny by resorption of central regions of the previously solid parietal. Although this is still controversial (e.g. Farke, 2011), opening of fenestrae through ontogeny has been proposed in both basal neoceratopsians (*Protoceratops*; Fastovsky et al., 2011) and the highly derived Late Maastrichtian ceratopsid *Triceratops* (Scannella and Horner, 2010). As such, it is probable that ontogeny influences the size and shape of parietal fenestrae in both the *Chasmosaurus* and *Pentaceratops* lineages, reflected in the width of the median, posterior and lateral bars.

In adult specimens of basal chasmosaurines, the median bar of the parietal either lacks lateral flanges that invade the fenestrae, or they are only weakly developed. Flanges are more strongly developed and conspicuous in Chasmosaurinae sp. taxon C (NMMNH P-33906) and more derived chasmosaurines like *Anchiceratops*. It is likely that development of the flanges occurs by paedomorphosis; ie. that flanges form as a result of the fenestrae opening less extensively during ontogeny (in more derived forms), rather than the flanges growing laterally from the median bar. It is expected therefore that juveniles of some of the more derived *Pentaceratops* lineage taxa (e.g. *Terminocavus* or taxon C) would exhibit relatively wider median bars with more developed lateral flanges, and smaller parietal fenestrae. In this respect, they might appear more similar to adults of derived chasmosaurines. This is seen in the *Chasmosaurus* lineage, where juvenile "*C.*

russelli" referred specimen AMNH 5656 has very weak lateral flanges on the median bar, whereas in more mature specimens (e.g. CMN 2280) lateral flanges are absent.

The development of the broad plate-like posterior bar (in *Pentaceratops* lineage) and lateral bars of the parietal is similarly expected to be a result of paedomorphosis. The posterior bar of immature aff. *Pentaceratops* sp. SDMNH 43470 comprises a bar-like posterior portion (typical of more basal members of the *Pentaceratops* lineage), which has small thin flanges extending anteriorly into the parietal fenestrae. These could be interpreted as remnants of a previously more extensive plate-like part of the posterior bar that is resorbed by adulthood in more basal chasmosaurines (thereby increasing the size of the fenestrae). Hypothesized paedomorphosis in more derived members of the *Pentaceratops* lineage might lead to retention of this flange.

In derived chasmosaurines (e.g. "*Torosaurus*", *Anchiceratops*, and *Kosmoceratops*), the lateral bars of the parietal are laterally broad and completely enclose the fenestrae within the parietal. In basal chasmosaurines the lateral bars are much narrower and might not fully enclose the fenestra (such that the squamosal forms part of the lateral margin). Within the *Chasmosaurus* lineage, "*Chasmosaurus russelli*" referred adult specimen CMN 2280 is illustrated by Godfrey and Holmes (1995) as exhibiting incomplete lateral rami (ie. the squamosal contributes to the fenestra), whereas in immature referred specimen AMNH 5656, the lateral bars are continuous, fully enclosing the fenestrae. This limited sample suggests that ontogenetic expansion of the parietal fenestrae may cause resorption of the central parts of the lateral bars, causing them to become discontinuous in adults. If so, this would be a paedomorphic trend as in

specimens of the slightly more derived *C. belli*, the fenestra is enclosed entirely within the parietal (Godfrey and Holmes, 1995). A similar paedomorphic trend is probably present in the *Pentaceratops* lineage where basal members have continuous but thin lateral bars, which are broad in *Anchiceratops* and more derived forms. This is only hypothetical as lateral bars are not preserved in *Navajoceratops*, *Terminocavus*, and "taxon C".

Origin of *Arrhinoceratops* and the Triceratopsini: a Second Speciation? The description of intermediate morphotaxa between *Pentaceratops* and *Anchiceratops* has implications for the origin of *Arrhinoceratops* and the Triceratopsini [*Ojoceratops* + *Eotriceratops* + "*Torosaurus*" + *Triceratops*]. In most phylogenetic analyses, *Arrhinoceratops* and the Triceratopsini are recovered as very closely related to *Anchiceratops* (e.g. Dodson et al., 2004; Sampson et al., 2010; Longrich, 2014; and the current analysis). Since *Anchiceratops* and *Arrhinoceratops* were contemporaneous (co-occurring in the Horsethief and Morrin members of the Horseshoe Canyon Formation, Alberta; ~72.4 - 71.6 Ma; Eberth et al., 2013; Mallon et al., 2014) then the phylogenetic relationship illustrated in Figures 4.19-4.21 require that a second speciation event splitting the two must have occurred prior to this time, but after the occurrence of the immediately basal *Terminocavus* (~74.7 Ma). However, taxa immediately basal to *Anchiceratops* do not resemble *Arrhinoceratops*, being generally characterized by a deep notch-like median embayment and large triangular epiparietals, neither of which are observed in *Arrhinoceratops* at any ontogenetic stage (Mallon et al., 2014). It is possible that character states shared between

Arrhinoceratops and *Anchiceratops* (for example, small circular parietal fenestrae) may be homoplastic rather than synapomorphic, and could instead reflect shared long term trends observed across Chasmosaurinae (see above). Although this is speculative, candidates for a different origin of *Arrhinoceratops* and the Triceratopsini are present in the poorly known *Coahuilaceratops* (Loewen et al., 2010) and "*Bravoceratops*"(Wick and Lehman, 2013; see Appendix C), from the lower Maastrichtian of Mexico and Texas, respectively. Although both taxa are known from only very scant remains, both exhibit anteriorly positioned nasal horns and retain bumps on the anterior end of the parietal relatively late in ontogeny, both features characteristic of Triceratopsini. Recovery of more complete specimens of *Coahuilaceratops* and "*Bravoceratops*" may be enlightening.

Regardless of their precise phylogenetic origin, the slightly embayed, cardioid shape of the frill in some specimens referred to "*Torosaurus*" (YPM 1831; TMM 41480-1) and *Triceratops* (e.g. AMNH 5116) may be a remnant feature of their ancestry; a plesiomorphy exhibited by a few members of the population, which is gradually being lost. This is supported by the fact that very few specimens of *Triceratops prorsus* exhibit any parietal midline embayment, despite many specimens having been collected.

Conclusions

Description of the new taxa *Navajoceratops sullivani* and *Terminocavus sealyi*, and the fragmentary taxon C, provides critical stratigraphic and morphologic links between the Campanian *Pentaceratops*, and the Maastrichtian *Anchiceratops*, reinstating

the phylogenetic hypothesis originally postulated by Lehman (1993, 1998). Combined with significant revision of other chasmosaurine taxa, this reveals a deep split of the Chasmosaurinae into *Chasmosaurus* and *Pentaceratops* clades, which are mostly arranged into stacks of stratigraphically successive taxa. Morphological divergence from similar basal forms suggests the clades evolved from a common ancestor, which was subject to a true speciation or cladogenetic event, probably in the early Campanian. After this initial speciation, stratigraphically successive taxa suggest that evolution proceeded mostly by unbranching anagenesis, with evidence for only one additional speciation event, that of *Arrhinoceratops* (and the Triceratopsini).

Analysis of paleogeographic maps suggest that high sea level in the Santonian through to middle Campanian may have segregated an ancestral chasmosaurine population into northern and southern subpopulations, which over time led to divergence and speciation. This lends support to a to recent hypotheses of latitudinally arrayed differences in terrestrial faunal composition (e.g. Lehman, 1987; 1997, 2001), but stops short of supporting the extreme version of these hypotheses which posit Campanian basinal-level endemism (e.g. Sampson et al., 2010).

Description of the new material places San Juan Basin chasmosaurines as among the best documented of their clade, second only to *Triceratops* in number of specimens and quality of accompanying data. Although this work presents significant revision of many chasmosaurine taxa, much reanalysis and redescription remains.

Acknowledgements

Grateful thanks extended to my committee: Jack Horner, David Bowen, David Varricchio, and David Eberth, as well as Liz Freedman Fowler, Warwick and Jackie Fowler, Mark Goodwin, Joe Hartman, Ray Butler, Arthur Bogan, Greg Wilson, Dean Pearson, John Hoganson, Kirk Johnson, MOR preparators and staff, Bob Sullivan, Spencer Lucas, and everyone at the Digital Library Project. Funding for the Museum of the Rockies graduate student fund was provided by Damaris Waggoner and David Sands. Additional funding was provided by the Welles Fund (UCMP), the Jurassic Foundation, Jackson School of Geosciences (SVP), MSU Dept. Cell Biology and Neuroscience, and MSU College of Letters and Science.

Table 4.1. List of specimens discussed in this study. Detailed descriptions of the cranial material preserved for each specimen, geologic and geographic locality information, and discussion of taxonomic assignments are available in Appendix C. Specimens are listed in the order in which they are discussed in the text and Appendix C. References in this table refer to publications that figure and/or describe this material.

Specimen	Taxonomic Assignment	Material Preserved	Geology	Locality	Notes and Original References
SMP VP-1500	*Navajoceratops sullivani* gen. et sp. nov.	parietal, squamosal fragments, jugal-epijugal	lower Hunter Wash Member of Kirtland Formation	San Juan Basin, New Mexico	Figures 4.9-4.12
NMMNH P-27468	*Terminocavus sealeyi* gen. et sp. nov.	parietal, jugal, epijugal, partial quadratojugal	middle of Hunter Wash Member of Kirtland Formation	San Juan Basin, New Mexico	Figures 4.13-4.15
NMMNH P-33906	Chasmosaurinae sp. "Taxon C"	parietal median bar, epijugal	De-na-zin Member of Kirtland Formation	San Juan Basin, New Mexico	Figure 4.16
AMNH 6325	*Pentaceratops sternbergii*	mostly complete skull missing posterior parietal	middle of Fossil Forest Member of Fruitland Formation	San Juan Basin, New Mexico	Holotype. (Osborn, 1923)
AMNH 1624	cf. *Pentaceratops sternbergii*	mostly complete skull missing posterior parietal	middle of Fossil Forest Member of Fruitland Formation	San Juan Basin, New Mexico	(Lehman, 1993; 1998; Sullivan and Lucas, 2011)
AMNH 1625	cf. *Pentaceratops sternbergii*	mostly complete frill missing anterior parietal and anterior squamosal	middle of Fossil Forest Member of Fruitland Formation	San Juan Basin, New Mexico	(Longrich, 2014)
UKVP 16100	aff. *Pentaceratops* n. sp.	skull with frill	between the uppermost coal of Fruitland Formation and top of Bisti Bed Sandstone of Kirtland Formation	San Juan Basin, New Mexico	(Rowe et al., 1980; Lehman, 1998)
MNA Pl.1747	aff. *Pentaceratops* n. sp.	skull with frill	between the uppermost coal of Fruitland Formation and top of Bisti Bed Sandstone of Kirtland Formation	San Juan Basin, New Mexico	(Rowe et al., 1980; Lehman, 1993)
NMMNH P-37880	aff. *Pentaceratops* n. sp.	half of right ramus of parietal posterior bar	upper Fossil Forest Member of Fruitland Formation	San Juan Basin, New Mexico	Figure 4.S2
OMNH 10165	aff. *Pentaceratops* sp.	skull with fragmentary frill	Fossil Forest Member of Fruitland Formation	San Juan Basin, New Mexico	"*Titanoceratops ouranos*" (Lehman, 1998; Longrich, 2011)
PMU 24923	"*Pentaceratops fenestratus*"	skull with frill	Kirtland Formation	San Juan Basin, New Mexico	Holotype. (Wiman, 1930)

Table 4.1, continued.

Specimen	Taxonomic Assignment	Material Preserved	Geology	Locality	Notes and Original References
PMU 24924	aff. *Navajoceratops* sp.	anterior parietal median bar	Kirtland Formation	San Juan Basin, New Mexico	Figure 4.S3C
NMMNH P-50000	Chasmosaurinae sp.	partial skull missing frill	Hunter Wash Member or Farmington Member of Kirtland Formation	San Juan Basin, New Mexico	(Sampson et al., 2010)
SDMNH 43470	aff. *Pentaceratops* sp.	partial skull with midline of parietal posterior bar	lower Williams Fork Formation	Colorado	(Diem and Archibald, 2005; Lucas et al., 2006; Longrich, 2014)
UMNH VP 16784	*Utahceratops gettyi*	skull with right ramus of parietal posterior bar	lower part of middle Kaiparowits Formation	Utah	Holotype. (Sampson et al., 2010)
UMNH VP 16671	*Utahceratops gettyi*	parietal posterior bar	middle Kaiparowits Formation	Utah	(Sampson et al., 2010)
CMN 9813	*Pentaceratops aquilonius*	distal squamosal and lateralmost parietal posterior bar	uppermost Dinosaur Park Formation	Alberta	Holotype. (Langston, 1959; Longrich, 2014)
CMN 9814	*Pentaceratops aquilonius*	fragment of right lateral ramus of parietal posterior bar and two isolated epiossifications	Lethbridge Coal Zone of Dinosaur Park Formation	Alberta	Paratype. (Langston, 1959; Longrich, 2014)
TMM 46015-1	*Bravoceratops polyphemus*	partial skull with partial parietal	lowermost Javelina Formation	Texas	Holotype. (Wick and Lehman, 2013)
TMP 1983.25.1	"*Mojoceratops perifania*"	partial skull with frill	Dinosaur Park Formation?	Alberta	Holotype. (Longrich, 2010)
CMN 491	*Chasmosaurus belli*	mostly complete parietal	Dinosaur Park Formation?	Alberta	Holotype. (Lambe, 1902; Hatcher, 1907; Lambe, 1914a and 1914b)
YPM 2016	*Chasmosaurus belli*	skull with frill	Dinosaur Park Formation	Alberta	Figure 4.S5
CMN 8800	"*Chasmosaurus russelli*"	complete skull with frill	upper Dinosaur Park Formation	Alberta	Holotype. (Sternberg, 1940)
CMN 2280	"*Chasmosaurus russelli*"	complete skull with frill	Dinosaur Park Formation	Alberta	(Godfrey and Holmes, 1995)
CMN 41357	*Vagaceratops* (*Chasmosaurus*) *irvinensis*	complete skull with frill	upper Dinosaur Park Formation below the Lethbridge Coal Zone	Alberta	Holotype. (Holmes et al., 2001; Sampson et al., 2010)
UMNH VP 17000	*Kosmoceratops richardsoni*	complete skull with frill	Kaiparowits Formation	Utah	Holotype. (Sampson et al., 2010)
UTEP P.37.7.086	*Agujaceratops* (*Chasmosaurus*) *mariscalensis*	partial skull missing frill	lower Upper Shale Member of Aguja Formation	Texas	Holotype. (Lehman, 1989; Lucas et al., 2006)
UTEP P.37.7.065	*Agujaceratops* (*Chasmosaurus*) *mariscalensis*	partial parietal	lower Upper Shale Member of Aguja Formation	Texas	(Lehman, 1989; Lucas et al., 2006)

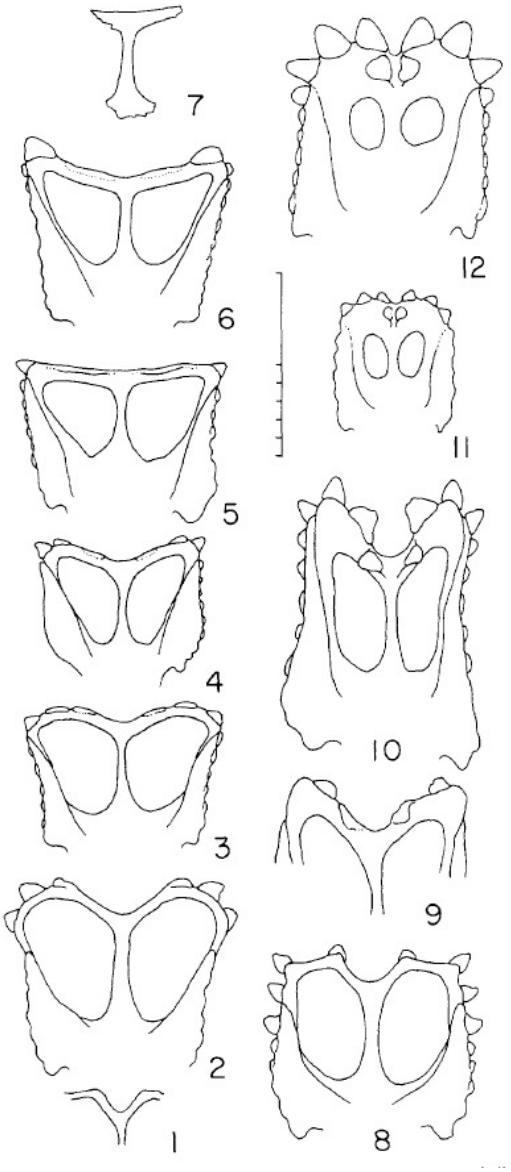

Figure 4.1. Hypothesis of chasmosaurine relationships from Lehman (1998). Lehman (1998) proposed that Campanian chasmosaurines belonged to two lineages evolving divergently from initially similar morphology. A *Chasmosaurus* lineage (left, *C. russelli* 1-3, *C. belli* 4-7) was characterized by progressive shallowing of the parietal median embayment, development of epiparietals into an elongate ridge at locus ep1, and lateral migration of loci ep2 and 3. In contrast, an *Agujaceratops* (8) - *Pentaceratops* (9, 10) -

Anchiceratops (11, 12) lineage (right) was characterized by a deepening median embayment which caused rotation of epiparietals at locus ep1 to form the butterfly-wing orientation characteristic of *Anchiceratops*. Lehman's hypothesis was consistent with the stratigraphic distribution of the depicted specimens, and was further supported by the subsequent discovery of new taxa. Facsimile of Lehman (1998).

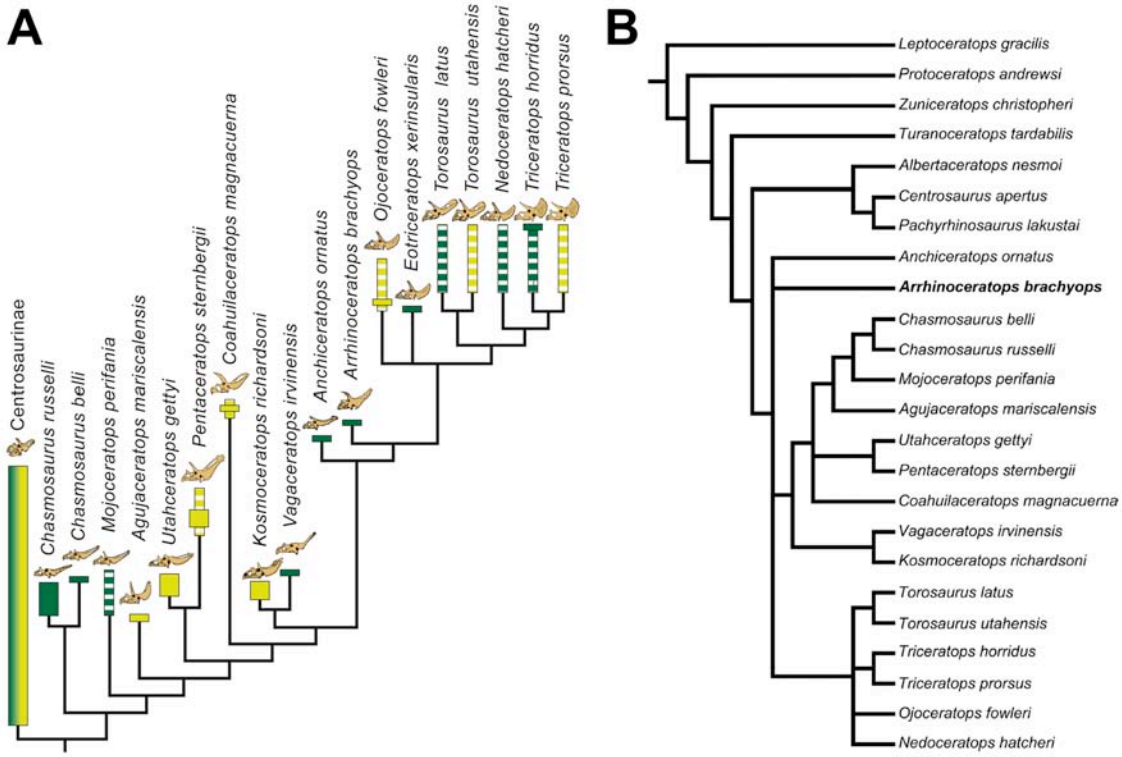

Figure 4.2. Alternative hypotheses of chasmosaurine phylogeny. Two recent phylogenetic analyses contrast the dual-lineage hypothesis of Lehman (1998). A, Sampson et al. (2010) recover a phylogeny where *Pentaceratops* is unrelated to *Anchiceratops*; where *Vagaceratops* is unrelated to *Chasmosaurus*; and where instead *Kosmoceratops* and *Vagaceratops* form an outgroup to *Anchiceratops* and all other more derived chasmosaurines. B, Mallon et al. (2014; drawing on the same phylogenetic matrix as Sampson et al., 2010) published a phylogeny where the Lower Maastrichtian taxa *Anchiceratops* and *Arrhinoceratops* occur in a basal polytomy, and some of the stratigraphically oldest taxa form the most derived clade (Middle to Upper Campanian *C. belli* + C. *russelli*). These new analyses require significant ghost lineages be present for most clades, for which there is currently no fossil evidence. A, B adapted from Sampson et al. (2010) and Mallon et al. (2014) respectively.

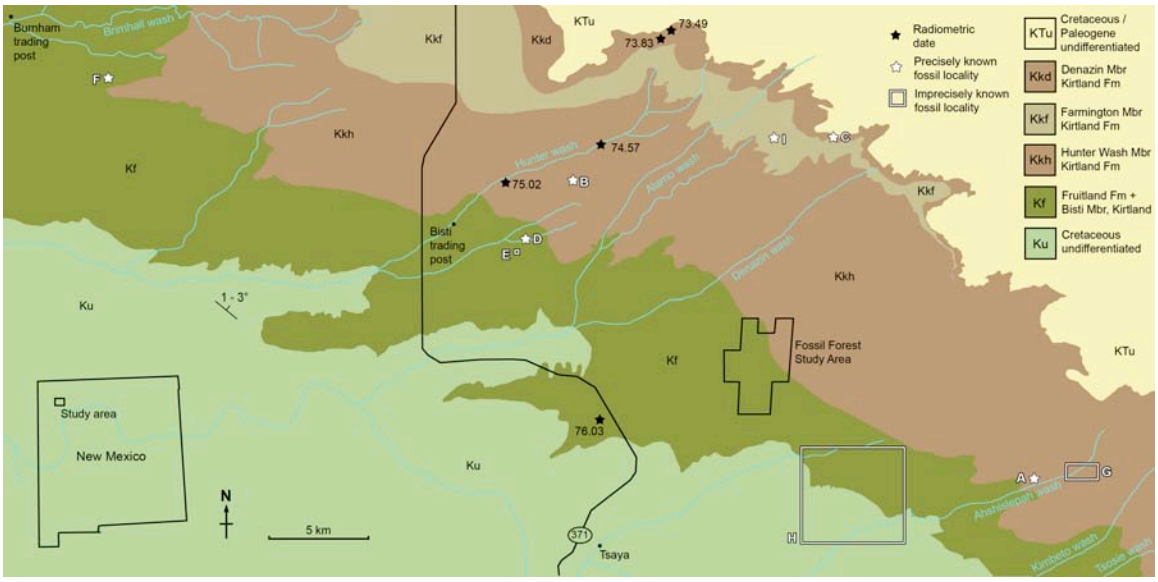

Figure 4.3. Geological map of the southeast San Juan Basin showing localities of radiometric dates and important fossil specimens mentioned in the text. Collection localities; A, SMP VP-1500, *Navajoceratops sullivani*, holotype; B, NMMNH P-27486, *Terminocavus sealeyi*, holotype; C, NMMNH P-33906, Denazin chasmosaurine; D, NMMNH P-37880, c.f. *Pentaceratops sternbergii*, parietal fragment; E, UKVP 16100, c.f. *P. sternbergii*, complete skull; F, MNA Pl.1747, c.f. *P. sternbergii*, complete skull; G, USNM 8604, Chasmosaurinae sp. anterior end of a parietal median bar; H, purported collection area of AMNH 6325, *P. sternbergii*, holotype. I, NMMNH P-50000, Chasmosaurinae sp., skull missing frill. Radiometric dates recalibrated from Fassett and Steiner (1997) by Fowler (Chapter 3) using Ar / Ar standard and decay constants of Kuiper et al. (2008) and Min et al. (2000). Bedrock geology altered from O'Sullivan and Beikman (1963).

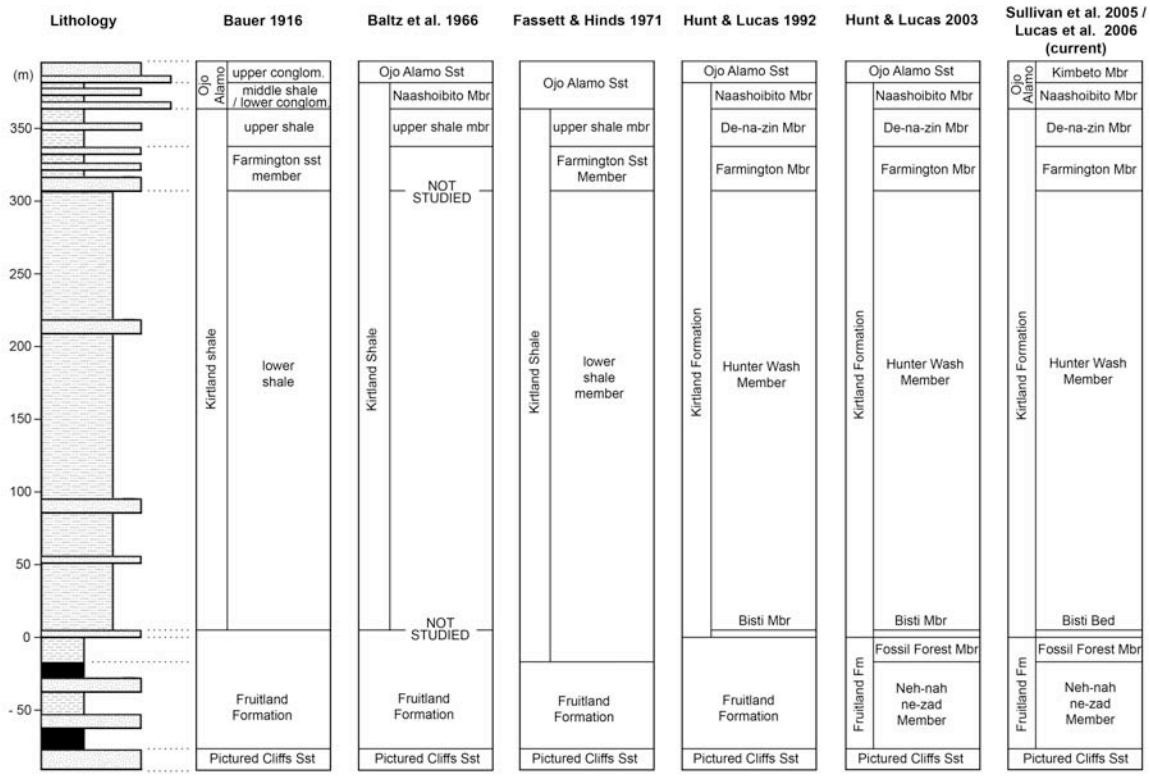

Figure 4.4. Historical stratigraphic terminology of the Fruitland and Kirtland Formations. The Fruitland and Kirtland Formations of the San Juan Basin have undergone many changes regarding terminology, and (more importantly) the definitions of member or formational contacts. Here I illustrate all the revisions in chronological order, ending with the current terminology and definitions used in this study. Adapted from Bauer (1916); Baltz et al. (1966); Fassett and Hinds (1971); Hunt and Lucas (1992; 2003); Sullivan et al. (2005) and Lucas et al. (2006). Section thickness in meters (m).

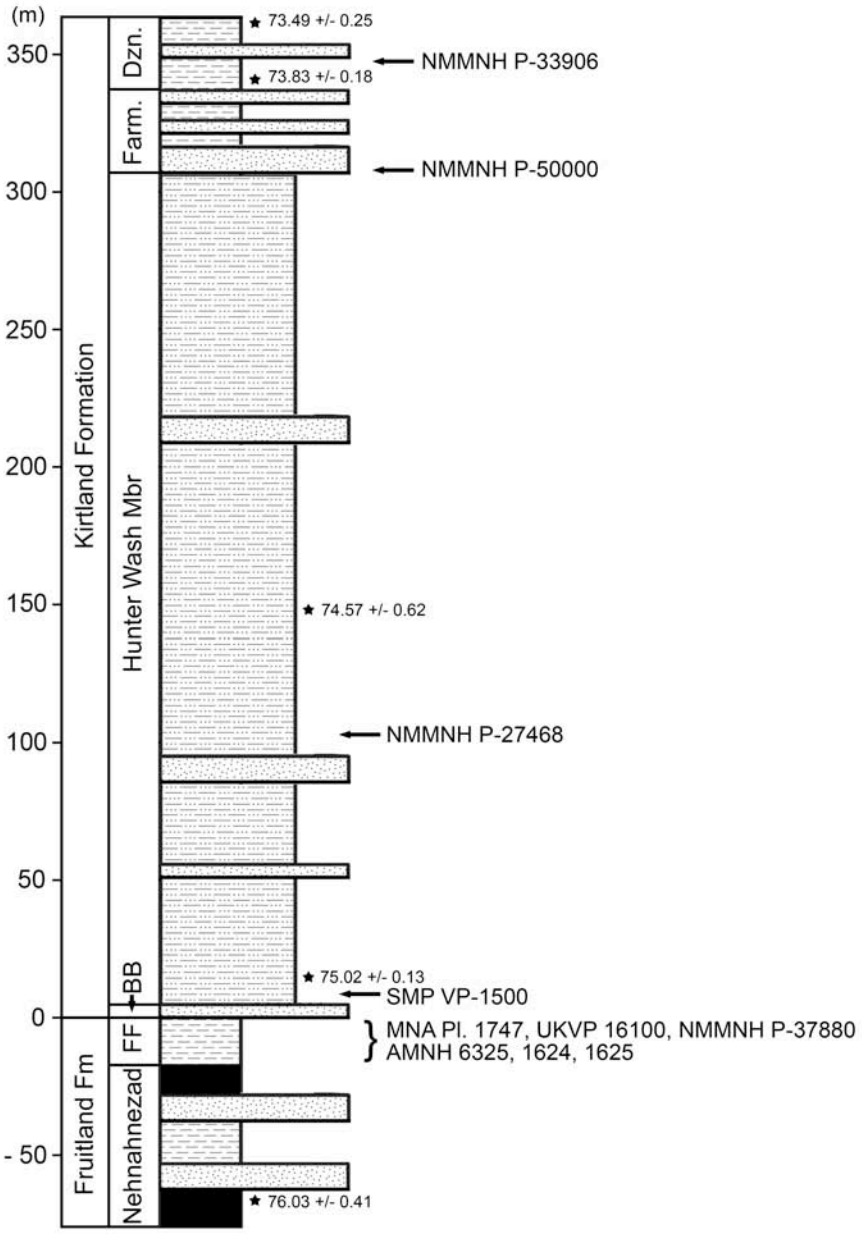

Figure 4.5. Generalized stratigraphic column of the Fruitland and Kirtland Formations with radiometric dates and fossil occurrences. Specimens mentioned in the main text or Appendix C: *Pentaceratops sternbergii* holotype, AMNH 6325; cf. *P. sternbergii*, AMNH 1624, 1625; aff. *Pentaceratops* n. sp., MNA Pl.1747, UKVP 16100, NMMNH P-37880; *Navajoceratops sullivani* holotype SMP VP-1500; *Terminocavus sealeyi* holotype, NMMNH P-27468; Chasmosaurinae sp., NMMNH P-50000; "Taxon C", NMMNH P-33906. Radiometric dates (★) recalibrated from Fassett and Steiner (1997) by Fowler (Chapter 3) using Ar / Ar standard and decay constants of Kuiper et al. (2008) and Min et al. (2000).

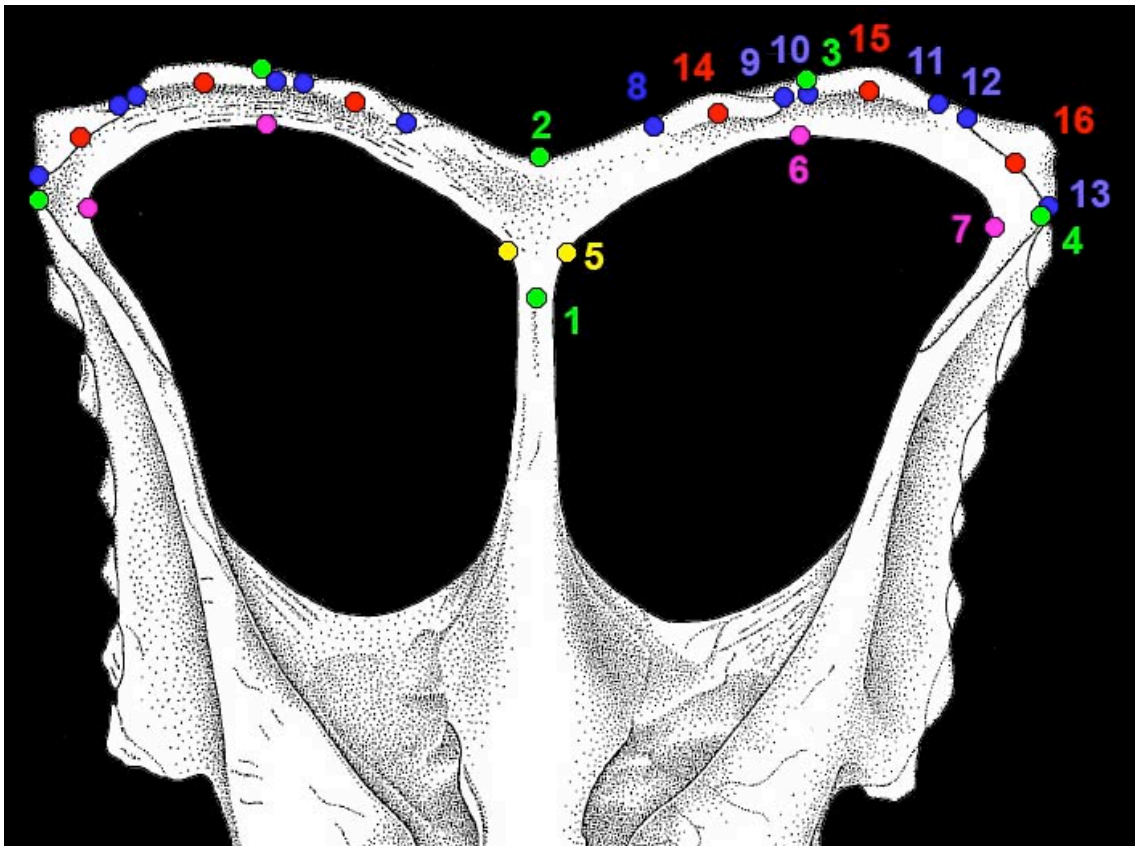

Figure 4.6. Morphological landmarks used in morphometric analysis of chasmosaurine parietals. All landmarks were measured on the parietal only. Points 1 and 2 are the same for both left and right sides, but all other points were mirrored for the right side and analysed along with the non-mirrored left side. Points are defined as follows: (1-4; green): 1, maximum constriction of the median bar, positioned on the midline; 2, posteriormost point of the parietal at the midline; 3, posteriormost point of the parietal anywhere along the posterior margin; 4, lateralmost point of the parietal; (5, yellow): 5, point at which the lateral ramus of the posterior bar meets the median bar as expressed on the posteriomedial border of the parietal fenestra, may be marked by a change in angle of the fenestra border; (6, 7; magenta): 6, posteriormost point of parietal fenestra; 7, lateralmost point of parietal fenestra; (8-13; blue): 8, contact point of the medial margin of epiparietal 1 with the parietal itself ; 9, contact point of the lateral margin of epiparietal 1 with the parietal itself; 10, contact point of the medial margin of epiparietal 2 with the parietal itself ; 11, contact point of the lateral margin of epiparietal 2 with the parietal itself; 12, contact point of the medial margin of epiparietal 3 with the parietal itself ; 13, contact point of the lateral margin of epiparietal 3 with the parietal itself; (14-16; red): 14, The contact point of the midpoint of epiparietal 1 with the parietal itself; 15, The contact point of the midpoint of epiparietal 2 with the parietal itself; 16, The contact point of the midpoint of epiparietal 3 with the parietal itself. Colors are intended to aid in visual distinction only. Points illustrated on *Chasmosaurus russelli* referred specimen CMN 2280, adapted from Godfrey and Holmes (1995).

Figure 4.7. *Navajoceratops sullivani* holotype SMP VP-1500 parietal exposed before collection. An area of rugose concreted bone occurred at locus ep1 and extended around the anterior border of the median embayment (em), but was mostly unrecoverable during preparation. This is interpreted here representing ep1. ep1, epiparietal 1. f, parietal fenestra. L-lr, Left lateral ramus of the posterior bar. Hammer for scale = 28 cm.

Figure 4.8. *Navajoceratops sullivani* holotype SMP VP-1500 parietal exposed before collection. The median bar (mb) of SMP VP-1500 was slightly displaced laterally and ventrally. em, median embayment of posterior bar. ep1, epiparietal 1. f, parietal fenestra. L-lr / R-lr, Left / Right lateral rami of the posterior bar. Hammer for scale = 28 cm.

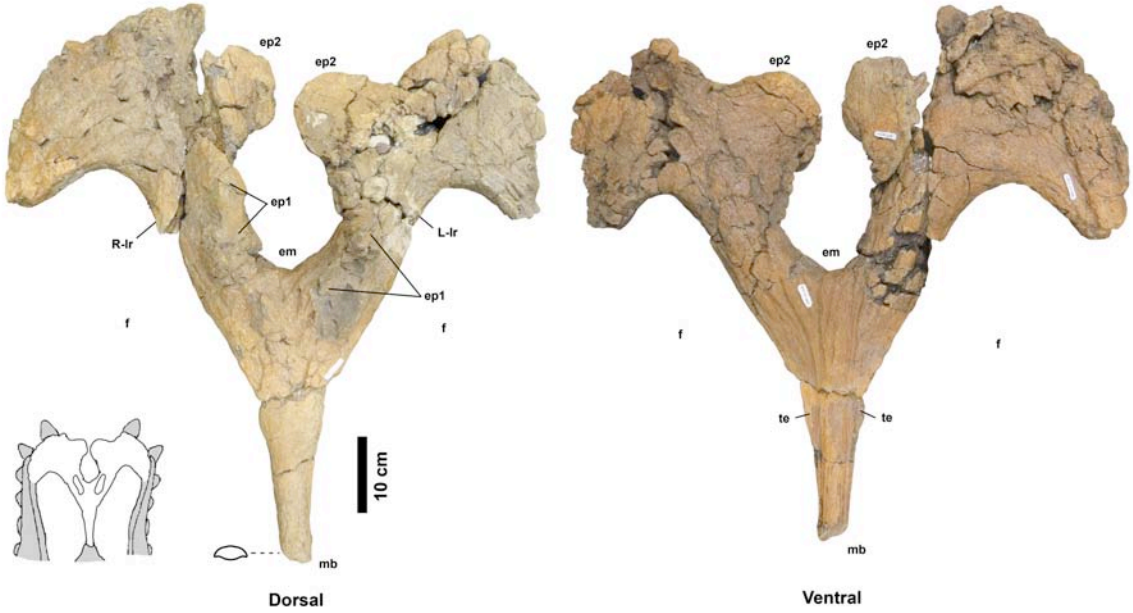

Figure 4.9. *Navajoceratops sullivani* holotype SMP VP-1500 parietal. Dorsal (left) and ventral (right) views. cross section of median bar (mb) illustrated on dorsal view. Ep1 mostly removed during extraction or preparation (see Figure 4.7 for original extent). em, median embayment of the posterior bar; ep, epiparietal loci numbered by hypothesized position (no epiossifications are fused to this specimen). f, parietal fenestra. L-lr / R-lr, Left / Right lateral rami of the posterior bar. te, tapering lateral edges of the median bar. Scalebar = 10 cm. Reconstruction adapted from Lehman (1998).

Figure 4.10. *Navajoceratops sullivani* holotype SMP VP-1500 isolated frill epiossification. Isolated frill epiossification found with parietal. Possibly an epiparietal, although squamosal fragments were found weathered out on the surface. Scalebar = 5 cm.

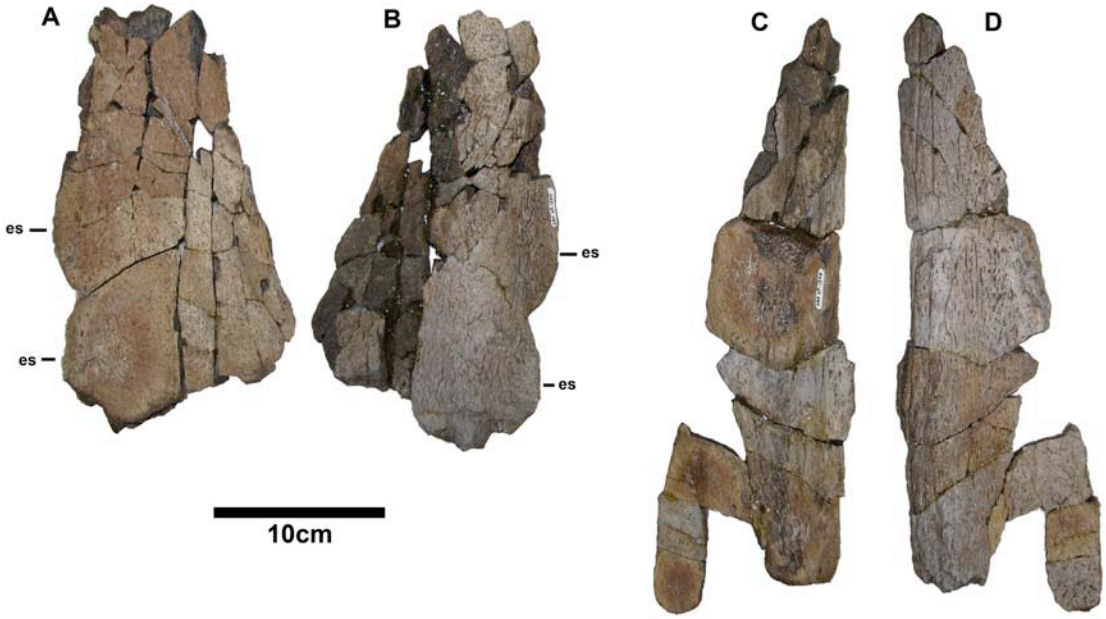

Figure 4.11. *Navajoceratops sullivani* holotype SMP VP-1500 squamosal fragments. Two of the largest fragments of the squamosal found weathered on the surface next to the parietal. A (dorsal), B (ventral; inferred orientations), squamosal fragment exhibiting two fused episquamosals (es). C, D, elongate fragment, possibly from the posterior end of the squamosal where it narrows. Both fragments exhibit characteristic ceratopsian vascular surface texture. Scalebar = 10 cm.

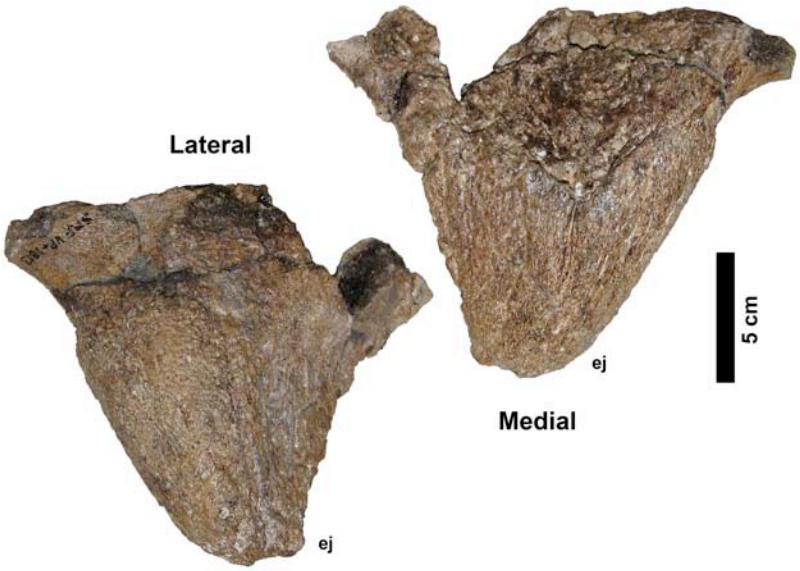

Figure 4.12. *Navajoceratops sullivani* holotype SMP VP-1500 jugal. Possible ventralmost end of a jugal with fused epijugal (ej), in lateral and medial views (inferred). Alternatively, this may be an episquamosal fused to a small part of the squamosal. Scalebar = 5 cm.

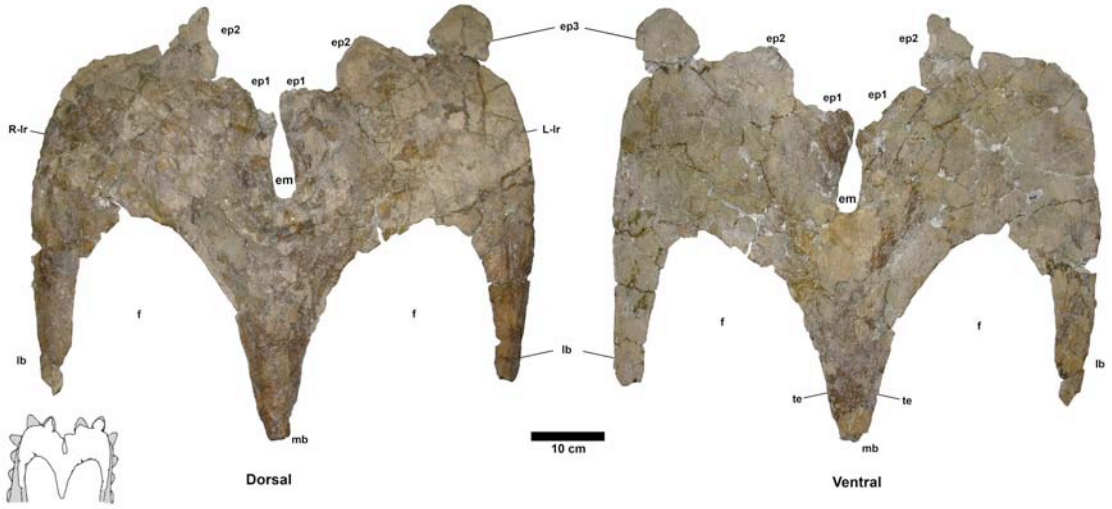

Figure 4.13. *Terminocavus sealeyi* holotype NMMNH P-27468 parietal. Dorsal (left) and ventral (right) views. Paired ep1 are deflected dorsally. em, median embayment of the posterior bar. ep, epiparietal loci numbered by hypothesized position (no epiossifications are fused to this specimen). f, parietal fenestra. lb, lateral bar. L-lr / R-lr, Left / Right lateral rami of the posterior bar. mb, median bar. te, tapering lateral edges of the median bar. Scalebar = 10 cm. Reconstruction adapted from Lehman (1998).

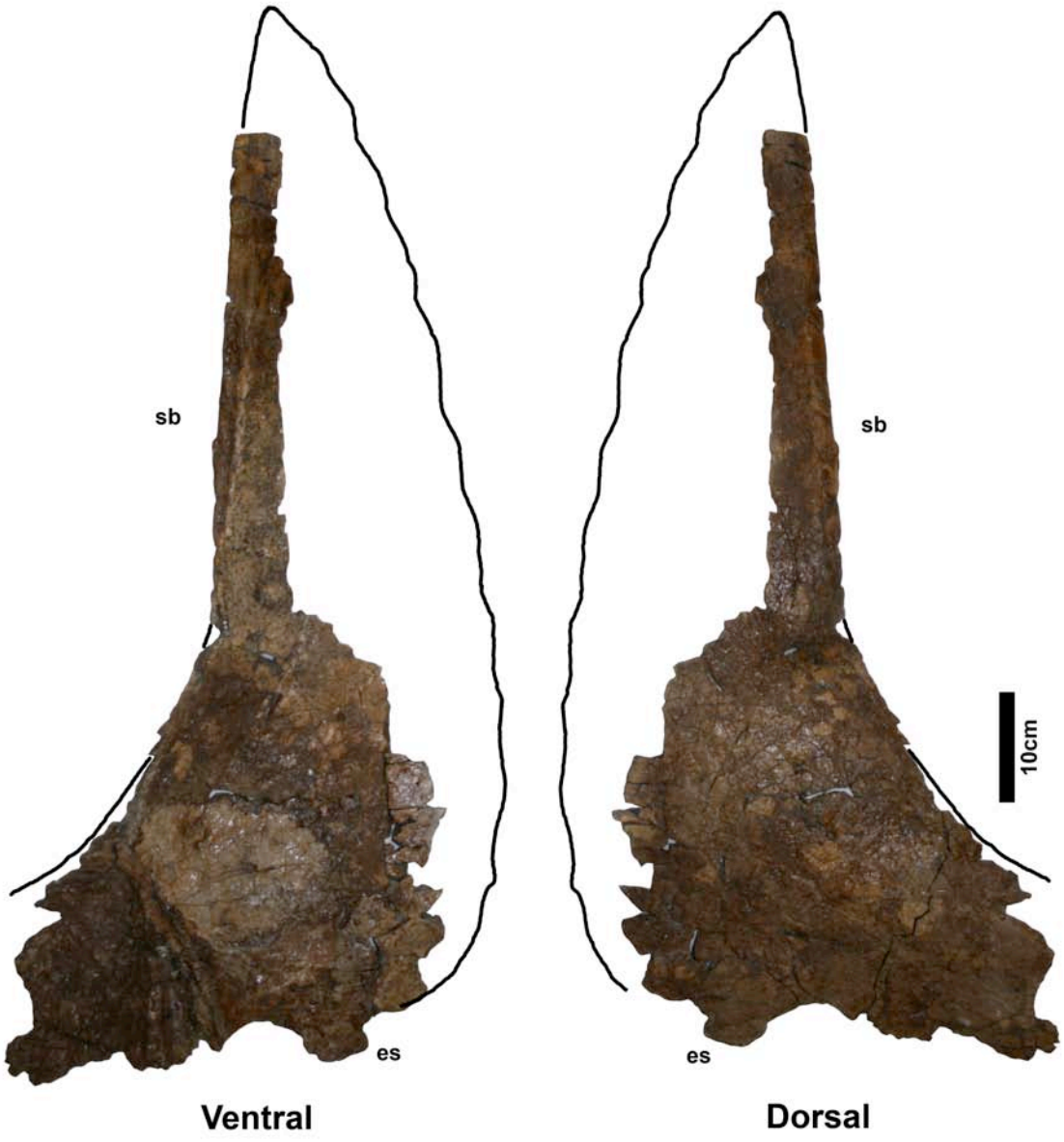

Figure 4.14. *Terminocavus sealeyi* holotype NMMNH P-27468 right squamosal. Ventral (left) and dorsal (right) views. sb, squamosal bar. es, episquamosal. Scalebar = 10 cm.

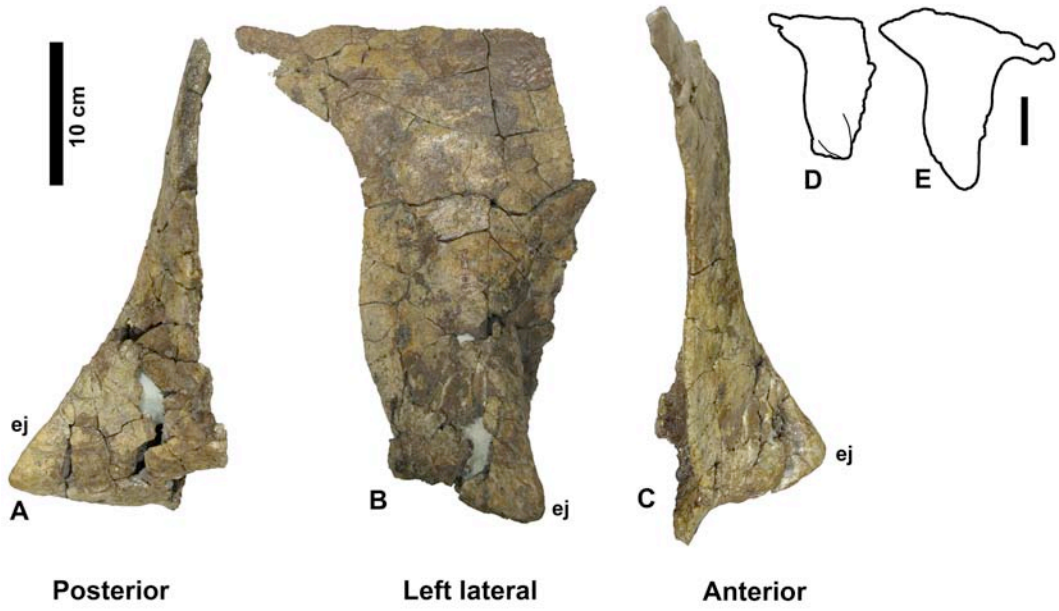

Figure 4.15. *Terminocavus sealeyi* holotype NMMNH P-27468 left jugal. Ventral two thirds of left jugal with fused epijual (ej) and partial quadratojugal in posterior (A), left lateral (B) and Anterior (C) views. A size comparison of NMMNH P-27468 (D) is compared with *Utahceratops gettyi* referred specimen UMNH VP-12198 (E). Scalebars = 10 cm.

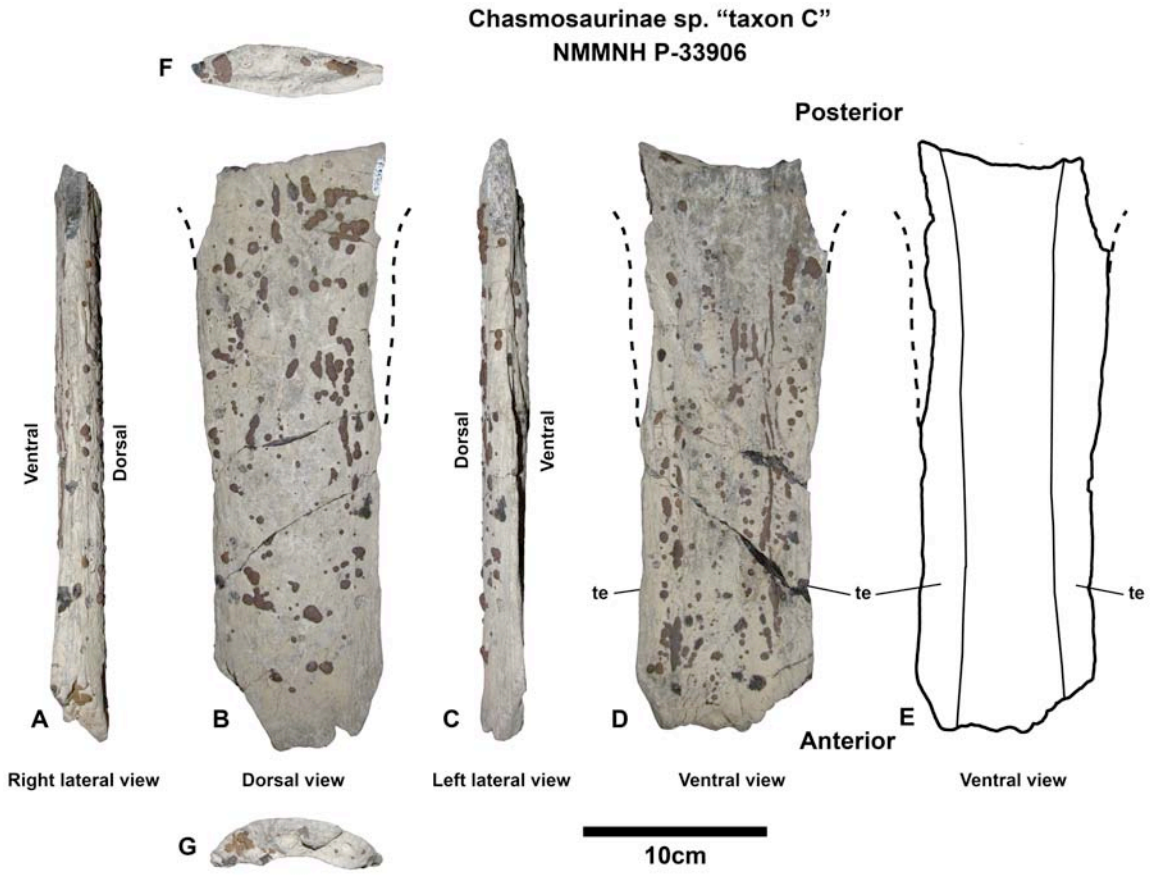

Figure 4.16. Chasmosaurinae sp. "Taxon C" NMMNH P-33906 parietal median bar. Near-complete parietal median bar in right lateral (A), dorsal (B), left lateral (C), ventral (D), and ventral outline (E) views. Cross sections in posterior (F) and anterior (G) inferred views. Subtle lateral expansion at both anterior and posterior ends suggests that the length of the median bar is complete, and as such is much wider than in stratigraphically preceding forms *Utahceratops*, *Pentaceratops*, *Navajoceratops*, and *Terminocavus*. The extra width is due to more extensive tapering lateral edges (te) of the median bar that extend out into the parietal fenestrae. Scalebar = 10 cm.

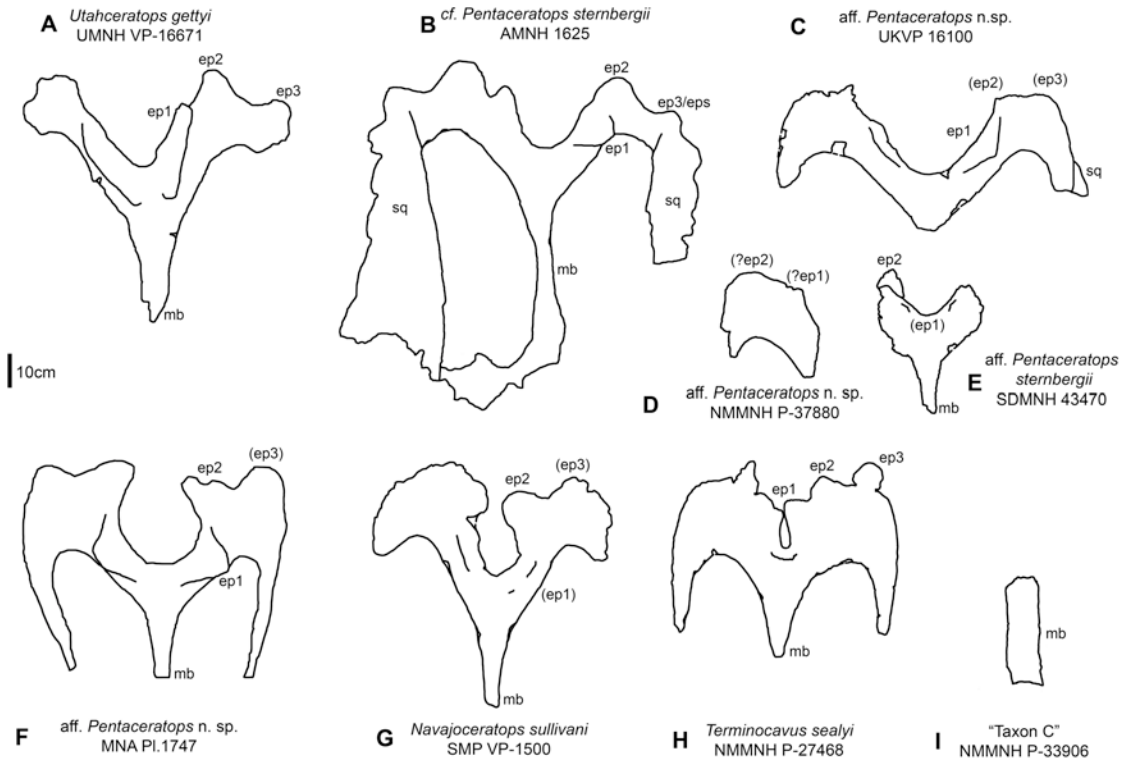

Figure 4.17. Parietal relative sizes among specimens of *Pentaceratops* and related chasmosaurines. Parietals of chasmosaurine taxa mentioned in the main text, all in dorsal view and to scale with each other to show relative size. Taxa shown in stratigraphic order (with the exception of E, SDMNH 43470). A, *Utahceratops gettyi* referred specimen UMNH VP-16671. B, cf. *Pentaceratops sternbergii* referred specimen AMNH 1625. Aff. *Pentaceratops* sp. referred specimens C, UKVP 16100; D, NMMNH P-37880, and F, MNA Pl. 1747. E, aff. *Pentaceratops sternbergii* referred specimen SDMNH 43470. G, *Navajoceratops sullivani* holotype SMP VP-1500. H, *Terminocavus sealeyi* holotype NMMNH P-27468. I, Chasmosaurinae sp. "Taxon C" specimen NMMNH P-33906. ep, epiparietal loci numbered by hypothesized position (no epiossifications are fused to this specimen). mb, median bar. Line drawings adapted from Longrich (2014), and Sampson et al. (2010). Scalebar = 10 cm.

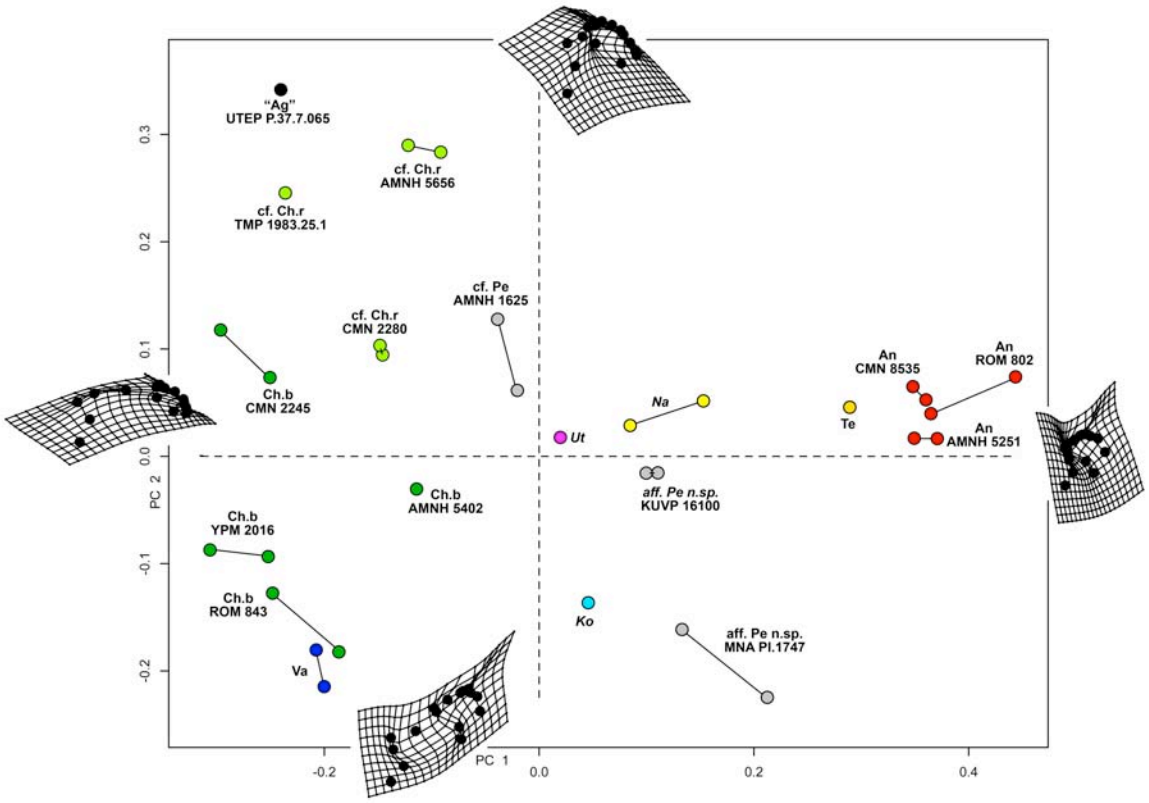

Figure 4.18. Morphometric analysis of chasmosaurine posterior parietals. Deformation grids illustrate shape of left lateral ramus of each specimen at the end of each principal component axis (PC). PC 1 (x axis) accounts for 50.5% of variation and assesses depth of the median embayment from shallow (negative) to deep (positive), and orientation of ep1 from mediolateral (negative) to anteroposterior (positive). PC 2 (y axis) accounts for 19.0% of variation. Points connected by a bar represent left and right sides of the same specimen (where adequately preserved). *Pentaceratops* through *Anchiceratops* plot along PC 1, demonstrating progressively deeper median embayment, and an increase in the angle of ep1. *Chasmosaurus* through to *Vagaceratops* are concentrated on the negative side of PC 1, following a trend from positive to negative along PC 2. Key: "Ag", *Agujaceratops*; An, *Anchiceratops*; Ch.b, *Chasmosaurus belli*; cf. Ch.r, cf. *Chasmosaurus russelli*; Ko, *Kosmoceratops*; Na, *Navajoceratops*; aff. Pe n.sp., aff. *Pentaceratops* n. sp.; cf. Pe, cf. *Pentaceratops sternbergii*; Te, *Terminocavus*; Ut, *Utahceratops*; Va, *Vagaceratops*. Color to aid in distinction only.

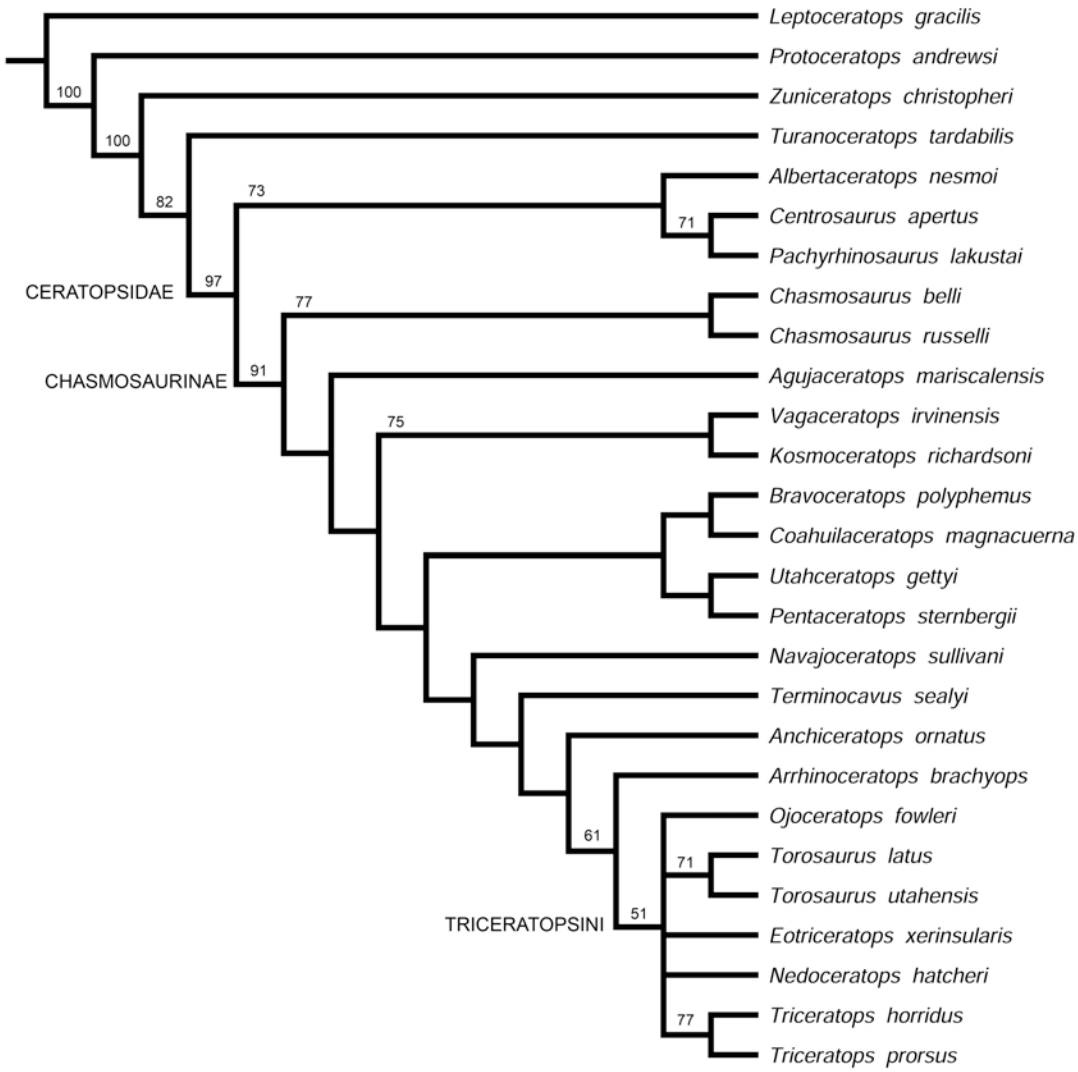

Figure 4.19. Strict consensus tree showing all taxa (MPT = 6; L = 319; CI = 0.72; RI = 0.79). Numbers on nodes indicate bootstrap values >50%; nodes without values had <50% support. Character matrix altered from Sampson et al. (2010) and Mallon et al. (2014).

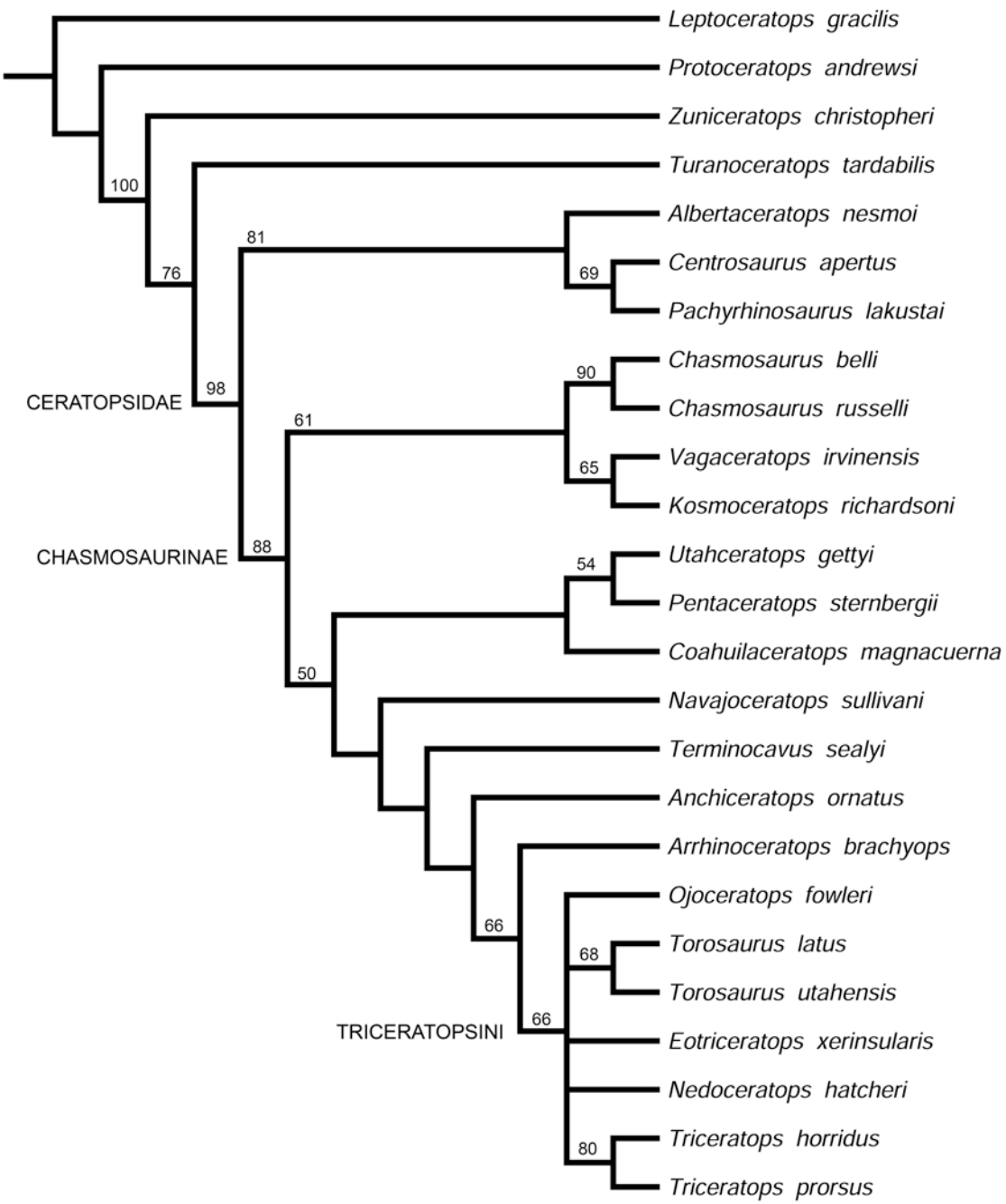

Figure 4.20. Reanalysis 1, strict consensus tree (MPT = 6; L = 310; CI = 0.72; RI = 0.79). *Bravoceratops*, *Agujaceratops* removed from the character matrix. Numbers on nodes indicate bootstrap values >50%; nodes without values had <50% support. Character matrix altered from Sampson et al. (2010) and Mallon et al. (2014).

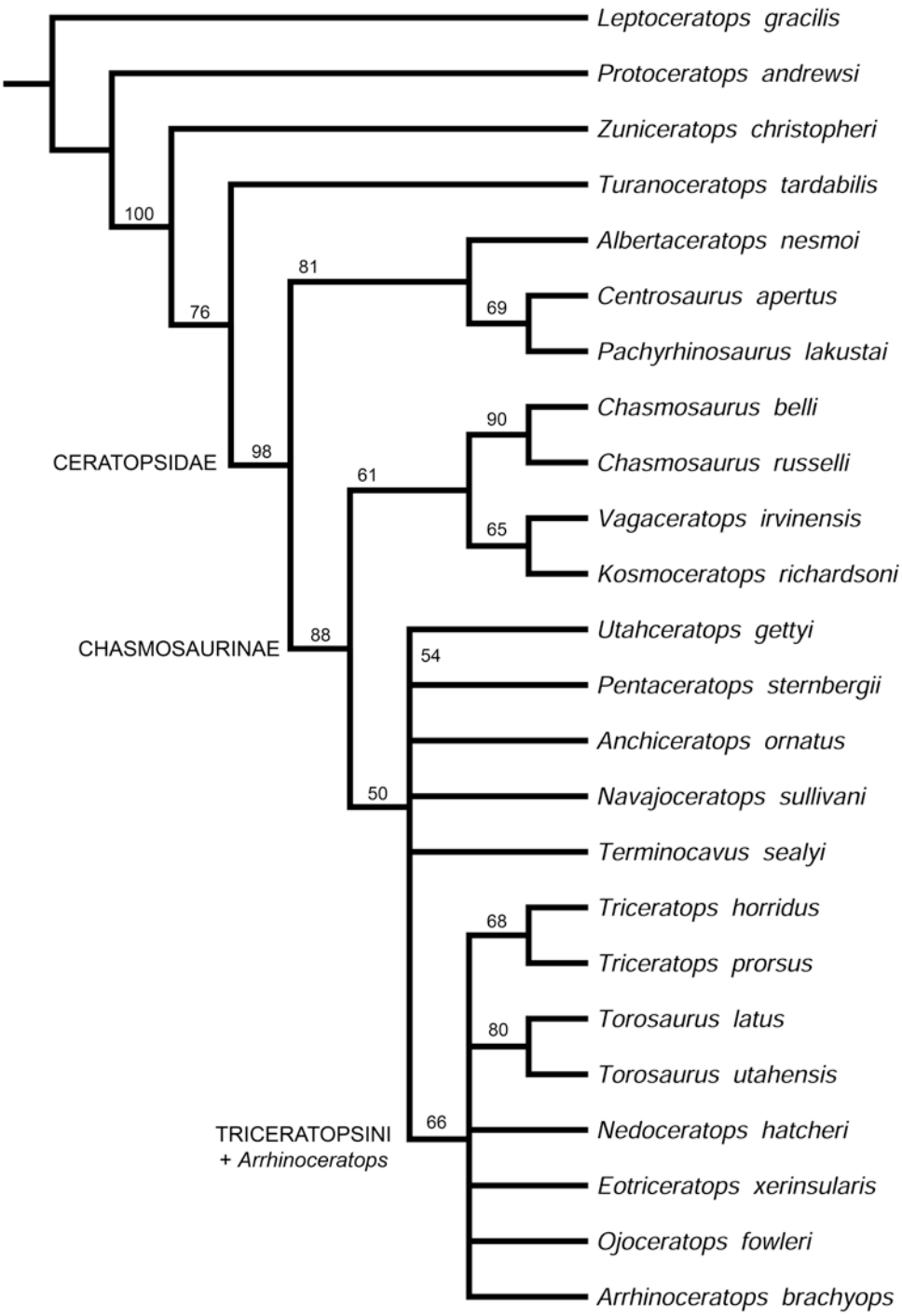

Figure 4.21. Strict consensus tree showing all taxa (MPT = 28; L = 308; CI = 0.72; RI = 0.79). Numbers on nodes indicate bootstrap values >50%; nodes without values had <50% support. Character matrix altered from Sampson et al. (2010) and Mallon et al. (2014)

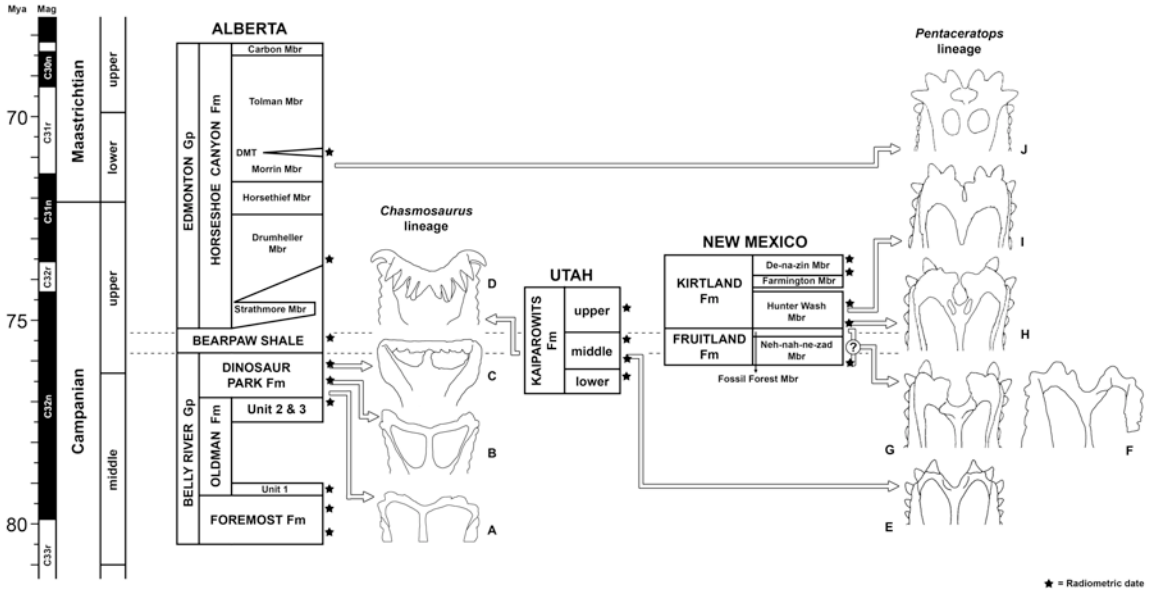

Figure 4.22. Stratigraphic positions of chasmosaurine taxa. Morphospecies of *Chasmosaurus* (A-D) and *Pentaceratops* (E-J) clades which do not overlap stratigraphically. These are hypothesized to form two anagenetic lineages which resulted from a cladogenetic branching event prior to the middle Campanian. A, *"Chasmosaurus russelli"*, lower Dinosaur Park Fm, ~76.8 Ma. B, *Chasmosaurus belli*, middle Dinosaur Park Fm, ~76.5 - 76.3 Ma. C, *Vagaceratops irvinensis*, upper Dinosaur Park Fm, ~76.1 Ma. D, *Kosmoceratops richardsoni*, middle Kaiparowits Fm, ~76.0 - 75.9 Ma. E, *Utahceratops gettyi*, middle Kaiparowits Fm, ~76.0 - 75.6 Ma. F, c.f. *Pentaceratops sternbergii*, unknown occurrence within "Fruitland Formation" ~76.0 - 75.1 Ma. G, aff. *Pentaceratops* n. sp., uppermost Fossil Forest Mbr, Fruitland Fm, ~75.1 Ma. H, *Navajoceratops sullivani*, lowermost Hunter Wash Mbr, Kirtland Fm, ~75.0 Ma. I, *Terminocavus sealyi*, middle Hunter Wash Mbr, Kirtland Fm, ~74.7 Ma. F, *Anchiceratops ornatus*, Drumheller to Morrin Mbr, Horseshoe Canyon Fm, ~71.7 - 70.7 Ma. Stratigraphic positions and recalibrated radiometric dates from Appendix C and Fowler (Chapter 3). Timescale from Gradstein et al. (2012). Specimens not to scale. Images adapted from Lehman (1998); Holmes et al., 2001; Sampson et al. (2010); Maidment and Barrett (2011); and Longrich (2014).

References Cited

Adams, D. C., and E. Otárola-Castillo. 2013. geomorph: an R package for the collection and analysis of geometric morphometric shape data. Methods in Ecology and Evolution 4:393-399.

Anderson, J. S., and H.-D. Sues eds. 2007. Major Transitions in Vertebrate Evolution. Indiana University Press, 432 pp.

Aze, T., T. H. Ezard, A. Purvis, H. K. Coxall, D. R. Stewart, B. S. Wade, and P. N. Pearson. 2011. A phylogeny of Cenozoic macroperforate planktonic foraminifera from fossil data. Biological Reviews 86:900–927.

Baltz, E. H., S. R. Ash, and R. Y. Anderson. 1966. History of nomenclature and stratigraphy of rocks adjacent to the Cretaceous-Tertiary boundary, western San Juan Basin, New Mexico. US Government Printing Office.

Bauer, C. M. 1916. Contributions to the Geology and Paleontology of San Juan County, New Mexico: Part 1. Stratigraphy of a Part of the Chaco River Valley. U.S. Geological Survey Professional Paper.

Brookins, D. G., and J. K. Rigby Jr. 1987. Geochronologic and geochemical study of volcanic ashes from the Kirtland Shale (Cretaceous), San Juan Basin, New Mexico. Geological Society of America Special Paper 209:105-110.

Brown, B. 1914. *Anchiceratops*, a new genus of horned dinosaurs from the Edmonton Cretaceous of Alberta. Bulletin of the American Museum of Natural History 33:539-548.

Brown, C. M., A. P. Russell, and M. J. Ryan. 2009. Pattern and transition of surficial bone texture of the centrosaurine frill and their ontogenetic and taxonomic implications. Journal of Vertebrate Paleontology 29:132-141.

Campbell, J. A. 2015. A reassessment of the horned dinosaur *Judiceratops tigris* (Ornithischia: Ceratopsidae) from the Upper Cretaceous (Campanian) of Montana, USA. Canadian Journal of Earth Sciences 52:85-95.

Campbell, J. A., M. J. Ryan, C. J. Schröder-Adams, and R. B. Holmes. 2015: Evolutionary trends in *Vagaceratops* (Ornithischia: Ceratopsidae) and the status of *Kosmoceratops* in the Upper Cretaceous (Campanian) Dinosaur Park Formation of Alberta. Society of Vertebrate Paleontology Annual Meeting, Dallas, Texas, 2015.

Campbell, J., M. J. Ryan, C. Schröder-Adams, R. B. Holmes, and D. C. Evans. 2013: A specimen-based phylogenetic analysis of the chasmosaurine ceratopsid *Chasmosaurus* (Ornithischia) form the Upper Cretaceous (Campanian) Dinosaur Park Formation of western Canada suggests the validity of only one species. Society of Vertebrate Paleontology 73rd Annual Meeting, Abstracts of Papers, Los Angeles, 2013.

Campione, N. E., K. S. Brink, E. A. Freedman, C. T. McGarrity, and D. C. Evans. 2013. '*Glishades ericksoni*', an indeterminate juvenile hadrosaurid from the Two Medicine Formation of Montana: implications for hadrosauroid diversity in the latest Cretaceous (Campanian-Maastrichtian) of western North America. Palaeobiodiversity and Palaeoenvironments 93:65-75.

Cook, O. F. 1906. Factors of species-formation. Science 23:506-507.

Currie, P. J., W. Langston Jr, and D. H. Tanke. 2008. A new species of *Pachyrhinosaurus* (Dinosauria, Ceratopsidae) from the Upper Cretaceous of Alberta, Canada; pp. 1-108 in P. J. Currie and W. Langston Jr (eds.), A New Horned Dinosaur from an Upper Cretaceous Bone Bed in Alberta. NRC Research Press, Ottawa, Ontario, Canada.

Daeschler, E. B., N. H. Shubin, and F. A. Jenkins. 2006. A Devonian tetrapod-like fish and the evolution of the tetrapod body plan. Nature 440:757-763.

DeCelles, P. G. 2004. Late Jurassic to Eocene evolution of the Cordilleral thrust belt and foreland basin system, western U.S.A. American Journal of Science 304:105-168.

Diem, S., and J. D. Archibald. 2005. Range extension of southern chasmosaurine ceratopsian dinosaurs into northwestern Colorado. Journal of Paleontology 79:251-258.

Dodson, P. 1997. Neoceratopsia; pp. 473-478 in P. J. Currie and K. Padian (eds.), Encyclopedia of Dinosaurs. Academic Press, San Diego.

Dodson, P., and P. J. Currie. 1988. The smallest ceratopsid skull - Judith River Formation of Alberta. Canadian Journal of Earth Sciences 25:926-930.

Dodson, P., C. A. Forster, and S. D. Sampson. 2004. Ceratopsidae; pp. 494-513 in D. B. Weishampel, P. Dodson, and H. Osmolska (eds.), The Dinosauria. University of California Press, Berkeley.

Eberth, D. A. 2005. The Geology; pp. 54-82 in P. J. Currie and E. B. Koppelhus (eds.), Dinosaur Provincial Park: A Spectacular Ancient Ecosystem Revealed. Indiana University Press, Bloomington, Indiana.

Eberth, D. A. 2011. A revised chronostratigraphy for Dinosaur Provincial Park, Alberta, Canada;in Speaker Series, Royal Tyrrell Museum, Drumheller, Alberta.

Eberth, D. A., D. C. Evans, D. B. Brinkman, F. Therrien, D. H. Tanke, and L. S. Russell. 2013. Dinosaur biostratigraphy of the Edmonton Group (Upper Cretaceous), Alberta, Canada: evidence for climate influence. Canadian Journal of Earth Sciences 50:701-726.

Eldredge, N., and S. J. Gould. 1972. Punctuated equilibria: an alternative to phyletic gradualism; pp. 82-115 in T. J. M. Schopf (ed.), Models in Paleobiology. Freeman, Cooper and Co., San Francisco.

Evans, D. C., L. M. Witmer, and J. R. Horner. 2011: A new low-crested lambeosaurine hadrosaurid from the Dinosaur Park Formation of Sandy Point, eastern Alberta. International Hadrosaur Symposium abstracts volume, 2011.

Farke, A. A. 2011. Anatomy and taxonomic status of the chasmosaurine ceratopsid *Nedoceratops hatcheri* from the Upper Cretaceous Lance Formation of Wyoming, U.S.A. PLoS ONE 6:e16196 p. 1-9. doi:10.1371/journal.pone.0016196.

Fassett, J. E. 2009. New geochronologic and stratigraphic evidence confirms the Paleocene age of the dinosaur-bearing Ojo Alamo Sandstone and Animas Formation in the San Juan Basin, New Mexico and Colorado. Palaeontologia Electronica 12:1-150.

Fassett, J. E., and J. S. Hinds. 1971. Geology and fuel resources of the Fruitland Formation and Kirtland Shale of the San Juan Basin, New Mexico and Colorado. United States Geological Survey Professional Paper 676:1-76.

Fassett, J. E., and M. B. Steiner. 1997. Precise age of C33N-C32R magnetic-polarity reversal, San Juan Basin, New Mexico and Colorado. New Mexico Geological Society Guidebook 48:239-247.

Fastovsky, D. E., D. B. Weishampel, M. Watabe, R. Barsbold, K. H. Tsogtbaatar, and P. Narmandakh. 2011. A nest of *Protoceratops andrewsi* (Dinosauria, Ornithischia). Journal of Paleontology 85:1035-1041.

Forster, C. A., P. C. Sereno, T. W. Evans, and T. Rowe. 1993. A complete skull of *Chasmosaurus mariscalensis* (Dinosauria: Ceratopsidae) from the Aguja Formation (Late Campanian) of West Texas. Journal of Vertebrate Paleontology 13:161-170.

Fowler, D. 2006. Terrestrial Late Cretaceous stratigraphy of North America and the utility of ceratopsids in biostratigraphy. Journal of Vertebrate Paleontology - Abstracts 26:63A.

Fowler, D. 2010: Anagenesis and long-term morphologic trends in Chasmosaurinae (Dinosauria: Ceratopsidae) revealed by a new high-resolution chronostratigraphic framework, ontogenetic analysis, and description of two new taxa. Journal of Vertebrate Paleontology 30:91A.

Fowler, D. W. in prep. Chapter 3. Dissertation.

Fowler, D. W., J. B. Scannella, and J. R. Horner. 2011: Reassessing ceratopsid diversity using unified frames of reference. Society of Vertebrate Paleontology Annual Meeting, Las Vegas, Nevada, 2011.

Francillon-Vieillot, H., V. de Buffrenil, J. Castanet, J. Geraudie, F. J. Meunier, J. Y. Sire, L. Zylberberg, and A. de Ricqlès. 1990. Microstructure and mineralization of vertebrate skeletal tissues.; pp. 471-548 in J. G. Carter (ed.), Skeletal Biomineralization: Patterns, Processes and Evolutionary Trends, Volume 1. Van Nostrand Reinhold, New York.

Gilmore, C. W. 1946. Reptilian fauna of the North Horn Formation of central Utah. United States Geological Survey Professional Paper 210-C:29-53.

Godfrey, S. J., and R. B. Holmes. 1995. Cranial morphology and systematics of *Chasmosaurus* (Dinosauria: Ceratopsidae) from the Upper Cretaceous of western Canada. Journal of Vertebrate Paleontology 15:726-742.

Goodwin, M. B., and A. L. Deino. 1989. The first radiometric ages from the Judith River Formation (Upper Cretaceous), Hill County, Montana. Canadian Journal of Earth Sciences 26:1384-1391.

Goodwin, M. B., W. A. Clemens, J. R. Horner, and K. Padian. 2006. The smallest known *Triceratops* skull: new observations on ceratopsid cranial anatomy and ontogeny. Journal of Vertebrate Paleontology 26:103-112.

Gradstein, F. M., J. G. Ogg, M. D. Schmitz, and G. M. Ogg eds. 2012. The Geologic Time Scale 2012. Elsevier, Amsterdam, 1144 pp.

Hatcher, J. B., O. C. Marsh, and R. S. Lull. 1907. The Ceratopsia. United States Geological Monograph 49:1-300.

Holmes, R. B., C. A. Forster, M. J. Ryan, and K. M. Shepherd. 2001. A new species of *Chasmosaurus* (Dinosauria: Ceratopsia) from the Dinosaur Park Formation of southern Alberta. Canadian Journal of Earth Sciences 38:1423-1438.

Horner, J. R., and M. B. Goodwin. 2006. Major cranial changes during *Triceratops* ontogeny. Proceedings of the Royal Society B 273:2757-2761.

Horner, J. R., and M. B. Goodwin. 2008. Ontogeny of cranial epi-ossifications in *Triceratops*. Journal of Vertebrate Paleontology 28:134-144.

Horner, J. R., and E.-T. Lamm. 2011. Ontogeny of the parietal frill of *Triceratops*: a preliminary histological analysis. Comptes Rendus Palevol 10:439-452.

Horner, J. R., D. J. Varricchio, and M. B. Goodwin. 1992. Marine transgressions and the evolution of Cretaceous dinosaurs. Nature 358:59-61.

Hull, P. M., and R. D. Norris. 2009. Evidence for abrupt speciation in a classic case of gradual evolution. Proceedings of the National Academy of Sciences 106:21224-21229.

Hunt, A. P., and S. G. Lucas. 1992. Stratigraphy, paleontology, and age of the Fruitland and Kirtland Formations (Upper Cretaceous), San Juan Basin, New Mexico. New Mexico Geological Society Guidebook 43:217-239.

Hunt, A. P., and S. G. Lucas. 2003. Origin and stratigraphy of historic dinosaur quarries in the Upper Cretaceous Fruitland Formation of the Fossil Forest Research Natural Area, northwestern New Mexico. New Mexico Geological Society Guidebook, 54th Field Conference, Geology of the Zuni Plateau:383-388.

Jinnah, Z. A. 2013. Tectonic and sedimentary controls, age, and correlation of the Upper Cretaceous Wahweap Formation, Southern Utah; pp. 57-73 in A. L. Titus and M. A. Loewen (eds.), At the Top of the Grand Staircase: the Late Cretaceous of Southern Utah. Indiana University Press, Bloomington, Indiana.

Kuiper, K. F., A. L. Deino, F. J. Hilgen, W. Krijgsman, P. R. Renne, and J. R. Wijbrans. 2008. Synchronizing rock clocks of Earth history. Science 320:500-504.

Lambe, L. M. 1915. On *Eoceratops canadensis*, gen. nov., with remarks on the other genera of Cretaceous horned dinosaurs. Geological Survery of Canada Museum Bulletin 12:1-49.

Lawson, D. A. 1976. *Tyrannosaurus* and *Torosaurus*, Maestrichtian dinosaurs from Trans-Pecos, Texas. Journal of Paleontology 50:158-164.

Lehman, T. M. 1987. Late Maastrichtian paleoenvironments and dinosaur biogeography in the Western Interior of North America. Palaeogeography, Palaeoclimatology, Palaeoecology 60:189-217.

Lehman, T. M. 1989. *Chasmosaurus mariscalensis*, sp. nov., a new ceratopsian dinosaur from Texas. Journal of Vertebrate Paleontology 9:137-162.

Lehman, T. M. 1990. The ceratopsian subfamily Chasmosaurinae: sexual dimorphism and systematics; pp. 211-229 in K. Carpenter and P. J. Currie (eds.), Dinosaur Systematics Approaches and Perspectives. Cambridge University Press, Cambridge.

Lehman, T. M. 1993. New data on the ceratopsian dinosaur *Pentaceratops sternbergii* Osborn from New Mexico. Journal of Paleontology 67:279-288.

Lehman, T. M. 1997. Late Campanian dinosaur biogeography in the western interior of North America. Dinofest International:223–240.

Lehman, T. M. 1998. A gigantic skull and skeleton of the horned dinosaur *Pentaceratops sternbergi* from New Mexico. Journal of Paleontology 72:894-906.

Lehman, T. M., F. McDowell, and J. Connelly. 2006. First isotopic (U-Pb) age for the Late Cretaceous *Alamosaurus* vertebrate fauna of West Texas, and its significance as a link between two faunal provinces. Journal of Vertebrate Paleontology 26:922-928.

Lillegraven, J. A., and L. M. Ostresh. 1990. Late Cretaceous (earliest Campanian/Maastrichtian) evolution of western shorelines of the North American Western Interior Seaway in relation to known mammalian faunas. Geological Society of America Special Paper 243.

Loewen, M. A., S. D. Sampson, E. K. Lund, A. A. Farke, M. C. Aguillón-Martínez, C. A. de Leon, R. A. Rodríguez-de la Rosa, M. A. Getty, and D. A. Eberth. 2010. Horned dinosaurs (Ornithischia: Ceratopsidae) from the Upper Cretaceous (Campanian) Cerro del Pueblo Formation, Coahila, Mexico; pp. 99-116 in M. J. Ryan, B. J. Chinnery-Allgeier, and D. A. Eberth (eds.), New Perspectives on Horned Dinosaurs: The Royal Tyrrell Museum Ceratopsian Symposium. Indiana University Press, Bloomington.

Lohmann, G. P., and B. A. Malmgren. 1983. Equatorward migration of *Globorotalia truncatulinoides* ecophenotypes through the late Pleistocene; gradual evolution or ocean change? Paleobiology 9:414-421.

Longrich, N. R. 2010. *Mojoceratops perifania*, a new chasmosaurine ceratopsid form the Late Campanian of western Canada. Journal of Paleontology 84:681-694.

Longrich, N. R. 2011. *Titanoceratops ouranos*, a giant horned dinosaur from the Late Campanian of New Mexico. Cretaceous Research 32:264-276.

Longrich, N. R. 2013. *Judiceratops tigris*, a new horned dinosaur from the middle Campanian Judith River Formation of Montana. Bulletin of the Peabody Museum of Natural History 54:51-65.

Longrich, N. R. 2014. The horned dinosaurs *Pentaceratops* and *Kosmoceratops* from the upper Campanian of Alberta and implications for dinosaur biogeography. Cretaceous Research 51:292-308.

Longrich, N. R., and D. J. Field. 2012. *Torosaurus* is not *Triceratops*: ontogeny in chasmosaurine ceratopsids as a case study in dinosaur taxonomy. PLoS ONE 7:e32623 p. 1-10. doi:10.1371/journal.pone.0032623.

Lucas, S. G., A. P. Hunt, and R. M. Sullivan. 2006. Stratigraphy and age of the Upper Cretaceous Fruitland Formation, west-central San Juan Basin, New Mexico. New Mexico Museum of Natural History and Science Bulletin 35:1–6.

Lucas, S. G., R. M. Sullivan, S. M. Cather, S. E. Jasinski, D. W. Fowler, A. B. Heckert, J. A. Spielmann, and A. P. Hunt. 2009. No definitive evidence of Paleocene dinosaurs in the San Juan Basin. Palaeontologia Electronica 12:1-10.

Lull, R. S. 1933. A revision of the Ceratopsia or horned dinosaurs. Peabody Museum of Natural History Bulletin 3:1-175.

Maddison, W. P., and D. R. Maddison. 2015. Mesquite: a modular system for evolutionary analysis. Version 3.02;http://mesquiteproject.org.

Maidment, S. C. R., and P. M. Barrett. 2011. A new specimen of *Chasmosaurus belli* (Ornithischia: Ceratopsidae), a revision of the genus, and the utility of postcrania in the taxonomy and systematics of ceratopsid dinosaurs. Zootaxa 2963:1-47.

Maiorino, L., A. A. Farke, T. Kotsakis, and P. Piras. 2013. Is *Torosaurus Triceratops*? Geometric morphometric evidence of Late Maastrichtian ceratopsid dinosaurs. PLoS ONE 8:e81608. doi:10.1371/journal.pone.0081608.

Mallon, J. C., D. C. Evans, M. J. Ryan, and J. S. Anderson. 2012. Megaherbivorous dinosaur turnover in the Dinosaur Park Formation (upper Campanian) of Alberta, Canada. Palaeogeography, Palaeoclimatology, Palaeoecology 350-352:124-138.

Mallon, J. C., R. B. Holmes, D. A. Eberth, M. J. Ryan, and J. S. Anderson. 2011. Variation in the skull of *Anchiceratops* (Dinosauria: Ceratopsidae) from the Horseshoe Canyon Formation (Upper Cretaceous) of Alberta. Journal of Vertebrate Paleontology 31:1047-1071.

Mallon, J. C., R. B. Holmes, J. S. Anderson, A. A. Farke, D. C. Evans, and H.-D. Sues. 2014. New information on the rare horned dinosaur *Arrhinoceratops brachyops* (Ornithischia: Ceratopsidae) from the Upper Cretaceous of Alberta, Canada. Canadian Journal of Earth Sciences 51:618-634.

Malmgren, B. A., W. A. Berggren, and G. P. Lohmann. 1984. Species Formation Through Punctuated Gradualism in Planktonic Foraminifera. Science 225:317-319.

Marsh, O. C. 1888. A new family of horned dinosaurs from the Cretaceous. American Journal of Science 3:477-478.

Marsh, O. C. 1890. Additional characters of the Ceratopsidae with notice of new Cretaceous dinosaurs. American Journal of Science 3:418-426.

Mateer, N. J. 1980. The reptilian megafauna from the Kirtland Shale (Late Cretaceous) of the San Juan Basin, New Mexico; pp. 49-75 in S. G. Lucas, J. K. Rigby Jr., and B. S. Kues (eds.), Advances in San Juan Basin Paleontology. University of New Mexico Press, Albuquerque.

Min, K., R. Mundil, P. R. Renne, and K. R. Ludwig. 2000. A test for systematic errors in 40Ar/39Ar geochronology through comparison with U/Pb analysis of a 1.1-Ga rhyolite. Geochimica et Cosmochimica Acta 64:73-98.

Ogg, J. G. 2012. Geomagnetic polarity time scale; pp. 85-113 in F. M. Gradstein, J. G. Ogg, M. D. Schmitz, and G. M. Ogg (eds.), The Geologic Time Scale 2012. Elsevier, Amsterdam.

Ogg, J. G., L. A. Hinnov, and C. Huang. 2012. Cretaceous; pp. 793-853 in F. M. Gradstein, J. G. Ogg, M. D. Schmitz, and G. M. Ogg (eds.), The Geologic Time Scale 2012. Elsevier, Amsterdam.

Osborn, H. F. 1923. A new genus and species of Ceratopsia from New Mexico, *Pentaceratops sternbergii*. American Museum Novitates 93:1-3.

O'Sullivan, R. B., and H. M. Beikman. 1963. Geology, structure, and uranium deposits of the Shiprock Quadrangle, New Mexico and Arizona, Report 345.

O'Sullivan, R. B., G. R. Scott, and J. S. Heller. 1979. Preliminary geologic map of the Bisti Trading Post Quadrangle, San Juan County, New Mexico, Report 1075.

Owen, R. 1842. Report on British fossil reptiles. Part II. Report of the Eleventh Meeting of the British Association for the Advancement of Science 11:60-204.

Padian, K., and C. L. May. 1993. The earliest dinosaurs. New Mexico Museum of Natural History and Science Bulletin 3:379-381.

Pearson, P. N., and T. H. G. Ezard. 2014. Evolution and speciation in the Eocene planktonic foraminifer Turborotalia. Paleobiology 40:130-143.

R_Core_Team. 2014. R: A language and environment for statistical computing. R Foundation for Statistical Computing, Vienna, Austria. ISBN 3-900051-07-0, URL http://www.R-project.org/.

Rambaut, A. 2014. FigTree, Tree Figure Drawing Tool, Version 1.4.2; http://mesquiteproject.org.

Rasband, W. S. 1997-2014. ImageJ. U. S. National Institutes of Health, Bethesda, Maryland, USA; http://imagej.nih.gov/ij/.

Rensch, B. 1959. Evolution Above the Species Level. English translation Edition, Columbia Biological Series. Columbia University Press, New York, 419 pp.

Roberts, E. M., S. D. Sampson, A. L. Deino, S. A. Bowring, and R. Buchwaldt. 2013. The Kaiparowits Formation: a remarkable record of Late Cretaceous terrestrial environments, ecosystems, and evolution in western North America; pp. 85-106 in A. L. Titus and M. A. Loewen (eds.), At the Top of the Grand Staircase: the Late Cretaceous of Southern Utah. Indiana University Press, Bloomington.

Rogers, R. R., and C. C. Swisher. 1996. The Claggett and Bearpaw transgressions revisited: new 40Ar/39Ar data and a review of possible drivers. Abstracts with programs - Geological Society of America, North-Central Section 28:62.

Rogers, R. R., C. C. Swisher, and J. R. Horner. 1993. 40Ar/39Ar age and correlation of the nonmarine Two Medicine Formation (Upper Cretaceous), northwestern Montana, USA. Canadian Journal of Earth Sciences 30:1066-1075.

Rowe, T., E. H. Colbert, and J. D. Nations. 1981. The occurrence of *Pentaceratops* (Ornithischia: Ceratopsia) with a description of its frill; pp. 29-48 in S. G. Lucas, J. K. Rigby, and B. S. Kues (eds.), Advances in San Juan Basin Paleontology. University of New Mexico Press, Albuquerque.

Ryan, M. J., and A. P. Russell. 2005. A new centrosaurine ceratopsid from the Oldman Formation of Alberta and its implications for centrosaurine taxonomy and systematics. Canadian Journal of Earth Sciences 42:1369-1387.

Ryan, M. J., D. C. Evans, P. J. Currie, and M. A. Loewen. 2014. A new chasmosaurine from northern Laramidia expands frill disparity in ceratopsid dinosaurs. Naturwissenschaften 101:505-512.

Sampson, S. D. 1995. Two new horned dinosaurs from the Upper Cretaceous Two Medicine Formation of Montana; with a phylogenetic analysis of the Centrosaurinae (Ornithischia: Ceratopsidae). Journal of Vertebrate Paleontology 15:743-760.

Sampson, S. D., and M. A. Loewen. 2010. Unraveling a radiation: a review of the diversity, stratigraphic distribution, biogeography, and evolution of horned dinosaurs (Ornithischia: Ceratopsidae); pp. 405-427 in M. J. Ryan, B. J. Chinnery-Allgeier, and D. A. Eberth (eds.), New Perspectives on Horned Dinosaurs. Indiana University Press, Bloomington, Indiana.

Sampson, S. D., M. J. Ryan, and D. H. Tanke. 1997. Craniofacial ontogeny in centrosaurine dinosaurs (Ornithischia: Ceratopsidae): taxonomic and behavioral implications. Zoological Journal of the Linnean Society 121:293-337.

Sampson, S. D., M. A. Loewen, E. M. Roberts, and M. A. Getty. 2013. A new macrovertebrate assemblage from the Late Cretaceous (Campanian) of Southern Utah; pp. 599-620 in A. L. Titus and M. A. Loewen (eds.), At the Top of the Grand Staircase: the Late Cretaceous of Southern Utah. Indiana University Press, Bloomington.

Sampson, S. D., M. A. Loewen, A. A. Farke, E. M. Roberts, C. A. Forster, J. A. Smith, and A. L. Titus. 2010. New horned dinosaurs from Utah provide evidence for intracontinental dinosaur endemism. PLoS ONE 5:e12292.

Sander, P. M., and N. Klein. 2005. Developmental plasticity in the life history of a prosauropod dinosaur. Science 310:1800-1802.

Scannella, J. B., and D. W. Fowler. 2014. A stratigraphic survey of Triceratops localities in the Hell Creek Formation, northeastern Montana (2006–2010). Geological Society of America Special Papers 503:313–332.

Scannella, J. B., and J. R. Horner. 2010. *Torosaurus* Marsh, 1891, is *Triceratops* Marsh, 1889 (Ceratopsidae: Chasmosaurinae): synonymy through ontogeny. Journal of Vertebrate Paleontology 30:1157-1168.

Scannella, J. B., and J. R. Horner. 2011. *'Nedoceratops'*: an example of a transitional morphology. PLoS ONE 6:e28705 p. 1-9. doi:10.1371/journal.pone.0028705.

Scannella, J. B., D. W. Fowler, M. B. Goodwin, and J. R. Horner. 2014. Evolutionary trends in *Triceratops* from the Hell Creek Formation, Montana. Proceedings of the National Academy of Sciences 111:10245-10250.

Scott, G. R., R. B. O'Sullivan, and J. S. Heller. 1979. Preliminary geologic map of the Burnham Trading Post Quadrangle, San Juan County, New Mexico, Report 1076.

Sealey, P., J. A. Smith, and T. E. Williamson. 2005: An unusual *Pentaceratops* from New Mexico. Society of Vertebrate Paleontology Annual Meeting, Mesa, Arizona, 2005.

Seeley, H. G. 1887. On the classification of the fossil animals commonly called Dinosauria. Proceedings of the Royal Society of London 43:165-171.

Sereno, P. C. 1998. A rationale for phylogenetic definitions, with application to the higher-level taxonomy of Dinosauria. Neues Jahrbuch für Geologie und Paläontologie - Abhandlungen 210:41-83.

Simpson, G. G. 1940. Types in modern taxonomy. American Journal of Science 238:413-431.

Simpson, G. G. 1961. Principles of Animal Taxonomy, Columbia Biological Series. Columbia University Press, New York, 247 pp.

Sternberg, C. M. 1929. A new species of horned dinosaur from the Upper Cretaceous of Alberta. Bulletin of the National Museum of Canada 54:34-37.

Sullivan, R. M. 2006. Ah-shi-sle-pah Wilderness Study Area (San Juan Basin, New Mexico): a paleontological (and historical) treasure and resource. New Mexico Museum of Natural History and Science Bulletin 34:169–174.

Sullivan, R. M., and S. G. Lucas. 2006. The Kirtlandian land-vertebrate "age" - faunal composition, temporal position and biostratigraphic correlation in the nonmarine Upper Cretaceous of Western North America. New Mexico Museum of Natural History and Science Bulletin 35:7-29.

Sullivan, R. M., and S. G. Lucas. 2010. A new Chasmosaurine (Ceratopsidae, Dinosauria) from the Upper Cretaceous Ojo Alamo Formation (Naashoibito Member), San Juan Basin, New Mexico; pp. 169-180 in M. J. Ryan, B. J. Chinnery, and D. A. Eberth (eds.), New Perspectives on Horned Dinosaurs. Indiana University Press, Bloomington, Indiana.

Sullivan, R. M., S. G. Lucas, and D. R. Braman. 2005. Dinosaurs, pollen, and the Cretaceous-Tertiary boundary in the San Juan Basin, New Mexico. New Mexico Geological Society, 56th Field Conference Guidebook, Geology of the Chama Basin:395-407.

Swofford, D. L. 2002. PAUP*. Phylogenetic analysis using parsimony (*and other methods). Version 4.0b10. Sinauer Associates, http://paup.csit.fsu.edu/, Sunderland, MA.

Tsai, C.-H., and R. E. Fordyce. 2015. Ancestor-descendant relationships in evolution: origin of the extant pygmy right whale, *Caperea marginata*. Biology Letters 11:1-4.

Vrba, E. S. 1985. Environment and evolution: alternative causes of the temporal distribution of evolutionary events. South African Journal of Science 81:229-236.

Weide, D. L., G. B. Schneider, J. W. Mytton, and G. R. Scott. 1979. Geologic map of the Pueblo Bonito Quadrangle, San Juan County, New Mexico, Report 1119.

Wellnhofer, P. 2010. A short history of research on Archaeopteryx and its relationship with dinosaurs. Geological Society, London, Special Publications 343:237-250.

Wick, S. L., and T. M. Lehman. 2013. A new ceratopsian dinosaur from the Javelina Formation (Maastrichtian) of West Texas and implications for chasmosaurine phylogeny. Naturwissenschaften 100:667-682.

Wiley, E. O. 1981. Phylogenetics. The Theory and Practice of Phylogenetic Systematics. Wiley- Interscience, New York, 439 pp.

Wiman, C. 1930. Uber Ceratopsia aus der oberen Kreide in New Mexico. Nova Acta Regiae Societatis Scientarum Upsaliensis 4-7:1-19.

Woodward, H. N., E. A. Freedman Fowler, J. O. Farlow, and J. R. Horner. 2015. *Maiasaura*, a model organism for extinct vertebrate population biology: a statistically robust assessment of growth dynamics and survivorship. Paleobiology 41:503-527.

Wu, X.-c., D. B. Brinkman, D. A. Eberth, and D. R. Braman. 2007. A new ceratopsid dinosaur (Ornithischia) from the uppermost Horseshoe Canyon Formation (upper Maastrichtian), Alberta, Canada. Canadian Journal of Earth Sciences 44:1243–1265.

Xu, X., K. Wang, X. Zhao, and D. Li. 2010. First ceratopsid dinosaur from China and its biogeographical implications. Chinese Science Bulletin 55:1631-1635.

CHAPTER FIVE

A STRATIGRAPHIC SURVEY OF *TRICERATOPS* LOCALITIES IN THE HELL CREEK FORMATION, NORTHEASTERN MONTANA (2006-2010)

Contribution of Authors and Co-Authors

Manuscript in Chapter 5

Author: John B. Scannella

Contributions: Conceived the study, collected data, interpreted results, and wrote the manuscript.

Co-author: Denver W. Fowler

Contributions: Conceived the study, collected data, correlated stratigraphic sections, interpreted results, and contributed to the manuscript.

Manuscript Information Page

John B. Scannella, Denver W. Fowler.
Journal: Geological Society of America Special Paper
Status of Manuscript:
___Prepared for submission to a peer-reviewed journal
___Officially submitted to a peer-reviewed journal
___Accepted by a peer-reviewed journal
_x_Published in a peer-reviewed journal

Published by the Geological Society of America
Scannella J.B., and D.W. Fowler. 2014. A stratigraphic survey of *Triceratops* localities in the Hell Creek Formation, northeastern Montana (2006-2010). pp. 313-332 in Through the End of the Cretaceous in the Type Locality of the Hell Creek Formation in Montana and Adjacent Areas, G.P. Wilson, W.A. Clemens, J.R. Horner, and J.H. Hartman (eds.) Geological Society of America Special Paper, Boulder, Colorado.

The following chapter (and supporting information in Appendix F) has been published in the Geological Society of America Special Paper 503 and appears in this dissertation with the permission of the Geological Society of America. The copyright is held by the Geological Society of America.

Abstract

Here we provide a survey of *Triceratops* localities and accompanying stratigraphic data from the Hell Creek Formation of northeastern Montana. The majority of the sites discussed here were relocated or discovered during the last five years of the Hell Creek Project (1999–2010); a multi-institutional effort to record a large volume of faunal, floral, and geologic data on the Hell Creek Formation in order to test evolutionary, paleoecological, and geological hypotheses. *Triceratops* is the most abundant dinosaur in the Hell Creek Formation and one of the most common non-avian dinosaurs of the Upper Cretaceous. It is known from hundreds of specimens, which have been collected since it was first described in 1889. Although these specimens provide a wealth of morphological data on *Triceratops*, many lack detailed stratigraphic information and context. Detailed stratigraphic and contextual data for more than 70 specimens of *Triceratops* collected during the Hell Creek Project make this data set among the most comprehensive for any non-avian dinosaur.

Introduction

It was the famous horned dinosaur *Triceratops* that first called paleontologists to the Hell Creek Formation. W.T. Hornaday, the director of the Bronx Zoölogical Garden, returned from a 1901 hunting trip to eastern Montana with a piece of fossil bone (Brown, 1907). Henry Fairfield Osborn, director of the American Museum of Natural History (AMNH) and Barnum Brown (AMNH) recognized the fossil as a segment of *Triceratops* horn (Brown, 1907; Dingus and Norell, 2010). By 1901, *Triceratops* was already known

from multiple impressive specimens collected from the Lance Formation of Wyoming and broadly contemporaneous Upper Cretaceous formations of Colorado (Hatcher et al., 1907; Ostrom and Wellnhofer, 1986; Carpenter and Young, 2002). The AMNH was seeking an exhibit-quality specimen of *Triceratops* for its dinosaur hall and the Hornaday horn (originally discovered by settler Max Sieber) seemed a promising lead (Dingus and Norell, 2010). Osborn dispatched Barnum Brown to the area, initiating over a century of fossil collecting in the uppermost Cretaceous deposits of eastern Montana. Brown would go on to discover and collect numerous dinosaur fossils from the Hell Creek Formation, including the holotype specimen of *Tyrannosaurus* (Osborn, 1905); however, it was *Triceratops* that he encountered most frequently. "During seven years' work, 1902–1909, in the Hell Creek Beds (Lance) of Montana I identified no less than five hundred fragmentary skulls and innumerable bones referable to this genus" (Brown, 1917, p. 281–282). Lull (1915) presented a stratigraphic survey of specimens of *Triceratops* from the Lance Formation of Wyoming. "I have arranged the skulls in their stratigraphic sequence, based upon all the data available at the present, but taken very largely from a study of the map . . ." (Lull, 1915, p. 341). As Ostrom and Wellnhofer (1986, p. 155) noted: " . . . the precise stratigraphic spacing of these specimens can no longer be established," and it has been difficult to assess the stratigraphic placement of these specimens due to the absence of more precise locality data (Farke, 1997). The detailed stratigraphy of the Hell Creek Formation in Montana is now well understood (e.g., Flight, 2004; Fowler, 2009; Horner et al., 2011; Hartman et al., 2014), allowing specimens of *Triceratops* to be placed in a high-resolution stratigraphic context.

Taxa known from greater numbers of specimens can reveal more details of systematics and development than those known from a few pristine specimens. *Triceratops* is now one of the best understood of all dinosaur taxa (e.g., Hatcher et al., 1907; Ostrom and Wellnhofer, 1986; Forster, 1996a; 1996b; Horner and Goodwin, 2006; 2008; Scannella and Horner, 2010; Horner and Lamm, 2011). This is, in part, due to the efforts of the Hell Creek Project, a large scale, multi-institutional (Museum of the Rockies [MOR], University of California Museum of Paleontology [UCMP], University of North Dakota [UND]) study of the fauna, flora, and geology of the Hell Creek Formation in northeastern Montana (e.g., Wilson, 2005; Goodwin and Horner, 2010; Horner et al., 2011, this volume). Since the initiation of the Hell Creek Project in 1999, field crews at the MOR alone have collected over 70 new specimens of *Triceratops* (Scannella and Horner, 2010; Horner et al., 2011; Appendix F). Dozens more poorly preserved specimens were discovered and recorded in the field but remain uncollected (Horner et al., 2011). Many of the specimens of *Triceratops* collected by the MOR represent previously unrecorded ontogenetic stages, revealing new details of the developmental biology of this animal (Horner and Goodwin, 2006; 2008; Scannella and Horner, 2010).

The MOR now houses one of the largest collections of *Triceratops* in the world, and, significantly, nearly every specimen has detailed locality records associated with it (Horner et al., 2011). In contrast, many of the specimens of *Triceratops* collected in the late nineteenth and early twentieth centuries have very little stratigraphic data associated with them (Farke, 1997). This makes it difficult to place those specimens in precise

stratigraphic position and thus test evolutionary hypotheses in detail. In many cases, fragmentary specimens with stratigraphic data can provide valuable insights unavailable from more complete skulls or skeletons lacking this data (e.g., Pearson et al., 2002; Horner et al., 2011).

Here, we present a review of some significant localities of *Triceratops* either relocated or discovered during the later years of the Hell Creek Project (1999–2010). Firsthand accounts from those who have visited sites can be critical to future quarry relocation (e.g., Tanke, 2010), and, as such, we provide contextual information for sites that we have personally visited (Fig. 5.1). For each locality, we provide details of the specimen(s) collected, its relative stratigraphic position, and, for many, a stratigraphic section. Precise locality data are on record at the respective institutions. This survey will facilitate reassessment of the stratigraphic positions of these specimens, thus helping to make systematic and evolutionary hypotheses testable now and in the future.

Institutional Abbreviations

AMNH—American Museum of Natural History, New York, New York, USA

MOR—Museum of the Rockies, Bozeman, Montana, USA

MSU—Montana State University, Bozeman, Montana, USA

NCSU—North Carolina State University, Raleigh, North Carolina, USA

UCMP—University of California Museum of Paleontology, Berkeley, California, USA

UND—University of North Dakota, Grand Forks, North Dakota, USA

UW-FDL—University of Wisconsin–Fond du Lac, Fond du Lac, Wisconsin, USA

USNM—National Museum of Natural History, Smithsonian Institution, Washington, D.C., USA

Materials and Methods

The stratigraphy of the Montanan Hell Creek Formation remained poorly resolved until recently (Flight, 2004; Fowler, 2009; Hartman et al., 2014; Horner et al., 2011). Analyses within a stratigraphic framework were largely dependent on finding a nearby exposure of either the top or the bottom of the formation and measuring the distance to that contact (e.g., Wilson, 2005). This methodology, however, does not always allow for reliable placement of specimens recovered from areas in which neither the top nor the bottom contact is exposed in relatively close proximity, nor does it allow for correlation of specimens traced to the bottom contact with specimens that have been traced to the top contact without making the assumption that all exposures of the Hell Creek Formation have a consistent preserved thickness (Fowler, 2009). While the Hell Creek Formation is commonly around 90 m thick in the Fort Peck area (Wilson, 2004), this can vary by 20 m, especially based on the presence or absence of the Basal Sandstone (Brown, 1907; Flight, 2004) or incised Paleocene channels (e.g., 20 m or more removed at Bug Creek; Lofgren, 1995).

The most accurate method of stratigraphic placement of localities is to measure their position relative to the upper and lower formational contacts and stratigraphic unit boundaries (Fig. 5.2; see Hartman et al., 2014; Horner et al., 2011). A sequence stratigraphic interpretation of facies shifts within the Hell Creek Formation is in preparation (Fowler, 2009). The majority of specimens included in this review are placed

stratigraphically relative to nearby exposures of either the upper or lower contacts. Placement relative to unit boundaries increases stratigraphic resolution. Nomenclature for unit boundaries follows Horner et al. (2011; see also Hartman et al., 2014). The Basal Sandstone is an informal name for the sandstone unit that marks the base of the lower unit of the formation. The Jen-rex Sandstone is an informal name for the sandstone unit that marks the base of the middle unit of the formation. The Apex Sandstone is an informal name for the sandstone unit that marks the base of the upper unit; it is typically located ~26–30 m below the Hell Creek–Fort Union formational contact. The 10-Meter Sandstone is the informal name for a sandstone that typically occurs ~10 m below the lower Z-coal.

A 1.5 m Jacob's staff and Brunton compass were used to take stratigraphic sections for *Triceratops* sites discovered by MOR crews during the Hell Creek Project from 2006 through 2010. The lower Z-coal was identified as the lowermost coal in the Fort Union Formation, although the precise stratigraphic position of this horizon can vary (Archibald et al., 1982; Swisher et al., 1993; Turner, 2010). These data were combined with stratigraphic information from the MOR archives as well as locality data for specimens from UCMP.

Triceratops Localities

UCMP Locality V88001 (High Ceratopsian): UCMP Specimen 137263

In 1987, along the southern margin of a local basin in close proximity to exposures of the Fort Union Formation referred to by UCMP and MOR paleontologists

as “the swamp” (for its organic-rich beds containing abundant champsosaurs and crocodiles), Mark Goodwin (UCMP) discovered a disarticulated skull of a subadult *Triceratops* weathering out of a bentonitic, dark-gray mudstone high in the underlying Hell Creek Formation (Goodwin and Horner, 2010). The site, UCMP locality V88001, “High Ceratopsian,” is stratigraphically a few meters below the base of the lower Z-coal, which defines the Hell Creek–Fort Union formational contact and, in this area, approximates the Cretaceous-Paleogene boundary. Crews from the UCMP returned to the site several times over the next few years, collecting a set of postorbital horn cores, much of the parietal-squamosal frill, a pair of unfused nasals, a jugal, and other cranial elements. In 2007, when we visited the locality with Mark Goodwin, a shallow depression was still visible in the mudstone where the skull had been removed. UCMP 137263 was not from a large individual of *Triceratops*, but the crews working the site had been thorough in expanding the quarry. In more recent years, it has been determined that *Triceratops* quarries often need to be expanded significantly to discover if more elements are preserved (Horner et al., 2011). The stratigraphic position of the locality is ~5 m below the lower Z-coal.

UCMP Locality V83224 (Dave’s Nose): UCMP Specimen 128561

UCMP 128561 was originally described as a new genus of latest Cretaceous ceratopsid, “*Ugrosaurus olsoni*” (Cobabe and Fastovsky, 1987). The specimen, which was discovered by David Fastovsky in the summer of 1983, consists of a partial premaxilla and rostral, a partial nasal with a low nasal boss, and fragments of dentary,

frill, and postcrania. Forster (1993) found that all the characters used to diagnose UCMP 128561 were within the range of variation seen in *Triceratops* and referred it to *Triceratops* sp.

We visited the site along with Mark Goodwin, Mary Schweitzer (NCSU), and Liz Johnson (NCSU) on 8 July 2007. Because the majority of the fossil material was collected as float, remnants of a quarry were not apparent. Based on maps and field notes, we narrowed the location of the site to a gray-green mudstone on one side of a small tributary. The locality falls within the middle unit of the Hell Creek Formation, roughly 30 m below the local formational contact as initially reported by Cobabe and Fastovsky (1987). The specimen exhibits a nasal boss morphology, which is similar to that seen in several specimens of *Triceratops* (e.g., MOR 981, MOR 1122) from the lower half of the Hell Creek Formation. Similar morphologies are also found in some specimens collected from the Lance Formation, for which detailed stratigraphic data are not available (USNM 2412, USNM 4720). Whether the boss morphology represents the ontogenetic transformation of a pre-existing nasal horn (as is seen in some centrosaurines [Sampson, 1995; Currie et al., 2008]), pathology (Horner and Goodwin, 2008), or individual variation are competing hypotheses that cannot be rejected at this time and are under study by Hell Creek Project participants.

UCMP Locality V88081 (Russell Basin *Triceratops*): UCMP Specimen 136092

In 1981, Dale Russell and Helen Michel discovered UCMP 136092, a nearly complete skull (missing the snout, jaws, and beak). We visited the area with Mark

Goodwin and Mary Schweitzer on 10 July 2007. With only the plotted location on a topographic map and the lithologic description, we were unable to locate any remnants of an old quarry. A deep excavation had not been required to collect the skull, which had been preserved on its side, laterally compressed and covered by very little overburden (W.A. Clemens, pers. comm, 2011; Fig. 5.3). On a previous visit to the UCMP, one of us (Scannella) had examined the jacket of UCMP 136092 and noted the dark gray mudstone partially covering the skull (Fig. 5.3). While in the field and the area of the Russell Basin *Triceratops*, we located a dark gray mudstone horizon and eventually came upon bits of old plaster that we believe are from the original quarry (Fig. 5.4). The quarry was positioned just below a prominent sandstone ~6–10 m below multiple thin organic rich horizons, one of which represents the lower Z-coal (Fig. 5.4, C). As noted by Goodwin and Horner (2010), several other specimens of *Triceratops* were found weathering out of the same mudstone horizon within a kilometer of UCMP locality V88081.

UCMP Locality V75046 (Ruben's *Triceratops*): UCMP Specimen 113697

In 1970, then graduate student John Ruben discovered the skull of a large specimen of *Triceratops* in the Hell Creek Formation in the Bug Creek area of McCone County, Montana (Fig. 5.5). The stratigraphy in the Bug Creek area is notoriously problematic (Lofgren, 1995). Specifically, the local contact between the Hell Creek and Fort Union formations is obscured by what is now understood to be a Paleocene sandstone channel deposit that formed by incision of latest Cretaceous-aged Hell Creek Formation deposits (Lofgren, 1995).

The *Triceratops* quarry was in a mudstone bed in the saddle of a low set of hills. Upon tracing the beds laterally across the area, we found a thin coal and a dinosaur-bearing sandstone stratigraphically above it that we identified as the Apex Sandstone, which marks the base of the upper sequence of the Hell Creek Formation (Horner et al., 2011). The lower Z-coal is not present in the area surrounding UCMP locality V75046, likely having been scoured out by a Paleocene channel that incised down some 30 m or more from the Fort Union Formation. UCMP locality V75046 is stratigraphically very high in the middle unit of the Hell Creek Formation, ~6 m below the Apex Sandstone.

MOR Locality HC-135
(MORT): MOR Specimen 004

MOR 004 is a specimen that represents a large individual of *Triceratops* from the upper part of the Hell Creek Formation. It was discovered by Norman Constenius and was collected by Mick Hager in 1981 (Fig. 5.6). MOR 004 was the first specimen of *Triceratops* collected by the MOR. The site name, "MORT," is an acronym for "Museum of the Rockies *Triceratops*." On 12 July 2007, we visited the locality, which is in a sandstone ~6 m stratigraphically below the lower Z-coal. We also located and recorded locality data for several other poorly preserved skulls of *Triceratops* within one half of a kilometer of MOR locality HC-135.

MOR Locality HC-425
(Afternoon Delight): MOR Specimen 2569

In 2006, MOR volunteer Sonya Scarff discovered the partial skull of a very young juvenile *Triceratops* (MOR 2569) in a gray mudstone ~6 m below the top of prominent

hill in the Lost Creek Bay area (MOR locality HC-425; "Afternoon Delight"). MOR 2569 is one of the most complete specimens of *Triceratops* known that represents this early stage of ontogeny. Material collected from the locality includes the parietal, squamosals, a postorbital horn core, quadrates, and a partial maxilla (see Goodwin and Horner, 2010). The locality is in the lower part of the middle unit of the Hell Creek Formation (Fig. 5.1).

MOR Locality HC-531
(Lauren's Trike): MOR Specimen 2938

Lauren Berg discovered a partial skull of *Triceratops* (MOR 2938) weathering out of a gray mudstone roughly 2 m above the base of a small hill (16 July 2007). Among the material collected from the site (MOR locality HC-531) were the nasal horn, a dentary, maxilla, partial parietal, and sections of other cranial bones. MOR locality HC-531 was measured at ~10 m below the lower Z-coal (Fig. 5.7, section 1). The drainage of Short Creek (~200 m south of MOR locality HC-531) is extremely productive, particularly for material of *Triceratops*.

MOR Locality HC-520 (Joe's
Half Day Trike): MOR Specimen 2923

A short distance from MOR locality HC-531, film director Joe Johnston discovered the skull of a large *Triceratops* (MOR 2923). MOR locality HC-520 is stratigraphically slightly lower than MOR locality HC-531; it was found in a prominent sandstone that we believe can be stratigraphically correlated with a sandstone that is typically ~10 m below the lower Z-coal (Fig. 5.7, section 1). The skull was lying with its ventral side up and the underside of the parietal exposed (Fig. 5.8A). Whereas MOR

2938, which was found in mudstone, was disarticulated and three-dimensionally distorted post mortem, MOR 2923 was articulated, largely undistorted, and in excellent condition (Fig. 5.8B). This taphonomic pattern (correlation between lithology and degree of articulation in specimens of *Triceratops*) was noted by Goodwin and Horner (2010). MOR locality HC-520 also produced a shed *Tyrannosaurus* tooth and leaf impressions.

MOR 2923 preserves six epiparietals adorning the parietal with no evidence of one straddling the midline (Scannella and Horner, 2010). *Triceratops* had previously been described as possessing five epiparietals, one of which caps the midline of the frill (Forster, 1996a; 1996b). It is relatively rare to find all of the epiparietals attached to the parietal margin as they were likely removed during postmortem transport and burial (Horner and Goodwin, 2008). MOR 1122, a specimen of *Triceratops* ("*Torosaurus*" morph; Scannella and Horner, 2010 originally described by Farke, 2007) from the lower part of the Hell Creek Formation (the locality [MOR locality HC-258] is positioned at the bottom of the Basal Sandstone), preserves 12 epiparietals. Whether variation in epiparietal count is indicative of stratigraphic, ontogenetic, or individual variation is a research question currently under study by researchers at the MOR.

MOR Locality HC-702 (JD Trike12):
MOR Specimen 3056 and MOR Locality
HC-541 (JD Trike14): MOR Specimen 2950

In 2007, we encountered numerous specimens of *Triceratops* of varying degrees of preservation. Those in poor shape were recorded and left uncollected in the field. Others that were collected provide information on ontogenetic changes in cranial morphology. MOR 3056 is a squamosal and postorbital horn core of a juvenile

Triceratops that was exposed on a small gray mudstone bluff ~7 m stratigraphically below the lower Z-coal (Fig. 5.9). MOR 3056, though only represented by two elements, exhibits morphologies that are useful for testing hypotheses about ontogenetic variation and documenting patterns of growth and development (Horner and Goodwin, 2006; Goodwin and Horner, 2010).

Less than 100 m from MOR locality HC-702, and ~2 m higher in section, we found a partially disarticulated skull of a subadult *Triceratops* (MOR 2950 at MOR locality HC-541; Fig. 5.10) weathering out of a mudstone. This specimen preserves most of a squamosal, section of parietal, braincase, quadrate, frill episossifications, and epijugal.

MOR Locality HC-426 (Mark's Scavenged Trike): MOR Specimen 2570 and MOR Locality HC-639 (Anky Breaky Heart): MOR Specimen 3011

In 2006, Mark Goodwin discovered MOR specimen 2570, a partial young adult skull, in a gray mudstone (MOR locality HC-426; Mark's Scavenged Trike"; see Goodwin and Horner, 2010). It was found in an area where the formational contacts are not visible. In 2009, we identified the middle to upper depositional unit boundary (Apex Sandstone) in this area and the lower Z-coal ~1.5 miles (2.4 km) farther south. MOR locality HC-426 is ~25 m stratigraphically below the base of the upper unit (Fig. 5.11, section 2).

In 2009, Holly Woodward discovered the partial skull of a *Triceratops* in a low mudstone bluff less than 0.5 km west of MOR locality HC-426. The specimen (MOR 3011) preserves a partial parietal, nasal, epinasal, maxilla and premaxilla. The locality

(MOR locality HC-639; “Anky Breaky Heart”) is at approximately the same stratigraphic level as MOR locality HC-426 (Fig. 5.11, section 2).

MOR Locality HC-430 (Quittin’ Time): MOR Specimens 2574 and 2702

The Quittin’ Time Bonebed was discovered by Laura Wilson in 2006. The specimens of *Triceratops* were found in a mudstone 17 m stratigraphically below the lower Z-coal. Collected material includes partial skulls of a juvenile, subadult, and large, young adult *Triceratops*. The taphonomy of this site is discussed in detail by Keenan and Scannella (2014).

MOR Locality HC-521 (Lon’s Trike): MOR Specimen 2924

In 2007, Lon Bolick, a retired psychology professor (UW-FDL), discovered a specimen of *Triceratops* north of Jordan near Brownie Butte. The Hell Creek Formation and overlying Fort Union Formation have been extensively studied in this area (e.g., Archibald, 1982; Fastovsky, 1987). Jack Horner (MOR, MSU), who initially inspected the site (MOR locality HC-521), collected a partial braincase that was found as float on the surface of a sandstone horizon from the Apex Sandstone. We later collected the remainder of a nearly complete skull of a subadult *Triceratops* (MOR 2924) as well as much of the right forearm, several vertebrae (including articulated caudals), and ribs. A nearly complete crocodile skull, invertebrates, and palm impressions were also found at the site. MOR 2924 preserves the skull and postcrania of a subadult *Triceratops*. This allows for study of correlations between skull and postcranial morphology in ontogeny.

Whereas *Triceratops* cranial material is common in the Hell Creek Formation, associated postcrania are rare (Horner et al., 2011). After the excavation was concluded, an isolated postorbital horn core (MOR 3057 from MOR locality HC-114) as well as other material of *Triceratops* was discovered in the upper unit of the Hell Creek Formation within one kilometer of MOR locality HC-521.

MOR Locality HC-571 (Seth's Trike):
MOR Specimen 2979 and MOR Locality
HC-543 (TriSarahTops): MOR Specimen 2980

On August 6, 2008, MOR volunteer Seth Bainbridge discovered weathered fossil bone scattered over a hard, gray mudstone in the upper unit of the Hell Creek Formation (Figs. 5.12, 5.13A). In the nearby hill, two *Triceratops* postorbital horn cores were discovered in situ (MOR locality HC-571; "Seth's Trike"; MOR 2979). MOR 2979 consists of a partial skull in good condition, preserving the postorbital horn cores, frontoparietal fontanelle morphology (sensu Farke, 2010), and braincase region as well as pieces of frill and premaxilla (Fig. 5.13B). About a hundred meters east of MOR locality HC-571, Sarah Keenan discovered a site with a poorly preserved specimen of *Triceratops* (MOR locality HC-543; "TriSarahTops"). The best-preserved bone at the site is a squamosal (MOR 2980) that was collected.

MOR Locality HC-544 (DFJuvieTrike3):
MOR Specimen 2951 and MOR Locality
HC-627 (Situ But Sad): MOR Specimen 2999

On 22 June 2008 Fowler discovered the most complete juvenile *Triceratops* so far reported (MOR 2951). The site was named "DFJuvieTrike3" (Fig. 5.14A). Small bone

fragments on the surface of a dark gray mudstone were identified as part of the jugal of a very young *Triceratops* (Fig. 5.14B). A fragmentary rib was found eroding out of the same horizon. Excavation of MOR locality HC-544 (2008, 2009) produced a nearly complete and well-preserved juvenile skull, along with postcranial material including limb bones, ribs, vertebrae, a scapula, and an ilium. The specimen was placed at ~4 m stratigraphically above the Apex Sandstone, in the upper unit of the formation (Fig. 5.7, section 3). MOR 2951, which is currently under study, will provide a wealth of information on the ontogeny of the skeleton of *Triceratops*.

Nearly 1.5 km southeast of MOR locality HC-544, Fowler and Michiel Pillet discovered what initially appeared to be the partial parietal of a *Triceratops* weathering out of a mudstone near the base of a small hill. The locality (MOR locality HC-627; "Situ but Sad") was excavated and produced a partial skull from a subadult *Triceratops* (MOR 2999). Most of the posterior of the skull was preserved, including both postorbital horn cores and the braincase. An unfused nasal was also found at the site. MOR locality HC-627 is very high in the upper unit of the Hell Creek Formation (~7 m below the lower Z-coal; Fig. 5.7, section 5).

MOR Locality HC-565 (Supernasal):
MOR Specimen 2972 and MOR Locality
HC-628 (Ashes Trike): MOR Specimen 3000

Several specimens of *Triceratops* were collected from within two kilometers of MOR locality HC-544. On 23 June 2008, Fowler found an isolated large juvenile horn core (MOR 2958; MOR locality HC-500; "DF Juvie-Horncore"). He subsequently discovered a very large nasal horn in the Apex Sandstone (MOR locality HC-565;

"Supernasal"; Fig. 5.7, section 3) within 200 km of MOR locality HC-500. In addition to the nasal horn, MOR locality HC-565 produced a partial squamosal, braincase, jugal, and postcranial elements (MOR 2972).

Near MOR locality HC-565, Scannella discovered the partial skull of a large *Triceratops* weathering out of a dark gray mudstone horizon ~14 m stratigraphically below the lower Z-coal (MOR 3000; MOR locality HC-628; "Ashes Trike"; Fig. 5.7, section 2). The locality, which was excavated in 2009, produced a postorbital horn core, partial parietal, squamosal, dentary, and scapula.

MOR Locality HC-573 (Three Amigos): MOR Specimen 2982 and MOR Locality HC-576 (Six O'Clock Trike): MOR Specimen 2985

In 2008, Lee Hall discovered a nasal horn weathering out of a dark gray mudstone horizon (MOR 3055; MOR locality HC-1026; "Brown Nose") ~1 km north of Pennick Coulee. The locality is ~100 m away from a partial skeleton of a *Tyrannosaurus* (MOR 2925) found weathering out of a gray mudstone (Hall and Keenan, 2010). MOR 2925 and MOR 3055 occur low in the middle unit of the formation (Fig. 5.15, section 2).

Several more specimens of *Triceratops* were found in this area, the most complete being a partial subadult skeleton discovered by Lee Hall and volunteers Seth Bainbridge and Michael Flowers (MOR 2982; MOR locality HC-573; "Three Amigos"; Fig. 5.15, section 2). MOR 2982 was collected from a dark gray bentonitic mudstone low in the middle unit and consists of a partial skull including postorbital horn core, nasal horn, partial squamosal, midline of the parietal, dentary, rostral, and associated postcrania.

Less than half a kilometer from the *Tyrannosaurus* quarry (MOR locality HC-522), Bob Harmon discovered a large squamosal of a *Triceratops* weathering out of a mudstone horizon. In addition to the squamosal, the site ("Six O'Clock Trike"; MOR locality HC-576) produced a partial parietal, and associated postcrania. This specimen (MOR 2985) is significant as it occurred ~12 m below MOR locality HC-522 ("Brown Nose"), in the upper part of the lower unit (Fig. 5.15, section 2; see Discussion).

MOR Locality HC-532 (Ducky Tail): MOR Specimen 6648

In 2007, Bob Harmon discovered articulated caudal vertebrae of an *Edmontosaurus* (MOR 2939) leading into a sandstone horizon within the upper unit of the formation. In 2009, during excavation at the locality (MOR locality HC-532; "Ducky Tail"), an MOR crew led by Alessandro Carpana discovered the parietal, squamosal, and ilium of a juvenile *Triceratops* amongst the hadrosaur material.

Several other specimens of *Triceratops* were found within two kilometers of MOR locality HC-532, most notably the complete skull of a large *Triceratops* (MOR 3004; MOR locality HC-633; "The Horn Resounding") discovered by Becky Schaff ~22 m stratigraphically below the Apex Sandstone (Fig. 5.11, section 1). HC-633 also produced some postcranial material. MOR 3004 awaits preparation at the MOR. Less than a hundred meters from MOR locality HC-633, Bobby Ebelhar found a disarticulated skull weathering from a stratigraphically lower dark gray mudstone layer. This site (MOR locality HC-634; "Antsy Trike"; MOR 3005; Fig. 5.11, section 1) produced an unfused nasal, partial parietal, and some postcranial material. Paul Ullmann collected an

isolated nasal horn (MOR 3008; MOR locality HC-636; “American Beauty”; Fig. 5.11, section 1) from the base of the Apex Sandstone in this area.

MOR Locality HC-638 (Golden Goose): MOR Specimen 3010

In 2009, Fowler and Bobby Ebelhar discovered an area (~400 m^2) that produced several fragmentary *Triceratops* and was called “Trikey Town”. A ~3 m-thick mudstone horizon, produced the majority of the material. The locality produced *Triceratops* from the lower part of the middle unit of the Hell Creek Formation (Fig. 5.11, section 3). MOR 3010 (“Golden Goose”), a partial skull of a small *Triceratops*, was the most complete specimen collected from the area. The quarry (MOR locality HC-638) produced a nasal horn, postorbital horn core, dentary and other more fragmentary material. In addition to *Triceratops*, the area contained a rich fossil macrosite with concentrated remains of several taxa including fish, turtles, crocodiles, and dinosaurs.

MOR Locality HC-668 (Yoshi’s Trike): MOR Specimen 3027 and MOR Locality HC-682 (Cliffhanger): MOR Specimen 3045

MOR 3027 is an exquisitely preserved large disarticulated skeleton of *Triceratops* discovered by Yoshi Katsura in 2010. The specimen was collected from a mudstone high in the middle unit of the Hell Creek Formation (~5.5 m stratigraphically below the Apex Sandstone; Fig. 5.15, section 5; Fig. 5.16). Although on the surface the specimen did not look very promising, excavation in 2010 and 2011 revealed one of the most productive MOR *Triceratops* localities (MOR locality HC-668).

Less than half a kilometer from MOR locality HC-668, Yoshi discovered a subadult *Triceratops* weathering out of a mudstone horizon in a shear hillside. This locality (MOR locality HC-682; “Cliffhanger”), like MOR locality HC-668, is positioned very high in the middle unit (Fig. 5.15, section 5). A disarticulated partial skull (MOR 3045) was collected from the site.

MOR Locality HC-716 (Little Horny Devil): MOR Specimen 3064

MOR 3064 is a partial skull of a small juvenile *Triceratops*, consisting of a brow horn, quadrate, partial squamosal, both jugals, partial quadratojugal, numerous frill epiossifications, and other cranial material. It was discovered by Fowler, Aaron Medford, Nick Resar and Rebecca Cook at the southern end of Pennick Coulee. The specimen was recovered from a horizon ~13 m stratigraphically below the Apex Sandstone (MOR loc HC-716; Fig. 5.15, section 4). MOR 3064 is approximately the size of MOR 2951, which is from above the Apex Sandstone, hence the specimens will facilitate comparison of ontogenetic trajectories between *Triceratops* from the upper middle and lower upper unit of the Hell Creek Formation. Approximately 100 m south of MOR locality HC-717, Fowler discovered a postorbital horn above the Apex Sandstone (MOR 3047; MOR locality HC-697; "Got the Horn"; Fig. 5.15, section 4).

Discussion and Conclusions

Lull (1933: p. 123) stated: “There is infinite variation in all *Triceratops* skulls.” Due to the morphological variability seen among specimens, *Triceratops* has been the

source of considerable systematic confusion since its initial description. As many as 16 species of *Triceratops* have been named, many of which are based on the slightest of variations in cranial morphology (Ostrom and Wellnhofer, 1986; 1990; Dodson, 1996). Forster (1996b) argued that the characters that had been used to erect these taxa likely represented intraspecific variation in only two species: *T. horridus* and *T. prorsus*. Much of the variation found in *Triceratops* is likely due to changes that occurred through ontogeny (Horner and Goodwin, 2006; 2008; Scannella and Horner, 2010). Another important consideration for dinosaur systematics is that morphology may vary with stratigraphy (e.g., Evans et al., 2006). Evolutionary change through the Hell Creek Formation may have contributed to morphological variation seen in *Triceratops* (Scannella and Fowler, 2009).

The database of *Triceratops* specimens compiled during the Hell Creek Project is among the most comprehensive for any non-avian dinosaur in a single study area. It includes not only a large sample of *Triceratops* specimens from multiple ontogenetic stages, but each specimen is accompanied by detailed stratigraphic positional data as well. This stratigraphic survey forms the basis for ongoing research into the evolution of *Triceratops* (e.g., Scannella and Fowler, 2009; Scannella, 2010). From this database, analyses may be able to tease apart the relative contributions of ontogeny and evolution to the morphological variation of *Triceratops* from the Hell Creek Formation. Every specimen of *Triceratops*, whether a complete skull or an isolated epinasal, might hold valuable research information if considered in stratigraphic context. Moreover, this survey suggests that a reliance on holotypes in phlyogenetic analyses may place undue

focus on a single morphologic variant and may actually obscure stratigraphic and ontogenetic variation (e.g., Mayr, 1959; Scannella and Horner, 2010).

This survey highlights the importance of targeted fossil collecting within a stratigraphic context. Ideally, an ontogenetic series of *Triceratops* specimens would be collected for each depositional unit of the Hell Creek Formation in order to detail evolutionary and heterochronic trends (Scannella, 2010). Several specimens of *Triceratops* have been collected from the lower unit of the Hell Creek Formation (Horner et al., 2011), including a nearly complete, disarticulated skull of a subadult (MOR 1120; MOR locality HC-256 [“Getaway Trike”]; see Goodwin and Horner, 2010) and the most complete skull of an adult known (= ”*Torosaurus*”; MOR 1122 [but see also Farke, 2011; Longrich and Field, 2012]); however, sampling of the ontogenetic series for the lower unit remains far less complete than those for the middle and upper units. A small juvenile from this stratigraphic interval, for example, would reveal insights into chasmosaurine heterochrony. Future field work will target the lower part of the Hell Creek Formation in order to increase resolution of trends in *Triceratops* morphological variation.

Acknowledgements

We are especially grateful to Jack Horner for advice, assistance, and constant support. Special thanks also to Mark Goodwin for assistance and encouragement throughout. Carrie Ancell, Susan Brewer, Bob Harmon, Patsy Hookey, Jamie Jette, and Linda Roberts prepared specimens. We thank all of the Museum of the Rockies (MOR)

field crews, who contributed to the findings of the Hell Creek Project, and everyone who has discovered or collected a *Triceratops* for the MOR collections. The Twitchell, Taylor, Trumbo, Holen, and Isaacs families granted access to lands. The Bureau of Land Management, U.S. Fish and Wildlife Service, Charles M. Russell National Wildlife Refuge, and the Montana Department of Natural Resources and Conservation granted collection permits to J. Horner and MOR over the course of the Hell Creek Project. Montana Fish Wildlife and Parks hosted MOR crews during the early years of the Hell Creek Project. Sarah Keenan and Leigha King provided invaluable field assistance. We thank Bill Clemens and Laura Wilson for sharing stratigraphic data. We thank Bobby Boessenecker, Lon Bolick, Bill Clemens, Peter Dodson, David Evans, Andy Farke, Liz Freedman, Mark Goodwin, Lee Hall, Joe Hartman, John Hoganson, Michael Holland, Jack Horner, Mark Loewen, Kevin Padian, Dean Pearson, Kari Scannella, Mary Schweitzer, Darrin Strosnider, Dave Varricchio, Dave Weishampel, Greg Wilson, and Holly Woodward for helpful comments and conversations. Two anonymous reviewers provided helpful comments that improved the manuscript. Editorial comments from Greg Wilson and W.A. Clemens improved the manuscript. Funding was provided by MOR Paleo, the donors to the Hell Creek Project, and the Smithsonian Institution. Grants from the Welles Fund of the University of California Museum of Paleontology to Scannella and Fowler are gratefully acknowledged. We are thankful for North American Paleontological Convention student travel grants (2009).

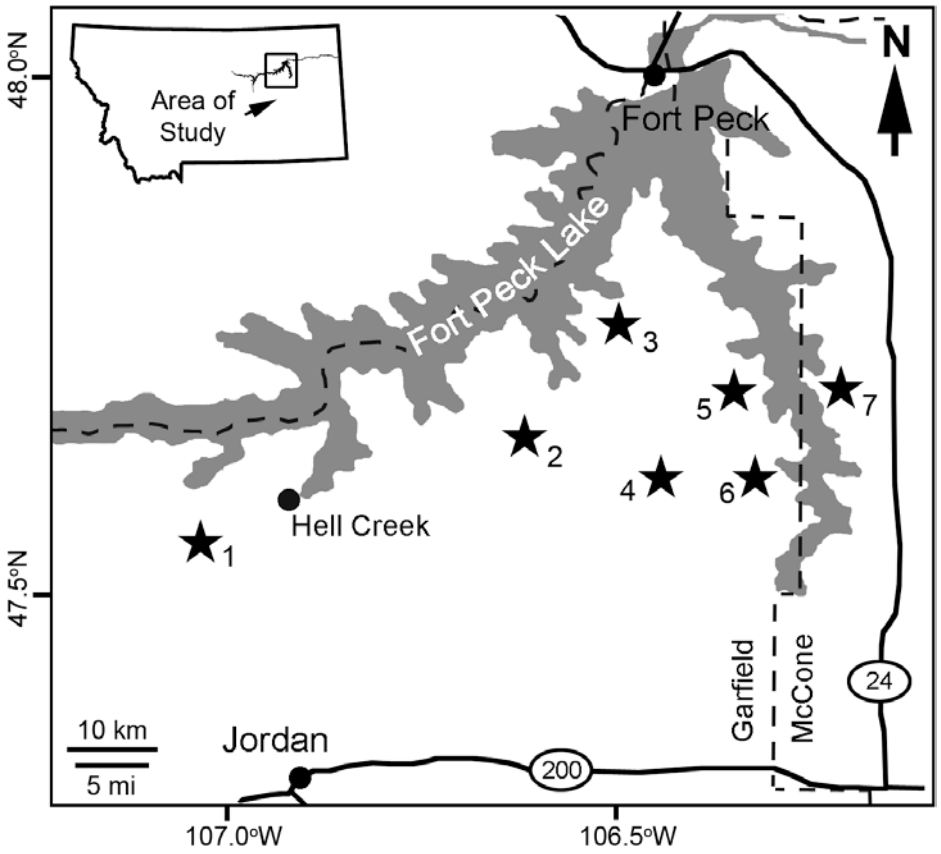

Figure 5.1. Collection areas for specimens of *Triceratops* discussed in the text, south Fort Peck Lake in Garfield and McCone Counties, Montana. 1—Brownie Butte; 2—Gilbert Creek; 3—Pennick Coulee; 4—Lone Tree Creek; 5—Lost Creek; 6—Short Creek; 7—Bug Creek. More detailed locality data are on file at the Museum of the Rockies and are available to qualified researchers upon request.

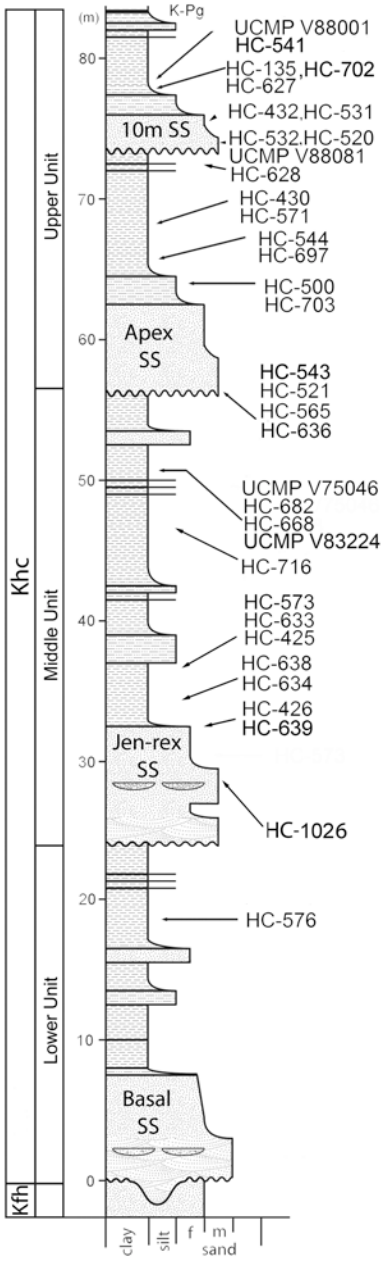

Figure 5.2. Relative positions of *Triceratops* localities discussed in the text superimposed on a generalized section. Localities are plotted based on stratigraphic position, not by facies. Because unit thicknesses vary among outcrops, the relative positions of localities from different sections are approximate at the meter scale. Placement of localities within subunits (e.g., middle unit–upper part; see Appendix F) is accurate. Position of the Cretaceous-Paleogene (K-Pg) boundary varies in northern Montana (Turner, 2010). Scale in meters. SS—sandstone. Kfh-Fox Hills Formation. Khc-Hell Creek Formation.

Figure 5.3. The Russell Basin *Triceratops* (University of California Museum of Paleontology [UCMP] 136092), photographed while still under preparation at the UCMP. Right lateral view of skull.

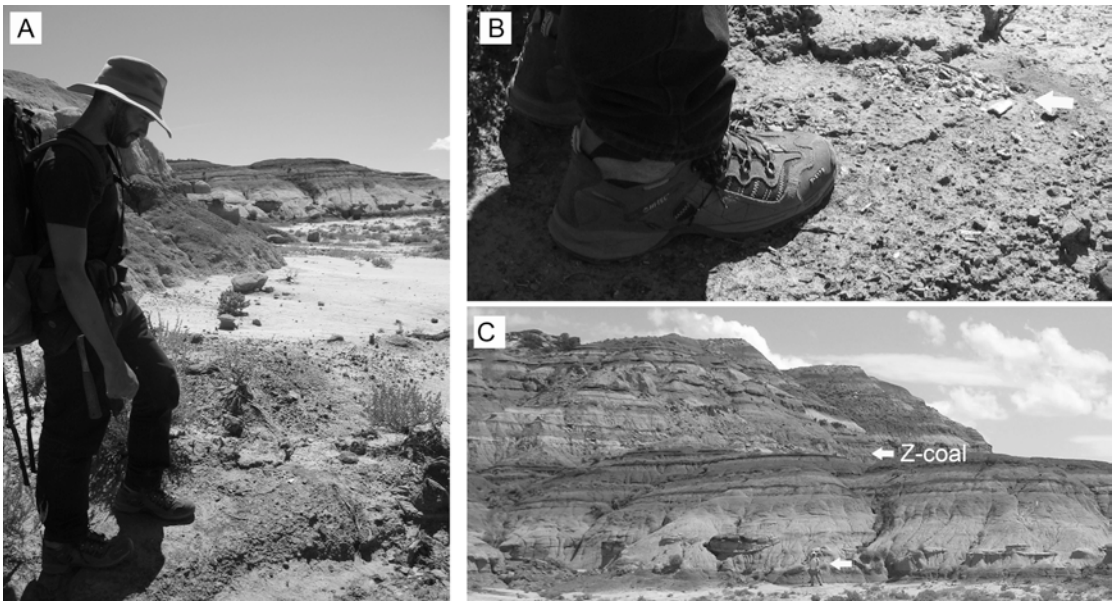

Figure 5.4. Relocating the Russell Basin *Triceratops* quarry (University of California Museum of Paleontology [UCMP] locality V88081). (A) Scannella standing at the site. (B) A small amount of plaster found at the site. (C) Fowler standing just above the stratigraphic level of UCMP locality V88081.

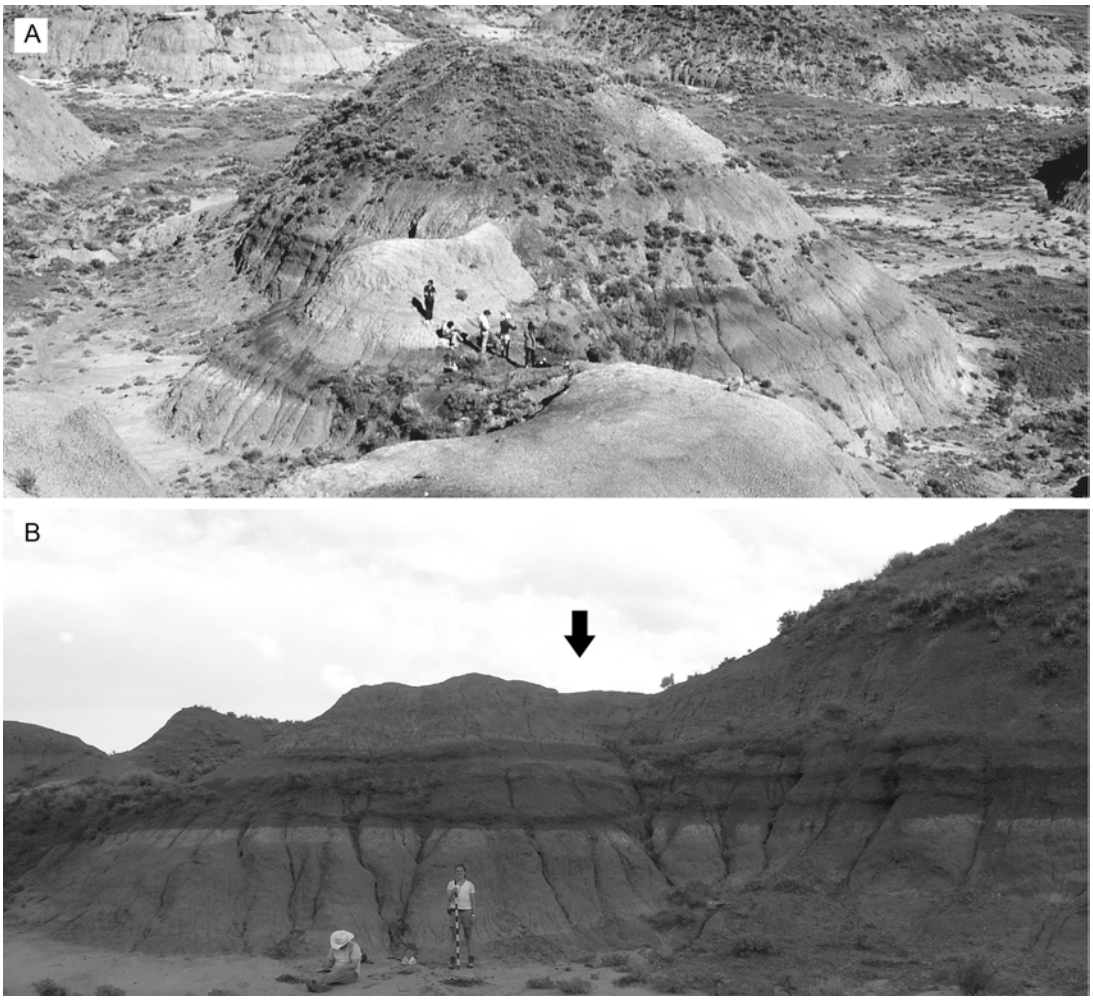

Figure 5.5. Ruben's *Triceratops* (University of California Museum of Paleontology [UCMP] locality V75046). (A) Excavation under way in 1970 (image by J.T. Gregory, courtesy of UCMP). (B) Fowler and Sarah Keenan taking a stratigraphic section at the site in 2007. Arrow indicates quarry site.

Figure 5.6. Museum of the Rockies (MOR) *Triceratops* (MORT; MOR 004), jacketed and awaiting collection in 1981. Note the prominent coals of the Fort Union Formation in the background. Image courtesy of MOR.

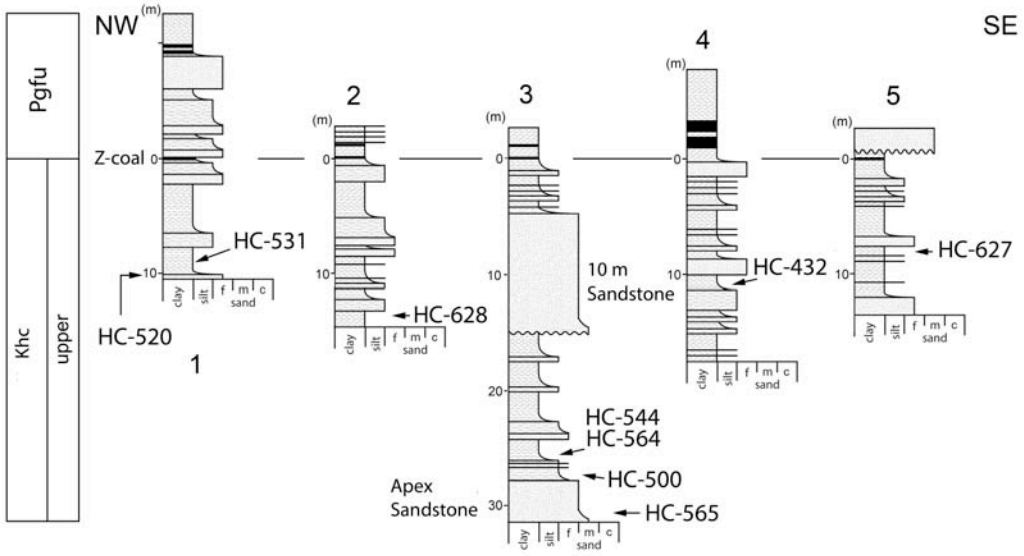

Figure 5.7. Correlation of measured sections and Museum of the Rockies (MOR) *Triceratops* localities, ~4.5 km across the Short Creek area (Garfield County, Fig. 5.1, locality 6) from northwest to southeast. This area includes exposures of the upper part of the Hell Creek Formation (Khc) up to the contact with the Fort Union Formation (Pgfu). Section 1 taken at HC-531. Section 2 taken at HC-628. Section 3 taken at HC-500. Section 4 taken at site HC-432 ("Snap Creek," which produced an isolated nasal horn [Museum of the Rockies (MOR) 2576]). Section 5 taken at site HC-627. Scale in meters.

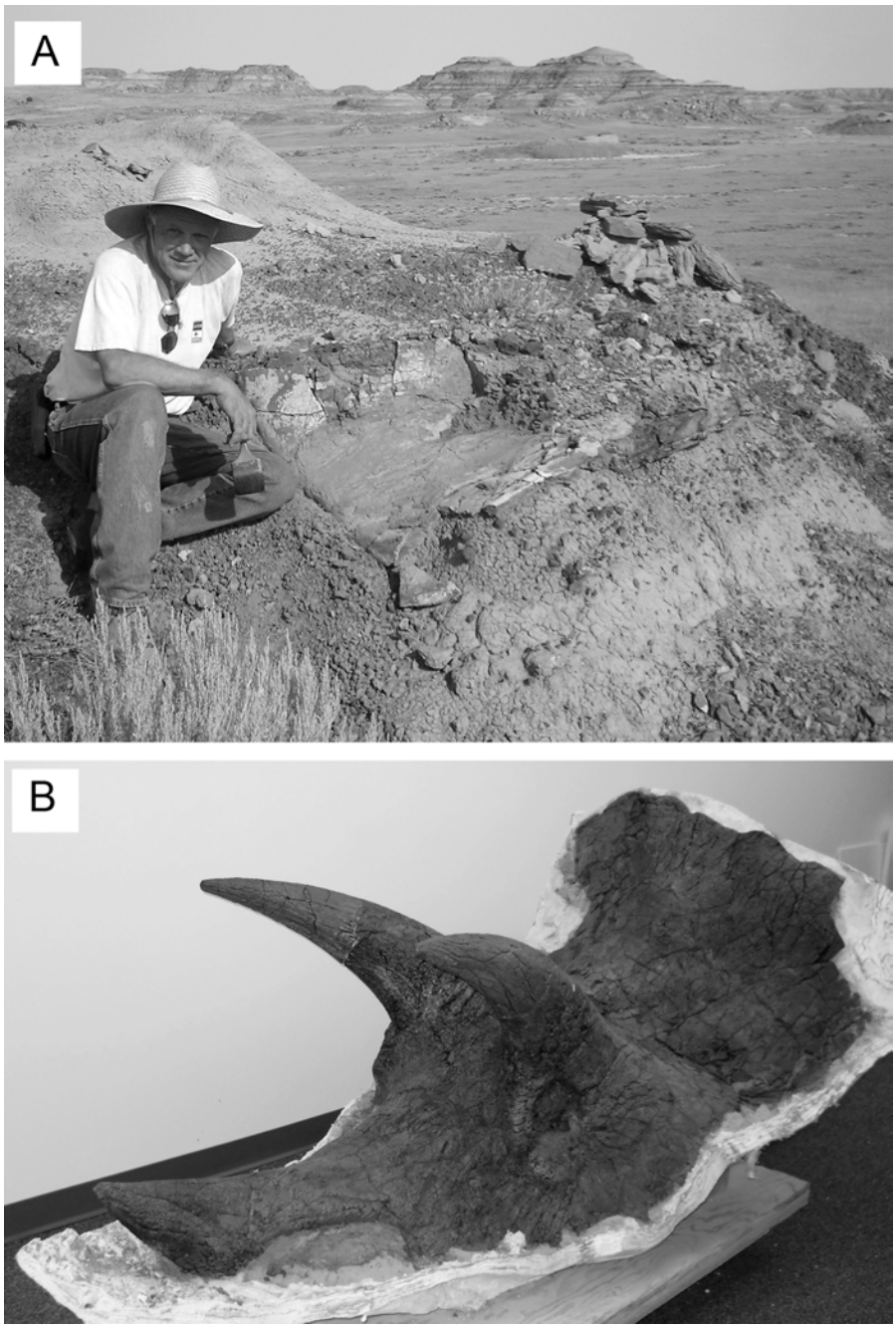

Figure 5.8. Joe's Half Day Trike (Museum of the Rockies [MOR] locality HC-520). (A) Joe Johnston uncovers MOR specimen 2923. It was preserved ventral side up (the ventral surface of its parietal is exposed here) in the 10-Meter Sandstone. The lower Z-coal is exposed in the hills in the background. Image by Kari Scannella, courtesy of MOR. (B) MOR 2923 after preparation. This specimen preserves a nearly complete posterior parietal margin; the remaining pieces are housed in a cabinet in collections at MOR.

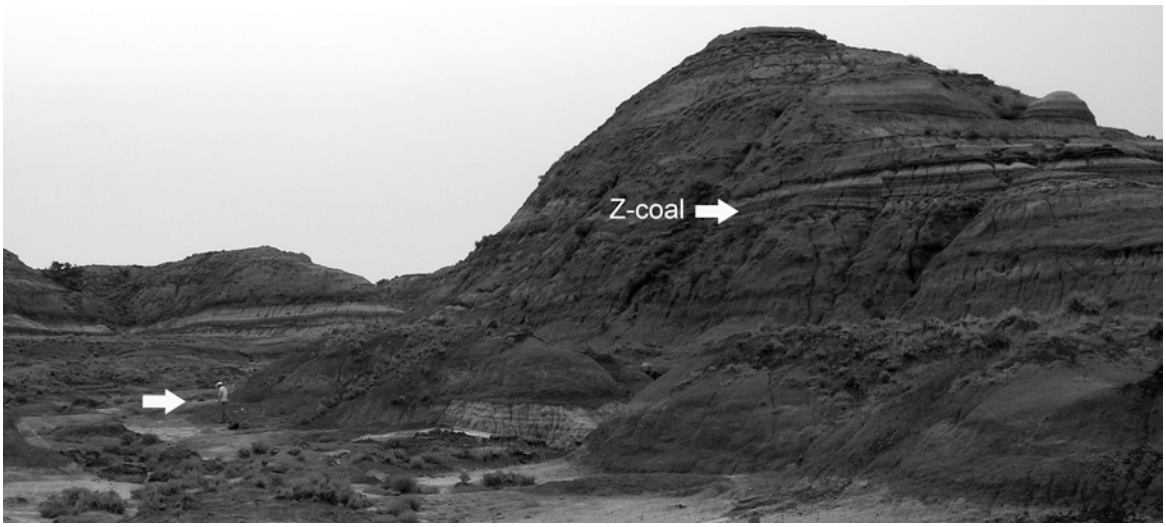

Figure 5.9. Fowler discovers JDTrike12 (Museum of the Rockies [MOR] specimen 3056) eroding from a gray mudstone stratigraphically high in the upper unit of the Hell Creek Formation.

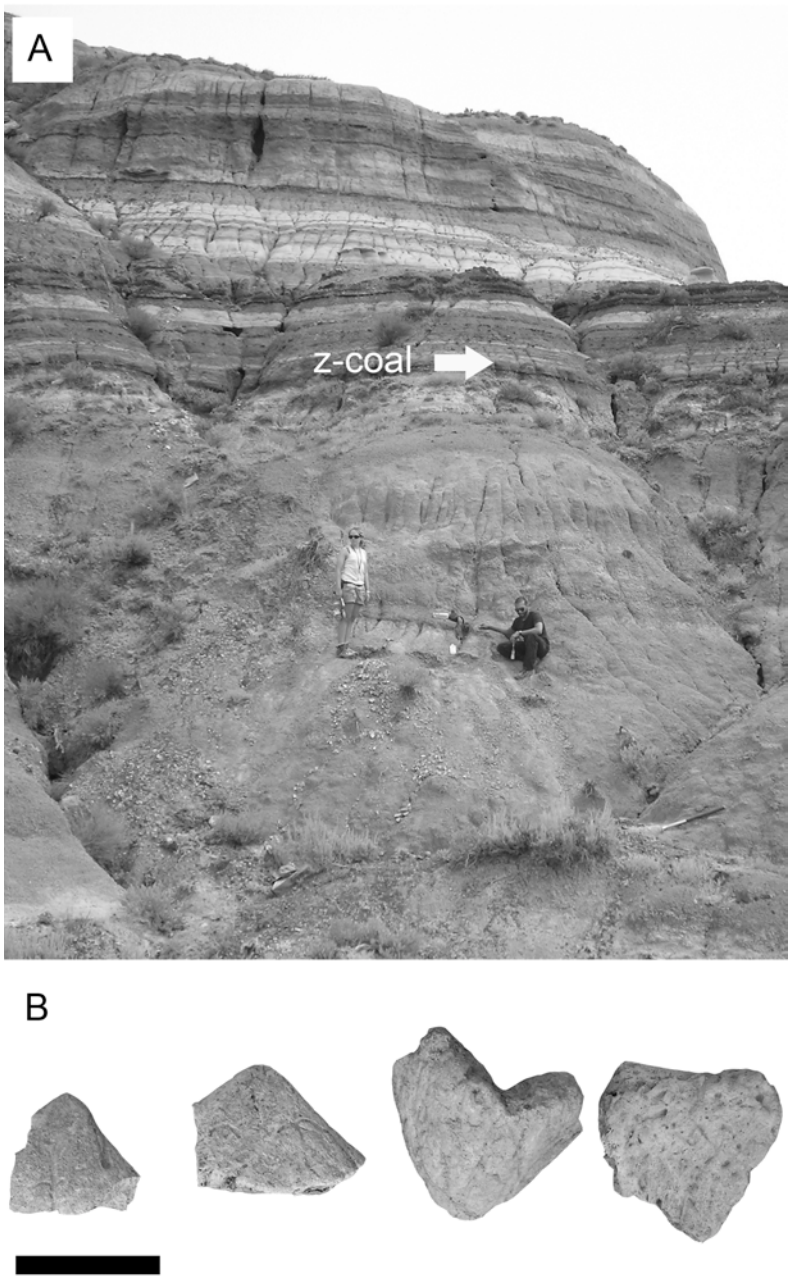

Figure 5.10. JDTrike14 (Museum of the Rockies [MOR] locality HC-541). (A) Scannella and Sarah Keenan at the quarry, only a few meters below the lower Z-coal. (B) Some of the elements originally surface collected from the site, including an epijugal and frill episossification, which provide information on the ontogenetic status of the individual (MOR 2950). The specimen represents a subadult *Triceratops*. Scale bar is 5 cm.

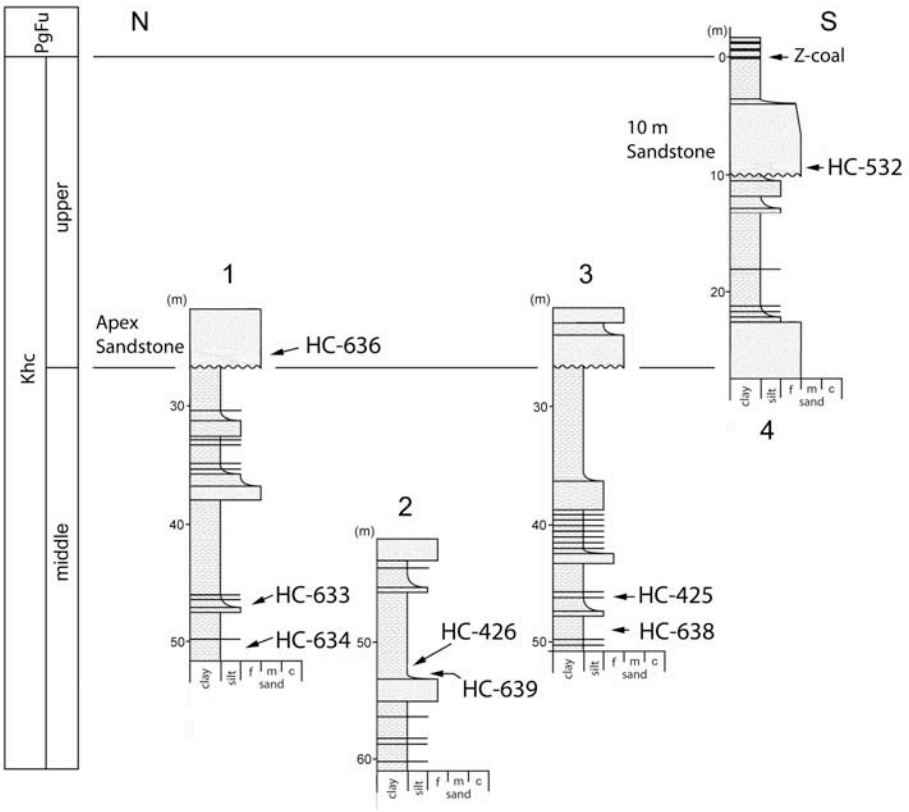

Figure 5.11. Correlation of measured sections and Museum of the Rockies (MOR) *Triceratops* localities ~2.5 km across Lost Creek Bay area (Garfield County, Fig. 5.1, locality 5) from north to south. This area exposes the lower middle part of the Hell Creek Formation (Khc), up to the contact with the Fort Union Formation (Pgfu). Section 1 taken at HC-633. Section 2 taken at HC-426. Section 3 taken at HC-638. Section 4 taken at HC-532. Scale in meters.

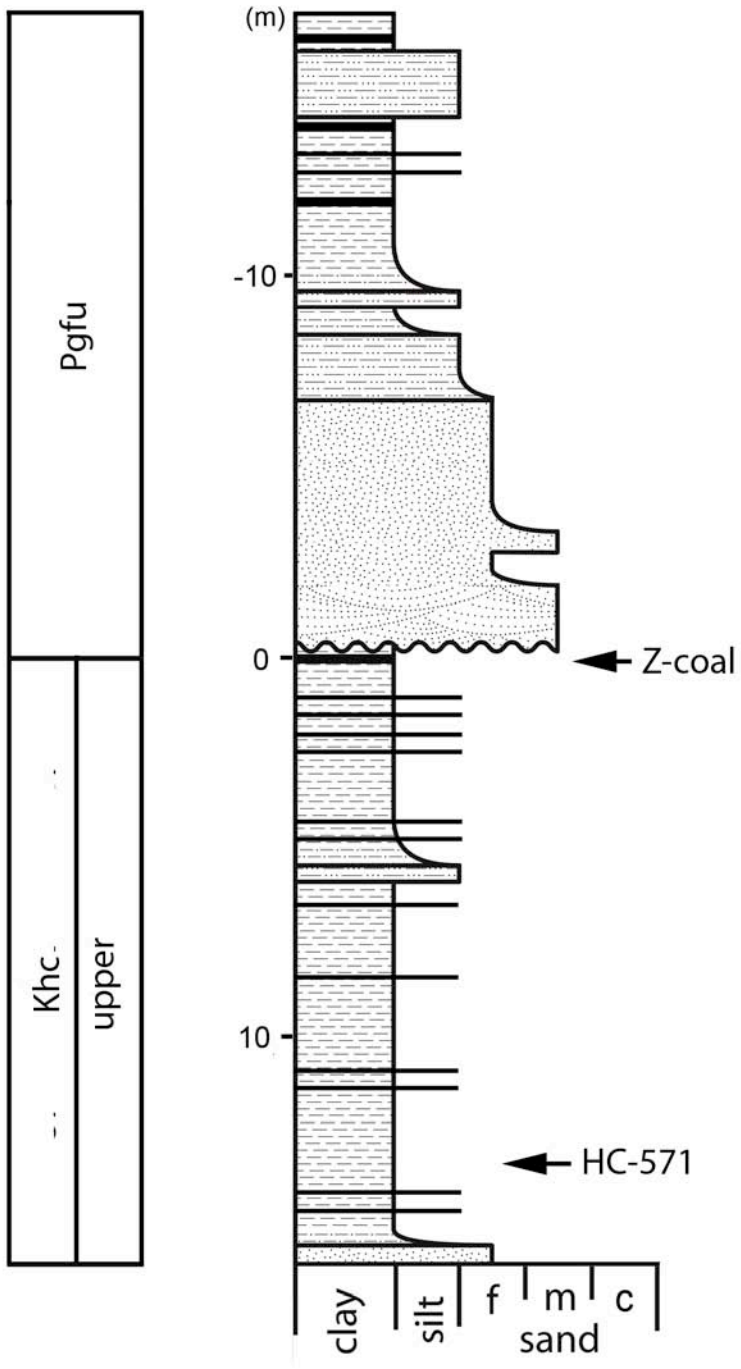

Figure 5.12. Museum of the Rockies (MOR) locality HC-571 plotted on measured section, Brownie Butte (Garfield County; Fig. 5.1, locality1). This area includes exposures of the upper part of the Hell Creek (Khc) and the lower part of the Fort Union Formations (Pgfu). Scale in meters.

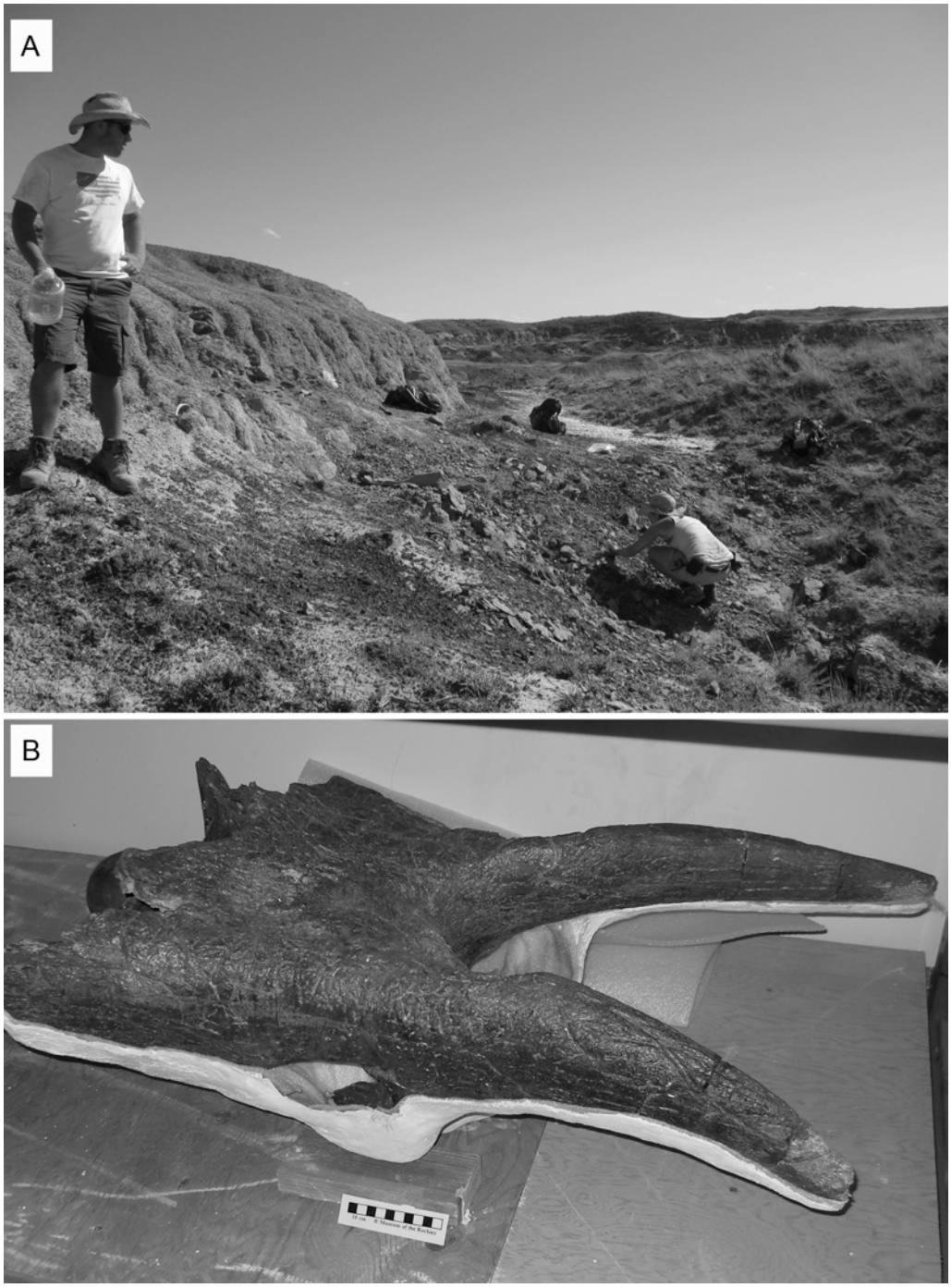

Figure 5.13. Seth's Trike (Museum of the Rockies [MOR] locality HC-571). (A) Seth Bainbridge and Sarah Keenan at the site. (B) MOR 2979 after preparation; additional cranial elements were also recovered from the site.

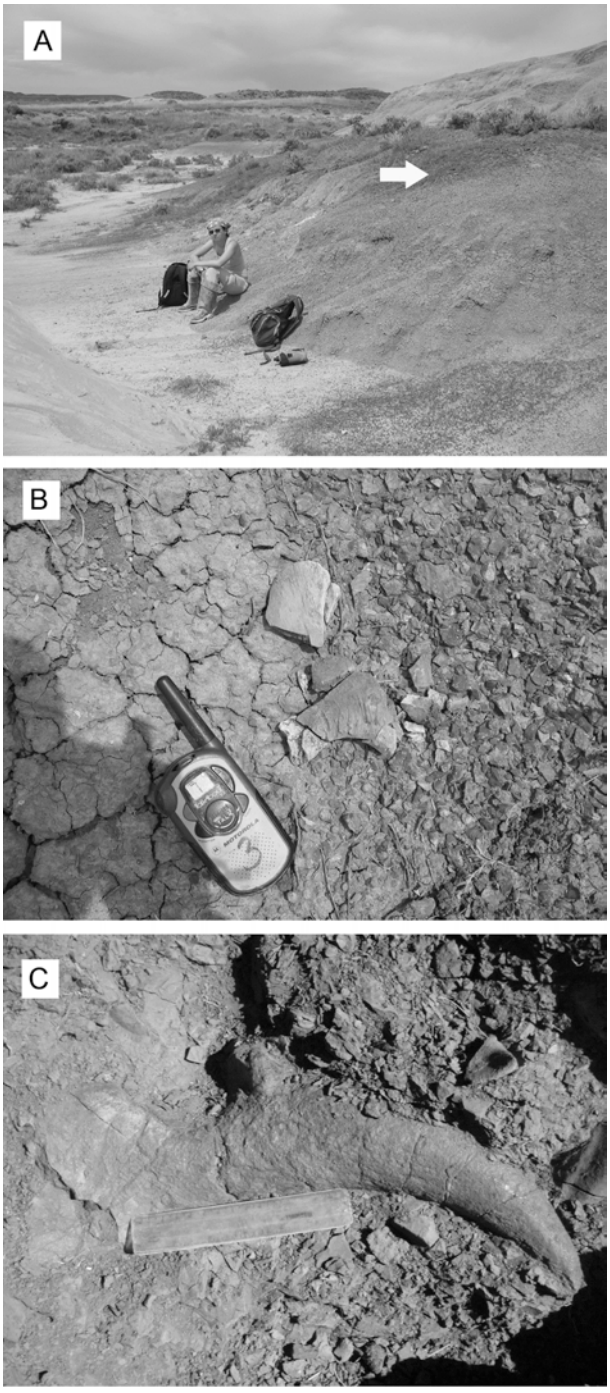

Figure 5.14. DFJuvieTrike3 (Museum of the Rockies [MOR] locality HC-544). (A) Liz Freedman at the site. (B) A partial jugal that was found as float at the site. (C) A left postorbital horn core is exposed during collection of the specimen. MOR 2951 is one of the most complete juvenile specimens of *Triceratops* ever discovered. Ruler is 15 cm in length.

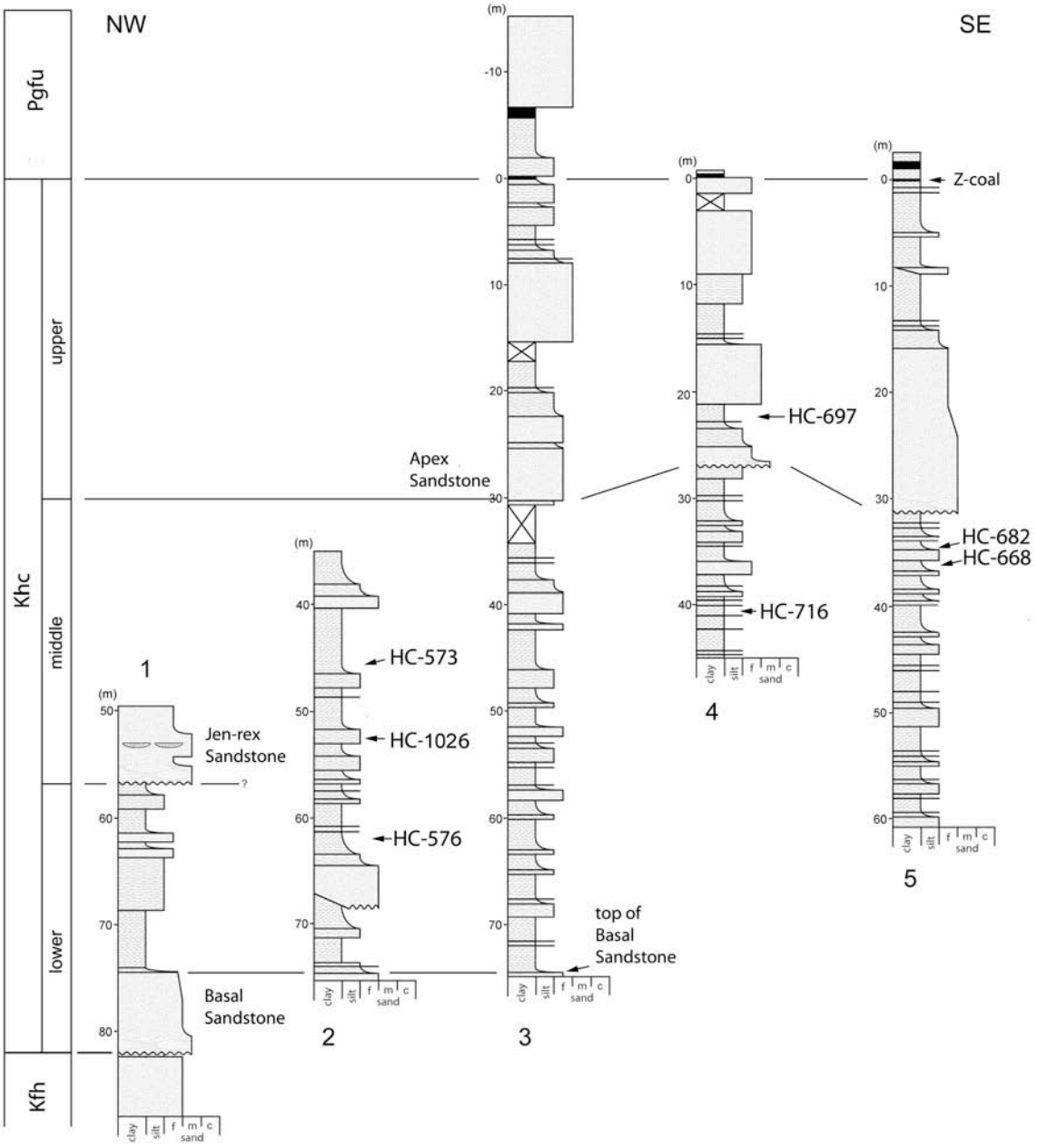

Figure 5.15. Correlation of measured sections and Museum of the Rockies (MOR) *Triceratops* localities across ~6.5 km of the Pennick Coulee area (Garfield County, Fig. 5.1, locality 3) from northwest to southeast. This area includes a complete section of the Hell Creek Formation (Khc). Section 1 taken at NW Pennick Coulee. Section 2 taken at N Pennick Coulee. Section 3 taken at E Pennick Coulee. Section 4 taken at HC-716. Section 5 taken at HC-668. Scale in meters. Kfh-Fox Hills Formation. Pgfu-Fort Union Formation.

Figure 5.16. Yoshi's Trike (Museum of the Rockies [MOR] locality HC-668). This locality is very high in the middle unit, ~5.5 m below the Apex Sandstone.

References Cited

Archibald, D.J. 1982. A Study of Mammalia and Geology across the Cretaceous-Tertiary Boundary in Garfield County, Montana. University of California Publications in Geological Sciences 122: 286 p.

Archibald, D.J., R.F. Butler, E.H. Lindsay, W.A. Clemens, and L. Dingus. 1982, Upper Cretaceous–Paleocene biostratigraphy and magnetostratigraphy, Hell Creek and Tullock Formations, northeastern Montana. Geology 10(3): 153–159

Brown, B. 1907. The Hell Creek beds of the Upper Cretaceous of Montana: American Museum of Natural History Bulletin 23:823–845.

Brown, B. 1917. A complete skeleton of the horned dinosaur Monoclonius, and a description of a second skeleton showing skin impressions. Bulletin of the American Museum of Natural History 37: 281–306.

Carpenter, K., and D.B. Young. 2002. Late Cretaceous dinosaurs from the Denver Basin, Colorado. Rocky Mountain Geology 37(2): 237–254.

Cobabe, E.A., and D.E. Fastovsky. 1987. *Ugrosaurus olsoni*, a new ceratopsian (Reptilia: Ornithischia) from the Hell Creek Formation of eastern Montana: Journal of Paleontology 61 (1):148–154.

Currie, P.J., W. Langston, and D.H. Tanke. 2008. A new species of *Pachyrhinosaurus* (Dinosauria, Ceratopsidae) from the Upper Cretaceous of Alberta Canada; pp. 1-108 in P.J. Currie, W. Langston, and D.H. Tanke (eds.) A New Horned Dinosaur from an Upper Cretaceous Bone Bed in Alberta. NRC Research Press, Ottawa, Ontario, Canada.

Dingus, L., and M.A. Norell 2010. Barnum Brown: The Man Who Discovered *Tyrannosaurus rex*. University of California Press, Berkeley, California, 368 pp.

Dodson, P. 1996. The Horned Dinosaurs. Princeton University Press, Princeton, New Jersey, 346 pp.

Evans, D., P. Currie, D. Eberth, and M. Ryan. 2006. High-resolution lambeosaurine dinosaur biostratigraphy, Dinosaur Park Formation: Sexual dimorphism reconsidered. Journal of Vertebrate Paleontology 26 Supplement: 59A.

Farke, A.A., 1997. The distribution and taxonomy of *Triceratops* p. 47-79 in Wolberg, D.L., E. Stump, and G.D. Rosenberg (eds.), Dinofest International Proceedings Volume. Philadelphia Academy of Natural Sciences, Philadelphia, Pennsylvania.

Farke, A.A., 2007. Cranial osteology and phylogenetic relationships of the chasmosaurine ceratopsid *Torosaurus latus*,p. 235-257 in Carpenter, K., (ed.), Horns and Beaks: Ceratopsian and Ornithopod Dinosaurs. Indiana University Press, Bloomington, Indiana.

Farke, A.A. 2010. Evolution, homology, and function of the supracranial sinuses in ceratopsian dinosaurs. Journal of Vertebrate Paleontology 30 (5): 1486–1500.

Farke, A.A. 2011. Anatomy and taxonomic status of the chasmosaurine ceratopsid *Nedoceratops hatcheri* from the Upper Cretaceous Lance Formation of Wyoming, U.S.A. PLoS ONE 6:e16196, doi:10.1371/journal.pone.0016196.

Fastovsky, D.E. 1987. Paleoenvironments of vertebrate-bearing strata during the Cretaceous-Paleogene transition, eastern Montana and western North Dakota. Palaios 2: 282–295, doi:10.2307/3514678.

Flight, J.N. 2004. Sequence stratigraphic analysis of the Fox Hills and Hell Creek Formations (Maastrichtian), Eastern Montana and its relationships to dinosaur paleontology [M.S. thesis]: Bozeman, Montana, State University, 164 pp.

Forster, C.A. 1993. Taxonomic validity of the ceratopsid dinosaur *Ugrosaurus olsoni* (Cobabe and Fastovsky). Journal of Paleontology 67(2): 316–318.

Forster, C.A. 1996a. New information on the skull of *Triceratops*. Journal of Vertebrate Paleontology 16(2): 246–258, doi:10.1080/02724634.1996.10011312.

Forster, C.A. 1996b. Species resolution in *Triceratops*: Cladistic and morphometric approaches. Journal of Vertebrate Paleontology 16(2): 259–270, doi:10.1080/02724634.1996.10011313.

Fowler, D.W. 2009. A sequence stratigraphic subdivision of the Hell Creek Formation: Beginnings of a high-resolution regional chronostratigraphic framework for the terminal Cretaceous, p. 136 in Storrs, G.W. (ed.) 9th North American Paleontological Convention Abstracts. University of Cincinnati, Cincinnati Museum Center Scientific Contributions 3, Cincinnati, Ohio.

Goodwin, M.B., and J.R. Horner. 2010. Historical collecting bias and the fossil record of *Triceratops* in Montana, p. 551-564 in Ryan, M.J., Chinnery-Allgeier, B.J., and Eberth, D.A. (eds.), New Perspectives on Horned Dinosaurs: The Royal Tyrrell Museum Ceratopsian Symposium. Indiana University Press, Bloomington, Indiana.

Hall, L., and S. Keenan 2010, Taphonomy of a new specimen of *Tyrannosaurus rex* from the Hell Creek Formation, Montana. Journal of Vertebrate Paleontology: SVP Program and Abstracts Book, v. 30: 100A-101A.

Hartman, J.H., R.D., Butler, M.W., Weiler, K.K., Schumaker. 2014. Context, naming, and formal designation of the Cretaceous Hell Creek Formation lectostratotype, Garfield County, Montana , in Wilson, G.P., Clemens, W.A., Horner, J.R., and Hartman, J.H., eds., Through the End of the Cretaceous in the Type Locality of the Hell Creek Formation in Montana and Adjacent Areas: Geological Society of America Special Paper 503, doi:10.1130/2014.2503(02).

Hatcher, J.B., Marsh, O.C., and Lull, R.S., 1907, The Ceratopsia. U.S. Geological Survey Monograph 49, 300 pp.

Horner, J. R., and M. B. Goodwin. 2006. Major cranial changes during *Triceratops* ontogeny. Proceedings of the Royal Society B: Biological Sciences 273:2757–2761, doi:10.1098/rspb.2006.3643.

Horner, J. R., and M. B. Goodwin. 2008. Ontogeny of cranial epi-ossifications in *Triceratops*. Journal of Vertebrate Paleontology 28:134–144.

Horner, J. R., and E.-T. Lamm. 2011. Ontogeny of the parietal frill of *Triceratops*: A preliminary histological analysis. Comptes Rendus Palevol 10:439–452 doi:10.1016/j.crpv.2011.04.006.

Horner, J. R., M. B. Goodwin, and N. Myhrvold. 2011. Dinosaur Census Reveals Abundant *Tyrannosaurus* and Rare Ontogenetic Stages in the Upper Cretaceous Hell Creek Formation (Maastrichtian), Montana, USA. PLoS ONE 6:e16574.

Keenan, S.W., and J.B. Scannella. 2014. Paleobiological implications of a *Triceratops* bonebed from the Hell Creek Formation, Garfield County, northeastern Montana, in Wilson, G.P., W.A. Clemens, J.R. Horner, and J.H. Hartman, (eds.) Through the End of the Cretaceous in the Type Locality of the Hell Creek Formation in Montana and Adjacent Areas: Geological Society of America Special Paper 503, doi:10.1130/2014.2503(14).

Lofgren, D.L. 1995. The Bug Creek Problem and the Cretaceous-Tertiary Transition at McGuire Creek, Montana. University of California Publications in Geological Sciences 140, 185 p.

Longrich, N.R., and D.J. Field. 2012. *Torosaurus* is not *Triceratops*: Ontogeny in chasmosaurine ceratopsids as a case study in dinosaur taxonomy: PLoS ONE 7(2) p. e32623, doi:10.1371/journal.pone.0032623.

Lull, R.S. 1915. The mammals and horned dinosaurs of the Lance formation of Niobrara County, Wyoming. American Journal of Science 4: 319–348, doi:10.2475/ajs.s4-40.238.319.

Lull, R.S. 1933. A Revision of the Ceratopsia or Horned Dinosaurs. Yale Peabody Museum of Natural History Memoir 3, 178 pp.

Mayr, E. 1959. Darwin and the evolutionary theory in biology, p. 1-10 in Meggers J., ed., Evolution and Anthropology: A Centennial Appraisal: Anthropological Society of Washington, Washington, D.C.

Osborn, H.F. 1905. *Tyrannosaurus* and other Cretaceous carnivorous dinosaurs. Bulletin of the American Museum of Natural History 22: 475–479.

Ostrom, J.H. and P. Wellnhofer. 1986. The Munich specimen of *Triceratops* with a revision of the genus. Zitteliana 14: 111–158.

Ostrom, J.H., and P. Wellnhofer. 1990. *Triceratops*: An example of flawed systematics, p. 245-254 in Carpenter, K., and Currie, P.J., eds., Dinosaur Systematics: Approaches and Perspectives. Cambridge University Press, New York, New York.

Pearson, D.A., T., Schaefer, K.R., Johnson, D.J., Nichols, and J.P., Hunter. 2002. Vertebrate biostratigraphy of the Hell Creek Formation in southwestern North Dakota and northwestern South Dakota, p. 145-167 in Hartman, J.H., K.R., Johnson, and D.J., Nichols (eds.) The Hell Creek Formation and the Cretaceous-Tertiary Boundary in the Northern Great Plains: An Integrated Continental Record of the End of the Cretaceous. Geological Society of America Special Paper 361.

Sampson, S.D. 1995. Two new horned dinosaurs from the Upper Cretaceous Two Medicine Formation of Montana; with a phylogenetic analysis of the Centrosaurinae (Ornithischia: Ceratopsidae). Journal of Vertebrate Paleontology 15 (4):743–760, doi:10.1080/02724634.1995.10011259.

Scannella, J. 2010. *Triceratops*: A model organism for deciphering dinosaur heterochrony. Journal of Vertebrate Paleontology, SVP Program and Abstracts Book 30 (2): 158A.

Scannella, J.B., and D.W., Fowler. 2009. Anagenesis in *Triceratops*: Evidence from a newly resolved stratigraphic framework for the Hell Creek Formation p. 148-149 in Storrs, G.W. (ed.), 9th North American Paleontological Convention Abstracts. University of Cincinnati, Cincinnati Museum Center Scientific Contributions 3, Cincinnati, Ohio.

Scannella, J.B., and J.R. Horner. 2010. *Torosaurus* Marsh, 1891 is *Triceratops* Marsh, 1889 (Ceratopsidae: Chasmosaurinae): Synonymy through ontogeny. Journal of Vertebrate Paleontology 30(4):1157–1168, doi:10.1080/02724634.2010.483632.

Swisher, C.C., L., Dingus. and R.F., Butler. 1993. 40Ar/39Ar dating and magnetostratigraphic correlation of the terrestrial Cretaceous-Paleogene boundary and Puercan mammal age, Hell Creek-Tullock Formations, eastern Montana. Canadian Journal of Earth Sciences 30(9):1981–1996, doi:10.1139/e93-174.

Tanke, D.H. 2010. Ceratopsian discoveries and work in Alberta, Canada: A historical review and census, in Ryan, M.J., B.J., Chinnery-Allgeier, and D.A., Eberth, (eds.), New Perspectives on Horned Dinosaurs: The Royal Tyrrell Museum Ceratopsian Symposium. Indiana University Press, Bloomington, Indiana, supplemental CD-ROM, 488 pp.

Turner, B.W. 2010. Testing the Local Diachroneity of the Terrestrial Lithostratigraphic KPg Boundary, Northern Montana [M.S. thesis]: Montana State University, Bozeman, Montana, 187 pp.

Wilson, G.P. 2004. A Quantitative Assessment of Evolutionary and Ecological Change in Mammalian Faunas Leading Up To and Across the Cretaceous-Tertiary Boundary, Northeastern Montana [Ph.D. dissertation]: University of California, Berkeley, California, 412 p.

Wilson, G.P. 2005. Mammalian faunal dynamics during the last 1.8 million years of the Cretaceous in Garfield County, Montana. Journal of Mammalian Evolution. 12(1-2): 53–76, doi:10.1007/s10914-005-6943-4.

CHAPTER SIX

EVOLUTIONARY TRENDS IN *TRICERATOPS* FROM THE HELL CREEK FORMATION, MONTANA

Contribution of Authors and Co-Authors

Manuscript in Chapter 6

Author: John B. Scannella

Contributions: Designed research, performed research, analyzed data, wrote the paper

Co-author: Denver W. Fowler

Contributions: Designed research, performed research, analyzed data, wrote the paper

Co-author: Mark B. Goodwin

Contributions: Designed research, performed research, wrote the paper

Co-author: John R. Horner

Contributions: Designed research, performed research, contributed new reagents/analytic tools

Manuscript Information Page

John B. Scannella, Denver W. Fowler, Mark B. Goodwin, John R. Horner
Journal: Proceedings of the National Academy of Sciences of the United States of America
Status of Manuscript:
___Prepared for submission to a peer-reviewed journal
___Officially submitted to a peer-reviewed journal
___Accepted by a peer-reviewed journal
_x_Published in a peer-reviewed journal

Published by the National Academy of Sciences.
Scannella, J. B., D. W. Fowler, M. B. Goodwin, and J. R. Horner. 2014. Evolutionary trends in *Triceratops* from the Hell Creek Formation, Montana. Proceedings of the National Academy of Sciences 111:10245–10250, doi: 10.1073/pnas.1313334111

The following chapter (and supporting information in Appendix G) has been published in the Proceedings of the National Academy of Sciences of the United States of America.

Abstract

The placement of over 50 skulls of the well-known horned dinosaur *Triceratops* within a stratigraphic framework for the Upper Cretaceous Hell Creek Formation (HCF) of Montana reveals the evolutionary transformation of this genus. Specimens referable to the two recognized morphospecies of *Triceratops*, *T. horridus* and *T. prorsus*, are stratigraphically separated within the HCF with the *T. prorsus* morphology recovered in the upper third of the formation and *T. horridus* found lower in the formation. Hypotheses that these morphospecies represent sexual or ontogenetic variation within a single species are thus untenable. Stratigraphic placement of specimens appears to reveal ancestor-descendant relationships. Transitional morphologies are found in the middle unit of the formation, a finding which is consistent with the evolution of *Triceratops* being characterized by anagenesis, the transformation of a lineage over time. Variation among specimens from this critical stratigraphic zone may indicate a branching event in the *Triceratops* lineage. Purely cladogenetic interpretations of the HCF dataset imply greater diversity within the formation. These findings underscore the critical role of stratigraphic data in deciphering evolutionary patterns in the Dinosauria.

Significance Statement

The deciphering of evolutionary trends in non-avian dinosaurs can be impeded by a combination of small sample sizes, low stratigraphic resolution, and lack of ontogenetic (developmental) details for many taxa. Analysis of a large sample (n>50) of the famous horned dinosaur *Triceratops* from the Hell Creek Formation of Montana incorporates

new stratigraphic and ontogenetic findings to permit the investigation of evolution within this genus. Our research indicates that the two currently recognized species of *Triceratops* (*T. horridus* and *T. prorsus*) are stratigraphically separated and that the evolution of this genus likely incorporated anagenetic (transformational) change. These findings impact interpretations of dinosaur diversity at the end of the Cretaceous and illuminate potential modes of evolution in the Dinosauria.

Introduction

The Hell Creek Project (1999-2010), a multi-institutional survey of the fauna, flora, and geology of the Upper Cretaceous Hell Creek Formation (HCF), provides insights into the paleobiology and evolution of the last non-avian dinosaurs (Horner et al., 2011). *Triceratops* (Ceratopsidae: Chasmosaurinae) is the most abundant dinosaur in the HCF; >50 skulls, including previously unknown or rare growth stages, have been collected throughout the entire formation (spanning ~ 1 to 2 million y) (Hicks et al., 20022) over the course of the Hell Creek Project (Horner and Goodwin, 2006; Horner et al., 2011; Scannella and Horner, 2010; Scannella and Fowler, 2014). The combination of a stratigraphically-controlled robust sample from the entire ~90 meter (m) thick HCF and identification of ontogenetic stages makes *Triceratops* a model organism for testing hypotheses proposed for the modes of dinosaur evolution (e.g. Horner et al., 1992, Sampson, 1995; Sampson and Loewen, 2010).

Since its initial discovery (Marsh, 1889), as many as 16 species of *Triceratops* were named based on variations in cranial morphology (Ostrom and Wellnhofer, 1986;

1990). Forster (1996) recognized only two species, *T. horridus* and *T. prorsus,* based on cranial features including differences in relative length of the postorbital horn cores (long in *T. horridus* and shorter in *T. prorsus*), morphology of the rostrum (elongate in *T. horridus* and shorter in *T. prorsus*), and closure of the frontoparietal fontanelle (sensu Farke) (2010); open in *T. horridus* and closed in *T. prorsus*). Marsh initially distinguished these two species by the morphology of the nasal horn (Marsh, 1890); the type specimen of *T. horridus* possesses a short, blunt nasal horn whereas the nasal horn in *T. prorsus* is elongate. Whether or not these taxa were largely biogeographically separated or represented ontogenetic variants or sexual dimorphs within a single species has remained unresolved (Ostrom and Wellnhofer, 1986; Dodson, 1996; Forster, 1996; Happ and Morrow, 1996; Farke, 1997; Lehman, 1998; Sampson and Loewen, 2010). A record of the stratigraphic distribution of *Triceratops* from the Upper Cretaceous Lance Formation of Wyoming compiled by Lull (1915; 1933) suggested that these taxa overlap stratigraphically. However, this assessment was likely based on limited stratigraphic data (Farke, 1997) and "the precise stratigraphic placement of these specimens can no longer be established" (Ostrom and Wellnhofer, p. 155). As such, consideration of morphological variation in a detailed stratigraphic context is necessary to reassess systematic hypotheses.

Results

Stratigraphic placement of *Triceratops* specimens within the HCF reveals previously undocumented shifts in morphology. The HCF is divided into three

stratigraphic units: the lower third (L3), middle third (M3), and upper third (U3) (Horner et al., 2011; Hartman et al., 2014). The stratigraphic separation of *Triceratops* morphospecies is apparent with specimens referable to *T. prorsus* (following Forster) (1996) found in U3 and *T. horridus* only recovered lower in the HCF. Specimens from the upper part of M3 exhibit a combination of *T. horridus* and *T. prorsus* features (Fig. 6.1, Appendix G).

L3 *Triceratops*.

Triceratops from the lowermost 15-30 m of the HCF (L3) possess either a small nasal horn (Fig. 6.2A; Appendix G) or a low nasal boss. The boss morphology appears in a large individual that histologically represents a mature specimen [="*Torosaurus*" ontogenetic morph [Scannella and Horner, 2010 (but see also: Farke, 2011; Longrich and Field, 2012; Maiorino et al., 2014); Museum of the Rockies (MOR) specimen 1122) (Appendix G)]. The nasal process of the premaxilla (NPP) in L3 *Triceratops* is narrow (Fig. 6.2B and Fig. 6.S2) and strongly posteriorly inclined; a pronounced anteromedial process is present on the nasal (Fig. 6.S3). The frontoparietal fontanelle remains open until late in ontogeny (MOR 1122). Specimens from the lower unit of the HCF bear a range of postorbital horn core lengths (ranging from ~ .45 to at least .74 basal-skull length) (Fig. 6.2D and Appendix G).

M3 *Triceratops*.

The mean nasal-horn length increases through M3 (Figs. 6.1E and F and Fig. 6.2A). University of California Museum of Paleontology (UCMP) specimen 113697

(collected ~ 6 m below the base of U3) possesses a nasal horn that is elongate (length/width: 2.12) (Appendix G) but retains a broad posterior surface, giving the horn a subtriangular cross section. Forster (1996) noted that UCMP 113697 exhibits a small nasal boss posterior to the nasal horn. Disarticulated specimens (e.g. MOR 3027 and MOR 3045) reveal that this protuberance posterior to the epinasal appears to be formed by the combination of a posterior projection on the epinasal (Appendix G Fig. 6.S4) and the anteriormost nasal. A homologous morphology is observed in specimens from L3 and the lower half of M3 (MOR 1120, MOR 2982, MOR 3010). UCMP 128561, from the upper half of M3, exhibits a low nasal boss (Cobabe and Fastovsky, 1987; Forster, 1993) (Appendix G). The anteromedial process of the nasal is pronounced in *Triceratops* from M3 and the NPP is more vertically inclined in specimens from upper M3, producing a more convex rostrum morphology which was previously found to characterize *T. prorsus* (Forster, 1996; Longrich and Field, 2012). The frontoparietal fontanelle is open in late stage subadults/young adults (UCMP 113697).

U3 *Triceratops*.

Specimens from U3 exhibit the features Forster (1996) found to characterize *T. prorsus*. U3 *Triceratops* possess an elongate, relatively narrow nasal horn (average length/width > 2) (Fig. 6.2A; Appendix G). The NPP is more vertically inclined, producing a convex rostrum lacking the low, elongate profile noted in *T. horridus* [although the largest, and presumably oldest, known specimens (e.g. MOR 004 and MOR 1625) exhibit proportionally longer rostra] (Fig. 6.2E and Appendix G). The NPP is antero-posteriorly expanded and the anteromedial process of the nasal is greatly reduced

(Fig. 6.S3) (Horner and Goodwin, 2008). The frontoparietal fontanelle becomes constricted and eventually closed in late stage subadults/young adults (e.g. MOR 2923 and MOR 2979), ontogenetically earlier than in L3 and M3. The postorbital horn cores are short (< 0.64 basal-skull length) (Fig. 6.2D). Further, U3 *Triceratops* appear to exhibit nasals which are more elongate than *Triceratops* from the lower half of the HCF (Fig. 6.2F and Appendix G).

Shifts in Morphology over Time.

Epinasals exhibit a directional morphologic trend; average length increases throughout the formation (Fig. 6.2A and Appendix G) (Spearman's rank coefficient = 0.824, p = 4.15E-07). A protuberance just posterior to the epinasal, observed in specimens from L3 and M3 (Fig. 6.1) is particularly pronounced in UCMP 113697 from the uppermost M3 (Fig. 6.1E). U3 *Triceratops* either do not exhibit this feature or express only a subtle ridge in the homologous location. Concurrent with elongation of the epinasal was an expansion of the NPP (Fig. 6.2B) (Spearman's rank coefficient = -0.969, *P*= 3.74E-06) and an increase in the angle between the NPP and the narial strut of the premaxilla (Fig. 6.2C and Appendix G) (Spearman's rank coefficient = .802, *P* = .000186). Nasals also become more elongate relative to basal skull length (although only three specimens with complete nasals have thus far been recorded from the lower half of the formation) (Fig 5.2F and Appendix G) (Spearman's rank coefficient = .804, *P* = .00894).

Postorbital horn-core length appears to be variable throughout L3 and M3 and is consistently short in U3 *Triceratops* (Fig. 6.2D and Appendix G) [Spearman's rank

coefficient is negative (-0.197) and not statistically significant (*P*=0.392)]. Large juvenile U3 *Triceratops* (e.g. MOR 1110) can possess more elongate postorbital horn cores (0.64 basal-skull length). Whereas U3 postorbital horn core length falls within the range of variation observed lower in the formation (Fig. 6.2D), elongate postorbital horn cores have thus far not been found in post-juvenile stage *Triceratops* from U3. Many large *Triceratops* (e.g. MOR 1122 and MOR 3000) (Scannella and Horner, 2010) exhibit evidence of postorbital horn core resorption, suggesting maximum length is reached earlier in ontogeny. Maximum postorbital horn core length may have been expressed later in development (or for a longer duration) in *Triceratops* from lower in the formation

Triceratops from the upper half of the HCF exhibit a more vertically inclined NPP (Fig. 6.2C), which contributes to a rostrum which appears shorter and more convex in lateral profile (a feature Forster [1996] noted in *T. prorsus*) (). However, we note that a Spearman's rank correlation test found apparent reduction in rostrum length to be statistically insignificant (Spearman rank's coefficient .018, *P*=.966). Large specimens from U3 (e.g. MOR 004) possess a more elongate rostrum relative to basal skull length (Fig. 6.2E and Appendix G), however the shape of U3 rostra appears to be consistently convex.

Eotriceratops xerinsularis, found in the stratigraphically older uppermost Horseshoe Canyon Formation (~ 68 Ma) (Wu et al., 2007), expresses morphologies (elongate postorbital horn cores, small nasal horn) consistent with its stratigraphic position relative to *Triceratops*.

Cladistic and Stratocladistic Analyses.

Initial cladistic analyses recovered a polytomy of all HCF specimens, with the 50% majority tree producing a succession of *Triceratops* that largely correlates with stratigraphic placement (Fig. 6.S5 and Appendix G). Removal of the more fragmentary material recovered *Torosaurus* specimens as basal to a stratigraphic succession of *Triceratops* including a polytomy of specimens from the upper half of the formation. A similar topology was recovered when specimens not exhibiting codeable features of the parietal squamosal frill were removed from the analysis (Fig. 6.3B). Removal of MOR 2924, a specimen from the base of U3 which does not preserve postorbital horn cores (Appendix G), recovers specimens from the upper part of M3 as basal to U3 *Triceratops*.

In the analysis of the most reduced data set, UCMP 113697 and MOR 3027 cluster together (Fig. 6.3C). These specimens exhibit a combination of characters found in *Triceratops* from L3 and M3. The epinasal of UCMP 113697 is morphologically intermediate between L3 and U3 *Triceratops* (the epinasal of MOR 3027 is incomplete). These specimens each exhibit large postorbital horn cores (a feature expressed in some L3 *Triceratops*) and a more vertically inclined NPP (found in U3 *Triceratops*). MOR 3045 is recovered as being more derived than UCMP 113697 and MOR 3027 (Fig. 3) based on its possession of relatively short postorbital horn cores, a more expanded NPP, and a pronounced step bordering the 'incipient fenestrae' (sensu Scannella and Horner, 2010) (Appendix G). This specimen exhibits the basal condition of the antero-medial nasal process and expresses a pronounced upturn of the posterior surface of the epinasal, suggesting the presence of a protuberance in life. MOR 3045 exhibits a fairly elongate

epinasal (est. length/width: ~ 1.88), with a posterior surface which is broader than is seen in most U3 specimens; and, like UCMP 113697, MOR 3027, and U3 *Triceratops*, exhibits a more vertically inclined NPP.

Stratocladistic analyses, in which specimens were grouped into operational units based on stratigraphic position, were performed in the program StrataPhy (Marcot and Fox, 2008). *Torosaurus* specimens were initially considered separately from other specimens (see Appendix G). Initial results suggested that specimens from the upper half of the HCF represented a sequence of ancestors and descendants but differed on the position of operational units from the lower half of the formation (Fig. 6.S6A). This result was likely influenced by missing data for specimens from the lower half of the formation; no specimens from lower M3 preserve frill characters which can distinguish them from the *Torosaurus* morphology. When *Torosaurus* specimens were incorporated into *Triceratops* operational units, three topologies were produced: a strictly cladogenetic result, a topology in which all operational units except lower M3 were recovered in a transformational sequence, and a topology in which the HCF operational units were recovered in two lineages (an upper L3/lower M3 lineage and an upper M3/U3 lineage) which had diverged at some point in the deposition of L3 (Fig. 6.S6B). Pruning of *Torosaurus* specimens from the dataset produced two topologies which incorporated morphological transformation: one topology in which all HCF operational units fell into a single lineage and another topology presenting two HCF lineages which diverged either in L3 or prior to deposition of the HCF (Fig. 6.S6C).

Discussion

Evolutionary Patterns.

One of the principle questions in evolutionary biology regards the modes of evolution: what evolutionary patterns are preserved in the fossil record and how prominent are these patterns (Simpson, 1944; 1953; Eldredge and Gould, 1972)? Small sample sizes for most non-avian dinosaur taxa complicate the investigation of evolutionary modes in this group. As such, it is unknown how prominent a role anagenesis (the transformation of lineages over time) (Fig. 6.4A) (e.g. Rensch, 1947; Malmgren et al., 1983; Gingerich, 1985; Macleod, 1991; Benton and Pearson, 2001) played in their evolution or whether the majority of morphologies recorded in the fossil record were a product of cladogenesis (evolution via branching events (Fig. 6.4B-D) (Rensch, 1947; Eldredge and Gould, 1972; Wagner and Erwin, 1995; Benton and Pearson, 2001; Sampson and Loewen, 2010).

Horner et al. (1992) presented evidence for anagenesis in several dinosaur clades within the Cretaceous Two Medicine Formation of Montana. It has been suggested that the sample size presented in that study was too small and that cladogenesis was a more conservative interpretation of the data (Sampson, 1995). A combination of large sample size, ontogenetic resolution, and detailed stratigraphic data makes *Triceratops* an ideal taxon for testing hypotheses regarding evolutionary mode in a non-avian dinosaur.

Restriction of the full *T. prorsus* morphology to U3 renders hypotheses that *T. horridus* and *T. prorsus* represent sexual or ontogenetic variation within a single taxon untenable. *Triceratops* from the upper part of M3 exhibit a combination of features found

in L3 and U3 *Triceratops*. This pattern suggests that the evolution of *Triceratops* incorporated anagenesis.

Strict consensus trees produced by cladistic analyses either recover upper M3 specimens in a polytomy with all HCF specimens, in a polytomy of HCF *Triceratops* from the upper half of the formation, or UCMP 113697 and MOR 3027 cluster together whereas MOR 3045 shares more features with U3 *Triceratops* (Fig. 6.3 and Fig. 6.S5). We will consider four alternative hypotheses for the morphological pattern recorded in the HCF:

i) *T. prorsus* evolved elsewhere and migrated into the HCF, eventually replacing the incumbent HCF *Triceratops* population by the beginning of the deposition of U3. Upper M3 specimens represent early members (or close relatives of) this group that would come to dominate the ecosystem.

ii) Variation between MOR 3045, MOR 3027, and UCMP 113697 represents intraspecific (or intrapopulation) variation. As the HCF *Triceratops* lineage evolved, some individuals expressed more of the features that would eventually dominate the population. Over time, these traits were selected for and characterized U3 *Triceratops*. This is a purely anagenetic scenario.

iii) A bifurcation event is recorded in the HCF and occurred at some point prior to the deposition of U3, resulting in two lineages which differ primarily in the morphology of the epinasal and rostrum (consistent with Forster's diagnoses for *T. horridus* and *T. prorsus*). MOR 3045 represents an early member of a lineage which evolved into U3

Triceratops. This scenario incorporates anagenesis (Wagner and Erwin, 1995) and is presented in some trees produced by the stratocladistic analysis (Fig. 6.S6).

iv) The evolution of *Triceratops* was characterized by a series of cladogenetic events that produced at least five taxa over the course of the deposition of the HCF (the L3 clade, the lower M3 clade, the MOR 3027 clade, the MOR 3045 clade, and the U3 clade). This strictly cladogenetic scenario suggests that no *Triceratops* found lower in the HCF underwent evolutionary transformation into forms found higher in the formation.

A Biogeographic Signal?

The Hell Creek Project's stratigraphic record of *Triceratops* is primarily restricted to northeastern Montana. It has been hypothesized that *T. horridus* and *T. prorsus* were largely biogeographically separated, with *T. prorsus* generally restricted to the Hell Creek and Frenchman Formations and *T. horridus* commonly found in the more southern Lance, Laramie, and Denver Formations (Happ and Morrow, 1996; Farke, 1997). However, this suggested biogeographic segregation may represent an artifact of the stratigraphic record. Specimens which have thus far been described from neighboring coeval formations exhibit morphologies consistent with their stratigraphic position relative to the HCF (Tokaryk, 1986; Carpenter and Young, 2002) (Appendix G).

Anagenesis and Cladogenesis.

If the morphological trends noted in *Triceratops* were purely the result of cladogenetic branching (consistent with punctuated equilibrium [Eldredge and Gould, 1972) (Fig. 6.4C and D), we would expect to find the full U3 morphology coexisting with

Triceratops found lower in the formation, or alternatively, specimens exhibiting the L3 morphology in U3. Such specimens have yet to be discovered (Appendix G). Specimens from the upper part of M3 exhibit transitional features relative to L3 and U3 *Triceratops*, a pattern consistent with anagenesis.

Some cladistic analyses distinguish MOR 3045 from other upper M3 *Triceratops* based on variation in the length of the postorbital horn cores, width of the NPP, and the thickened regions of the parietal (Fig. 6.3, Fig. 6.S5, and Appendix G). *Triceratops* collected from a multi-individual bonebed in U3 (MOR locality no. HC-430; Keenan and Scannella, 2014) show variable morphology of the premaxillae and parietal between individuals (Fig 5.S2). This finding suggests that the variation between upper M3 specimens may represent intrapopulational, not taxonomic, variation (Ostrom and Wellnhofer, 1986). Individuals exhibiting more pronounced U3 character states may have become increasingly abundant in the HCF *Triceratops* population over time until, by the end of the Cretaceous, all *Triceratops* exhibited these character states (Fig. 6.4A). Alternatively, MOR 3045 may represent an early member of a U3 (*T. prorsus*) lineage with MOR 3027 representing a separate lineage. Stratocladistic analyses suggest the possibility of two lineages in the HCF (Fig. 6.4B and 5.S6), however this scenario would require the independent evolution of an enlarged epinasal-nasal protuberance. A purely cladogenetic interpretation of the HCF *Triceratops* dataset suggests the presence of at least five stratigraphically overlapping taxa in the formation (Fig. 6.4C and D). This scenario is possible, but we would argue that interpretations that incorporate populational transformation (anagenesis) are more conservative..

Specimens from upper M3 exhibit a combination of primitive and derived characters, as well as more developed states of characters expressed in L3 *Triceratops*. Forster (1996) noted that, whereas *T. prorsus* exhibited derived characters, no autapomorphic characters were recognized in *T. horridus*. This finding is consistent with the hypothesis that the evolution of *Triceratops* incorporated anagenesis and illustrates the potential difficulties with defining species in evolving populations (Gingerich, 1985; Horner et al., 1992). The HCF dataset underscores the importance of considering morphologies in a populational, rather than typological context (Simpson, 1951).

Conclusions

The documented changes in *Triceratops* morphology occurred over a geologically short interval of time (1-2 million y) (Hicks et al., 2002). High-resolution stratigraphy is necessary for recognizing fine scale evolutionary trends. If cladogenesis is considered the primary mode of dinosaur evolution, a problematic inflation of dinosaur diversity occurs.

Current evidence suggests that the evolution of *Triceratops* incorporated anagenesis as there is currently no evidence for biogeographic segregation of contemporaneous *Triceratops* morphospecies and there is evidence for the morphological transformation of *Triceratops* throughout the HCF. This dataset supports hypotheses that the evolution of other Cretaceous dinosaurs may have incorporated phyletic change (Horner et al., 1992; Evans et al., 2006; Campione and Evans, 2011) and suggests that many speciation events in the dinosaur record may represent bifurcation events within anagenetic lineages (Wagner and Erwin, 1995).

Materials and Methods

Most specimens in this study were placed in section relative to either the upper and /or lower formational contacts, respectively marked by the overlying Fort Union or underlying Fox Hills Formations (Scannella and Fowler, 2014). For some specimens, stratigraphic precision was increased by measuring position relative to marker sandstones (Horner et al., 2011). The base of each unit in the HCF near Fort Peck Lake is marked by a prominent amalgamated channel sandstone that consistently occurs in the same stratigraphic position (Horner et al., 2011). The Basal sand, Jen-rex sand, and Apex sand mark the bases of the Lower, Middle, and Upper units respectively (Horner et al., 2011; Hartman et al., 2014) (Fig. 6.1C). Each sandstone complex fines upwards into overbank mudstones and siltstones. MOR 981 was collected from a mudstone horizon above the basal sandstone; more detailed stratigraphic data is unavailable for this specimen.

The boundary between the C30N and C29R magnetozones occurs either at the base, or in the middle of the Apex sand (base of U3) (Fig. 6.1). Samples taken within the sandstone do not produce a signal, but samples from above the sandstone are of reversed polarity (C29r), while those below are normal polarity (C30n) (Lerbekmo and Braman, 2002; Lecain et al., 2014).

A cladistic analysis of HCF *Triceratops* specimens was conducted in PAUP* 4.0b10 (Swofford, 2003) (Appendix G) initially using the heuristic search command with *Arrhinoceratops* (Parks, 1925) designated as the outgroup. The matrix was assembled in Mesquite 2.75 (Maddison and Maddison, 2011) and cladograms were displayed using

FigTree (Rambaut, 2012). Analyses were conducted using the random addition sequence (Appendix G). The most complete post-juvenile stage specimens were included in the analysis (Appendix G; see Campione et al., 2013). Characters found to vary within *Triceratops,* and between *Triceratops* and *Eotriceratops,* (Fig. 6.S7 and Appendix G), were included. Strongly ontogenetically influenced characters (e.g. postorbital horn core orientation; frill epiossification shape) were excluded from the analysis, however characters often used to distinguish *Triceratops* and *Torosaurus* (e.g. parietal fenestrae, epiossification position) were retained. Specimens exhibiting multiple character states (e.g. differing numbers of episquamosals on each squamosal) were coded as polymorphic. All characters were left unordered; maxtrees was set to 250,000. Bremer support indices were calculated using TreeRot v3 (Sorenson and Franzosa, 2007). Analyses of the reduced dataset were conducted using the branch and bound search command. Stratocladistic analyses were performed in the program StrataPhy (Marcot and Fox, 2008) with maxtrees set to 250,000. Specimens with some ambiguity regarding stratigraphic position (MOR 981, MOR 1604, MOR 2978) were excluded from the analysis (Appendix G). Spearman's rank correlation analyses were performed in R (R Core Team, 2013) using the 'cor.test' function [cor.test(x,y, method='spear', exact = FALSE)]. Juvenile specimens were excluded from these analyses as were specimens exhibiting significant taphonomic distortion (see Fig. 6.2 and Appendix G). Additional calculations were performed in Microsoft Office Excel 2007.

Acknowledgements

We thank D. Barta, B. Boessenecker, N. Campione, T. Carr, W. Clemens, W. Clyde, P. Dodson, D. Evans, A. Farke, C. Forster, E. Fowler, J. Frederickson, J. Hartman, L. Hall, J. Hoganson, M. Holland, F. Jackson, S. Keenan, M. Lavin, M. Loewen, J. Mallon, K. Olson, C. Organ, K. Padian, A. Poust, D. Pearson, P. Renne, D. Roberts, K. Scannella, J. Stiegler, D. Varricchio, D. Woodruff, H. Woodward, and B. Zorigt for helpful discussions, without implying their agreement with our conclusions. Comments and suggestions from G. Hunt, P.D. Polly, and three anonymous reviewers were very helpful. Thanks to D. Fox, A. Huttenlocker, and J. Marcot for help using StrataPhy. D. Evans, K. Seymour, and B. Iwama provided access to the holotype of *Arrhinoceratops* at the Royal Ontario Museum. B. Strilisky and G. Housego provided access to the holotype of *Eotriceratops* at the Royal Tyrrell Museum and additional images of its premaxilla. J. Sertich provided access to specimens at the Denver Museum of Nature and Science. P. Sheehan provided access to and locality data for Milwaukee Publich Museum (MPM) specimen VP6841. R. Scheetz and B. Britt provided access to a cast of Museum of Western Colorado (MWC) specimen 7584 at BYU; W. Clemens shared stratigraphic data for this specimen. The Bureau of Land Management, Charles M. Russell National Wildlife Refuge, and the Department of Natural Resources and Conservation provided access to land under their management and collection permits. We are grateful to the Twitchell, Taylor, Trumbo, Holen, and Isaacs families for land access. We thank the Museum of the Rockies (MOR) volunteers, staff, and all participants in the Hell Creek Project. We thank the MOR and the University of California Museum of Paleontology

(UCMP) for support of this research. Funding for the Hell Creek Project was provided by donations from J. Kinsey, C.B. Reynolds, H. Hickam, and Intellectual Ventures. The Windway Foundation and the Smithsonian Institution provided grants (to JRH). UCMP provided funding (to MBG). The Theodore Roosevelt Memorial Fund of the American Museum of Natural History, the Fritz Travel Grant of the Royal Ontario Museum, and the Jurassic Foundation provided grants (to J.B.S.). The Evolving Earth Foundation and the Doris O. and Samuel P. Welles Research Fund of the UCMP provided grants (to J.B.S. and D.W.F.).

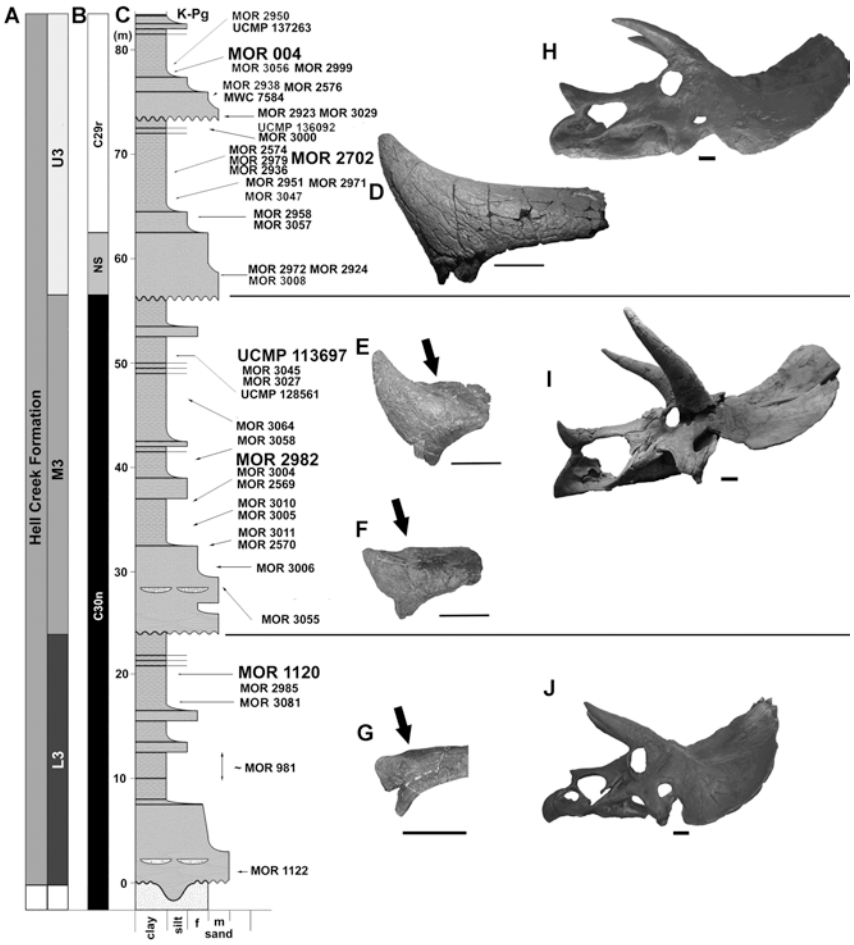

Figure 6.1. Stratigraphic placement of HCF *Triceratops* reveals trends in cranial morphology including elongation of the epinasal and change in morphology of the rostrum. (*A*) HCF stratigraphic units. (*B*) Magnetostratigraphic correlation (Lerbekmo and Braman, 2002; Lecain et al., 2014); NS: no signal, so precise position of C29R-C30n boundary is unknown. (*C*) Stratigraphic positions of *Triceratops* specimens within a generalized section. Specimens plotted by stratigraphic position, not by facies. Relative position of specimens from different areas are approximate at the meter scale (Scannella and Fowler, 2014). See Horner et al. (2011) and Scannella and Fowler (2014) for further specimens for which more precise position (beyond HCF unit) is to be determined. Scale in meters. (*D*) MOR 2702 nasal horn from U3. (*E*) UCMP 113697 nasal horn from upper part of M3; black arrow indicates epinasal-nasal protuberance. (*F*) MOR 2982 nasal horn from lower part of M3 (image mirrored). (*G*) MOR 1120 nasal horn from L3. (*H*) MOR 004 young adult *Triceratops* skull from U3 (cast; image mirrored). Postorbital horn cores reconstructed to approximate average length of young adult specimens from this unit. (*I*) UCMP 113697 late stage subadult/young adult *Triceratops* skull from the upper part of M3. (*J*) MOR 1120 (cast) subadult *Triceratops* skull from L3. Figure modified from Scannella and Fowler (2014). f, fine sand; m, medium sand (Scale bars: 10 cm).

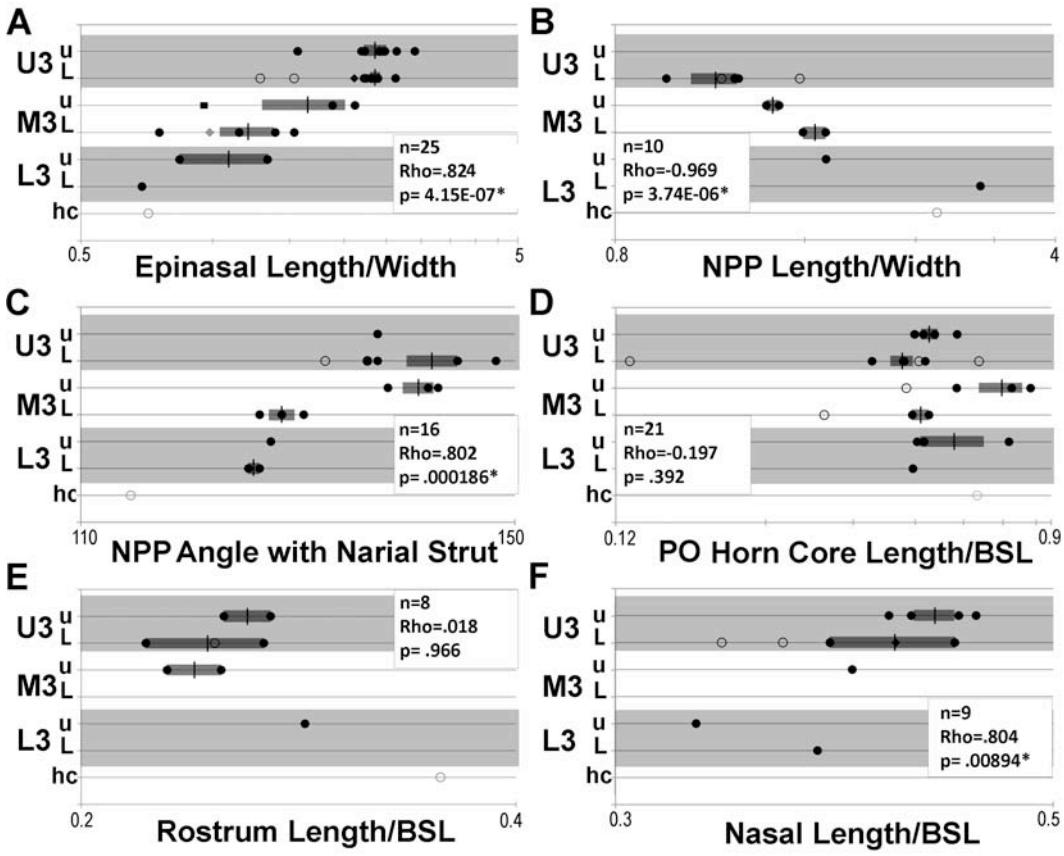

Figure 6.2. Stratigraphic variation in cranial morphology. Each unit of the HCF is divided into upper and lower sections. For L3, the upper part is here designated as strata above the basal sandstone. For M3, the upper part is here considered the upper 15 m of the unit. The 10-m sandstone and above is here considered the upper section of U3. (*A*) Epinasal length/width. MOR 3011 denoted by a gray diamond as the fragmentary nature of this specimen obscures its ontogenetic status. Square represents UCMP 128561. Results of Spearman's rank correlation analysis in white box. (*B*) Nasal process of the premaxilla (NPP) height/width. *(C*) Angle between the NPP and the narial strut of the premaxilla. (*D*) Postorbital horn core length/basal skull length. Estimated total lengths are used here for postorbital horn core length (see Appendix G). (*E*) Rostrum length/basal skull length. (*F*) Nasal length/basal skull length. Vertical lines denote the mean (not including juvenile or taphonomically deformed specimens; Appendix G). Dark gray bars represent standard error. Black rings denote juveniles. Gray ring represents RTMP 2002.57.7. Spearman's rank correlation analyses exclude juveniles and taphonomically distorted specimens (indicated by diamonds). Asterisks indicate statistically significant *P* values. Scale on x-axes are logarithmic.

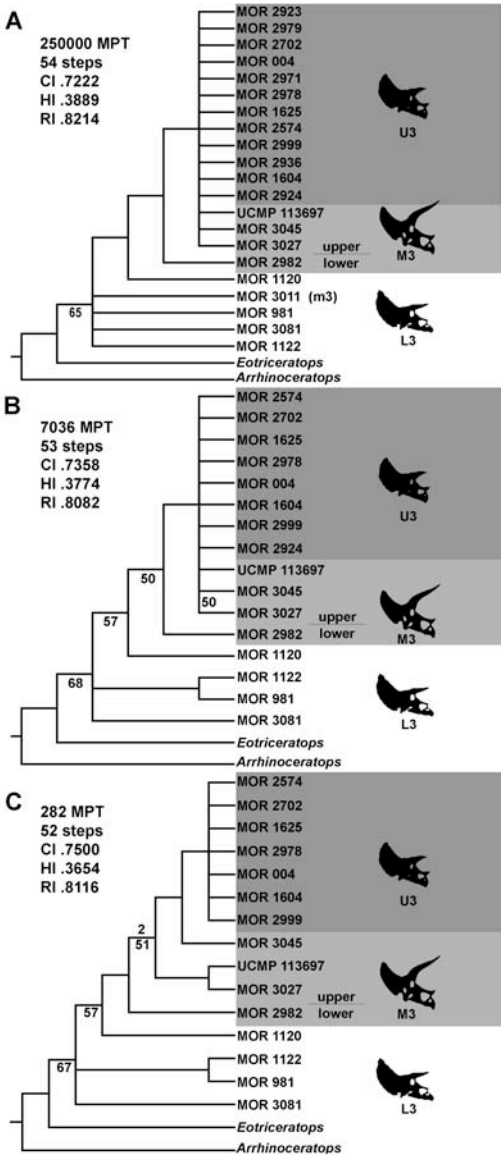

Figure 6.3. Results of cladistic analysis of HCF *Triceratops*. (*A*) Strict consensus tree produced by analysis of HCF specimens using a heuristic search and multistate coding once the most fragmentary specimens were removed (See Appendix G and Fig. 6.S5 for additional results). Bootstrap support values below nodes. Bremer support values greater than 1 above nodes. *Torosaurus* specimens are recovered as basal to a stratigraphic succession of specimens. MOR 3011 does not preserve characters of the parietal-squamosal frill. (Appendix G). *(B)* Analysis (multistate coding, branch-and-bound search) excluding specimens that could not be coded for at least 10 cranial characters or characters of the frill. *(C*) Analysis (multistate coding, branch-and-bound search) after removal of MOR 2924 (Appendix G).

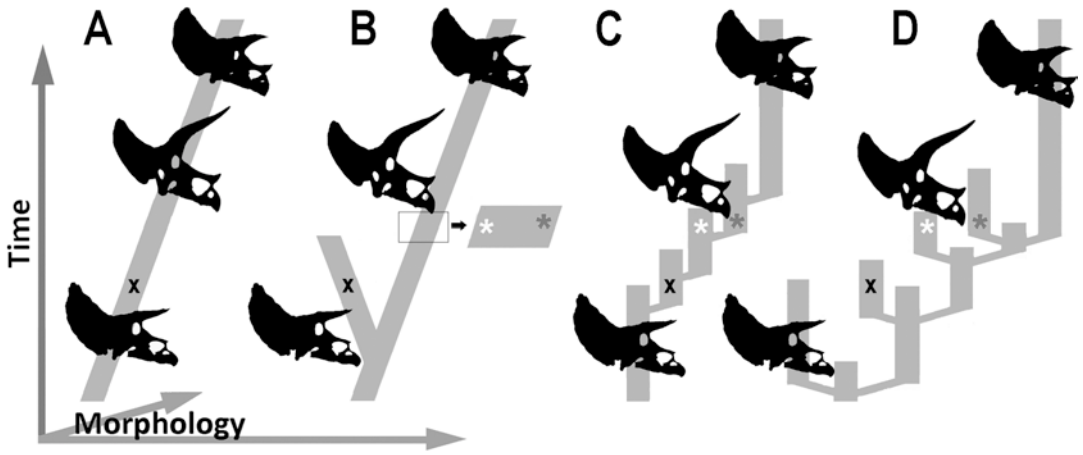

Figure 6.4. Potential patterns of HCF *Triceratops* evolution. *(A)* Anagenesis, or transformation of a lineage over time. *(B)* Bifurcation of an anagenetic lineage in which the ancestor becomes pseudoextinct through evolution (sensu Wagner and Erwin, 1995). Wagner and Erwin (1995) distinguish bifurcation from "true" cladogenesis, which includes no anagenetic component. *(C,D)* True cladogenesis implies the coexistence of ancestral and descendant clades for at least a short period of time. The presented modes represent points on a spectrum of potential evolutionary patterns. The gray and white asterisks represent potential positions for MOR 3045 and MOR 3027, respectively; black X represents MOR 2982. X and Y axes represent morphospace.

References

Benton M.J., and P.N. Pearson. 2001. Speciation in the fossil record. Trends in Ecology and Evolution 16(7): 405-411.

Campione N.E., and D.C. Evans. 2011. Cranial growth and variation in edmontosaurs (Dinosauria: Hadrosauridae): Implications for Latest Cretaceous megaherbivore diversity in North America. *PLoS ONE* 6(9): e25186. doi:10.1371/journal.pone.0025186

Campione, N.E., K.S. Brink, E.A. Freedman, T. McGarrity, and D.C. Evans. 2013. '*Glishades ericksoni'*, an indeterminate juvenile hadrosaurid from the Two Medicine Formation of Montana: implications for hadrosauroid diversity in the latest Cretaceous (Campanian-Maastrichtian) of western North America. Paleobiodiversity and Paleoenvironments 93: 65-75.

Carpenter K., and D.B. Young. 2002. Late Cretaceous dinosaurs from the Denver Basin, Colorado. Rocky Mountain Geology 37(2): 237-254.

Cobabe E.A., and D.E. Fastovsky. 1987. *Ugrosaurus olsoni*, a new ceratopsian (Reptilia: Ornithischia) from the Hell Creek Formation of eastern Montana. Journal of Paleontology 61(1): 148–154.

Dodson P. 1996. *The Horned Dinosaurs.* Princeton, Princeton University Press.

Eldredge N., and S.J. Gould. 1972. Punctuated equilibria: an alternative to phyletic gradualism. pp. 82-115 in Models in Paleobiology, T.J.M. Schopf (ed.) Freeman, Cooper & Co., San Francisco.

Evans D., P. Currie, D. Eberth, and M. Ryan. 2006. High-resolution lambeosaurine dinosaur biostratigraphy, Dinosaur Park Formation, Alberta: sexual dimorphism reconsidered. Journal of Vertebrate Paleontology 26: 59A.

Farke A.A. 1997. The distribution and taxonomy of Triceratops. pp. 47-49 in Dinofest International Proceedings Volume, D.L. Wolberg, E. Stump, G.D. Rosenberg (eds.) Philadephia Academy of Natural Sciences, Philadelphia.

Farke A.A. 2010. Evolution, homology, and function of the supracranial sinuses in ceratopsian dinosaurs. Journal of Vertebrate Paleontology 30(5): 1486-1500.

Farke A.A. 2011. Anatomy and taxonomic status of the chasmosaurine ceratopsid *Nedoceratops hatcheri* from the Upper Cretaceous Lance Formation of Wyoming, U.S.A. PLoS One 6(1): e16196.doi:10.1371/journal.pone.0016196.

FigTree v 1.4.0. http://tree.bio.ed.ac.uk/software/figtree/

Forster C.A. 1993. Taxonomic validity of the ceratopsid dinosaur *Ugrosaurus olsoni* (Cobabe and Fastovsky). Journal of Paleontology 67(2): 316–318.

Forster C.A. 1996. Species resolution in *Triceratops*: cladistic and morphometric approaches. Journal of Vertebrate Paleontology 16(2): 259-270.

Gingerich P.D. 1985. Species in the fossil record: concepts, trends, and transitions. Paleobiology 11(1): 27-41.

Happ J.W., and C.M. Morrow. 1996. Separation of *Triceratops* (Dinosauria: Ceratopsidae) into two allopatric species by cranial morphology. Journal of Vertebrate Paleontology 16: 40A.

Hartman J.H., R.D. Butler, M.W. Weiler, and K.K. Schumaker. 2014. Context, naming, and formal designation of the Cretaceous Hell Creek Formation lectostratotype, Garfield County, Montana. pp. 89-122 in Through the End of the Cretaceous in the Type Locality of the Hell Creek Formation in Montana and Adjacent Areas. G.P. Wilson, W.A. Clemens, J.R. Horner, and J.H. Hartman (eds.) Geological Society of America Special Paper, Boulder, Colorado.

Hicks J.F., K.R. Johnson, J.D. Obradovich, L. Tauxe, and D. Clark. 2002. Magnetostratigraphy and geochronology of the Hell Creek and basal Fort Union Formations of southwestern North Dakota and a recalibration of the age of the Cretaceous-Tertiary boundary, pp. 35-55 in The Hell Creek Formation and the Cretaceous -Tertiary boundary in the northern Great Plains: an integrated continental record of the end of the Cretaceous, J.H. Hartman, K.R. Johnson, and D.J. Nichols (eds.) Geological Society of America Special Paper 361, Boulder, Colorado.

Horner J.R. and, M.B. Goodwin. 2006. Major cranial changes during *Triceratops* ontogeny. Proceedings of the Royal Society B 273: 2757-2761.

Horner J.R. and, M.B. Goodwin. 2008. Ontogeny of cranial epi-ossifications in *Triceratops*. Journal of Vertebrate Paleontology 28(1): 134–144.

Horner J.R., Varricchio D.J., and M.B. Goodwin. 1992. Marine transgressions and the evolution of Cretaceous dinosaurs. Nature. 358: 59-61.

Horner J.R, M.B. Goodwin, and N. Myhrvold. 2011. Dinosaur census reveals abundant *Tyrannosaurus* and rare ontogenetic stages in the Upper Hell Creek Formation (Maastrichtian), Montana, USA. *PLoS One* 6: e16574 (doi:10.1371/journal.pone.0016574).

Keenan, S.W., and J.B. Scannella. 2014. Paleobiological implications of a *Triceratops* bonebed from the Hell Creek Formation, Garfield County, northeastern Montana, in Wilson, G.P., W.A. Clemens, J.R. Horner, and J.H. Hartman, (eds.) Through the End of the Cretaceous in the Type Locality of the Hell Creek Formation in Montana and Adjacent Areas: Geological Society of America Special Paper 503, doi:10.1130/2014.2503(14).

LeCain R., W. Clyde, G.P. Wilson, and J. Riedel. 2014. Magnetostratigraphy of the Hell Creek and lower Fort Union formations in northeastern Montana. pp. 137-148 in Through the End of the Cretaceous in the Type Locality of the Hell Creek Formation in Montana and Adjacent Areas, G.P. Wilson, W.A. Clemens, J.R. Horner, J.H. Hartman (eds.) Geological Society of America Special Paper, Boulder, Colorado.

Lehman T.M. 1998. A gigantic skull and skeleton of the horned dinosaur *Pentaceratops* from New Mexico. Journal of Paleontology 72(5): 894–906.

Lerbekmo J.F., and D.R. Braman. 2002. Magnetostratigraphic and biostratigraphic correlation of late Campanian and Maastrichtian marine and continental strata from the Red Deer Valley to the Cypress Hills, Alberta, Canada. Canadian Journal of Earth Sciences 39: 539-557.

Longrich N.R., and D.J. Field. 2012. *Torosaurus* Is Not *Triceratops*: Ontogeny in chasmosaurine ceratopsids as a case study in dinosaur taxonomy. PLoS ONE 7(2): e32623.doi:10.1371/journal.pone. 00326

Lull R.S. 1915. The mammals and horned dinosaurs of the Lance formation of Niobrara County, Wyoming. American Journal of Science 4(40): 319-348.

Lull R.S. 1933. A revision of the Ceratopsia or horned dinosaurs. Yale Peabody Museum Memoir 3: 1–175.

Macleod N. 1991. Punctuated anagenesis and the importance of stratigraphy to paleobiology. Paleobiology 17(2): 167-188.

Maddison, W.P., and D.R. Maddison. 2011. Mesquite: a modular system for evolutionary analysis. Version 2.75. http://mesquiteproject.org/

Maiorino L., A.A. Farke, T. Kotsakis, and P. Piras. 2013. Is *Torosaurus Triceratops*? Geometric morphometric evidence of Late Maastrichtian ceratopsid dinosaurs. PLoS ONE 8(11): e81608: doi:10.1371/journal.pone.0081608

Malmgren B.A., W.A. Berggren, and G.P. Lohmann. 1983. Evidence for punctuated gradualism in the Late Neogene *Globorotalia tumida* lineage of planktonic foraminifera. Paleobiology 9(4): 377-389.

Marcot, J.D., and D.L. Fox. 2008. StrataPhy: a new computer program for stratocladistic analysis. Palaeontologica Electronica 11:5A.

Marsh O.C. 1889. Notice of gigantic horned Dinosauria from the Cretaceous. American Journal of Science 3(38): 173-175.

Marsh O.C. 1890. Description of new dinosaurian reptiles. American Journal of Science 3(39): 81-86.

Ostrom J.H., and P. Wellnhofer. 1986. The Munich specimen of *Triceratops* with a revision of the genus. Zitteliana 14: 111-158.

Ostrom, J.H., and P. Wellnhofer. 1990. *Triceratops*: an example of flawed systematics. pp. 245-254 in Dinosaur Systematics: Approaches and Perspectives, K. Carpenter, and P.J. Currie (eds.) Cambridge University Press, New York.

Parks, W.A. 1925. *Arrhinoceratops brachyops*, a new genus and species of Ceratopsia from the Edmonton Formation of Alberta. University of Toronto Studies, Geological Series 19: 5-15.

R Core Team. 2013. R: A language and environment for statistical computing. R Foundation for Statistical Computing, Vienna, Austria. URL http://www.R-project.org/.

Rensch B. 1947. Neure Probleme der Abstammungslehre. Die transspezifische evolution. Ferdinand Enke, Stuttgart.

Sampson S.D. 1995. Two new horned dinosaurs from the Upper Cretaceous Two Medicine Formation of Montana; with a phylogenetic analysis of the Centrosauriane (Ornithischia: Ceratopsidae). Journal of Vertebrate Paleontology 15(4): 743-760.

Sampson S.D., and M.A. Loewen. 2010. Unraveling a radiation: a review of the diversity, stratigraphic distribution, biogeography, and evolution of horned dinosaurs (Ornithischia: Ceratopsidae). pp. 405-427 in New Perspectives on Horned Dinosaurs: The Royal Tyrell Museum Ceratopsian Symposium, M.J. Ryan, B.J. Chinnery-Allgeier, and D.A. Eberth (eds.) Indiana University Press, Bloomington and Indianapolis.

Scannella J.B., and J.R. Horner. 2010. *Torosaurus* Marsh, 1891, is *Triceratops* Marsh, 1889 (Ceratopsidae: Chasmosaurinae): synonymy through ontogeny. Journal of Vertebrate Paleontology 30(4): 1157-1168.

Scannella J.B., and D.W. Fowler. 2014. A stratigraphic survey of *Triceratops* localities in the Hell Creek Formation, northeastern Montana (2006-2010). pp. 313-332 in Through the End of the Cretaceous in the Type Locality of the Hell Creek Formation in Montana and Adjacent Areas, G.P. Wilson, W.A. Clemens, J.R. Horner, and J.H. Hartman (eds.) Geological Society of America Special Paper, Boulder, Colorado.

Simpson G.G. 1944. Tempo and mode in evolution. Columbia University Press, New York.

Simpson G.G. 1951. The species concept. Evolution 5: 285-298.

Simpson G.G. 1953. The major features of evolution. New York, Columbia University Press, New York.

Sorenson M.D., and E.A. Franzosa. 2007. TreeRot, version 3. Boston University, Boston, MA.

Swofford D. L. 2003. PAUP*. Phylogenetic Analysis Using Parsimony (*and Other Methods). Version 4. Sinauer Associates, Sunderland, Massachusetts.

Tokaryk T.T. 1986. Ceratopsian dinosaurs from the Frenchman Formation (Upper Cretaceous) of Saskatchewan. Canadian Field-Naturalist 100(2): 192-196.

Wagner P.J., and D.H. Erwin. 1995. Phylogenetic patterns as tests of speciation models. pp. 87-122 in *New Approaches to Speciation in the Fossil Record*, D.H. Erwin, and R.H. Anstey (eds.) Columbia University Press, New York.

Wu X., D.B. Brinkman, D.A. Eberth, and D.R. Braman. 2007. A new ceratopsid dinosaur (Ornithischia) from the uppermost Horseshoe Canyon Formation (upper Maastrichtian), Alberta, Canada. Canadian Journal of Earth Sciences 44: 1243-1265.

CHAPTER SEVEN

REANALYSIS OF "*RAPTOREX KRIEGSTEINI*": A JUVENILE TYRANNOSAURID DINOSAUR FROM MONGOLIA

Contribution of Authors and Co-Authors

Manuscript in Chapter 7

Author: Denver W. Fowler

Contributions: Conceived and designed the study, performed experiments, analyzed data, and wrote and compiled the manuscript.

Co-author: HollyNoelle W. Ballard

Contributions: Conceived and designed the study, performed experiments, analyzed data, and wrote a section of the manuscript.

Co-author: Elizabeth A. Freedman

Contributions: Conceived and designed the study, performed experiments, analyzed data, and wrote a section of the manuscript.

Co-author: Peter L. Larson

Contributions: Conceived and designed the study, performed experiments, analyzed data, and contributed to sections of the manuscript.

Co-author: John R. Horner

Contributions: Analyzed data, contributed materials and analytical tools.

Manuscript Information Page

Denver W. Fowler, Holly N. Woodward, Elizabeth A. Freedman, Peter L. Larson, John R. Horner
Journal Name: PLOS ONE
Status of Manuscript:
___Prepared for submission to a peer-reviewed journal
___Officially submitted to a peer-reviewed journal
___Accepted by a peer-reviewed journal
_x_Published in a peer-reviewed journal

Published by Public Library of Science
Issue 6(6): e31376. 2011.
The following chapter has been published in PLOS ONE and appears in this dissertation under the terms of the Creative Commons Distribution License.

Abstract

The carnivorous Tyrannosauridae are among the most iconic dinosaurs: typified by large body size, tiny forelimbs, and massive robust skulls with laterally thickened teeth. The recently described small-bodied tyrannosaurid *Raptorex kreigsteini* is exceptional as its discovery proposes that many of the distinctive anatomical traits of derived tyrannosaurids were acquired in the Early Cretaceous, before the evolution of large body size. This inference depends on two core interpretations: that the holotype (LH PV18) derives from the Lower Cretaceous of China, and that despite its small size, it is a subadult or young adult. Here we show that the published data is equivocal regarding stratigraphic position and that ontogenetic reanalysis shows there is no reason to conclude that LH PV18 has reached this level of maturity. The probable juvenile status of LH PV18 makes its use as a holotype unreliable, since diagnostic features of *Raptorex* may be symptomatic of its immature status, rather than its actual phylogenetic position. These findings are consistent with the original sale description of LH PV18 as a juvenile *Tarbosaurus* from the Upper Cretaceous of Mongolia. Consequently, we suggest that there is currently no evidence to support the conclusion that tyrannosaurid skeletal design first evolved in the Early Cretaceous at small body size.

Key Words

Dinosauria; Theropoda; Tyrannosauridae; *Raptorex*; *Tarbosaurus*; Lycopteridae; histology; ontogeny; growth; stratigraphy; Mongolia; China.

Introduction

The Tyrannosauridae are probably the most famous of all dinosaurs. They are characterized by Upper Cretaceous taxa such as the iconic *Tyrannosaurus rex* from North America (Osborn, 1905) and *Tarbosaurus bataar* from Mongolia (Maleev, 1955; Rozhdestvensky, 1965): stocky carnivores of enormous size, with massive heads, huge laterally thickened teeth, and diminutive forelimbs. These and many other distinctive features are instantly recognizable and largely set tyrannosaurids apart from other theropods (Holtz Jr., 2004). Finds of relatively small, basal tyrannosauroids in the Upper Jurassic and Lower Cretaceous of North America (Madsen, 1974; Carpenter et al., 2005), Europe (Hutt et al., 2001; Rauhut, 2003; Benson, 2008), Asia (Xu et al., 2004; Xu et al., 2006), and possibly Australia ((Benson et al., 2010); although see (Herne et al., 2010)) indicated that these characteristics were gradually acquired through time, along with an increase in body size.

An intriguing twist to the evolutionary history of Tyrannosauridae was proposed in 2009 when Sereno et al. (2009) described *Raptorex kreigsteini* as a small-bodied tyrannosaurid from the Lower Cretaceous of China. The beautifully preserved holotype skeleton (LH PV18; Long Hao Institute of Geology and Paleontology, Hohhot, Nei Mongol, China) first surfaced at the Tucson Gem Mineral and Fossil Show several years ago where it was purchased by Dr. Henry Kriegstein, an American ophthalmologist and private fossil collector (Clark, 2009). Dr. Kriegstein showed the specimen to Paul Sereno, who recognized its scientific value and arranged to coauthor its description on the condition that it should be repatriated to China, from which it was assumed that it had

been illegally removed (Sereno et al., 2009). LH PV18 was important as it seemed to indicate that tyrannosaurid skeletal design first evolved at small body size in the Early Cretaceous. This inference depends on two core interpretations, that LH PV18 derives from the Lower Cretaceous, and that despite its small size, it is a subadult or young adult.

In the original description, LH PV18 is referred to as having been "discovered in the Lujiatun Beds (Hauterivian-Barremian, ca. 130 Ma) of the Lower Cretaceous Jehol Group" (Sereno et al., 2009; p. 419). However, uncertainty is indicated in the Supporting Online Material, and news articles (Achenbach, 2009; Boyle, 2009; Mullen, 2009) including the Chicago Tribune (Mullen, 2009) where Sereno is quoted: "From sediments, fossil fish bones, turtles, clam shells and other fauna we recovered from the rock matrix alongside the *Raptorex* fossil, we could generally pinpoint where it had been dug up in an area along the border with Inner Mongolia". Contrary to this statement (Mullen, 2009), published associated fossils (Sereno et al., 2009; Supporting Online Material) consist only of a crushed pelecypod and a fish centrum. As the crushed pelecypod is unidentified, the age of LH PV18 is based primarily on the fish centrum which is identified as "cf. *Lycoptera*" (Sereno et al., 2009; Supporting Online Material). This is used to suggest LH PV18 derives from the Lower Cretaceous, since the known stratigraphic range of Lycopteridae is ~122-135 Ma (Li et al., 1994). LH PV18 is suggested to have been collected from the Lujiatun Beds of the Yixian Formation, China, as this unit commonly yields articulated dinosaurs along with fossils of pelecypods and *Lycoptera,* as opposed to other potential units in China (e.g. the Iren Dabasu Formation).

LH PV18 was diagnosed as a subadult or young adult based on osteological analysis and a histological section of the right femur (Sereno et al., 2009). Osteological evidence cited as indicative of maturity includes complete obliteration of the internasal suture, partial coossification of several cranial sutures, coossification of some vertebral neural arches to centra, and partial fusion of the pelvis. In their histological analysis, spacing of Line(s) of Arrested Growth (LAGs) led the authors to suggest that LH PV18 had undergone an exponential growth period, and that growth was possibly slowing at death. From reconstructed LAG history it was suggested that LH PV18 died at an age of 5-6 years, as a subadult or young adult.

Herein, we show that the stratigraphic evidence provided (Sereno et al., 2009; Supporting Online Material) is uninformative and cannot be used to infer provenance. We demonstrate that the fish centrum is not of Lycopteridae and therefore the proposed stratigraphic position is not supported. Using histological and osteological analysis, we show there is no reason to believe that LH PV18 has reached subadult or young adult ontogenetic status. Further, we reveal that the specimen was originally sold as a juvenile *Tarbosaurus* from Mongolia, a diagnosis consistent with its morphology and the results of our independent analysis.

Materials and Methods

Identification of associated fossil material and histological analysis was conducted by reference to photographs provided in the Sereno et al. (2009) Supporting Online Material and comparison to adult and subadult tyrannosaurid specimens held at

the Museum of the Rockies and the Black Hills Institute. Consultation with Hollis Butts (pers. comm. to PL), who sold LH PV18 to Henry Kriegstein, was conducted at Tuscon Mineral Fair, Arizona, January 2011.

Here we follow Brochu (1996; p. 51-52) in his definition of vertebral neural arch fusion. A "closed" vertebra is defined as "one in which the neurocentral suture is no longer visible" (i.e. the suture is obliterated). An open vertebra is defined as "completely visible from all aspects, and the centrum and neural arch can be separated easily". A partially closed vertebra is "one in which the suture has started closing, but is still discernible".

Results and Discussion

Stratigraphy

The stratigraphic evidence (fish vertebra; rarity of articulated skeletons in the Iren Dabasu Formation; (Sereno et al., 2009; Supporting Online Material)) is uninformative and cannot be used to reliably infer provenance. The LH PV18 fish centrum was assigned to *Lycoptera* without comment on how this diagnosis was made (Sereno et al., 2009; Supporting Online Material). Because isolated *Lycoptera* centra have never been described in detail, such positive identification is difficult. The only published account of *Lycoptera* vertebrae is Zhang 2002 (not cited by Sereno et al. (2009)), whose morphological description is so different from the LH PV18 fish vertebra that this specimen cannot be a *Lycoptera*. Several features of the LH PV18 fish centrum that strongly differ from those of *Lycoptera* and related Osteoglossiformes, are instead more

consistent with centra of Ellimmichthyiformes (double-armored herrings; Figure 7.1) or Hiodontiformes. *Lycoptera* centra are highly unusual in being thin-walled and tubular with a large notochordal foramen (Zhang, 2002), whereas the LH PV18 fish centrum (Sereno et al., 2009), Ellimmichthyiformes, and Hiodontiformes (Brinkman and Neuman, 2002; Newbrey et al., 2010) are deeply amphicoelous, with thicker walls relative to the notochordal foramen. The LH PV18 fish centrum and Ellimmichthyiformes possess mid-dorsal and lateral-dorsal fossae posterior to the neural pits (Brinkman and Neuman, 2002; Newbrey et al., 2010); *Lycoptera* lacks these fossae (M. G. Newbrey pers. comm. 2010). A full description of *Lycoptera* vertebrae and comparison to Ellimmichthyiformes and Hiodontiformes is in preparation (Newbrey et al., in review).

In addition, the LH PV18 fish centrum is far larger than any centra found in an articulated *Lycoptera* specimen. *Lycoptera* are small fish, generally ranging in size from 7 to 13 cm, and their centra are typically <1 mm to 2 mm long (Ma, 1987; Zhang, 2002). By contrast, the LH PV18 centrum (Sereno et al., 2009) is 4 mm in diameter and approximately 4 mm in length. This would be anomalously large for a *Lycoptera* centrum, but is fully within the size range expected for ellimmichthyiform centra, which are commonly up to 7 mm in diameter (Newbrey et al., 2010; Figure 7.1).

Although the LH PV18 fish centrum cannot be more precisely identified without further comprehensive comparisons, its morphology and size exclude the possibility of it being *Lycoptera*, but are consistent with centra of Ellimmichthyiformes. As Ellimmichthyiformes in China range from the Early Cretaceous to the Eocene (Zaragüeta, 2004; Newbrey et al., 2010), the LH PV18 fish centrum cannot be used as definitive

evidence of an Early Cretaceous age for the specimen. Therefore there is no biostratigraphic evidence for placement of the specimen in the Lower Cretaceous.

The presence of pelecypod and *Lycoptera* fish fossils in the Jehol Biota is used by Sereno et al. (2009) as supporting evidence for assignment of LH PV18 to the Lujiatun beds of the Yixian Fm. We have shown that the fish vertebra does not pertain to Lycopteridae, so this argument is reduced to the presence of pelecypods and fish, which is typical for many if not most Mesozoic terrestrial formations and cannot be used as supporting evidence. Further, taphonomic data cannot exclude the possibility of a Late Cretaceous age, since articulated and partly articulated dinosaur remains are known from the Iren Dabasu Formation (Currie and Eberth, 1993).

We suggest that other methods of chronostratigraphic analysis might provide independent age assessment of LH PV18. Analysis of palynomorphs or detrital zircons, extracted from the enclosing "tuffaceous sandstone" matrix (which might be expected to have potential for such analyses) could be used to assess stratigraphic position. While these methods provide only rough ages, often variably accurate within a range of ~5 million years, this would still be adequate considering the ~60my disparity between potential Early and Late Cretaceous ages. Conceivably, analyzing Rare Earth Element content of fossil bone might also help elucidate provenance (Trueman and Benton, 1997; Trueman et al., 2006).

Independent testimony states that the specimen was collected in Mongolia, not China. Before its final sale in the United States, LH PV18 was purchased from a Mongolian fossil collector by one of the brokers, an American businessman residing in

Tokyo, Japan: at no time had the specimen been represented as coming from China (seller Hollis Butts pers. comm. to PL). Dr. Kriegstein confirmed (pers. comm. to PL) that he discussed the origin of LH PV18 with Mr. Butts and that upon purchase it was tentatively identified as a juvenile *Tarbosaurus*, a tyrannosaurid known only from the Late Cretaceous (Campanian and/or Maastrichtian; (Holtz Jr., 2004)). Variability in personal communications regarding the specimen makes it difficult to ascertain exact details that were known at the time of purchase, highlighting the problems of dealing with commercial specimens that have been illegally collected. It is unclear how the specimen came to be considered as having originated from the Lower Cretaceous of China, but a Mongolian (Upper Cretaceous) origin is consistent with other aspects of our stratigraphic reanalysis. Regardless of independent testimony, published stratigraphic data are uninformative. LH PV18 is of currently unknown provenance.

Ontogeny

Ontogeny has an enormous influence on the skeletal morphology of dinosaurs, most obviously affecting both proportions and ornament of the skull (Brown and Schlaikjer, 1940; Rozhdestvensky, 1965; Russell, 1970; Dodson, 1975, 1976; Maryanska and Osmolska, 1979; Horner, 1983; Dodson and Currie, 1988; Horner and Currie, 1994; Sampson, 1995; Sampson et al., 1997; Carr, 1999; Ryan et al., 2001; Currie, 2003a; Carr and Williamson, 2004; Evans et al., 2005; Horner and Goodwin, 2006; Evans et al., 2007; Currie et al., 2008; Horner and Goodwin, 2008; Brown et al., 2009; Horner and Goodwin, 2009; Knoll et al., 2010; Scannella and Horner, 2010; Whitlock et al., 2010; Tsuihiji et al., 2011), but also postcrania (Russell, 1970; Dilkes, 2001; Wedel, 2003; Reisz et al.,

2005; Tsuihiji et al., 2011). While it has long been recognized that immature individuals can appear morphologically more basal than adults of the same species (Rozhdestvensky, 1965), only relatively recently has this begun to be acknowledged in taxonomic studies (Rozhdestvensky, 1965; Russell, 1970; Dodson, 1975; Sampson et al., 1997; Carr, 1999; Currie, 2003a; Horner and Goodwin, 2009; Knoll et al., 2010; Scannella and Horner, 2010; Tsuihiji et al., 2011). Historically, many specimens of immature dinosaurs have been described as unique taxa, only later being recognized as juveniles and subsequently synonymized with a different taxon (Russell, 1970; Dodson, 1975; Dodson and Currie, 1988; Sampson et al., 1997; Carr, 1999; Currie and Dong, 2001; Currie, 2003a; Carr and Williamson, 2004; Horner and Goodwin, 2009; Knoll et al., 2010; Scannella and Horner, 2010; Margottini, 2011). The emerging view of dinosaur ontogeny is that fully derived cranial and postcranial characters are typically only gained near to and/or upon reaching maturity (potentially beyond skeletal maturity), hence juvenile dinosaurs exhibit morphological characters that might make them appear more basal than they really are (Brown and Schlaikjer, 1940; Rozhdestvensky, 1965; Russell, 1970; Dodson, 1975, 1976; Maryanska and Osmolska, 1979; Horner, 1983; Dodson and Currie, 1988; Horner and Currie, 1994; Sampson, 1995; Sampson et al., 1997; Carr, 1999; Ryan et al., 2001; Currie, 2003a; Carr and Williamson, 2004; Evans et al., 2005; Horner and Goodwin, 2006; Evans et al., 2007; Currie et al., 2008; Horner and Goodwin, 2008; Brown et al., 2009; Horner and Goodwin, 2009; Knoll et al., 2010; Scannella and Horner, 2010; Whitlock et al., 2010; Margottini, 2011; Tsuihiji et al., 2011). This is illustrated in Tyrannosauridae by MPC-D 107/7 (Mongolian Paleontological Center, Ulaan Bataar,

Mongolia), a recently described (Tsuihiji et al., 2011) juvenile *Tarbosaurus bataar* (Nemegt Formation, Mongolia), nearly identical in size to LH PV18 (skull length 290 mm and 300 mm, respectively) and extremely similar in morphology. Cladistic analysis recovers MPC-D 107/7 as the sister taxon to Tyrannosauridae (with LH PV18 as the next more basal node) rather than the sister taxon to *Tarbosaurus*. Consequently, if LH PV18 is shown to be non-mature, then it is possible that purported basal characteristics do not reflect a true phylogenetic position, but rather its immature status. Assessing whether LH PV18 is a juvenile *Tarbosaurus* (as stated at its original sale) requires reanalysis of ontogenetic data, as the specimen was originally described as a subadult or young adult (Sereno et al., 2009).

Osteological Indications of Maturity

Reanalysis of the published osteological data demonstrates that the specimen should not be considered as close to mature. Partial fusion of the internasal suture of LH PV18 (Sereno et al., 2009) is not indicative of maturity as the nasal suture begins to fuse very early in the ontogeny of tyrannosaurids (Carr and Williamson, 2004; Tsuihiji et al., 2011).

"Closed and coossified" neurocentral sutures in the cervical, anterior dorsal, and sacral vertebrae were used to infer a near mature condition for LH PV18 (Sereno et al., 2009), but this diagnosis is at odds with personal examination of the specimen by one of the present authors (PL), where (using the definition of Brochu (1996)) neurocentral sutures of anterior dorsal and cervical vertebrae were observed to be only partially closed. Moreover, neurocentral sutures remain open in the anterior caudal and posterior dorsal

vertebrae, some of which have become slightly disarticulated. The ontogenetic pattern for neurocentral closure has not yet been fully studied for tyrannosaurid dinosaurs (Carr et al., 2005), but the initially observed pattern does not match that described for crocodylians, where the caudal series can be closed before hatching, and fusion proceeds cranially (Brochu, 1996). Moreover, neurocentral fusion is an inconsistently observed character in tyrannosaurids suggesting that it is unreliable in determining maturity. The very large *Tyrannosaurus* FMNH PR2081 ("Sue"; (Brochu, 2003); Field Museum of Natural History, Chicago) exhibits unobliterated neurocentral sutures through the presacral and sacral series, as well as the first 15 caudal vertebrae. The juvenile *Tarbosaurus* IVPP V4878, (=*Shanshanosaurus huoyanshanensis*; Subashi Formation, Upper Cretaceous, Xinjiang, China; (Dong, 1977; Currie and Dong, 2001); Institute of Vertebrate Paleontology and Paleoanthropology, Beijing, China) is of near-identical size to LH PV18 and exhibits variable states of fusion in preserved cervical and dorsal vertebrae with some apparently closed, and others with visible sutures (Currie and Dong, 2001). Neurocentral sutures also appear closed in the cervical vertebrae of the juvenile tyrannosaurid IGM 100/1844 (Institute of Geology, Ulaan Baatar, Mongolia), described as the holotype of *Alioramus altai* (Brusatte et al., 2010). This demonstrates that neurocentral closure is known in tyrannosaurids that are not close to being mature, making it difficult to use this feature to support an adult status for LH PV18. Finally, in the recently described dromaeosaurid theropod *Balaur* (Csiki et al., 2010), extensive postcranial fusion is noted in both the holotype and paratype specimens, yet the paratype pertains to an individual 45% larger than the holotype. Csiki et al. (2010) were not able to

conduct independent histological analysis of ontogenetic status, but acknowledge that one hypothesis to account for this observation is that "growth continued after fusion of numerous regions of the skeleton". Partial neurocentral fusion is therefore an unreliable indicator of maturity in theropods, at least without further study.

The narrow maxillary tooth crowns of LH PV18 are suggested to be different from "mature tyrannosaurids" (Sereno et al., 2009). Narrow crowns are typical of both immature Late Cretaceous tyrannosaurids (Carr, 1999; Currie, 2003a) and basal tyrannosauroids (Hutt et al., 2001; Xu et al., 2004; Xu et al., 2006). Since narrow crowns would be expected in both immature and basal tyrannosaurids then we suggest this feature is of equivocal use for determining ontogenetic status.

Histology

Histological sectioning of limb bones remains the only reliable assessment of ontogenetic status. Sereno et al. (2009) conclude that LH PV18 is a nearly mature subadult based on a histological section of the right femur. However, the section exhibits typically juvenile histological features. If LH PV18 was nearly mature then bone remodeling in the form of secondary osteons should be widespread in the histologic section (Francillon-Vieillot et al., 1990; Horner et al., 2001; Klein and Sander, 2008). However, secondary osteons are only seen in two very small areas, both associated with migration of adductor muscle attachment (Figure 7.2). Furthermore, the femur is composed entirely of plexiform fibro-lamellar bone indicating rapid growth and consistent with an immature status.

Sereno et al.'s (2009) suggestion that the distance between LAG 2 and the surface records a transition to exponential growth compared to the distance between LAGs 1 and 2 is questionable as the spacing between LAG 1 and the missing LAGs was just as large if not larger. The amount of growth represented by the distance between LAG 1 and 2 is anomalous as it is bound on either side by bone thicknesses representing larger amounts of growth. In addition, if the distance between LAG 2 and the surface represents the beginning of an exponential growth phase, then this individual should be considered immature because a subadult would be characterized by a reducing, not increasing, growth rate. There is no indication from tissue organization or LAG spacing that suggests growth is slowing down or that adult or subadult size has been approached. Because a fibro-lamellar tissue complex is consistent throughout, even up to the periosteal surface, growth was still proceeding rapidly at time of death.

The outer layer described as a possible third LAG is difficult to fully trace around the circumference in the images available, and may be an artifact of diagenetic staining. The close-up image using transmitted light (Sereno et al., 2009; Fig. S7b) supports this, as the image shows that the cortex near the periosteal surface is less clearly preserved and there is no "well-defined" third LAG. Sereno et al. interpret this possible LAG, so close to the periosteal surface, to indicate a decrease in bone deposition associated with approaching skeletal maturity. For this to be true, a corresponding and permanent change from plexiform tissue to slowly deposited parallel-fibered or lamellar bone tissue is necessary. If there is indeed a third LAG near the surface, the few lamellae deposited after it remain plexiform like the rest of the section. In this case, a single LAG so close to

the surface means only that this animal died shortly after its deposition, not that growth was slowing down.

It has been suggested that the long bone histology of small dinosaurs (i.e. those of small adult size) and basal birds is different from that of large dinosaurs (Case, 1978; Padian et al., 2001; Ricqlès et al., 2003; Horner and Padian, 2004; Padian et al., 2004). Padian et al. (2001; p. 405) state: "In contrast to large dinosaurs and pterosaurs, small ones apparently grew more slowly. Their long bone cortices were less well vascularized, the vessels were primarily longitudinal, and the bones may show more closely spaced growth lines". If LH PV18 was a near-mature individual of a small tyrannosaur species we would expect to observe the aforementioned histological features in the section. However, LH PV18 exhibits histology more consistent with that of an immature large dinosaur, rather than a mature (or even immature) small dinosaur.

Histology also indicates that the original age estimate of 5-6 years (Sereno et al., 2009) is an overestimate. We suggest that an age of 3-6 years is more accurate, with strong suspicion of a true age closer to 3 years. The annual periodicity of cortical growth marks (LAGs) has been demonstrated in extant archosaurs (e.g. Hutton, 1986; Tucker, 1997), thus allowing their use in estimating age at death for dinosaurs. Sereno et al. determined the age of LH PV18 by counting the LAGs present within the cortex, and adding to that the number of LAGs estimated to be missing due to bone resorption during medullary cavity expansion. Because the distance between two LAGs reveals the amount of cortical growth in one year, Sereno et al. (2009) use the spacing (or growth "zone") between LAG 1 and 2 to assess the number of missing LAGs by determining how many

of those zones would fit within the medullary cavity. However, this method is problematic. The deep cortex shown on the left side of the section is less affected by medullary expansion than the right side, affording a more complete record of cortical growth. Here the distance from the edge of the medullary cavity to LAG 1 is greater than the distance between LAG 1 and 2 (Figure 7.2), and equivalent to the spacing between LAG 2 and the surface. Therefore the amount of cortical growth in the year separating LAG 1 and LAG 2 is actually less than the amount of cortical growth from the previous year (edge of medullary cavity to LAG 1), as well as less than the cortical growth from the year after (the zone between LAG 2 and the surface). Therefore, the distance between LAG 1 and LAG 2 should not be used to estimate the number of missing LAGs. Despite being incomplete due to resorption, the innermost growth zone is approximately twice as large as the distance between LAG 1 and LAG 2, and would be a better estimate of the width of the missing growth zones. It is also equally plausible that the bone tissue destroyed by medullary expansion was free of additional LAGs. Ontogenetic histology studies of large dinosaurs demonstrate a rapid increase in body size prior to the deposition of the first LAG (Horner et al., 2000; Erickson et al., 2004; Bybee et al., 2006). Following this model of growth, missing LAGs destroyed by medullary expansion would not be expected in LH PV18 and the actual age at death was 2-3 years. This is supported by the ontogenetic analysis of the near-identically sized juvenile *Tarbosaurus* MPC-D 107/7. Histological analysis of the fibula and tibia from MPC-D 107/7 revealed an age of 2-3 years with no possibility of missing LAGs (Tsuihiji et al., 2011). Therefore, given the presence of a rapidly deposited bone tissue typical of an immature animal, and

because in general LAG spacing decreases throughout ontogeny as growth rate slows, we consider an age estimate of 2-3 years most likely for LH PV18.

Taxonomy

It is not the main purpose of this study to reassess the taxonomic status and possible affinities of LH PV18; however, some comment is appropriate. In their description of a juvenile *Tarbosaurus bataar* (MPC-D 107/7), Tsuihiji et al. (2011) discuss morphology of juvenile tyrannosaurs, including characters considered diagnostic of "*Raptorex*" which are also seen in MPC-D 107/7. They conclude that it can be challenging to discriminate juvenile characters from plesiomorphic characters, with which we concur. Tsuihiji et al. (2011) tentatively suggest that LH PV18 is not assignable to *T. bataar* for two reasons. Firstly, LH PV18 has "reportedly very different stratigraphic age and provenance", which we show here to be based on incorrect interpretation by Sereno et al. (2009). Secondly, there are some morphological differences between LH PV18 and MPC-D 107/7, including cranial characters (dorsoventral extension of the rostroventral lamina of the ventral ramus of the lacrimal, and size of caudal surangular foramen) and significantly, that LH PV18 is reported as lacking a vertical crest on the ilium (a character seen in all other tyrannosauroids (Holtz Jr., 2001, 2004)). However, personal observation of LH PV18 by one of us (PL) found that a subtle crest is visible on the ilium (as expected). Thus, the only definable differences between a juvenile *Tarbosaurus bataar* and LH PV18 are two minor skull characters, which Tsuihiji et al. (2011) suggest could be intraspecific variation (although intraspecific variation in tyrannosaurids (Carr, 1999; Currie, 2003a, b; Hurum and Sabath, 2003), especially

juveniles, requires further study). Morphological and histological consistency between the two specimens supports our conclusion that LH PV18 is a juvenile of a much larger tyrannosaurid species, and may indicate affinity with *Tarbosaurus,* although not necessarily being assignable to *T. bataar*. Comparison to the tyrannosaurid record of North America (Holtz Jr., 2004) over the equivalent time frame (Late Cretaceous; Campanian - Maastrichtian; ~83 - 66 Ma; (Weishampel et al., 2008; Hone et al., 2011)) suggests that some diversity might be expected in Asian taxa. North American dinosaur taxa often form lineages of non-overlapping chronospecies, even within the same formation (Holmes et al., 2001; Currie and Russell, 2005; Ryan and Evans, 2005; Ryan and Russell, 2005; Scannella and Fowler, 2009). Small changes seen among Asian tyrannosaurids may similarly be the result of slight stratigraphic variation. However, as demonstrated with *Triceratops* (Scannella and Fowler, 2009; Scannella and Horner, 2010), making sense of multiple morphologies first requires knowledge of ontogenetic change as well as relative stratigraphic position of specimens, emphasizing the necessity for such data in specimen descriptions.

The lack of provenance data and juvenile status of LH PV18 make its use as a holotype problematic. When sample sizes are extremely limited, all specimens may appear to be useful records of morphology, even if they lack essential locality data. However, specimens without stratigraphic data can be extremely difficult to compare properly with newly discovered material for which stratigraphic position is known. Thus, many historically collected specimens (even holotypes) will eventually become morphologies without context and mostly useless for any detailed scientific investigation

(something we have personally encountered while studying historical collections of *Triceratops*). This can only be countered by relocation (where possible) of the original collection quarries (Tanke, 2005; Scannella and Fowler, 2009; Everhart, 2011). Similarly, definition of taxa from juvenile specimens may not be useful because they are notoriously difficult to associate with adult morphologies (without intermediate forms for reference), which can result in their eventual designation as nomina dubia (e.g. *Brachyceratops montanensis*; *Monoclonius crassus*; (Sampson et al., 1997)). Tsuihiji et al (2011) had great difficulty assigning the juvenile MPC-D 107/7 to *Tarbosaurus bataar*, finding only three characters shared by both juvenile and adult (including number of tooth positions which varies even between left and right sides of a single individual (Tsuihiji et al., 2011), and is thought to change through ontogeny; (Carr, 1999)). Given that MPC-D 107/7 is morphologically dissimilar to an adult *T. bataar*, and that it is of almost identical ontogenetic status as LH PV18, we would not expect the adult morphology of "*Raptorex*" to look overly similar to LH PV18. Thus, even if "*Raptorex*" is a genuine taxon, it cannot be reliably compared to other species that are diagnosed based on adult specimens.

Conclusions

LH PV18 cannot be demonstrated to be from the Lower Cretaceous, therefore the conclusion that derived features of tyrannosaurids evolved before the Late Cretaceous cannot be supported. As histology demonstrates that LH PV18 is immature then the conclusion that typical tyrannosaurid features evolved at a small size also cannot be

supported, since the small size of LH PV18 is more likely the result of its immature status. Furthermore, the probable juvenile status of LH PV18 makes its use as a holotype unreliable, since diagnostic features of *Raptorex* may be symptomatic of its immature status, rather than its actual phylogenetic position. Unless stronger evidence is presented, *Raptorex* should be considered a *nomen dubium*. LH PV18 more likely represents the juvenile of a larger tyrannosaurid from the Late Cretaceous of Mongolia, such as *Tarbosaurus* (as per its original sale description), although testing of this hypothesis awaits description of new specimens of immature tyrannosaurids.

Misidentification of immature dinosaur specimens as new taxa is a persistent and increasingly pervasive problem that can be detected and diagnosed only by thorough and proper histological analysis. Combined ontogenetic and stratigraphic analyses have great potential to reveal new information on the mode and tempo of dinosaur evolution, but as this reanalysis exemplifies, such studies must be based upon solid and replicable data.

Acknowledgements

Our gratitude is extended to Michael Newbrey (Tyrell Museum of Paleontology, TMP) for detailed consultation on fish vertebrae, and comments on the manuscript. Donald Brinkman (TMP) provided helpful comments on an early draft of the manuscript. Ellen Lamm (MOR) prepared histology slides used for comparison. Hollis Butts and Dr. Henry Kriegstein are thanked for their communications regarding the LH PV18 specimen. Thanks to John Scannella for discussion and help with references. Special thanks to Paul Sereno for unimpeded access to LH PV18.

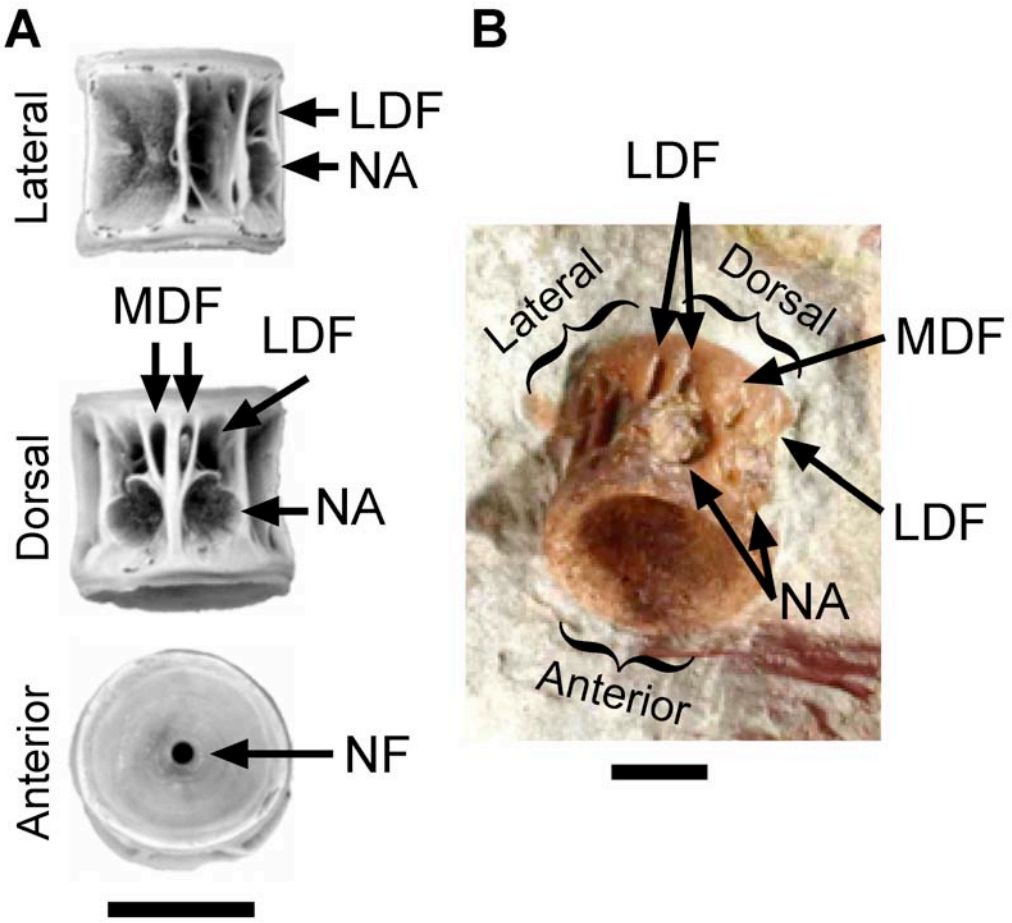

Figure 7.1 Comparison of the LH PV18 fish centrum (D) to an ellimmichthyiform centrum (A-C) (Horseshoeichthyes) from the Dinosaur Park Formation (Campanian) of Alberta. The notochordal foramen (NF) in the LH PV18 fish centrum (D) is so small that it cannot be seen from the angle of the photograph. The exact number and positions of mid-dorsal fossae (MDF) and laterodorsal fossae (LDF) are variable within the same taxon (Brinkman and Neuman, 2002). Photos (A-C) have been rotated to align with the general orientation of the obliquely figured LH PV18 fish centrum. Picture (A) was also flipped horizontally to simulate the right lateral view. Additional abbreviations: NA: neural arch articular pit. (A-C) adapted from Newbrey et al. (2010; Figure 9h). (D) adapted from Sereno et al. (2009; Figure S8B).

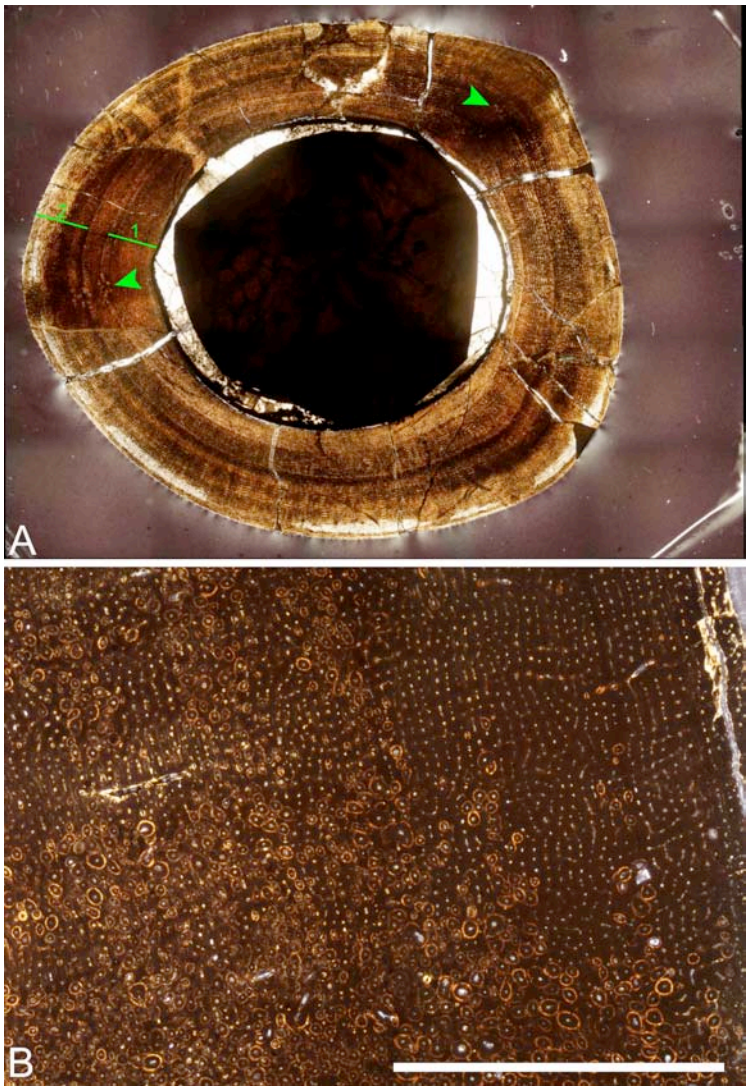

Figure 7.2. Osteohistological features of LH PV18 and a near adult *Tyrannosaurus rex* for comparison. A) Femur cross section of LH PV18 modified from Sereno et al. (2009; Figure S7A). Only two small clusters of secondary osteons (arrows) are visible, associated with adductor muscle attachment sites. The width of cortical bone from the edge of the medullary cavity to LAG 1 (green bar labeled 1) is nearly the same as the width of cortical bone from LAG 2 to the outer surface (green bar labeled 3). B) Mid to outer cortex of a femur cross section from a *Tyrannosaurus rex* (MOR 1198; Museum of the Rockies, Bozeman, Montana) described (Horner and Padian, 2004) as approaching adult length. The bone surface is located to the right of the picture. Several generations of secondary osteons nearly obliterate primary tissue within the deeper cortex and become scattered close to the surface. This pattern is typical of dinosaurs approaching asymptotic size. Scale bars, 5 mm.

References Cited

Achenbach, J. Unveiled: The Surprisingly Small Precursor of T. Rex. Washington Post 18th September 2009. http://www.washingtonpost.com/wp-dyn/content/article/2009/09/17/AR2009091702573.html?hpid=topnews&sid=ST2009091800725. Retrieved 2011 March 8.

Benson, R. B. J. 2008. New information on *Stokesosaurus*, a tyrannosauroid (Dinosauria: Theropoda) from North America and the United Kingdom. Journal of Vertebrate Paleontology 28:732-750.

Benson, R. B. J., P. M. Barrett, T. H. Rich, and P. Vickers-Rich. 2010. A Southern Tyrant Reptile. Science 327:1613.

Boyle, A. Tiny T. rex? Big surprise! MSNBC News. http://cosmiclog.msnbc.msn.com/archive/2009/09/17/2072603.aspx. Retrieved 2011 March 8.

Brinkman, D. B., and A. G. Neuman. 2002. Teleost centra from uppermost Judith River Group (Dinosaur Park Formation, Campanian) of Alberta. Canadian Journal of Paleontology 76:138-155.

Brochu, C. A. 1996. Closure of neurocentral sutures during crocodilian ontogeny: implications for maturity assessment in fossil archosaurs. Journal of Vertebrate Paleontology 16:49-62.

Brochu, C. A. 2003. Osteology of *Tyrannosaurus rex*: Insights from a nearly complete skeleton and high-resolution computed tomographic analysis of the skull. Journal of Vertebrate Paleontology Memoir 7:1-138.

Brown, B., and E. Schlaikjer. 1940. The structure and relationships of *Protoceratops*. Annals of the New York Academy of Sciences 40:133-266.

Brown, C. M., A. P. Russell, and M. J. Ryan. 2009. Pattern and transition of surficial bone texture of the Centrosaurine frill and their ontogenetic and taxonomic implications. Journal of Vertebrate Paleontology 29:132-141.

Brusatte, S. L., T. D. Carr, G. M. Erickson, G. S. Bever, and M. A. Norell. 2010. A long-snouted, multihorned tyrannosaurid from the Late Cretaceous of Mongolia. Proceedings of the National Academy of Science 106:17261-17266.

Bybee, P. J., A. H. Lee, and E. Lamm. 2006. Sizing the Jurassic theropod dinosaur *Allosaurus*: assessing growth strategy and evolution of ontogenetic scaling of limbs. Journal of Morphology 267:347-359.

Carpenter, K., C. Miles, and K. Cloward. 2005. New small theropod from the Upper Jurassic Morrison Formation of Wyoming; pp. 23-48 in K. Carpenter (ed.), The Carnivorous Dinosaurs. Indiana University Press, Bloomington.

Carr, T. D. 1999. Craniofacial ontogeny in Tyrannosauridae (Dinosauria, Coelurosauria). Journal of Vertebrate Paleontology 19:497-520.

Carr, T. D., and T. E. Williamson. 2004. Diversity of Late Maastrichtian Tyrannosauridae (Dinosauria: Theropoda) from western North America. Zoological Journal of the Linnean Society-London 142:419-523.

Carr, T. D., T. E. Williamson, and D. E. Schwimmer. 2005. A new genus and species of tyrannosaurid from the Late Cretaceous (Middle Campanian) Demopolis Formation of Alabama. Journal of Vertebrate Paleontology 25:119-143.

Case, T. J. 1978. Speculation on the growth rate and reproduction of some dinosaurs. Paleobiology 4:320-328.

Clark, J. 2009. Becoming *T. rex*. Science 326:373-374.

Csiki, Z., M. Vremir, S. L. Brusatte, and M. A. Norell. 2010. An aberrant island-dwelling theropod dinosaur from the Late Cretaceous of Romania. Proceedings of the National Academy of Science 107:15357-15361.

Currie, P. J. 2003a. Allometric growth in tyrannosaurids (Dinosauria: Theropoda) from the Upper Cretaceous of North America and Asia. Canadian Journal of Earth Sciences 40:651-665.

Currie, P. J. 2003b. Cranial anatomy of tyrannosaurid dinosaurs from the Late Cretaceous of Alberta, Canada. Acta Palaeontolgica Polonica 48:191-226.

Currie, P. J., and Z. Dong. 2001. New information on *Shanshanosaurus huoyanshanensis*, a juvenile tyrannosaurid (Theropoda, Dinosauria) from the Late Cretaceous of China. Canadian Journal of Earth Sciences 38:1729-1737.

Currie, P. J., and D. A. Eberth. 1993. Palaeontology, sedimentology, and palaeoecology of the Iren Dabasu Formation (Upper Cretaceous), Inner Mongolia, People's Republic of China. Cretaceous Research 14:127-144.

Currie, P. J., and D. A. Russell. 2005. The geographic distribution of articulated and associated dinosaur remains; pp. 537-569 in P. J. Currie and E. B. Koppelhaus (eds.), Dinosaur Provincial Park. Indiana University Press, Bloomington.

Currie, P. J., W. Langston, and D. H. Tanke. 2008. A new species of *Pachyrhinosaurus* (Dinosauria, Ceratopsidae) from the Upper Cretaceous of Alberta, Canada; pp. 1-108 in P. J. Currie, W. Langston, and D. H. Tanke (eds.), A New Horned Dinosaur from an Upper Cretaceous Bone Bed in Alberta. NRC Research Press, Ottawa.

Dilkes, D. W. 2001. An ontogenetic perspective on locomotion in the Late Cretaceous dinosaur Maiasaura peeblesorum (Ornithischia: Hadrosauridae). Canadian Journal of Earth Sciences 38:1205-1227.

Dodson, P. 1975. Taxonomic implications of relative growth in Lambeosaurine hadrosaurs. Systematic Zoology 24:37-54.

Dodson, P. 1976. Quantitative aspects of relative growth and sexual dimorphism in *Protoceratops*.

Dodson, P., and P. J. Currie. 1988. The smallest ceratopsid skull - Judith River Formation of Alberta. Canadian Journal of Earth Sciences 25:926-930.

Dong, Z. 1977. On the dinosaurian remains from Turpan, Xinjiang. Vertebrata PalAsiatic 15:59-66.

Erickson, G. M., P. J. Makovicky, P. J. Currie, M. A. Norell, S. A. Yerby, and C. A. Brochu. 2004. Gigantism and comparative life-history parameters of tyrannosaurid dinosaurs. Nature 430:772-775.

Evans, D. C., C. A. Forster, and R. R. Reisz. 2005. The type specimen of *Tetragonosaurus erectofrons* (Ornithischia: Hadrosauridae) and the identification of juvenile Lambeosaurines; pp. 349-366 in P. J. Currie and E. B. Koppelhaus (eds.), Dinosaur Provincial Park. Indiana University Press, Bloomington.

Evans, D. C., R. R. Reisz, and K. Dupuis. 2007. A juvenile *Parasaurolophus* (Ornithischia: Hadrosauridae) braincase from Dinosaur Provincial Park, Alberta, with comments on crest ontogeny in the genus. Journal of Vertebrate Paleontology 27:642-650.

Everhart, M. J. 2011. Rediscovery of the *Hesperornis regalis* Marsh 1871 holotype locality indicates an earlier stratigraphic occurrence. Transactions of the Kansas Academy of Science 114:59-68.

Francillon-Vieillot, H., V. d. Buffrenil, J. Castanet, J. Geraudie, F. J. Meunier, J. Y. Sire, L. Zylberberg, and A. d. Ricqlès. 1990. Microstructure and mineralization of vertebrate skeletal tissues; pp. 471-548 in J. G. Carter (ed.), Skeletal biomineralization patterns, processes and evolutionary trends. Van Nostrand Reinhold, New York.

Herne, M. C., J. P. Nair, and S. W. Salisbury. 2010. Comment on "A Southern Tyrant Reptile". Science 329:1013.

Holmes, R. B., C. A. Forster, M. Ryan, and K. M. Shepherd. 2001. A new species of *Chasmosaurus* from the Dinosaur Park Formation of Southern Alberta. Canadian Journal of Earth Sciences 38:1423-1438.

Holtz Jr., T. R. 2001. The phylogeny and taxonomy of the Tyrannosauridae; pp. 64-83 in D. H. Tanke and K. Carpenter (eds.), Mesozoic Vertebrate Life. Indiana University Press, Bloomington.

Holtz Jr., T. R. 2004. Tyrannosauroidea; pp. 111-136 in D. Weishampel, P. Dodson, and H. Osmolska (eds.), The Dinosauria. University of California Press, Berkeley.

Hone, D. W., K. Wang, C. Sullivan, X. Zhao, S. Chen, D. Li, S. Ji, Q. Ji, and X. Xu. 2011. A new tyrannosaurine theropod, *Zhuchengtyrannus magnus* is named based on a maxilla and dentary. Cretaceous Research doi: 10.1016/j.cretres.2011.03.005.

Horner, J. R. 1983. Cranial osteology and morphology of the type specimen of *Maiasaura peeblesorum* (Ornithischia: Hadrosauridae), with discussion of its phylogenetic position. Journal of Vertebrate Paleontology 3:29-38.

Horner, J. R., and P. J. Currie. 1994. Embryonic and neonatal morphology and ontogeny of a new species of *Hypacrosaurus* (Ornithischia, Lambeosauridae) from Montana and Alberta; pp. 312-336 in K. Carpenter, K. F. Hirsch, and J. R. Horner (eds.), Dinosaur Eggs and Babies. Cambridge University Press, New York.

Horner, J. R., and K. Padian. 2004. Age and growth dynamics of *Tyrannosaurus rex*. Proceedings of the Royal Society of London Series B 271:1875-1880.

Horner, J. R., and M. B. Goodwin. 2006. Major cranial changes during *Triceratops* ontogeny. Proceedings of the Royal Society of London Series B 273:2757-2761.

Horner, J. R., and M. B. Goodwin. 2008. Ontogeny of cranial epi-ossifications in *Triceratops*. Journal of Vertebrate Paleontology 28:134-144.

Horner, J. R., and M. B. Goodwin. 2009. Extreme cranial ontogeny in the Upper Cretaceous dinosaur *Pachycephalosaurus*. Public Library of Science ONE 4:e7626.

Horner, J. R., A. d. Ricqlès, and K. Padian. 2000. Long bone histology of the hadrosaurid dinosaur *Maiasaura peeblesorum*: growth dynamics and physiology based on an ontogenetic series of skeletal elements. Journal of Vertebrate Paleontology 20:115-129.

Horner, J. R., K. Padian, and A. d. Ricqlès. 2001. Comparative osteohistology of some embryonic and perinatal archosaours: developmental and behavioral implications for dinosaurs. Paleobiology 27:39-58.

Hurum, J. H., and K. Sabath. 2003. Giant theropod dinosaurs from Asia and North America: skulls of *Tarbosaurus bataar* and *Tyrannosaurus rex* compared. Acta Palaeontolgica Polonica 48:161-190.

Hutt, S., D. W. Naish, D. M. Martill, M. J. Barker, and P. Newberry. 2001. A preliminary account of a new tyrannosauroid theropod from the Wessex Formation (Early Cretaceous) of southern England. Cretaceous Research 22:227-242.

Hutton, J. M. 1986. Age determination of living Nile crocodiles from the cortical stratification of bone. Copeia 2:332-341.

Klein, N., and P. M. Sander. 2008. Ontogenetic stages in the long bone histology of sauropod dinosaurs. Paleobiology 34:248-264.

Knoll, F., K. Padian, and A. d. Ricqlès. 2010. Ontogenetic change and adult body size of the early ornithischian dinosaur *Lesothosaurus diagnosticus*: implications for basal ornithischian taxonomy. Gondwana Research 17:171-179.

Li, P.-X., D.-Y. Su, Y.-G. Li, and J.-X. Yu. 1994. Age assignment of the *Lycoptera*-bearing bed. Acta Geologica Sinica-English Edition 7:329-349.

Ma, F. 1987. Review of *Lycoptera davidi*. Vertebrata PalAsiatic 25:8-19.

Madsen, J. H. 1974. A new theropod dinosaur from the Upper Jurassic of Utah. Journal of Paleontology 48:27-31.

Maleev, E. A. 1955. Giant carnivorous dinosaurs of Mongolia. Doklady Akademii Nauka SSSR+ 104:634-637.

Margottini, L. 2011. Is it time to declutter the dinosaur roster? Science 332:782.

Maryanska, T., and H. Osmolska. 1979. Aspects of hadrosaurian cranial anatomy. Lethaia 12:265-273.

Mullen, W. Fossil identified as mini-T.rex. Chicago Tribune, 18th September 2009. http://articles.chicagotribune.com/2009-09-18/news/0909170802_1_fossil-bones-tyrannosaurus-rex-chicago-paleontologist-paul-sereno. Retrieved 2011 March 8.

Newbrey, M. G., A. M. Murray, D. B. Brinkman, M. V. H. Wilson, and A. G. Neuman. 2010. A new articulated freshwater fish (Clupeomorpha, Ellimmichthyiformes) from the Horseshoe Canyon Formation, Maastrichtian, of Alberta, Canada. Canadian Journal of Earth Sciences 47:1183-1196.

Osborn, H. F. 1905. *Tyrannosaurus* and other Cretaceous carnivorous dinosaurs. Bulletin of the American Museum of Natural History 21:259-265.

Padian, K., A. d. Ricqlès, and J. R. Horner. 2001. Dinosaurian growth rates and bird origins. Nature 412:405-408.

Padian, K., J. R. Horner, and A. d. Ricqlès. 2004. Growth in small dinosaurs and pterosaurs: the evolution of archosaurian growth strategies. Journal of Vertebrate Paleontology 24:555-571.

Rauhut, O. W. M. 2003. A tyrannosauroid dinosaur from the Upper Jurassic of Portugal. Palaeontology 46:903-910.

Reisz, R. R., D. Scott, H.-D. Sues, D. C. Evans, and M. A. Raath. 2005. Embryos of an early Jurassic prosauropod dinosaur and their evolutionary significance. Science 309:761-764.

Ricqlès, A. d., K. Padian, and J. R. Horner. 2003. On the bone histology of some Triassic pseudosuchian archosaurs and related taxa. Annales de Paléontologie 89:67-101.

Rozhdestvensky, A. K. 1965. Growth changes in Asian dinosaurs and some problems of their taxonomy. Paleontologicheskii Zhurnal 3:95-109.

Russell, D. A. 1970. Tyrannosaurs from the Late Cretaceous of western Canada. National Museums of Canada Publications in Paleontology 1:1-34.

Ryan, M. J., and D. C. Evans. 2005. Ornithischian dinosaurs; pp. 312-348 in P. J. Currie and E. B. Koppelhaus (eds.), Dinosaur Provincial Park. Indiana University Press, Bloomington.

Ryan, M. J., and A. P. Russell. 2005. A new centrosaurine ceratopsid from the Oldman Formation of Alberta and its implications for centrosaurine taxonomy and systematics. Canadian Journal of Earth Sciences 42:1369-1387.

Ryan, M. J., A. P. Russell, D. A. Eberth, and P. J. Currie. 2001. The taphonomy of a Centrosaurus (Ornithischia: Ceratopsidae) bone bed from the Dinosaur Park Formation (Upper Campanian), Alberta, Canada, with comments on cranial ontogeny. Palaios 16:482-506.

Sampson, S. D. 1995. Two new horned dinosaurs from the Upper Cretaceous Two Medicine Formation of Montana; with a phylogenetic analysis of Centrosaurinae (Ornithischia: Ceratopsidae). Journal of Vertebrate Paleontology 15:743-760.

Sampson, S. D., M. J. Ryan, and D. Tanke. 1997. Craniofacial ontogeny in centrosaurine dinosaurs (Ornithischia: Ceratopsidae): taxonomic and behavioral implications. Zoological Journal of the Linnean Society 121:293-337.

Scannella, J. B., and D. W. Fowler. 2009. Anagenesis in *Triceratops*: evidence from a newly resolved stratigraphic framework for the Hell Creek Formation. Cincinnati Museum Center Science Contributions.

Scannella, J. B., and J. R. Horner. 2010. *Torosaurus* Marsh, 1891, is *Triceratops* Marsh, 1889 (Ceratopsidae: Chasmosaurinae): synonymy through ontogeny. Journal of Vertebrate Paleontology 30:1157-1168.

Sereno, P. C., L. Tan, S. L. Brusatte, H. J. Kriegstein, X. Zhao, and K. Cloward. 2009. Tyrannosaurid skeletal design first evolved at small body size. Science 326:418-422.

Tanke, D. H. 2005. Identifying lost quarries; pp. 34-53 in P. J. Currie and E. B. Koppelhaus (eds.), Dinosaur Provincial Park. Indiana University Press, Bloomington.

Trueman, C. N., and M. J. Benton. 1997. A geochemical method to trace the taphonomic history of reworked bones in sedimentary settings. Geology 25:263-266.

Trueman, C. N., A. K. Behrensmeyer, R. Potts, and N. Tuross. 2006. High-resolution records of location and stratigraphic provenance from the rare earth element composition of fossil bones. Geochimica et Cosmochimica Acta 70:4343-4355.

Tsuihiji, T., M. Watabe, K. Tsogtbaatar, R. Barsbold, S. Suzuki, A. H. Lee, R. C. Ridgely, Y. Kawahara, and L. M. Witmer. 2011. Cranial osteology of a juvenile specimen of *Tarbosaurus bataar* from the Nemegt Formation (Upper Cretaceous) of Bugin Tsav, Mongolia. Journal of Vertebrate Paleontology 31:497-517.

Tucker, A. D. 1997. Validation of skeletochronology to determine age of freshwater crocodiles (*Crocodylus johnstoni*). Australian Journal of Marine and Freshwater Research 48:343-351.

Wedel, M. J. 2003. The evolution of vertebral pneumaticity in sauropod dinosaurs. Journal of Vertebrate Paleontology 23:344-357.

Weishampel, D. B., D. E. Fastovsky, M. Watabe, D. Varricchio, F. Jackson, K. Tsogtbaatar, and R. Barsbold. 2008. New oviraptorid embryos from Bugin-Tsav, Nemegt Formation (Upper Cretaceous), Mongolia, with insights into their habitat and growth. Journal of Vertebrate Paleontology 28:1110-1119.

Whitlock, J. A., J. A. Wilson, and M. C. Lamanna. 2010. Description of a nearly complete juvenile skull of *Diplodocus* (Sauropoda: Diplodocoidea) from the Late Jurassic of North America. Journal of Vertebrate Paleontology 30:442-457.

Xu, X., C. A. Forster, M. A. Norell, G. M. Erickson, D. A. Eberth, C. Jia, and Q. Zhao. 2006. A basal tyrannosauroid dinosaur from the Late Jurassic of China. Nature 439:715-718.

Xu, X., M. A. Norell, X. Kuang, X. Wang, Q. Zhao, and C. Jia. 2004. Basal tyrannosauroids from China and evidence for protofeathers in tyrannosauroids. Nature 431:680-684.

Zaragüeta, B. 2004. Basal clupeomorphs and ellimmichthyiform phylogeny; pp. 391-404 in G. Arratia and A. Tintori (eds.), Mesozoic Fishes 3 - Systematics, Paleoenvironments, and Biodiversity. Verlag Dr. Friedrich Pfeil, Munich.

Zhang, J.-Y. 2002. A new species of *Lycoptera* from Liaoning, China. Vertebrata PalAsiatic 40:257-266.

CHAPTER EIGHT

SPECIATION OF LATE CRETACEOUS DINOSAURS OF THE WESTERN INTERIOR: INITIATED BY TRANSGRESSION/CLIMATE-INDUCED ALLOPATRY, AND COMPLETED BY REINFORCEMENT-DRIVEN ANAGENESIS

Abstract

There has been recent debate as to the function of 'bizarre structures' observed in Late Cretaceous dinosaurs of the Western interior. A better understanding of the phylogenetic, ontogenetic, stratigraphic, and geographic contexts of taxa bearing bizarre structures reveals the curious finding that ornithischian sister taxa consistently evolve cranial display organs in opposite directions in morphospace. This might be unexpected under some proposed functional hypotheses, but is a predicted outcome of speciation combined with the evolutionary process of reinforcement (currently undergoing a renaissance in genetics), with important implications for our understanding of dinosaur evolution of the North American Western Interior. Reinforcement may provide an explanation for apparent "endemism" and diversity patterns and adds fuel to the argument that vertebrate diversity patterns seen in the Late Cretaceous of North America are probably strongly correlated to its peculiar geography (orogenic activity and cyclic seaway transgression / regression), and may not be expected on a global scale.

Introduction

Although this chapter begins by addressing the function of bizarre structures, it is really an attempt at a holistic explanation for patterns of phylogeny (speciation and diversity), biogeography, and biostratigraphy of Late Cretaceous dinosaurs of the Western Interior. This is achieved by application of key concepts and results established in Chapters 2 to 4, and review of critical terminology:

- From Chapter 2: patterns of transgression & regression occur over various orders of cyclicity and may affect the biota in the following ways:
    - Distance from the shoreline (inland vs coastal habitats)
    - Basin drainage regimes (low vs high accommodation and associated changes in habitat and environment), and related aridity or wet climate regimes.
    - During maximum transgression, the Western Interior Seaway (WIS) may abut the Sevier thrust front, physically separating northern and southern zones of Laramidia
        - Habitat space may bottleneck during maximum transgression (*sensu* Horner et al, 1992), limiting available resources and potentially altering selection.
        - The continent may be divided into northern and southern areas inviting allopatric speciation

- Climate bands may migrate north-south correspondingly with regression / transgression if cyclicity in WIS shoreline position is related to climate-forced eustasy (especially polar ice; Miller et al. 2011).

- From Chapters 3 and 4: In order to understand evolutionary patterns and processes it is essential to fundamentally separate speciation (= cladogenesis, under most definitions; branching evolution) and anagenesis (= evolution; "phyletic evolution", non-branching evolution), which are often proposed as alternative modes of evolution; this is a misconception which is a result of slightly differing perspectives or definitions of key terms:
  - All evolution occurs only by anagenesis, as the definition of evolution and anagenesis are refer to the same result (descent with modification [Darwin]; change in allele frequency between generations within a breeding population [modern synthesis]).
    - Straw-man mischaracterizations of anagenesis as constant-rate "phyletic gradualism" (*sensu* Eldredge and Gould, 1972; Vrba, 1980) are unhelpful and only muddy the water as to what evolution is, and processes that drive it (Dawkins, 1986).
    - "Turnover" turnover is often inappropriately asserted in studies of Western Interior dinosaurs. Evolution from one form to the next is not turnover: anagenesis was specifically excluded from the definition of turnover given by Vrba (1985).

- Speciation (cladogenesis) is a branching or divergence event, creating two species from one. It is the result of anagenesis in at least one of two or more isolated (allopatric) breeding populations that were originally united as a single breeding population. By definition, speciation is not evolution (Cook, 1906), but is a *result* of evolution (*contra* Cook, 1906).
    - Because speciation demands isolation of a gene pool it must be associated with an isolating mechanism, typically allopatry. Therefore, investigations of speciation in Late Cretaceous dinosaurs of the Western interior naturally impact current hypotheses of their geographic isolation: the endemism hypotheses of Lehman (1987; 1997; 2001) and Sampson et al. (2010).

- From Chapter 3. Precise stratigraphic placement of different formations facilitates precise stratigraphic placement of taxa
    - Many taxa are stacked up into stratigraphically separated "species", which is most consistent with anagenesis of a single lineage (e.g. Horner et al., 1992).
        - They are not real species under the biological definition (Hausdorf, 2011), as they are not the result of a speciation event.
    - The combination of precise stratigraphic placement of taxa, and understanding their respective sister group relationships, infers the timing of genuine speciation events, after which two sister taxa/lineages are

present at the same time (though not necessarily the same geographic location).

- Recognizes a time period when speciation occurs, and helps align this with abiotic events (barriers to geneflow) that potentially drive divergence (Court Jester hypothesis; Barnosky, 2001).
- May reveal association of multiple speciation events at roughly the same time, in unrelated taxa; this would be in support of the turnover-pulse hypothesis (Vrba, 1985; 1993).
- Reveals that over many millions of years most functional features (especially postcrania) are in effective equilibrium (*sensu* Eldredge and Gould 1972), while display characters are subject to rapid (and maybe constant) change.

Bizarre Structures

There has been much recent discussion on the function of the various horns and crests ("bizarre structures") seen in many Late Cretaceous dinosaur clades from the North American Western Interior (e.g. the horns crests and frills of Ceratopsidae and Hadrosauridae). Functional suggestions have included both inter- and intraspecific defense, or display (Sampson, 1997; Goodwin, 2005; Forster and Farke, 2005; Padian and Horner, 2011a,b; 2013; Knell and Sampson, 2011; Hone et al., 2012; Knell et al., 2013; Hone and Naish, 2013). A display function of some kind is preferred by most current workers, but there has been debate regarding whether such structures function primarily for "sexual selection" or "species recognition" (Padian and Horner, 2011a,b;

2013; Knell and Sampson, 2011; Hone et al., 2012; Knell et al., 2013; Hone and Naish, 2013).

Following Padian and Horner (2013), functions or behaviors related to the disputed meaning of sexual selection and species recognition are probably better broken up into a hierarchy of terms:

- *Species recognition* – the ability of individual animals to recognize their own species, for a variety of purposes.
    - *Reproductive benefits* – (syn. *sexual selection* [broad sense]; *sensu* Ryan & Rand, 1993; Knell & Sampson, 2011; Hone and Naish (2013); and others) – a general term where positively selected traits offer a reproductive advantage; whether or not to use "sexual selection" in this general context is up to the individual researcher, but it is useful to have an overarching term that denotes reproductive benefits. However, the fact that reproductive advantage is ultimately achieved by all forms of selection (see above) means that limiting use of this term to mating benefits is paraphyletic.
        - *mate recognition* – an individual (the observer) considers another individual (the signaler) as an appropriate mate (even if erroneously; Paterson, 1985; in Ryan and Rand, 1993). This can be a selection process if: 1. potential mates vary slightly phenotypically such that one is more easily recognized as a potential mate than another (though not necessarily preferred, nor

more fit); 2. if the observer is specifically trying to avoid a particular phenotype for some reason (e.g. deleterious hybridization).

- *mate choice* - (syn. *intersexual selection*) – where the observer is presented with multiple individuals of the opposite sex. Sometimes synonymized with *mate discrimination*.
    - *mate preference* – a behavioral response by the observer indicating that an individual intends to mate with one individual rather than another (Ryan and Rand, 1993); may be seen as the result of assessment for mate choice.

- *mate competition* - (syn. *intrasexual selection*) – individuals of the same sex compete for access to the opposite sex, who may or may not be presented with any choice (ie. the victor is their only choice). This term is invented by Sampson (1999).
    - *sexual selection* (strict sense)– a trait or behaviour that is exhibited by one gender but not the other, and which increases reproductive potential by attracting potential mates and / or repelling rivals (Darwin, 1871).

- *social selection* – where positively selected traits offer a social but not reproductive advantage to the individual possessing these traits (Tibbetts

and Dale, 2007). Varying definitions of this in the literature (e.g. West-Eberhard, 1983; Sampson, 1999; where it is synonymized with sexual selection) mean that *social signaling* may be preferable (Padian et al., 2010; SVP abstract).

- *kin selection* – (syn. *group selection*) – where close relatives are afforded altruistic behavior by an individual (Marshall, 2011). This requires recognition of shared kinship, though not necessarily to the level of recognition of individuals.
- *individual recognition* – where an individual can recognize other individuals within a population (Tibbetts and Dale, 2007).

Both sides of the debate seem to agree that "mate recognition" (as defined above) was probably an important function for bizarre structures, and both sides appear to be working with the same general taxonomic and phylogenetic framework. From this, hypotheses explaining the evolution and function of bizarre structures can be formulated by deconstructing analysis into phylogenetic distribution, ontogenetic development, stratigraphic distribution, and geographic context. Phylogeny is especially important as many of the most extravagant and rapidly evolving bizarre structures are exhibited by extremely closely related taxa (sister-lineages). Indeed, many taxa are typically only distinguishable from each other by their cranial adornments. This suggests that the processes of speciation (as opposed to mere taxonomic assignment) play an important if not defining role in the origin and function of bizarre structures.

Padian and Horner (2010, p. 12; using a figure from Main et al., 2005) make an interesting suggestion regarding the different expected patterns of morphological evolution from divergence (speciation) when it occurs purely working under natural selection (or "Fisherian sexual selection") compared to divergence incorporating species recognition. They suggest that selection-based morphological change should be directional (i.e. toward a fitness peak), whereas species recognition should be essentially random.

I agree with the idea that the direction (or otherwise) of morphological change is informative, but do not think that if bizarre structures evolved for species recognition then this would necessarily produce a random pattern. Bizarre structures exhibited in pairs of dinosaur sister taxa often show opposite or perpendicular morphological trends (i.e. they are non-random with respect to each other), especially in those taxa that appear to have diverged relatively recently within North America. This is consistent with the hypothesis that species are actively selecting for the evolution of bizarre structures that are morphologically opposite to that of their sister taxon (and potentially, other related taxa). Examples include:

- Basal Ceratopsidae split into the Centrosaurinae & Chasmosaurinae (Lower to Middle Campanian):
    - Centrosaurinae generally characterized by:
        - brown horns that are reducing in size phylogenetically
        - a short broad squamosal
        - an enlarged rostral region

        - an enlarged nasal horn
    - Chasmosaurinae are characterized by:
        - long brow horns
        - an elongate squamosal
        - reduced but elongated rostral region
        - small nasal horn.
- Chasmosaurinae underwent a further cladogenetic split (Middle Campanian; partly covered in Chapter 4) into the *Chasmosaurus* & *Pentaceratops* lineages:
    - *Chasmosaurus* lineage ("*Chasmosaurus russelli" – C. belli – YPM – Vagaceratops – Kosmoceratops*):
        - Shallowing parietal embayment
        - Development of array of epiparietals
        - Brow horn reduction
    - *Pentaceratops* lineage (*Utahceratops – Pentaceratops – Navajoceratops – Terminocavus – Anchiceratops*):
        - Progressively deepening parietal embayment
        - Increase in size of epiparietals
        - Maintain long brow horns
- In the Lower to Middle Campanian, there was a cladogenetic split within Hadrosaurinae where *Brachylophosaurus* and *Maiasaura* diverged:
    - *Brachylophosaurus* has a broad, flat, paddle-shaped crest formed from the nasals extending posteriorly over the frontal-parietal area.

- *Maiasaura* has a short erect crest at the nasal-frontal contact
- In the more basal Brachylophosaurini gen. et sp. nov. (MOR 2919; Freedman Fowler and Horner, 2015) the crest is smaller, implying that the crest becomes larger through the lineage, ie. it is continuously selected for size increase
    - The morphology of an equivalently basal *Maiasaura* is unknown, although the closely related *Acristavus* (Gates et al., 2011) has no crest and may represent a basal *Maiasaura* (e.g. Gates et al., 2011) or the sister taxon (and potential ancestor) to both *Brachylophosaurus* and *Maiasaura* (e.g. Godefroit et al., 2012; Prieto-Marquez and Wagner, 2012).

- In the Middle Campanian there is evidence for at least one divergence within Lambeosaurinae between *Lambeosaurus* and *Corythosaurus* lineages.
    - *Corythosaurus* / *Hypacrosaurus*
    - *Lambeosaurus*
- There are potentially more pairings, but phylogenetic resolution is poor for other taxa (e.g. *Gryposaurus*-*Kritosaurus*, *Edmontosaurus*, *Prosaurolophus*)

Furthermore, there is evidence that morphological divergence is continuous in many clades. We do not observe rapid (sub- 1m.y.) divergence into two distinct morphospecies, followed by morphological stasis; rather we see the same morphological trends continuing within individual lineages, exacerbating the morphological differences between sister lineages (e.g. *Chasmosaurus* vs *Pentaceratops* lineages; see Chapter 4).

Note that this line of thinking utilizes anagenetic lineage evolutionary hypotheses, where true cladogenesis is represented by two contemporaneous morphospecies, and anagenesis is suggested by non-overlapping stratigraphically separated morphologies. This is an alternative to the always-cladogenesis philosophy (as proposed by Sampson, 1997; although this is largely an artifact of methodology).

Taxa that possess bizarre structures are contrasted with those that apparently lack such structures (for example, the Maastrichtian hadrosaurid *Edmontosaurus*) or taxa that possess elaborate structures that do not seem to change much (e.g. the Late Campanian lambeosaurine *Parasaurolophus;* and hadrosaurine *Prosaurolophus,* McGarrity et al., 2013).

Neither of the currently suggested hypotheses satisfactorily explain the observed patterns. If bizarre structures evolved only for mate choice (the "sexual selection" of Knell, Sampson, Hone, etc), then this would well-explain the continuously changing nature of display structure morphology, but it would not explain why sister taxa exhibit opposite morphological trends, nor why non-speciose clades exhibit relatively restricted adornments. Conversely, the "species recognition" hypothesis (as characterized by Knell and Sampson etc.) well-explains sister-taxon differences, but cannot account for why structures continue to evolve beyond the point at which a level of morphological distinction has been achieved ("signal redundancy"; Rand & Williams, 1970; highlighted by West-Eberhard, 1983, p. 166).

Furthermore, neither hypothesis presents a viable selection pathway that explains the origin of either a species recognition allele, or a mate choice allele. It is not enough to

merely state (for example) that a species may have a sexual preference for bigger horns: why? How is such a preference selected for?

Hone and Naish (2013, p. 6) state [*italics* my emphasis]:

> "Critically, it is not clear how [a bizarre structure] would evolve to separate putative species through mate identification. Given that extant taxa do not appear to be using these structures for species recognition, a plausible mechanism is required to explain their origin, retention and propagation […]. If speciation occurred allopatrically, an exaggerated structure would be unnecessary because the populations would not be at risk of interbreeding. Ergo, such structures could only be generated during sympatric speciation events. A single interbreeding population would likely have relatively little variance in structure, size and form (be that a small crest vs. none, or two versions of a single crest). Individuals of the population might prefer one form of crest over another, or a crest over none, but this would represent mate choice, not mate recognition. *We may, of course, have overlooked an obvious and simple mechanism for this, but the previously hypothesized example would appear to be a problem for the species recognition hypothesis*."

The particular phylogenetic distribution and patterns of bizarre structures in dinosaurs of the Western Interior are potentially better explained by allopatric speciation combined with the evolution of prezygotic barriers, potentially through the selection process of reinforcement.

Reinforcement

Reinforcement is an evolutionary process that strengthens divergence, helping to complete speciation. It does so through selection for prezygotic barriers to reproduction (preventing mating) in divergent populations that can still produce hybrids, especially including fertile hybrids (Dobzhansky, 1940; Blair, 1955). Reinforcement is innately attractive to biologists (Servedio, 2004) as it is a form of Darwinian selection through which speciation can be initiated and / or completed, thereby linking speciation

("macroevolutionary change") with selection ("microevolutionary change"). Reinforcement is also often invoked as a strong selection process for sympatric speciation, but it may operate equally in incomplete allopatric speciation, or parasympatry.

Example. To illustrate how and when reinforcement comes into play, let us take the idealized example of hypothetical species A, through time, T.

T_0. At time 0, species A enjoys uninterrupted geneflow throughout its breeding population that resides on a continental landmass.

T_1. Now imagine that some physical barrier arises that divides species A into two separate populations (population Ab and Ac), and preventing geneflow between them: this is a vicariance event, the first stage 0of allopatric speciation.

T_{1+}. If the environmental conditions for population Ab are different from Ac, then natural selection may favor different adaptations or alleles in each population. Even if conditions are the same, genetic drift will cause gradual accumulation of genetic differences between populations.

T_6 (long time after T_1). Under the classic allopatric speciation model, these accumulated changes (either by natural selection or genetic drift) build up over time (T_1 to T_6) such that the two populations become so different that if presented with the opportunity to interbreed, hybrids would be inviable. This is the definition of the biological species concept (BSC), and at this point the two populations would be considered as two different species (B and C).

T_3 (short time after T_1). However, it is possible that removal of the physical barrier between populations Ab and Ac occurs after only a low number of generations (T_1 to T_3) such that upon reintroduction, populations Ab and Ac may still be able to produce viable offspring (ie. offspring that could go on to reproduce themselves). Thus, the two populations would not yet have reached the BSC definition of a species, and hence would still be considered populations Aa and Ab of species A. In this situation, the reintroduced populations may simply continue as a single species, perhaps as two varieties, but enjoying geneflow between the populations. However, in this situation it is also possible that hybrids would be less fit than "pure breeds" of either population Ab or Ac. This can occur for a number of reasons: 1. If the different populations live in different environments and have adapted slightly: maybe population Ab has a small beak for procuring seeds from the common food plant in its habitat, whereas population Ac has a large beak adapted to a different plant: hybrids with medium sized beaks (say) would be less competitive in either environment. 2. Reproductive behavior & structures may have changed between populations, such that hybrids either lack or weakly develop an appropriate structure or behavior and are less able to compete for mates. 3. Genetic drift may simply have accumulated enough genetic differences such that hybrids suffer deleterious combinations of alleles and reproduce less successfully than pure breeds (neutral evolution).

Situation T_3 is where the selection process of *reinforcement* comes into play. When hybrids of the two populations are viable, but are less competitive than 'pure' breeds of either population, then selection will therefore favor individuals that breed

within their own population (assortative mating). This occurs by increased selection for pre-zygotic barriers that prevent or dissuade mating with the sister population (or encourage mating within your own population), thus *reinforcing* their separation (Marshall et al., 2002; Johnson, 2008). Potential pre-zygotic barriers include differences in display structures (including color), sound or scent cues, behavior (especially courtship behavior), physical incompatibility of reproductive structures, timing of reproduction, and many more. Importantly, reinforcement acts upon formerly recently separated breeding populations that already have some kind of division that came into existence by some other means. Although the given idealized example above demonstrates reinforcement acting on small changes accumulated during a brief period of allopatry, reinforcement may also occur in sympatry, when a species is subjected to strong disruptive selection (e.g. Feder et al., 2003; Matute, 2010).

It is notable that reinforcement (which is fundamentally a "mate recognition" subprocess of "species recognition") may act to select for and strengthen traits considered as "sexual selection" by Knell and Sampson (2011; etc.), and especially "mutual sexual selection" (Hone et al., 2011; etc.). Further, it seems common for authors to be implicitly describing reinforcement when discussing mechanisms of increased selection for prezygotic barriers in parapatric or sympatric species (e.g. the discussion of divergent mating signals and speciation in West-Eberhard, 1983, p.177). This strengthens the view that "species recognition" and "sexual selection" may have a hierarchal or a continuous relationship (e.g. Padian and Horner, 2013; Boake et al., 1997; see above).

Technically, reinforcement occurs in the area between the extremes of species concept definitions. Reinforcement only acts after the point of phylogenetic speciation (i.e. separated genepools; early allopatry) but before the point of biological speciation (beyond which hybrids are not viable; Hausdorf, 2011). Technically this is close to the definition of the "differential fitness" species concept: where species are "characterized by features that would have negative fitness effects in other groups and that cannot be regularly exchanged between groups upon contact" (Hausdorf, 2011). This is also probably just beyond the point of a subspecies status (under the Biological Species Concept): where interbreeding is possible, but the subspecies population has been reproductively isolated for a period of time sufficient to accumulate notable allele frequency differences.

Reinforcement has a related selection process: *the Wallace effect* (Johnson, 2008; sometimes synonymized with reinforcement under either name) which concerns the selection for postzygotic barriers (ie. barriers to hybridization that occur after mating). These generally refer to some level of hybrid inviability, where the hybrid either fails to develop properly, or develops to adulthood but is sterile in one or both genders. To most workers, this represents divergence that has proceeded beyond the biological species concept.

After Dobzhansky (1940) through to the early 1970's, the idea of reinforcement as a speciation mechanism became very popular among biologists. However, there was a decline in support and interest through the late 1970's and 1980's as theoretical models suggested that reinforcement was statistically unlikely (Marshall et al., 2002).

Specifically, the "two-allele model" (see review in Johnson, 2008) suggested that reinforcement required two simultaneous allele changes in order to work: 1. a mutation that changes a trait of one gender (typically the male), and 2. a mutation that makes the opposite gender desire such a trait (ie. mate choice). The apparent necessity of two simultaneous mutations that serendipitously corroborate was considered so improbable that reinforcement could only be very rare at best. However, since the mid 1990's reinforcement has once again been reconsidered as an important force, mainly due to the development of "one-allele" models, and the identification of reinforcement acting in many extant animals (Marshall et al., 2002; Johnson, 2008).

The Hypothesis Regarding Dinosaurs of the Western Interior

Here I suggest that the opposite morphological trends observed in stratigraphically successive taxa within recently diverged dinosaur lineages are potentially best explained by the evolutionary process of reinforcement. This proposal has two main aspects or hypotheses, drawn from the findings of Chapters 2 through 4:

1. That true speciation events (represented by lineage divergence) are relatively infrequent and initiated by movement of paleoshorelines. This primarily concerns periods where transgression means that the shoreline immediately abuts the Sevier thrust front, reducing or preventing geneflow between northern and southern dinosaur populations, and inducing allopatric speciation by vicariance.

2. That the bizarre structures which distinguish sister-lineages evolve via selection processes related to speciation. Particular interest is focused on the possibility of reinforcement and the formation and strengthening of prezygotic barriers.

Methods

Testing the Evolution of Prezygotic Barriers in the Extant and Fossil Record

It is worth re-emphasizing that pre- and post- zygotic barriers may either be directly selected for (via the Wallace effect or reinforcement; example T_3, above), or may be a byproduct of divergence (e.g. example T_6, above). The question is how to differentiate among these origins in both the extant and fossil record, if indeed this is possible.

By definition, reinforcement acts between two breeding populations that are at least partially sympatric or parapatric. The area where the two population ranges overlap (or touch) is known as the hybrid zone as it is here that there is a risk of less-fit hybridization. It follows that under reinforcement, assortative mating must be higher in the hybrid zone than in areas where hybridization is not a risk, and that this should be inferred by understanding "the genetics of trait differences, patterns of mating in the field, the cost of a heterospecific mating, and the discriminatory abilities of females and/or males" (Marshall et al., 2002, p. 558).

The fossil record does not immediately lend itself to studies of reinforcement as most of these strict criteria are not knowable from fossils, primarily because they were set up by biologists to test for reinforcement in the extant record. However, the advantage of

the fossil record is that we can use it to analyze phenotypes generated under natural conditions (ie. not in a laboratory setting) over geological time, an alternative method which is not available to biological workers. This sets up a number of predictions as to what you would expect to see in the fossil record of a given lineage or taxon if selection for prezygotic barriers was occurring (related predictions are outlined in Padian and Horner 2011a).

1. Phylogeny

Phylogenetic analysis should show study taxa as sister lineages that can therefore be inferred to have diverged from a common ancestor at some point in the past (preferably, with stratigraphically successive stem taxa along each divergent lineage).

2. Morphology

Display structure morphology should be divergent between sister-lineages; i.e. they should be selecting in opposite directions in morphospace. If full BSC speciation has occurred already, then hybrids are infertile and the only selective pressure to look different from another “group” remains a late form of reinforcement.

3. Geography

During the time of morphological divergence, sister lineages should be sympatric, partially sympatric or parapatric. However, initially they would have comprised a single ancestral population that becomes divided, probably by a physical barrier (i.e. allopatry).

4. Stratigraphy

The timing of the emergence and removal of physical barriers and the first time that morphological divergence is detected, relies upon precise stratigraphy. The physical barriers that cause vicariance should precede morphological divergence. The strongest pressure for morphological divergence should occur upon reintroduction (or at least this is when the rate of change might be observed to dramatically increase); i.e. the physical barrier may be removed before morphological divergence is detected.

5. Ontogeny

Potentially, the onset of morphological divergence only occurring at the point of reproductive maturity (e.g. hadrosaurs); or if through ontogeny as a whole may be indicative of social signaling. This is interesting ecologically, but is mostly peripheral to the intended main subject of reinforcement.

Results

The above predictions were tested against the 3 clades suspected to be candidates for reinforcement-supported speciation: Centrosaurinae vs Chasmosaurinae subfamilies within Ceratopsidae; *Chasmosaurus* vs *Pentaceratops* lineages within Chasmosaurinae; and *Brachylophosaurus* vs *Maiasaura* lineages within hadrosauridae.

1. Phylogeny

All major phylogenetic analyses of ceratopsids recover Centrosaurines and Chasmosaurines as sister taxa (e.g. Sampson et al., 2010; Longrich, 2015);

Chasmosaurus and *Pentaceratops* are sister lineages (Fowler, Chapter 4), thereby the phylogenetic criterion is satisfied for these first two groupings. In their description of a new brachylophosaurin, *Probrachylophosaurus bergei*, Freedman Fowler and Horner (2015) present two phylogenies; one shows *Brachylophosaurus* and *Maiasaura* as sister taxa, with *Probrachylophosaurus* as the immediate stem taxon (which would not meet the criterion), the other recovers *Probrachylophosaurus* and *Brachylophosaurus* as sister taxa, satisfying the phylogenetic criterion.

2. Morphology

Geometric morphometric analysis (Fowler, Chapter 4) shows that display structure morphology is divergent between the *Chasmosaurus* and *Pentaceratops* sister-lineages, satisfying this criterion. A detailed morphometric analysis has not been conducted for either of the other proposed groupings, however, qualitative analysis (as stated in detail in the introduction, above) shows opposite morphological trends in both Centrosauinae vs Chasmosaurinae, and to a more limited extent in *Brachylophosaurus* vs *Maiasaura*.

3. Geography

Centrosaurinae and Chasmosaurinae clades show evidence of slight geographic segregation, with centrosaurines having a more northern range, and chasmosaurines more southern, although with considerable overlap. Derived centrosaurine remains are undocumented further south than southern Utah (Kaiparowits Formation; Loewen et al., 2013), whereas chasmosaurine remains are documented as far south as Northern Mexico

(e.g. Loewen et al., 2010). Conversely, Centrosaurine remains have been recovered as far north as northern Alaska (Fiorillo et al., 2010), whereas chasmosaurines are not known further north than southern Alberta (e.g. Ryan and Evans, 2007).

It has been suggested (e.g. Lehman, 2001) that *Chasmosaurus* and *Pentaceratops* clades might be geographically segregated, with *Chasmosaurus* limited to the north (Dinosaur Park Formation, Alberta) and *Pentaceratops*-related taxa limited to the south (Utah and New Mexico). However, the phylogenetic analysis of Fowler (Chapter 4) shows that the northern chasmosaurine *Anchiceratops* (Horseshoe Canyon Formation, Alberta, uppermost Campanian) is a derived member of the *Pentaceratops* lineage (which had not been previously considered). Moreover, recent fragmentary specimens (Longrich, 2014) suggest that a *Pentaceratops* lineage chasmosaurine is present in the Dinosaur Park Formation of Alberta (Middle Campanian). It is notable however, that in general, *Pentaceratops*-lineage chasmosaurines are rare in northern North America before the Early Maastrichtian, which may suggest an originally more southern range (see Chapter 4 for discussion). In support of this, the southernmost known member of the *Chasmosaurus* lineage is *Kosmoceratops* from the middle unit of the Kaiparowits Formation (Sampson et al., 2010). Thus it can be shown that *Chasmosaurus* and *Pentaceratops* lineages have an overlapping geographic range, but that they are more abundant in the north and south, respectively.

Brachylophosaurus and *Maiasaura* clades are more difficult to assess as they are known from a more restricted geographic area. The derived form *Maiasaura* is only recorded from the Two Medicine Formation of western Montana (Horner et al., 2001). In

Brachylophosaurini, the basal *Probrachylophosaurus* is only recorded from the lower Judith River Formation of north central Montana, whereas the more derived *Brachylophosaurus* is slightly more cosmopolitan, being recorded from the Oldman Formation, southern Alberta, and equivalent middle to upper part of the Judith River Formation in north central Montana (Freedman Fowler and Horner, 2015). It is notable that the ranges of *Maiasaura* and *Brachylophosaurus* are adjacent but not known to overlap. Furthermore, unlike the previous example, *Maiasaura* and *Brachylophosaurus* show no indication of latitudinal segregation; rather *Maiasaura* is known from more inland deposits, whereas *Brachylophosaurus* are recovered from coastal plain sediments closer to the Western Interior Seaway. However, given the relative rarity of fossils from these groups, this interpretation can only be tentative.

4. Stratigraphy

Unfortunately, the fossil record of Ceratopsidae is relatively poor around the time when Centrosaurinae diverged from Chasmosaurinae (?Santonian), and also the divergence point of *Chasmosaurus* and *Pentaceratops* lineages (probably Early Campanian; see Chapters 3 and 4). However, this corresponds to a period of relatively high sealevel when the Western Interior Seaway directly abutted the thrust front of the incipient Rocky Mountains from southern Utah as far north as Montana; roughly the dividing line between purported northern and southern faunal provinces (e.g. Lehman, 2001). This is elaborated further in the discussion.

A possible ancestral taxon to both *Maiasaura* and *Brachylophosaurus* is the non-crested basal taxon *Acristavus*, described from the Lower Campanian of Montana and

Utah (Gates et al., 2011; Freedman Fowler and Horner, 2015). The stratigraphic position of *Acristavus* would be consistent with it being an ancestor (e.g. Freedman Fowler and Horner, 2015), although in some phylogenetic analyses it is recovered as the sister taxon to *Maiasaura* (Gates et al., 2011). There are no obvious physical barriers that might explain the segregation of *Maiasaura* and *Brachylophosaurus*. However, I suspect that the relatively restricted fossil record of these taxa might be obscuring their true geographical ranges, such that full assessment is not possible.

5. Ontogeny

Detailed ontogenetic series are still rare for most dinosaurs. However, it has been shown that cranial display organs in ceratopsids develop through ontogeny at a fairly constant rate, rather than remaining static then developing quickly upon acquisition of sexual maturity (e.g. see Horner and Goodwin, 2006; Brown et al., 2009; Fowler, Chapter 4). The situation for the hadrosaurid examples is less clear. Although a good ontogenetic series is known for *Maiasaura* (Horner and Makela, 1979; Horner, 1983), development of cranial display organs has not been described. In *Brachylophosaurus*, the paddle-shaped crest develops through ontogeny relatively constantly (Freedman Fowler and Horner, 2015), similar to changes in ceratopsids.

Other Potential Causes of the Same Patterns

Although the fossil records of the three studied groups largely conform to the patterns expected of reinforcement, it should be noted that there are other potential explanations for these patterns:

"Neutral evolution" or genetic drift – where non-adaptive changes accumulate in allopatry. This can account for notable morphological variation among sister-species or subspecies (e.g. as recently documented for the "ring species" greenish warbler of the Tibetan Plateau; Martins et al., 2013) and may account for directionless morphological change, but it cannot account for "species" evolving in opposite directions in morphospace

Ecological Character Displacement (ECD) – Where species with similar resource requirements appear morphologically similar in allopatry, but strongly diverge in sympatry; a form of in situ coevolution (see critical review by Stuart & Losos 2013). ECD and reinforcement are potentially differentiable as reinforcement should only affect prezygotic characters (mainly display), whereas ECD may affect other characters associated with non-reproductive functional morphology. Also, ECD does not require a close phylogenetic relationship between competing organisms. The related term "reproductive character displacement" (e.g. West-Eberhard, 1983) is an alternative term for prezygotic barriers and reinforcement.

Correlated evolutionary response (CER) – Where there is no active selection for divergence of trait X, but it changes because it is correlated with trait Y that is under divergent selection (Nosil et al., 2009). If reinforcement was not active, and species evolved completely in allopatry (ie. completion from PSC to beyond the point of BSC), then it is difficult to explain the opposite nature of display organs unless these organs are somehow correlated with other characters (CER).

The fact that it is difficult to differentiate reinforcement from other related processes should not dissuade its use as a potential explanatory tool in understanding evolutionary patterns in the fossil record, especially as these other processes have been given much consideration recently. I think that reinforcement potentially reconciles many apparently disparate views regarding the evolution of dinosaurs of the Late Cretaceous Western Interior.

Discussion

Geographic Barriers

Previous publications on Western Interior dinosaur dispersal and vicariance patterns have suffered from a combination of mismatched or poor stratigraphic resolution, taxonomic confusion caused by oversplitting (often due to ontogenetic variation), and misunderstanding of the difference between anagenetic lineages and true speciation events (Lehman, 1987; 1997; 2001; Sampson and Loewen, 2010; Sampson et al. 2010; Gates et al., 2010; 2012).

The studies on speciation and biogeography by Gates et al. (2010; 2012) and Horner et al. (1992) have a similar basis to what I am proposing in that they look for barriers to geneflow. Gates et al (2010) performed quantitative biogeographic comparisons of six roughly contemporaneous "Late Campanian" formations, using a number of statistical methods. They found strong support for divergent northern and southern faunas (with a possible central mixing zone), suggesting that this was due to latitudinal climate variation as there was no evidence for a physiographic barrier between the units. However, this study used incomparable radiometric dates which had the result

of misrepresenting diversity, and overestimated species-level diversity due to a lack of lineage-thinking. I agree with some of the broad findings, but I find the taxonomic and stratigraphic shortcomings too severe for the results to be considered reliable. In notable contrast to their previous paper, Gates et al. (2012) suggested that physiographic barriers did in fact exist within Laramidia, and that incipient Laramide orogenic uplifts in the Campanian subdivided the subcontinent of Laramidia into separate sub-basins, which subdivided populations of dinosaurs, encouraging allopatric speciation. This hypothesis is more closely related to the "extreme faunal endemism" of Sampson et al. (2010). However, this hypothesis is unsatisfactory for a number of reasons. 1, there is no geological evidence for significant Laramide uplifts in the Campanian that may have divided the Western Interior Basin. Indeed Lawton (2008) suggests that despite incipient Laramide orogenic uplifts through the Late Campanian-Maastrichtian, Laramide-style basins were not present in the Western Interior until after the K-Pg boundary. 2, the proposed geographic barriers appear to restrict distribution of some Late Campanian clades (e.g. *Chasmosaurus*; *Nasutuceratops*), yet other clades (e.g. *Gryposaurus*, *Parasaurolophus,* and eventually *Anchiceratops*) suffer no such impediment. 3, a number of speciation events are expected to have occurred in the Lower to earliest Middle Campanian, not the Middle to Upper Campanian as suggested, by which time, lineages are merely undergoing anagenetic change.

Horner et al. (1992) observed a succession of dinosaur morphospecies from the uppermost Two Medicine Formation (Upper Campanian, Montana), deposited during the T9 Bearpaw cyclothem (Kauffman and Caldwell, 1993). They suggested that

transgression and regression of the Western Interior Seaway alternately restricted and expanded (respectively) available habitat space in Laramidia, and that in the case of the Two Medicine dinosaurs, transgression caused habitat bottlenecking with the resultant stress stimulating evolutionary (anagenetic) change in multiple lineages of dinosaurs (Centrosaurinae; Lambeosaurinae; Pachycephalosauridae; and Tyrannosauridae). I agree that constant cycles of transgression and regression probably had significant effects on dinosaur evolution in the Western Interior, but I do not think that the Two Medicine dinosaurs were undergoing an unusual pulse of evolution; since the publication of Horner et al. (1992) it has been recognized that many other clades of Western Interior dinosaurs show similar rapid change (e.g. Holmes et al., 2001; Fowler, 2006; Horner & Goodwin, 2006; Scannella & Horner, 2010; Mallon et al., 2012; Part 3 of this proposal), including centrosaurines and lambeosaurines that immediately precede, and were probably ancestral to, the Two Medicine forms (Ryan & Russell, 2005; Eberth & Evans, 2011). As such I suspect that the anagenesis observed by Horner et al. (1992) may represent normal rather than unusual conditions. However, it is interesting that there is variation in rates of change between clades; this is potentially explained by the effects of repeated speciation events.

Allopatry and Endemism

There has been much debate over the past 20 years over the significance of apparent differences between dinosaur faunas in northern and southern regions of North America (Lehman, 1997; 2001; Sampson et al., 2010). While some purported endemism is undoubtedly the result of stratigraphic incongruence (e.g. Sullivan and Lucas, 2006),

there do appear to be genuine latitudinal biogeographic patterns for many clades of vertebrates (including marine vertebrates; Kauffman, 1984; Nicholls and Russell, 1990; Gates et al., 2010; Brinkman, 2003), albeit not as extreme as some have suggested (Sampson et al., 2010; Gates et al., 2012). Many clades also exhibit distributions that vary from east (distal coastal plain / swamp) to west (upper coastal plain / inland), in particular ceratopsids (Brinkman et al., 1998), and turtles (Holroyd and Hutchison, 2002), but also faunas in general (e.g. broad differences between the Two medicine and Judith River faunas; Gates et al., 2010).

It is probably useful to conceptually separate the potential effects of latitudinal climate variation from the after-effects of allopatric speciation. Clades may be separated into northern and southern taxa as a result of differing habitat requirements, or as a result of an earlier phase of allopatry (or a combination of both).

Preliminary work further suggests a relationship between transgressive-regressive events and periods of immigration/migration and isolation (leading to speciation). Detailed maps of paleoshorelines, and their position relative to the Sevier thrust front are provided by Lillegraven and Ostresh (1990), Cobban et al. (1994), and Robinson-Roberts and Kirschbaum (1995; none of which are cited by Gates et al., 2010; 2012, who instead use the popular maps of Ron Blakey). These maps (especially Lillegraven and Ostresh, 1990) show that from the Santonian to Lower Campanian, the shoreline of the Western Interior Seaway abutted the Sevier orogenic thrust front from mid-Utah (~38^{o}) through to mid-Wyoming (~43^{o}). This would be a considerable barrier to geneflow between northern and southern terrestrial vertebrates, including populations of dinosaurs, and also

correlates with the rough boundaries of northern and southern faunas (e.g. Gates et al., 2010), and the expected timing of divergence between Centrosaurinae-Chasmosaurinae (?Santonian), and *Chasmosaurus-Pentaceratops* lineages (Early Campanian).

If Vrba (1985) is correct, then periods of isolation leading to speciation may be only very brief. Such periods may or may not be represented by deposition in the terrestrial geologic record. The suggestion that we see repeated, almost continuous divergence events (ie. Sampson, 1999; Sampson et al., 2010) is at odds with biological thinking that these punctuations are relatively rare (i.e. Vrba, 1985).

It follows that clades of dinosaurs that have been separated by some physical barrier to geneflow may then become susceptible to reinforcement upon reintroduction after removal of the barrier. This predicts that while in allopatry, newly divergent populations may look similar to each other (assuming that geographic separation is merely "inconvenient" for geneflow), and that only after reconciliation (probably related to an abiotic event, e.g. regression) will we see significant morphological divergence (although this may depend on how long each lineage has been in isolation). Another prediction is that reproductive display morphology will trend in the opposite direction to a sister taxon, something that is observed in all three of the examined groups (see above), and that is unexplainable by a classic allopatry or other model (other than ECD). Moreover, there appears to be little functional difference between sister-lineages. If we were observing a single population that got split into two reproductively isolated populations (i.e. classic allopatry), assuming that the selection pressures for each population are fairly similar, we might expect to see parallel morphologic trends (i.e.

parallel evolution). Indeed this is generally what we see in functional aspects of morphology (feeding adaptations in the skull; locomotor adaptations of the postcrania). However, in display organs we instead observe divergent evolution, the selection for which is difficult to explain other than by the presence of something against which to contrast your own morphology.

Potentially, if the initial function of a dinosaur's crest is avoiding mating with a parapatric or sympatric sister taxon, then a “mutual sexual selection” or social signaling preference may then get hard-wired into the genetics of the population. If initially it is advantageous to avoid breeding with the sister lineage, then any way of doing so will be selected for, ie. the signaler is positively selected for having a species-distinctive crest (probably the initial trigger), and the signal receiver is positively selected for having a preference for its own specific type of crest. Thus in the second case, this reproductive preference for your own crest becomes genetically based, and future populations may continue to select for the crest (a form of phylogenetic inertia), simply because of genetically-based preferred mate choice unless the crest somehow becomes disadvantageous (perhaps too large), or selection changes direction for some reason. Thus, once selection for consistent morphological change away from a sister taxon is hardwired into the genome, it may persist even if selection is relaxed.

Another prediction would be that taxa which do not share their environment with a sister taxon (or at least, a closely related taxon) would be expected to exhibit either reduced propensity for display organs, or a slower or relatively static rate of change in a display organ (West-Eberhard, 1983). If reinforcement and/or prezygotic barriers are an

explanation for the bizarre display structures, then this may suggest that clades that exhibit relatively muted display structures (e.g. *Edmontosaurus*), may have (anagenetically) evolved in relative isolation with little risk of deleterious hybridization, and hence no need for pre or post-zygotic isolation. Alternatively, taxa that exhibit no bizarre structures (e.g. *Edmontosaurus*) or have structures that seem to have changed little over the same time frame as related taxa have changed much (e.g. *Parasaurolophus*) may represent *relaxation* of selection for possession or enhancement of bizarre structures. Such taxa may have undergone speciation elsewhere (perhaps before entering North America), and therefore experienced strong selection for change in the past, but the pressure is relaxed when they are no longer living alongside a sister lineage. This may also have some biogeographic importance.

Significance of These Concepts for Dinosaur Paleontology

Most significantly, this chapter draws together many currently disparate viewpoints of dinosaur paleobiology in the Late Cretaceous of North America. It potentially gives a functional explanation and viable selection pathway for bizarre structures that incorporates both "sexual selection" (*sensu* Knell & Sampson, 2011; etc.) and "species recognition" (*sensu* Padian & Horner, 2011ab, 2013).

Selection for reproductive barriers may explain the origin of increased "intensity" of evolution of bizarre structures in some clades (intensity of "sexual selection", *sensu* Sampson, 1999). Sampson (1999, HB, p179-180) suggests that if sexual selection is more intense in one clade (rather than another; using Vrba's antelope as an example) then

mating signals may diverge faster, causing more frequent speciation. It is possible that sexual selection is more intense because of reinforcement, which if hard-wired into the genome, will naturally predispose particular clades to speciation. Clades that undergo reduced sexual selection (because of no need for reinforcement), will be able to undergo longer periods of isolation with less likelihood of having undergone enough change to force speciation. Thus, reinforcement induced sexual selection may be self-perpetuating, especially so in environments where environmental perturbations / geographic isolation mechanisms are common.

Reinforcement potentially explains patterns of "diversity" of Laramidian dinosaurs, where speciation is initiated by occasional short periods of isolation caused by the combined effects of transgression/regression and climate. This is in agreement with Vrba's (1980; 1985; 1993; 2005) hypothesis that speciation is initiated by "physical change" (abiotic events; i.e. the Court Jester hypothesis; Barnosky 2001; Benton 2009), but "fine tuned" by natural selection (biotic interaction; Red Queens; Van Valen, 1973; Benton, 2009). Firstly, reinforcement presents a viable selection pathway for the origin of apparent differences in northern and southern taxa, which incorporates both biogeographic endemism (e.g. Lehman, 2001; Sampson et al., 2010) and the perspective that this represents stratigraphic patterns of occurrence (Sullivan and Lucas, 2006; Fowler, 2006). Second, it has often been noted that diversity of Campanian dinosaurs appears to be higher than that of the Maastrichtian, and some authors have suggested this is indicative of a gradual decline in diversity towards the K-Pg boundary extinction (e.g. Archibald, 2011). In contrast, reinforcement potentially supports the view that apparent

decline in dinosaur diversity from the Campanian to Maastrichtian may be peculiar to, or exacerbated in, North America as an artifact of its unusual geographic setting; combining the effects of an isolated subcontinent subjected to intermittent immigration and speciation due to the effects of eustasy and/or shoreline position with a north-south orientation of a narrow ecospace, enhancing the effects of a normal latitudinal environmental gradient.

Impact of These Concepts on Speciation Studies

There has been a recent revival on the topic of speciation in the biological literature; most notably, more advanced computer capabilities and increased genetic sampling have facilitated modeling and direct testing of selection processes. However, while geneticists have identified the expected allele frequency changes occurring through selection and speciation, they have had a much more difficult job identifying the initial triggers or agents of isolation that prevent geneflow between populations sufficient to initiate and complete speciation (Albert & Schluter, 2005). Potentially this is because these events may be so infrequent that they are typically not observed over human timescales. The geological record has much to offer in this respect.

From this perspective, it is possible that study of extant systems may offer only a limited view of speciation processes. It follows that if abiotic factors (environmental cycles or perturbations) are a significant but infrequent factor in creating barriers to geneflow, then study of extant animals may be relatively uninformative for understanding long term evolutionary patterns. Study of microevolutionary fluctuations in a modern stable system may only be looking at the after-effects of isolating mechanisms or

macroevolutionary events; i.e. organismal interaction (Red queens hypothesis) may drive evolution, but typically only abiotic events (court jester) may initiate speciation. Of course, extant taxa that have shorter generation times and potentially smaller species ranges (e.g. insects) may still provide useful models for larger organisms.

Conservation and Environment

The study has implications for modern conservation biology as it investigates how changing climate bands interacting with habitat fragmentation can affect terrestrial ecosystems and speciation, perhaps allegorical to what is occurring today with climate change. How long can species exist in fragmented environments before the seeds of speciation are sown? If there is no geneflow between isolated forest patches, how many generations must pass before a species will develop limited genepools and upon reintroduction (perhaps due to conservationist efforts planting forested corridors) select for pre-zygotic reproductive barriers? Taxa with long generational turnover times (e.g. large bodied vertebrates) may not be as strongly affected, but short-turnover taxa such as insects may be more susceptible. If a keystone species happens to be a short-generation-turnover taxon, then splitting the species into units too small for long-term survival may be very dangerous for long-term survival. In this way, habitat fragmentation can lead to multiple pre-zygotic barriers becoming emplaced, forcing speciation, with the result that a previously ubiquitous single species may be highly fragmented into many more local species. This cascade speciation effect may increase extinction susceptibility if emergent species' populations are too small for long-term survival. Future research should

investigate whether the most speciose clades go extinct more readily than slow change, low diversity clades.

References Cited

Archibald, J. D. 2011. Extinction and Radiation: How the Fall of Dinosaurs Led to the Rise of Mammals, 1st ed. The Johns Hopkins University Press, 120 pp.

Barnosky, A. D. 2001. Distinguishing the effects of the Red Queen and Court Jester on Miocene mammal evolution in the northern Rocky Mountains. Journal of Vertebrate Paleontology 21:172–185.

Benton, M. J. 2009. The Red Queen and the Court Jester: Species Diversity and the Role of Biotic and Abiotic Factors Through Time. Science 323:728–732.

Blair, W. F. 1955. Mating Call and Stage of Speciation in the Microhyla olivacea-M. carolinensis Complex. Evolution 9:469.

Boake, C. R. B., M. P. DeAngelis, and D. K. Andreadis. 1997. Is sexual selection and species recognition a continuum? Mating behavior of the stalk-eyed fly Drosophila heteroneura. Proceedings of the National Academy of Sciences 94:12442–12445.

Brinkman, D. B. 2003. A review of nonmarine turtles from the Late Cretaceous of Alberta. Canadian Journal of Earth Sciences 40:557–571.

Brinkman, D. B., M. J. Ryan, and D. A. Eberth. 1998. The paleogeographic and stratigraphic distribution of ceratopsids (Ornithischia) in the upper Judith River Group of Western Canada. Palaios 13:160–169.

Brown, C. M., A. P. Russell, and M. J. Ryan. 2009. Pattern and transition of surficial bone texture of the centrosaurine frill and their ontogenetic and taxonomic implications. Journal of Vertebrate Paleontology 29:132–141.

Castellano, S., and P. Cermelli. 2006. Reconciling sexual selection to species recognition: A process-based model of mating decision. Journal of Theoretical Biology 242:529–538.

Cook, O. F. 1906. Factors of species-formation. Science 23:506–507.

Darwin, C. 1859. The Origin of Species by Means of Natural Selection. John Murray, London.

Darwin, C. 1871. The Descent of Man and Selection in Relation to Sex. John Murray, London.

Dawkins, R. 1986. The Blind Watchmaker: Why the Evidence of Evolution Reveals a Universe without Design. WW Norton & Company, 227 pp.

Dobzhansky, T. 1940. Speciation as a stage in evolutionary divergence. American Naturalist 74:312–321.

Eldredge, N., and S. J. Gould. 1972. Punctuated equilibria: an alternative to phyletic gradualism; pp. 82–115 in T. J. M. Schopf (ed.), Models in Paleobiology. Freeman Cooper, San Francisco.

Evans, D. C., L. M. Witmer, and J. R. Horner. 2011. A new low-crested lambeosaurine hadrosaurid from the Dinosaur Park Formation of Sandy Point, eastern Alberta. International Hadrosaur Symposium Abstracts Volume 48–49.

Feder, J. L., J. B. Roethele, K. Filchak, J. Niedbalski, and J. Romero-Severson. 2003. Evidence for Inversion Polymorphism Related to Sympatric Host Race Formation in the Apple Maggot Fly, Rhagoletis pomonella. Genetics 163:939–953.

Fiorillo, A. R., P. J. McCarthy, P. P. Flaig, E. Brandlen, D. W. Norton, P. Zippi, L. Jacobs, and R. A. Gangloff. 2010. Paleontology and Paleoenvironmental Interpretation of the Kikak-Tegoseak Quarry (Prince Creek Formation: Late Cretaceous), Northern Alaska: a Multi-Disciplinary Study of a High-Latitude Ceratopsian Dinosaur Bonebed; pp. 456–477 in New Perspectives on Horned Dinosaurs. The Royal Tyrrell Museum Ceratopsian Symposium. Indiana University Press.

Forster, C. A., and A. A. Farke. 2005. Dinosaur disputes, What good was all that headgear: for defense. Natural History May 2005:48–49.

Fowler, D. W., and L. E. Hall. 2011. Scratch-digging sauropods, revisited. Historical Biology 23:27–40.

Fox, R. C. 1978. Upper Cretaceous terrestrial vertebrate stratigraphy of the Gobi Desert (Mongolian People's Republic) and western North America. Geological Association of Canada Special Paper 18:571–594.

Freedman Fowler, E. A., and J. R. Horner. 2015. A New Brachylophosaurin Hadrosaur (Dinosauria: Ornithischia) with an Intermediate Nasal Crest from the Campanian Judith River Formation of Northcentral Montana. PLOS ONE 10:e0141304.

Gates, T. A., A. Prieto-Márquez, and L. E. Zanno. 2012. Mountain Building Triggered Late Cretaceous North American Megaherbivore Dinosaur Radiation. PLoS ONE 7:e42135.

Gates, T. A., J. R. Horner, R. R. Hanna, and C. R. Nelson. 2011. New unadorned hadrosaurine hadrosaurid (Dinosauria, Ornithopoda) from the Campanian of North America. Journal of Vertebrate Paleontology 31:798–811.

Gates, T. A., S. D. Sampson, L. E. Zanno, E. M. Roberts, J. G. Eaton, R. L. Nydam, J. H. Hutchison, J. A. Smith, M. A. Loewen, and M. A. Getty. 2010. Biogeography of terrestrial and freshwater vertebrates from the late Cretaceous (Campanian) Western Interior of North America. Palaeogeography, Palaeoclimatology, Palaeoecology 291:371–387.

Godefroit, P., F. Escuillié, Y. L. Bolotsky, and P. Lauters. 2012. A new basal hadrosauroid dinosaur from the Upper Cretaceus of Kazakhstan; pp. 335–338 in P. Godefroit (ed.), Bernissart Dinosaurs and Early Cretaceous Terrestrial Ecosystems. Indiana University Press, Bloomington, Indiana.

Goodwin, M. A. 2005. Dinosaur disputes, What good was all that headgear: for decoration. Natural History May 2005:48–49.

Hausdorf, B. 2011. Progress Toward a General Species Concept. Evolution 65:923–931.

Holmes, R. B., C. A. Forster, M. Ryan, and K. M. Shepherd. 2001. A new species of Chasmosaurus (Dinosauria: Ceratopsia) from the Dinosaur Park Formation of southern Alberta. Canadian Journal of Earth Sciences 38:1423–1438.

Holroyd, P. A., and J. H. Hutchison. 2002. Patterns of geographic variation in latest Cretaceous vertebrates: Evidence from the turtle component. Geological Society of America Special Papers 361:177–190.

Hone, D. W. E., and D. Naish. 2013. The "species recognition hypothesis" does not explain the presence and evolution of exaggerated structures in non-avialan dinosaurs. Journal of Zoology 290:172-180.

Hone, D. W. E., D. Naish, and I. C. Cuthill. 2012. Does mutual sexual selection explain the evolution of head crests in pterosaurs and dinosaurs? Lethaia 45:139–156.

Horner, J. R. 1983. Cranial osteology and morphology of the type specimen of *Maiasaura peeblesorum* (Ornithischia: Hadrosauridae), with a discussion of its phylogenetic position. Journal of Vertebrate Paleontology 3:29–38.

Horner, J. R., and R. Makela. 1979. Nest of juveniles provides evidence of family structure among dinosaurs. Nature 282:296–298.

Horner, J. R., and M. B. Goodwin. 2006. Major cranial changes during Triceratops ontogeny. Proceedings of the Royal Society B: Biological Sciences 273:2757–2761.

Horner, J. R., D. J. Varricchio, and M. B. Goodwin. 1992. Marine transgressions and the evolution of Cretaceous dinosaurs. Nature 358:59–61.

Horner, J. R., J. G. Schmitt, F. Jackson, and R. Hanna. 2001. Bones and rocks of the Upper Cretaceous Two Medicine-Judith River clastic wedge complex, Montana. Field Trip Guidebook, Society of Vertebrate Paleontology 61st Annual Meeting: Mesozoic and Cenozoic Paleontology in the Western Plains and Rocky Mountains. Museum of the Rockies Occasional Paper 3:3–14.

Johnson, N. A. 2008. Direct Selection for Reproductive Isolation: The Wallace Effect and Reinforcement; pp. 114–124 in C. H. Smith and G. Beccaloni (eds.), Natural selection and beyond: the intellectual legacy of Alfred Russel Wallace. Oxford University Press, Oxford, UK.

Kauffman, E. G. 1984. Paleobiogeography and evolutionary response dynamic in the Cretaceous Western Interior Seaway of North America. Geological Association of Canada, Special Paper 27:273–306.

Kauffman, E. G., and W. G. E. Caldwell. 1993. The Western Interior Basin in space and time. Geological Association of Canada, Special Paper 39:1–30.

Knell, R. J., and S. Sampson. 2011a. Bizarre structures in dinosaurs: species recognition or sexual selection? A response to Padian and Horner. Journal of Zoology 283:18–22.

Knell, R. J., and S. Sampson. 2011b. Bizarre structures in dinosaurs: species recognition or sexual selection? A response to Padian and Horner. Journal of Zoology 283:18–22.

Knell, R. J., D. Naish, J. L. Tomkins, and D. W. E. Hone. 2013a. Sexual selection in prehistoric animals: detection and implications. Trends in Ecology & Evolution 28:38–47.

Knell, R. J., D. Naish, J. L. Tomkins, and D. W. E. Hone. 2013b. Is sexual selection defined by dimorphism alone? A reply to Padian and Horner. Trends in Ecology & Evolution 28:250–251.

Lehman, T. M. 2001. Late Cretaceous dinosaur provinciality; pp. 310–328 in D. H. Tanke and K. Carpenter (eds.), Mesozoic Vertebrate Life. Indiana University Press, Bloomington, Indiana.

Lillegraven, J. A., and L. M. Ostresh. 1990. Late Cretaceous (earliest Campanian/Maastrichtian) evolution of western shorelines of the North American Western Interior Seaway in relation to known mammalian faunas. Geological Society of America Special Papers 243:1–30.

Loewen, M. A., A. A. Farke, S. D. Sampson, M. A. Getty, E. K. Lund, and P. M. O'Connor. 2013. Ceratopsid dinosaurs from the Grand Staircase of southern Utah. At the Top of the Grand Staircase: The Late Cretaceous of Southern Utah. Indiana University Press, Bloomington 488–503.

Loewen, M. A., S. D. Sampson, E. K. Lund, A. A. Farke, M. C. Aguillón-Martínez, C. A. de Leon, R. A. Rodríguez-de la Rosa, M. A. Getty, and D. A. Eberth. 2010. Horned dinosaurs (Ornithischia: Ceratopsidae) from the Upper Cretaceous (Campanian) Cerro del Pueblo Formation, Coahuila, Mexico; pp. 99–116 in New Perspectives on Horned Dinosaurs: The Royal Tyrrell Museum Ceratopsian Symposium. Indiana University Press.

Longrich, N. R. 2014. The horned dinosaurs Pentaceratops and Kosmoceratops from the upper Campanian of Alberta and implications for dinosaur biogeography. Cretaceous Research 51:292–308.

Longrich, N. 2015. Systematics of Chasmosaurus - new information from the Peabody Museum skull, and the use of phylogenetic analysis for dinosaur alpha taxonomy. F1000Research.

Main, R. P., A. R. De, J. R. Horner, and K. Padian. 2005. The evolution and function of thyreophoran dinosaur scutes: implication for plate function in stegosaurs. Paleobiology 294–314.

Mair, W. 2010. Reinforcing Reinforcement. PLoS Biology 8:e1000340.

Marshall, J. A. R. 2011. Group selection and kin selection: formally equivalent approaches. Trends in Ecology & Evolution 26:325–332.

Marshall, J. L., M. L. Arnold, and D. J. Howard. 2002. Reinforcement: the road not taken. Trends in Ecology & Evolution 17:558–563.

Martins, A. B., M. A. de Aguiar, and Y. Bar-Yam. 2013. Evolution and stability of ring species. Proceedings of the National Academy of Sciences.

Matute, D. R. 2010. Reinforcement can overcome gene flow during speciation in Drosophila. Current Biology: CB 20:2229–2233.

Mendelson, T. C., and K. L. Shaw. 2012. The (mis)concept of species recognition. Trends in Ecology & Evolution 27:421–427.

Miller, K. G., G. S. Mountain, J. D. Wright, and J. V. Browning. 2011. A 180-Million-Year Record of Sea Level and Ice Volume Variations from Continental Margin and Deep-Sea Isotopic Records. Oceanography 24:651–655.

Nicholls, E. L., and A. P. Russell. 1990. Paleobiogeography of the Cretaceous Western Interior Seaway of North America: the vertebrate evidence. Palaeogeography, Palaeoclimatology, Palaeoecology 79:149–169.

Padian, K., and J. R. Horner. 2011a. The definition of sexual selection and its implications for dinosaurian biology. Journal of Zoology 283:23–27.

Padian, K., and J. R. Horner. 2011b. The evolution of "bizarre structures" in dinosaurs: biomechanics, sexual selection, social selection or species recognition? Journal of Zoology 283:3–17.

Padian, K., and J. R. Horner. 2013. Misconceptions of sexual selection and species recognition: a response to Knell et al. and to Mendelson and Shaw. Trends in Ecology & Evolution 28:249–250.

Paterson, H. E. 1985. The recognition concept of species. Species and Speciation 4:21–29.

Prieto-Márquez, A., and J. Wagner. 2013. Saurolophus morrisi, a new species of hadrosaurid dinosaur from the Late Cretaceous of the Pacific coast of North America. Acta Palaeontologica Polonica.

Rand, A. S., and E. E. Williams. 1970. An estimation of redundancy and information content of anole dewlaps. The American Naturalist 104:99–103.

Roberts, L. N. R., and M. A. Kirschbaum. 1995. Paleogeography and the Late Cretaceous of the Western Interior of Middle North America; Coal Distribution and Sediment Accumulation. United States Geological Survey.

Ryan, M. J., and D. C. Evans. 2005. Ornithischian dinosaurs; pp. 312–348 in Dinosaur Provincial Park: A spectacular ancient ecosystem revealed. Indiana University Press.

Ryan, M. J., and A. S. Rand. 1993. Sexual Selection and Signal Evolution: The Ghost of Biases past. Philosophical Transactions of the Royal Society of London. Series B: Biological Sciences 340:187–195.

Sampson, S. D., and M. A. Loewen. 2010. Unraveling a radiation: a review of the diversity, stratigraphic distribution, biogeography, and evolution of horned dinosaurs. (Ornithischia: Ceratopsidae); pp. 405–427 in M. J. Ryan, B. J. Chinnery, and D. A. Eberth (eds.), New Perspectives on Horned Dinosaurs. Indiana University Press, Bloomington, Indiana.

Sampson, S. D., M. J. Ryan, and D. H. Tanke. 1997. Craniofacial ontogeny in centrosaurine dinosaurs (Ornithischia: Ceratopsidae): taxonomic and behavioral implications. Zoological Journal of the Linnean Society 121:293–337.

Sampson, S. D., M. A. Loewen, A. A. Farke, E. M. Roberts, C. A. Forster, J. A. Smith, and A. L. Titus. 2010. New Horned Dinosaurs from Utah Provide Evidence for Intracontinental Dinosaur Endemism. PLoS ONE 5:e12292.

Servedio, M. R. 2004. The What and Why of Research on Reinforcement. PLoS Biol 2:e420.

Stuart, Y. E., and J. B. Losos. 2013. Ecological character displacement: glass half full or half empty? Trends in Ecology & Evolution.

Sullivan, R. M., and S. G. Lucas. 2006. The Kirtlandian land-vertebrate "age"–faunal composition, temporal position and biostratigraphic correlation in the nonmarine Upper Cretaceous of western North America. New Mexico Museum of Natural History and Science Bulletin 35:7–29.

Tibbetts, E. A., and J. Dale. 2007. Individual recognition: it is good to be different. Trends in Ecology & Evolution 22:529–537.

van Valen, L. 1973. A new evolutionary law. Evolutionary Theory 1:1–30.

Vrba, E. S. 1980. Evolution, species and fossils: how does life evolve. South African Journal of Science 76:61–84.

Vrba, E. S. 1985. Environment and evolution: alternative causes of the temporal distribution of evolutionary events. South African Journal of Science 81:229–236.

Vrba, E. S. 1993. Turnover-pulses, the Red Queen, and related topics. American Journal of Science 293:418–452.

West-Eberhard, M. J. 1983. Sexual selection, social competition, and speciation. Quarterly Review of Biology 155–183.

CHAPTER NINE

CONCLUSION

This dissertation centered around the importance of stratigraphy to paleobiological interpretation, comprising a number of studies each of which addressed a different aspect of this core question. The first set of studies concerned the Hell Creek Formation of Montana. Here I showed how terrestrial sequence stratigraphic methods can be used to subdivide the Hell Creek Formation into three depositional sequences and related surfaces which can be traced over at least 120 km, and potentially across the region. Incorporated into this work were corrections to lithostratigraphic interpretation (particularly of the cryptic lower contacts), and magnetostratigraphic correlations. This chronostratigraphic framework was subsequently used to plot the stratigraphic position of over 50 skulls of the chasmosaurine ceratopsid *Triceratops* (including detailed locality data not typically published), showing that the two recognized morphospecies are stratigraphically separated with *T. prorsus* present in the upper third, and *T. horridus* found lower in the formation. Transitional *Triceratops* morphologies in the middle unit of the formation were interpreted as evidence of anagenesis, or linear evolution, with *T. horridus* evolving through the unnamed transitional form into *T. prorsus*. A similar study of more basal chasmosaurine ceratopsids named two new taxa from the Upper Campanian Kirtland Formation, New Mexico, *Navajoceratops sullivani* and *Terminocavus sealyi*, which formed stratigraphic and morphologic intermediates between the older taxon *Pentaceratops* (Fruitland Formation, New Mexico) and younger

Anchiceratops (Horseshoe Canyon Formation, Alberta). Lack of overlap between stratigraphically successive taxa similarly suggested anagenesis as the primary mode of morphological change in a "*Pentaceratops*" lineage characterized by deepening and eventual closure of the posterior embayment of the parietal. This was contrasted with the sister-lineage of *Chasmosaurus* which follows an opposite morphological trajectory, shallowing the posterior embayment. Phylogenetic analysis of these basal chasmosaurine clades suggests a deep split within Chasmosaurinae that occurs before the Middle Campanian, creating *Chasmosaurus* and *Pentaceratops* lineages. This is supportive of true speciation (branching) by vicariance occurring relatively basally within Chasmosaurinae, followed by more prolonged periods of anagenetic (unbranching) evolution. Recent hypotheses of extreme faunal endemism are not supported; however, it appears likely that continental-scale latitudinal faunal variation occurred in the Campanian.

The largest single project is a broad-ranging and comprehensive stratigraphic correlation chart comprising the major terrestrial geological formations of the North American Western Interior. Notably, this study recalibrated nearly two hundred ^{40}Ar / ^{39}Ar radiometric dates, including many that had been previously incorrectly recalibrated. This chart represents the most precise and comprehensive correlation currently available for terrestrial geological formations of the North American Western Interior. In combination with fossil locality data, the stratigraphic ranges for dinosaur taxa were plotted on the chart. This revealed that many dinosaur clades comprises stacks of morphospecies that do not overlap stratigraphically, interpreted as most parsimoniously

representing anagenesis. By contrast, true branching events are evidenced by the co-occurrence of more than one species at a single point in time. In combination with high-resolution stratigraphic data, and knowledge of mode of evolution (provided by the stratigraphic chart), here I suggest that the evolutionary process of reinforcement provides the strongest explanation for opposite morphological trends seen in the display organs of some dinosaur sister lineages, reconciling previously disparate viewpoints over whether dinosaur cranial display structures functioned for species recognition or sexual selection. The overarching conclusion of this work is that the interplay of transgression cyclicity with speciation explains patterns of diversity, mode of evolution, and morphologic variation in dinosaurs of the Late Cretaceous Western Interior.

APPENDICES

APPENDIX A

SUPPLEMENTARY INFORMATION FOR CHAPTER 2

Methods: Lithofacies Descriptions

Facies descriptions follow methodology laid out in Miall (1985). Descriptions mostly follow those of Flight (2004) for the Bearpaw Shale and Fox Hills Sandstone. Additional lithofacies are described for the Colgate sandstone, ?Battle Formation, an undivided Hell Creek Formation, and the lowermost 5-10 m of the Fort Union Formation. It was desirable to stay as close to Flight's (2004) definitions as possible in order to facilitate cross comparison between measured sections and interpretation; however I have also chosen to remain true to the intentions of Brown (1906) in keeping the Basal Sandstone (and associated basal scour) as the first unit of the Hell Creek Formation, rather than the tidal flats identified by Flight (2004). This analysis is not as concerned with the nature of the basal contacts as much as internal stratigraphy within the Hell Creek Formation itself, hence some of the stratal and facies relationships described by Flight (2004) were not directly observed by myself, but I have included them here to ease comparisons.

The current work builds on rather than repeats the previous analyses of Flight (2004) and to a lesser extent, Behringer (2008). It is unfortunate that there are so few adequate or accurate analyses of Hell Creek stratigraphy to cite other than unpublished theses, but this is reflective of the few narrowly-focused stratigraphic surveys conducted by paleontologists historically working in the region. It would be intellectually dishonest for me not to acknowledge the strong influence of Flight (2004) on my own analysis. I do so here unreservedly.

Bearpaw Shale

The Bearpaw Shale is the basalmost formation considered in this study; as such only the uppermost 10-20 m have been observed in outcrop. In this upper 20 m or so, the Bearpaw Shale generally coarsens upwards, predominantly comprising shale with occasional interbedded sandstone. All lithofacies display sheet-like geometries.

Geomorphologically, shale units form low, rounded hills, conspicuously different from the cliff forming lithologies of the overlying units. Beds of pale grey to tan, fine grained silty sandstone, up to 1 m thick, become increasingly common in the upper 5-10 m of the formation, where they are interbedded with shale. Sandstones are massive, planar bedded or occasionally hummocky-cross-stratified, weather a pale grey color, and form steeper slopes than the underlying shale. Sandy units within the Bearpaw eventually grade into the overlying Fox Hills Sandstone.

Massive to Laminated Mudstone (Mml)

Lithofacies Mml is a massive to laminated fissile shale, typically mid-dark grey, weathering to dark grey with occasional zones of iron oxidation.

Hydrodynamic Interpretation. Mml is interpreted as representing deposition by fine grains of sediment falling out of suspension in quiet water (Boggs, 2001).

Facies Associations. Mml typically grades vertically into facies Sh or Sm, but may abruptly overlie Sh or Sm. At some localities Mml is erosively overlain by Se of the Basal sand or Jen Rex sand of the Hell Creek Formation. Flight (2004) states that Se of

the Colgate Sandstone may also overlie Mml of the Bearpaw. Although probable, this was not observed in any sections which I measured.

Depositional Process. The gradational contact of overlying facies Sh or Sm is indicative of hemipelagic deposition gradually coming under the influence of higher energy deposition, indicative of shallowing water depth. At localities where Sh or Sm are abruptly overlain by Mml, this is taken to indicate a change from higher energy deposition back to hemipelagic deposition.

Horizontally Stratified Silty Sandstone (Sh)

Lithofacies Sh is a light grey colored, poorly consolidated siltstone or silty sandstone. Grain size is silt-sized to very fine sand. Horizontally stratified beds are usually less than 30 cm in thickness and coarsen upwards. Adapted from Flight (2004).

Hydrodynamic Interpretation. Sh is interpreted as representing upper or lower flow regime deposition, where flows are shallow or of low enough velocity as to not form ripples (Boggs, 2001; Flight, 2004).

Facies Associations. Sh either abruptly overlies Mml, or the contact is gradational. Sh is overlain abruptly by Mml, or gradationally coarsens into Shcs, or Sm of the Fox Hills Formation.

It is noted here that this transitional facies is variably considered as either part of the Bearpaw Shale or Fox Hills Sandstone, depending on which state or region is being

studied (e.g. see Jensen and Varnes, 1964; Landman and Waage, 1993; Landman and Cobban, 2003; Fowler, Chapter 3).

Depositional Process. A gradational contact of Sh over Mml is indicative of hemipelagic deposition gradually coming under the influence of higher energy deposition, indicative of shallowing water depth. An abrupt contact may be more indicative of deposition during storm events (Carr et al., 2003; Flight, 2004). At localities where Sh or Sm are abruptly overlain by Mml, this is taken to indicate a change from higher energy deposition back to hemipelagic deposition.

Massive Silty Sandstone (Sm)

Lithofacies Sm is a light grey colored, poorly consolidated siltstone or silty sandstone. Grain size is silt-sized to very fine sand. Bedding is massive and up to 1-2 meters in thickness. Adapted from Flight (2004).

Hydrodynamic Interpretation. Lack of sedimentary structures in Sm is interpreted as representing either bioturbation by burrowing organisms; rapid deposition; or homogeneity of grain size and sediment type (Flight, 2004).

Facies Associations. Sm either abruptly overlies Mml, or the contact is gradational. Sm is overlain abruptly by Mml, or gradationally coarsens into Shcs, or Sm of the Fox Hills Formation.

It is noted here that this transitional facies is variably considered as either part of the Bearpaw Shale or Fox Hills Sandstone, depending on which state or region is being

studied (e.g. see Landman and Waage, 1993; Landman and Cobban, 2003; Fowler, Chapter 3).

Depositional Process. A gradational contact of Sm over Mml is indicative of hemipelagic deposition gradually coming under the influence of higher energy deposition, indicative of shallowing water depth. At localities where Sm is abruptly overlain by Mml, this is taken to indicate a change from higher energy deposition back to hemipelagic deposition.

Fox Hills Sandstone (Excluding the Colgate Sandstone)

The Fox Hills Sandstone is a complex unit that generally coarsens upwards and exhibits a sheet-like geometry with considerable variation in thickness. Lithologies are typically fine grained sandstones (hummocky cross-stratified, trough cross-bedded, planar bedded, ripple cross laminated, and massively bedded) with less common interbedded mudstone. Flight (2004) notes a number of facies which can be medium or coarse grained, but I did not observe medium or coarse grained sand within the Fox Hills Formation, although sandstones of the overlying Hell Creek Formation are commonly medium grained at their bases, fining upwards. This is corroborated in the definition of the Fox Hills Sandstone given by Jensen and Varnes (1964) who suggest the unit comprises only lower to upper fine sand.

The Fox Hills Sandstone is conspicuous in outcrop by its yellow-orange coloration (Figure 2.4-2.6); generally distinct from the more pale grey sandstones of the

underlying Bearpaw Shale, or overlying Colgate Sandstone and Hell Creek Formation (although the latter are often tan colored).

The gradational transition from the Bearpaw Shale to Fox Hills Sandstone has led to variable lithostratigraphic definitions of the position of the contact (e.g. Landman and Waage, 1993; Landman and Cobban, 2003). For consistency, here the basalmost bed of the Fox Hills Sandstone follows Flight (2004) as being either the first amalgamated hummocky cross-stratified sandstone (in contrast to the isolated units of the Bearpaw Shale), first massive sandstone, or first trough cross-stratified sandstone. Typically the Fox Hills Sandstone is 4-6 m thick, but can reach up to 15 m thick locally (Flight, 2004). Massive bedding and hummocky cross stratification is more common near the base of the formation, with trough cross bedding and ripple cross lamination more common higher up. *Thalassinoides* and *Planolites* burrows are recorded in trough cross-stratified sands by Flight (2004). Large carbonate-concretions are common throughout (Jensen and Varnes, 1964), but especially in the upper part of the unit, which is typically capped by prominent bench-forming cemented sandstones.

Hummocky Cross-Stratified Sandstone (Shcs)

Lithofacies Shcs comprises hummocky cross-stratified well -sorted, well-cemented, fine-grained tan-colored sandstone. Adapted from Flight (2004).

Hydrodynamic Interpretation. Hummocky cross-stratification forms under oscillatory flow conditions, generally taken to represent deposition during storm events (Harms et al., 1975; Dott and Bourgeios, 1982).

Facies Associations. Flight (2004) records that facies Shcs is gradationally overlain by St, Sm, Sr, and Sl, or abruptly overlain by Mml of the Bearpaw Shale. Shcs gradationally overlies Sm, or abruptly overlies Mml of the Bearpaw Shale.

Depositional Process. Shcs is interpreted as representing deposition during storm events (Harms et al., 1975; Dott and Bourgeios, 1982). Abrupt contact with Mml of the Bearpaw Shale represents transition from. Flight (2004) reports that the larger bedform size and bedset thickness of Shcs in the Fox Hills Formation (compared to the Bearpaw Shale) indicates that it was deposited under higher energy conditions (note that Shcs was not noted in the Bearpaw Shale by me here).

Massive Sandstone (Sm)

Lithofacies Sm is a tan to orange colored well-sorted fine-grained sandstone. Bedding is massive and up to 1-5 meters in thickness. Adapted from Flight (2004).

Hydrodynamic Interpretation. Lack of sedimentary structures in Sm is interpreted as representing either bioturbation by burrowing organisms; rapid deposition; or homogeneity of grain size and sediment type (Flight, 2004).

Facies Associations. Sm gradationally overlies Shcs, St, or Sl of the Fox Hills Formation, or Mml of the Bearpaw Shale. Sm is overlain gradationally by Shs, St, Sl, Sr, and Mm of the Fox Hills Formation, or is overlain abruptly by Mml of the Bearpaw Shale. Sm may be erosively overlain by Se of either the Colgate Sandstone or Hell Creek Formation.

Depositional Process. Sm is considered as representing a transitional unit from other sand bodies (St, Hhcs, Sr) which have more defined structure, suggesting that lack of structure in Sm may not be primary. Structure may have been eliminated by bioturbation (Flight, 2004).

Trough Cross-Stratified Sandstone (St)

Trough cross stratified sandstone (St) is recorded as present in the Fox Hills Sandstone by Flight (2004) and Jensen and Varnes (1964), but was not personally noted by myself as the emphasis of my work is not focused on the Fox Hills Formation; this account is therefore based on the observations of these authors. Lithofacies St is a light gray to tan colored well-sorted, poorly to moderately cemented medium grained sandstone. Troughs are 1-2 m wide and ~0.5 m in height. Bed sets are up to 8 m in thickness. Invertebrate feeding traces *Thalassenoides*, *Planolites*, and *Ophiomorpha* are reported as occasionally present by Flight (2004).

Hydrodynamic Interpretation. Trough cross stratification represents dune migration in a lower flow regime with a unidirectional current (Boggs, 2001).

Facies Associations. Flight (2004) observes that St gradationally overlies Shcs, Sm, Sr, or Mm of the Fox Hills Formation, or abruptly overlies Mml of the Bearpaw Formation. St is interbedded or overlain gradationally by Sm, Sr, and Mm, or abruptly by Se of the Hell Creek Formation. Flight (2004) suggests that St might also be gradational above to Fml of the Hell Creek Formation, but this is not shown in any of her measured

sections (in her appendix), and is probably not possible based on the depositional hiatus that exists between the Fox Hills and Hell Creek formations; given that this relationship is not shown in any of the measured sections, then I suspect that this is a misstatement, rather than misidentification of Hell Creek Basal Sand as Fox Hills Formation.

Depositional Process. St represents higher energy deposition than Shcs and Sr. Unlike St of the Hell Creek Formation, St of the Fox Hills is not associated with channel forms, and tends to be found at the top of coarsening upward sequence. In comparison, St of the Hell Creek Formation is associated with large channel forms, and is typically the basal unit in a fining upward sequence that ends with a terrestrial mudstone.

Ripple Cross-Laminated Sandstone (Sr)

Lithofacies Sr is a yellow colored well-sorted fine-grained sandstone with asymmetric ripples. Beds are typically ~0.2 m in thickness, but observed up to 0.5 m.

Hydrodynamic Interpretation. Sr is interpreted as forming in a lower flow regime.

Facies Associations. Sr gradationally overlies Shcs, Sm, or Mm of the Fox Hills Formation, or Mml of the Bearpaw Shale (Flight, 2004). Sr is overlain gradationally or interbedded with Sm and Mm, or abruptly overlain by St of the Fox Hills Formation; Fsm of the Colgate Sandstone, or erosively overlain by Se of either the Colgate Sandstone or Hell Creek Formation.

Flight (2004) states that this facies is not abundant in the Fox Hills Formation. My own observation is that is encountered commonly as the uppermost facies of the Fox

Hills Formation. Often it is Sr that forms the concreted bench-forming horizon commonly encountered at the upper contact of the Fox Hills Formation.

Depositional Process. Sr represents lower energy or shallower deposition than St within the lower flow regime. Prominence of Sr in the uppermost Fox Hills Formation might be expected as the unit overall records shallowing depositional conditions as it coarsens upwards from the conformable underlying Bearpaw Shale.

Massive Mudstone (Mm)

Mm is a massive dark brown or grey, well-sorted, poorly-consolidated silty mudstone. It is a very minor facies, rarely encountered in the Fox Hills Formation. Where it occurs it is limited to beds 10cm or less in thickness, lenticular, and laterally discontinuous over more than a few meters (Flight, 2004).

Hydrodynamic Interpretation. Mm is interpreted as representing deposition by fine grains of sediment falling out of suspension in quiet water (Boggs, 2001). Lack of primary structure may indicate reworking or rapid deposition.

Facies Associations. Mm typically is interbedded with St, Sm, or Sr (Flight, 2004).

Depositional Process. The fine grain size of Mm suggests deposition in low energy setting. This probably occurs within typical Fox Hills depositional cycles as high energy conditions, progress to waning flow, and eventual quiet water conditions whereupon mud can settle out of suspension.

Low Angle Planar Sandstone (Sl)

Flight (2004) notes that lithofacies Sl is rarely observed in the field and combines her own noted with those of Shoup (2001). As the emphasis of my own project does not concern the Fox Hills Formation, I include it here only out of completeness. Sl is a light tan to grey, low angle planar laminated well-sorted medium to coarse grained sandstone.

Hydrodynamic Interpretation. Sl is interpreted as representing upper flow regime deposition, where flows are shallow or of low enough velocity as to not form ripples (Boggs, 2001; Flight, 2004).

Facies Associations. Sl grades upwards intp Sm, or is abruptly overlain by Se or St of the Hell Creek Formation. Sl grades from Sm or Shcs below (Flight, 2004).

Depositional Process. Sl represents swash and backwash; higher energy conditions than observed in Shcs, St, Sr, and probably Sm. (Boggs, 2001; Flight, 2004)

Colgate Sandstone

The Colgate Sandstone is most easily distinguished from the underlying Fox Hills Sandstone by its grey to white weathering color, and greenish-grey fresh surfaces (Figure 2.7; Calvert, 1912; Thom and Dobbin, 1924; Murphy et al., 2002, although see below). Where present, the Colgate Sandstone rests on an erosive scour that is typically shallow (0-2 m), but sometimes incises up to 25 m into the Fox Hills Sandstone, or even into the underlying Bearpaw Shale (Flight, 2004; Behringer, 2008). A coarse grained basal lag was recorded by Wheeler (1983) although this is rarely encountered (Flight, 2004;

Behringer, 2008). Otherwise, the Colgate Sandstone is a micaceous, clay-rich fine grained sandstone, with occasional thin interbedded mudstones, and rare, laterally restricted coals. Bedding is typically massive, occasionally planar, although trough cross stratification is visible in particularly thick sections. Total thickness of the Colgate Sandstone varies, and is typically 2-5 m, but up to 15m in geographically restricted areas (see main manuscript; Flight, 2004).

Sandstone facies of the Colgate sandstone (Sm, St, Sh) are not typically laterally extensive and the unit exhibits mostly restricted channelized geometry (Flight, 2004; Behringer, 2008). The Colgate Sandstone is generally poorly cemented, and large concretions are notably absent, unlike the underlying Fox Hills Sandstone and overlying Basal Sand of the Hell Creek Formation (which may aid in distinguishing the Colgate Sandstone from these units; although note that Waage, 1968, suggests calcareous concretions are present in Colgate Sandstone exposures of South Dakota, none were observed by myself in Montana). *Skolithos* burrows are recorded in sandstones by Flight (2004). Although the bold white weathered color is considered characteristic of the Colgate Sandstone (Calvert, 1912; c; Waage, 1968; Murphy et al., 2002; Flight, 2004; Behringer, 2008), this is variable geographically, and not commonly seen in the Hell Creek type area (Jensen and Varnes, 1964), although it is conspicuous at the northern edge of "Best Butte" (see section description of the Marina Road exposures). The Colgate Sandstone typically exhibits conspicuous dual color banding (Figures 2.5, 2.7, 2.8), with a lower pale tan unit, and a less colorful but brighter pale grey upper unit. The upper unit exhibits more thin interbedded mudstones than the lower unit, and it is the upper unit that

sometimes weathers to a bold white color (Figure 2.7). In a fresh surface, the contact between the two bands is marked by a thin (~1-2 mm) iron-rich horizon, while the initial 2-3 cm above the contact are notably gleyed (Figure 2.9).

The Colgate Sandstone fines rapidly or abruptly in the upper 1-2 meters into a grey siltstone (Fsm) which in all observed sections is overlain by an organic-rich horizon (C1). These two lithofacies are included here within the Colgate Sandstone, mainly due to the transitional contact of Sm with Fsm making separation difficult. Previous authors (e.g. Dobbin and Reeside, 1929; Flight, 2004; Behringer, 2008) have included these units as the basalmost facies of the Hell Creek Formation. but again, the transitional nature of Sm to Fsm makes this undesirable. Further discussion of this issue occurs in the main manuscript.

Erosional Scour (Se)

The basal contact of the Colgate Sandstone is marked by an erosive scour that is typically shallow (0-2 m), but sometimes incises up to 25 m into the Fox Hills Sandstone, or even into the underlying Bearpaw Shale (Flight, 2004; Behringer, 2008).

Hydrodynamic Interpretation. Se is interpreted as representing a scour formed by current activity removing underlying sediment.

Facies Associations. Se is very rarely overlain by a coarse grained basal lag (recorded by Wheeler, 1983; but not observed here, nor by Flight, 2004; or Behringer, 2008). Typically Se is overlain by Sm or St of the Colgate Sandstone. Where sandstone

facies of the Colgate Sandstone are absent, Se is either overlain by Fsm of the Colgate Sandstone, or probably compunded with Se at the base of the Hell Creek Formation.

Depositional Process. Flight (2004) and Behringer (2008) suggest the erosive scour represents a broad incised valley formed by fall in accommodation (in this case, linked to sea-level fall). Evidence in support of this diagnosis includes depth (up to 25 m); lateral continuity of the erosive scour; a non-Waltheran facies shift from marine Bearpaw Shale to estuarine deposits of the Colgate Sandstone, and onlap of the Colgate Sandstone to incised valley walls (Flight, 2004; Behringer, 2008).

Massive Sandstone (Sm)

Sm is the most characteristic facies of the Colgate Sandstone, being a greenish-grey, well-sorted, fine to medium grained, micaceous, clay-rich, fining upward sandstone that weathers to a grey or notably conspicuous white color. Bedding is massive, although faint remains of primary bedding are sometimes visible. Sm occasionally exhibits the U-shaped burrow trace fossil *Skolithos* (Flight, 2004).

Hydrodynamic Interpretation. Due to the presence of *Skolithos*, massive bedding is likely to be the result of biogenic reworking destroying primary structures. However, see depositional process.

Facies Associations. Sm overlies Se of the Colgate Sandstone or is transitional from St. Sm is overlain either gradationally or abruptly by Fsm of the Colgate Sandstone, or is erosively overlain by Se of the Hell Creek Formation.

Depositional Process. Without primary structure, it is difficult to ascertain a depositional process for Sm specifically. Massively bedded sandstones may form from sediment gravity flows (Miall, 1996); however, lack of primary structures may also be due to biogenic reworking. The presence of faint vestiges of primary structures is also suggestive that the Colgate Sandstone may have originally had primary structure. It has been suggested that lack of primary structure may be the result of the Colgate Sandstone being composed of a large proportion of lithic fragments, the feldspars of which have been altered diagenetically into clay (explaining the high clay content of this unit, despite the fine to medium sand grain size; Dobbin and Reeside, 1929; Waage, 1968). Flight (2004) notes that other than the lack of structure, the similarity of Sm to St suggests a similar depositional process; ie. that Sm represents fluvial deposition in estuarine, delta mouth-bar, or other marginal marine setting. The upper transition to Fsm (then Fc) represents a decrease in energy and a change in depositional environment to tidal flats.

Trough Cross-Stratified Sandstone (St)

I did not personally observe lithofacies St, but it is included here as it was noted as present at one locality (westernmost Garfield County) by Flight (2004; upon which this account is based) and is important for interpretation of the Colgate Sandstone. St is a well-sorted, fine to medium grained, micaceous, clay-rich sandstone that weathers to a grey or notably conspicuous white color. Troughs are 1 - 2 m wide and 0.5 - 1 m deep. St occasionally exhibits the U-shaped burrow trace fossil *Skolithos* (Flight, 2004).

Hydrodynamic Interpretation. Trough cross-stratification represents sand transported in traction currents, forming dunes which migrate in a lower flow regime with a unidirectional current (Miall, 1998; Boggs, 2001).

Facies Associations. Flight (2004) states that in the one section in which she observed it, St directly superposed Se and was overlain by Sm.

Depositional Process. *Skolithos*-dominated ichnofacies are indicative of medium to high-energy wave-dominated foreshore, estuarine, and delta mouth-bars (Buatois and Mangano, 2004). As trough cross-stratification is indicative of unidirectional current, this suggests St represents estuarine, delta mouth-bar, or other marginal marine fluvial deposition. Flight (2004) suggests that the vertical transition from St to Sm may represent change from unidirectional to variable currents (ie. perhaps more tidal or wave-based influence), but I do not see any reason to think that Sm is not simply the result of increased biogenic disruption on St.

Planar Horizontally Bedded Sandstone (Sh)

I did not personally observe lithofacies Sh, but it is included here as it was noted as present at one locality (north of Winnett, Petroleum County) by Flight (2004; upon which this account is based). Sh is a well-sorted, fine to medium grained, micaceous, clay-rich sandstone that weathers to a grey or notably conspicuous white color. Troughs are 1 - 2 m wide and 0.5 - 1 m deep. The U-shaped burrow trace fossil *Skolithos* is abundant (Flight, 2004).

Hydrodynamic Interpretation. Planar horizontally bedded sandstone can be deposited under two different conditions (Miall, 1996); within an upper flow regime at the transition from subcritical to supercritical flow for fine to medium grained sand; and in coarse to very coarse sand at low flow speeds (rarely preserved).

Facies Associations. Flight (2004) states that in the single section in which she observed it, Sh is transitional from Sm below, subsequently being abruptly overlain by Fml of her lower Hell Creek Formation. I find the suggestion that Fml overlies Sh to be unlikely as this suggests absence of both Se and the basal sand. Indeed, consultation of the Flight (2004) appendix (containing the measured sections) demonstrates that Fml identified by Flight (2004) is the facies I identify here as Fsm and C1 of the Colgate Sandstone (grey siltstone overlain by an organic rich purple mudstone).

Depositional Process. *Skolithos*-dominated ichnofacies are indicative of medium to high-energy wave-dominated foreshore, estuarine, and delta mouth-bars (Buatois and Mangano, 2004). Transition from Sm to Sh suggests an increase in energy from probable lower flow regime (Sm), to higher flow regime (Sh). The overlying contact with transitional facies Fsc represents decrease in energy to a tidal flat setting.

Massive Mudstone (Mm)

Massively bedded silty mudstone lenses occur interbedded within the Colgate Sandstone. These mudstones are dark brown or grey, well sorted and poorly consolidated. Bed thicknesses are 5 cm or less and are not laterally extensive, typically 10 m or less. I

did not observe this facies in the field and its inclusion here follows Flight (2004), who records it at one locality.

Hydrodynamic Interpretation. Mm was deposited as suspension dropout in quiet water.

Facies Associations. Flight records a single locality where Mm occurs interbedded within Sm or Sh. The contacts between lithofacies are undulatory, but with no ripples.

Depositional Process. Thin interbeds of Mm within sandstone facies with undulatory contacts is similar to descriptions of flaser or wavy bedding (Martin, 2000). This is generally taken to represent deposition under periods of intermittent flow, from slackwater (mud deposition) to a stronger current (sand or silt) most notably in a tidally-influenced setting (Martin, 2000; Boggs, 2001).

Massive to Laminated Siltstone (Fsm)

The first of my new lithofacies of the Colgate Sandstone is a massive siltstone or mudstone (Fsm) which in association with the overlying organic rich mudstone (C1), usually forms the uppermost bed of the Colgate Sandstone. This unit was assigned (in part) to Fml of the lower Hell Creek Formation by Flight (2004), but I move it into the Colgate Sandstone, because at some localities Sm of the Colgate sandstone fines upwards into Fsm, suggesting that it should be considered part of the Colgate depositional cycle.

Fsm is a medium to pale grey, well sorted siltstone. Bedding is massive, with beds up to 50 cm thick, although typically closer to 10cm, and sometimes as little as 2 - 5 cm. Flight (2004) suggests that Fsm (her Fml) may reach up to 3 m in thickness at some localities (in combination with the overlying lithofacies C1). Root traces are present which may penetrate completely through Fsm into the underlying Sm (Flight, 2004). Flight (2004) records occasional *Skolithos* burrows occurring in lower parts of Fsm. Fsm occurs with sheet-like geometry as a single horizon at or near the top of the Colgate depositional cycle. Fsm is sometimes present even if underlying Colgate Sandstone St, Sm, or Sh are absent.

Hydrodynamic Interpretation. Massive to laminated silt or mudstone represents deposition from suspension or weak traction currents (Miall, 1996). It is possible that massive bedding is a result of rapid deposition of uniform grain size, or a sediment gravity flow. However, presence of laminae in some sections, and presence of rootlets and *Skolithos* traces (Flight, 2004) suggest that any lack of primary structures is due to secondary biogenic reworking.

Facies Associations. Fsm overlies Sm abruptly or gradationally. It can also occur in the absence of sandstone facies, therefore directly overlying Sm or Sr of the Fox Hills Formation; in this situation there is not evidence of an erosive scour (Se) of the Colgate Sandstone. Fsm is overlain abruptly by the organic rich horizon C1.

Depositional Process. The transitional or abrupt contact between underlying Sm and Fsm suggests decrease in energy combined with flooding. Presence of *Skolithos* in

lower parts of Fsm, being replaced by root traces is consistent with a decrease in energy being associated with a change from fluvial or estuarine conditions to tidal flat (Flight, 2004).

Coal or Organic-Rich Shale (C1 and C2)

The second of my new lithofacies of the Colgate Sandstone refers to two separate organic rich lithofacies both included as classification code C (Miall, 1985).

The first lithofacies (C1) is a purple, or reddish brown siltstone or silty mudstone almost always encountered as the uppermost unit of the Colgate Sandstone. Bedding is massive or laminated, and sheet-like in geometry. The unit rarely exceeds 40 cm in thickness, but is typically much less (<10 cm) and can be as little as 1cm. Bed thickness is generally related to thickness of the Colgate Sandstone overall; in areas where the Colgate Sandstone is thick, unit thicknesses of lithofacies Fsm and C1 also tend to be thicker. The unit is organic rich with plant detritus, although fragments are small enough such that the type of plant cannot be discerned.

The second use of lithofacies C2 refers to a more typical coal which is rarely encountered interbedded within Sm. Flight (2004) does not record the presence of coal within the Colgate, but coals are present (albeit very rarely) as thin (<50cm) lenses (Figure 2.8) within massively bedded sandstone. Lenticular coals have not been observed more than ~10 m in width, and were only observed at Crooked Creek, north of the small town of Winnett (Petroleum County, ~120 km west of Jordan; Figure 2.1).

Hydrodynamic Interpretation. Massive to laminated silt or mudstone represents deposition from suspension or weak traction currents (Miall, 1996). Coal deposition occurs in quiet water settings.

Facies Associations. C1 overlies Fsm abruptly, and is overlain by Se, Sihs, Sm, or St of the Hell Creek Formation. C2 occurs as laterally discontinuous interbeds within Sm of the Colgate Sandstone.

Depositional Process. Presence of organic fragments, in combination with rootlet traces into and through the underlying Fsm supports interpretation of Fsm through C1 as tidal flats. C2 represents accumulation and burial of peat or a concentration of woody materials in a quiet water setting. However, as lenticular interbeds of coal within Sm, C2 probably does not represent extensive coal swamps; rather coal beds are either reworked from elsewhere, or represent quiet water deposition in abandoned chutes or ox-bows.

?Battle Formation

An unusual set of lithofacies up to 10 m in thickness occurs between the underlying Colgate Sandstone (C1), and erosively overlying Basal Sand of the Hell Creek Formation (Se, followed by Sm, Shcs, or St). The set of lithofacies comprise a basal pale colored siltstone (seatearth, Fr), an organic rich silt or sandstone (C), and mauve or green-grey banded mudstone (Fml).

These lithofacies were assigned (in part) to Fml of the lower Hell Creek Formation by Flight (2004). However, here I very tentatively refer them to the Battle Formation (otherwise only recorded in southern Alberta and Saskatchewan). This referral

is based on lithological similarity to description of the Battle Formation given by Irish (1970), and the occurrence of palynomorphs which have correlated with the Battle Formation in Alberta and Saskatchewan (Lerbekmo, 2009).

These facies show similarity to the organic rich C1 facies as defined above as the uppermost facies of the underlying Colgate Sandstone. However, I chose to include C1 within the Colgate Sandstone (rather than the Battle Formation) as C1 is encountered overlying Fsm of the Colgate Formation in sections where neither the sandstone facies of the Colgate Sandstone, nor the Battle Formation facies are present. In the future it might be desirable to remove both Fsm and C1 from the Colgate Sandstone and place them within the Battle Formation, although definition of the boundary between these units is not clear, and I am unable to find good photographs; for example, it is not clear if the basal bed of the Battle Formation is one of the organic-rich horizons, or the underlying pale siltstone (Irish, 1970; Eberth and Braman, 2012).

It is necessary to separate these possible Battle Formation facies mainly due to the confusion that their inclusion in either the Colgate or Hell Creek formations might cause concerning the age of these units and their contacts. I also consider that the basal unit of the Hell Creek Formation should be maintained as the Basal Sandstone as originally defined by Brown (1907), and consistent with current understanding of depositional cyclicity.

I have only encountered these probable Battle Formation facies in the area around Hell Creek itself, most easily observable at Manaige Spring (see main manuscript), but also in the cliffs visible on both sides of the usually flooded tributary of Hell Creek itself

("Battle Butte"). Combined thickness of the Battle Formation lithofacies is 10 m at Manaige Spring, but thins northwards such that it is only ~ 5 m thick at Battle Butte (~ 1 km north of Manaige Spring), and absent at "Best Butte" (~3 km NE of Manaige Spring; see main manuscript). I suspect that this represents considerable northwards thinning and hence consider the Battle Formation as lenticular in geometry.

These facies descriptions are only preliminary as a more detailed investigation of these specific beds has not been conducted.

Seatearth (Fr)

A conspicuous pale cream-colored silt or silty mudstone which is massively bedded, up to 30 cm thick, well sorted and poorly consolidated. This facies was only observed at two localities where it has a sheet-like geometry. The facies was not analysed closely enough to ascertain if rootlets were present.

Hydrodynamic Interpretation. Massive silt or mudstone represents deposition from suspension or weak traction currents (Miall, 1996). It is possible that massive bedding is a result of rapid deposition of uniform grain size, or a sediment gravity flow.

Facies Associations. Fr abruptly overlies C1 of the Colgate Sandstone and abruptly underlies C of the Battle Formation.

Depositional Process. Based on its position underlying the organic rich horizon C, lithofacies Fr is tentatively interpreted as a seatearth.

Organic-Rich Silt, Silty Mud, or Sandstone (C)

Lithofacies C is a dark brown to black, organic rich horizon with grain size varying from silt or silty mud, to fine sandstone. The most easily observable section exposing this facies at Manaige Spring on the Hell Creek Marina road (see main manuscript), where C is a massive to laminated silt or silty mud. However, ~2 km to the east in Jordan Coulee (47°34'2" N, 106°55'39" W; NAD27CONUS), C is a fine grained silty sandstone. Large cm-scale fragments of wood are occasionally present, especially so when C is a sandstone. C reaches a maximum thickness of ~30 cm and has a sheet-like geometry.

Hydrodynamic Interpretation. Massive to laminated silt or mudstone represents deposition from suspension or weak traction currents (Miall, 1996). The more sandy occurrence of this facies represents deposition in higher energy conditions.

Facies Associations. C abruptly overlies Fr, and is abruptly overlain by Fml of the Battle Formation.

Depositional Process. Presence of organic fragments, in combination with rootlet traces into and through the underlying Fsm supports interpretation of Fsm through C1 as tidal flats.

Massive Mudstone (Fml)

Fml is a massively bedded mudstone. It is variable in coloration, although generally dominated by mauve purple and green-grey bands. It has only been observed in

detail at the Manaige Spring locality where it is ~11 m thick, but is also visible northwards along the east and west valley walls of Hell Creek itself where it is eroded by incision by the overlying Se of the Hell Creek Formation. This limited exposure suggests a sheet-like geometry.

Hydrodynamic Interpretation. Mm was deposited as suspension dropout in quiet water.

Facies Associations. Mm abruptly overlies C of the Battle Formation and is erosively overlain by Se, Sm, Sihs, or St of the Hell Creek Formation.

Depositional Process. The abrupt contact of Mm with underlying C suggests a change from tidal flat to floodplain deposition. The erosive contact of Se (then Sm, Shcs, or St) of the Hell Creek Formation suggests an increase in energy; in the case of Sm or St to a fluvial channel; in the case of Shcs, fluctuating flow strength possibly indicative of tidal influence or seasonal variation.

Hell Creek Formation

The ~80-90 m thick Hell Creek Formation consists of seven lithofacies comprising an erosional scour (Se), Inclined heterolithic strata (Sihs), trough cross-bedded (St), massive (Sm), and ripple cross-laminated sandstones (Sr), massive to laminated siltstones and mudstones (Fml), and organic rich facies (C). Lithofacies are for the most part fluvial in origin, although there is some indication of possible marine or tidal influence in basal beds. Here I differ from Flight (2004) in that I do not consider the

Basal Sandstone as a subdivision separate from the rest of the Hell Creek Formation. A detailed overview of the Hell Creek Formation is given in the main manuscript.

Erosional Scour (Se)

Erosional scours can be found within the Hell Creek Formation at the bases of the four major amalgamated sandstone units (Basal Sand; Jen Rex Sand; Apex Sand; Ten Meter Sand; Hartman et al., 2014), but also at the bases of isolated channels.

Normally the basal contact of the Hell Creek Formation with the underlying unit (various) is not strongly erosive (Figures 2.4, 2.5, 2.10), but is occasionally up to 5m depth (Figure 2.10). However, scouring is relatively rare and very localized in nature, perhaps explaining how it was not observed by Flight (2004), although it was mentioned by Brown (1907; 1914) and Jensen and Varnes (1964), who suggested incisions up to 10 m are known. The exceptionally thick Basal Sand at the type section (Hartman et al., 2014; as reinterpreted here) represents at least ~15 m of relief.

The base of the Jen Rex Sand is usually marked by an erosive scour, with depth variation highly localized, typically from 0-5 m, but up to 15 m (Flight, 2004). The scour at the base of the Apex Sand usually shows very little relief but has been observed to incise up to 5 m into the Middle Hell Creek Formation, to the top of the Null Coal (East Gilbert Creek; see main manuscript). Typically, the least relief is seen for Se at the base of the 10 m sand, which was only observed with any notable incision at the south side of East Gilbert Creek where it incises ~10 m into the top of the Apex Sand.

At some localities, Se is overlain by a lag of gravel to cobble-sized clasts. This has been observed for both the basal Se and that of the Jen Rex Sand. Even in the absence of a conglomerate, Se is commonly overlain by a lag deposit of dinosaur bones.

Hydrodynamic Interpretation. Se is interpreted as representing a scour formed by current activity removing underlying sediment.

Facies Associations. At the basal contact, since the depth of Se can be up to 25m, then it can erosively overlie any of the facies down to Mml of the Bearpaw Shale. I have not personally observed this relationship however; the deepest incision of Se that I have observed is at the new type section where Se erosively overlies Sm of the Bearpaw Shale.

Se is typically overlain by a medium grained sandstone of the Hell Creek Formation, either Sm or St. More rarely, Se is overlain by Sihs (only observed at the basal contact; Flight, 2004).

Depositional Process. Erosive scours can represent major regional events, or localized channel scouring. Regional erosive scours (present at the bases of major amalgamated sandstone units) are evidence of stillstand or fall in accommodation, and may represent significant periods of time (tens of thousands to millions of years). Localized scouring at the bases of isolated channels is representative of an order of magnitude less time, centuries to thousands of years.

Inclined Heterolithic Strata (Sihs)

Flight (2004) describes Inclined Heterolithic Strata (IHS) as a relatively common lithofacies (Sihs) encountered as part of the Basal Sand, although no convincing photograph is provided. However, Sihs is recorded at Site #10 of Flight (2004: Figure 13 and appendices therein), which is the same as what I call "Best Butte" (see main manuscript). I did not have the opportunity to measure a section at Best Butte, but I did take a series of photographs (see main manuscript). The facies described by Flight (2004) as IHS are low angle inclined beds which occur overlying Sm at the top of the first package of sandstones (immediately overlying C1 of the Colgate Sandstone), alternating in lithology between sandstone and mudstone; consistent with description of IHS given by Thomas et al. (1987).

The following description is adapted from Flight (2004). Sihs comprises shallowly inclined beds of sandstone and mudstone with sporadic, often large iron concretions. Sand beds are typically ~30 cm thick, well sorted, fine grained, and exhibit ripples and occasional flaser bedding. Bimodal current direction was recorded at one section (best butte) by Flight (2004). Mudstone beds are ~5-10 cm thick, dark brown to black (this coloration is not immediately obvious based on photographs of best butte) and contain plant fossils.

Sihs is recorded only as a component lithofacies of the Basal Sand, and is not observed higher up in the Hell Creek Formation (e.g. Jen Rex Sand, Apex Sand, 10 Meter Sand). Sihs is not laterally extensive, even within the Basal Sand, and should be considered as channelized geometry.

Hydrodynamic Interpretation. Alternating beds of sandstone and mudstone indicate cyclic deposition between higher energy flow (sand) to suspension fallout (mud; Thomas et al., 1987).

Facies Associations. Other than the alternating beds that define the lithofacies, Sihs gradationally overlies Sm, and is gradationally overlain by St or Fml of the Hell Creek Formation.

Depositional Process. IHS represents environments that experience cyclic variation in depositional conditions. As such, IHS is often considered as indicative of tidally influenced deposition (Thomas, 1987). This was contested by Eberth (2005) who suggested that IHS encountered far inland from the shoreline may instead be indicative of seasonal variation in climate, or other forcing factors.

Trough Cross-Stratified Sandstone (St)

St is a well-sorted, medium to fine-grained, clay-rich sandstone that weathers to a grey or tan color, often in a distinctive rilled pattern. Bedsets were observed up to 25 m thick, comprised of individual beds typically 1-2 m in thickness. Troughs are typically 1 - 2 m wide, but up to 5m (Flight, 2004) and 0.5 - 2 m deep. Bedsets and individual beds fine upwards. St contains calcareously cemented concretions, which are frequent and sometimes large, on the scale of meters. St can be of either channelized or sheet-like geometry. Channelized geometry is more commonly observed in the Basal Sand or Jen Rex Sand in the lower half of the Hell Creek Formation.

Conglomerate lags are occasionally observed within the lower 2-3 m of the Basal Sand and Jen Rex Sand, but have not been observed in stratigraphically higher amalgamated sandstones. Conglomerates comprise weathered bone and mudstone clasts typically <2cm in diameter, but occasionally up to 10cm.

Hydrodynamic Interpretation. Trough cross stratification represents sand transported in traction currents, forming dunes which migrate in a lower flow regime with a unidirectional current (Miall, 1998; Boggs, 2001).

Facies Associations. St abruptly overlies Se, Sm, Sihs, Sr, or Fml. St is overlain often gradationally by Sm, Sr, Fml or (rarely) abruptly by Se.

Depositional Process. Transition from St to Sr or Sm represents decrease in energy, but within a channel environment. Transition from St to Fml represents decrease in energy and a change from traction-based transport in a channel to suspension fallout in a floodplain environment.

Massive Sandstone (Sm)

Sm is a medium to fine-grained, clay-rich massively bedded sandstone that weathers to a grey or tan color, often in a distinctive rilled pattern. Bedsets are up 10m, with individual beds 1-3 m thick, fining upwards. Sm contains calcareously cemented concretions, which are frequent and sometimes large, on the scale of meters. Smaller (up to ~25cm) spherical or irregular iron concretions are also common, although notably much more rare or absent in the upper half of the Hell Creek Formation. Sm can be of

either channelized or sheet-like geometry. Channelized geometry is more commonly observed in the Basal Sand or Jen Rex Sand in the lower half of the Hell Creek Formation.

Hydrodynamic Interpretation. Lack of sedimentary structures in Sm is interpreted as representing either bioturbation by burrowing organisms; rapid deposition; or homogeneity of grain size and sediment type (Miall, 1998; Boggs, 2001). However, vestiges of primary structure (typically cross-bedding) are sometimes visible, especially when iron staining or small nodules are present.

Facies Associations. Sm gradationally overlies St, or abruptly overlies Se or Fml. St is overlain often gradationally by Sm, Sr, Fml or (rarely) abruptly by Se.

Depositional Process. Similar to Sm of the Colgate Sandstone, it is possible that lack of primary structure may be the result of diagenesis, due to feldspathic degradation into clay (Dobbin and Reeside, 1929; Waage, 1968). Presence of root casts noted by Flight (2004) may indicate that bioturbation is at least in part responsible for the lack of primary structures.

Transition from St to Sm represents decrease in energy, but within a channel environment. Transition from Sm to Fml represents decrease in energy and a change from traction-based transport in a channel to suspension fallout in a floodplain environment.

Ripple Cross-Laminated Sandstone (Sr)

Lithofacies Sr is a grey to tan colored well-sorted fine-grained sandstone with ripple cross lamination. Ripples are asymmetric, up to 5cm in height and <10cm wavelength. Beds are typically quite thin ~0.2 m or less in thickness. Sr is most conspicuous in the broken edges of large concretions where they are emphasized by slight variation in resistance to erosion between laminae.

Hydrodynamic Interpretation. Sr is interpreted as forming in a lower flow regime. Asymmetrical ripples are indicative of unidirectional current.

Facies Associations. Sr gradationally overlies Sm, or St of the Hell Creek Formation. It is gradationally overlain by St, Sm, or Fml.

Depositional Process. Sr represents lower energy or shallower deposition than St or Sm within the lower flow regime.

Massive to Laminated Mudstone or Siltstone (Fml)

Lithofacies Fml makes up the majority of the thickness of the Hell Creek Formation, comprising massive or laminated grey, grey-green, grey-blue, purple and brown mudstones, silty mudstones, and occasional siltstones. Fml are low-chroma colors, described as "somber" by Brown (1907), and alternations of different color beds leads to banding in outcrop. Beds are variable in thickness, up to 3m, but typically less. High smectite content in some beds (particularly dark grey, and grey-green) leads to "popcorn" weathering. Where present, laminations are planar. Slickensides are common. Rootlets

and organic debris are common, but mostly restricted to dark grey or brown mudstones. Iron concentrations, staining, and gypsum crystals are common.

Hydrodynamic Interpretation. Fml was deposited as suspension dropout in quiet water.

Facies Associations. Fml gradationally overlies Sm, Sr, or St of the Hell Creek Formation. It is gradationally overlain by C, or abruptly overlain by St, or Sm.

Depositional Process. Transition from Sm to Fml represents decrease in energy and a change from traction-based transport in a channel to suspension fallout in a floodplain environment, probably due to periodic sheetwash flooding (Fastovsky, 1987). An abrupt transition from Fml to Se, Sm, or St represents an increase in energy from floodplain suspension fallout to traction transport in a channel.

Coal or Organic-Rich Shale (C)

Lithofacies C is usually represented by red-brown fissile laminated silty mudstones, very rich in organic debris. Laminations are planar. Bed thickness is typically ~20 cm but can be up to 50 cm. Beds are lenticular and typically laterally persistent only ~100 m, although they may form clusters of lenticular beds at particular horizons. Some C facies are more laterally persistent and may extend over a kilometre.

Thin coals comprised of a greater proportion of organic debris are generally absent from the Hell Creek Formation in Montana. An exception is the Null Coal which occurs at the top of the middle depositional sequence. This unit is ~50 cm thick in

western McCone County, but thins slightly to the east, the lower part changing from a true coal to a red organic rich shale. This is determinable by the presence of two persistent ash horizons the lower of which is preserved within a coal in McCone County, but in a red organic rich shale in eastern Garfield County.

Hydrodynamic Interpretation. Organic rich shale facies of C was deposited as suspension dropout in quiet water. Coal deposition occurs in quiet water settings.

Facies Associations. C gradationally overlies Fml, and is abruptly overlain by Se, St, Sm, or Fml. Although not observed directly, the Null Coal probably grades laterally into red fissile shale.

Depositional Process. C represents accumulation and burial of peat or a concentration of woody materials in a quiet water setting. Although rare in the Hell Creek, lateral persistence over ~20-30 km of (for example) the Null Coal shows that some coal horizons represent extensive coal swamps; rather than lenticular localized concentrations, perhaps representing quiet water deposition in abandoned chutes or ox-bows.

Fort Union Formation

The Fort Union Formation is not the main emphasis of this study, however, facies in the lowermost Fort Union Formation are included here as they represent the first ~5-10 m of sediment above the formational contact, coincident with the K-Pg boundary. These described facies comprise an erosional scour (Se), Trough cross-bedded sandstone (St),

laminated siltstone and mudstone (Fl), Massive mudstone (Fm) and Coal (C). Unlike most other formational contacts in this study, that of the Hell Creek and Fort Union formations is usually non-erosive, recording a transition from massive mudstone (Fml) of the uppermost Hell Creek Formation to coal (C) of the Fort Union Formation.

Erosional Scour (Se)

Erosional scours can be found at the bases of major sandstone units within the lowermost Fort Union Formation. Relief is generally 1-2 m or less; however a notable deep incision occurs at Bug Creek in McCone County, where Paleogene channels incise at least ~30 m into the Hell Creek Formation (Lofgren, 1995), and at Penick Coulee in Garfield County where incision is at least ~10 m into the Hell Creek Formation (see main manuscript).

Hydrodynamic Interpretation. Se is interpreted as representing a scour formed by current activity removing underlying sediment.

Facies Associations. Se erosively overlies C, or Fml of the Hell Creek Formation, and C, Fm or Fl of the Fort Union Formation. Se is typically overlain by St.

Depositional Process. Erosive scours can represent major regional events, or localized channel scouring. Regional erosive scours (present at the bases of major amalgamated sandstone units) are evidence of stillstand or fall in accommodation, and may represent significant periods of time (tens of thousands to millions of years).

Localized scouring at the bases of isolated channels is representative of an order of magnitude less time, centuries to thousands of years.

Trough Cross-Stratified Sandstone (St)

St is a well-sorted, medium to fine grained sandstone that weathers to a yellow or brown color of notably higher chroma than sandstones of the underlying Hell Creek Formation. Bedsets were observed up to 30 m thick, comprised of individual beds typically 1-2 m in thickness, fining upwards. Troughs are typically 1 - 2 m wide, and 0.5 - 2 m deep. St can be of either channelized or sheet-like geometry.

Hydrodynamic Interpretation. Trough cross stratification represents sand transported in traction currents, forming dunes which migrate in a lower flow regime with a unidirectional current (Miall, 1998; Boggs, 2001).

Facies Associations. St abruptly overlies Se, or Fl (of either the Fort Union or Hell Creek Formation). St is overlain gradationally by Fl.

Depositional Process. Transition from Fl to St represents an increase in energy, from quiet water floodplain deposition to a fluvial channel environment. Transition from St to Fl represents gradual decrease in energy and a change from traction-based transport in a channel to suspension fallout in a floodplain environment.

Laminated Siltstone or Mudstone (Fl)

Lithofacies Fl of the lowermost Fort Union Formation is a distinctive banded siltstone or mudstone. These beds are high chroma shades of yellow, brown, tan, and

brownish grey, in notable contrast to the low chroma Fml of the Hell Creek Formation. Fl is typically finely laminated (1-3mm thickness), exhibits conspicuous iron staining (especially in the more pale colored bands), and was described as "variegated" by Archibald (1982). Plant detritus is occasionally abundant, along with occasional rootlets. Individual bands are typically up to 50 cm in thickness. Packages of banded facies can be up to 5 m thick, and are sheet-like in geometry, being laterally extensive over kilometers.

Hydrodynamic Interpretation. Fl was deposited as suspension dropout in quiet water.

Facies Associations. Fl abruptly overlies C of the Fort Union Formation, gradationally overlies Sm, Sr, or St of the Hell Creek Formation. Fl is abruptly overlain by C, St, or Sm.

Depositional Process. Fl represents low energy floodplain deposition; banded siltstones are considered to represent paludal deposition on a floodplain with overall high water tables, supported by the presence of articulated remains of aquatic vertebrates (Fastovsky, 1987).

Massive Mudstone (Fm)

Lithofacies Fm is less commonly encountered in the lowermost Fort Union Formation than Fl. Fm is a massively bedded high-chroma brown mudstone. Beds are often quite thick, up to 3 m, but more typically ~ 1 m.

Hydrodynamic Interpretation. Fm was deposited as suspension dropout in quiet water.

Facies Associations. Fm gradationally overlies St, or abruptly overlies C or Fl of the Fort Union Formation. It is abruptly overlain by C, St or Fl.

Depositional Process. Transition from Sm to Fm represents decrease in energy and a change from traction-based transport in a channel to suspension fallout in a floodplain environment, probably due to periodic sheetwash flooding. An abrupt transition from Fm to Se, Sm, or St represents an increase in energy from floodplain suspension fallout to traction transport in a channel.

Coal (C)

One of the most conspicuous changes from the Hell Creek Formation to the Fort Union Formation is that the lower part of the Fort Union contains a large number of thick coals (lithofacies C). Coals are well developed and typically 0.5 - 2 m in thickness, and sometimes up to 3m. Many contain cream to pink colored ash horizons that have been dated most recently by Sprain et al. (2015). Some coal horizons are lenticular, but many are laterally extensive over a kilometer or more.

Hydrodynamic Interpretation. Coal deposition occurs in quiet water settings.

Facies Associations. C abruptly overlies Fml of the Hell Creek Formation or Fml of the Fort Union Formation. C is abruptly overlain by Se, St, or Fml.

Depositional Process. C represents accumulation and burial of peat or a concentration of woody materials in a quiet water setting. Many lower Fort Union Formation coal horizons extend laterally over many kilometers, suggesting extensive coal swamp environments were present.

References Cited

Archibald, J. D. 1982. A study of Mammalia and geology across the Cretaceous-Tertiary boundary in Garfield County, Montana. University of California Publications in the Geological Sciences 122:1–286.

Behringer, D. H. 2008. Geometry, genesis and sequence stratigraphic framework of the Colgate Sandstone Member of the Fox Hills, Garfield County, MT. M.S., Montana State University, Bozeman, Montana, 134 pp.

Boggs, S. 2001. Principles of Sedimentology and Stratigraphy. Prentice Hall, Upper Saddle River, N.J., 568 pp.

Brown, B. 1907. The Hell Creek beds of the Upper Cretaceous of Montana: their relation to contiguous deposits, with faunal and floral lists, and a discussion of their correlation. Bulletin of the American Museum of Natural History 823–845.

Buatois, L. A., and M. G. Mángano. 2004. Animal-substrate interactions in freshwater environments: applications of ichnology in facies and sequence stratigraphic analysis of fluvio-lacustrine successions. Geological Society, London, Special Publications 228:311–333.

Calvert, W. R., C. F. Bowen, F. A. Herald, J. H. Hance, E. Stebinger, and A. L. Beekly. 1912. Geology of Certain Lignite Fields in Eastern Montana. US Government Printing Office, pp.

Carr, I. D., R. L. Gawthorpe, C. A. Jackson, I. R. Sharp, and A. Sadek. 2003. Sedimentology and sequence stratigraphy of early syn-rift tidal sediments: the Nukhul Formation, Suez Rift, Egypt. Journal of Sedimentary Research 73:407–420.

Dobbin, C. E., and J. B. Reeside. 1929. The Contact of the Fox Hills and Lance Formations. US Government Printing Office, pp.

Eberth, D. A. 2005. The geology. Dinosaur Provincial Park: A Spectacular Ancient Ecosystem Revealed 54–82.

Eberth, D. A., and D. R. Braman. 2012. A revised stratigraphy and depositional history for the Horseshoe Canyon Formation (Upper Cretaceous), southern Alberta plains. Canadian Journal of Earth Sciences 49:1053–1086.

Fastovsky, D. E. 1987. Paleoenvironments of Vertebrate-Bearing Strata during the Cretaceous-Paleogene Transition, Eastern Montana and Western North Dakota. PALAIOS 2:282.

Flight, J. N. 2004. Sequence stratigraphic analysis of the Fox Hills and Hell Creek Fms (Maastrichtian), Eastern Montana and its relationship to dinosaur paleontology. MS, Montana State University, Bozeman, Montana, 164 pp.

Hartman, J. H., R. D. Butler, M. W. Weiler, and K. K. Schumaker. 2014. Context, naming, and formal designation of the Cretaceous Hell Creek Formation lectostratotype, Garfield County, Montana. Geological Society of America Special Papers 503:89–121.

Irish, E. J. W. 1970. The Edmonton Group of South-Central Alberta. Bulletin of Canadian Petroleum Geology 18:125–155.

Jensen, F. S., and H. D. Varnes. 1964. Geology of the Fort Peck Area, Garfield, McCone and Valley Counties, Montana. USGS Professional Paper 414-F, 49 pp.

Landman, N. H., and K. M. Waagé. 1993. Scaphitid ammonites of the Upper Cretaceous (Maastrichtian) Fox Hills Formation in South Dakota and Wyoming. Bulletin of the AMNH□; no. 215. Bulletin of the American Museum of Natural History 215:1–257.

Landman, N. H., and W. A. Cobban. 2003. Ammonites from the upper part of the Pierre Shale and Fox Hills Formation of Colorado. American Museum Novitates 1–45.

Lofgren, D. L. 1995. The Bug Creek Problem and the Cretaceous-Tertiary Transition at McGuire Creek, Montana. University of California Press, 204 pp.

Martin, A. J. 2000. Flaser and wavy bedding in ephemeral streams: a modern and an ancient example. Sedimentary Geology 136:1–5.

Miall, A. D. 1985. Architectural-element analysis: a new method of facies analysis applied to fluvial deposits.

Miall, A. D. 1996. The Geology of Fluvial Deposits. Springer Verlag Berlín, 582 pp.

Murphy, E. C., J. W. Hoganson, and K. R. Johnson. 2002. Lithostratigraphy of the Hell Creek Formation in North Dakota. Geological Society of America Special Papers 361:9–34.

Thom, W. T., and C. E. Dobbin. 1924. Stratigraphy of Cretaceous-Eocene transition beds in eastern Montana and the Dakotas. Geological Society of America Bulletin 35:481–506.

Thomas, R. G., D. G. Smith, J. M. Wood, J. Visser, E. A. Calverley-Range, and E. H. Koster. 1987. Inclined heterolithic stratification—terminology, description, interpretation and significance. Sedimentary Geology 53:123–179.

Waagé, K. M. 1968. The Type Fox Hills Formation, Cretaceous (Maestrichtian), South Dakota. Peabody Museum of Natural History, Yale University, pp.

Wheeler, K. L. 1983. Maestrichtian shoreline sedimentation in northeastern Montana. University of Iowa pp.

APPENDIX B

SUPPLEMENTARY INFORMATION FOR CHAPTER 3

Supplementary Files for Chapter 3: A New Correlation of the Cretaceous Formations of the Western Interior of the United States, I: Santonian-Maastrichtian Formations and Dinosaur Biostratigraphy.

Chapter 3 of this dissertation has three parts to its supplementary information. Part 1 is the stratigraphic chart that forms the bulk of this work; it is provided as a Microsoft Excel file (Electronic Supplementary File 1) as a supplement to this dissertation PDF. Part 2 is the recalibration chart for the radiometric dates used in constructing the stratigraphic chart; it is provided as a Microsoft Excel file (Electronic Supplementary File 2) as a supplement to this dissertation PDF. Part 3 is the list of references used in the stratigraphic chart and recalibration chart Microsoft Excel files; it is provided here in Appendix B of this dissertation PDF.

References Cited in Supplementary Files

Alexander, E. C., G. M. Mickelson, and M. A. Lanphere. 1978. Mmhb-1: a new 40Ar/39Ar dating standard. Short Papers of the Fourth International Conference, Geochronology, Cosmochronology, and Isotope Geology: US Geological Survey Open-File Report 78–701.

Arbour, V. M., M. E. Burns, and R. L. Sissons. 2009. A redescription of the ankylosaurid dinosaur Dyoplosaurus acutosquameus Parks, 1924 (Ornithischia: Ankylosauria) and a revision of the genus. Journal of Vertebrate Paleontology 29:1117–1135.

Archibald, J. D., R. F. Butler, E. H. Lindsay, W. A. Clemens, and L. Dingus. 1982. Upper Cretaceous–Paleocene biostratigraphy and magnetostratigraphy, Hell Creek and Tullock Formations, northeastern Montana. Geology 10:153–159.

Atchley, S. C., L. C. Nordt, and S. I. Dworkin. 2004. Eustatic Control on Alluvial Sequence Stratigraphy: A Possible Example from the Cretaceous-Tertiary Transition of the Tornillo Basin, Big Bend National Park, West Texas, U.S.A. Journal of Sedimentary Research 74:391–404.

Baadsgaard, H., J. F. Lerbekmo, J. R. Wijbrans, C. C. Swisher III, and M. Fanning. 1993. Multimethod radiometric age for a bentonite near the top of the Baculites reesidei Zone of southwestern Saskatchewan (Campanian–Maastrichtian stage boundary?). Canadian Journal of Earth Sciences 30:769–775.

Baksi, A. K., D. A. Archibald, and E. Farrar. 1996. Intercalibration of 40Ar39Ar dating standards. Chemical Geology 129:307–324.

Bauer, C. M. 1916. Contributions to the Geology and Paleontology of San Juan County, New Mexico: Part 1. Stratigraphy of a Part of the Chaco River Valley. U.S. Geological Survey Professional Paper.

Bauer, C. M., and J. B. Reeside. 1921. Contributions to Economic Geology, 1920, Part II, Mineral Fuels--Coal in the Middle and Eastern Parts of San Juan County, New Mexico. United States Geological Survey, pp.

Beaumont, E. C., and G. K. Hoffman. 1992. Interrelationships between the upper coal member of the Menefee Formation, the La Ventana Tongue, and the Lewis Shale in the southeastern San Juan Basin, New Mexico. New Mexico: New Mexico Geological Society 43rd Guidebook 207–216.

Beckinsale, R. D., and N. H. Gale. 1969. A reappraisal of the decay constants and branching ratio of 40K. Earth and Planetary Science Letters 6:289–294.

Befus, K. S., R. E. Hanson, T. M. Lehman, and W. R. Griffin. 2008. Cretaceous basaltic phreatomagmatic volcanism in west Texas: maar complex at Pena Mountain, Big Bend National park. Journal of Volcanology and Geothermal Research 173:245–264.

Behringer, D. H. 2008. Geometry, genesis and sequence stratigraphic framework of the Colgate Sandstone Member of the Fox Hills, Garfield County, MT. M.S., Montana State University, Bozeman, Montana, 134 pp.

Bell, P. R. 2011. Cranial Osteology and Ontogeny of Saurolophus angustirostris from the Late Cretaceous of Mongolia with Comments on Saurolophus osborni from Canada. Acta Palaeontologica Polonica 56:703–722.

Benammi, M., C. M. Ramos, and E. C. Garcia. 2006. Preliminary Magnetostratigraphic Study of the Upper Cretaceous Dinosaur Site from La Barranca Los Bonites, Tiquicheo (Michoacan State, Southern Mexico). Geophysical Research Abstracts 8:10656.

Bouligand, C., J. Dyment, Y. Gallet, and G. Hulot. 2006. Geomagnetic field variations between chrons 33r and 19r (83–41 Ma) from sea-surface magnetic anomaly profiles. Earth and Planetary Science Letters 250:541–560.

Braman, D. R. 2001. Terrestrial palynomorphs of the upper santonian-? Lowest campanian milk river formation, Southern Alberta, Canada. Palynology 25:57–107.

Braman, D. R., and A. R. Sweet. 1999. Terrestrial palynomorph biostratigraphy of the Cypress Hills, Wood Mountain, and Turtle Mountain areas (Upper Cretaceous-Paleocene) of western Canada. Canadian Journal of Earth Sciences 36:725–741.

Braman, D. R., and A. R. Sweet. 2012. Biostratigraphically useful Late Cretaceous–Paleocene terrestrial palynomorphs from the Canadian Western Interior sedimentary basin. Palynology 36:8–35.

Braman, D. R., A. R. Sweet, and J. F. Lerbekmo. 1999. Upper Cretaceous - lower Tertiary lithostratigraphic relationships of three cores from Alberta, Saskatchewan, and Manitoba, Canada. Canadian Journal of Earth Sciences 36:669–683.

Breyer, J. A., A. B. Busbey III, R. E. Hanson, K. E. Befus, W. R. Griffin, U. S. Hargrove, and S. C. Bergman. 2007. Evidence for Late Cretaceous Volcanism in Trans-Pecos Texas. The Journal of Geology 115:243–251.

Brink, K. S., D. K. Zelenitsky, D. C. Evans, J. R. Horner, and F. Therrien. 2014. Cranial morphology and variation in Hypacrosaurus stebingeri; pp. 245–266 in Hadrosaurs. Indiana University Press.

Brinkman, D. B. 2003. A review of nonmarine turtles from the Late Cretaceous of Alberta. Canadian Journal of Earth Sciences 40:557–571.

Brookins, D. G., and J. K. Rigby. 1987. Geochronologic and geochemical study of volcanic ashes from the Kirtland Shale (Cretaceous), San Juan Basin, New Mexico. Geological Society of America Special Papers 209:105–110.

Brown, B. 1907. The Hell Creek beds of the Upper Cretaceous of Montana: their relation to contiguous deposits, with faunal and floral lists, and a discussion of their correlation. Bulletin of the American Museum of Natural History 823–845.

Brown, B. 1910. The Cretaceous Ojo Alamo Beds of New Mexico: With Description of the New Dinosaur Genus Kritosaurus. Bulletin of the American Museum of Natural History 267–274.

Brown, B. 1913a. A new trachodont dinosaur, Hypacrosaurus, from the Edmonton Cretaceous of Alberta. Bulletin of the American Museum of Natural History 32:395–406.

Brown, B. 1913b. The Skeleton of Saurolophus: A Crested Duck-billed Dinosaur from the Edmonton Cretaceous. Bulletin of the American Museum of Natural History 32:387–393.

Brown, B. 1914a. Anchiceratops, a New Genus of Horned Dinosaurs from the Edmonton Cretaceous of Alberta. With Discussion of the Origin of the Ceratopsian Crest and the Brain Casts of Anchiceratops and Trachodon. Bulletin of the American Museum of Natural History 33:539–548.

Brown, B. 1914b. Corythosaurus Casuarius, a New Crested Dinosaur from the Belly River Cretaceous: With Provisional Classification of the Family Trachodontidae. Bulletin of the American Museum of Natural History.

Brown, B. 1914c. Leptoceratops, a new genus of Ceratopsia from the Edmonton Cretaceous of Alberta. Bulletin of the American Museum of Natural History 33:567–580.

Brown, B. 1916. A new crested trachodont dinosaur Prosaurolophus maximus. Bulletin of the American Museum of Natural History 35:701–708.

Brown, B., and E. M. Schlaikjer. 1942. The skeleton of Leptoceratops with the description of a new species. American Museum Novitates 1169:1–15.

Brown, C. M., and D. M. Henderson. 2015. A New Horned Dinosaur Reveals Convergent Evolution in Cranial Ornamentation in Ceratopsidae. Current Biology 25:1641–1648.

Brownfield, M. E., and E. A. Johnson. 2008. The Yampa Bed-A Regionally Extensive Tonstein in the Williams Fork Formation, Northwestern Piceance Creek and Southern Sand Wash Basins, Colorado. Geological Survey (US), pp.

Butler, R. F., and E. H. Lindsay. 1985. Mineralogy of Magnetic Minerals and Revised Magnetic Polarity Stratigraphy of Continental Sediments, San Juan Basin, New Mexico. The Journal of Geology 93:535–554.

Calvert, W. R., C. F. Bowen, F. A. Herald, J. H. Hance, E. Stebinger, and A. L. Beekly. 1912. Geology of certain lignite fields in eastern Montana. U.S. Geological Survey Bulletin 471:187–201.

Campbell, J. A., M. J. Ryan, R. B. Holmes, and C. J. Schröder-Adams. 2016. A Re-Evaluation of the Chasmosaurine Ceratopsid Genus Chasmosaurus (Dinosauria: Ornithischia) from the Upper Cretaceous (Campanian) Dinosaur Park Formation of Western Canada. PLoS ONE 11:e0145805.

Campione, N. E., and D. C. Evans. 2011. Cranial Growth and Variation in Edmontosaurs (Dinosauria: Hadrosauridae): Implications for Latest Cretaceous Megaherbivore Diversity in North America. PLoS ONE 6:e25186.

Cantrell, A. K., T. L. Suazo, S. G. Lucas, and R. M. Sullivan. 2013. Preliminary Report Of A Nearly Complete Juvenile Pentaceratops From The Upper Cretaceous Kirtland Formation (Hunter Wash Member), San Juan Basin, New Mexico. New Mexico Geological Society 17.

Catuneanu, O., and A. R. Sweet. 1999. Maastrichtian-Paleocene foreland-basin stratigraphies, western Canada: a reciprocal sequence architecture. Canadian Journal of Earth Sciences 36:685–703.

Cebula, G. T., M. J. Kunk, H. H. Mehnert, C. W. Naeser, J. D. Obradovich, and J. F. Sutter. 1986. The Fish Canyon Tuff, a potential standard for the 40Ar-39Ar and fission-track dating methods. Terra Cognita 6:139–140.

Chen, D., C. W. Langenberg, and A. P. Beaton. 2005. Horseshoe Canyon-Bearpaw Transition and Correlation of Associated Coal Zones across the Alberta Plains.

Alberta Energy and Utilities Board: Alberta Geological Survey, Edmonton, Alberta, 22 pp.

Chinnery, B. 2004. Description of Prenoceratops pieganensis gen. et sp. nov. (Dinosauria: Neoceratopsia) from the Two Medicine Formation of Montana. Journal of Vertebrate Paleontology 24:572–590.

Chinnery, B. J., and D. B. Weishampel. 1998. Montanoceratops cerorhynchus (Dinosauria: Ceratopsia) and relationships among basal neoceratopsians. Journal of Vertebrate Paleontology 18:569–585.

Chinnery, B. J., and J. R. Horner. 2007. A new neoceratopsian dinosaur linking North American and Asian taxa. Journal of Vertebrate Paleontology 27:625–641.

Christensen, A. E. 2005. Sequence Stratigraphy, Sedimentology and Provenance of the Drip Tank Member, Straight Cliffs Formation, Kaiparowits Plateau, Southwestern Utah. .

Christensen, W. K. 1996. A review of the Upper Campanian and Maastrichtian belemnite biostratigraphy of Europe. Cretaceous Research 17:751–766.

Cifelli, R. L., J. J. Eberle, D. L. Lofgren, J. A. Lillegraven, and W. A. Clemens. 2004. Mammalian biochronology of the latest Cretaceous; pp. 21–42 in M. O. Woodburne (ed.), Late Cretaceous and Cenozoic Mammals of North America. Columbia University Press, New York.

Clemens, W. A. 1994. Continental vertebrates from the Late Cretaceous of the North Slope, Alaska. 1992 Proceedings International Conference on Arctic Margins: Outer Continental Shelf Study, Mineral Management Service 94–0040.

Cobban, W. A. 1950. Telegraph Creek Formation of Sweetgrass Arch, north-central Montana. American Association of Petroleum Geologists Bulletin 34.

Cobban, W. A. 1955. Cretaceous Rocks of Northwestern Montana. Billings Geological Society: Guidebook: Sixth Annual Field Conference 107–119.

Cobban, W. A. 1969. The Late Cretaceous ammonites Scaphites leei Reeside and Scaphites hippocrepis (DeKay) in the western interior of the United States. United States Geological Survey, Professional Paper.

Cobban, W. A. 1993. Diversity and distribution of Late Cretaceous ammonites, Western Interior, United States. Evolution of the Western Interior Basin: Geological Association of Canada Special Paper 39:435–451.

Cobban, W. A., and J. B. Reeside. 1952. Correlation of the Cretaceous formations of the Western Interior of the United States. Geological Society of America Bulletin 63:1011–1044.

Cobban, W. A., I. Walaszczyk, J. D. Obradovich, and K. C. McKinney. 2006. USGS Zonal Table for the Upper Cretaceous Middle Cenomanian-Maastrichtian of the Western Interior of the United States Based on Ammonites, Inoceramids, and Radiometric Ages. United States Geological Survey.

Cochran, J. K., N. H. Landman, K. K. Turekian, A. Michard, and D. P. Schrag. 2003. Paleoceanography of the late cretaceous (Maastrichtian) Western Interior Seaway of North America: evidence from Sr and O isotopes. Palaeogeography, Palaeoclimatology, Palaeoecology 191:45–64.

Collier, A. J., and M. M. Knechtel. 1939. Coal resources of McCone County, Montana. U.S. Geological Survey Bulletin 905:1–80.

Conrad, J. E., E. H. Mackee, and B. D. Turrin. 1992. Age of Tephra Beds at the Ocean Point Dinosaur Locality, North Slope, Alaska, Based on K-Ar and 40Ar/39Ar Analyses. U.S. Geological Survey Bulletin, pp.

Cross, A. T., and M. S. Yi. 1997. Palynology and a review of vertebrate faunas of the Late Cretaceous-Paleocene North Horn Formation, Price Canyon, Wasatch Plateau and environs, Utah, USA. Dinofest International, Academy of Natural Sciences, Philadelphia 417–455.

Cullins, H. L. 1971. Geologic Map of the Rangely Quadrangle, Rio Blanco County, Colorado. United States Geological Survey, pp.

Currie, P. J., and D. A. Russell. 2005. The geographic and stratigraphic distribution of articulated and associated dinosaur remains; pp. 537–569 in P. J. Currie and E. B. Koppelhus (eds.), Dinosaur Provincial Park. Indiana University Press, Bloomington, Indiana.

Currie, P. J., W. Langston Jr, and D. H. Tanke. 2008. A new species of Pachyrhinosaurus (Dinosauria, Ceratopsidae) from the Upper Cretaceous of Alberta, Canada; pp. 1–108 in P. J. Currie and W. Langston Jr (eds.), A New Horned Dinosaur from an Upper Cretaceous Bone Bed in Alberta. NRC Research Press, Ottawa, Ontario, Canada.

Dalrymple, G. B., and W. A. Duffield. 1988. High precision 40Ar/39Ar dating of Oligocene rhyolites from the Mogollon-Datil Volcanic Field using a continuous laser system. Geophysical Research Letters 15:463–466.

Davies, J. H. F. L., J.-F. Wotzlaw, A. P. Wolfe, and L. M. Heaman. 2014. Assessing the age of the Late Cretaceous Danek Bonebed with U–Pb geochronology. Canadian Journal of Earth Sciences 51:982–986.

Davies, K. L. 1983. Hadrosaurian dinosaurs of Big Bend National Park, Brewster County, Texas. M.A., The University of Texas at Austin, 235 pp.

Dawson, F. M., W. D. Kalkreuth, and A. R. Sweet. 1994a. Stratigraphy and Coal Resource Potential of the Upper Cretaceous to Tertiary Strata of Northwestern Alberta. Geological Survey of Canada, pp.

Dawson, F. M., C. G. Evans, R. Marsh, and R. Richardson. 1994b. Uppermost Cretaceous and Tertiary strata of the Western Canada sedimentary basin. Geological Atlas of the Western Canadian Sedimentary Basin. G. Mossop and I. Shetsen (comps.). Canadian Society of Petroleum Geologists and Alberta Research Council 387–406.

Decker, P. L. 2007. Brookian Sequence Stratigraphic Correlations, Umiat Field to Milne Point Field, West-Central North Slope, Alaska. Division of Geological & Geophysical Surveys, 19 pp.

Deibert, J. E., and B. H. Breithaupt. 2006. Ferdinand v. Hayden's 1868 "huge bird" tracks in the upper Cretaceous Almond Formation: field evidence for the first dinosaur fossil discovered in Wyoming. Late Cretaceous Vertebrates from the Western Interior: Bulletin 35 35:69.

Diem, S., and J. D. Archibald. 2005. Range extension of southern chasmosaurine Ceratopsian dinosaurs into northwestern Colorado. Journal of Paleontology 79:251–258.

Difley, R. 2007. Biostratigraphy of the North Horn Formation at North Horn Mountain, Emery County, Utah. Central Utah: Diverse Geology of a Dynamic Landscape 439–454.

Difley, R., and A. A. Ekdale. 1999. Biostratigraphic aspects of the Cretaceous-Tertiary (KT) boundary interval at North Horn Mountain, Emery County, Utah. Vertebrate Paleontology in Utah. Utah Geological Survey Miscellaneous Publication. Utah Geological Survey, Salt Lake City 389–398.

Difley, R. L., and A. A. Ekdale. 2002. Footprints of Utah's Last Dinosaurs: Track Beds in the Upper Cretaceous (Maastrichtian) North Horn Formation of the Wasatch Plateau, Central Utah. PALAIOS 17:327–346.

Dodson, P. 1986. Avaceratops lammersi: A New Ceratopsid from the Judith River Formation of Montana. Proceedings of the Academy of Natural Sciences of Philadelphia 138:305–317.

Dodson, P., and P. J. Currie. 1990. Neoceratopsia; pp. 593-618 in in D. B. Weishampel, P. Dodson, and H. Osmolska (eds.), The Dinosauria. Univ. Calif. Press, Berkeley, CA.

Doelling, H. H. 1997. Interim geologic map of the Smoky Mountain 30'x 60'Quadrangle. Utah Geological Survey Open-File Report 359.

Duffield, W. A., and G. B. Dalrymple. 1990. The Taylor Creek Rhyolite of New Mexico: a rapidly emplaced field of lava domes and flows. Bulletin of Volcanology 52:475–487.

Eaton, J. G. 1991. Biostratigraphic framework for the Upper Cretaceous rocks of the Kaiparowits Plateau, southern Utah. Geological Society of America Special Papers 260:47–64.

Eaton, J. G. 2002. Multituberculate Mammals from the Wahweap (Campanian, Aquilan) and Kaiparowits (Campanian, Judithian) Formations, within and near Grand Staircase-Escalante National Monument, Southern Utah. Utah Geological Survey Miscellaneous Publication 02-4, 66 pp.

Eaton, J. G. 2006. Santonian (late Cretaceous) mammals from the John Henry Member of the Straight Cliffs Formation, Grand Staircase-Escalante National Monument, Utah. Journal of Vertebrate Paleontology 26:446–460.

Eaton, J. G., and R. L. Cifelli. 1988. Preliminary report on Late Cretaceous mammals of the Kaiparowits Plateau, southern Utah. Rocky Mountain Geology 26:45–55.

Eaton, J. G., S. Diem, J. D. Archibald, C. Schierup, and H. Munk. 1999. Vertebrate paleontology of the Upper Cretaceous rocks of the Markagunt Plateau, southwestern Utah. Vertebrate Paleontology in Utah 99:323–334.

Eaton, J. G., J. Laurin, J. I. Kirkland, N. E. Tibert, R. M. Leckie, B. B. Sageman, P. M. Goldstrand, D. W. Moore, A. W. Straub, W. A. Cobban, and others. 2001. Cretaceous and Early Tertiary Geology of Cedar and Parowan Canyons, Western Markagunt Plateau, Utah Utah Geological Association Field Trip Road Log September, 2001. The Geologic Transition, High Plateaus to Great Basin - A Symposium and Field Guide.

Eberth, D. A. 2005. The geology; pp. 54–82 in Dinosaur Provincial Park: A spectacular ancient ecosystem revealed. Indiana University Press.

Eberth, D. A. 2010. A revised regional stratigraphy and stratigraphic architecture for the Horseshoe Canyon Formation: outcrop and subsurface. Field Trip 14, May 17–18, 2010.

Eberth, D. A. 2011. A Revised Chronostratigraphy for the Oldman, Dinosaur Park and Bearpaw formations at Dinosaur Provincial Park, Alberta, Canada. .

Eberth, D. A., and A. L. Deino. 1992. A geochronology of the non-marine Judith River Formation of southern Alberta. SEPM Theme Meeting, Mesozoic of the Western Interior 24–25.

Eberth, D. A., and A. P. Hamblin. 1993. Tectonic, stratigraphic, and sedimentologic significance of a regional discontinuity in the upper Judith River Group (Belly River wedge) of southern Alberta, Saskatchewan, and northern Montana. Canadian Journal of Earth Sciences 30:174–200.

Eberth, D. A., and A. Deino. 2005. New 40Ar/39Ar ages from three bentonites in the Bearpaw, Horseshoe Canyon, and Scollard formations (Upper Cretaceous-Paleocene) of southern Alberta, Canada. Dinosaur Park Symposium: Short Papers, Abstracts, and Program. Royal Tyrrell Museum of Paleontology, Drumheller, Alberta 23–24.

Eberth, D. A., and D. R. Braman. 2012. A revised stratigraphy and depositional history for the Horseshoe Canyon Formation (Upper Cretaceous), southern Alberta plains. Canadian Journal of Earth Sciences 49:1053–1086.

Eberth, D. A., and P. R. Bell. 2014. Stratigraphy of the Danek Bonebed (Upper Cretaceous Horseshoe Canyon Formation, central Alberta) and correlations with strata in the Drumheller and Grande Prairie regions. Canadian Journal of Earth Sciences 51:975–981.

Eberth, D. A., R. G. Thomas, and A. Deino. 1992. Preliminary K-Ar dates from bentonites in the Judith River and Bearpaw Formations (Upper Cretaceous) of Dinosaur Provincial park, southern Alberta, Canada. Aspects of Nonmarine Cretaceous Geology. China Ocean Press, Beijing 296–304.

Eberth, D. A., C. R. D. de Jesús, R. A. R. de la Rosa, J. F. Lerbekmo, D. B. Brinkman, and S. D. Sampson. 2004. Cerro del Pueblo Fm (Difunta Group, Upper Cretaceous), Parras Basin, southern Coahuila, Mexico: reference sections, age, and correlation. Revista Mexicana de Ciencias Geológicas 21:335–352.

Eberth, D. A., D. C. Evans, D. B. Brinkman, F. Therrien, D. H. Tanke, and L. S. Russell. 2013. Dinosaur biostratigraphy of the Edmonton Group (Upper Cretaceous),

Alberta, Canada: evidence for climate influence. Canadian Journal of Earth Sciences 50:701–726.

Eberth, D. A., D. B. Brinkman, P.-J. Chen, F.-T. Yuan, S.-Z. Wu, G. Li, and X.-S. Cheng. 2001. Sequence stratigraphy, paleoclimate patterns, and vertebrate fossil preservation in Jurassic–Cretaceous strata of the Junggar Basin, Xinjiang Autonomous Region, People's Republic of China. Canadian Journal of Earth Sciences 38:1627–1644.

Endt, P. M. 1990. Energy levels of A= 21–44 nuclei (VII). Nuclear Physics A 521:1–400.

Endt, P. M., and C. Van der Leun. 1973. Energy levels of A= 21-44 nuclei (V). Nuclear Physics A 214:1–625.

Evans, D. C., and M. J. Ryan. 2015. Cranial Anatomy of Wendiceratops pinhornensis gen. et sp. nov., a Centrosaurine Ceratopsid (Dinosauria: Ornithischia) from the Oldman Formation (Campanian), Alberta, Canada, and the Evolution of Ceratopsid Nasal Ornamentation. PLOS ONE 10:e0130007.

Evans, D. C., R. R. Reisz, and K. Dupuis. 2007. A juvenile Parasaurolophus (Ornithischia: Hadrosauridae) Braincase from Dinosaur Provincial Park, Alberta, with comments on crest ontogeny in the genus. Journal of Vertebrate Paleontology 27:642–650.

Evans, D. C., R. Bavington, and N. E. Campione. 2009. An unusual hadrosaurid braincase from the Dinosaur Park Formation and the biostratigraphy of Parasaurolophus (Ornithischia: Lambeosaurinae) from southern Alberta. Canadian Journal of Earth Sciences 46:791–800.

Evans, D. C., R. K. Schott, D. W. Larson, C. M. Brown, and M. J. Ryan. 2013. The oldest North American pachycephalosaurid and the hidden diversity of small-bodied ornithischian dinosaurs. Nature Communications 4:1828.

Fanti, F., and O. Catuneanu. 2009. Stratigraphy of the Upper Cretaceous Wapiti Formation, west-central Alberta, Canada. Canadian Journal of Earth Sciences 46:263–286.

Fanti, F., and O. Catuneanu. 2010. Fluvial Sequence Stratigraphy: The Wapiti Formation, West-Central Alberta, Canada. Journal of Sedimentary Research 80:320–338.

Fanti, F., P. J. Currie, and M. E. Burns. 2015. Taphonomy, age, and paleoecological implication of a new Pachyrhinosaurus (Dinosauria: Ceratopsidae) bonebed from the Upper Cretaceous (Campanian) Wapiti Formation of Alberta, Canada. Canadian Journal of Earth Sciences 52:250–260.

Farke, A. A. 2004. Ceratopsid dinosaurs from the Upper Cretaceous Almond Formation of southwestern Wyoming. Rocky Mountain Geology 39:1–5.

Farke, A. A., D. J. Chok, A. Herrero, B. Scolieri, and S. Werning. 2013. Ontogeny in the tube-crested dinosaur Parasaurolophus (Hadrosauridae) and heterochrony in hadrosaurids. PeerJ.

Farke, A. A., M. J. Ryan, P. M. Barrett, D. H. Tanke, D. R. Braman, M. A. Loewen, and M. R. Graham. 2011. A New Centrosaurine from the Late Cretaceous of Alberta, Canada, and the Evolution of Parietal Ornamentation in Horned Dinosaurs. Acta Palaeontologica Polonica 56:691–702.

Fassett, J. E. 1973. The saga of the Ojo Alamo Sandstone; or the rock-stratigrapher and the paleontologist should be friends. Cretaceous and Tertiary Rocks of the Southern Colorado Plateau 123–130.

Fassett, J. E., and J. S. Hinds. 1971. Geology and fuel resources of the Fruitland Formation and Kirtland shale of the San Juan Basin, New Mexico and Colorado. U.S. Geological Survey Professional Paper 676.

Fassett, J. E., and M. B. Steiner. 1997. Precise age of C33N-C32R magnetic-polarity reversal, San Juan Basin, New Mexico and Colorado. New Mexico Geological Society Guidebook 48:239–247.

Fiorillo, A. R. 1991. Taphonomy and depositional setting of Careless Creek Quarry (Judith River Formation), Wheatland County, Montana, U.S.A. Palaeogeography, Palaeoclimatology, Palaeoecology 81:281–311.

Fiorillo, A. R., and R. S. Tykoski. 2012. A New Maastrichtian Species of the Centrosaurine Ceratopsid Pachyrhinosaurus from the North Slope of Alaska. Acta Palaeontologica Polonica 57:561–573.

Fiorillo, A. R., and R. S. Tykoski. 2014. A Diminutive New Tyrannosaur from the Top of the World. PLOS ONE 9:e91287.

Fiorillo, A. R., P. J. McCarthy, P. P. Flaig, E. Brandlen, D. W. Norton, P. Zippi, L. Jacobs, and R. A. Gangloff. 2010. Paleontology and Paleoenvironmental Interpretation of the Kikak-Tegoseak Quarry (Prince Creek Formation: Late Cretaceous), Northern Alaska: a Multi-Disciplinary Study of a High-Latitude Ceratopsian Dinosaur Bonebed; pp. 456–477 in New Perspectives on Horned Dinosaurs. The Royal Tyrrell Museum Ceratopsian Symposium. Indiana University Press.

Flight, J. N. 2004. Sequence stratigraphic analysis of the Fox Hills and Hell Creek Fms (Maastrichtian), Eastern Montana and its relationship to dinosaur paleontology. MS, Montana State University, Bozeman, Montana, 164 pp.

Flores, R. M., M. D. Myers, D. W. Houseknecht, G. D. Stricker, D. W. Brizzolara, T. J. Ryherd, and K. I. Takahashi. 2007. Stratigraphy and Facies of Cretaceous Schrader Bluff and Prince Creek Formations in Colville River Bluffs, North Slope, Alaska. Geological Survey (U.S.), pp.

Foreman, B. Z., R. R. Rogers, A. L. Deino, K. R. Wirth, and J. T. Thole. 2008. Geochemical characterization of bentonite beds in the Two Medicine Formation (Campanian, Montana), including a new< sup> 40</sup> Ar/< sup> 39</sup> Ar age. Cretaceous Research 29:373–385.

Forster, C. A., P. C. Sereno, T. W. Evans, and T. Rowe. 1993. A complete skull of Chasmosaurus mariscalensis (Dinosauria: Ceratopsidae) from the Aguja Formation (late Campanian) of West Texas. Journal of Vertebrate Paleontology 13:161–170.

Fouch, T. D., T. F. Lawton, D. J. Nichols, W. B. Cashion, and W. A. Cobban. 1983. Patterns and Timing of Synorogenic Sedimentation in Upper Cretaceous Rocks of Central and Northeast Utah. Mesozoic Paleogeography of the West-Central United States: Rocky Mountain Symposium 2 305–336.

Fowler, D. 2006. Terrestrial Late Cretaceous stratigraphy of North America and the utility of ceratopsids in biostratigraphy. Society of Vertebrate Paleontology Annual Meeting 26:63A.

Fowler, D. 2010. Anagenesis and long-term morphologic trends in Chasmosaurinae (Dinosauria: Ceratopsidae) revealed by a new high-resolution chronostratigraphic framework, ontogenetic analysis, and description of two new taxa. Journal of Vertebrate Paleontology 30:91A.

Franczyk, K. J., J. K. Pitman, and D. J. Nichols. 1990. Sedimentology, Mineralogy, Palynology, and Depositional History of Some Uppermost Cretaceous and Lowermost Tertiary Rocks along the Utah Book and Roan Cliffs East of the Green River. pp.

Frederiksen, N. O. 1991. Pollen Zonation and Correlation of Maastrichtian Marine Beds and Associated Strata, Ocean Point Dinosaur Locality, North Slope of Alaska. US Department of the Interior, US Geological Survey, pp.

Frederiksen, N. O., D. J. McIntyre, and T. P. Sheehan. 2002. Palynological dating of some Upper Cretaceous to Eocene outcrop and well samples from the region

extending from the easternmost part of NPRA in Alaska to the western part of ANWR. North Slope of Alaska: US Geological Survey, Open-File Report 02–405.

Freedman Fowler, E. A., and J. R. Horner. 2015. A New Brachylophosaurin Hadrosaur (Dinosauria: Ornithischia) with an Intermediate Nasal Crest from the Campanian Judith River Formation of Northcentral Montana. PLOS ONE 10:e0141304.

Gaffney, E. S., H. Tong, and P. A. Meylan. 2006. Evolution of the side-necked turtles: the families bothremydidae, euraxemydidae, and araripemydidae. Bulletin of the American Museum of Natural History 1–698.

Gangloff, R. A., and A. R. Fiorillo. 2010. Taphonomy and Paleoecology of a Bonebed from the Prince Creek Formation, North Slope, Alaska. PALAIOS 25:299–317.

Gangloff, R. A., A. R. Fiorillo, and D. W. Norton. 2005. The first pachycephalosaurine (dinosauria) from the paleo-arctic of alaska and its paleogeographic implications. Journal of Paleontology 79:997–1001.

Gates, T. A. 2007. Taxonomy, Biogeography, and Paleoecology of North American Hadrosaurid (Ornithopoda) Dinosaurs. University of Utah, 290 pp.

Gates, T. A., and S. D. Sampson. 2007. A new species of Gryposaurus (Dinosauria: Hadrosauridae) from the late Campanian Kaiparowits Formation, southern Utah, USA. Zoological Journal of the Linnean Society 151:351–376.

Gates, T. A., J. R. Horner, R. R. Hanna, and C. R. Nelson. 2011. New unadorned hadrosaurine hadrosaurid (Dinosauria, Ornithopoda) from the Campanian of North America. Journal of Vertebrate Paleontology 31:798–811.

Gates, T. A., S. D. Sampson, C. R. D. D. Jesús, L. E. Zanno, D. Eberth, R. Hernandez-Rivera, M. C. A. Martínez, and J. I. Kirkland. 2007. Velafrons coahuilensis, a new lambeosaurine hadrosaurid (Dinosauria: Ornithopoda) from the late Campanian Cerro del Pueblo Formation, Coahuila, Mexico. Journal of Vertebrate Paleontology 27:917–930.

Gates, T. A., S. D. Sampson, L. E. Zanno, E. M. Roberts, J. G. Eaton, R. L. Nydam, J. H. Hutchison, J. A. Smith, M. A. Loewen, and M. A. Getty. 2010. Biogeography of terrestrial and freshwater vertebrates from the late Cretaceous (Campanian) Western Interior of North America. Palaeogeography, Palaeoclimatology, Palaeoecology 291:371–387.

Gates, T. A., E. K. Lund, C. A. Boyd, D. D. DeBlieux, A. L. Titus, D. C. Evans, M. A. Getty, J. I. Kirkland, J. G. Eaton, A. L. Titus, and others. 2013. Ornithopod

dinosaurs from the Grand Staircase-Escalante National Monument region, Utah and their role in paleobiogeographic and macroevolutionary studies. Advances in Late Cretaceous Western Interior Basin Paleontology and Geology; pp. 463–481 in At the top of the Grand Staircase: The Late Cretaceous of southern Utah. Indiana University Press.

Gee, J. S., and D. V. Kent. 2007. Source of Oceanic Magnetic Anomalies and the Geomagnetic Polarity Timescale; pp. 455–507 in Treatise on Geophysics. Elsevier.

Gill, J. R., and W. A. Cobban. 1973. Stratigraphy and Geologic History of the Montana Group and Equivalent Rocks, Montana, Wyoming, and North and South Dakota. U.S. Geological Survey Professional Paper 776. 37 pp.

Gill, J. R., and W. J. Hail Jr. 1975. Stratigraphic Sections across Upper Cretaceous Mancos Shale-Mesaverde Group Boundary, Eastern Utah and Western Colorado. U.S. Geological Survey Oil and Gas Investigation Chart 68. 1 pp.

Gill, J. R., W. A. Cobban, and L. G. Schultz. 1972. Correlation, Ammonite Zonation, and a Reference Section for the Montana Group, Central Montana. Montana Geological Society, Twenty-First Annual Geological Conference: Crazy Mountains Basin 21:91–97.

Gilmore, C. W. 1922. A New Sauropod Dinosaur from the Ojo Alamo Formation of New Mexico(with Two Plates). Smithsonian Miscellaneous Collections 72:1–9.

Gilmore, C. W. 1924. On the skull and skeleton of Hypacrosaurus, a helmet-crested dinosaur from the Edmonton Cretaceous of Alberta. Canada Geological Survey Bulletin 38:49–89.

Gilmore, C. W. 1930. On dinosaurian reptiles from the Two Medicine Formation of Montana. Proceedings of the United States National Museum 77:1–39.

Gilmore, C. W. 1939. Ceratopsian dinosaurs from the Two Medicine Formation, Upper Cretaceous of Montana. Proceedings of the United States National Museum 87:1–18.

Gilmore, C. W. 1946a. A new carnivorous dinosaur from the Lance Formation of Montana. Smithsonian Miscellaneous Collections 106:1–19.

Gilmore, C. W. 1946b. Reptilian fauna of the North Horn Formation of central Utah. U.S. Geological Survey Professional Paper 210-C 1–52.

Godfrey, S. J., and R. Holmes. 1995. Cranial morphology and systematics of Chasmosaurus (Dinosauria: Ceratopsidae) from the Upper Cretaceous of western Canada. Journal of Vertebrate Paleontology 15:726–742.

Goodwin, M. B., and A. L. Deino. 1989. The first radiometric ages from the Judith River Formation (Upper Cretaceous), Hill County, Montana. Canadian Journal of Earth Sciences 26:1384–1391.

Gradstein, F., and J. Ogg. 2004. Geologic Time Scale 2004 – why, how, and where next! Lethaia 37:175–181.

Gradstein, F. M., J. G. Ogg, and A. G. Smith. 2004. A Geologic Time Scale 2004. Cambridge University Press, 589 pp.

Gradstein, F. M., J. G. Ogg, M. Schmitz, and G. Ogg. 2012. The Geologic Time Scale 2012 2-Volume Set, 1st ed. Elsevier, 1176 pp.

Gradstein, F. M., F. P. Agterberg, J. G. Ogg, J. Hardenbol, P. van Veen, J. Thierry, and Z. Huang. 1994. A Mesozoic time scale. Journal of Geophysical Research: Solid Earth 99:24051–24074.

Hamblin, A. P. 1998. Edmonton Group/St. Mary River Formation: summary of literature and concepts. Geological Survey of Canada Open File Report 3578. 36 pp.

Hamblin, A. P. 2010. Scollard/Willow Creek/Coalspur Formations: Summary of Literature and Concepts. Natural Resources Canada, 25 pp.

Hamblin, A. P., and B. W. Abrahamson. 1996. Stratigraphic Architecture of "Basal Belly River" Cycles, Foremost Formation, Belly River Group, Subsurface of Southern Alberta and Southwestern Saskatchewan. Bulletin of Canadian Petroleum Geology 44:654–673.

Haq, B. U., J. Hardenbol, and P. R. Vail. 1987. Chronology of fluctuating sea levels since the Triassic. Science 235:1156–1167.

Haq, B. U., J. Hardenbol, and P. R. Vail. 1988. Mesozoic and Cenozoic Chronostratigraphy and Cycles of Sea-Level Change. Society of Economic Paleontologists and Mineralogists Special Publication No. 42:71-108.

Harrell, T. L. J., and J. e. Martin. 2015. A mosasaur from the Maastrichtian Fox Hills Formation of the northern Western Interior Seaway of the United States and the synonymy of Mosasaurus maximus with Mosasaurus hoffmanni (Reptilia: Mosasauridae). Netherlands Journal of Geosciences 94:23–37.

Hartman, J. H., and J. I. Kirkland. 2002. Brackish and marine mollusks of the Hell Creek Formation of North Dakota: Evidence for a persisting Cretaceous seaway. Geological Society of America Special Papers 361:271–296.

Hatcher, J. B., H. F. Osborn, and O. C. Marsh. 1907. The Ceratopsia. Monographs of the United States Geological Survey 49:300 pp.

Heckert, A. B., C. Lewis, S. Lucas, and T. Williamson. 2007. New Mixed Marine-Nonmarine Microvertebrate Fauna From The Upper Cretaceous (Late Santonian-Early Campanian) Menefee Formation, Northwestern New Mexico. Abstracts with Programs - Geological Society of America 39:73.

Hettinger, R. D., and M. A. Kirschbaum. 2002. Stratigraphy of the Upper Cretaceous Mancos Shale (upper part) and Mesaverde Group in the southern part of the Uinta and Piceance basins, Utah and Colorado. U.S. Geological Survey 1–21.

Hicks, J. F., J. D. Obradovich, and L. Tauxe. 1995. A New Calibration Point for the Late Cretaceous Time Scale: The (40)Ar/(39)Ar Isotopic Age of the C33r/C33n Geomagnetic Reversal from the Judith River Formation (Upper Creataceous), Elk Basin, Wyoming, USA. Journal of Geology 103:243–256.

Hicks, J. F., D. Fastovsky, D. J. Nichols, and M. Watabe. 2001. Magnetostratigraphic correlation of Late Cretaceous dinosaur-bearing localities in the Nemegt and Ulan Nuur basins, Gobi Desert, Mongolia. Abstracts with Programs - Geological Society of America 33:323.

Hicks, J. F., K. R. Johnson, J. D. Obradovich, L. Tauxe, and D. Clark. 2002. Magnetostratigraphy and geochronology of the Hell Creek and basal Fort Union Formations of southwestern North Dakota and a recalibration of the age of the Cretaceous-Tertiary boundary. The Hell Creek Formation and the Cretaceous-Tertiary Boundary in the Northern Great Plains: An Integrated Continental Record of the End of the Cretaceous 35–55.

Hicks, J. F., K. R. Johnson, J. D. Obradovich, D. P. Miggins, and L. Tauxe. 2003. Magnetostratigraphy of upper Cretaceous (Maastrichtian) to lower Eocene strata of the Denver Basin, Colorado. Rocky Mountain Geology 38:1–27.

Hicks, J. F., M. Watabe, D. E. Fastovsky, K. R. Johnson, D. J. Nichols, and Anonymous. 1999. Magnetostratigraphic correlation of Late Cretaceous dinosaur-bearing localities, Nemegt Basin, Gobi Desert, Mongolia. Abstracts with Programs - Geological Society of America 31:234.

Hofmann, M. H., A. Wroblewski, and R. Boyd. 2011. Mechanisms Controlling the Clustering of Fluvial Channels and the Compensational Stacking of Cluster Belts. Journal of Sedimentary Research 81:670–685.

Hoganson, J. W., and E. C. Murphy. 2002. Marine Breien Member (Maastrichtian) of the Hell Creek Formation in North Dakota: Stratigraphy, vertebrate fossil record, and age. Geological Society of America Special Papers 361:247–269.

Holmes, R. B., C. A. Forster, M. Ryan, and K. M. Shepherd. 2001. A new species of Chasmosaurus (Dinosauria: Ceratopsia) from the Dinosaur Park Formation of southern Alberta. Canadian Journal of Earth Sciences 38:1423–1438.

Holroyd, P. A., G. P. Wilson, and J. H. Hutchison. 2014. Temporal changes within the latest Cretaceous and early Paleogene turtle faunas of northeastern Montana. Geological Society of America Special Papers 503:299–312.

Horner, J. R. 1979. Upper Cretaceous Dinosaurs from the Bearpaw Shale (Marine) of South-Central Montana with a Checklist of Upper Cretaceous Dinosaur Remains from Marine Sediments in North America. Journal of Paleontology 53:566–577.

Horner, J. R. 1984. Three ecologically distinct vertebrate faunal communities from the Late Cretaceous Two Medicine Formation of Montana, with discussion of evolutionary pressures induced by interior seaway fluctuations. Field Conference Guidebook 299–304.

Horner, J. R. 1992. Cranial Morphology of Prosaurolophus (Ornithischia: Hadrosauridae): With Descriptions of Two New Hadrosaurid Species and an Evaluation of Hadrosaurid Phylogenetic Relationships. Museum of the Rockies Occasional Paper 119.

Horner, J. R., and R. Makela. 1979. Nest of juveniles provides evidence of family structure among dinosaurs. Nature 282:296–298.

Horner, J. R., and P. J. Currie. 1994. Embryonic and neonatal morphology and ontogeny of a new species of Hypacrosaurus (Ornithischia, Lambeosauridae) from Montana and Alberta; pp. 312–336 in Dinosaur Eggs and Babies. Cambridge University Press.

Horner, J. R., D. J. Varricchio, and M. B. Goodwin. 1992. Marine transgressions and the evolution of Cretaceous dinosaurs. Nature 358:59–61.

Horner, J. R., J. G. Schmitt, F. Jackson, and R. Hanna. 2001. Bones and rocks of the Upper Cretaceous Two Medicine-Judith River clastic wedge complex, Montana. Field Trip Guidebook, Society of Vertebrate Paleontology 61st Annual Meeting:

Mesozoic and Cenozoic Paleontology in the Western Plains and Rocky Mountains. Museum of the Rockies Occasional Paper 3:3–14.

Hunt, A. P. 1986. “Bisti member” of the Kirtland Shale, San Juan Basin, New Mexico: implications for basin development. Geological Society of America, Abstracts with Programs 24:26–27.

Hunt, A. P., and S. G. Lucas. 1992. Stratigraphy, paleontology and age of the Fruitland and Kirtland formations (Upper Cretaceous), San Juan Basin, New Mexico. New Mexico Geological Society Guidebook 43:217–239.

Hunt, A. P., and S. G. Lucas. 1993. Cretaceous Vertebrates of New Mexico. New Mexico Museum of Natural History and Science Bulletin 2:77–91.

Hunt, A. P., and S. G. Lucas. 2003. Origin and stratigraphy of historic dinosaur quarries in the Upper Cretaceous Fruitland Formation of the Fossil Forest research Natural Area, northwestern New Mexico. New Mexico Geological Society Guidebook 54:383–388.

Hunter, J. P., R. E. Heinrich, and D. B. Weishampel. 2010. Mammals from the St. Mary River Formation (Upper Cretaceous), Montana. Journal of Vertebrate Paleontology 30:885–898.

Hunt, R. K., and T. M. Lehman. 2008. Attributes of the ceratopsian dinosaur Torosaurus, and new material from the Javelina Formation (Maastrichtian) of Texas. Journal of Paleontology 82:1127–1138.

Ifrim, C., W. Stinnesbeck, and J. F. Ventura. 2013. An endemic cephalopod assemblage from the lower Campanian (Late Cretaceous) Parras Shale, western Coahuila, Mexico. Journal of Paleontology 87:881–901.

Ifrim, C., W. Stinnesbeck, R. R. Garza, and J. F. Ventura. 2010. Hemipelagic cephalopods from the Maastrichtian (Late Cretaceous) Parras Basin at La Parra, Coahuila, Mexico, and their implications for the correlation of the lower Difunta Group. Journal of South American Earth Sciences 29:597–618.

Imhof, M., and L. B. Albright. 2003. Preliminary Magnetostratigraphic Analysis Of The Upper Cretaceous Kaiparowits Formation, Southern Utah. Journal of Vertebrate Paleontology 23:65A–65A.

Izett, G. A., and J. D. Obradovich. 1994. 40Ar/39Ar age constraints for the Jaramillo Normal Subchron. Journal of Geophysical Research 99:2925–2934.

Izett, G. A., W. A. Cobban, J. D. Obradovich, and G. B. Dalrymple. 1998. 40Ar/39Ar age of the Manson impact structure, Iowa, and correlative impact ejecta in the Crow Creek Member of the Pierre Shale (Upper Cretaceous), South Dakota and Nebraska. Geological Society of America Bulletin 110:361–376.

Jeletzky, J. A., and W. A. Clemens. 1965. Comments on Cretaceous Eutheria, Lance Scaphites, and Inoceramus? ex gr. tegulatus. Journal of Paleontology 39:952–959.

Jerzykiewicz, T., and D. K. Norris. 1994. Stratigraphy, structure and syntectonic sedimentation of the Campanian "Belly River" clastic wedge in the southern Canadian Cordillera. Cretaceous Research 15:367–399.

Jinnah, Z. A. 2011. Tectonic and sedimentary controls, age and correlation of the Upper Cretaceous Wahweap Formation, southern Utah, USA. Faculty of Science, University of the Witwatersrand pp.

Jinnah, Z. A. 2013. Tectonic and Sedimentary Controls, Age, and Correlation of the Upper Cretaceous Wahweap Formation, Southern Utah; pp. 57–73 in At the Top of the Grand Staircase: The Late Cretaceous of Southern Utah. Indiana University Press.

Jinnah, Z. A., and E. M. Roberts. 2011. Facies Associations, Paleoenvironment, and Base-Level Changes in the Upper Cretaceous Wahweap Formation, Utah, U.S.A. Journal of Sedimentary Research 81:266–283.

Jinnah, Z. A., E. M. Roberts, A. L. Deino, J. S. Larsen, P. K. Link, and C. M. Fanning. 2009. New 40Ar-39Ar and detrital zircon U-Pb ages for the Upper Cretaceous Wahweap and Kaiparowits formations on the Kaiparowits Plateau, Utah: implications for regional correlation, provenance, and biostratigraphy. Cretaceous Research 30:287–299.

Jourdan, F., C. Verati, and G. Féraud. 2006. Intercalibration of the Hb3gr 40 Ar/39 Ar dating standard. Chemical Geology 231:177–189.

Kauffman, E. G., B. B. Sageman, J. I. Kirkland, W. P. Elder, P. J. Harries, and T. Villamil. 1993. Molluscan biostratigraphy of the Cretaceous western interior basin, North America. Evolution of the Western Interior Basin: Geological Association of Canada Special Paper 39:397–434.

Kennedy, W. J., N. H. Landman, W. K. Christensen, W. A. Cobban, and J. M. Hancock. 1998. Marine connections in North America during the late Maastrichtian: palaeogeographic and palaeobiogeographic significance ofJeletzkytes nebrascensisZone cephalopod fauna from the Elk Butte Member of the Pierre Shale, SE South Dakota and NE Nebraska. Cretaceous Research 19:745–775.

Kirkland, J. I. 2001. The quest for new dinosaurs at Grand Staircase–Escalante National Monument: Utah Geological Survey Notes, v. 33. Utah Geological Survey Survey Notes 33:4.

Kirkland, J. I., and D. D. DeBlieux. 2007. New horned dinosaurs from the Wahweap Formation. Utah Geological Survey Survey Notes 39:4–5.

Kirkland, J. I., and D. D. DeBlieux. 2010. New basal centrosaurine ceratopsian skulls from the Wahweap Formation (Middle Campanian), Grand Staircase-Escalante National Monument, southern Utah; pp. 117–140 in New Perspectives on Horned Dinosaurs: The Royal Tyrrell Museum Ceratopsian Symposium. Indiana University Press Bloomington.

Kirkland, J. I., R. Hernández-Rivera, M. C. Aguillón Martínez, C. R. Delgado de Jesús, R. Gómez-Nuñez, and I. Vallejo. 2000. The Late Cretaceous Difunta Group of the Parras Basin, Coahuila, Mexico, and its vertebrate fauna. Society of Vertebrate Paleontology Annual Meeting 133–172.

Kirkland, J. I., R. Hernández-Rivera, T. Gates, G. S. Paul, S. J. Nesbitt, C. I. Serrano-Brañas, and J. P. Garcia-de la Garza. 2006. Large hadrosaurine dinosaurs from the latest Campanian of Coahuila, Mexico. New Mexico Museum of Natural History and Science Bulletin 35:299–315.

Kirschbaum, M. A., and R. D. Hettinger. 2004. Facies Analysis and Sequence Stratigraphic Framework of Upper Campanian Strata (Neslen and Mount Garfield Formations, Bluecastle Tongue of the Castlegate Sandstone, and Mancos Shale), Eastern Book Cliffs, Colorado and Utah. pp.

Krystinik, L. F., and B. B. DeJarnett. 1995. Lateral Variability of Sequence Stratigraphic Framework in the Campanian and Lower Maastrichtian of the Western Interior Seaway. American Association of Petroleum Geologists, Memoir 64:11–25.

Kuiper, K. F., A. Deino, F. J. Hilgen, W. Krijgsman, P. R. Renne, and J. R. Wijbrans. 2008. Synchronizing Rock Clocks of Earth History. Science 320:500–504.

Kwon, J., K. Min, P. J. Bickel, and P. R. Renne. 2002. Statistical Methods for Jointly Estimating the Decay Constant of 40K and the Age of a Dating Standard. Mathematical Geology 34:457–474.

Lambe, L. M. 1902. New genera and species from the Belly River series (Mid-Cretaceous). Contributions to Canadian Palaeontology 3:25–81.

Lambe, L. M. 1904. On the Squamoso-parietal Crest of the Horned Dinosaurs Centrosaurus Apertus and Monoclonius Canadensis from the Cretaceous of Alberta. The Ottawa Naturalist 18:81–84.

Lambe, L. M. 1913. A New Genus and Species of Ceratopsia from Belly River Formation of Alberta. The Ottawa Naturalist 27:109–116.

Lambe, L. M. 1914. On Gryposaurus notabilis, a new genus and species of trachodont dinosaur from the Belly River Formation of Alberta, with a description of the skull of Chasmosaurus belli. The Ottawa Naturalist 27:145–155.

Lambe, L. M. 1917. A new genus and species of crestless hadrosaur from the Edmonton Formation of Alberta. The Ottawa Naturalist 31:65–73.

Landman, N. H., and K. M. (Karl M. Waagé. 1993. Scaphitid ammonites of the Upper Cretaceous (Maastrichtian) Fox Hills Formation in South Dakota and Wyoming. Bulletin of the AMNH. Bulletin of the American Museum of Natural History 215:1–257.

Landman, N. H., R. O. Johnson, and L. E. Edwards. 2004. Cephalopods from the Cretaceous/Tertiary boundary interval on the Atlantic Coastal Plain, with a description of the highest ammonite zones in North America. Part 2. Northeastern Monmouth County, New Jersey. Bulletin of the American Museum of Natural History 1–107.

Langston, W. 1959. Anchiceratops from the Oldman Formation of Alberta. Natural History Papers 3:11.

Langston, W. 1975. The Ceratopsian Dinosaurs and Associated Lower Vertebrates from the St. Mary River Formation (Maestrichtian) at Scabby Butte, Southern Alberta. Canadian Journal of Earth Sciences 12:1576–1608.

Langston, W. 1976. A Late Cretaceous vertebrate fauna from the St. Mary River Formation in Western Canada. Essays on Palaeontology in Honour of Loris Shano Russell. Edited by CS Churcher. Royal Ontario Museum, Life Sciences Miscellaneous Publications 114–133.

Lanphere, M. A., G. B. Dalrymple, R. J. Fleck, and M. S. Pringle. 1990. Intercalibration of mineral standards for K-Ar and 40Ar/39Ar age measurements. EOS, Transactions of the American Geophysical Union 71:1–658.

Larson, D. W. 2008. Diversity and variation of theropod dinosaur teeth from the uppermost Santonian Milk River Formation (Upper Cretaceous), Alberta: a

quantitative method supporting identification of the oldest dinosaur tooth assemblage in Canada. Canadian Journal of Earth Sciences 45:1455–1468.

Lawson, D. A. 1976. Tyrannosaurus and Torosaurus, Maastrichtian dinosaurs from Trans-Pecos, Texas. Journal of Paleontology 50:158–164.

Lawton, T. F. 2008. Chapter 12 Laramide Sedimentary Basins; pp. 429–450 in A. D. Miall (ed.), Sedimentary Basins of the World. vol. 5. Elsevier.

Lawton, T. F., and A. E. Christensen. 2005. Sequence Boundaries in Terrestrial Foreland-Basin Strata: Do They Lie Above or Below the Amalgamated Fluvial Facies Tract? American Association of Petroleum Geologists Annual Meeting Abstracts.

Lawton, T. F., S. L. Pollock, and R. A. J. Robinson. 2003. Integrating sandstone petrology and nonmarine sequence stratigraphy: application to the Late Cretaceous fluvial systems of Southwestern Utah, USA. Journal of Sedimentary Research 73:389–406.

Leahy, G. D., and J. F. Lerbekmo. 1995. Macrofossil magnetobiostratigraphy for the upper Santonian-lower Campanian interval in the Western Interior of North America: comparisons with European stage boundaries and planktonic foraminiferal zonal boundaries. Canadian Journal of Earth Sciences 32:247–260.

LeCain, R., W. C. Clyde, G. P. Wilson, and J. Riedel. 2014. Magnetostratigraphy of the Hell Creek and lower Fort Union Formations in northeastern Montana. Geological Society of America Special Papers 503:137–147.

Lehman, T. M. 1981. The Alamo Wash local fauna: a new look at the old Ojo Alamo fauna. Advances in San Juan Basin Paleontology. New Mexico University Press, Albuquerque, New Mexico 189–221.

Lehman, T. M. 1987. Late Maastrichtian paleoenvironments and dinosaur biogeography in the western interior of North America. Palaeogeography, Palaeoclimatology, Palaeoecology 60:189–217.

Lehman, T. M. 1989. Chasmosaurus mariscalensis, sp. nov., a new ceratopsian dinosaur from Texas. Journal of Vertebrate Paleontology 9:137–162.

Lehman, T. M. 1990a. The ceratopsian subfamily Chasmosaurinae: sexual dimorphism and systematics; pp. 356 in Dinosaur Systematics: Approaches and Perspectives. Cambridge University Press.

Lehman, T. M. 1990b. Paleosols and the Cretaceous/Tertiary transition in the Big Bend region of Texas. Geology 18:362–364.

Lehman, T. M. 1993. New data on the ceratopsian dinosaur Pentaceratops sternbergii Osborn from New Mexico. Journal of Paleontology 67:279–288.

Lehman, T. M. 2001. Late Cretaceous Dinosaur Provinciality; pp. 310–328 in D. H. Tanke and K. Carpenter (eds.), Mesozoic Vertebrate Life. Indiana University Press, Bloomington, Indiana.

Lehman, T. M., and A. B. Coulson. 2002. A juvenile specimen of the sauropod dinosaur Alamosaurus sanjuanensis from the Upper Cretaceous of Big Bend National Park, Texas. Journal of Paleontology 76:156–172.

Lehman, T. M., and S. L. Tomlinson. 2004. Terlinguachelys fischbecki, a new genus and species of sea turtle (Chelonioidea: Protostegidae) from the Upper Cretaceous of Texas. Journal of Paleontology 78:1163–1178.

Lehman, T. M., F. W. Mcdowell, and J. N. Connelly. 2006. First isotopic (U-Pb) age for the Late Cretaceous Alamosaurus vertebrate fauna of West Texas, and its significance as a link between two faunal provinces. Journal of Vertebrate Paleontology 26:922–928.

Lerbekmo, J. F. 1985. Magnetostratigraphic and Biostratigraphic Correlations of Maastrichtian to Early Paleocene Strata Between South-Central Alberta and Southwestern Saskatchewan. Bulletin of Canadian Petroleum Geology 33:213–226.

Lerbekmo, J. F. 1989. The stratigraphic position of the 33-33r (Campanian) polarity chron boundary in southeastern Alberta. Bulletin of Canadian Petroleum Geology 37:43–47.

Lerbekmo, J. F. 1999. Magnetostratigraphy of the Canadian Continental Drilling Program Cretaceous-Tertiary (KT) Boundary Project core holes, western Canada. Canadian Journal of Earth Sciences 36:705–715.

Lerbekmo, J. F. 2002. The Dorothy bentonite: an extraordinary case of secondary thickening in a late Campanian volcanic ash fall in central Alberta. Canadian Journal of Earth Sciences 39:1745–1754.

Lerbekmo, J. F. 2005. Paleomagnetostratigraphy; pp. 83–87 in Dinosaur Provincial Park. Indiana University Press.

Lerbekmo, J. F. 2009. Glacioeustatic sea level fall marking the base of supercycle TA-1 at 66.5 Ma recorded by the kaolinization of the Whitemud Formation and the

Colgate Member of the Fox Hills Formation. Marine and Petroleum Geology 26:1299–1303.

Lerbekmo, J. F. 2014. The Chicxulub-Shiva extraterrestrial one-two killer punches to Earth 65 million years ago. Marine and Petroleum Geology 49:203–207.

Lerbekmo, J. F., and K. C. Coulter. 1985. Late Cretaceous to early Tertiary magnetostratigraphy of a continental sequence: Red Deer Valley, Alberta, Canada. Canadian Journal of Earth Sciences 22:567–583.

Lerbekmo, J. F., and D. R. Braman. 2002. Magnetostratigraphic and biostratigraphic correlation of late Campanian and Maastrichtian marine and continental strata from the Red Deer Valley to the Cypress Hills, Alberta, Canada. Canadian Journal of Earth Sciences 39:539–557.

Lerbekmo, J. F., and D. R. Braman. 2005. Magnetostratigraphic and Palynostratigraphic Correlation of Late Campanian to Early Maastrichtian strata of the Bearpaw and Horseshoe Canyon formations between the CPOG Strathmore Corehole and the Red Deer Valley Section, Alberta, Canada. Bulletin of Canadian Petroleum Geology 53:154–164.

Lerbekmo, J. F., and N. Lehtola. 2011. Magnetostratigraphy of the Bearpaw and Blood Reserve formations on the St. Mary River: Evidence for the effect of the Sweetgrass Arch. Bulletin of Canadian Petroleum Geology 59:1–6.

Lerbekmo, J. F., and M. E. Evans. 2012. Cryptochrons and tiny wiggles: New magnetostratigraphic evidence from chrons 32 and 33 in Western Canada. Physics of the Earth and Planetary Interiors 202:8–13.

Lerbekmo, J. F., A. R. Sweet, and M. J. Duke. 1996. A normal polarity subchron that embraces the K/T boundary: A measure of sedimentary continuity across the boundary and synchroneity of boundary events. Geological Society of America Special Papers 307:465–476.

Lerbekmo, J. F., D. R. Braman, O. Catuneanu, and N. C. Humphrey. 2003. Magnetostratigraphic and Palynostratigraphic Correlation of Late Campanian Strata of the Bearpaw and Horseshoe Canyon Formations of the RCA Castor Corehole to the Red Deer Valley, Alberta. Bulletin of Canadian Petroleum Geology 51:70–77.

Lewis, C., A. Heckert, S. Lucas, and T. Williamson. 2007. A diverse new microvertebrate fauna from the Upper Cretaceous (late Santonian-early Campanian) Menefee Formation of New Mexico. 27:105A–105A.

Lillegraven, J. A., and M. C. McKenna. 1986. Fossil mammals from the “Mesaverde” Formation (late Cretaceous, Judithian) of the Bighorn and Wind River basins, Wyoming : with definitions of late Cretaceous North American land-mammal “ages”. American Museum novitates ; no. 2840. American Museum Novitates 2840:1–68.

Lindsay, E. H., R. F. Butler, and N. M. Johnson. 1981. Magnetic polarity zonation and biostratigraphy of Late Cretaceous and Paleocene continental deposits, San Juan Basin, New Mexico. American Journal of Science 281:390–435.

Loewen, M. A., R. B. Irmis, J. J. W. Sertich, P. J. Currie, and S. D. Sampson. 2013a. Tyrant Dinosaur Evolution Tracks the Rise and Fall of Late Cretaceous Oceans. PLOS ONE 8:e79420.

Loewen, M. A., A. A. Farke, S. D. Sampson, M. A. Getty, E. K. Lund, and P. M. O’Connor. 2013b. Ceratopsid dinosaurs from the Grand Staircase of southern Utah. At the Top of the Grand Staircase: The Late Cretaceous of Southern Utah. Indiana University Press, Bloomington 488–503.

Loewen, M. A., S. D. Sampson, E. K. Lund, A. A. Farke, M. C. Aguillón-Martínez, C. A. de Leon, R. A. Rodríguez-de la Rosa, M. A. Getty, and D. A. Eberth. 2010. Horned dinosaurs (Ornithischia: Ceratopsidae) from the Upper Cretaceous (Campanian) Cerro del Pueblo Formation, Coahuila, Mexico; pp. 99–116 in New Perspectives on Horned Dinosaurs: The Royal Tyrrell Museum Ceratopsian Symposium. Indiana University Press.

Longrich, N. 2015. Systematics of Chasmosaurus - new information from the Peabody Museum skull, and the use of phylogenetic analysis for dinosaur alpha taxonomy. F1000Research.

Longrich, N. R. 2010. Mojoceratops perifania, A New Chasmosaurine Ceratopsid from the Late Campanian of Western Canada. Journal of Paleontology 84:681–694.

Longrich, N. R. 2014. The horned dinosaurs Pentaceratops and Kosmoceratops from the upper Campanian of Alberta and implications for dinosaur biogeography. Cretaceous Research 51:292–308.

Longrich, N. R., and P. J. Currie. 2009. Albertonykus borealis, a new alvarezsaur (Dinosauria: Theropoda) from the Early Maastrichtian of Alberta, Canada: implications for the systematics and ecology of the Alvarezsauridae. Cretaceous Research 30:239–252.

Lorenz, J. C., and W. Gavin. 1984. Geology of the Two Medicine Formation and the sedimentology of a dinosaur nesting ground. Montana Geological Society 1984 Field Conference Guidebook 1984:175–186.

Lucas, S. G., and R. M. Sullivan. 2000. The sauropod dinosaur Alamosaurus from the Upper Cretaceous of the San Juan Basin, New Mexico. New Mexico Museum of Natural History and Science Bulletin 17:147–156.

Lucas, S. G., A. P. Hunt, and R. M. Sullivan. 2006a. Stratigraphy and age of the Upper Cretaceous Fruitland Formation, west-central San Juan Basin, New Mexico. New Mexico Museum of Natural History and Science Bulletin 35:1–6.

Lucas, S. G., R. M. Sullivan, and A. P. Hunt. 2006b. Re-evaluation of Pentaceratops and Chasmosaurus (Ornithischia: Ceratopsidae) in the Upper Cretaceous of the Western Interior. New Mexico Museum of Natural History and Science Bulletin 35:367–370.

Lucas, S. G., R. M. Sullivan, and J. A. Spielmann. 2012. Cretaceous vertebrate biochronology, North American Western Interior. Journal of Stratigraphy 36:436–461.

Lucas, S. G., J. A. Spielmann, J. I. Kirkland, J. R. Foster, and R. M. Sullivan. 2006c. A juvenile hadrosaurine from the middle Campanian (Late Cretaceous) interval of the Mancos Shale, western Colorado. Late Cretaceous Vertebrates from the Western Interior: New Mexico Museum of Natural History and Science Bulletin 35:281–292.

Lucas, S. G., R. M. Sullivan, S. M. Cather, S. E. Jasinski, D. W. Fowler, A. B. Heckert, J. A. Spielmann, and A. P. Hunt. 2009. No definitive evidence of Paleocene dinosaurs in the San Juan Basin. Paleontologia Electronica 12:1–10.

Lull, R. S. 1933. A revision of the Ceratopsia or horned dinosaurs. Memoirs of the Peabody Museum of Natural History 3:175.

Lull, R. S., and N. E. Wright. 1942. Hadrosaurian Dinosaurs of North America. Geological Society of America Special Papers 40:1–272.

Machalski, A., J. W. M. Jagt, N. H. Landman, and N. Motchurova-Dekova. 2007. The highest records of North American scaphitid ammonites in the European Maastrichtian (Upper Cretaceous) and their stratigraphic implications. Acta Geologica Polonica 57:169–185.

Maidment, S. C. R., and P. M. Barrett. 2011. A new specimen of Chasmosaurus belli (Ornithischia: Ceratopsidae), a revision of the genus, and the utility of postcrania in the taxonomy and systematics of ceratopsid dinosaurs. Zootaxa 2963:1–47.

Mallon, J. C., D. C. Evans, M. J. Ryan, and J. S. Anderson. 2012. Megaherbivorous dinosaur turnover in the Dinosaur Park Formation (upper Campanian) of Alberta, Canada. Palaeogeography, Palaeoclimatology, Palaeoecology 350–352:124–138.

Mallon, J. C., R. Holmes, D. A. Eberth, M. J. Ryan, and J. S. Anderson. 2011. Variation in the skull of Anchiceratops (Dinosauria, Ceratopsidae) from the Horseshoe Canyon Formation (Upper Cretaceous) of Alberta. Journal of Vertebrate Paleontology 31:1047–1071.

Mallon, J. C., R. Holmes, J. S. Anderson, A. A. Farke, D. C. Evans, and H.-D. Sues. 2014. New information on the rare horned dinosaur Arrhinoceratops brachyops (Ornithischia: Ceratopsidae) from the Upper Cretaceous of Alberta, Canada. Canadian Journal of Earth Sciences 51:618–634.

Marsh, O. C. 1892. Notice of new reptiles from the Laramie Formation. American Journal of Science s3-43:449–453.

Mason, I. P., M. T. Heizler, and T. E. Williamson. 2013. 40 Ar/39 Ar Sanidine Chronostratigraphy Of K-Pg Boundary Sediments Of The San Juan Basin, Nm. New Mexico Geological Society 2013 Spring Meeting 42.

McDougall, I., and T. M. Harrison. 1999. Geochronology and Thermochronology by the 40Ar/39Ar Method, 2nd ed. Oxford University Press, 288 pp.

McKenna, M. C., and J. D. Love. 1970. Local stratigraphic and tectonic significance of Leptoceratops, a Cretaceous dinosaur in the Pinyon Conglomerate, northwestern Wyoming. United States Geological Survey, Professional Paper 700:55–61.

Meek, F. B., and F. V. Hayden. 1861. Descriptions of New Lower Silurian,(Primordial), Jurassic, Cretaceous and Tertiary Fossils: Collected in Nebraska, by the Exploring Expeditions Under the Command of Capt. Wm. F. Raynolds,... Proceedings of the Academy of Natural Sciences of Philadelphia 415–447.

Meyers, S. R., S. E. Siewert, B. S. Singer, B. B. Sageman, D. J. Condon, J. D. Obradovich, B. R. Jicha, and D. A. Sawyer. 2012. Intercalibration of radioisotopic and astrochronologic time scales for the Cenomanian-Turonian boundary interval, Western Interior Basin, USA. Geology 40:7–10.

Miall, A. D., O. Catuneanu, B. K. Vakarelov, and R. Post. 2008. The Western Interior Basin; pp. 329–362 in Andrew D. Miall (ed.), Sedimentary Basins of the World. vol. 5. Elsevier.

Min, K., R. Mundil, P. R. Renne, and K. R. Ludwig. 2000. A test for systematic errors in 40 Ar/39 Ar geochronology through comparison with U/Pb analysis of a 1.1-Ga rhyolite. Geochimica et Cosmochimica Acta 64:73–98.

Molenaar, C. M., W. A. Cobban, E. A. Merewether, C. L. Pillmore, D. G. Wolfe, and J. M. Holbrook. 2002. Regional Stratigraphic Cross Sections of Cretaceous Rocks from East-Central Arizona to the Oklahoma Panhandle. U.S. Geological Survey, pp.

Montgomery, P., E. A. Hailwood, A. S. Gale, and J. A. Burnett. 1998. The magnetostratigraphy of Coniacian-Late Campanian chalk sequences in southern England. Earth and Planetary Science Letters 156:209–224.

Mori, H., P. S. Druckenmiller, and G. M. Erickson. 2015. A new Arctic hadrosaurid from the Prince Creek Formation (lower Maastrichtian) of northern Alaska. Acta Palaeontologica Polonica.

Mull, C. G., D. W. Houseknecht, and K. J. Bird. 2003. Revised Cretaceous and Tertiary Stratigraphic Nomenclature in the Colville Basin, Northern Alaska. US Department of the Interior, US Geological Survey, pp.

Murphy, E. C., J. W. Hoganson, and K. R. Johnson. 2002. Lithostratigraphy of the Hell Creek Formation in North Dakota. Geological Society of America Special Papers 361:9–34.

Nambudiri, E. M. V., and P. L. Binda. 1991. Paleobotany, palynology and depositional environment of the Maastrichtian Whitemud Formation in Alberta and Saskatchewan, Canada. Cretaceous Research 12:579–596.

Newman, K. R. 1987. Biostratigraphic correlation of Cretaceous-Tertiary boundary rocks, Colorado to San Juan Basin, New Mexico. Geological Society of America Special Papers 209:151–164.

Nichols, D. J. 1995. Palynostratigraphy in Relation to Sequence Stratigraphy, Straight Cliffs Formation (Upper Cretaceous), Kaiparowits Plateau, Utah. U.S. G.P.O., pp.

Nichols, D. J. 1997. Palynology and ages of some Upper Cretaceous formations in the Markagunt and northwestern Kaiparowits Plateaus, southwestern Utah. US Geological Survey Bulletin.

Nordt, L., S. Atchley, and S. Dworkin. 2003. Terrestrial evidence for two greenhouse events in the latest Cretaceous. GSA Today 13:4–9.

Obradovich, J. D. 1993. A Cretaceous time scale. Evolution of the Western Interior Basin 39:379–396.

Obradovich, J. D. 2002. Geochronology of Laramide synorogenic strata in the Denver Basin, Colorado. Rocky Mountain Geology 37:165–171.

Obradovich, J. D., and W. A. Cobban. 1975. A Time-Scale For The Late Cretaceous Of The Western Interior Of North America. Geological Association of Canada Special Paper 13:31–54.

O'Connor, P. M., E. M. Roberts, L. Tapanila, A. L. Deino, T. Hieronymous, and Z. A. Jinnah. 2009. Reconnaissance paleontology in the Straight Cliffs and Wahweap formations (Turonian– Campanian), Grand Staircase–Escalante National Monument, Utah. Advances in Western Interior Late Cretaceous Paleontology and Geology, St. George, Utah, Abstracts with Program.

Ogg, J. G. 2012. Geomagnetic Polarity Time Scale; pp. 85–113 in The geologic time scale. vol. 1. Elsevier.

Ogg, J. G., and A. G. Smith. 2004. The geomagnetic polarity time scale; pp. 63–86 in F. M. Gradstein, J. G. Ogg, and A. G. Smith (eds.), A Geologic Time Scale. Cambridge University Press, Cambridge, UK.

Ogg, J. G., and L. A. Hinnov. 2012. Cretaceous; pp. 793–853 in The geologic time scale. vol. 2. Elsevier.

Ogg, J. G., F. P. Agterberg, and F. M. Gradstein. 2004. The Cretaceous Period; pp. 344–383 in A Geologic Time Scale.

Olsen, T., R. Steel, K. Hogseth, T. Skar, and S. L. Roe. 1995. Sequential architecture in a fluvial succession; sequence stratigraphy in the Upper Cretaceous Mesaverde Group, Prince Canyon, Utah. Journal of Sedimentary Research 65:265–280.

Osborn, H. F. 1923. A new genus and species of Ceratopsia from New Mexico, Pentaceratops sternbergii. American Museum Novitates 93:3.

Ostrom, J. H. 1961. A New Species of Hadrosaurian Dinosaur from the Cretaceous of New Mexico. Journal of Paleontology 35:575–577.

Ott, C. J. 2006. Cranial anatomy and biogeography of the first Leptoceratops gracilis (Dinosauria: Ornithischia) specimens from the Hell Creek Formation, southeast

Montana; pp. 213–233 in Horns and Beaks. Ceratopsian and Ornithopod Dinosaurs. Indiana University Press.

Parks, W. A. 1919. Preliminary description of a new species of trachodont dinosaur of the genus Kritosaurus, Kritosaurus incurvimanus. Transactions of the Royal Society of Canada, Series 3:51–59.

Parks, W. A. 1920. The osteology of the trachodont dinosaur Kritosaurus incurvimanus. University of Toronto Studies 5–74.

Parks, W. A. 1922. Parasaurolophus Walkeri: A New Genus and Species Of Crested Trachodont Dinosaur. University of Toronto Studies 5–32.

Parks, W. A. 1925. Arrhinoceratops brachyops, a new genus and species of Ceratopsia from the Edmonton Formation of Alberta. University of Toronto Studies 5–15.

Payenberg, T. H., D. R. Braman, D. W. Davis, and A. D. Miall. 2002. Litho-and chronostratigraphic relationships of the Santonian Campanian Milk River Formation in southern Alberta and Eagle Formation in Montana utilising stratigraphy, U Pb geochronology, and palynology. Canadian Journal of Earth Sciences 39:1553–1577.

Penkalski, P., and P. Dodson. 1999. The morphology and systematics of Avaceratops, a primitive horned dinosaur from the Judith River Formation (Late Campanian) of Montana, with the description of a second skull. Journal of Vertebrate Paleontology 19:692–711.

Peterson, F. 1969. Four New Members of the Upper Cretaceous Straight Cliffs Formation in the Southeastern Kaiparowits Region, Kane County, Utah. United States Geological Survey, pp.

Powell, J. S. 1973. Paleontology and sedimentation models of the Kimbeto Member of the Ojo Alamo Sandstone. Cretaceous and Tertiary Rocks of the Southern Colorado Plateau 111–122.

Prieto-Marquez, A. 2008. Phylogeny and historical biogeography of hadrosaurid dinosaurs. Florida State University, 861 pp.

Prieto-Marquez, A. 2010. The braincase and skull roof of Gryposaurus notabilis (Dinosauria, Hadrosauridae), with a taxonomic revision of the genus. Journal of Vertebrate Paleontology 30:838–854.

Prieto-Márquez, A. 2012. The skull and appendicular skeleton of Gryposaurus latidens, a saurolophine hadrosaurid (Dinosauria: Ornithopoda) from the early Campanian (Cretaceous) of Montana, USA. Canadian Journal of Earth Sciences 49:510–532.

Prieto-Márquez, A. 2013. Skeletal morphology of Kritosaurus navajovius (Dinosauria: Hadrosauridae) from the Late Cretaceous of the North American south-west, with an evaluation of the phylogenetic systematics and biogeography of Kritosaurini. Journal of Systematic Palaeontology 12:133–175.

Ramírez-Velasco, A. A., M. Benammi, A. Prieto-Márquez, J. A. Ortega, and R. Hernández-Rivera. 2012. Huehuecanauhtlus tiquichensis, a new hadrosauroid dinosaur (Ornithischia: Ornithopoda) from the Santonian (Late Cretaceous) of Michoacán, Mexico. Canadian Journal of Earth Sciences 49:379–395.

Raynolds, R. G. 2002. Upper Cretaceous and Tertiary stratigraphy of the Denver Basin, Colorado. Rocky Mountain Geology 37:111–134.

Raynolds, R. G., and K. R. Johnson. 2003. Synopsis of the stratigraphy and paleontology of the uppermost Cretaceous and lower Tertiary strata in the Denver Basin, Colorado. Rocky Mountain Geology 38:171–181.

Reeside, J. B. 1924. Upper Cretaceous and Tertiary Formations of the Western Part of San Juan Basin, Colorado, and New Mexico. United States Geological Survey, pp.

Reeside, J. B. 1927. The cephalopods of the Eagle Sandstone and related formations in the Western Interior of the United States. United States Geological Survey, Professional Paper 151.

Renne, P. R., R. Mundil, G. Balco, K. Min, and K. R. Ludwig. 2010. Joint determination of 40K decay constants and 40Ar□/40K for the Fish Canyon sanidine standard, and improved accuracy for 40Ar/39Ar geochronology. Geochimica et Cosmochimica Acta 74:5349–5367.

Renne, P. R., G. Balco, K. R. Ludwig, R. Mundil, and K. Min. 2011. Response to the comment by WH Schwarz et al. on "Joint determination of 40 K decay constants and 40 Ar□/40 K for the Fish Canyon sanidine standard, and improved accuracy for 40 Ar/39 Ar geochronology" by PR Renne et al.(2010). Geochimica et Cosmochimica Acta 75:5097–5100.

Renne, P. R., C. C. Swisher, A. L. Deino, D. B. Karner, T. L. Owens, and D. J. DePaolo. 1998. Intercalibration of standards, absolute ages and uncertainties in 40Ar/39Ar dating. Chemical Geology 145:117–152.

Renne, P. R., A. L. Deino, R. C. Walter, B. D. Turrin, C. C. Swisher, T. A. Becker, G. H. Curtis, W. D. Sharp, and A.-R. Jaouni. 1994. Intercalibration of astronomical and radioisotopic time. Geology 22:783–786.

Rivera, T. A., M. Storey, C. Zeeden, F. J. Hilgen, and K. Kuiper. 2011. A refined astronomically calibrated 40 Ar/39 Ar age for Fish Canyon sanidine. Earth and Planetary Science Letters 311:420–426.

Roberts, E. M. 2007. Facies architecture and depositional environments of the Upper Cretaceous Kaiparowits Formation, southern Utah. Sedimentary Geology 197:207–233.

Roberts, E. M., A. L. Deino, and M. A. Chan. 2005. 40Ar/39Ar age of the Kaiparowits Formation, southern Utah, and correlation of contemporaneous Campanian strata and vertebrate faunas along the margin of the Western Interior Basin. Cretaceous Research 26:307–318.

Roberts, E. M., S. D. Sampson, A. L. Deino, S. Bowring, and R. Buchwaldt. 2013. The Kaiparowits Formation: a remarkable record of Late Cretaceous terrestrial environments, ecosystems and evolution in Western North America; pp. 85–106 in At the Top of the Grand Staircase: The Late Cretaceous of Southern Utah. Edited by AL Titus and MA Loewen. Indiana University Press, Bloomington. Indiana University Press.

Roehler, H. W. 1990. Stratigraphy of the Mesaverde Group in the Central and Eastern Greater Green River Basin, Wyoming, Colorado, and Utah. United States Geological Survey, Professional Paper 1508.

Rogers, R. R. 1993. Marine facies of the Judith River Formation (Campanian) in the type area, north-central Montana. Montana Geological Society: 1993 Field Conference Guidebook: Old Timers' Rendezvous Edition: Energy and Mineral Resources of Central Montana 61–69.

Rogers, R. R. 1994. Nature and origin of through-going discontinuities in nonmarine foreland basin strata, Upper Cretaceous, Montana: Implications for sequence analysis. Geology 22:1119–1122.

Rogers, R. R. 1998. Sequence analysis of the Upper Cretaceous Two Medicine and Judith River formations, Montana; nonmarine response to the Claggett and Bearpaw marine cycles. Journal of Sedimentary Research 68:615–631.

Rogers, R. R., and C. C. Swisher. 1996. The Claggett and Bearpaw transgressions revisited; new 40Ar/39Ar data and a review of possible drivers. Geological Society of America 28:62.

Rogers, R. R., and M. E. Brady. 2010. Origins of microfossil bonebeds: insights from the Upper Cretaceous Judith River Formation of north-central Montana. Paleobiology 36:80–112.

Rogers, R. R., C. C. Swisher III, and J. R. Horner. 1993. 40Ar/39Ar age and correlation of the nonmarine Two Medicine Formation (Upper Cretaceous), northwestern Montana, U.S.A. Canadian Journal of Earth Sciences 30:1066–1075.

Rowe, T., E. H. Colbert, and J. D. Nations. 1981. The occurrence of Pentaceratops with a description of its frill; pp. 29–48 in S. G. Lucas, J. K. Rigby, and B. S. Kues (eds.), Advances in San Juan Basin Paleontology. University of New Mexico Press, Albuquerque.

Rowe, T., R. L. Cifelli, T. M. Lehman, and A. Weil. 1992. The Campanian Terlingua local fauna, with a summary of other vertebrates from the Aguja Formation, Trans-Pecos Texas. Journal of Vertebrate Paleontology 12:472–493.

Russell, L. S. 1964. Cretaceous non-marine faunas of northwestern North America. Life Sciences Contributions, Royal Ontario Museum 61:1–21.

Russell, L. S. 1975. Mammalian faunal succession in the Cretaceous System of western North America. Geological Association of Canada Special Paper 13:137–161.

Russell, L. S. 1983. Evidence for an unconformity at the Scollard–Battle contact, Upper Cretaceous strata, Alberta. Canadian Journal of Earth Sciences 20:1219–1231.

Russell, L. S., and R. W. Landes. 1940. Geology of the southern Alberta plains. Geological Survey of Canada, Memoir 221.

Ryan, M., D. Tanke, D. Brinkman, D. Eberth, and P. Currie. 2006. A New Pachyrhinosaurus-Like Ceratopsian From The Upper Dinosaur Park Formation (Late Campanian) Of Southern Alberta, Canada. 117A.

Ryan, M. J. 2003. Taxonomy, systematics and evolution of centrosaurine ceratopsids of the Campanian Western Interior Basin of North America. Ph.D, University of Calgary, Calgary, 578 pp.

Ryan, M. J. 2007. A new basal centrosaurine ceratopsid from the Oldman Formation, southeastern Alberta. Journal of Paleontology 81:376–396.

Ryan, M. J., and D. C. Evans. 2005. Ornithischian dinosaurs; pp. 312–348 in Dinosaur Provincial Park: A spectacular ancient ecosystem revealed. Indiana University Press.

Ryan, M. J., and A. P. Russell. 2005. A new centrosaurine ceratopsid from the Oldman Formation of Alberta and its implications for centrosaurine taxonomy and systematics. Canadian Journal of Earth Sciences 42:1369–1387.

Ryan, M. J., R. Holmes, and A. P. Russell. 2007. A revision of the late campanian centrosaurine ceratopsid genus Styracosaurus from the Western Interior of North America. Journal of Vertebrate Paleontology 27:944–962.

Ryan, M. J., A. P. Russell, and S. Hartman. 2010a. A new chasmosaurine ceratopsid from the Judith River Formation, Montana; pp. 181–188 in New Perspectives on Horned Dinosaurs. The Royal Tyrrell Museum Ceratopsian Symposium. Indiana University Press.

Ryan, M. J., D. C. Evans, and K. M. Shepherd. 2012a. A new ceratopsid from the Foremost Formation (middle Campanian) of Alberta. Canadian Journal of Earth Sciences 49:1251–1262.

Ryan, M. J., D. A. Eberth, D. B. Brinkman, P. J. Currie, and D. H. Tanke. 2010b. A new Pachyrhinosaurus-like ceratopsid from the upper Dinosaur Park Formation (late Campanian) of southern Alberta, Canada; pp. 141–155 in New Perspectives on Horned Dinosaurs. The Royal Tyrrell Museum Ceratopsian Symposium. Indiana University Press.

Ryan, M. J., D. C. Evans, P. J. Currie, C. M. Brown, and D. Brinkman. 2012b. New leptoceratopsids from the Upper Cretaceous of Alberta, Canada. Cretaceous Research 35:69–80.

Sageman, B. B., B. S. Singer, S. R. Meyers, S. E. Siewert, I. Walaszczyk, D. J. Condon, B. R. Jicha, J. D. Obradovich, and D. A. Sawyer. 2014. Integrating 40Ar/39Ar, U-Pb, and astronomical clocks in the Cretaceous Niobrara Formation, Western Interior Basin, USA. Geological Society of America Bulletin 126:956–973.

Sahni, A. 1972. The vertebrate fauna of the Judith River Formation, Montana. Bulletin of the American Museum of Natural History 147:325–412.

Sampson, S. D. 1995. Two new horned dinosaurs from the upper Cretaceous Two Medicine Formation of Montana; with a phylogenetic analysis of the Centrosaurinae (Ornithischia: Ceratopsidae). Journal of Vertebrate Paleontology 15:743–760.

Samspon, S. D., and E. C. Alexander Jr. 1987. Calibration of the interlaboratory 40Ar/39Ar dating standard, MMhb-1. Chemical Geology: Isotope Geoscience Section 66:27–34.

Sampson, S. D., and M. A. Loewen. 2005. Tyrannosaurus rex from the Upper Cretaceous (Maastrichtian) North Horn Formation of Utah: biogeographic and paleoecologic implications. Journal of Vertebrate Paleontology 25:469–472.

Sampson, S. D., and M. Loewen. 2010. Unraveling a radiation: a review of the diversity, stratigraphic distribution, biogeography, and evolution of horned dinosaurs. (Ornithischia□: Ceratopsidae); pp. 405–427 in M. J. Ryan, B. J. Chinnery, and D. A. Eberth (eds.), New Perspectives on Horned Dinosaurs. The Royal Tyrrell Museum Ceratopsian Symposium. Indiana University Press, Bloomington, Indiana.

Sampson, S. D., E. K. Lund, M. A. Loewen, A. A. Farke, and K. E. Clayton. 2013. A remarkable short-snouted horned dinosaur from the Late Cretaceous (late Campanian) of southern Laramidia. Proceedings of the Royal Society of London B: Biological Sciences 280:20131186.

Sampson, S. D., M. A. Loewen, A. A. Farke, E. M. Roberts, C. A. Forster, J. A. Smith, and A. L. Titus. 2010. New Horned Dinosaurs from Utah Provide Evidence for Intracontinental Dinosaur Endemism. PLoS ONE 5:e12292.

Sankey, J. T. 2001. Late Campanian southern dinosaurs, Aguja Formation, Big Bend, Texas. Journal of Paleontology 75:208–215.

Sankey, J. T. 2006. Turtles of the upper Aguja Formation (late Campanian), Big Bend National Park, Texas. New Mexico Museum of Natural History and Science Bulletin 35:235–243.

Sankey, J. T. 2010. Faunal composition and significance of high-diversity, mixed bonebeds containing Agujaceratops mariscalensis and other dinosaurs, Aguja Formation (Upper Cretaceous), Big Bend, Texas. New Perspectives on Horned Dinosaurs. The Royal Tyrrell Museum Ceratopsian Symposium 520–37.

Sankey, J. T., and W. A. Gose. 2001. Late Cretaceous mammals and magnetostratigraphy, Big Bend, Texas. Occasional Papers of the Museum of Natural Science, Louisiana State University 77:1–16.

Sarna-Wojcicki, A. M., and M. S. Pringle Jr. 1992. Laser-fusion 40 Ar/39 Ar ages of the Tuff of Taylor Canyon and Bishop Tuff, E. California-W. Nevada. Eos Trans. AGU 73:43.

Scannella, J. B., and D. W. Fowler. 2009. Anagenesis in Triceratops: evidence from a newly resolved stratigraphic framework for the Hell Creek Formation. Cincinnati Mus Cent Sci Contrib 3:148–149.

Scannella, J. B., and J. R. Horner. 2010. Torosaurus Marsh, 1891, is Triceratops Marsh, 1889 (Ceratopsidae: Chasmosaurinae): synonymy through ontogeny. Journal of Vertebrate Paleontology 30:1157–1168.

Scannella, J. B., D. W. Fowler, M. B. Goodwin, and J. R. Horner. 2014. Evolutionary trends in Triceratops from the Hell Creek Formation, Montana. Proceedings of the National Academy of Sciences 111:10245–10250.

Schiebout, J. A., C. A. Rigsby, S. D. Rapp, J. A. Hartnell, and B. R. Standhardt. 1987. Stratigraphy of the Cretaceous-Tertiary and Paleocene-Eocene transition rocks of Big Bend National Park, Texas. The Journal of Geology 95:359–375.

Schmitz, M. D. 2012a. Radiogenic isotope geochronology; pp. 115–125 in The Geological Time Scale. Elsevier.

Schmitz, M. D. 2012b. Radiometric Ages used in GTS2012; pp. 1045–1082 in The Geological Time Scale. Elsevier.

Schmitz, M. D., and S. A. Bowring. 2001. U-Pb zircon and titanite systematics of the Fish Canyon Tuff: an assessment of high-precision U-Pb geochronology and its application to young volcanic rocks. Geochimica et Cosmochimica Acta 65:2571–2587.

Schoene, B., J. L. Crowley, D. J. Condon, M. D. Schmitz, and S. A. Bowring. 2006. Reassessing the uranium decay constants for geochronology using ID-TIMS U–Pb data. Geochimica et Cosmochimica Acta 70:426–445.

Schoene, B., K. M. Samperton, M. P. Eddy, G. Keller, T. Adatte, S. A. Bowring, S. F. R. Khadri, and B. Gertsch. 2015. U-Pb geochronology of the Deccan Traps and relation to the end-Cretaceous mass extinction. Science 347:182–184.

Schwarz, W. H., K. Kossert, M. Trieloff, and J. Hopp. 2011. Comment on the “Joint determination of 40K decay constants and 40Ar□/40K for the Fish Canyon sanidine standard, and improved accuracy for 40Ar/39Ar geochronology” by Paul R. Renne et al. (2010). Geochimica et Cosmochimica Acta 75:5094–5096.

Shelton, J. A. 2007. Application of sequence stratigraphy to the nonmarine Upper Cretaceous Two Medicine Formation, Willow Creek anticline, northwestern Montana. M.S., Montana State University, Bozeman, Montana, 238 pp.

Singer, B. S., B. R. Jicha, R. S. Coe, and N. Mochizuki. 2012. An Earthtime Chronology for the Matuyama-Brunhes Geomagnetic Field Reversal. AGU Fall Meeting Abstracts 21.

Soegaard, K., H. Ye, N. Halik, A. T. Daniels, J. Arney, and S. Garrick. 2003. Stratigraphic evolution of latest Cretaceous to early Tertiary Difunta foreland basin in northeast Mexico: Influence of salt withdrawal on tectonically induced subsidence by the Sierra Madre Oriental fold and thrust belt. AAPG Memoir 79:364–394.

Spear, B., and M. A. Kirschbaum. 2012. Re-evaluation of depositional environments of the Neslen Formation from subsurface and surface data, Book Cliffs, Utah. 2012 AAPG Rocky Mountain Section Meeting.

Speiker, E. M. 1946. Late Mesozoic and early Cenozoic history of central Utah. United States Geological Survey Prof. Paper 205:117–161.

Sprain, C. J., P. R. Renne, G. P. Wilson, and W. A. Clemens. 2014. High-resolution chronostratigraphy of the terrestrial Cretaceous-Paleogene transition and recovery interval in the Hell Creek region, Montana. Geological Society of America Bulletin 127:393–409.

Steiger, R., and E. Jäger. 1977. Subcommission on geochronology: convention on the use of decay constants in geo-and cosmochronology. Earth and Planetary Science Letters 36:359–362.

Sternberg, C. M. 1929. A new species of horned dinosaur from the Upper Cretaceous of Alberta. Bulletin of the National Museum of Canada 54:34–37.

Sternberg, C. M. 1935. Hooded Hadrosaurs of the Belly River Series of the Upper Cretaceous: Canada Department of Mines Bulletin. Bulletin of the National Museum of Canada 52:1–37.

Sternberg, C. M. 1940. Ceratopsidae from Alberta. Journal of Paleontology 14:468–480.

Sternberg, C. M. 1950. Pachyrhinosaurus canadensis, representing a new family of the Ceratopsia, from southern Alberta. National Museum of Canada Bulletin 118:109–120.

Sternberg, C. M. 1951. Complete Skelton of Leptoceratops Gracilis Brown from the Upper Edmonton Member on Red Deer River, Alberta. Bulletin of the National Museum of Canada 225–255.

Sternberg, C. M. 1953. A new hadrosaur from the Oldman Formation of Alberta: discussion of nomenclature. Bulletin of the National Museum of Canada 1–12.

Sues, H.-D., and D. W. Larson. 2008. Diversity and variation of theropod dinosaur teeth from the uppermost Santonian Milk River Formation (Upper Cretaceous), Alberta: a quantitative method supporting identification of the oldest dinosaur tooth assemblage in Canada. Canadian Journal of Earth Sciences 45:1455–1468.

Sullivan, R. M., and T. E. Williamson. 1999. A new skull of Parasaurolophus (Dinosauria: Hadrosauridae) and a revision of the genus. New Mexico Museum of Natural History and Science. New Mexico Museum of Natural History and Science Bulletin 15:52.

Sullivan, R. M., and G. E. Bennett. 2000. A juvenile Parasaurolophus (Ornithischia: Hadrosauridae) from the Upper Cretaceous Fruitland Formation of New Mexico. New Mexico Museum of Natural History and Science Bulletin 17:215–220.

Sullivan, R. M., and S. G. Lucas. 2003. The Kirtlandian, a new land-vertebrate "age" for the Late Cretaceous of western North America. New Mexico Geological Society Guidebook 54:369–377.

Sullivan, R. M., and S. G. Lucas. 2006. The Kirtlandian land-vertebrate "age"–faunal composition, temporal position and biostratigraphic correlation in the nonmarine Upper Cretaceous of western North America. New Mexico Museum of Natural History and Science Bulletin 35:7–29.

Sullivan, R. M., and S. G. Lucas. 2010. A New Chasmosaurine (Ceratopsidae, Dinosauria) from the Upper Cretaceous Ojo Alamo Formation (Naashoibito Member), San Juan Basin, New Mexico; pp. 169–180 in M. J. Ryan, B. J. Chinnery, and D. A. Eberth (eds.), New Perspectives on Horned Dinosaurs. The Royal Tyrrell Museum Ceratopsian Symposium. Indiana University Press, Bloomington, Indiana.

Sullivan, R. M., A. C. Boere, and S. G. Lucas. 2005a. Redescription of the ceratopsid dinosaur Torosaurus utahensis (Gilmore, 1946) and a revision of the genus. Journal of Paleontology 79:564–582.

Sullivan, R. M., S. G. Lucas, and D. R. Braman. 2005b. Dinosaurs, pollen, and the Cretaceous-Tertiary boundary in the San Juan Basin, New Mexico. New Mexico Geological Society Guidebook 56:395–407.

Sullivan, R. M., S. E. Jasinkski, M. Guenther, and S. G. Lucas. 2011. The first lambeosaurin (Dinosauria, Hadrosauridae, Lambeosaurinae) from the Upper Cretaceous Ojo Alamo Formation (Naashoibito Member), San Juan Basin, New Mexico. New Mexico Museum of Natural History and Science Bulletin 53:405–417.

Swisher, C. C., Y. Wang, X. Wang, X. Xu, and Y. Wang. 1999. Cretaceous age for the feathered dinosaurs of Liaoning, China. Nature 400:58–61.

Swisher, C. C., X. Wang, Z. Zhou, Y. Wang, F. Jin, J. Zhang, X. Xu, F. Zhang, and Y. Wang. 2002. Further support for a Cretaceous age for the feathered-dinosaur beds of Liaoning,China:New 40Ar/39Ar dating of the Yixian and Tuchengzi Formations. Chinese Science Bulletin 47:136–139.

Talling, P. J., D. W. Burbank, T. F. Lawton, R. S. Hobbs, and S. P. Lund. 1994. Magnetostratigraphic Chronology of Cretaceous-to-Eocene Thrust Belt Evolution, Central Utah, USA. The Journal of Geology 102:181–196.

Tanke, D. H. 2004. The 2003 Royal Tyrrell Museum of Palaeontology Expedition to the Grande Prairie Region (Northwestern Alberta, Canada). Alberta Palaeontological Society Bulletin 19:3–31.

Tanke, D. H. 2006. Sixty years of pachyrhinosaur (Dinosauria: Ceratopsidae) discoveries in North America. Alberta Paleontological Society, 10th Annual Symposium, Abstract Volume. Alberta Paleontological Society, Calgary, Alta 33–35.

Tanke, D. H. 2010. Ceratopsian discoveries and work in Alberta, Canada: A historical review and census; pp. in M. J. Ryan and B. J. Chinnery-Allgeier (eds.), New Perspectives on Horned Dinosaurs: The Royal Tyrrell Museum Ceratopsian Symposium. Indiana University Press.

Thomas, R. G., D. A. Eberth, A. L. Deino, and D. Robinson. 1990. Composition, radioisotopic ages, and potential significance of an altered volcanic ash (bentonite) from the Upper Cretaceous Judith River Formation, Dinosaur Provincial Park, southern Alberta, Canada. Cretaceous Research 11:125–162.

Thomson, T. J., R. B. Irmis, and M. A. Loewen. 2013. First occurrence of a tyrannosaurid dinosaur from the Mesaverde Group (Neslen Formation) of Utah: Implications for upper Campanian Laramidian biogeography. Cretaceous Research 43:70–79.

Thom, W. T., and C. E. Dobbin. 1924. Stratigraphy of Cretaceous-Eocene transition beds in eastern Montana and the Dakotas. Geological Society of America Bulletin 35:481–506.

Trexler, D. 2001. Two Medicine Formation, Montana: geology and fauna; pp. 298–309 in Mesozoic Vertebrate Life. Indiana University Press.

Tsujita, C. J. 1995. Origin of Concretion-Hosted Shell Clusters in the Late Cretaceous Bearpaw Formation, Southern Alberta, Canada. PALAIOS 10:408–423.

Tyson, H. 1981. The structure and relationships of the horned dinosaur Arrhinoceratops Parks(Ornithischia: Ceratopsidae). Canadian Journal of Earth Sciences 18:1241–1247.

Upchurch, P., P. M. Barrett, and P. Dodson. 2004. Sauropoda; pp. 259–322 in The Dinosauria II. University of California Press.

Varricchio, D. J., C. Koeberl, R. F. Raven, W. S. Wolbach, W. C. Elsik, and D. P. Miggins. 2010. Tracing the Manson impact event across the Western Interior Cretaceous Seaway. Geological Society of America Special Papers 465:269–299.

Villeneuve, M. 2004. Radiogenic Isotope Geochronology; pp. in A Geologic Time Scale 2004. Cambridge University Press.

Waagé, K. M. 1968. The Type Fox Hills Formation, Cretaceous (Maestrichtian), South Dakota. Peabody Museum of Natural History, Yale University Bulletin, pp.

Wagner, J. R. 2001. The hadrosaurian dinosaurs (ornithiscia: hadrosauria) of Big Bend National Park, Brewster County, Texas, with implications for late Cretaceous paleozoogeography. Thesis, Texas Tech University pp.

Wagner, J. R., and T. M. Lehman. 2009. An enigmatic new lambeosaurine hadrosaur (Reptilia: Dinosauria) from the Upper Shale member of the Campanian Aguja Formation of Trans-Pecos Texas. Journal of Vertebrate Paleontology 29:605–611.

Wagoner, J. C. V., R. M. Mitchum, K. M. Campion, and V. D. Rahmanian. 1990. Siliciclastic Sequence Stratigraphy in Well Logs, Cores, and Outcrops: Concepts for High-Resolution Correlation of Time and Facies. American Association of Petroleum Geologists, Methods in Exploration 174:55.

Wall, W. P., and P. M. Galton. 1979. Notes on pachycephalosaurid dinosaurs (Reptilia: Ornithischia) from North America, with comments on their status as ornithopods. Canadian Journal of Earth Sciences 16:1176–1186.

Weimer, R. J. 1960. Upper Cretaceous stratigraphy, Rocky Mountain area. AAPG Bulletin 44:1–20.

Weishampel, D. B., and J. A. Jensen. 1979. Parasaurolophus (Reptilia: Hadrosauridae) from Utah. Journal of Paleontology 53:1422–1427.

Wick, S. L., and T. M. Lehman. 2013. A new ceratopsian dinosaur from the Javelina Formation (Maastrichtian) of West Texas and implications for chasmosaurine phylogeny. Naturwissenschaften 100:667–682.

Williamson, T. E. 1996. ?Brachychampsa sealeyi, sp nov., (Crocodylia, Alligatoroidea) from the Upper Cretaceous (lower Campanian) Menefee Formation, northwestern New Mexico. Journal of Vertebrate Paleontology 16:421–431.

Williamson, T. E. 1997. A new Late Cretaceous (early Campanian) vertebrate fauna from the Allison Member, Menefee Formation, San Juan Basin, New Mexico. New Mexico Museum of Natural History and Science Bulletin 11:51–59.

Williamson, T. E. 2000. Review of Hadrosauridae (Dinosauria, Ornithischia) from the San Juan Basin, New Mexico. Dinosaurs of New Mexico. SG Lucas and AB Heckert (eds.). New Mexico Museum of Natural History and Science, Bulletin 17:191–213.

Williamson, T. E., and A. Weil. 2008. Stratigraphic distribution of sauropods in the Upper Cretaceous of the San Juan Basin, New Mexico, with comments on North America's Cretaceous "sauropod hiatus." Journal of Vertebrate Paleontology 28:1218–1223.

Wiman, C. 1931. Parasaurolophus tubicen n. sp. aus der Kreide in New Mexico. Nova Acta Regiae Scientiarum Upsaliensis 7:3–11.

Wolfe, D. G., and J. I. Kirkland. 1998. Zuniceratops christopheri n. gen. & n. sp., a ceratopsian dinosaur from the Moreno Hill Formation (Cretaceous, Turonian) of west-central New Mexico. Lower and Middle Cretaceous Terrestrial Ecosystems. New Mexico Museum of Natural History and Science Bulletin 14:303–317.

Wu, X., D. B. Brinkman, D. A. Eberth, and D. R. Braman. 2007. A new ceratopsid dinosaur (Ornithischia) from the uppermost Horseshoe Canyon Formation (upper Maastrichtian), Alberta, Canada. Canadian Journal of Earth Sciences 44:1243–1265.

Xing, H., X. Zhao, K. Wang, D. Li, S. Chen, J. C. Mallon, Y. Zhang, and X. Xu. 2014. Comparative Osteology and Phylogenetic Relationship of Edmontosaurus and Shantungosaurus (Dinosauria: Hadrosauridae) from the Upper Cretaceous of North America and East Asia. Acta Geologica Sinica - English Edition 88:1623–1652.

Yi, M.-S., and A. T. Cross. 1997. Palynostratigraphy of Upper Cretaceous-Lower Tertiary strata, Price Canyon, Utah. Review of Palaeobotany and Palynology 97:53–66.

Zanno, L. E., D. J. Varricchio, P. M. O'Connor, A. L. Titus, and M. J. Knell. 2011. A new troodontid theropod, Talos sampsoni gen. et sp. nov., from the Upper Cretaceous Western Interior Basin of North America. PLOS ONE 6:e24487.

APPENDIX C

SUPPLEMENTARY INFORMATION 1 FOR CHAPTER 4:

REVIEW OF FOSSIL MATERIALS AND FIGURES

Here I review fossil materials of chasmosaurines relevant to the current study, including observations not previously published. Detailed descriptions are given for Campanian chasmosaurine specimens from the San Juan Basin, New Mexico, which are most comparable to the new specimens. Attention is also given to chasmosaurines from elsewhere in North America that preserve the parietal posterior bar, being therefore comparable to the newly described specimens, and can be included in the morphometric analysis. I also review problematic or fragmentary taxa (including many recently described taxa) that require reassessment or comment. Specimens described here are listed in Table 4.1 of the main manuscript.

The following morphological features of the parietal are given special attention as they are most important when considering differences among chasmosaurines:

1. Presence and shape of an embayment on the posterior bar, including whether the embayment extends anterior to the posteriormost border of the parietal fenestrae.
2. Angle at which the lateral rami of the posterior bar meet medially.
3. Relative and absolute anteroposterior thickness of the posterior bar lateral rami from medial to lateral.
4. Number, shape, size, and orientation of epiparietals (typically 3), especially ep1, which is the most diagnostic.
5. Anteroposterior position of the maximum constriction of the median bar.
6. Development of lateral flanges of the median bar that invade the parietal fenestrae.
7. Development of the lateral bars to completely enclose the parietal fenestrae.

The precise stratigraphic position of specimens is also given special attention as this information is critical when assessing morphological change through time and its implications for the mode of evolution. Ontogenetic development is assessed where relevant or possible, although this is largely limited to size, parietosquamosal frill texture, and shape and fusion of frill epiossifications.

Institutional Abbreviations

AMNH, American Museum of Natural History, New York; CMN, Canadian Museum of Nature, Ottawa (was NMC, National Museum of Canada); MNA, Museum of Northern Arizona, Flagstaff; NHMUK, Natural History Museum, London (was BMNH, British Museum Natural History); NMMNH, New Mexico Museum of Natural History and Science, Albuquerque; OMNH, Oklahoma Museum of Natural History, Norman; PMU, Paleontologiska Museet, Uppsala University, Sweden; ROM, Royal Ontario Museum, Toronto; SDNHM, San Diego Natural History Museum, California; SMP, State Museum of Pennsylvania, Harrisburg; TMP, Tyrrell Museum of Paleontology, Drumheller, Alberta; UALP, University of Arizona Laboratory of Paleontology; UKVP, University of Kansas, Lawrence; UMNH, Utah Museum of Natural History, Salt Lake City; UNM, University of New Mexico, Albuquerque; USNM, United States National Museum, Smithsonian Institution, Washington D.C.; UTEP, University of Texas at El Paso.

Campanian San Juan Basin Chasmosaurine Specimens

Pentaceratops sternbergii Holotype AMNH 6325, and cf. *P. sternbergii* Referred Specimens AMNH 1624, 1625

The holotype of *Pentaceratops sternbergii* (AMNH 6325; Osborn, 1923) was collected in the San Juan Basin by Charles H. Sternberg in 1922, and comprises a mostly complete skull that unfortunately lacks the diagnostic posterior bar of the parietal. A second near-complete skull (AMNH 1624, currently undescribed but figured as a line drawing by Lehman, 1993; 1998; and numerous photographs in Sullivan and Lucas, 2011) was collected by C.H. Sternberg in the San Juan Basin in June 1923 (*contra* Lull, 1933; see C.H. Sternberg's letters in Sullivan and Lucas, 2011; p. 455; see below), but similarly lacks the distal part of the parietal. Both of these specimens were reconstructed for display based on a third specimen (AMNH 1625, also undescribed but figured by Longrich, 2014) collected by C.H. Sternberg in 1923 (*contra* Lull, 1933; see below), which is a near-complete frill missing only the anterior ends of the parietal and squamosal; as such it can be directly compared with the new specimens described here. Osborn (1923) does not mention the existence of AMNH 1624 or AMNH 1625 (nor AMNH 1622, a set of brow horns), as they were not acquired by the AMNH until 1924 (see letters in Sullivan and Lucas, 2011). After the specimens were acquired by the AMNH, it appears likely that they were labeled as *P. sternbergii* in the AMNH collections, as Lull (1933) includes them in a list of *Pentaceratops sternbergii* specimens without any specific comment on them not being previously described or figured, nor listing characters that would permit referral.

Stratigraphy. As AMNH 6325 is the type specimen of *P. sternbergii*, it is clearly important to establish its provenance. All available data suggests that the holotype of *Pentaceratops sternbergii* (AMNH 6325), and probably the referred specimens AMNH 1624 and 1625 were collected from the Fossil Forest Member of the Fruitland Formation, probably from a sandstone in the middle of the Fossil Forest Member. In the original description (Osborn, 1923), the holotype (AMNH 6325) was described as having been collected from the Fruitland Formation, but no further details are given. This was later expanded upon by Lull (1933) who stated that AMNH 6325 was collected from 9 miles east of Tsaya (a trading post). Using this description, Rowe et al. (1981) suggest that the collection locality is "probably NW 1/4 T22N R11W", however, this defined area (Figure 4.3H) has very little to no outcrop visible on Google Earth satellite images, consisting instead of flat scrubland. It is unlikely that vegetation cover and topography have changed significantly since the specimen was collected in 1922, so the locality suggested by Rowe et al. (1981) is probably incorrect. Hunt and Lucas (2003) suggest that the holotype might have been collected from one of the many old quarries (up to 12; Wolberg et al., 1988; only 5 described by Hunt and Lucas, 2003) located in the Fossil Forest study area (Figure 4.3), which they point out is 8-9 miles northeast of Tsaya (i.e. mostly matching the descriptions of Lull, 1933; and Rowe et al., 1981), and from which it is generally accepted that C.H. Sternberg collected fossil material. All of the historical quarries described by Hunt and Lucas (2003) were excavated into a sandstone horizon approximately in the middle of the Fossil Forest Member of the Fruitland Formation. Furthermore, the Fossil Forest study area has little to no outcrop that occurs above the

Bisti Bed (the lowermost member of the Kirtland Formation), such that specimens collected from this locality are all likely to have originated from the Fruitland Formation. The referred partial skull AMNH 1624 is described as having been "collected by CH Sternberg in 1923 from the Fruitland Formation, near Tsaya" (Lull, 1933). The diagnostic nearly complete frill (AMNH 1625) was "collected by CH Sternberg from the Fruitland Formation in 1924" (Lull, 1933). Rowe et al. (1981) acknowledge the existence of AMNH 1625 but state that they had not seen the specimen. Further information is provided in Sternberg's letters to the AMNH documented by Sullivan and Lucas (2011); in their appendices (p. 447), Sullivan and Lucas (2011) suggest that a ceratopsid frill found by C.H. Sternberg in the Fruitland Formation (mentioned by Sternberg in a letter to Prof. Carl Wiman of the Paleontologiska Museet at Uppsala University; dated 4th Sept 1921) is AMNH 1625. However, this is probably in error as all material collected during 1921 should have been shipped to Uppsala (the 1921 specimen is probably therefore one of the other pieces of ceratopsian frill that Sternberg sent to Uppsala, likely incomplete left squamosal PMU 24944 (was PMU R.220), as this is the only frill piece from the Fruitland Formation in the Uppsala University collection). In a later letter from Sternberg to W.D. Matthew of the AMNH (June 27th, 1923; in Sullivan and Lucas, 2011, p. 456), Sternberg refers to a newly discovered frill as "the entire distal margin of the crest and the central bar are entire, also part of both squamosals and margin of crest." Unfortunately, no locality details are given, but this accurately describes the preserved material of AMNH 1625. Indeed, Sternberg had found AMNH 1624 a few weeks previously (documented in his letter dated June 17th 1923; Sullivan and Lucas, 2011) and

offered both specimens to the AMNH as a set. Based on this information, AMNH 1625 was presumably found and collected in 1923, not 1924 (as stated by Lull, 1933). Sternberg's 1923 letters were sent from Tsaya, but other than that no locality information is available for AMNH 1625, however it seems likely that he was working in the same area in which he discovered AMNH 1624 only weeks previously. Regardless, AMNH 6325, 1624, and 1625 are all described as having been collected in the Fruitland Formation.

Morphology. As AMNH 6325 (holotype, *Pentaceratops sternbergii*) lacks the posterior end of the frill, it cannot be compared with the new specimens described here. Some comparisons can be made between the new specimens and AMNH 1624 as it preserves the right posterolateral corner of the parietal (at its contact with the squamosal). AMNH 1625 is a nearly complete frill so can be fully compared with the new specimens. Morphological assessment of AMNH 1624 and 1625 is based on images and description provided in Lehman (1998), Sullivan and Lucas (2011), and Longrich (2014).

Specimen AMNH 1625 is as large or larger than other specimens of previously referred to *Pentaceratops* (Figure 4.17). The lateral rami of the posterior bar meet at an angle of 83° (Figure 4.S1). The anteroposterior thickness of the posterior bar of AMNH 1625 is either relatively consistent mediolaterally, making it appear strap-like, or is actually thicker medially than laterally (also seen in *Utahceratops* referred specimen UMNH VP-16671 and coded as a new character by Longrich, 2014). This is unlike specimens of aff. *Pentaceratops* n. sp. (UKVP 16100, MNA Pl.1747, and NMMNH P-37880), *Navajoceratops*, and *Terminocavus*, where the lateral rami of the posterior bar

are anteroposteriorly narrower medially than laterally. The lateral rami of AMNH 1624 are also unexpanded anteroposteriorly at the contact with the squamosal. Each lateral ramus of the posterior bar is bent at an obtuse angle at the ep2 locus. This is not observed in specimens referred to aff. *Pentaceratops* n. sp. (UKVP 16100; MNA Pl.1747; NMMNH P-37880), however, an obtuse angle at the ep2 locus is present in *Utahceratops gettyi* (referred specimen UMNH VP-16671, and probably the holotype UMNH VP-16784; Sampson et al., 2010), and also possibly *C. russelli* referred specimen TMP 1999.55.292 (Longrich, 2010). A similarly angular posterior bar is also seen in *C. russelli* referred specimen CMN 8803 (Sternberg, 1940; Longrich, 2010), and *Agujaceratops* specimen UTEP P.37.7.065 (Lehman, 1989), although in these specimens the angular deflection occurs at the locus labeled as ep1. It is unclear if this angular shape for the posterior bar has taxonomic significance, or might simply represent individual variation.

The median bar of AMNH 1625 is narrow and strap-like with the point of maximum constriction occurring approximately half way along its length. The ventral side of AMNH 1625 was not figured by Longrich (2014) so it is unknown whether or not there are any lateral flanges that extend into the fenestrae; however, the narrowness of the bar suggests that they are not present. The median bar of AMNH 6325 is similarly narrow and strap-like, but the specimen is encased in a wall mount and so further comparisons are not possible.

The parietal lateral bars of AMNH 1625 are either broken, imperceptibly fused to the squamosal bar, or are simply less encompassing of the parietal fenestrae than in specimens of aff. *Pentaceratops* n. sp. (and later chasmosaurines). The degree to which

the parietal fenestrae are entirely enclosed within the parietal is noted as variable even between left and right sides of the same individual in *Chasmosaurus belli* (Godfrey and Holmes, 1995). However, given that in more derived chasmosaurines the parietal fenestrae are completely enclosed by a thick parietal lateral bar (e.g. *Anchiceratops*, "*Torosaurus*"), then variability in this character is probably phylogenetically important (see main text).

AMNH 1625 is one of the few frills to exhibit all epiparietals fused to the posterior bar. Although the typical six epiparietals are present, the lateralmost epiparietals (ep3) on both sides straddle the parietal-squamosal contact such that under some classification systems (e.g. Sampson et al., 2010) they might be considered as "eps" rather than ep3. Most other specimens of cf. *P. sternbergii* do not preserve an epiossification fused to locus ep3 (although one presumably existed there in life). The exception is AMNH 1624, which has the lateralmost part of the parietal preserved and an ep3 that abuts but does not appear to straddle the parietal-squamosal contact. *Terminocavus* preserves a fused ep3 on the left side which does not straddle the squamosal-parietal contact. This suggests that, as in *Triceratops*, the "eps" is an individually variable feature (perhaps strongly influenced by ontogeny), and might not be a reliable character for phylogenetic analysis. However, it remains an interesting source of variation within a population.

Ep1 is interesting in AMNH 1625 as on the left side it projects anterodorsally (as seen in c.f. *Pentaceratops* sp. UKVP 16100 and MNA Pl.1747) but on the right side only dorsally. Longrich (2014) suggests that this is a preservational artifact, but it is hard to

imagine a burial process where the left ep1 remains as normal, whereas the right side is distorted to deflect dorsally, especially in this case where there is otherwise no unusual distortion elsewhere on the frill. I therefore interpret the difference in orientation of left and right ep1 in AMNH 1625 as genuine, which has repercussions for the validity of *P. aquilonius* (Longrich, 2014; see later).

In AMNH 1625 ep2 projects posteriorly, as in *Utahceratops* referred specimen UMNH VP-16671, but unlike c.f. *Pentaceratops* sp. MNA Pl.1747, *Navajoceratops,* and *Terminocavus*, in which ep2 projects medioposteriorly. Ep2 is damaged in UKVP 16100, but would appear to be intermediate in orientation between that of AMNH 1625 and MNA Pl.1747, being mostly posteriorly oriented, but slightly medially deflected (Rowe et al., 1981; Lehman, 1998). In the new specimen c.f. *P. sternbergii* NMMNH P-37880, ep2 is similarly unfused, but the ep2 locus is oriented either posteriorly or slightly medioposteriorly (see later).

In AMNH 1625 (and almost certainly AMNH 1624), the angular shape of the posterior bar means that the posteriormost epiparietal is ep2, with ep3 either subequal or anterior to ep2. This condition is also seen in *Utahceratops* specimens UMNH VP 16784 (holotype) and UMNH VP 16671. However, in aff. *Pentaceratops* n. sp. specimens MNA Pl.1747 and UKVP 16100, *Navajoceratops* holotype SMP VP-1500, and *Terminocavus* holotype NMMNH 27468, ep3 is the posteriormost locus.

In summary, cf. *P. sternbergii* referred specimen AMNH 1625 exhibits morphology intermediate between *Utahceratops* referred specimen UMNH VP-16671 and specimens referred to aff. *Pentaceratops* n. sp. (UKVP 16100 and MNA Pl.1747).

aff. *Pentaceratops* n. sp.; UKVP 16100.

UKVP 16100 was collected in 1966 by the University of Kansas Museum of Natural History and comprises a skull with frill. Most of the skull has not been described, but the critical posteromedial area of the parietal was briefly described and figured by Rowe et al. (1981), and Lehman (1998), who both referred it to *Pentaceratops sternbergii*. The specimen has recently been completely reprepared and is currently being described (J. Fry, pers. comm.).

Stratigraphy. Rowe et al. (1981) report that UKVP 16100 was collected from the upper part of the Fruitland Formation in the SW 1/4, Sec. 34, T24N R13W, Hunter Wash, New Mexico. This is refined to the SE 1/4 of the SW 1/4 of the SW 1/4, Sec. 34, T24N R13W (Figure 4.3E; RM Sullivan, pers. comm. 2015). This quarter-mile square plots entirely within the uppermost part of the Fruitland Formation in the USGS 100k bedrock geology map (O'Sullivan and Beikman, 1963), or alternatively in the lowermost part of the Kirtland lower shale (Hunter Wash Member) in the USGS 24k surficial geology map (O'Sullivan et al., 1979). From this, it can be inferred that UKVP 16100 occurs stratigraphically between the uppermost coal of the Fruitland Formation and the top of the Bisti Bed sandstone (sensu Lucas et al., 2006). This is supported by reference to aerial photography of the area in Google Earth, which reveals extensive dark red-brown sandstones matching the description of the Bisti Bed sandstone (Hunt and Lucas, 1992; Lucas et al., 2006). Finally, this specific area was illustrated in an aerial photograph by Hunt and Lucas (1992) and identified as outcrop of the Fossil Forest Member of the Fruitland Formation and the Bisti Bed sandstone (indeed, this is the type area for the Bisti

Bed; Hunt and Lucas, 1992). From this information it is considered that UKVP 16100 was collected from the Fossil Forest Member of the Fruitland Formation.

Morphology. UKVP 16100 is currently under study (J. Fry, pers. comm.) so discussion of its morphology is brief and limited to the parietal, that being the element relevant to description of the new specimens, and the only element previously figured or described (in ventral view by Rowe et al., 1981; in dorsal view by Lehman, 1998). The figured portion of the parietal comprises a complete posterior bar, and the posterior ends of the lateral bars. A median bar is figured by Rowe et al. (1981), but may not be correctly identified, and so it will not be further discussed here.

The lateral rami of the posterior bar meet at an angle of 87° forming a deep embayment that extends anteriorly slightly further than the posteriormost edge of the fenestrae (Figure 4.S1). The posterior bar is of similar anteroposterior thickness from the midpoint to the lateral edges, although the lateral edges are slightly anteroposteriorly thickened at the apex. With regards to anteroposterior thickness, UKVP 16100 is intermediate between AMNH 1625 (where the posterior bar is of uniform thickness) and MNA PL.1747 (which is significantly thicker at the lateral margins). This represents an interesting trend in San Juan Basin chasmosaurines where the anteroposterior thickness of the posterior bar changes stratigraphically, culminating in the condition seen in *Navajoceratops* and *Terminocavus* (see main text).

Only the posteriormost ends of the parietal lateral bars are figured by Rowe et al. (1981), but this at least demonstrates that the lateral bars are more substantial than in *P.*

sternbergii specimen AMNH 1625. However, the extent to which they might enclose the parietal fenestrae must await full description of the specimen.

UKVP 16100 preserves loci for three epiparietals on each side, with some epiparietals fused in place (Rowe et al., 1981; Lehman, 1998; J. Fry, pers. comm.). Both ep1 are recurved to point anterolaterally (Lehman, 1998) as seen in other specimens of *Pentaceratops*. Lehman (1998) illustrates fused epiparietals at locus ep2, but it would appear that this is only visible on the right side (J. Fry, pers. comm.). Ep3 loci do not bear fused epiparietals and are positioned immediately lateral to ep2.

The parietal of UKVP 16100 exhibits characters consistent with a subadult status in that only ep1 has fused epiossifications. Unfused epiossifications at loci ep2 and ep3 are supportive of a subadult status (based on ontogenetic analysis of *Triceratops*; Horner and Goodwin, 2006). Ontogenetic assessment of elements other than the parietal await full description of the specimen by J. Fry.

aff. *Pentaceratops* n. sp.; MNA Pl.1747

MNA Pl.1747 was collected in 1975 by the Museum of Northern Arizona. It comprises a mostly complete skull, including the diagnostic posterior bar of the parietal. The specimen has never been completely described, although partial descriptions have been given by Rowe et al. (1981), and Lehman (1993), and a full description is in preparation (J. Fry, pers. comm.).

Stratigraphy. The collection locality of MNA Pl.1747 has been previously misreported and is corrected here. Rowe et al. (1981) give the locality as the NW 1/4, SW

1/4, Sec. 28, T24N, R13W; ~5km east of the Burnham Trading Post (destroyed by fire in 1978). However, this is in error as the township/range coordinates are inconsistent with the locality description. The township range coordinates plot a one-sixteenth-mile square within the southwesternmost part of the Bisti-Denazin wilderness, along Hunter Wash, ~2.1 km ENE of the old Bisti trading post (Figure 4.3). By comparison, the Burnham trading post was located ~25 km northwest of this position, in Brimhall Wash (Figure 4.3). A locality map on file at the Museum of Northern Arizona resolves this problem, showing that MNA Pl.1947 was collected from section 4, T24N R15W, ~5 km southeast of Burnham trading post (Figure 4.3F). The locality data of Rowe et al. (1981) should therefore be disregarded. Qualified researchers can request more precise locality data from the Museum of Northern Arizona.

The locality of MNA Pl.1747 plots within the upper part of the Fruitland Formation in the USGS 100k bedrock geology map (O'Sullivan and Beikman, 1963; Figure 4.3), and in the lowermost part of the Kirtland lower shale (Hunter Wash Member) in the USGS 24k surficial geology map (Scott et al., 1979). From this, it can be inferred that MNA Pl.1747 occurs stratigraphically between the uppermost coal of the Fruitland Formation and the top of the Bisti Bed sandstone (sensu Lucas et al., 2006).

Morphology. MNA Pl.1747 is currently under study (J. Fry, pers. comm.) so discussion of its morphology is brief and mostly limited to the parietal, that being the element relevant to description of the new specimens, and the only element previously well figured or described (Rowe et al., 1981; Lehman, 1993).

The parietal of MNA Pl.1747 is complete and well preserved. The posterior bar is anteroposteriorly narrow medially, but thickens laterally (although this may be partly an artifact of fusion of epiparietal 3; see later). The lateral rami of the posterior bar meet at an angle of 88° (Figure 4.S1) forming a deep embayment that extends slightly (4 cm) more anteriorly than the posteriormost edge of the fenestrae (Rowe et al., 1981).

The median bar is narrow and strap-like with the point of maximum constriction occurring approximately half way along its length. The ventral side was figured by Rowe et al. (1981) and does not exhibit the lateral flanges present in Taxon C (and to a lesser extent in *Navajoceratops* and *Terminocavus*; see main manuscript).

The parietal lateral bars are figured by Rowe et al. (1981), and completely enclose the fenestra on the left side. The right side is incompletely preserved.

MNA Pl.1747 preserves loci for three epiparietals on each side, with ep1 and ep2 fused on both sides (Rowe et al., 1981; Lehman, 1993). Both ep1 are recurved such that their tips point anterolaterally (Lehman, 1993). Both ep2 are preserved attached to the posterior bar (the suture is still visible), and are oriented dorsomedially, with their distal tips separated by only 12cm (Rowe et al., 1981). The medial edges of both ep2 are twisted slightly, being directed anterodorsally. Ep3 loci are described by Rowe et al. (1981) and Lehman (1993) as not bearing a fused epiparietal. This is how the specimen is reconstructed in my figures. However, J. Fry (pers. comm.) has suggested that ep3 is actually fully fused to the posterior bar on both sides, being distinguished only by a barely perceptible textural change (also implied in the reconstruction provided by Forster et al., 1993). If true, it would mean that the shape of the posterior bar would be very close

to that of UKVP 16100 and NMMNH P-37880, but less similar to *Navajoceratops*. This issue will remain open until the complete redescription of MNA Pl.1747 is published by J. Fry.

MNA Pl.1747 exhibits characters consistent with an adult or subadult status (in comparison to ontogenetic indicators in *Triceratops*; Horner and Goodwin 2006; 2008). Epiparietals ep1, ep2, and possibly ep3 are fused to the parietal. In contrast only the anterior episquamosals are fused (see Rowe et al., 1981). Ontogenetic assessment of other elements awaits full description of the specimen by J. Fry.

aff. *Pentaceratops* n. sp.; NMMNH P-37880

NMMNH P-37880 comprises ~50% of the right ramus of a parietal posterior bar (Figure 4.S2). Although incomplete, it preserves enough morphology to be compared to other chasmosaurine parietals, and so is figured and described here for the first time.

Stratigraphy. NMMNH P-37880 was collected in 1998 by Paul Sealey from NMMNH locality L-4010 and has been plotted from accurate UTM coordinates held on file at NMMNH (Figure 4.3D). L-4010 occurs in the base of a white silty sand at the southwestern end of the south branch of Hunter Wash. The locality plots high in the Fruitland Formation, close to the boundary with the Kirtland Formation on the USGS 100k bedrock geology map (O'Sullivan and Beikman, 1963; Figure 4.3), and within the lowermost part of the Kirtland lower shale (Hunter Wash Member) on the USGS 24k surficial geology maps (O'Sullivan et al., 1979). It is listed as having been collected from

the Fruitland Formation, and the map plot suggests that it occurs high in the Fossil Forest Member.

Morphology. NMMNH P-37880 comprises ~50% of the right ramus of the parietal posterior bar, and derives from an individual approximately the same size as UKVP 16100 and MNA Pl.1747 (Figure 4.17). The posterior bar is embayed medially, but is broken and missing the midline. Similarly the lateralmost edge of the posterior bar is broken, such that the articulation surface with the squamosal is missing. No epiparietals are fused to the posterior bar, although two or three shallow bumps (loci) project from the posterior margin to which epiparietals are presumed to have attached. The medialmost locus (?ep1) is deflected slightly dorsally and divided into three smaller bumps, reminiscent of the irregular shape of ep1 in *Utahceratops* UMNH VP 16671. The next lateralmost locus (?ep2) is directed posteriorly, lying within the plane of the parietal itself. Further lateral to ?ep2, the posterior border is raised to a bump which would appear to be ep3, then is broken. In other specimens of *Pentaceratops*, only ep1 is typically dorsally deflected, supporting the identification that the medialmost locus of NMMNH P-37880 is locus ep1. However, it is possible that ep1 is not preserved on this portion of the parietal, and that instead the medialmost preserved locus is in fact ep2 (with the lateral most locus ep3). The posterior edge within the median embayment is slightly curved dorsally, perhaps indicative of attachment of ep1 more medially, but which is not preserved. The posterior bar is anteroposteriorly thicker laterally, and narrows medially (as seen in UKVP 16100, MNA Pl. 1747, *Navajoceratops*, and *Terminocavus*).

The large size of the specimen might be taken as an indication of maturity. However, as no epiparietals are fused to the posterior bar (which is an indication of subadult status in *Triceratops*; Horner and Goodwin, 2006; Scannella and Horner, 2010), it is likely that the specimen should be considered a subadult or younger. This is supported by the surface texture which exhibits only a few shallowly indented blood vessel grooves, and instead preserves vestiges of a long grain texture, which has been associated with immaturity in ontogenetic studies of centrosaurines and *Triceratops* (Brown et al., 2009; Scannella and Horner, 2010).

NMMNH P-37880 is here referred to aff. *Pentaceratops* n. sp., based on the presence of the following characters exhibited by MNA Pl.1747 and UKVP 16100 (see main text): Arches of the M-shaped parietal posterior bar rounded rather than angular. Lateral rami of the parietal posterior bar become more anteroposteriorly broad from medial to lateral, rather than being uniform thickness.

aff. *Pentaceratops* sp. ("*Titanoceratops ouranos*") OMNH 10165

OMNH 10165 was collected in July 1941, probably from the Fruitland Formation, New Mexico, by Wann Langston, Jr., D.E. Savage, and J.W. Stovall for the Oklahoma Museum of Natural History (Lehman, 1998). The original description of OMNH 10165 (Lehman, 1998) referred it to *Pentaceratops sternbergii*. However, Longrich (2011) recently redescribed it as the holotype of the new taxon *Titanoceratops ouranos*. Longrich (2011) further suggested that *Titanoceratops* is much more derived than *Pentaceratops*, representing a very early-occurring representative of the *Triceratopsini*,

which are otherwise only known from the Maastrichtian [*Eotriceratops* + "*Torosaurus*" + *Triceratops*]. However, many of the characters later used by Longrich (2011) to diagnose *Titanoceratops* were originally noted by Lehman (1998) as subject to a high level of intraspecific variability, and thus not useful in species-level discrimination among chasmosaurines. Furthermore, recent work on chasmosaurine ontogeny has highlighted that characters used by Longrich (2011) to distinguish "*Titanoceratops*" from *Pentaceratops* are known to change ontogenetically in other chasmosaurines, notably characters: 1, large size; 3, anterior squamosal epioccipitals low and with a dorsal ridge; 6, extensive cornual sinuses; 8, postorbital horns strongly curved anteriorly; 9, postorbital horns extremely elongate; 14 premaxillae extremely elongate (Lehman, 1998; Farke, 2006; Horner and Goodwin, 2006; Horner and Goodwin, 2008; Scannella and Horner, 2010; Scannella et al., 2014). It is therefore possible (if not probable) that differences between OMNH 10165 and other specimens referred to *Pentaceratops* might be due to OMNH 10165 being an especially large and old individual, as per its original description (Lehman, 1998). A reanalysis of this specimen is currently being undertaken by other researchers (H. N. Woodward, pers. comm. 2014), so its morphology will not be addressed in detail here.

Stratigraphy. The collection locality of OMNH 10165 is suggested to be 40 miles south of Aztec, New Mexico, ~5 miles south of former headquarters of Wood Ranch, in headwaters of Coal Creek (Longrich, 2011; citing Lehman, 1998, and Wann Langston's unpublished field notes). However, Hunt & Lucas (2003; not cited by Longrich, 2011) express some doubts, as Wolberg et al. (1988) relocated the Wood Ranch headquarters as

being in the SE 1/4, NW 1/4, sec. 36, T24N R12W, therefore the location of the OMNH specimen quarry should be in sec. 25, T23N, R12W, which has no outcrop. Hunt & Lucas (2003) therefore suggest that the section immediately north of this (sec. 24, T23N, R12W) could be the true location of the quarry; it is this section that contains the famous "Fossil Forest" Study Area (Figure 4.3; Fossil Forest Member of the Fruitland Formation; Hunt and Lucas, 2003; Lucas et al., 2006) which has a number of large historical quarries from which the specimen might have been extracted (Hunt and Lucas, 2003).

Note that in the description of OMNH 10165 by Longrich (2011) the relative position of the radiometric date 74.11 Ma (unrecalibrated, Ash 4 of Fassett and Steiner, 1997) is misplotted as occurring at the top of the Fruitland Formation. This was indeed the original described stratigraphic position (Fassett and Steiner, 1997), however, the sample horizon was relocated by Sullivan and Lucas (2006) and found to occur relatively high in the Hunter Wash Member of the Kirtland Formation, rather than the uppermost Fruitland Formation (confirmed here by plotting the coordinates given by Fassett and Steiner, 1997; see Figure 4.3). Thus the cited age range for OMNH 10165 (Longrich, 2011) is incorrect regardless of whether or not it is possible to assert a collection locality.

Morphology. The type specimen of *Titanoceratops* OMNH 10165 lacks the diagnostic posteromedial part of the parietal, therefore it is not possible to fully compare the specimen with other San Juan Basin chasmosaurines. However, it can be noted that the parietal median bar of OMNH 10165 is relatively narrow and lacks lateral flanges; i.e. it is unlike the condition seen in Taxon C (NMMNH P-33906), and all later chasmosaurines (*Anchiceratops*, *Arrhinoceratops* and all Triceratopsini, sensu Longrich,

2011). This is consistent with the suggestion that the specimen was collected from the Fruitland Formation (see above), and it is likely that it pertains to the same taxon as other specimens from the Fruitland, i.e. cf. *Pentaceratops sternbergii* (AMNH 1624, 1625, 6325) or cf. *P*. n. sp. (MNA Pl.1747; UKVP 16100; NMMNH P-37880).

I further make note here that Longrich (2011) proposes that the scapula of OMNH 10165 is different from *Pentaceratops*, but this is based on the postcranium (PMU R.268; now recatalogued as PMU 24922; Kear pers. comm. 2015) described by Wiman (1930), and attributed to *P. fenestratus*. This postcranium (with an associated dentary) is not diagnostic to species, and has not been demonstrated to contain overlapping diagnostic material with the skull attributed to *P. fenestratus*, nor any other chasmosaurine specimen from the Fruitland or Kirtland Formations, with the exception of OMNH 10165. This postcranium cannot therefore be referred to *Pentaceratops* and should be considered as Ceratopsidae sp.. Hence any differences between the postcranial skeletons cannot be used to infer that OMNH 10165 is different from *Pentaceratops*.

"Pentaceratops fenestratus", Holotype PMU 24923

The holotype of *Pentaceratops fenestratus* (Wiman, 1930) is a near-complete skull (PMU 24923; number reassigned from PMU R200; Kear pers. comm. 2015) collected by Charles H. Sternberg in 1921 from the Kirtland Formation, New Mexico (Sullivan and Lucas, 2011). The skull was designated a new species of *Pentaceratops* based on fenestration of the squamosal (Wiman, 1930). This was later deemed pathological by Lull (1933), as such extraneous squamosal fenestrae are relatively common in ceratopsids (e.g. see Tanke and Rothschild, 2002) and may be related to

thinning of the squamosal through ontogeny rather than being strictly pathological. However, Lull (1933) never went so far as to sink *P. fenestratus* into *P. sternbergii*; indeed, Lull commented that *P. fenestratus* was probably a distinct form (based on it being recovered from younger sediments than *P. sternbergii),* just that he was not convinced by the diagnosis. More recently, Rowe et al. (1981) similarly discussed the diagnosis of Wiman (1930), but did not synonymize the species. However, more recently *P. fenestratus* has generally been treated as a junior synonym of *P. sternbergii* by most researchers (e.g. Dodson et al., 2004).

Stratigraphy. In his letters to Prof. Carl Wiman (Paleontologiska Museet at Uppsala University, which purchased the specimen; Sullivan and Lucas, 2011; p. 446), Sternberg specifically notes that PMU 24923 was collected from "what our geologists call the Kirtland Shales" and references Bauer (1916) and Gilmore (1919). If this is correct, then PMU 24923 was recovered from higher in section than other San Juan Basin specimens for which data is available (UKVP 16100; MNA Pl.1747; NMMNH P-37880; all confirmed as from the Fruitland Formation; AMNH 6325, 1624, 1625; reported as from the Fruitland Formation by Sternberg; see above). As such PMU 24923 may derive from a stratigraphic position in the Kirtland Formation equivalent to *Navajoceratops* or *Terminocavus*. Preservation (bone color and mineralization) of the PMU 24923 specimen is inconsistent with the specimen being derived from the stratigraphically higher De-na-zin Member (ie. the collection horizon of Taxon C).

Morphology. Morphological assessment is based on the description and figures of Wiman (1930) and photographs of specimens provided by R.M. Sullivan (SMP; NMMNH) and B. Kear (PMU). PMU 24923 is laterally compressed and slightly crushed such that the morphology of the posterior border of the parietal is difficult to ascertain. However, the diagnostic midline of the posterior bar is preserved and is more comparable to Kirtland Formation taxa *Navajoceratops* and *Terminocavus,* than to c.f. *Pentaceratops sternbergii* from the Fruitland Formation. The median embayment of the posterior bar is deep, notch-shaped and bordered by a raised rim, from which the paired epiparietals (locus ep1) project anterodorsally. Although the narrowness and depth of the notch may be affected by post-burial compression, it seems unlikely that this distortion is severe enough for the original morphology to have resembled *P. sternbergii*, and so it was probably more similar in life to *Navajoceratops* or *Terminocavus*. As preserved, the posterior bar is anteroposteriorly broad, unlike the narrow strap-like condition of Fruitland Formation c.f. *Pentaceratops* (AMNH 1625 and UKVP 16100) and more similar to *Terminocavus*. The morphology is otherwise mostly difficult to determine; although the parietal-squamosal contact is preserved, it is difficult to judge what the morphology of this area would be like as the bone is too distorted.

Similarity of PMU 24923 to *Navajoceratops* and *Terminocavus* is unsurprising since these specimens were all recovered from the Kirtland Formation. However, I concur with Lull (1933) in concluding that although *P. fenestratus* is probably distinct from *P. sternbergii*, distortion of the preserved material is too great to permit an accurate

diagnosis. Either *Navajoceratops* or *Terminocavus* might be referable to the same taxon as PMU 24923, but it is impossible to demonstrate this based on current material.

Other Uppsala Specimens: PMU 24924

It is worth noting that during the 1920's, Sternberg collected a number of other chasmosaurine elements from the Fruitland and Kirtland Formations that were sent to Paleontologiska Museet at Uppsala University (Wiman, 1930; Sullivan and Lucas, 2011). Most of these specimens are probably not diagnostic to the same level as the posterior bar of the parietal. However, PMU 24924 (was PMU R.223; Kear, pers. comm. 2015) is an anterior part of the parietal preserving the median bar which is quite robust and bears small flanges directed laterally into the fenestrae, forming a broad T-shape in cross section (Figure 4.S3C). The flanges are not as well developed as in Taxon C from the De-na-zin Member, but are more developed than in *Pentaceratops sterbergii* and cf. *P.* n. sp., and similar to that observed in *Navajoceratops*. This is consistent with the collection locality which is recorded as being in the Kirtland Formation, rather than the Fruitland Formation (Wiman, 1930), and supports the hypothesis that the lateral flanges of the median bar become more prominent through time (see main text).

Chasmosaurinae sp. NMMNH P-50000 (Formerly UALP 13342)

NMMNH P-50000 (formerly UALP 13342) is a partial skull collected in 1975 by the University of Arizona, and is currently under study (J. Fry, S. G. Lucas, pers. comm.). The skull has a well-preserved facial region, but lacks the frill and postorbital horns (although originally present, the right postorbital horn was apparently lost at some point

prior to the specimen's transferral to NMMNH). Since it lacks a frill, it is not comparable to the new specimens described here, however, it is relevant because it was collected from high in section (see below) and because it was used to code character states for *Pentaceratops sternbergii* by Sampson et al. (2010).

Stratigraphy. Rowe et al. (1981) report that NMMNH P-50000 was collected from the SE 1/4 of the NE 1/4, Section 14, T24N R12W, Alamo Wash, New Mexico (see Figure 4.3). This plots within the Farmington Sandstone Member of the Kirtland Formation using the USGS 100k bedrock geology map (O'Sullivan and Beikman, 1963; Figure 4.3), or on the boundary of the Kirtland lower shale (Hunter Wash Member) and overlying Farmington Sandstone Member using the USGS 24k surficial geology map (Brown, 1982). Thus NMMNH P-50000 occurs stratigraphically between *Terminocavus* holotype NMMNH P-27468, and the De-na-zin Member chasmosaurine fragment NMMNH P-33906. As such, NMMNH P-50000 is the stratigraphically highest reasonably complete skull known from the Campanian of the San Juan Basin.

Morphology. Because NMMNH P-50000 occurs high in the Kirtland Formation, then it might be expected to exhibit morphology intermediate between *Pentaceratops* and *Anchiceratops,* rather than simply being the same as *Pentaceratops*. Some features seem to support this: notably, the nasal horn is positioned more anteriorly than in *Pentaceratops*, and the narial strut of the premaxilla is oriented closer to vertical than the anteriorly inclined condition seen in c.f. *Pentaceratops* (see character matrix of Sampson et al., 2010), although this character may be influenced by ontogenetic elongation of the

rostrum. Further information regarding morphology will be available upon completion of the description by J. Fry or S.G. Lucas.

Taxa Similar to *Pentaceratops*, from Outside the San Juan Basin

aff. *Pentaceratops* sp.; SDMNH 43470

Diem and Archibald (2005) described SDMNH 43470, a partial skull (including the midline of the parietal posterior bar) of a chasmosaurine from the Williams Fork Formation, Colorado. Despite similarities with *Pentaceratops*, Diem and Archibald (2005) refrained from referring the specimen to a specific genus. Later, Lucas et al. (2006) assigned SDMNH 43470 to *Pentaceratops sternbergii*, whereas Longrich (2014) suggested it may belong to the newly named taxon *P. aquilonius* (see later).

Stratigraphy. Diem and Archibald (2005) illustrate SDMNH 43470 as having been collected from the lower part of the Williams Fork Formation (Piceance basin, Rio Blanco County, Colorado), although no explanation is given in the text other than a note in the figure caption that this stratigraphic position is approximate (consultation of Diem's 1999 MS thesis reveals no additional data). Age of the Williams Fork Formation is constrained by the ammonites *Exiteloceras jenneyi* (75.08 - 74.60 Ma; Ogg and Hinnov, 2012) at the top of the underlying Iles Formation; *Didymoceras cheyennense* (74.60 - 74.21 Ma; Ogg and Hinnov, 2012), in the lower part of the Williams Fork Formation; and *Baculites reesidei* (73.63 - 73.27 Ma; Ogg and Hinnov, 2012) from a marine shale (below the Twenty Mile Sandstone Member) in the upper part of the Williams Fork Formation (Newman, 1987). Brownfield and Johnson (2008) published a

K-Ar date of 72.5 ± 5.1 Ma from the Yampa bed tonstein, which occurs 0-80 m above the base of the Williams Fork Formation (ie. very low) in more eastern exposures. For more discussion on age of the Williams Fork Formation, see Fowler (Chapter 3). From this data, it is likely that SDMNH 43470 derives from the *D. cheyennense* zone (74.60 - 74.21 Ma; Ogg and Hinnov, 2012), which is correlative with the upper half of the Hunter Wash Member (~75-74 Ma; Fowler, Chapter 3) of the Kirtland Formation, in the San Juan Basin, New Mexico. However, the morphology of the specimen is more similar to chasmosaurines from stratigraphically lower (see below).

Morphology. Description and comparisons of SDMNH 43470 were given by Diem and Archibald (2005), and Lucas et al. (2006), so discussion here will be brief. The specimen was described as a subadult based on frill texture, a squamosal that is less elongate than other chasmosaurines, and visible cranial sutures (especially at the base of frill epiossifications). To this we can add the shape of the frill epiossifications, which are quite pointed, suggesting a relative maturity between juvenile and subadult ("adult" epiossifications are more broad and blunt; based on *Triceratops*; Horner and Goodwin, 2008). Despite its immaturity, the medial portion of the parietal is comparable in size to specimens of *Pentaceratops* and related chasmosaurines (Figure 4.17). However, the squamosal is not as elongate as in (for example) aff. *Pentaceratops* n. sp. MNA PL.1747; this pattern is similarly seen in *Chasmosaurus russelli* specimen TMP 1983.25.1, which also has a large parietal of comparable size to (probable) adult *Chasmosaurus* specimens, but exhibits more pointed epiparietals, and a much shorter and broader squamosal. The presence of a flange protruding into the parietal fenestra from the ventral part of the

posterior bar probably indicates that the parietal fenestrae are still opening; in all neoceratopsians with documented growth series, parietal fenestrae open and enlarge through ontogeny (e.g. Brown et al., 2009; Scannella and Horner, 2010; Fastovsky et al., 2011).

Parietal morphology of SDMNH 43470 is most similar to cf. *Pentaceratops sternbergii* material from the Fruitland Formation, and older chasmosaurines such as *Utahceratops* (Sampson et al., 2010). The median bar has a rounded cross section; the anteroposterior thickness of the (albeit incomplete) posterior bar is relatively uniform and strap-like, most similar to *Utahceratops* specimen UMNH VP-16671; the angle formed by the lateral rami of the posterior bar is 98°, slightly shallower than Fruitland Formation c.f. *Pentaceratops* (83 - 88°) but much shallower than either of the new taxa (*Navajoceratops*, SMP VP1500, 60°; *Terminocavus* NMMNH P-27468, 73°). It is worth noting that Longrich (2014; p. 302) states that SDMNH 43470 "lacks the strongly U-shaped parietal emargination seen in [*Utahceratops gettyi* and *P. sternbergii*]". However, SDMNH 43470 clearly exhibits a U-shaped embayment (emargination), comparable to *Utahceratops* and cf. *P. sternbergii* (Figure 4.17). What Longrich (2014, p. 297) actually refers to here is that in *Utahceratops* and *Pentaceratops* "the posterior margin of the parietal actually extends forward ahead of the end of the parietal fenestrae"; which is here interpreted as meaning that the deepest (anteriormost) point of the parietal emargination (which is positioned at the midline on the posterior edge of the posterior bar) is more anterior than the posteriormost edge of the parietal fenestrae (as measured on the anterior edge of the posterior bar). It is possible that this is exhibited by SDMNH 43470, although

the posterior extent of the parietal fenestrae is not known as the lateral rami are not preserved more laterally than locus ep2. Regardless, the significance of this feature is difficult to assess as it is not observed in any other specimens of cf. or aff. *Pentaceratops* (contra. Longrich, 2014; see entry on *P. aquilonius*), and might be affected by ontogeny. However, the anterior depth of the median embayment is particularly deep in *Navajoceratops* (more so than in any cf. or aff. *Pentaceratops*) and development of this feature may be important in the eventual enclosure of the median embayment (as seen in *Terminocavus* through *Anchiceratops*; see main text). The position of the attached right ep2 may give indication as to the shape of the lateralmost parts of the lateral rami of the posterior bar. The anteriormost edge of the right lateralmost corner of the right ep2 must lie on the posterior edge of the right lateral ramus of the posterior bar. In which case, the posterior bar cannot have continued laterally at the same angle as seen in specimens referred to aff. *P*. n. sp. (MNA Pl.1747 and UKVP 161000). Instead, this morphology suggests that the posterior bar must have been angled at the ep2 locus, as seen in *Utahceratops* and cf. *P. sternbergii* (AMNH 1625). This might not be indicative of phylogenetic similarity with *Utahceratops* and cf. *P. sternbergii* as immature dinosaurs often exhibit character states more similar to the ancestral form than to an adult of their own species. However, it is a subtle but useful feature, which aids in interpretation of the specimen.

The significance of the morphological similarity of SDMNH 43470 with Fruitland Formation (and more basal) chasmosaurines is twofold. Firstly, as currently understood, the stratigraphic position of the specimen (*D. cheyennense* zone; 74.60 - 74.21 Ma; Ogg

and Hinnov, 2012) correlates with the upper half of the Hunter Wash Member (~75-74 Ma; Fowler, Chapter 3) of the Kirtland Formation; i.e. stratigraphically equivalent to *Terminocavus*, and therefore higher than the Fruitland Formation (and older) chasmosaurines with which it is most similar morphologically. This is unexpected and may be indicative that the correlation of either or both units is incorrect; given the tentative nature of the Williams Fork stratigraphy, and the age of the analyses that produced the San Juan Basin radiometric dates, this seems likely. Secondly, the morphology of SDMNH 43470 may be reflective of its relative immaturity; young dinosaurs often appear more basal than adults of the same species (Fowler et al., 2011; Rozhdestvensky 1965). However, I do not think that this is the case, as the overall stratigraphic and phylogenetic trend in chasmosaurine parietal morphology is paedomorphism. Therefore, SDMNH 43470 cannot be confidently assigned to *Pentaceratops sternbergii* (*sensu* Lucas et al., 2006) nor *P. aquilonius* (Longrich, 2014; possibly a nomen dubium, see below). Instead, I suggest a more conservative approach in considering it as aff. *Pentaceratops* sp., consistent with the original description (Diem and Archibald, 2005). Discovery of immature chasmosaurines from the Fruitland and Kirtland Formations, or more mature material from the Williams Fork Formation, may help clear up the issue.

Utahceratops gettyi

Sampson et al. (2010) described the new taxon *Utahceratops gettyi* based on material from seven localities (including two multi individual bonebeds), spread over

~0.5 - 1 million years, of the lower to middle Kaiparowits Formation (Sampson et al., 2010; Loewen et al., 2013).

There are potential complications in that some of the characters that diagnose *Utahceratops gettyi* are not observable in all referred specimens. Sampson et al. (2010) do not explicitly state which elements overlap among specimens (and do not list which elements are present in the holotype UMNH 16784), making it unclear what justification there is for assigning each specimen to *Utahceratops gettyi*. Most critical here is the character "supraorbital horncores short", which is observed in the fragmentary skull UMNH 12198, but is not figured as occurring in the holotype. Loewen et al. (2013) nebulously state that an "orbit" is known for the holotype, but do not figure the specimen. For the time being, I am going to follow the diagnosis of Sampson et al. (2010), but this will need to be reviewed in the future.

Two specimens preserve the middle part of the parietal posterior bar and are thus relevant to this study; holotype UMNH VP 16784 and UMNH VP 16671. These specimens are comparable in morphology (see below) and so for the purposes of this study they will be considered as representative of *Utahceratops*.

Stratigraphy. The stratigraphic position of specimens referred to *U. gettyi* were plotted by Loewen et al. (2013) relative to a series of radiometrically dated bentonites, the precise positions and ages of which are most recently summarized in Roberts et al. (2013). The stratigraphic position of the holotype specimen (UMNH VP 16784, locality UMNH 960) is shown by Roberts et al. (2013) as occurring in the lower part of the middle unit of the Kaiparowits Formation, slightly above an ash dated at 75.97 Ma (the

distance in meters is unclear); however, what is presumably the same locality (mislabeled as "UMNH VP 16748") is shown by Loewen et al. (2013) as occurring ~175m above the base of the Kaiparowits Formation, slightly below the same radiometric date. The complete posterior bar, UMNH VP 16671, derives from a bonebed (locality UMNH 942; Sampson et al., 2010) that is ~105m higher than the holotype in the middle Kaiparowits Formation, ~280m above the base, and ~140 m below an ash horizon dated at 75.51 Ma (Loewen et al., 2013; Roberts et al., 2013). A conservative view (based on parietal morphology) of the stratigraphic range of *U. gettyi* is therefore ~75.97 Ma to ~75.6 Ma.

Morphology. Partial skull UMNH VP 16784 includes a near complete right ramus of the parietal posterior bar. UMNH VP 16671 is an isolated parietal, but is more complete, comprising a nearly complete posterior bar. Neither specimen preserves the lateralmost edge of the posterior bar where it would articulate with the squamosal. Both UMNH VP 16784 and 16671 exhibit a central embayment medial to the ep2 locus, which in both specimens extends anteriorly beyond the posteriormost border of the fenestrae. Only UMNH 16671 preserves both lateral rami, which meet at an angle of 75°. This is relatively acute, more so than in specimens of c.f. *Pentaceratops sternbergii* (83 - 88°). The posterior bar is of similar anteroposterior thickness from medial to lateral. However, this varies somewhat, with the right side of UMNH VP 16671 being narrower at the point between ep1 and ep2, and the left side being narrower at the lateralmost preserved point (at ep3). In both specimens, three epiparietals are preserved fused to each lateral ramus of the posterior bar, although the right ramus of UMNH VP 16671 is broken before the ep3 locus. Ep1 is an elongate dorsally-deflected ridge that extends along the medial edges of

the embayment. Ep2 is triangular in shape, and projects posteriorly from the posterior bar, which forms an obtuse angle at the ep2 locus, similar to that seen in *Pentaceratops sternbergii* specimen AMNH 1625. Ep3 is triangular in shape and projects posterolaterally. The median bar is incomplete and it is not possible to confidently determine the point of maximum constriction. Narrow lateral flanges extend from the median bar into the parietal fenestrae. These are similar in extent to *Navajoceratops*, but less developed than Taxon C. Although a fragment of a parietal lateral bar is preserved in UMNH VP 12198, it is not complete enough to tell whether the lateral bars completely enclosed the fenestrae.

Pentaceratops aquilonius

Longrich (2014) recently named a new species of *Pentaceratops, P. aquilonius*, based on two specimens (holotype CMN 9813; paratype CMN 9814) from the uppermost Dinosaur Park Formation, Alberta, and possible referred specimen (SDMNH 43470) from the Williams Fork Formation, Colorado.

Holotype CMN 9813 comprises the distal end of a squamosal (bearing four episquamosals) and lateralmost part of the posterior bar of the parietal (bearing two fused epiparietals, probably ep3, and ep2). Paratype CMN 9814 comprises one fragment of the right lateral ramus of the posterior parietal bar, with two fused epiparietals (probably ep1 and ep2), and two isolated epiossifications labeled as ep1 and ep2 of the left side (Longrich, 2014). CMN 9813 and CMN 9814 were originally described by Langston (1959) and referred to *Anchiceratops* based on the large triangular epiparietals. SDMNH 43470 is a partial skull (including the midline of the parietal posterior bar) originally

described by Diem and Archibald (2005) and referred to Chasmosaurinae sp., then to *P. sternbergii* by Lucas et al. (2006), and is here considered as aff. *Pentaceratops*. Here I show that the autapomorphies used to diagnose *P. aquilonius* are invalid, and it should be considered a nomen dubium.

Stratigraphy. CMN 9813 and CMN 9814 were collected at different localities that expose the uppermost Dinosaur Park Formation, near Manyberries in southeast Alberta; i.e. outside of the well-studied exposures in Dinosaur Provincial Park itself (details provided in Langston, 1959; and Longrich, 2014). Langston (1959) described the CMN 9813 locality as being "but a few feet" stratigraphically below an outlier of the Bearpaw Shale that conformably overlies the upper part of the Dinosaur Park Formation (then referred to as an undivided Oldman Formation), and described CMN 9814 as having been collected one meter below the Bearpaw Shale. He therefore equated both localities as occurring within the Lethbridge Coal Zone, which occurs at the top of the Dinosaur Park Formation. CMN 9813 and 9814 are thus most likely constrained in age by two radiometric dates; the base of the Lethbridge Coal Zone (LCZ Tuff; 76.10 ± 0.5 Ma; Eberth, 2011) and the base of the Bearpaw Shale (Bearpaw Tuff; 75.46 ± 0.24 Ma; Eberth, 2011). This overlaps with the range of the morphologically similar *Utahceratops gettyi* from the middle unit of the Kaiparowits Formation, Utah (~75.97 Ma to ~75.6 Ma ; see above; Sampson et al., 2010; Loewen et al., 2013; Roberts et al., 2013), which, along with *P. sternbergii*, was recovered as the sister taxon to *P. aqulilonius* by Longrich (2014). However, it is possible that the Lethbridge Coal Zone at Manyberries is slightly older than in Dinosaur Provincial Park (from which the radiometric dates are derived),

since the coal zone tracks the shoreline of the westerly transgressing Bearpaw Seaway (Eberth, 2005), and Manyberries is ~80 km east of Dinosaur Provincial Park (and ~150 km east of Lethbridge).

Morphology. Longrich (2014) diagnosed *P. aquilonius* based on four autapomorphies, which are shown here as invalid, rendering *P. aquilonius* a nomen dubium:

1. Weak emargination [embayment] of parietal, with lateral rami meeting at an angle of approximately 90° and U-shaped emargination [embayment] not strongly extended anteriorly.

This autapomorphy cannot be assessed on *P. aquilonius* holotype CMN 9813 as it does not preserve the medial part of the posterior bar. Although the provided reconstruction (Longrich, 2014; Figure 4.6) suggests that enough of the posterior bar is preserved in CMN 9813 to accurately reconstruct the embayment, when shown to the same scale as AMNH 1625 (Figure 4.S4) it can be seen that the reconstruction probably overestimates the mediolateral extent of the posterior bar that is preserved in CMN 9813. Paratype CMN 9814 preserves the right lateralmost edge of the embayment, but it is not possible to assert its shape. Neither CMN 9813 nor 9814 preserve both lateral rami so the angle at which the rami meet is not measurable. None of these features can therefore be reliably observed in either the holotype or paratype.

2. [E]p1 projects dorsally, rather than anteriorly.

This autapomorphy cannot be assessed on the *P. aquilonius* holotype (CMN 9813) as it does not preserve the ep1 epiossification, or an ep1 locus (Langston, 1959;

Longrich, 2014). For referred specimen CMN 9814, the isolated epiossification labeled as the left ep1 (Longrich, 2014) is unattached to the parietal and so cannot be assessed for orientation. The small preserved fragment of the right posterior bar of CMN 9814 exhibits ep1 and ep2 fused to the posterior margin and indeed, ep1 projects dorsally, rather than anteriorly. However, this character is variable in specimens of cf. *P. sternbergii*. The orientation of ep1 in CMN 9814 is compared (Longrich, 2014) with cf. *P. sternbergii* specimen AMNH 1625, which preserves left and right ep1 in different orientations: the left ep1 projects anterolaterally, whereas the right ep1 is almost identical to CMN 9814 in projecting dorsally. It is suggested that the dorsal projection of the right ep1 of AMNH 1625 is a preservational artifact, whereas that of the left ep1 is natural (Longrich, 2014). It is hard to imagine a burial process where the left ep1 remains as normal, whereas the right side is distorted to deflect dorsally, especially in this case where there is otherwise no unusual distortion elsewhere on the frill. Furthermore, it would seem easier if not more likely for a burial process to force down a dorsally projected epiossification to make it anteriorly projecting, rather than raising an anteriorly projecting epiossification into a dorsally projecting orientation. This character is therefore shown to be individually and/or taphonomically variable and not taxonomically informative.

3. Lateral epoccipitals [episquamosals] <100 mm in length.

This character refers to the length of the bases of the four episquamosals present on CMN 9813. It has been shown in *Triceratops* that the shape of frill epiossifications changes through ontogeny; in young animals the epiossifications are narrow-based and

more pointed, which then broaden at the base and become blunt through to adulthood (Horner and Goodwin 2006; 2008; Scannella and Horner, 2010). It is possible, therefore, that the small size of the episquamosals in CMN 9813 is because the specimen is not fully mature. Morphology of the episquamosals is slightly pointed (more so than in AMNH 1625), which supports the hypothesis that CMN 9813 is relatively less mature than AMNH 1625. Furthermore, although episquamosal size follows general patterns based on position (ie. the posteriormost episquamosal is usually the largest, seen in CMN 9813), absolute size of lateral episquamosals is variable, even within individuals (e.g. CMN 2280), such that this is probably not a very reliable character upon which to base a species diagnosis.

4. Caudal [posterior] bar of parietal anteroposteriorly broad relative to *P. sternbergii* or *Utahceratops gettyi*.

This character can only be assessed in holotype CMN 9813 as the paratype CMN 9814 is too incomplete. Longrich (2014) reconstructs CMN 9813 with a posterior bar that appears to be anteroposteriorly thicker than cf. *P. sternbergii* AMNH 1625, to which it is being compared. However, this is at least partly an artifact of scaling issues between the specimens. Figure 4.S4 shows both CMN 9813 and AMNH 1625 at the same scale, whereupon it is clear that the posterior bar of CMN 9813 is comparable in anteroposterior thickness to AMNH 1625 (and other specimens of cf. *P. sternbergii*; see Figure 4.17). Furthermore, in all neoceratopsians with documented growth series, the parietal fenestrae open and enlarge through ontogeny by resorption of bone at the margins of the fenestra (e.g. Brown et al., 2009; Scannella and Horner, 2010; Fastovsky et al., 2011). If CMN

9813 is not yet fully mature, then the fenestrae might be enlarged by further resorption of the anterior margin of the posterior bar.

In conclusion, I agree with Longrich (2014) that CMN 9813 and 9814 are morphologically more similar to material referred to *Utahceratops gettyi* and cf. *Pentaceratops sternbergii*, than to *Anchiceratops ornatus* (as suggested by Langston, 1959), and probably represent a northern representative of the *Utahceratops* - *Pentaceratops* clade. However, the type and referred specimens are extremely fragmentary, making a specific diagnosis difficult; the autapomorphies used to diagnose *P. aquilonius* are here shown to be invalid, and it should be considered a nomen dubium. Given that *P. aquilonius* overlaps stratigraphically with *Utahceratops gettyi*, then it seems likely that the two taxa might be very closely related, if not conspecific. However, it is not possible to assert this based on currently published material.

Bravoceratops polyphemus

Wick and Lehman (2013) recently described a partial chasmosaurine skull (TMM 46015-1) from the lowermost Javelina Formation, Texas, as the holotype of *Bravoceratops polyphemus*. The characters that diagnose *B. polyphemus* almost all occur on the parietal posterior bar and median bar: described as fan-shaped, lacking a median embayment, and exhibiting a raised midline area with a shallow depression suggested to represent a missing midline epiparietal (Wick and Lehman, 2013). Although I sympathize with the overall conclusions of this paper, I believe that the median bar is misidentified, and as such none of the characters used to diagnose *B. polyphemus* are actually present in the material.

Morphology and Reassessment. The element identified as the posterior half of the median bar of the parietal is almost certainly the anterior half (Figure 4.S3), comparing favorably with anterior median bars of other chasmosaurines, including well-figured specimens USNM 8604 (c.f. *Pentaceratops*; Kirtland Formation, New Mexico; Gilmore, 1919); PMU R223 (c.f. *Pentaceratops*; Kirtland Formation, New Mexico; Wiman, 1930; Figure 4.1 frills 5 and 6); CMN 491 (the holotype of *Chasmosaurus belli*; as illustrated in Hatcher et al., 1907; Pl. XXI), and NHMUK R4948 (*C. belli*; Maidment and Barrett, 2011). In these specimens the median bar expands laterally at its anterior end, and on the ventral side hosts a shallow rounded fossa, bordered by distinctive longitudinal grooves typical of the ventral side of chasmosaurine parietals (most obvious in Hatcher et al., 1907, Pl. XXI; well-described by Maidment and Barrett, 2011). This matches the morphology of TMM 46015-1 if the element is rotated 180 degrees anteroposteriorly. By contrast, the midpoint and posterior end of chasmosaurine median bars are flat to convex ventrally (i.e. unlike the described condition of TMM 46015-1 in the incorrect orientation). Furthermore, a raised midline ridge on the posterior end of the median bar (as proposed for *Bravoceratops* Wick & Lehman, 2013) is not observed in other chasmosaurines, but a ridge is commonly observed on the anterior end (e.g. *Anchiceratops*; Brown, 1914; Mallon et al., 2011; "*Torosaurus*" *utahensis*; Gilmore, 1946; Lawson, 1976; Sullivan et al., 2005; c.f. *Pentaceratops*; Gilmore, 1919; "*Titanoceratops*" c.f. *Pentaceratops*; Longrich, 2011; *Arrhinoceratops*; Mallon et al., 2014; and subtly in *Chasmosaurus belli*; Hatcher et al., 1907; Maidment and Barrett, 2011). A series of raised bumps along the midline of the parietal is typical of immature

Triceratops ("raised bony prominences"; Goodwin et al., 2006), which become less pronounced through to adulthood, and are also seen *Coahuilaceratops* (Loewen et al., 2010; Cerro del Pueblo Formation, Mexico), which is closely related to, and possibly contemporaneous with *Bravoceratops*. I therefore suggest here that the pit present on the midline of TMM 46015-1 does not represent attachment of an epiparietal, rather, it is a posterior midline bump in the process of being remodeled (a similar depression on a raised midline is visible on the dorsal surface on USNM 8604; Gilmore, 1919; see Figure 4.S4). Contrary to the reconstruction given by Wick and Lehman (2013; their Figure 6F; see my Figure 4.S4), there does not appear to be any indication of an epiparietal present on what is described as the posterior margin of the parietal. Finally, a bifurcated quadratojugal (articulation surface of the squamosal) is given as an autapomorphy of *Bravoceratops*, allying it to "*Torosaurus*" and *Triceratops* (Wick and Lehman, 2013). However, a bifurcated quadratojugal-squamosal articulation surface is not visible in any of the *Triceratops* specimens held at MOR examined by D. Fowler and J. Scannella; the bifurcation seen in the illustrated examples is probably the result of the squamosal overlapping the quadratojugal, and might not be a genuine anatomical feature of *Bravoceratops*. Although *Bravoceratops polyphemus* should therefore be considered a *nomen dubium*, TMM 465015-1 remains important as it is morphologically most similar to chasmosaurines from the Upper Campanian.

Re-identification of the parietal fragment means that there is relatively little remaining diagnostic morphology of TMM 46015-1 for comparison. However, the preserved portion of the parietal shows that the median bar is relatively narrow,

suggesting that quite large parietal fenestrae were present. These large parietal fenestrae are unlike the reduced fenestrae seen in derived chasmosaurines from the Maastrichtian (*Anchiceratops*, *Arrhinoceratops*, and Triceratopsini) or that of Campanian chasmosaurines *Vagaceratops* and *Kosmoceratops*. The lack of lateral flanges to the median bar is also unlike Kirtland Formation Taxon C (NMMNH P-33906). This suggests that TMM 46015-1 is a chasmosaurine less derived than Kirtland Taxon C, and therefore probably older than the De-na-zin Member of the Kirtland Formation (73.8 - 73.5 Ma; Fowler, Chapter 3; see below).

Stratigraphy. The age of TMM 46015-1 remains uncertain, and can only be constrained to between the Middle Campanian to Early Maastrichtian by bounding radiometric dates and/or ammonite biostratigraphy. Wick and Lehman (2013) state that TMM 465015-1 derives from the lowermost Javelina Formation, ~3 m above the contact with the underlying Upper Shale Member of the Aguja Formation, and therefore suggest that the specimen is likely to be from the Late Campanian to Early Maastrichtian. Although I agree with this interpretation, the age of the Aguja and Javelina formations are imprecisely known, and might be of longer (or more intermittent) duration than is typically shown (see Fowler, Chapter 3, for a detailed discussion). The Upper Shale Member of the Aguja Formation rests upon the Terlingua Creek Sandstone, which is dated by the presence of the ammonite *Baculites mclearni* (Rowe et al., 1992; 80.67 - 80.21 Ma; lowermost part of the Middle Campanian; Ogg & Hinnov, 2012). Two U-Pb radiometric dates related to phreatomagmatic volcanism have been published as from within the Upper Shale Member of the Aguja Formation; 76.9 +/- 1.2 Ma (Befus et al.,

2008), and 72.6 +/- 1.5 Ma (Breyer et al., 2007). As the only radiometric dates reported from the Aguja Formation, it seems reasonable to report these dates as representing the age of the Upper Shale Member. However, Befus et al. (2008) present a model showing that two explosive volcanic events created craters within what would traditionally be considered as the Upper Shale Member; i.e. that the volcanism occurred after the Upper Shale Member had been deposited. As such, these dates might not in fact be representative of the age of the Upper Shale Member of the Aguja Formation. Elsewhere in the Big Bend region of southern Texas, the Javelina Formation overlies the Upper Shale Member of the Aguja Formation. Although the Javelina Formation is often cited as being ~69 Ma in age (due to a U-Pb date of 69+/- 0.9 reported by Lehman et al., 2006), it is entirely possible that the base of the Javelina is older as the 69 Ma datum occurs approximately mid-way through the Javelina Formation. Thus the age of TMM 46015-1 can really only be constrained as between the top of the *B. mclearni* zone (80.21 Ma) to the 69 Ma datum.

Based on the revised morphology of *Bravoceratops* (see above), I suspect that TMM 46015-1 is probably from the Upper Campanian, older than Kirtland Formation Taxon C (Denazin Member, 73.8 - 73.5 Ma; Fowler, Chapter 3). This is important as it would suggest that the basal part of the Javelina is older than previously assumed and might bear a fauna comparable to similarly aged units in Utah and New Mexico, potentially adding new data to the debate surrounding northern and southern biogeography.

Chasmosaurus and Related Chasmosaurines from the Western Interior

Chasmosaurus is a genus of ceratopsid dinosaur from the Middle to Upper Campanian Dinosaur Park Formation of Alberta, Canada (and Aguja Formation, Texas). It is important as it is one of the oldest well-known representatives of the Chasmosaurinae. *Chasmosaurus* has an incredibly complex taxonomic history (especially recently) due to synonymization of many historical taxa (*C. belli*; *C. brevirostris*; *Eoceratops canadensis*/ *C. canadensis*; *C. kaiseni*; *C. russelli*), followed by the erection of many new taxa, some of which are based on historical specimens (*C. mariscalensis*; *C. irvinensis*/ *Vagaceratops irvinensis*; *Mojoceratops perifania*; *Kosmoceratops richardsoni*; *Kosmoceratops* sp.). A detailed review of the taxonomic history of *Chasmosaurus* can be found in Godfrey and Holmes, 1995, and Maidment and Barrett, 2011. This taxonomic complexity is a result of multiple fragmentary specimens combined with morphological variability that, as with other dinosaurs, is probably strongly influenced by differences in stratigraphic position and ontogenetic age. The stratigraphic distribution of *Chasmosaurus* (and closely related taxa) is relatively well understood (see below, and main text); however, a detailed investigation into ontogeny in *Chasmosaurus* remains to be attempted (although see Lehman, 1989; 2007).

Godfrey and Holmes (1995) reviewed specimens assigned to *Chasmosaurus* and reduced the genus to two valid species; *C. belli* and *C. russelli*, based on the morphology of the posterior bar of the parietal. Later, Holmes et al. (2001) described a third species, *C. irvinensis*, which was renamed as *Vagaceratops irvinensis* by Sampson et al. (2010)

and is therefore discussed later in this document. To begin with I will review the recently named taxon *Mojoceratops perifania* (Longrich, 2010)

"*Mojoceratops perifania*"

Longrich (2010) recently described the chasmosaurine ceratopsid *Mojoceratops perifania* based on eight cranial specimens (holotype, TMP 1983.25.1; referred specimens, TMP 1999.55.292; NMC 8803; AMNH 5656; AMNH 5401; CMN 1254; CMN 34893; TMP 1979.11.147) previously assigned to *Chasmosaurus russelli*, *C. belli*, *C. kaiseni* (considered a junior synonym of *C. belli*) and *C.* (*Eoceratops*) *canadensis* (also considered a junior synonym of *C. belli*). This has invoked a discussion over the validity of *M. perifania*, with complex issues surrounding taxonomic priority, morphological change through ontogeny, and stratigraphic consistency, among others.

Taxonomy. Two taxonomic issues concern *Mojoceratops perifania*. Firstly, Longrich (2010) refers the nearly complete skull AMNH 5401 and partial skull CMN 1254 to *M. perifania*. However, since AMNH 5401 was originally described as the holotype of *Chasmosaurus kaiseni* (Brown, 1933), and CMN 1254 was described as the holotype of *Eoceratops canadensis* (Lambe 1902; 1915; later *C. canadensis*; Lehman, 1990) then if either specimen is indeed the same taxon as the *M. perifania* holotype (TMP 1983.25.1) at the least the new taxon should have become some taxonomic combination of *E. canadensis* and *C. kaiseni* (probably *E. canadensis* has priority). Secondly, the validity of *M. perifania* itself was questioned by both Mallon et al. (2011), and Maidment and Barrett (2011), who considered it a junior synonym of *C. russelli*, thereby potentially

avoiding the aforementioned taxonomic issue. Indeed the holotype of *M. perifania* resembles closely a referred specimen of *C. russelli* (NMC 2280; see later). However, this proposed synonymy is complicated by the recent finding that the holotype of *C. russelli* may not be the same taxon as the referred specimens to which *M. perifania* is compared (see later).

Stratigraphy. Of the eight specimens referred by Longrich (2010) to *M. perifania*, only TMP 1979.11.147 can be placed stratigraphically with any precision, and this is of little use as the specimen comprises only a set of brow horns that should probably be considered as Chasmosaurinae sp. (Godfrey and Holmes, 1995). NMC 8803 was collected in Saskatchewan from a locality thought to be equivalent to the middle part of the Dinosaur Park Formation. All other specimens have either only general provenance data, or lack locality data altogether. However, the holotype of *M. perifania* (TMP 1983.25.1) compares most favorably with specimens previously attributed to *C. russelli* from the lowermost part of the Dinosaur Park Formation, Alberta, and was considered a junior synonym of *C. russelli* by Maidment and Barrett (2011) and Mallon et al. (2011).

As stated below, the holotype of *C. russelli* is from the uppermost part of the Dinosaur Park Formation; this is much higher in section than all the referred specimens, which derive from the lower part of the Dinosaur Park Formation. If these lower specimens are eventually considered a different taxon from the holotype of *C. russelli,* and from *C. belli*, then either *M. perifania*, *C. kaiseni,* or *E. canadensis* (or some combination thereof) might become valid.

Morphology and Ontogeny. The holotype (TMP 1983.25.1) and at least one of the referred specimens (AMNH 5656, a small but complete frill and basicranium) of *Mojoceratops perifania* are probably from young individuals (small size, lack of cranial fusion, pointed and/or unfused frill epiossifications; crenulated frill margin; squamosal only weakly elongated; lack of resorption of postorbital horns; Lehman, 1990; Ryan and Evans, 2005; Horner and Goodwin, 2006; 2008; Scannella and Horner, 2010). As such, their morphology might reflect an immature status rather than their "true" adult state, and similarities between specimens may be due to a similar ontogenetic stage rather than truly representing the same taxon. This is especially important for AMNH 5656 as its stratigraphic and geographic provenance is unknown (Tanke, 2010); although it is similar in morphology to TMP 1983.25.1 (referred to *C. russelli* by Maidment et al., 2011 and Mallon et al., 2012), it is nearly half the size and could instead represent an immature individual from a stratigraphically higher taxon such as *C. belli*.

Regardless of these many issues, here I follow Maidment et al. (2011) and Mallon et al. (2012) in considering *Mojoceratops perifania* a synonym of *Chasmosaurus russelli*.

Chasmosaurus belli, "Chasmosaurus russelli", and *Chasmosaurus* sp.

Taxonomy. *Chasmosaurus belli* was originally described as *Monoclonius belli* by Lambe (1902) based on a relatively complete parietal (CMN 491), including the midline of the posterior bar. This was later placed into *Ceratops* by Hatcher (1907), then *Protorosaurus belli* by Lambe (1914a), but this was found to be preoccupied, so Lambe (1914b) changed it to *Chasmosaurus belli* while describing a new skull and skeleton

(CMN 2245). Since this time many specimens have been referred to *C. belli* (see revision by Lull, 1933; Godfrey and Holmes, 1995). However, only six specimens have the diagnostic parietal posterior bar intact; holotype CMN 491 (Lambe, 1914a), CMN 2245 (Lambe, 1914b), AMNH 5402 (Lull, 1933); NHMUK R4948 (Maidment and Barrett, 2011); ROM 843 (Godfrey and Holmes, 1995), and YPM 2016 (Lull, 1933).

Chasmosaurus russelli was described by Sternberg (1940) based on a very large complete skull (holotype CMN 8800), and referred specimens CMN 8801 (paratype; anterior part of a skull, no frill), CMN 8802 (partial skull without frill, destroyed in 1941; Tanke, 2010), and CMN 8803 (medial part of the parietal posterior bar). Godfrey and Holmes (1995) later referred the following specimens to *C. russelli* (some tentatively): AMNH 5656 (posterior half of a small skull with frill), CMN 2280 (large complete skull), TMP 1983.25.1 (posterior part of a skull, including frill), TMP 1981.19.175 (most of a skull, missing the posterior frill), and CMN 41933 (posterolateral corner of parietal). Longrich (2010) reassigned a number of specimens from *C. russelli* and *C. belli* into his new taxon, *Mojoceratops perifania*, which was considered invalid by Maidment and Barrett (2011; see section on *Mojoceratops*).

The taxonomy of *Chasmosaurus russelli* is currently in a state of flux as the holotype (CMN 8800) probably does not pertain to the same genus as most of the referred specimens (including the holotype of "*Mojoceratops perifania"* previously referred to *C. russelli*; Godfrey and Holmes, 1995; Longrich, 2010), indeed CMN 8800 may be unrelated to *Chasmosaurus* (Longrich, 2014; M. Loewen and D. Evans, pers. comm.). This is currently under study by other researchers. In reference to this issue,

Longrich (2014) refers to *C. russelli* referred specimen CMN 2280 as *Chasmosaurus* n. sp. in his phylogenetic analysis, and does not include "*C. russelli*". I am avoiding any issues associated with this situation by referring to "*Chasmosaurus russelli*" specimens by specimen number (I also do not refer to the holotype specimen since it is poorly figured and rarely referred to by other researchers), thereby avoiding any confusion while we await publication of new research that resolves the matter.

Stratigraphy. Stratigraphic positions of specimens (Table S1) are based on the topographic height of the localities given by Currie and Russell (2005). This data was reanalyzed by Mallon et al. (2012; supp. info.) to compensate for structural dip, and presented as the number of meters above the basal contact of the Dinosaur Park Formation with the underlying Oldman Formation. Mallon et al., (2012) state that there is an error of ±7 m for their stated measurements.

Precise stratigraphic position is only known for one specimen of *C. russelli* that exhibits the posterior parietal bar: CMN 2280 was recovered from 667 m above sea level (Currie and Russell, 2005), estimated at 15.9 m above the Oldman - Dinosaur Park Formation contact (Mallon et al., 2012), and therefore ~21.1 m below a bentonite dated at 76.39 Ma that occurs 36 m above the formational contact (dates from Eberth, 2011; see Fowler, Chapter 3). The holotype of *C. russelli* (CMN 8800) has more vague locality data, having been collected from high in the Dinosaur Park Formation from an area outside of Dinosaur Provincial Park itself (Sternberg, 1940; recently restudied with greater resolution by Campbell et al., 2013). However as previously mentioned, CMN 8800 probably does not pertain to the same genus as many or all of the referred

specimens (Longrich, 2014; M. Loewen and D. Evans, pers. comm.). Of all other specimens referred to *C. russelli* only TMP 81.19.175 has locality data, which places it 659 m above sea level (Currie and Russell, 2005), estimated at 10.5 m above the Oldman - Dinosaur Park Formation contact (Mallon et al., 2012).

Stratigraphic position is only known for four specimens of *C. belli* that exhibit the posterior parietal bar, all of which derive from the middle to upper part of the Dinosaur Park Formation (given here in stratigraphic order), straddling a 76.39 Ma bentonite at 36 m above the Oldman - Dinosaur Park Formation contact, and below a 76.10 Ma bentonite at 61.5 m (both dates from Eberth, 2011; see Fowler, Chapter 3). NHMUK R4948 was recovered from an estimated 20.1 m above the Oldman - Dinosaur Park Formation contact (Mallon et al., 2012; NHMUK R4948 is not mentioned by Currie and Russell 2005). YPM 2016 was recovered at 684 m above sea level (Currie and Russell, 2005), estimated at 24.5 m above the Oldman - Dinosaur Park Formation contact (Currie and Russell, 2005; Mallon et al., 2012). ROM 843 was recovered from 682 m above sea level (Currie and Russell, 2005), estimated at 33.4 m above the Oldman - Dinosaur Park Formation contact (Mallon et al., 2012). Finally, CMN 2245 was recovered at 692 m above sea level (Currie and Russell, 2005), estimated at 41.0 m above the Oldman - Dinosaur Park Formation contact (Mallon et al., 2012).

Specimen	Taxon	Sternberg 1950	Godfrey & Holmes 1995	Currie & Russell 2005	Mallon et al. 2012
CMN 2245	*C. belli*	691.90	43.89	692	41.0
ROM 843	*C. belli*	681.78	35.77	682	33.4
YPM 2016	*C. belli*	686.41	31.4	684	24.5
NHMUK R4948	*C. belli*	668.58	N/A	N/A	20.1
CMN 8801	*c.f. C. russelli*	670.04	23.04	N/A	N/A
CMN 2280	*"C. russelli"*	674.71	14.7	667	15.9

Table S1. Stratigraphic heights of *Chasmosaurus* specimens, which preserve the diagnostic posterior border of the parietal. Godfrey and Holmes (1995) and Mallon et al. (2012) estimated the height in meters above the base of the Dinosaur Park Formation based on topographic maps. The Currie and Russell (2005) measurements are elevation in meters above modern sea level. Sternberg (1950) measurements are also in meters above sea level, converted from their original measurements in feet.

Chasmosaurus has been presented as a good example of a stratigraphically separated morphospecies (Holmes et al., 2001); *C. russelli* specimens are limited to the lower part of the Dinosaur Park Formation; *C. belli* occurs in the middle to upper part, and *C. irvinensis* (later referred to a new genus *Vagaceratops irvinensis*; Sampson et al., 2010; see later) is restricted to the uppermost few meters (below the Lethbridge Coal Zone). The realization that the holotype of *C. russelli* is from the upper part of the

Dinosaur Park Formation (Sternberg, 1940; Campbell et al., 2013) would change this, except that the holotype is suspected to be a different taxon from the referred specimens. Therefore the stratigraphic segregation of Holmes et al. (2001) is maintained. It should be noted that Mallon et al. (2012) show slight stratigraphic overlap between *C. russelli* and *C. belli*. This is based on the uppermost specimen referred to *C. russelli* (CMN 8801), which occurs at 670 m above sea level (Currie and Russell, 2005), estimated at 21 m above the Oldman - Dinosaur Park Formation contact (Mallon et al., 2012), and therefore overlaps with lowermost *C. belli* specimen NHMUK R4948. However, CMN 8801 comprises a well preserved anterior half of a skull, but lacks the frill and as such was not considered diagnostic to species level by Godfrey and Holmes (1995), who referred it only to *Chasmosaurus* sp.. This conservative view therefore preserves the stratigraphic distinction of *C. russelli* and *C. belli*. Alternatively, CMN 8801 was assigned to *Kosmoceratops* sp. by Longrich (2014). Amid this disagreement, the taxonomic identity of CMN 8801 awaits detailed new work on Campanian chasmosaurines from Alberta.

Morphology. The morphology of *Chasmosaurus russelli* and *C. belli* is described by Godfrey and Holmes (1995) and Maidment and Barrett (2011) such that a detailed treatment is not required here. However, variation in the parietal among specimens warrants discussion, particularly with regards to phylogenetic and ontogenetic variability in characters considered important in *Pentaceratops* (and relatives), and a possible transitional specimen (YPM 2016) between typical *C. belli* and *Vagaceratops* (*Chasmosaurus*) *irvinensis*.

Chasmosaurus russelli Referred Specimens

CMN 2280 is the most complete of the specimens referred to *Chasmosaurus russelli* and is typically used as the reference for the morphology of the species (e.g. Godfrey and Holmes, 1995). However, the referred specimens vary slightly with regards to the shape of the posterior bar, the angle of the lateral rami, and the position of the epiparietals (Figure 4.S5). In all referred specimens the anteroposterior thickness of the posterior bar is either uniform mediolaterally, or tapers slightly from medial to lateral. The posterior bar is anteroposteriorly relatively narrow overall, similar to *Utahceratops*, but unlike that of more derived chasmosaurines where the posterior bar is more anteroposteriorly broad. In CMN 2280 the paired lateral rami of the posterior bar form a rounded M-shape, similarly seen in referred specimens AMNH 5656 and TMP 1983.25.1. Referred specimens TMP 1999.55.292 and CMN 8803 have M-shaped lateral rami that are more angular or subangular, similar to *Utahceratops*. In CMN 2280, AMNH 5656 and TMP 1983.25.1, the median embayment is formed from gradual medially inclined curvature of the lateral rami. By contrast, in CMN 8803 (and to a lesser extent, isolated right lateral ramus, TMP 1999.55.292) the median embayment is demarcated by a sharp change in angle of the lateral rami (more similar to *Utahceratops*, and especially the reconstruction of *Agujaceratops* provided by Lehman, 1989). The degree to which the median embayment extends anteriorly beyond the posteriormost extent of the parietal fenestrae is gradational and related to the angle of the lateral rami. In CMN 2280 the lateral rami of the posterior bar meet medially at 131°. By comparison the angle between the lateral rami is 99° in referred specimen AMNH 5656, 106° in TMP 1983.25.1, but

only 87° in CMN 8803. Furthermore, in both CMN 8803 and TMP 1999.55.292, the anteriormost point of the median embayment extends only slightly beyond the posteriormost extent of the fenestrae in CMN 2280, extends moderately anteriorly in TMP 1983.25.1 and AMNH 5656, and further still in CMN 8803 and TMP 1999.55.292 (similar to the deeper embayments exhibited by *Agujaceratops* and *Utahceratops*).

The median bar is narrow and strap-like in *Chasmosaurus russelli* referred specimens CMN 2280, TMP 1983.25.1, and AMNH 5656, with the point of maximum constriction occurring in the posterior third, close to the point of contact with the posterior bar. There are no well-developed lateral flanges that invade the parietal fenestrae (as seen in *Terminocavus*, Taxon C, or *Anchiceratops*). Godfrey and Holmes (1995) note that in *C. russelli* referred specimens CMN 2280, TMP 1981.19.175, and TMP 1983.25.1, the lateral bars do not fully enclose the fenestrae, with the squamosals therefore composing part of the mediolateral borders of the fenestrae. Godfrey and Holmes (1995) note that in AMNH 5656 the lateral bars do enclose the fenestrae.

Each referred specimen of *Chasmosaurus russelli* exhibits up to three pairs of epiparietals. Locus ep1 is positioned at the edge of the median embayment of the posterior bar in TMP 1983.25.1, AMNH 5656, and CMN 8803, but is slightly within the embayed area in CMN 2280 and TMP 1999.55.292 (i.e. more similar to *Utahceratops* and *Pentaceratops*, where ep1 is fully within the embayment). The basal length of ep1 is slightly more elongate than ep2 and ep3 in some referred specimens of *C. russelli* (CMN 2280; TMP 1983.25.1; AMNH 5656), although it is not as extremely elongated as seen in specimens of *C. belli* (see below). In some specimens, locus ep1 exhibits a possible

accessory process (as noted by Longrich, 2010), with a small bump present medial to a fused ep1 in TMP 1983.25.1, and a double process at the ep1 locus in CMN 8803 (to which no epiparietal is yet fused). The epiparietal at locus ep1 is a scalene triangle with the posterior apex of the triangle displaced laterally. Ep2 is of similar or smaller size than ep1 and is similarly shaped like a scalene triangle with the apex displaced laterally and pointing posterolaterally. Ep3 is slightly smaller than ep1 and 2 and is shaped like an isosceles triangle with the apex placed centrally. The apex of ep3 points laterally in TMP 1983.25.1 and AMNH 5656, but posterolaterally in CMN 2280 (especially on the left side).

Some characteristics indicate that *Chasmosaurus russelli* referred specimens AMNH 5656 and TMP 1983.25.1 represent immature individuals (more pointed epiparietals; unfused or pointed episquamosals, weak elongation of the squamosal, small size in the case of AMNH 5656). This may account for the slight differences between their parietal morphology and that of the most complete referred specimen, CMN 2280. Curiously, the fact that the smallest referred specimen of *C. russelli*, AMNH 5656, has parietal lateral bars that completely enclose the parietal fenestrae (whereas in all other specimens the lateral bars are open), suggests that the lateral bars may be closed early in ontogeny, but open up with maturity. This would be consistent with the hypothesis that parietal fenestrae open and enlarge through ontogeny (Brown et al., 2009; Scannella and Horner, 2010; Fastovsky et al., 2011; see main text for further discussion).

Chasmosaurus belli

Variation in parietal morphology is more notable among specimens referred to *Chasmosaurus belli* than in *C. russelli*. This is especially important concerning *C. belli* referred specimen YPM 2016 which in many ways is a morphological intermediate between more typical specimens of *C. belli* (e.g. CMN 2280) and *Vagaceratops* (*Chasmosaurus*) *irvinensis*.

The parietal of *Chasmosaurus belli* is unlike referred specimens of *C. russelli* in that the lateral rami of the posterior bar are straight giving a more triangular or chevron shape to the parietal, rather than forming a rounded M-shape. In most specimens referred to *C. belli* the anteroposterior thickness of the posterior bar is equal from medial to lateral, with the exception of NHMUK R4948, which tapers slightly from medial to lateral. The posterior bar is relatively narrow anteroposteriorly, although less so than in *C. russelli*. The lateral rami of the posterior bar meet medially at an angle forming a broad shallow embayment, which mostly does not extend anteriorly beyond the posteriormost extent of the fenestrae (with the possible exception of slight overlap observed in AMNH 5402, although this specimen is distorted). The angle between the lateral rami is shallower than that seen in *C. russelli*, and is relatively consistent at 149°-152° in *C. belli* holotype CMN 491, and referred specimens NHMUK R4948, ROM 843, and CMN 2245 (Figure 4.S5). However, YPM 2016 exhibits a posterior bar that is closer to straight, with the angle between the lateral rami at 167° (Figure 4.S5). This is interesting as it is therefore intermediate between typical *C. belli* specimens (149°-152°)

and *Vagaceratops* (*Chasmosaurus*) *irvinensis*, which succeeds *C. belli* stratigraphically and has an almost horizontal posterior bar (177°; Figure 4.S5).

The median bar of *C. belli* is narrow and strap-like with the point of maximum constriction occurring in the posterior third, close to the point of contact with the posterior bar. There are no well-developed lateral flanges that invade the parietal fenestrae (as seen in *Terminocavus*, Taxon C, or *Anchiceratops*).

The positioning and size of epiparietals varies more among referred specimens of *Chasmosaurus belli* than *C. russelli* (see Figure 4.S6). Understanding epiparietal morphology is critical as their correct identification provides additional synapomorphies linking *C. belli* specimens with more derived, stratigraphically younger taxa (*Vagaceratops* and *Kosmoceratops*), and helps highlight stratigraphic morphological trends over 2-4 million years. It is likely that specimens of *C. belli* exhibit three epiparietals (ep1-ep3) on each lateral ramus of the posterior bar, however, assignment of numbers to epiparietal loci is confounded by variation among specimens (especially regarding ep2 and ep3), and some specimens are either incomplete or lack epiparietal fusion (possibly due to being non-adult ontogenetic status; Horner and Goodwin, 2008). In all specimens referred to *C. belli*, locus ep1 is occupied by an elongate ridge, recurving anteriorly, occupying 50% or more of each lateral ramus of the posterior bar. Typically the ep1 ridge is relatively unornamented (e.g. ROM 843, CMN 2245, AMNH 5402; although this may be an ontogenetic artifact), such that it might not even be considered an epiparietal locus; however, in YPM 2016 the ridge bears the rugose texture characteristic of epiossifications, forming an undulating surface comprised of 3 to 4 processes, best

developed on the right side (Lehman, 1998). YPM 2016 is therefore intermediate in morphology between other specimens of *C. belli* (e.g. ROM 843) and that of *Vagaceratops* (*Chasmosaurus*) *irvinensis* (and *Kosmoceratops richardsoni*) in which the processes are more developed and differentiated into individual spikes (see later).

The size and position of loci ep2 and ep3 is particularly variable. In CMN 2245, AMNH 5402, and YPM 2016, the largest epiparietal is located immediately medial to the parietal-squamosal contact, occupying locus ep3, with ep2 more weakly developed. However, in ROM 843, the epiparietal immediately medial to the squamosal contact is small and described as "unfused (and presumably recently attached)" by Godfrey and Holmes (1995; p. 738). It is not clear if this is ep3, or (as suggested by Godfrey and Holmes, 1995) an additional fourth epiparietal (ep4) peculiar to ROM 843, although it is worth noting that it is more similar morphologically to episquamosals. Godfrey and Holmes (1995) suggest that the particularly large triangular epiparietals positioned between ep1 and the possible ep4 might represent ep2 and ep3 fused together. This hypothesis is supported by the double-peaked epiparietal exhibited on the left side of ROM 843 (but not the right side; Godfrey and Holmes, 1995). Although ROM 843 is often viewed as a typical example of *C. belli* (e.g. Godfrey and Holmes, 1995) it is unusual in the number and morphology of epiparietals for loci other than ep1. It is possible that this is an ontogenetic artifact, as ROM 843 is noted as being particularly large and might therefore represent an aged individual.

Vagaceratops (*Chasmosaurus*) *irvinensis* and *Kosmoceratops richardsoni*

Holmes et al. (2001) described *Chasmosaurus irvinensis* from two relatively complete skulls (holotype CMN 41357; referred specimen TMP 1987.45.1) and an exploded skull (TMP 1998.102.8; of which only a fragment of a parietal was diagnosable) from the Dinosaur Park Formation, Alberta. *Chasmosaurus irvinensis* was recovered as the sister taxon of *C. belli* by Holmes et al. (2001). Later, Sampson et al. (2010) described the new taxon *Kosmoceratops richardsoni* (now known from two specimens; holotype UMNH VP 17000; and a smaller referred specimen, UMNH VP 16878; Loewen et al., 2013) from the Kaiparowits Formation, Utah, and renamed *C. irvinensis* as *Vagaceratops irvinensis* to avoid paraphyly issues; their phylogenetic analysis placed [*Vagaceratops* + *Kosmoceratops*] as a separate clade that was recovered as much more derived than the clade comprising other species of *Chasmosaurus* (*C. belli* and *C. russelli*). Longrich (2014; using a different character matrix) recovered *V. irvinensis* as the sister taxon to *C. belli* (ie. the same relationship as recovered in the original analysis by Holmes et al., 2001), and therefore returned the taxon name to *C. irvinensis*. Notably, Longrich's analysis does not recover *Kosmoceratops* as the sister taxon to *Vagaceratops*. Although I agree with Holmes et al. (2001) and Longrich (2014) that *V. irvinensis* is probably a derived form of *Chasmosaurus* (based on strong similarity of the parietal), for the same reason I think it is likely that *Kosmoceratops* is the sister taxon of *V. irvinensis* (as recovered by Sampson et al., 2010, and in phylogenetic analyses in this paper based on the Sampson et al., 2010 character matrix). For the time being, it is probably desirable to maintain the name *Vagaceratops* as it seems likely that

the results of phylogenetic analyses will remain unstable for the foreseeable future, pending more detailed critical analysis of character matrices, and the description of new specimens of basal chasmosaurines.

In 2014, Longrich reassigned CMN 8801 (a large, nearly complete face lacking the frill and brow horns, although it is not clear if the brow horns have been broken or resorbed as is typical for many basal chasmosaurines) to *Kosmoceratops* n. sp.. The specimen was previously designated as the paratype of *C. russelli* by Sternberg (1940), but considered only as Chasmosaurinae sp. by Godfrey and Holmes (1995; with whom I agree) due to the lack of the posterior part of the frill. Better understanding of morphological characters in the anterior half of the skull (especially the premaxilla, and change through ontogeny) may make a more reliable referral possible in the future. Finally, it is worth noting here that Longrich (2014) states that the stratigraphic position of the CMN 8801 locality (quarry no. 63) had not been measured, and suggested that it occurred ~24 m above the Oldman - Dinosaur Park Formation contact. However, the stratigraphic position of CMN 8801 was stated by Godfrey and Holmes (1995) as 23.04 m above the Oldman - Dinosaur Park Formation contact (although Godfrey and Holmes do not state whether or not these are direct measurements, or extrapolations based on topographic height).

Stratigraphy. *Vagaceratops* was collected from the uppermost part of the Dinosaur Park Formation, Alberta, just below the Lethbridge Coal Zone (Holmes et al., 2001). The holotype (CMN 41357) and one of the referred specimens (TMP 98.102.8) were found outside of Dinosaur Provincial Park, so their stratigraphic position is not as

precisely known as the third specimen (TMP 1987.45.1). Holmes et al. (2001; p. 1433) state that the holotype (CMN 41357) derives from a layer "within 20m of the Lethbridge Coal Zone". The referred specimens derive from "within 20m and 10m, respectively, of the Lethbridge Coal Zone" (Holmes et al., 2001; p. 1433) although it is not made clear which of the referred specimens is which. However, Currie et al. (2005) and Mallon et al. (2014) provide some stratigraphic data for the referred skull TMP 1987.45.1, showing the quarry (no. 184) at 712 m above sealevel, and 50.4 m (± 7 m) above the Oldman - Dinosaur Park formational contact (respectively). This places *V. irvinensis* ~11.1 m below a 76.10 Ma bentonite (which occurs 61.5 m above the formational contact; 3.5 m into the Lethbridge Coal Zone) and 24.4 m above a 76.39 Ma bentonite (occurring at 36 m above the formational contact; dates from Eberth, 2011; see Fowler, Chapter 3).

The stratigraphic positions of *Kosmoceratops* specimens were plotted by Loewen et al. (2013) relative to a series of radiometrically dated bentonites, the precise positions and ages of which are most recently summarized in Roberts et al. (2013). The holotype (UMNH VP 17000) was recovered ~170 m above the base of the Kaiparowits Formation between a 76.46 Ma bentonite at 80 m, and a 75.97 Ma bentonite at 190 m. Referred specimen UMNH VP 16878 was collected at ~200 m above the base of the Kaiparowits Formation, between the 75.97 Ma bentonite at 190 m, and a 75.51 Ma bentonite at 420 m. Thus both specimens occur close to the 75.97 Ma datum.

Vagaceratops is therefore shown to occur at ~76. 2 Ma (no younger than 76.1 Ma), and *Kosmoceratops* at ~76 - 75.9 Ma. Thus the taxa do not overlap stratigraphically.

Morphology. The lateral rami of the posterior bar are virtually horizontal in *Vagaceratops*, meeting at an angle of 177° in the holotype CMN 41357 (Figure 4.S5), and therefore lacking any kind of embayment. In the *Kosmoceratops* holotype (UMNH VP 17000), this angle is more acute, being measured as 123° based on the drawing of the skull in dorsal view in Sampson et al. (2010). However, this is probably slightly exaggerated as an artifact of the curvature of the parietal, as when the skull is observed in anterior view the posterior bar appears more straight (indeed, "transverse parietal bar straight" is a character listed by Sampson et al., 2010, in the diagnosis). In a smaller (presumably immature) specimen (UMNH VP 16878) referred to *Kosmoceratops* by Loewen et al. (2013), the lateral rami meet at 142°. Thus, the posterior bar of *Kosmoceratops* is slightly embayed, to a similar extent to most specimens of *Chasmosaurus belli* (149-167°).

The median bar is only preserved in the holotypes of *Vagaceratops* (CMN 41357) and *Kosmoceratops* (UMNH VP17000). In *Vagaceratops* the median bar is broader than in specimens of *Chasmosaurus russelli* or *C. belli*, but less broad than *Kosmoceratops*. The point of maximum constriction of the median bar is difficult to assess in *Vagaceratops* as the median bar is partly broken on both sides. The reconstruction of *Kosmoceratops* in Sampson et al. (2010) shows the point of maximum constriction occurring in the posterior third. *Vagaceratops* exhibits lateral flanges of the median bar which are similarly intermediate between the condition in *C. belli* and the more developed flanges of *Kosmoceratops*. In *Vagaceratops* the lateral bars fully enclose the parietal fenestra on the left side of both the holotype and referred specimen TMP

1987.45.1, but on the right side of the holotype it is discontinuous, with ~ the squamosal forming ~5 cm of the lateral border of the fenestra (Holmes et al., 2001). In *Kosmoceratops* (UMNH VP 17000) the lateral bar fully encloses the fenestra on the right side, but the left side is not preserved. In *Vagaceratops* the lateral bars are thin, as in *C. belli*, whereas in *Kosmoceratops* they are much broader, more similar to *Anchiceratops*, and more derived chasmosaurines.

In the figures provided by Holmes et al. (2001), the parietal fenestrae (and squamosals) of *Vagaceratops* appear anteroposteriorly short compared to *Chasmosaurus russelli* and *C. belli* (see Figure 4.S6). This is an artifact of the higher angle at which the frill is held relative to the face, which was specifically noted by Holmes et al., 2001, and also observed in *Kosmoceratops* (Sampson et al., 2010). Holmes et al. (2001) figure the *Vagaceratops* frill in both anterior and dorsal views, but neither of these is comparable to the more typical "plan-type" view where the anteroposterior length of the squamosal lies flat on the resting surface. Consultation of photographs of the *Vagaceratops* holotype (CMN 41357) demonstrate that when oriented flat, the fenestrae are much longer and comparable to those of *C. belli* specimen YPM 2016 (see later).

The configuration of epiparietals and posterior episquamosals for *Vagaceratops* and *Kosmoceratops* differs among the original descriptions (Holmes et al., 2001; Sampson et al., 2010; also Loewen et al, 2013; Figure 4.S6). The identification of these epiossifications is important in phylogenetic analysis, and I have revised the numbering systems offered by previous authors based on comparisons with specimens of *Chasmosaurus belli*.

In the description of *Vagaceratops* (*Chasmosaurus*) *irvinensis*, Holmes et al. (2001) describe two specimens which preserve the squamosal-parietal contact (holotype CMN 41357 and referred specimen TMP 87.45.1). In the holotype, the parietal is described as exhibiting five epiparietals on each side (numbered ep1, medialmost through ep5, lateralmost; Figure 4.S6; Holmes et al., 2001). Ep1-4 are described as being imperceptibly fused to one another, and formed of two thin laminae curving anteriorly from the parietal posterior bar (Holmes et al., 2001). In contrast, referred specimen TMP 87.45.1 only preserves an ep4 (ep1-3 are missing) but it is described as well-preserved and triangular (Holmes et al., 2001). In the holotype CMN 41357, the lateralmost epiparietal (ep5) is "stout, shield-shaped, and forms a firm broad attachment to the [lateral ramus of the parietal posterior] bar adjacent to the parietal-squamosal suture" (Holmes et al., 2001; p. 1429). Ep5 is missing in TMP 87.45.1, with an oval facet in its place to which presumably the unfused epiparietal would have attached in life. It is important to note that ep5 is mounted on the posterolateralmost corner of the parietal which forms a small triangular extension over the posterior end of the squamosal (especially clear in Figure 4.S6H). In the holotype CMN 41357, the ep5 locus very closely abuts the posteriormost end of the squamosal, such that it might be considered as an eps (epi-parietal-squamosal; referring to an episossification that straddles the parietal-squamosal contact). This is significant as the large hook-shaped posterolateralmost frill episossification present in *Kosmoceratops* is in a similar position, but is considered as the posteriormost episquamosal (es1; Figure 4.S6C) by Sampson et al., (2010).

The configuration of epiparietals in *Kosmoceratops richardsoni* (Sampson et al., 2010) is strikingly similar to *Vagaceratops*, although the numbering system is slightly different (Figure 4.S6). As in *Vagaceratops*, four processes project anteriorly from the posterior border of the parietal posterior bar. However, in *Kosmoceratops* these processes form elongate spikes, whereas in *Vagaceratops* they are more modest triangular processes. It is notable that the spikes are relatively even more elongate in juvenile *Kosmoceratops* UMNH VP 16878 than in the larger more mature holotype UMNH VP 17000. These are numbered as ep1 through ep3, with what is considered as ep4 in *Vagaceratops* labeled as an eps. The epiossification present at the posterolateralmost corner of the *Kosmoceratops* frill is labeled as es1, (ie. the first episquamosal), rather than ep5 (as in *Vagaceratops*; Holmes et al., 2001). In their character matrix, Sampson et al. (2010) renumber the frill epiossifications of *Vagaceratops* to match *Kosmoceratops*. I agree that it is probable that the epiossifications are homologous, but I disagree with the numbering system.

Based on comparison to *Chasmosaurus*, especially *C. belli* specimen YPM 2016, I suggest that the epiossification numbering system of *Vagaceratops* and *Kosmoceratops* should be revised (Figure 4.S6). This is important as epiossification numbering directly affects 17 phylogenetic characters, and my proposed renumbering suggests previously unrecognized synapomorphies shared by *C. belli* and *Vagaceratops*. Campanian chasmosaurines typically exhibit three paired epiparietals, which are numbered from the midline laterally as ep1 to ep3 on each side, making a total of six. This is easily observed in *C. russelli* specimen CMN 2280 (Figure 4.S6D) where three epiparietals with elongate

bases are attached to the posterior margin of the parietal posterior bar. The positioning and numbering of epiparietals in *C. belli* is not as obvious, and varies slightly among individuals (as described above; Figure 4.S6E, 4.S6F). Locus ep1 is occupied by an elongate ridge, recurving anteriorly, that occupies 50% or more of each lateral ramus of the posterior bar. In most specimens the ep1 ridge is relatively unornamented, but in YPM 2016 the ridge bears the rugose texture characteristic of epiossifications, forming an undulating surface comprised of three to four short processes. I propose that the multiple processes present at locus ep1 on YPM 2016 are homologous with the first three processes of *Vagaceratops* and *Kosmoceratops*, i.e. that the majority of the posterior bar is occupied by an expanded ep1 locus, rather than representing individual loci (as numbered by Holmes et al., 2001, and Sampson et al., 2010). This is supported by the observation of Holmes et al. (2001) that the bases of these first three epiparietals are imperceptibly fused; if they are in fact outgrowths from the same locus, then it is reasonable to suggest that they do not represent discrete ossifications. This is further supported by the similar fusion seen in both specimens of *Kosmoceratops* (holotype UMNH VP 17000; juvenile UMNH VP 16878). Locus ep3 is reidentified as the lateralmost epiparietal in both *Vagaceratops* (previously identified as ep5 by Holmes et al., 2001) and *Kosmoceratops* (previously identified as es1 by Sampson et al., 2010, and Loewen et al., 2013). The epiparietal in this position abuts the squamosal and is in the expected position for ep3. Locus ep2 is designated to the epiparietal that occurs between the elongate ep1 and ep3 (see Figure 4.S6). This is the only epiparietal to be preserved in

Vagaceratops referred specimen TMP 87.45.1, supporting its designation as a discrete epiossification.

I acknowledge that this revision might be controversial, but it is the best representation of the hypothesis that the epiparietals of *Vagaceratops* and *Kosmoceratops* are homologous to the three paired epiparietals of *Chasmosaurus*.

Agujaceratops (*Chasmosaurus*) *mariscalensis*

Lehman (1989) described *Chasmosaurus mariscalensis* from a range of material collected from the Aguja Formation, Texas. Most of the cranial material (including that of the holotype, UTEP P.37.7.086; an associated braincase, brow horn, maxilla, and dentary) was recovered in the late 1930's from locality WPA1 (Works Progress Administration), a multi-individual bonebed, which occurs low in the Upper Shale Member (Lehman, 1989; Lehman and Busbey, 2007). However, the only specimen figured by Lehman (1989) that preserves the diagnostic midline of the parietal posterior bar is UTEP P.37.7.065 (an isolated fragmentary parietal associated with two humeri) which was collected from locality WPA3 (shown as stratigraphically equivalent to WPA1 by Lehman, 1989; Lehman and Busbey, 2007). Although Lehman (1989) mentions fragmentary parietal specimens from the WPA1 bonebed (UTEP P.37.7.063, 064, 089, and 093), these are neither described nor figured. In 1991, a nearly complete chasmosaurine skull was collected from higher in the Upper Shale Member of the Aguja Formation (Lehman and Busbey, 2007). This skull (TMM 43098-1) was referred to *C. mariscalensis* by Forster et al. (1993). Finally, the taxon was renamed as *Agujaceratops*

mariscalensis by Lucas et al. (2006), which has been followed by most workers since, and is the name used in the current study.

Stratigraphy. Lehman (1989) states that quarries WPA1 and WPA3 are located in the lower part of the Upper Shale Member of the Aguja Formation, "less than 70 m" above the underlying Terlingua Creek Sandstone, upon which the Upper Shale Member rests. A series of more detailed measured sections illustrated by Lehman and Busbey (2007; their Figure 35) show WPA1 as occurring immediately (<5m) above the Terlingua Creek Sandstone, and WPA3 as being stratigraphically equivalent (although the Terlingua Creek Sandstone is not present at the WPA3 section). By contrast, the locality from which the more complete skull (TMM 43098-1) was recovered is from much higher in the Upper Shale Member, ~50-70 m above the Terlingua Creek Sandstone, and positioned among a series of channel sandstones (Forster et al., 1993; Lehman and Busbey, 2007; their Figure 19).

The Terlingua Creek Sandstone is dated by the presence of the ammonite *Baculites mclearni* (Rowe et al., 1992; 80.67 - 80.21 Ma; lowermost part of the Middle Campanian; Ogg & Hinnov, 2012). As noted previously (see *Bravoceratops* entry), two U-Pb radiometric dates related to phreatomagmatic volcanism have been published as from within the Upper Shale Member of the Aguja Formation; 76.9 +/- 1.2 Ma (Befus et al., 2008), and 72.6 +/- 1.5 Ma (Breyer et al., 2007), although it is likely that the volcanism occurred after the Upper Shale Member had been deposited (Befus et al., 2008; see above).

The age of the quarries from which *A. mariscalensis* material was collected is not precisely known, but can be constrained as to between 80.21 and 76.9 Ma (probably closer to the older date; see above). It is therefore possible that *A. mariscalensis* is among the stratigraphically oldest known chasmosaurines. The higher stratigraphic position of TMM 43098-1 demonstrates that this specimen is younger than the WPA1 and WPA3 specimens, although by how much is difficult to assert, especially given that it occurs within a stratigraphic interval illustrated as being sand dominated, perhaps suggestive of having been deposited under a low accommodation setting rather than the high accommodation setting of the mud-dominated parts (e.g. Atchley et al., 2007). I am therefore not confident in asserting a stratigraphic placement for TMM 43098-1.

Morphology. As the only figured specimen that includes the diagnostic midline of the parietal posterior bar, only UTEP P.37.7.065 can be compared to *Navajoceratops* and *Terminocavus*. UTEP P.37.7.065 is fragmentary and in three pieces (Figure 4.S1). The largest piece comprises the middle part of the posterior bar, the medialmost parts of the lateral rami, and the posterior end of the median bar. Two other pieces comprise the lateralmost edge of the left lateral ramus of the posterior bar, and part one of the lateral bars. The lateral rami of the posterior bar are narrow struts of bone, meeting at an angle of 80° (Figure 4.S1) forming a median embayment that extends anterior to the posteriormost edge of the parietal fenestrae. The lateral rami are broken, but the lateral fragment is of similar anteroposterior thickness to the medial parts.

The median bar narrows anteriorly; the point of maximum constriction is unknown, but it is not immediately below the confluence of the lateral rami of the

posterior bar; i.e., it is not similar to species of *Chasmosaurus*, being more like the condition in specimens of c.f. *Pentaceratops sternbergii*. The median bar bears small lateral flanges that extend into the parietal fenestrae. Although Lehman (1989) suggests that these are present on the ventral side of the median bar, it would be more consistent with other chasmosaurine specimens if this was actually the dorsal side. The fragment of the lateral bar is too incomplete to establish to what extent it may have enclosed the parietal fenestrae.

A single epiparietal locus is preserved at the edge of the median embayment on the right side, this is presumed to represent ep1, although no epiparietal is fused to the locus; another epiparietal locus is preserved on the lateral fragment, and is presumed to represent ep3. Orientation of the loci is not discernible from published images (Lehman, 1989).

Comparisons. UTEP P.37.7.065, the holotype of *Agujaceratops*, exhibits a mosaic of characters variably seen in other relatively basal chasmosaurines. The median embayment is deeper than in *Chasmosaurus*, *Vagaceratops*, and *Kosmoceratops,* but similar to *Utahceratops* and cf. *Pentaceratops sternbergii*. Although the point of maximum constriction of the medial bar is not precisely knowable (due to incompleteness), it does not occur immediately anterior to the contact with the posterior bar, as in most *Chasmosaurus* specimens (especially, *C. belli*). In contrast, the position of ep1 outside of the embayed area is more consistent with *Chasmosaurus* than *Utahceratops*, *Pentaceratops*, and more derived forms. Indeed, UTEP P.37.7.065 bears strongest similarity to CMN 8803 (Figure 4.S5), an aberrant isolated midline parietal

fragment first referred to *C. russelli* by Sternberg (1940), then to *Mojoceratops perifania* by Longrich (2010). Given the current revision of *C. russelli*, the taxonomic affinity of CMN 8803 is unclear, so the significance of its similarity to UTEP P.37.7.065 is difficult to assess. It is tempting to suggest that UTEP P.37.7.065 may represent a more basal form of the *Utahceratops* clade, which would be consistent with its biogeography and probable stratigraphic occurrence. However, testing of such a hypothesis requires the discovery of better material.

Discussion

It is not the intent of this current study to revise the diagnoses of every chasmosaurine. Nevertheless, there are important taxonomic issues affecting *Agujaceratops mariscalensis* that need to be highlighted, especially because of its inclusion in phylogenetic analyses.

Firstly, no overlapping diagnostic elements were described between the holotype bonebed material (site WPA1), and the referred parietal midline specimen UTEP P.37.7.065 (site WPA3). Lehman (1989) does note that some parietal fragments were collected from WPA1 (UTEP P.37.7.063, 064, 089, and 093), but these are not described or figured, and no justification is given for referring UTEP P.37.7.065 to *A. mariscalensis*. Two humeri were collected from WPA3 and are comparable to humeri from WPA1 in that they are more slender than other ceratopsids with a deltopectoral crest that is more restricted than other chasmosaurines (Lehman, 1989). However, the taxonomic value of chasmosaurine postcrania is not well understood, and it would be

tentative at best to assign the WPA3 material to *A. mariscalensis* on the basis of postcrania alone. Therefore, it is not technically possible for UTEP P.37.7.065 to be referred to the same taxon as the holotype, especially as it is not from the same multi-individual bonebed as the other specimens. However, given that both localities occur at the same stratigraphic level, low in the Aguja Formation, then it is at least possible if not likely that the specimens belong to the same taxon. It is also notable that the material from the WPA3 quarry (parietal, two humeri) is from a larger individual than all or most material from the holotype bonebed WPA1, suggesting that it may be from a more mature individual.

A second problem is that the characters used by Lehman (1989) to diagnose *Agujaceratops mariscalensis* include some that are now recognized as being either undiagnostic or indicative of immature status rather than taxonomic distinction. All specimens from the WPA1 bonebed (including the largest purportedly adult specimens; Lehman, 1989) exhibit morphological characteristics indicative of varying degrees of immaturity in chasmosaurines (small size; unelongated premaxilla; posteriorly curving postorbital horncores; short postorbital horncores relative to long-horned chasmosaurines; relatively short and broad squamosals; fewer episquamosals than larger individuals with elongate squamosals; pointed episquamosals; weakly fused or unfused frill epiossifications; crenulated squamosal lateral margin; Lehman, 1990; Godfrey and Holmes, 1995; Horner and Goodwin 2006; 2008; Scannella and Horner, 2010). Indeed, immaturity of the WPA1 material was recognized by Forster et al. (1993) in their description of a more complete skull (TMM 43098-1; although this specimen has its own

problems, see below). The issue with the immaturity of the WPA1 material is that juvenile dinosaurs typically exhibit different character states than adults of their own species, often appearing more basal (Rozhdestvensky, 1965; Fowler et al., 2011; Campione et al., 2013). Thus, the diagnosis of *Agujaceratops mariscalensis* by Lehman (1989) includes characters that are consistent with the immature status of the type material rather than diagnostic of an adult (short broad squamosal; fewer episquamosals than larger individuals with elongate squamosals; premaxilla without posterodorsal extension, i.e. premaxilla is anteroposteriorly short). Other characters used by Lehman (1989) to diagnose *A. mariscalensis* (supraorbital horncores longer than in adults of other species of *Chasmosaurus*; maxilla without lateral horizontal shelf) may distinguish *A. mariscalensis* from species of *Chasmosaurus* (as was Lehman's intent), but do not distinguish *A. mariscalensis* from other long-horned chasmosaurines such as *Pentaceratops sternbergii* (indeed, Lehman, 1989, notes the similarity of *A. mariscalensis* to *P. sternbergii*, suggesting that they may be closely related). Therefore, the diagnosis of *A. mariscalensis* by Lehman (1989) is invalid. An attempt to rectify this is provided by Forster et al. (1993) in their description of a more complete skull (TMM 430981-1), however this specimen has its own problems (see next paragraph).

The third problem is that there is little justification for referring TMM 43098-1 (the partial skull described by Forster et al., 1993) to the same taxon (i.e. *A. mariscalensis*) as material from the WPA1 (holotype) or WPA3 (referred parietal) quarries. Firstly, as TMM 43098-1 does not preserve any part of the parietal, it cannot be compared with the WPA3 parietal (UTEP 037.7.065). On the basis of the new skull,

Forster et al. (1993) rediagnose *A. mariscalensis*. However, characters in the new diagnosis and in the discussion of Forster et al. (1993) are either not observable in the WPA1 type material, represent symplesiomorphies, or are known to vary ontogenetically.

Character 1, a "strong anteromedian nasal process extending between the premaxillae on the internarial bar" (Forster et al., 1993; p.162) is an unusual feature so far reported only in TMM 43098-1 (among chasmosaurines). However, this condition is not recorded for the type WPA1 bonebed material as no nasals were recovered. Furthermore, the single known premaxilla present in the WPA1 material is not figured in medial view by Lehman (1989), so any recessed articulation surface that might have received an anteromedian process of the nasal has not been observed, and no comment on this is provided by Forster et al. (1993). The holotype of *Pentaceratops sternbergii* (AMNH 6325) has similar grooves visible on the dorsal surface of the rostrum, suggesting that it too might exhibit a tongue-like extension of the nasals extending a short distance anteriorly between the premaxillae. However, this is difficult to see in the AMNH mount as it is covered by reflective glass. Regardless, this character is not demonstrable in the type material and so cannot be used to refer TMM 43098-1 to the same taxon as the WPA1 material.

Character 2, "erect supraorbital horncores that attain an angle of 85° to the maxillary tooth row in adults" (Forster et al., 1993; p.162) is observed in TMM 43098-1, and some of the larger postorbital horns from the holotype WPA1 quarry (UTEP P.37.7.082; 086, and 091; Lehman, 1989). However, the apparent erectness is an artifact of the posterior curvature of the horn tip (an indication of immaturity; Horner and

Goodwin, 2006); when measured at the base (Figure 4.S7), the postorbital horns are equally erect in the holotype of *Pentaceratops sternbergii* (AMNH 6325). Since equally erect postorbital horns are exhibited by other Campanian chasmosaurines then this character cannot be considered autapomorphic of *Agujaceratops mariscalensis*, and cannot be used to refer the TMM 43098-1 skull to the same taxon as the WPA1 material.

Character 3, "squamosal with a convex lateral frill margin" (Forster et al., 1993; p.162) is an important morphological feature of TMM 43098-1, but whether or not it is diagnostic (and can therefore be used to unite TMM 43098-1 with WPA1 material) is clouded by variability in the WPA1 material, and the fact that this character is known to vary ontogenetically in other chasmosaurines. In two of the WPA1 squamosal fragments, the posterior end has a lateral margin that is relatively straight (UTEP P37.7.046; 052; Lehman, 1989), which might indicate that their morphology is unlike that of TMM 43098-1; however, other specimens from the WPA1 bonebed do have a lateral margin that is convex (e.g. UTEP P37.7.062; Lehman, 1989). Convexity of the lateral margin of the squamosal is influenced by ontogeny in other chasmosaurines; in the derived chasmosaurine *Triceratops*, the squamosal is short and broad for most of ontogeny, and similarly has a convex lateral margin (Scannella and Horner, 2010). If the WPA1 material is all immature then it is not possible to determine whether the lateral convexity observed in some specimens is due to ontogeny or a genuine taxonomic feature. Similarly, the condition in TMM 430981-1 may therefore be more reflective of ontogeny rather than phylogeny, supported by the posteriorly curving postorbital horns that are also indicative of immaturity (Horner and Goodwin, 2006). Nevertheless it is interesting that

the squamosal of TMM 43098-1 is not as "bladed" (elongated) as squamosals of other Campanian chasmosaurines such as *Chasmosaurus belli* and *Pentaceratops sternbergii*. This complicates matters regarding *A. mariscalensis* as the other WPA1 squamosals are all from immature individuals which might be expected to have a short broad squamosal with a convex lateral margin.

As a result of the invalid diagnosis of *Agujaceratops mariscalensis*, TMM 43098-1 cannot be shown to share any diagnostic features with the type (WPA1) or referred (WPA2) material. TMM 43098-1 is also from a stratigraphic level that is ~50-70 m higher in the Aguja Formation than the WPA1 and WPA2 quarries, over which there is a change in depositional style from mud- to sand-dominated; this might reasonably be interpreted as representing a change in overall depositional conditions including available accommodation space, which further suggests that a considerable amount of time might be represented by the stratigraphic gap between the specimens. It has been shown (Horner et al., 1992; Mallon et al., 2012; Scannella et al., 2014) that dinosaur species (especially ceratopsids) evolve rapidly over as little as a few hundred thousand years, so it might not be expected that chasmosaurine morphospecies would be the same at the bottom and top of the Upper Shale Member. Therefore it does not seem appropriate to assign TMM 43098-1 to *A. mariscalensis*.

This proposal creates a problem in that the phylogenetic dataset of Sampson et al. (2010; and presumably, subsequent modifications) use an amalgam of "TMM 43098-1 and UTEP bonebed specimens" (in their supporting information, p. 2). Use of an amalgam of immature (type material from WPA1) and mature material (WPA2 referred

parietal and TMM 430981-1), which cannot be demonstrated to be from the same taxon, is clearly not ideal, and may explain the disruptive nature of *Agujaceratops* on cladistic analysis (see main text). The solution to this problem is probably to ignore the probable juvenile material from the WPA1 bonebed, and to code TMM 43098-1 and UTEP P.37.7.065 separately.

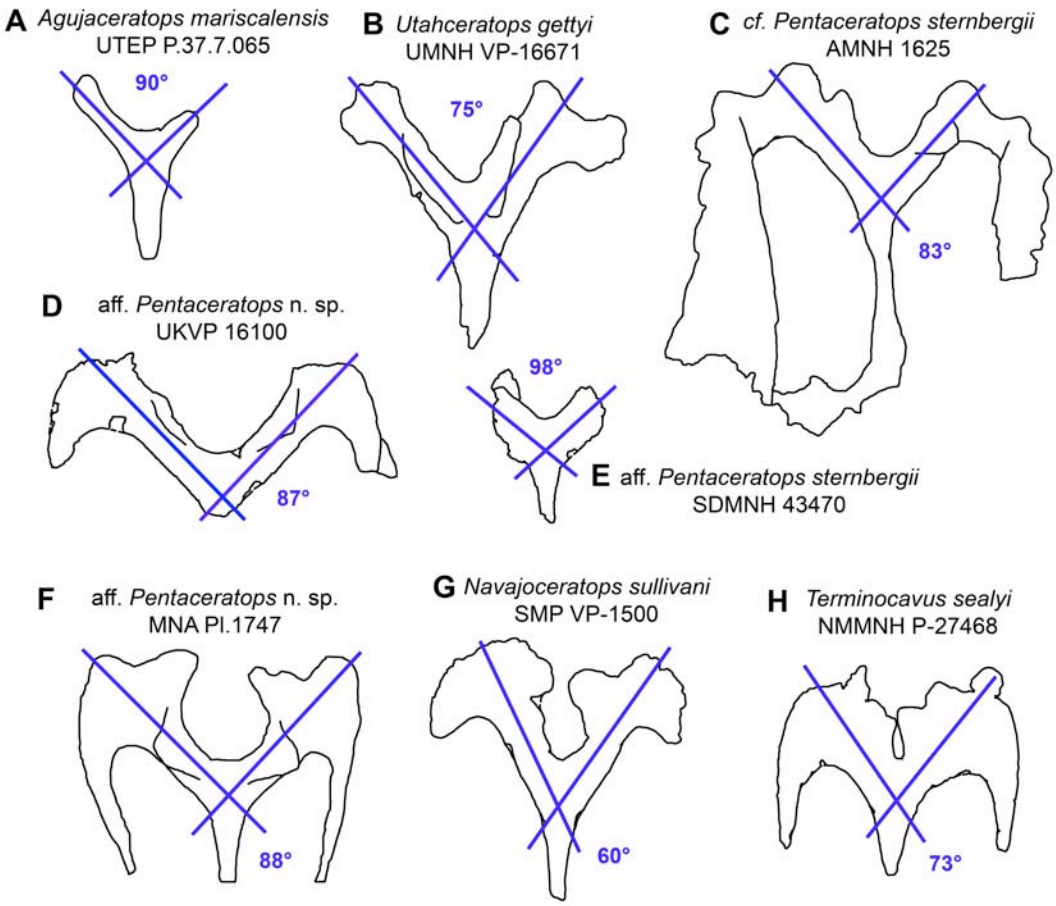

Figure 4.S1. Angle formed by the lateral rami of the parietal posterior bar in *Pentaceratops* and close relatives. In most chasmosaurines the lateral rami of the parietal posterior bar meet medially at an angle, forming an embayment. Specimens are shown here in stratigraphic order where possible. (A) is probably the stratigraphically oldest specimen illustrated. The stratigraphically separated taxa *Utahceratops* (B), *Pentaceratops* (C, D, F), *Navajoceratops* (G), to *Terminocavus* (H) form a morphologic spectrum, recording overall decrease in the angle of the lateral rami of the posterior bar, deepening and narrowing the median embayment. *Agujaceratops* specimen UTEP P.37.7.065 SDMNH 43470 (E) is of uncertain stratigraphic position, but may be roughly equivalent to the Hunter Wash Member of the Kirtland Formation, New Mexico, from which *Navajoceratops* (G) and *Terminocavus* (H) were collected. Specimens not shown to scale (see main text Figure 4.17 for relative sizes).

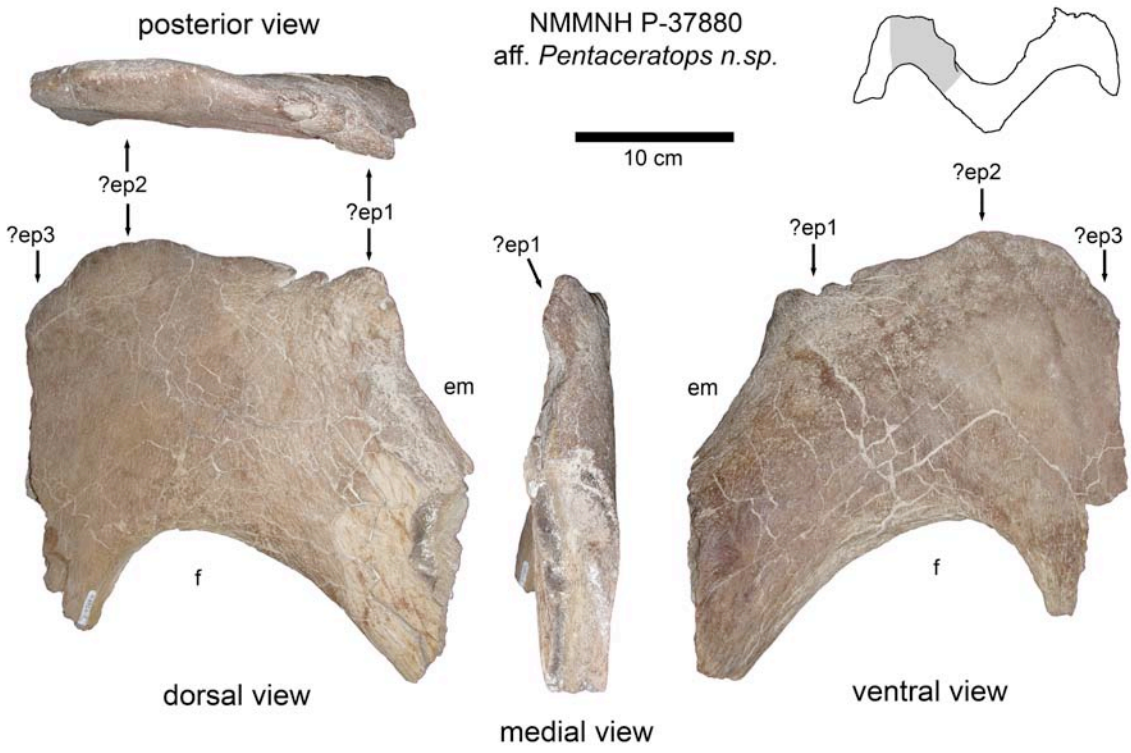

Figure 4.S2. Previously undescribed specimen, c.f. *Pentaceratops sternbergii*, NMMNH P-37880. NMMNH P-37880, a partial right lateral ramus of parietal posterior bar in posterior, dorsal, medial, and ventral views. Although an isolated skull fragment, the posterior bar of the parietal is the most diagnostic element in Campanian chasmosaurines. Specimen recovered from the Fossil Forest Member, Fruitland Formation (San Juan Basin, New Mexico) and is morphologically most similar to other specimens referred to c.f. *P. sternbergii*. Abbreviations: em, median embayment of the posterior bar; ep, epiparietal loci numbered by hypothesized position (no epiossifications are fused to this specimen). f, parietal fenestra. Scalebar equals 10 cm. Reconstruction line drawing based on c.f. *P. sternbergii* specimen UKVP 16100.

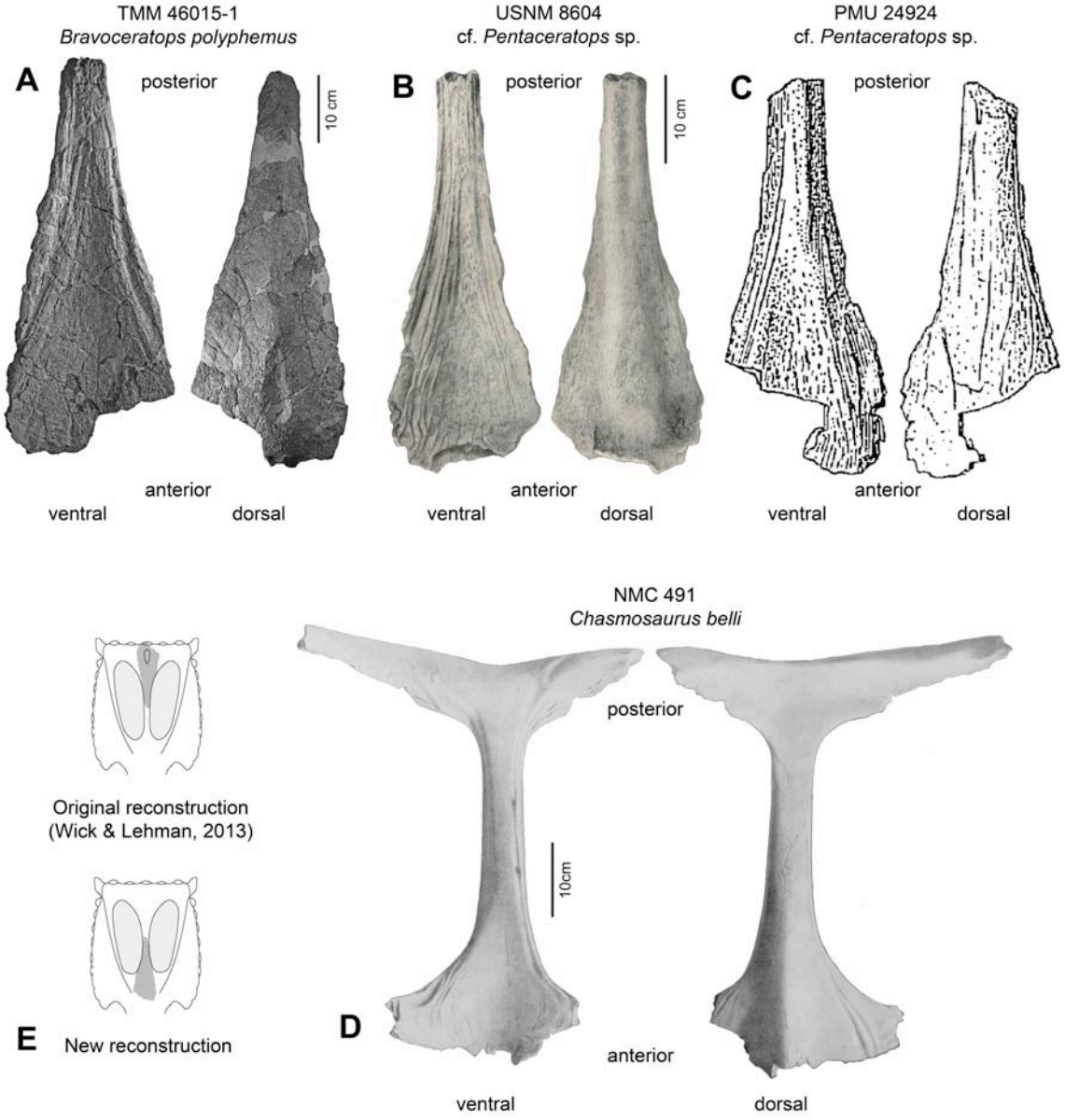

Figure 4.S3. Reidentification of parietal median bar of *Bravoceratops polyphemus* (Wick and Lehman, 2013). The parietal fragment of TMM 46015-1 (*Bravoceratops polyphemus*, A) is reidentified here as representing the anterior half of the parietal median bar as it compares favorably with the anterior median bars of c.f. *Pentaceratops* (USNM 8604, B; PMU 24924, C) and *Chasmosaurus belli* (CMN 491; D). The specimen was previously identified as the posterior half of the parietal median bar by Wick and Lehman (2013, E), and interpreted as such bore most of the morphological features which distinguished this new taxon. Scalebars equal 10 cm. No scale available for PMU 24924 (C). (A, E) adapted from Wick and Lehman (2013); (B) adapted from Gilmore (1919); (C) adapted from Wiman (1930); (D) adapted from Hatcher et al. (1907).

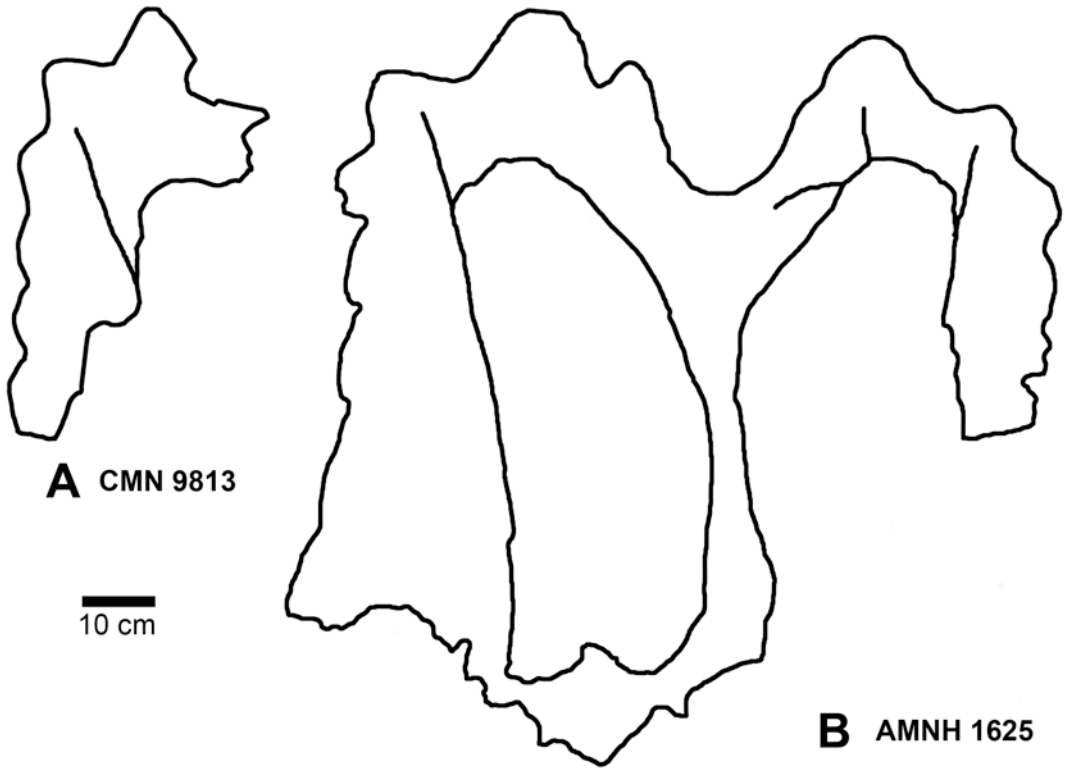

Figure 4.S4. "*Pentaceratops aquilonius*" (CMN 9813) shown to scale with c.f. *P. sternbergii* (AMNH 1625). Longrich (2014) proposed the new taxon *Pentaceratops aquilonius* (holotype CMN 9813, A) based in part on the suggestion that compared to c.f. *Pentaceratops sternbergii* (AMNH 1625, B), the parietal posterior bar is anteroposteriorly broad and only weakly embayed. This is based on inaccurate reconstruction of CMN 9813, mainly because of inappropriate scaling. This figure shows CMN 9813 is comparable to AMNH 1625 in the anteroposterior thickness of the posterior bar, and that CMN 9813 is too incomplete to infer size or shape of the median embayment. (A, B) Adapted from Longrich (2014). Scalebar equals 10 cm.

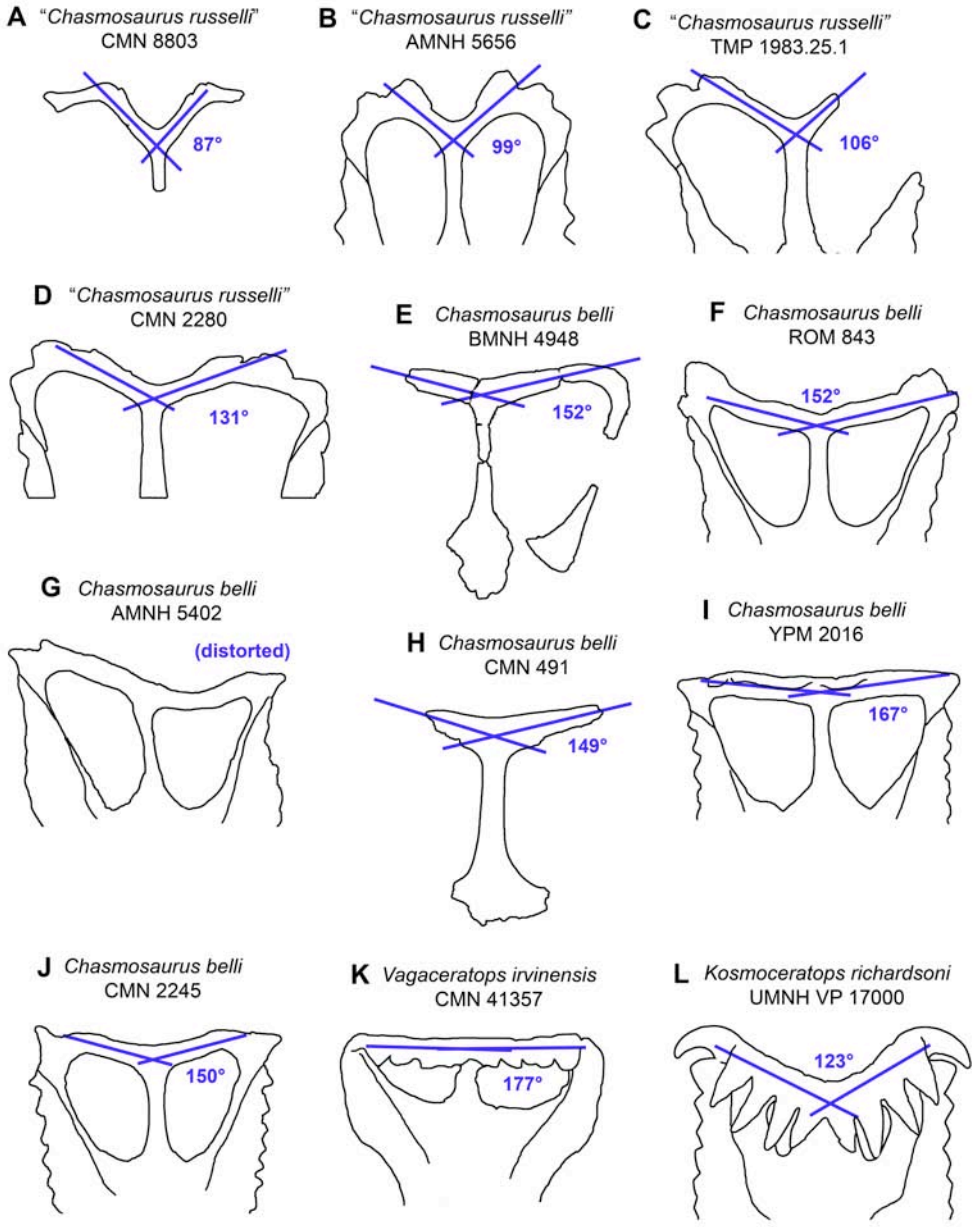

Figure 4.S5. Angle formed by the lateral rami of the parietal posterior bar in *Chasmosaurus* and close relatives. In most chasmosaurines the lateral rami of the parietal posterior bar meet medially at an angle, forming an embayment. Taxa are illustrated in stratigraphic order where possible. The stratigraphically separated taxa "*Chasmosaurus russelli*" (B-D), *C. belli* (E-J), *Vagaceratops irvinensis* (K), and *Kosmoceratops richardsoni* (H) form a morphologic spectrum, recording overall increase in the angle of the lateral rami of the posterior bar, shallowing the median embayment. Specimens not shown to scale.

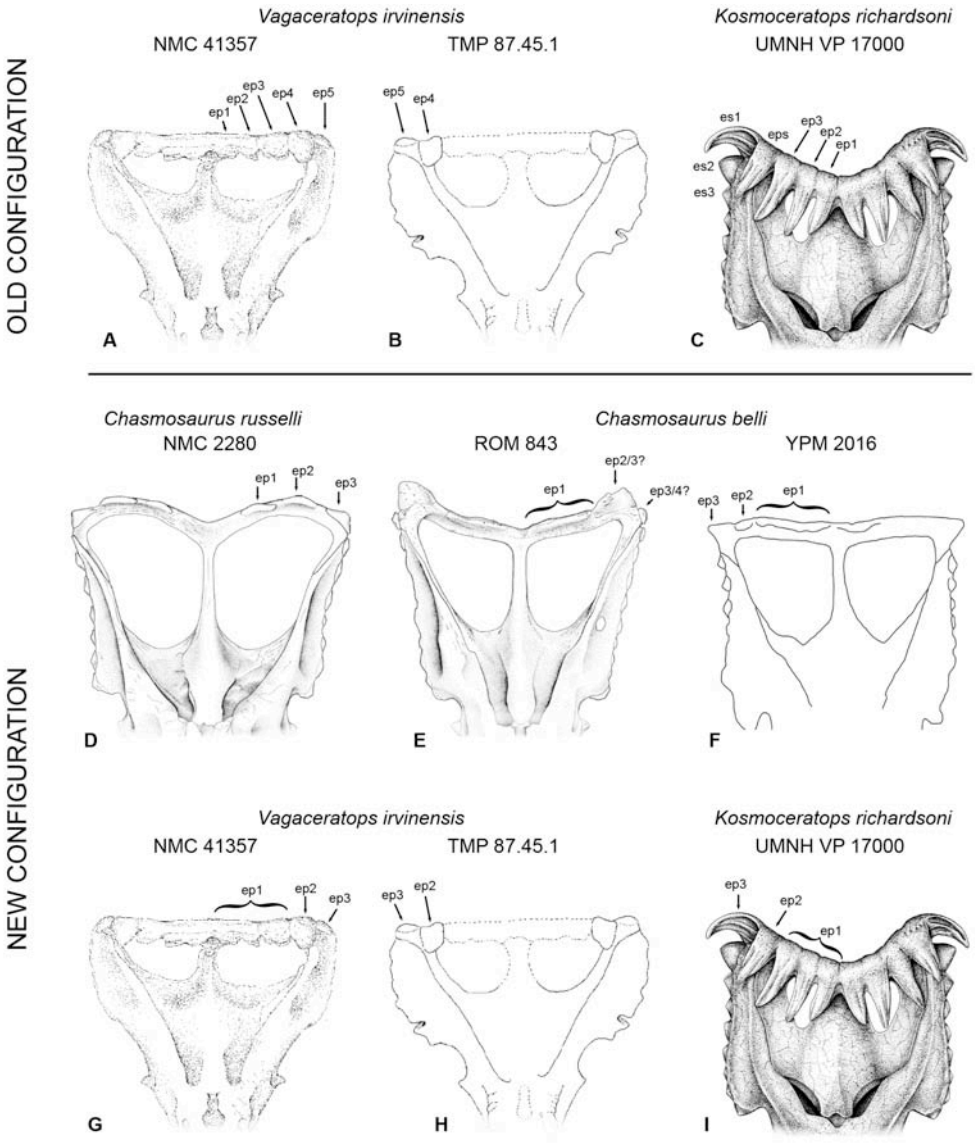

Figure 4.S6. Proposed reconfiguration of epiparietal numbering system in *Chasmosaurus* and related chasmosaurines. The original epiparietal numbering systems of Holmes et al. (2001; A, B) and Sampson et al. (2010, C) are reconfigured (G-I) based on comparison to stratigraphically preceding chasmosaurines c.f. *Chasmosaurus russelli* (CMN 2280, D), and *C. belli* (ROM 843, E; YPM 2016, F). Most notably, locus ep1 develops from a spindle shaped epiparietal in c.f. *C. russelli* (D) to an elongate and anteriorly curving ridge in *C. belli* (E, F). In YPM 2016 the ep1 ridge bears 3-4 anteriorly projecting processes which are here interpreted to be homologous with the anteriorly projecting processes also in this position in the stratigraphically succeeding taxa *Vagaceratops* (*Chasmosaurus*) *irvinensis* (G, H) and *Kosmoceratops richardsoni* (I). Specimens not shown to scale.

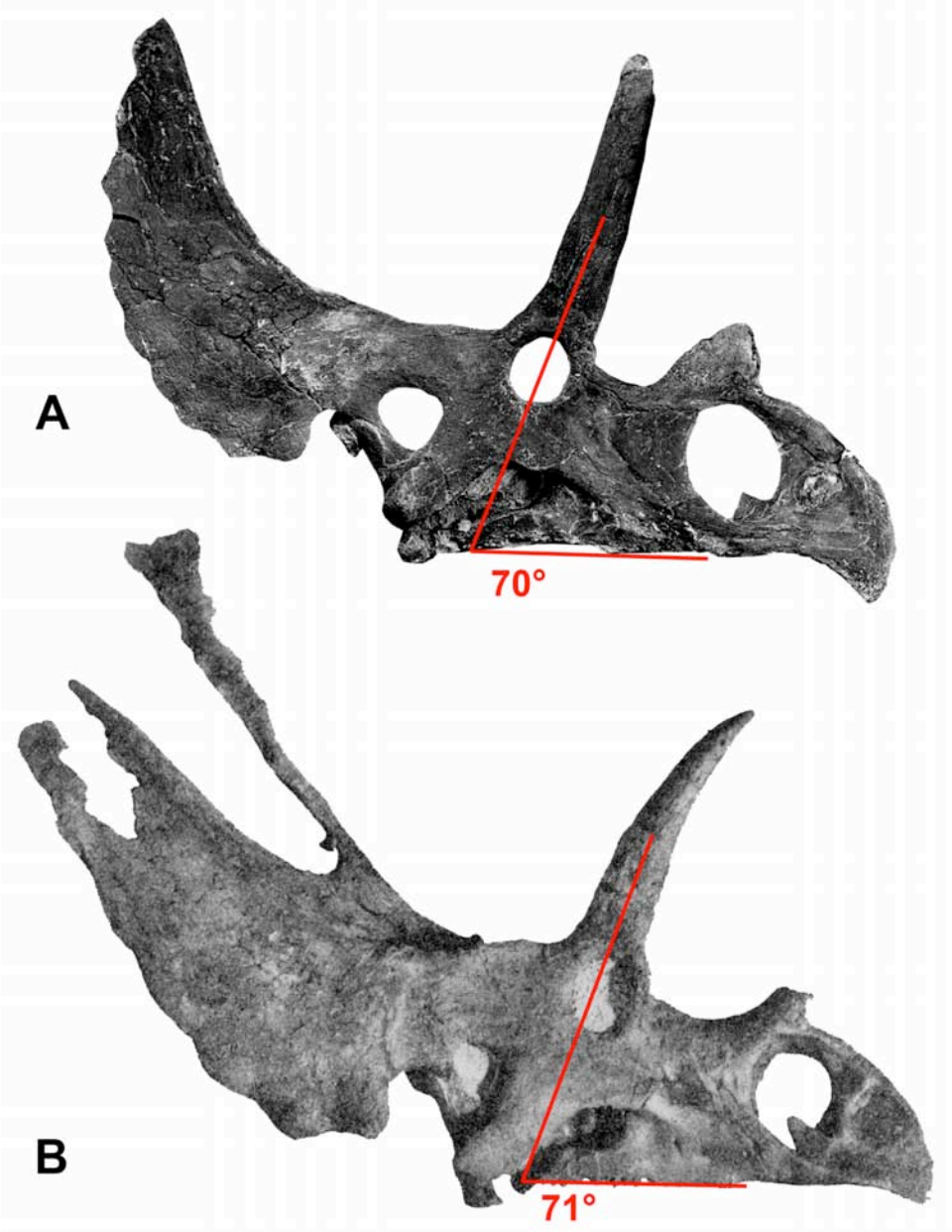

Figure 4.S7. Angle of postorbital horn relative to maxillary tooth row in Chasmosaurinae sp. "*Agujaceratops mariscalensis*" TMM 43098-1 (A) and *Pentaceratops sternbergii* AMNH 6325 (B). In their rediagnosis of *Agujaceratops mariscalensis*, Forster et al. (1993) suggest "erect supraorbital horncores that attain an angle of 85° to the maxillary tooth row in adults" as a new autapomorphy, based on TMM 43098-1 (A). This figure shows that the postorbital horns of TMM 43098-1 are no more erect than those of *Pentaceratops sternbergii* holotype AMNH 6325 (B). The posterior curvature of the postorbital horns in TMM 43098-1 create the illusion of more erect horns. (A) adapted from Forster et al., (1993); (B) adapted from Osborn (1923).

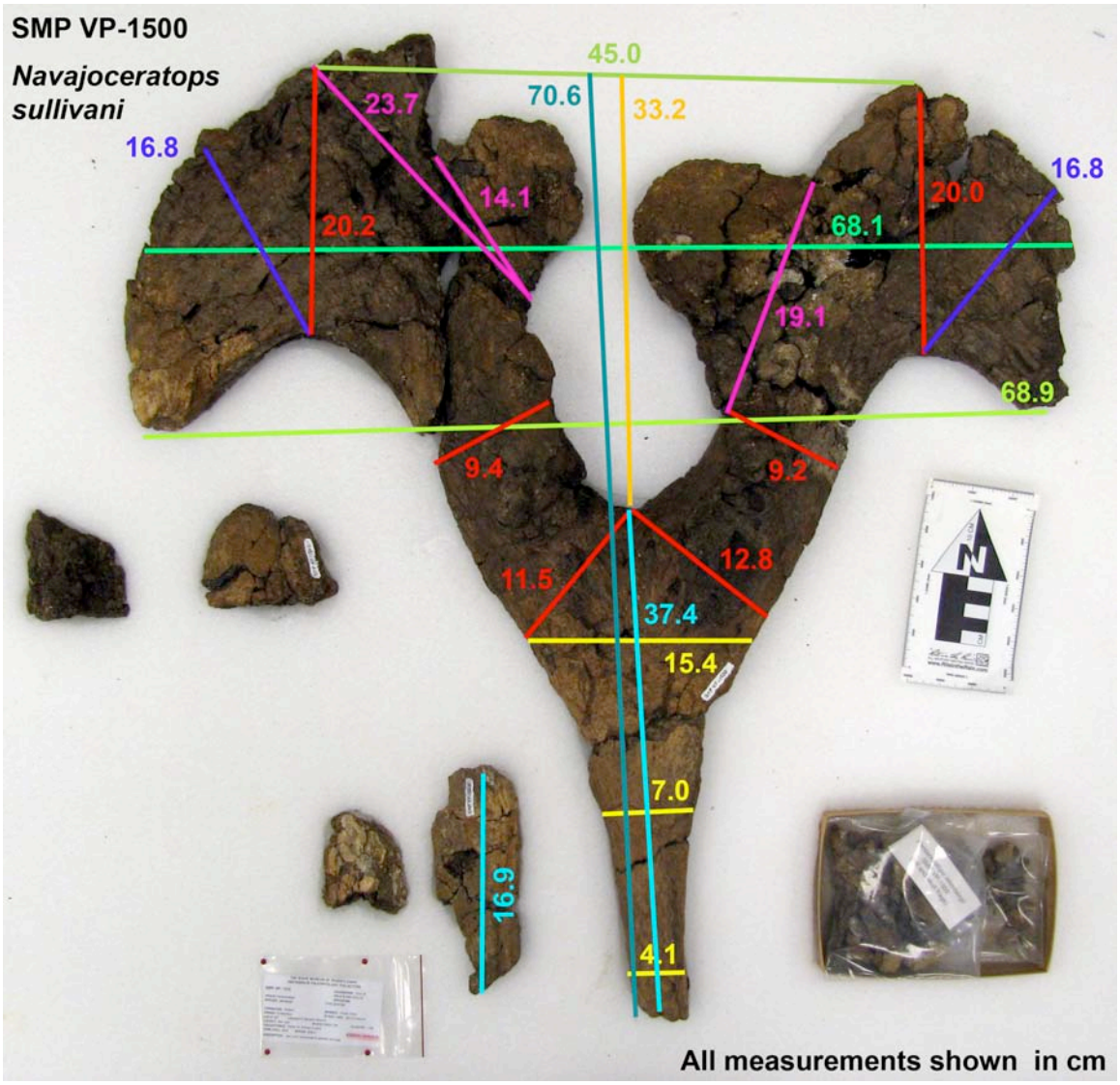

Figure 4.S8. Selected measurements of *Navajoceratops sullivani* holotype SMP VP-1500. Parietal shown in dorsal view. Measurements in cm (1.d.p).

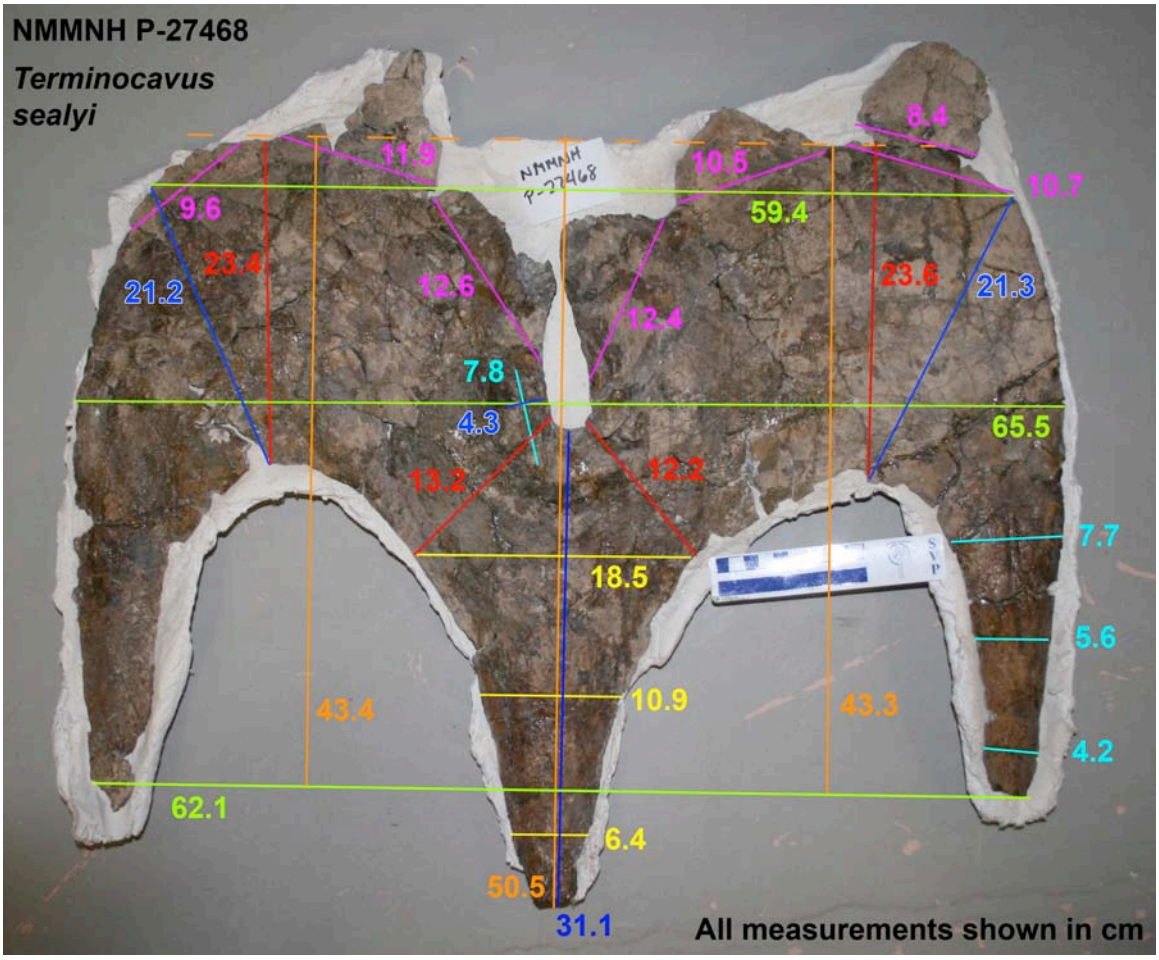

Figure 4.S9. Selected measurements of *Terminocavus sealyi* holotype NMMNH P-27468. Parietal shown in dorsal view. Measurements in cm (1.d.p).

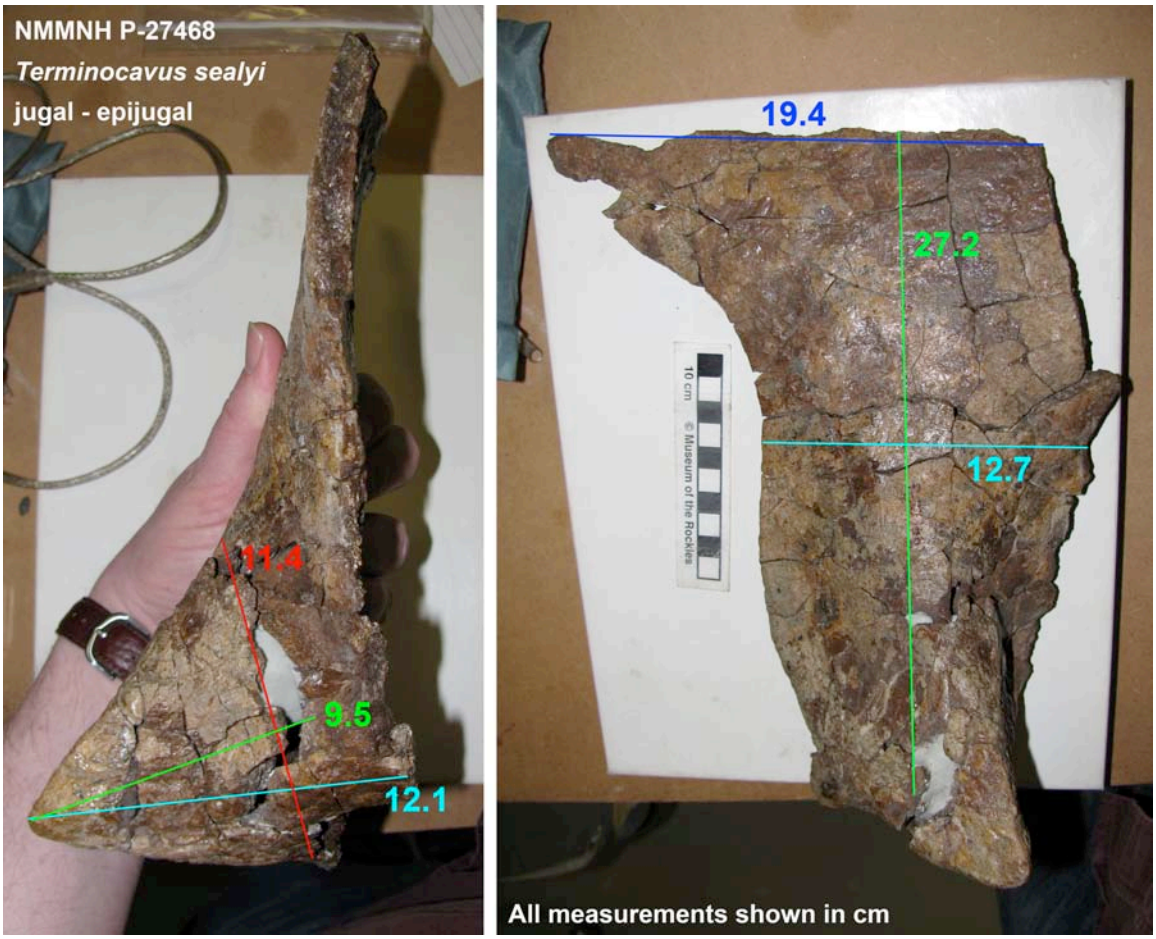

Figure 4.S10. Selected measurements of *Terminocavus sealyi* holotype NMMNH P-27468. Jugal - epijugal shown in posterior (left) and left lateral (right) views. Measurements in cm (1.d.p).

References Cited in Appendix C

Atchley, S. C., L. C. Nordt, and S. I. Dworkin. 2004. Eustatic Control on Alluvial Sequence Stratigraphy: A Possible Example from the Cretaceous-Tertiary Transition of the Tornillo Basin, Big Bend National Park, West Texas, U.S.A. Journal of Sedimentary Research 74:391–404.

Bauer, C. M. 1916. Contributions to the Geology and Paleontology of San Juan County, New Mexico: Part 1. Stratigraphy of a Part of the Chaco River Valley. US Government Printing Office, 8 pp.

Befus, K. S., R. E. Hanson, T. M. Lehman, and W. R. Griffin. 2008. Cretaceous basaltic phreatomagmatic volcanism in west Texas: maar complex at Pena Mountain, Big Bend National Park. Journal of Volcanology and Geothermal Research 173:245–264.

Brown, B. 1914. *Anchiceratops*, a new genus of horned dinosaurs from the Edmonton Cretaceous of Alberta. Bulletin of the American Museum of Natural History 33:539-548.

Brown, B. 1933. A new longhorned Belly River ceratopsian. American Museum Novitates 669:1-3.

Brown, C. M. 2009. Pattern and transition of surficial bone texture of the centrosaurine frill and their ontogenetic and taxonomic implications. Journal of Vertebrate Paleontology 29:132-141.

Brownfield, M. E., and E. A. Johnson. 2008. The Yampa Bed-A Regionally Extensive Tonstein in the Williams Fork Formation, Northwestern Piceance Creek and Southern Sand Wash Basins, Colorado. Geological Survey (US), pp.

Campbell, J., M. J. Ryan, C. Schröder-Adams, R. B. Holmes, and D. C. Evans. 2013: A specimen-based phylogenetic analysis of the chasmosaurine ceratopsid Chasmosaurus (Ornithischia) from the Upper Cretaceous (Campanian) Dinosaur Park Formation of western Canada suggests the validity of only one species. Society of Vertebrate Paleontology 73rd Annual Meeting, Abstracts of Papers, Los Angeles, 2013.

Campione, N. E., K. S. Brink, E. A. Freedman, C. T. McGarrity, and D. C. Evans. 2013. '*Glishades ericksoni*', an indeterminate juvenile hadrosaurid from the Two Medicine Formation of Montana: implications for hadrosauroid diversity in the latest Cretaceous (Campanian-Maastrichtian) of western North America. Palaeobiodiversity and Palaeoenvironments 93:65-75.

Currie, P. J., and D. A. Russell. 2005. The geographic and stratigraphic distribution of articulated and associated dinosaur remains; pp. 537-569 in P. J. Currie and E. B. Koppelhus (eds.), Dinosaur Provincial Park: A Spectacular Ancient Ecosystem Revealed. Indiana University Press, Bloomington, Indiana.

Diem, S., and J. D. Archibald. 2005. Range extension of southern chasmosaurine ceratopsian dinosaurs into northwestern Colorado. Journal of Paleontology 79:251-258.

Dodson, P., C. A. Forster, and S. D. Sampson. 2004. Ceratopsidae; pp. 494-513 in D. B. Weishampel, P. Dodson, and H. Osmolska (eds.), The Dinosauria. University of California Press, Berkeley.

Eberth, D. A. 2005. The Geology; pp. 54-82 in P. J. Currie and E. B. Koppelhus (eds.), Dinosaur Provincial Park: A Spectacular Ancient Ecosystem Revealed. Indiana University Press, Bloomington, Indiana.

Eberth, D. A. 2011. A revised chronostratigraphy for Dinosaur Provincial Park, Alberta, Canada;in Speaker Series, Royal Tyrrell Museum, Drumheller, Alberta.

Farke, A. A. 2006. Morphology and ontogeny of the cornual sinuses in chasmosaurine dinosaurs (Ornithischia: Ceratopsidae). Journal of Paleontology 80:780-785.

Fassett, J. E., and M. B. Steiner. 1997. Precise age of C33N-C32R magnetic-polarity reversal, San Juan Basin, New Mexico and Colorado. New Mexico Geological Society Guidebook 48:239-247.

Fastovsky, D. E., D. B. Weishampel, M. Watabe, R. Barsbold, K. H. Tsogtbaatar, and P. Narmandakh. 2011. A nest of *Protoceratops andrewsi* (Dinosauria, Ornithischia). Journal of Paleontology 85:1035-1041.

Forster, C. A., P. C. Sereno, T. W. Evans, and T. Rowe. 1993. A complete skull of *Chasmosaurus mariscalensis* (Dinosauria: Ceratopsidae) from the Aguja Formation (Late Campanian) of West Texas. Journal of Vertebrate Paleontology 13:161-170.

Fowler, D. W., H. N. Woodward, E. A. Freedman, P. L. Larson, and J. R. Horner. 2011. Reanalysis of *Raptorex kriegsteini*: A Juvenile Tyrannosaurid Dinosaur from Mongolia. PLoS ONE 6:e21376.

Gilmore, C. W. 1919. Reptilian faunas of the Torrejon, Puerco, and underlying Upper Cretaceous formations of San Juans County, New Mexico. United States Geological Survey Professional Paper 119:1-71.

Gilmore, C. W. 1946. Reptilian fauna of the North Horn Formation of central Utah. United States Geological Survey Professional Paper 210-C:29-53.

Godfrey, S. J., and R. B. Holmes. 1995. Cranial morphology and systematics of *Chasmosaurus* (Dinosauria: Ceratopsidae) from the Upper Cretaceous of western Canada. Journal of Vertebrate Paleontology 15:726-742.

Goodwin, M. B., W. A. Clemens, J. R. Horner, and K. Padian. 2006. The smallest known *Triceratops* skull: new observations on ceratopsid cranial anatomy and ontogeny. Journal of Vertebrate Paleontology 26:103-112.

Hatcher, J. B., O. C. Marsh, and R. S. Lull. 1907. The Ceratopsia. United States Geological Monograph 49:1-300.

Holmes, R. B., C. A. Forster, M. J. Ryan, and K. M. Shepherd. 2001. A new species of *Chasmosaurus* (Dinosauria: Ceratopsia) from the Dinosaur Park Formation of southern Alberta. Canadian Journal of Earth Sciences 38:1423-1438.

Horner, J. R., and M. B. Goodwin. 2006. Major cranial changes during *Triceratops* ontogeny. Proceedings of the Royal Society B 273:2757-2761.

Horner, J. R., and M. B. Goodwin. 2008. Ontogeny of cranial epi-ossifications in *Triceratops*. Journal of Vertebrate Paleontology 28:134-144.

Horner, J. R., D. J. Varricchio, and M. B. Goodwin. 1992. Marine transgressions and the evolution of Cretaceous dinosaurs. Nature 358:59-61.

Hunt, A. P., and S. G. Lucas. 1992. Stratigraphy, paleontology, and age of the Fruitland and Kirtland Formations (Upper Cretaceous), San Juan Basin, New Mexico. New Mexico Geological Society Guidebook 43:217-239.

Hunt, A. P., and S. G. Lucas. 2003. Origin and stratigraphy of historic dinosaur quarries in the Upper Cretaceous Fruitland Formation of the Fossil Forest Research Natural Area, northwestern New Mexico. New Mexico Geological Society Guidebook, 54th Field Conference, Geology of the Zuni Plateau:383-388.

Lambe, L. M. 1902. New genera and species from the Belly River Series (mid-Cretaceous). Contributions to Canadian Paleontology 3:25-81.

Lambe, L. M. 1914a. On the fore-limb of a carnivorous dinosaur from the Belly River Formation of Alberta, and a new genus of Ceratopsia from the same horizon, with remarks on the integument of some Cretaceous herbivorous dinosaurs. The Ottawa Naturalist 27:130-135.

Lambe, L. M. 1914b. On *Gryposaurus notabilis*, a new genus and species of trachodont dinosaur from the Belly River Formation of Alberta, with a description of the skull of *Chasmosaurus belli*. The Ottawa Naturalist 27:145-155.

Lambe, L. M. 1915. On *Eoceratops canadensis*, gen. nov., with remarks on the other genera of Cretaceous horned dinosaurs. Geological Survery of Canada Museum Bulletin 12:1-49.

Langston, W., Jr. 1959. *Anchiceratops* from the Oldman Formation of Alberta. Natural History Papers, National Museum of Canada 3:1-11.

Lawson, D. A. 1976. *Tyrannosaurus* and *Torosaurus*, Maestrichtian dinosaurs from Trans-Pecos, Texas. Journal of Paleontology 50:158-164.

Lehman, T. M. 1989. *Chasmosaurus mariscalensis*, n. sp., a new ceratopsian dinosaur from Texas. Journal of Vertebrate Paleontology 9:137-162.

Lehman, T. M. 1990. The ceratopsian subfamily Chasmosaurinae: sexual dimorphism and systematics; pp. 211-229 in K. Carpenter and P. J. Currie (eds.), Dinosaur Systematics Approaches and Perspectives. Cambridge University Press, Cambridge.

Lehman, T. M. 1993. New data on the ceratopsian dinosaur *Pentaceratops sternbergii* Osborn from New Mexico. Journal of Paleontology 67:279-288.

Lehman, T. M. 1998. A gigantic skull and skeleton of the horned dinosaur *Pentaceratops sternbergi* from New Mexico. Journal of Paleontology 72:894-906.

Lehman, T. M. 2007. Growth and population age structure in the horned dinosaur *Chasmosaurus*; pp. 259-317 in K. Carpenter (ed.), Horns and Beaks: Ceratopsian and Ornithopod Dinosaurs. Indiana University Press, Bloomington.

Lehman, T. M., and A. B. Busbey III. 2007. Big Bend Field Trip Guidebook. Society of Vertebrate Paleontology, 67th Annual Meeting Field Trip Guidebook:1-69.

Lehman, T. M., F. McDowell, and J. Connelly. 2006. First isotopic (U-Pb) age for the Late Cretaceous *Alamosaurus* vertebrate fauna of West Texas, and its significance as a link between two faunal provinces. Journal of Vertebrate Paleontology 26:922-928.

Loewen, M. A., A. A. Farke, S. D. Sampson, M. A. Getty, E. K. Lund, and P. M. O'Connor. 2013. Ceratopsid dinosaurs from the Grand Staircase of southern Utah; pp. 488-503 in A. L. Titus and M. A. Loewen (eds.), At the Top of the Grand

Staircase: the Late Cretaceous of Southern Utah. Indiana University Press, Bloomington.

Loewen, M. A., S. D. Sampson, E. K. Lund, A. A. Farke, M. C. Aguillón-Martínez, C. A. de Leon, R. A. Rodríguez-de la Rosa, M. A. Getty, and D. A. Eberth. 2010. Horned dinosaurs (Ornithischia: Ceratopsidae) from the Upper Cretaceous (Campanian) Cerro del Pueblo Formation, Coahila, Mexico; pp. 99-116 in M. J. Ryan, B. J. Chinnery-Allgeier, and D. A. Eberth (eds.), New Perspectives on Horned Dinosaurs: The Royal Tyrrell Museum Ceratopsian Symposium. Indiana University Press, Bloomington.

Longrich, N. R. 2010. *Mojoceratops perifania*, a new chasmosaurine ceratopsid form the Late Campanian of western Canada. Journal of Paleontology 84:681-694.

Longrich, N. R. 2011. *Titanoceratops ouranos*, a giant horned dinosaur from the Late Campanian of New Mexico. Cretaceous Research 32:264-276.

Longrich, N. R. 2014. The horned dinosaurs *Pentaceratops* and *Kosmoceratops* from the upper Campanian of Alberta and implications for dinosaur biogeography. Cretaceous Research 51:292-308.

Lucas, S. G., R. M. Sullivan, and A. P. Hunt. 2006. Re-evaluation of *Pentaceratops* and *Chasmosaurus* (Ornithischia: Ceratopsidae) in the Upper Cretaceous of the Western Interior. New Mexico Museum of Natural History and Science Bulletin 35:367-370.

Lull, R. S. 1933. A revision of the Ceratopsia or horned dinosaurs. Peabody Museum of Natural History Bulletin 3:1-175.

Maidment, S. C. R., and P. M. Barrett. 2011. A new specimen of *Chasmosaurus belli* (Ornithischia: Ceratopsidae), a revision of the genus, and the utility of postcrania in the taxonomy and systematics of ceratopsid dinosaurs. Zootaxa 2963:1-47.

Mallon, J. C., D. C. Evans, M. J. Ryan, and J. S. Anderson. 2012. Megaherbivorous dinosaur turnover in the Dinosaur Park Formation (upper Campanian) of Alberta, Canada. Palaeogeography, Palaeoclimatology, Palaeoecology 350-352:124-138.

Mallon, J. C., R. B. Holmes, D. A. Eberth, M. J. Ryan, and J. S. Anderson. 2011. Variation in the skull of *Anchiceratops* (Dinosauria: Ceratopsidae) from the Horseshoe Canyon Formation (Upper Cretaceous) of Alberta. Journal of Vertebrate Paleontology 31:1047-1071.

Mallon, J. C., R. B. Holmes, J. S. Anderson, A. A. Farke, D. C. Evans, and H.-D. Sues. 2014. New information on the rare horned dinosaur *Arrhinoceratops brachyops*

(Ornithischia: Ceratopsidae) from the Upper Cretaceous of Alberta, Canada. Canadian Journal of Earth Sciences 51:618-634.

Newman, K. R. 1987. Biostratigraphic correlation of Cretaceous–Tertiary boundary rocks, Colorado to San Juan Basin, New Mexico; pp. 151-163 in J. E. Fassett and J. K. Rigby Jr. (eds.), Cretaceous–Tertiary Boundary in the San Juan and Raton Basins, New Mexico and Colorado. Geological Society of America Special Paper.

Ogg, J. G., L. A. Hinnov, and C. Huang. 2012. Cretaceous; pp. 793-853 in F. M. Gradstein, J. G. Ogg, M. D. Schmitz, and G. M. Ogg (eds.), The Geologic Time Scale 2012. Elsevier, Amsterdam.

Osborn, H. F. 1923. A new genus and species of Ceratopsia from New Mexico, *Pentaceratops sternbergii*. American Museum Novitates 93:1-3.

O'Sullivan, R. B., and H. M. Beikman. 1963. Geology, Structure, and Uranium Deposits of the Shiprock Quadrangle, New Mexico and Arizona. pp.

O'Sullivan, R. B., G. R. Scott, and J. S. Heller. 1979. Preliminary Geologic Map of the Bisti Trading Post Quadrangle, San Juan County, New Mexico. pp.

Roberts, E. M., S. D. Sampson, A. L. Deino, S. A. Bowring, and R. Buchwaldt. 2013. The Kaiparowits Formation: a remarkable record of Late Cretaceous terrestrial environments, ecosystems, and evolution in western North America; pp. 85-106 in A. L. Titus and M. A. Loewen (eds.), At the Top of the Grand Staircase: the Late Cretaceous of Southern Utah. Indiana University Press, Bloomington, Indiana.

Rowe, T., E. H. Colbert, and J. D. Nations. 1981. The occurrence of *Pentaceratops* (Ornithischia: Ceratopsia) with a description of its frill; pp. 29-48 in S. G. Lucas, J. K. Rigby Jr., and B. S. Kues (eds.), Advances in San Juan Basin Paleontology. University of New Mexico Press, Albuquerque.

Rowe, T., R. L. Cifelli, T. M. Lehman, and A. Weil. 1992. The Campanian Terlingua Local Fauna, with a summary of other vertebrates from the Aguja Formation, Trans-Pecos Texas. Journal of Vertebrate Paleontology 12:472-493.

Rozhdestvensky, A. K. 1965. Growth changes in Asian dinosaurs and some problems of their taxonomy. Paleontologischeskii Zhurnal 3:95-109.

Ryan, M. J., and D. C. Evans. 2005. Ornithischian Dinosaurs. Dinosaur Provincial Park: A Spectacular Ancient Ecosystem Revealed:312-348.

Sampson, S. D., M. A. Loewen, A. A. Farke, E. M. Roberts, C. A. Forster, J. A. Smith, and A. L. Titus. 2010. New horned dinosaurs from UTah provide evidence for intracontinental dinosaur endemism. PLoS ONE 5:e12292.

Scannella, J. B., and J. R. Horner. 2010. *Torosaurus* Marsh, 1891, is *Triceratops* Marsh, 1889 (Ceratopsidae: Chasmosaurinae): synonymy through ontogeny. Journal of Vertebrate Paleontology 30:1157-1168.

Scannella, J. B., D. W. Fowler, M. B. Goodwin, and J. R. Horner. 2014. Evolutionary trends in *Triceratops* from the Hell Creek Formation, Montana. Proceedings of the National Academy of Sciences 111:10245-10250.

Scott, G. R., R. B. O'Sullivan, and J. S. Heller. 1979. Preliminary Geologic Map of the Burnham Trading Post Quadrangle, San Juan County, New Mexico. Report 1076.

Sternberg, C. M. 1940. Ceratopsidae from Alberta. Journal of Paleontology 14:468-480.

Sternberg, C. M. 1950. Steveville - west of the fourth meridian, Alberta. Geological Survey of Canada Topographic Map A.

Sullivan, R. M., and S. G. Lucas. 2006. The pachycephalosaurid dinosaur *Stegoceras validum* from the Upper Cretaceous Fruitland Formation, San Juan Basin, New Mexico. New Mexico Museum of Natural History and Science Bulletin 35:329-330.

Sullivan, R. M., and S. G. Lucas. 2011. Charles Hazelius Sternberg and his San Juan Basin Cretaceous dinosaur collections: correspondence and photographs (1920-1925). New Mexico Museum of Natural History and Science Bulletin 53:429-471.

Sullivan, R. M., S. G. Lucas, and D. R. Braman. 2005. Dinosaurs, pollen, and the Cretaceous-Tertiary boundary in the San Juan Basin, New Mexico. New Mexico Geological Society, 56th Field Conference Guidebook, Geology of the Chama Basin:395-407.

Tanke, D. H. 2010. Ceratopsian discoveries and work in Alberta, Canada: historical review and census; pp. 488 (CD-ROM) in M. J. Ryan, B. J. Chinnery-Allgeier, and D. A. Eberth (eds.), New Perspectives on Horned Dinosaurs: The Royal Tyrrell Museum Ceratopsian Symposium. Indiana University Press, Bloomington.

Tanke, D. H., and B. M. Rothschild. 2002. Dinosores: an annotated bibliography of dinosaur paleopathology and related topics - 1838-2001. New Mexico Museum of Natural History and Science Bulletin 20:1-97.

Wick, S. L., and T. M. Lehman. 2013. A new ceratopsian dinosaur from the Javelina Formation (Maastrichtian) of West Texas and implications for chasmosaurine phylogeny. Naturwissenschaften 100:667-682.

Wiman, C. 1930. Uber Ceratopsia aus der oberen Kreide in New Mexico. Nova Acta Regiae Societatis Scientarum Upsaliensis 4-7:1-19.

Wolberg, D. L., J. P. Hall, and D. Bellis. 1988. First record of dinosaur footprints from the Fruitland Formation, San Juan County, New Mexico. New Mexico Bureau of Mines and Mineral Resources, Bulletin 122:33–34.Breyer, J. A., A. B. Busbey III, R. E. Hanson, K. E. Befus, W. R. Griffin, U. S. Hargrove, and S. C. Bergman. 2007. Evidence for Late Cretaceous Volcanism in Trans-Pecos Texas. The Journal of Geology 115:243-251.

APPENDIX D

SUPPLEMENTARY INFORMATION 2 FOR CHAPTER 4:

PHYLOGENETIC ANALYSIS

The data matrix for the phylogenetic analysis was adapted from Mallon et al. (2014), which was itself adapted from Sampson et al. (2010).

Phylogenetic Character Alterations

It has not been possible to review all character states for every taxon listed by Sampson et al. (2010) and Mallon et al. (2014). However, I have made corrections in cases where I am familiar with the specimens (especially *Chasmosaurus*, *Pentaceratops*, and *Triceratops*). All corrections are noted below, and most concern parietal morphology.

Notes on Specimens and Data Used for Analysis

Additional specimens used to code character states are noted where appropriate.

Bravoceratops

The matrix has been amended to reflect the re-identification of the parietal median bar of *Bravoceratops polyphemus* (Wick and Lehman, 2013) as representing the anterior rather than posterior end (see main text). This results in characters 65, 68, 72, 76, 82-84, 95, 96, 98, 99, and 104-107 all being recoded as unknown (?).

Vagaceratops and *Kosmoceratops*

The character matrix for *Vagaceratops* (*Chasmosaurus*) *irvinensis* and *Kosmoceratops richardsoni* (Holmes et al., 2001; Sampson et al., 2010; Loewen et al., 2013) has been altered to reflect reinterpretation of epiparietals and episquamosals. This

is discussed in the main text, and results in changes for character states 88-90, 92, 96, 97, 102, and 103.

Notes and Alterations to Existing Characters

Character 7

"Premaxilla, narial strut orientation (Dodson et al., 2004, character 6)"

0: 'rostrally inclined'

1: 'caudally inclined'

Coahuilaceratops recoded from (1) to (?) as the premaxillary strut is heavily damaged and might not be caudally inclined. *Chasmosaurus belli* recoded from (0) to (0&1) as YPM 2016 has a caudally inclined narial strut.

Character 60

"Squamosal, length relative to parietal (Holmes et al., 2001, character 19, modified)"

0: 'squamosal much shorter than parietal, large portion of posterolateral frill made up of parietal'

1: 'squamosal slightly shorter than parietal, pmn;y posterolaterl-most [sic] margin of frill formed by the parietal'

2: 'squamosal and parietal equal in length'

Pentaceratops sternbergii is recoded from (1) to (1&2). *P. sternbergii* specimens AMNH 1624 and 1625 exhibit a squamosal that is the same length as the parietal, although in other speicmens (UKVP 16100, MNA Pl.1747) the squamosal is slightly

shorter (state 1). *Anchiceratops* is recoded from (2) to (1&2), as some specimens have squamosals that are equal in length to the parietal (e.g. ROM 802), whereas others the squamosal is shorter (e.g. AMNH 5251). *Ojoceratops* is originally coded as (2), however no squamosal has been collected with an associated parietal so that this cannot be asserted (Sullivan and Lucas, 2010). *Ojoceratops* is therefore recoded as (?).

Character 61

Squamosal forms part of posterior margin of frill (new)

0: 'present '

1: 'absent '

Ojoceratops changed from (1) to (?) for the same reason as the above character 60.

Character 66

"Parietal, concave median embayment on caudal margin (new)"

0: 'absent '

1: 'present '

Torosaurus latus and *Triceratops horridus* both changed from state (0) to (0&1). YPM 1831 (holotype of *Torosaurus* "*gladius*"=*latus*) has a clear embayment on the midline of the posterior parietal, as does *Triceratops horridus* specimen AMNH 5116. However, other specimens of *Torosaurus latus* (e.g. MOR 1122) and *Triceratops horridus* (e.g. MOR 1120) lack a medial embayment (state 0). A possible very weak embayment is present in isolated parietals MOR 2946 and MOR 6647, which probably

both pertain to *Triceratops prorsus*; MOR 2946 exhibits a stepped margin to the incipient fenestra on the ventral side (only seen in *T. prorsus*; Scannella and Horner, 2010); and MOR 6647 is from the upper third of the Hell Creek Formation (pers. obs.), from which only *T. prorsus* remains are known (Scannella et al., 2014). However, given that the embayment in these specimens is not very pronounced, I am going to leave *Triceratops prorsus* as state (0).

Chasmosaurus belli is recoded from (0) to (1). It is noted that in the original coding, *C. belli* is coded as lacking an embayment in character 66 (state 0), but in the following character (67) is coded as character state (1): 'shallow, entire transverse bar is a V-shaped embayment' (ie. that it possesses an embayment). The lateral rami of the parietal posterior bar are inclined in all specimens attributed to *C. belli*, meeting at the midline as a shallowly concave embayment (ie. character 66, state 1). It is noted here that the angle at which the lateral rami meet is almost flat in YPM 2016, being intermediate between the condition seen in other *C. belli*, and that of *Vagaceratops* (*Chasmosaurus*) *irvinensis*.

Although *Anchiceratops* is coded as lacking a medial embayment, if Lehman (1993, 1998) is correct then this is because the embayment has closed, rather than it never having existed in the ancestor. Furthermore, in all *Anchiceratops* specimens, the midline of the parietal posterior bar (point 2 in my morphometric analysis) is notably more anterior than the posteriormost part of the parietal (excluding epiparietals); i.e. it is embayed. This narrow notch-like embayment occurs between the epiparietals. Why this is not therefore coded as possession of an embayment is not clear. *Pachyrhinosaurus*

lakustai and *Centrosaurus apertus* are both coded for the possession of a median embayment, yet it is very shallow, and in at least two specimens of *P. lakustai* (TMP 1987.55.141 and 1988.55.46; Currie et al., 2009) it is extremely shallow to absent. In Version 2 of the matrix, *Anchiceratops* was coded as present (1) for this character.

Character 67

"Parietal, shape of concave median embayment (Forster, 1990, character 83, modified) PROBLEM WITH NUMBERS ON SHEET" [sic]

0: 'shallow, restricted to center of margin '

1: 'shallow, entire transverse bar is a V-shaped embayment '

2: 'notch-like, restricted to center of margin'

As with character 66, *Torosaurus latus* (YPM 1831) and *Triceratops horridus* (AMNH 5116) both exhibit a shallow median embayment and hence these taxa are recoded from(?) to (0). Note that the "PROBLEM" part of the description was in the original nexus file from Mallon et al. (2014). In Version 2 of the matrix, *Anchiceratops* was coded as (2) for this character.

Character 68

"Parietal, location of caudalmost point of caudal ramus (Holmes et al., 2001, character 18, modified)"

0: 'on midline '

1: 'between midline and lateral-most corner '

2: 'at lateral-most corner adjacent to squamosal'

Pentaceratops has been recoded from state (2) to (1&2). AMNH 1625 is like *Utahceratops* (coded as 1) in that the caudalmost part of the parietal posterior bar is not adjacent to the squamosal. It could be argued that other *Pentaceratops* specimens coded as state 2 (MNA Pl.1747 and UKVP 16100) are in fact intermediate between states 1 and 2, and unlike the condition in *Chasmosaurus belli*, which is more definitively coded as state 2. *Triceratops horridus* has also been recoded from (0) to (0&1) as the mounted exhibit specimen AMNH 5116 clearly exhibits a central embayment in the parietal (hence character state 1; the midline is embayed so cannot be state 0).

Character 74

"Parietal, rim on medial margin of dorsotemporal fenestra (Forster, 1990, character 86). CORRECTED."

0: 'absent '

1: 'present, well-defined, laterally projecting rim defines medial margin of fenestra'

Mojoceratops, *Chasmosaurus russelli* and *C. belli* are recoded from (0) to (1). All specimens attributed to these taxa have a rim on the medial margin of the dorsotemporal fenestra.

Both species of *Torosaurus* and of *Triceratops* were originally coded as (0). This is partly understandable as the dorsotemporal fenestrae are not as prominent in *Torosaurus* and *Triceratops*, and the ridge is weak in large (probably mature) specimens. Nevertheless, a rim on the dorsotemporal fenestra is visible in *Torosaurus latus* specimen MOR 1122; in *Triceratops horridus* specimens USNM 2100 and AMNH 5116; in

immature specimens of *Triceratops prorsus* held at MOR, and in the holotype (YPM 1822; see Hatcher et al., 1907; pl. 35). This region of the parietal is fragmentary in *Torosaurus utahensis*, but appears to preserve a rim (Scannella, pers. comm.). Hence *Torosaurus* and *Triceratops* are recoded from (0) to (1).

Character 76

"Parietal, rostrocaudal thickness of transverse bar at narrowest point (Holmes et al., 2001, character 22)"

0: 'narrow and straplike, less than 10% total parietal length'.

1: 'broad, 20% or more of total parietal length.'

Despite being incomplete, *Navajoceratops* and *Terminocavus* are coded for this character based on reconstruction of the parietal (see figures in main text), and the assertion that the rostrocaudal thickness of the narrowest point of the lateral ramus of *Terminocavus* cannot be 10% or less of total parietal length without the parietal being unusually elongate.

Character 77

"Parietal, relative rostrocaudal depth of broad transverse bar (new)"

0: 'subequal medial to lateral'.

1: 'tapering so that the narrowest point occurs medially'.

This was recoded as (0&1) for *Pentaceratops sternbergii* (previously 1) because AMNH 1625 records state 0 as it does not notably taper mediolaterally. Tapering is noted, however, in UKVP 10161, and MNA Pl.1747 (both state 1). This has also been

recoded for *Utahceratops*, which was coded as (1) and is recoded as (0). Despite being incomplete, the parietal of *Utahceratops* does not narrow notably medially. Indeed, in the reconstruction offered by Sampson et al. (2010), if anything the parietal is rostrocaudally deeper medially rather than laterally (although only very slightly).

Character 78

"Parietal, cross-sectional shape of median bar (Holmes et al., 2001, character 24, modified)"

0: 'diamond-shaped, tapers laterally'

1: 'rectangular or subrectangular, margin facing parietal fenestrae thick and oriented sub-perpendicular to parietal surface '

2: 'round to lenticular'

3: 'v-shaped, opening ventrally'

Pentaceratops altered to state 0 and 2 (previously only 2) as the MNA Pl.1747 specimen of *Pentaceratops* possesses a lenticular cross section with slight lateral flanges, similarly seen in *Navajoceratops* and *Terminocavus*.

This character state is poorly defined. None of the defined character states adequately describe the condition seen in *Navajoceratops*, *Terminocavus,* or indeed Taxon C; furthermore, the cross section of the median bar changes along its length and the character as defined makes no claim as to where it should be sampled. *Navajoceratops* and *Terminocavus* are therefore each coded as (0&2).

Character 86

"Episquamosal, location of largest/longest example (new)"

0: 'episquamosals subequal in size '

1: 'rostralmost episquamosal by far the largest '

2: 'caudalmost episquamosal by far the largest'

There is a serious issue with this character in that the size of the anteriormost (rostralmost) episquamosal (aes) can often appear large because it is mounted on an anteroventral extension of the squamosal, and because (in *Triceratops* at least; Forster, 1996) this es is one of the first to fuse to the squamosal, and can therefore be difficult to delineate its actual size. The aes is often more pointed than other episquamosals (es), but is not obviously by far the largest in size (it is not clear if this means basal width, total area, etc).

A review of *Chasmosaurus belli* and *C. russelli* specimens does not reveal any specimens which unequivocally bear an aes in this position that is "by far the largest". Illustrations of *C. russelli* specimen NMC 2280 (Godfrey and Holmes, 1995) show the aes is roughly the same size as many other es (especially on the left squamosal). *C. russelli* specimen TMP 81.19.175 (Godfrey and Holmes, 1995) bears an aes that is slightly larger than the next most anterior es, but lacks the posteriormost es for comparison and so cannot be coded. *C. belli* specimen ROM 843 bears an aes that is larger than the next most anterior es, but comparable to some of the more posterior es. CMN 2245 bears an episquamosal that is well fused to the anteroventral projection such that it is not possible to tell how big it is based on photographs; regardless, the posterior

es are quite large and it is not likely that the aes was by far the largest in this specimen. AMNH 5402 does not bear an aes that is any larger than other es positions. Based on these observations, *C. belli* and *C. russelli* are coded as (0).

The holotype of "*Mojoceratops*" *perfania* (TMP 1983.25.1) bears no obviously fused episquamosals and so should be coded as (?). Referred specimen AMNH 5656 has episquamosals that are of similar size along the squamosal, and so would be coded as (0) (although it is noted that this specimen is very small, and thus likely represents a juvenile, which may make its morphology unreliable).

Bravoceratops is recoded from (1) to (?). In their figure 8, Wick and Lehman (2013) illustrate the anterior end of the squamosal, which shows that the aes is actually small relative to other es. It appears large as it is mounted on the anteroventral extension of the squamosal. Although fragmentary, the squamosal of *Bravoceratops* bears six observable es, all of which are similar in size (ie. state 0). However, the posterior end of the squamosal is missing, such that it is not possible to exclude character state (2). As such, *Bravoceratops* must be coded as (?). In contrast, the posteriormost episquamosal is often notably larger than other episquamosals, as recorded in the original dataset.

Character 88

Episquamosal locus S1 shape (new)

0: 'small and crescentic'

1: 'low raised D-shaped process'

2: 'well developed larger triangular process'

3: 'elongate hook'

Reconfiguration of the frill epiossifications of *Kosmoceratops* changes its state from (3) to (2).

Character 89

"Episquamosal locus S2 shape (new)"

0: 'small and crescentic'

1: 'low raised D-shaped process'

2: 'well developed larger triangular process'

Vagaceratops (*Chasmosaurus*) *irvinensis* is coded as (2), but this is inaccurate. The holotype (NMC 41357; Holmes et al., 2001) bears no episquamosals that can be considered as "a well developed larger triangular process" and should therefore be coded as (1). Referred specimen TMP 87.45.1 has some more triangular projections of the squamosal margin visible in photographs (Holmes et al., 2001), but these are in the middle of the squamosal, not in locus s2. Finally, *Vagaceratops* is originally coded as (0) for character 86 (Episquamosal, location of largest/longest example), suggesting that its episquamosals are all of similar size, which would contradict a coding of (2). *Vagaceratops* is here recoded from (2) to (1).

Reconfiguration of the frill epiossifications of *Kosmoceratops* changes its state from (2) to (1). Note that in the holotype of *Kosmoceratops* UMNH VP 17000, the reconfigured es2 (es3 in the original configuration) is a D-shape, whereas it is more pointed in referred specimen UMNH VP 16878 (Loewen et al., 2013).

Character 90

"Episquamosal locus S2 size relative to other episquamosals (new)"

0: 'subequal'

1: 'second only to S1 in size, larger than S3'

Reconfiguration of the frill epiossifications (es3 is renumbered here as es2) of *Kosmoceratops* changes its state from (1) to (0).

Character 91

"Marginal ossification crossing squamosal-parietal contact (Dodson et al., 2004, character 43)"

0: 'absent'

1: 'present'

This character refers to the presence/absence of a frill epiossification that straddles the squamosal-parietal contact (referred to hereafter as an eps).

The character is of dubious utility for two reasons. Firstly, in many specimens epiossifications are not fused on to the frill border such that lack of a visible eps does not mean that one was absent in life. The only way that state (0) can be unequivocally asserted is if a specimen has epiossifications fused to either the squamosal or parietal such that there is no available space for an eps. Secondly, even if it is possible to assess the absence of an eps in one specimen, possession of an eps is observed to be very variable individually in some taxa. For example, the most well-known chasmosaurine, *Triceratops* typically exhibits 5-7 epiparietals (Scannella et al., 2014). In specimens with 5 epiparietals, an eps (or space for one) is typically present. In specimens with 7

epiparietals, an eps is typically absent (i.e. in some specimens the eps might "jump" on to the parietal).

In light of these issues, this character is miscoded for many taxa, so I have made a number of revisions. *Pentaceratops sternbergii* was previously coded as (0) but is here recoded as (0&1). Only *P. sternbergii* specimen AMNH 1624 can be reliably coded as (0) as it preserves fused epiossifications which do not straddle the parietal-squamosal contact, nor is there a space for an eps. However, *P. sternbergii* frill AMNH 1625 (not included in the observed specimen list of Sampson et al., 2010) clearly possesses a triangular epiossification that straddles the parietal-squamosal contact. *Nedoceratops* is recoded from (1) to (?) as the parietal-squamosal contact is only preserved on the right side of the skull, and even here it is incomplete and may or may not preserve an eps (Farke, 2011).

Eotriceratops and *Torosaurus latus* are treated inconsistently. *Eotriceratops* was originally coded as (1), which is probably true as there seems to be a space at the distal end of the squamosal where an eps might have occurred (and is inferred to have been by Wu et al., 2007). The parietal of *Eotriceratops* is unknown, but presumably on the basis of this space, and the logic outlined in the above paragraph, Sampson et al. (2010) code an eps as present. However, *Torosaurus latus* is coded as (0), despite possessing a notable gap at the parietal-squamosal contact in MOR 1122 (which was studied by Sampson et al., 2010). Furthermore, *Torosaurus latus* specimen ANSP 15192 exhibits an eps (Scannella and Horner, 2010), but this is not noted by Sampson et al. (2010; who also studied this specimen). Therefore I have recoded *Torosaurus latus* as (0&1). As

mentioned above, specimens of *Triceratops* exhibit both conditions and should therefore be recoded from (1) to (0&1).

Reconfiguration of the frill epiossifications of *Kosmoceratops* and *Vagaceratops* does not change the character state, but what was previously considered as es1 is here coded as an ep3 that is possibly partly borne on the squamosal as an eps.

Character 92

"Shape of marginal ossification crossing squamosal-parietal contact (new)"

0: 'small and crescentic'

1: 'present strongly recurved process or gnarled process'

2: 'well developed triangular process sometimes with a small peak'

Note that no taxa are coded as state (0), hence this character state is redundant. More importantly, the description of the morphology of eps is inconsistent with morphological description of other epiossifications. For example:

Character 102

"Epiparietal locus P3 shape (new)"

0: 'low D-shaped process '

1: 'elongate flattened process or spike '

2: 'strongly recurved triangular or recurved low gnarled triangular process'

3: 'well developed triangular process'

4: 'elongate low process sometimes with a small peak'

This is significant as the current definition of character 92 conflates "well-developed triangular process" with the "elongate low process" as a single character. I suggest that if the eps were coded using the morphological definitions of character 102, some taxa would not be lumped together as state (2); for example, the eps of *Anchiceratops* and *Pentaceratops* (see below) is triangular in shape and unlike the spindle-shaped eps seen in *Triceratops* and *Arrhinoceratops* (which is basically the same morphology as most other epiossifications of the frill). Therefore I have revised the character state definitions of character 92 as follows:

Character 92 (Revised)

"Shape of marginal ossification (eps) crossing squamosal-parietal contact (new)"

0: 'small and crescentic'

1: 'present strongly recurved process or gnarled process'

2: 'well developed triangular process'

3: 'elongate base, spindle-shaped low process sometimes with a small peak'

4: 'elongate hook'

State (0) is conserved as presumably this permits comparison with other datasets.

Albertaceratops and *Centrosaurus* were both coded as (0) for character state 91 (i.e. they do not possess an eps), but were coded (0) for character 92. This is in error. I have recoded *Albertaceratops* and *Centrosaurus* as (?) for character 92. *Pentaceratops sternbergii* was previously coded as (?) but is here recoded as (2). *P. sternbergii* frill AMNH 1625 (not included in the observed specimen list of Sampson et al., 2010) clearly possesses a triangular epiossification that straddles the parietal-squamosal contact.

Anchiceratops remains as (2). *Eotriceratops* was previously coded as (2), i.e. the same as other triceratopsins. However, although the presence of an eps is inferred (see Wu et al., 2007), the actual eps is not present, hence its morphology cannot be known. *Eotriceratops* is therefore recoded as (?). *Arrhinoceratops* and all species of *Triceratops* and *Torosaurus* are recoded from (2) to (3).

A further problem exists in that the identity of the epiossification at position eps might vary, and in at least some cases, character 92 might be coding for the morphology of ep3, which is already covered by character 103. This is probably the case with P. sternbergii specimen AMNH 1625 as it possesses an ep1 within the parietal embayment, an ep2 approximately halfway along the lateral rami, and an epiossification positioned as eps, which should probably be considered as ep3. Unfortunately no other specimens of *P. sternbergii* exist which preserve three epiossifications contacting the parietal such that comparisons can be made. Further discussion of the identity of ep3/eps can be found in the discussion in main text. I have chosen to leave character 92 in the analysis (in its revised form), but acknowledge a case can be made for its removal.

Reconfiguration of the frill epiossifications of *Kosmoceratops* changes the character state from (1) to the new state (4). Note that the laterally curving hook-shaped epiossification previously considered as es1 is here coded as an ep3 that is possibly partly borne on the squamosal as an eps.

Reconfiguration of the frill epiossifications of *Vagaceratops* changes the character state from (1) to state (2).

Character 96

"Epiparietal locus DPP1 (Sampson, 1995, character 14, modified)"

0: 'absent '

1: 'present '

This character refers to the possession of epiparietal locus "DPP1" but is not referred to as this in Sampson (1995) from which it is supposedly modified (a paper concerned with the description of new centrosaurine taxa). Character 14 of Sampson (1995, p. 760) is defined as "Posterior parietal hooks (Process 1): (0) absent; (1) present, abbreviated; (2) present, well-developed". Subsequent characters follow the same format for epiparietals 2 to 6; for example character 15 is defined as "Process 2 on parietal margin: (0) absent; (1) small; (2) large, medially-directed horn. Therefore it is established here that character 14 of Sampson (1995) refers to the possession and (if present) morphology of an epiparietal (parietal process) at position 1 (all in one character).

The current character 96 only has two character states (0) absent, and (1) present, hence it is not fully comparable to character 14 of Sampson (1995). If character 96 is simply supposed to record the presence / absence of epiparietal 1 (ep1), then this is understandable, however, epiparietals 2 and 3 are not afforded their own presence-absence character (although there is less variability in ep2 and ep3). Curiously, *Utahceratops* and *Pentaceratops* are the only chasmosaurines coded as state (1) for character 96, which might therefore suggest that the ep1 locus is missing from other chasmosaurine taxa. This might be understandable, as *Chasmosaurus belli* exhibits an elongate ridge in the position of ep1, so it could be arguable that the ep1 locus is

therefore absent in this taxon (I would disagree; I think the ridge is an laterally expanded ep1). However *C. belli*, and indeed all chasmosaurines (for which the posterior bar of the parietal is preserved) are coded for morphology of ep1 in character 97, which therefore shows that according to the original coding, they indeed possess the ep1 locus (I agree). This confusing issue would appear to be solved by either coding all chasmosaurines as state (1) for character 96, or deleting / altering character 96.

Note that *Pachyrhinosaurus lakustai* (Currie et al., 2009) is coded by Sampson et al. 2010 and Mallon (2014) as state (1), ie. that it possesses an ep1. However, in the original description, the parietal of *P. lakustai* is shown as lacking ep1. Therefore I have recoded *P. lakustai* as state (0).

Character 96 (Revised)

"Epiparietal locus ep1, position (New configuration)"

0: absent

1: present; locus ep1 is positioned at the lateral edge of the parietal embayment or the space usually occupied by an ep0, but not within this space; this is usually where there is a change of angle in the posterior bar.

2: present, locus ep1 is elongate, and extends laterally from the midline (or near the midline) over 50% or more of each lateral ramus of the parietal posterior bar.

3: present, locus ep1 is limited to the central third of the posterior bar, such that the medialmost edge of locus ep1 immediately abuts the midline (or nearly so).

Leptoceratops, *Protoceratops*, *Albertaceratops* and *Pachyrhinosaurus* are coded as (0). *Centrosaurus* is coded as (3). *Chasmosaurus russelli*, *Mojoceratops perfania*, and *Agujaceratops mariscalensis* all exhibit character state (1).

Chasmosaurus belli, *Vagaceratops* (*Chasmosaurus*) *irvinensis* and *Kosmoceratops richardsoni* exhibit character state (2). This is part of the reconfiguration of epiparietal classification within this study. Most specimens of *C. belli* exhibit a simple anteriorly recurved elongate ridge in the ep1 locus position, however one specimen (YPM 2016) has a what appears to be an array of protuberances developed along this ridge, but is otherwise like other specimens of *C. belli*. These protuberances are here suggested to develop into the prominent processes seen on the parietal of *Vagaceratops* (*Chasmosaurus*) *irvinensis*, and further developed into more elongate spikes in *Kosmoceratops*.

Utahceratops, *Pentaceratops sternbergii*, *Anchiceratops*, *Navajoceratops*, and *Terminocavus* all exhibit character state (3). *Arrhinoceratops*, *Ojoceratops* (based on the parietal described by Farke and Williamson, 2006; also used by Sampson et al. 2010), *Torosaurus latus*, and both species of *Triceratops* are coded as (1).

Character 97

"Epiparietal, locus P1 shape (Sampson, 1995, character 15, modified)"

0: 'low D-shaped process '

1: 'elongate flattened process or spike '

2: 'strongly recurved triangular or recurved low gnarled triangular process'

3: 'well developed triangular process'

4: 'elongate low process sometimes with a small peak'

Albertaceratops (Ryan, 2007) is coded by Sampson et al. 2010 and Mallon (2014) as state (1), ie. that it possesses an ep1. However, in the original description, the parietal of *Albertaceratops* is shown as lacking ep1, and is coded as such in the data matrix (Ryan, 2007). *Albertaeratops* is also coded as lacking an ep1 in character 96. I have therefore coded *Albertaceratops* as (?) for character 96 (it should really be "-", but in this analysis absent characters are coded as ?; see note). Similarly, epiparietal 1 is not present in *Pachyrhinosaurus lakustai* (Currie et al., 2009), hence I have recoded this from (1) to (?). Note that no taxa in the current matrix possess character state (0); presumably this is a result of culling other taxa from the matrix in a dataset prior to Sampson et al. (2010).

Character 97 has problems as most chasmosaurine frill epiossifications broaden and become less pointed through ontogeny; this has been demonstrated unequivocally in *Triceratops* (Horner and Goodwin, 2006; 2008) and is observable in other chasmosaurines (e.g. Lehman, 1990; Godfrey and Holmes, 1995; Mallon et al., 2014). However, in *Anchiceratops* and possibly *Pentaceratops*, parietal epiossifications remain triangular and pointed even in the largest and presumably oldest individuals (Mallon et al., 2011; see specimen descriptions in Appendix C). Moreover, it is not very clear what the difference is between character state 1 and 4 (for example). By reference to the codings (*Centrosaurus* is the only taxon coded as state 1) it can be seen that character state (1) refers to anteroposterior elongation, whereas state (4) refers to the broadening of the base of the epiossifications (in the case of the parietal this would usually be lateral

broadening, but on the squamosal, usually anteroposterior). These issues are reflected in the revised character 97.

Character 97 (Revised)

"Epiparietal, locus P1 morphology (revised)"

0: 'low D-shaped process '

1: 'anteroposteriorly elongate flattened process or spike '

2: 'strongly recurved triangular or recurved low gnarled triangular process'

3: 'well developed triangular process'

4: 'elongate base, spindle-shaped low process sometimes with a small peak'

5: 'very elongate and differentiated into an array of (typically 3) protuberances'

Note the addition of state (5): *Vagaceratops irvinensis* and *Kosmoceratops richardsoni* both exhibit an array of anteriorly projecting protuberances along the posterior bar of the parietal; this is coded as state (5). One specimen of *Chasmosaurus belli* (YPM 2016) has what appears to be an incipient development of this character (the protuberances are less pronounced, but clearly present). Other specimens of *C. belli* (e.g. CMN 491, ROM 843, BMNH 4948) exhibit an elongated ridge in the position of ep1, but it is an undifferentiated single ridge. Therefore *C. belli* is coded as (2&5). *Mojoceratops* is recoded as (2).

Character 98

"Epiparietal, locus P1 orientation (Sampson, 1995, character 15, modified)"

0: 'caudally, epiparietal oriented in the plane of the frill '

1: 'directed rostrodorsally '

2: 'P1 occurs on dorsal surface of parietal'

Again, both *Albertaceratops* and *Pachyrhinosaurus* lack an epiparietal 1, so should be coded as (?) instead of the original coding of (0). Also, since the parietal of *Bravoceratops* was misidentified (see main text), then it is now coded as (?), leaving only one taxon (*Anchiceratops*) that would exhibit character state (2) (which was added by Wick and Lehman, 2013, and maintained by Mallon et al., 2014). This makes character state (2) redundant. I am therefore reverting the character back to as it was in Sampson et al. (2010).

Character 98 (Revised)

"Epiparietal, locus P1 orientation (Sampson, 1995, character 15, modified)"

0: 'caudally, epiparietal oriented in the plane of the frill '

1: 'directed rostrodorsally '

Reconfiguration of the frill epiossifications of *Kosmoceratops* and *Vagaceratops* does not result in a change in character state, although what was previously considered as ep1, ep2, and ep3 by (Sampson et al., 2010; Loewen et al., 2013) are here considered as an array of processes hosted on locus ep1.

Character 99

"Epiparietal, locus P1 curvature (Sampson, 1995, character 15, modified)"

0: 'straight '

1: 'laterally curved '

2: 'medially curved'

3: 'dorsally curved'

Reconfiguration of the frill epiossifications of *Kosmoceratops* and *Vagaceratops* does not result in a change in character state, although what was previously considered as ep1, ep2, and ep3 by (Sampson et al., 2010; Loewen et al., 2013) is here considered as an array of processes hosted on ep1.

Character 100

"Epiparietal, locus P2 shape (Sampson, 1995, character 16, modified)"

0: 'low raised D-shaped process'

1: 'elongate spike'

2: 'strongly recurved triangular or recurved low gnarled triangular process'

3: 'well developed triangular process'

4: 'elongate low process sometimes with a small peak'

This character was then revised for clarity.

Character 100 (Revised)

"Epiparietal, locus P2 shape (Sampson, 1995, character 16, modified)"

0: 'low D-shaped process'

1: 'anteroposteriorly elongate flattened process or spike'

2: 'strongly recurved triangular or recurved low gnarled triangular process'

3: 'well developed triangular process'

4: 'elongate base, spindle-shaped low process sometimes with a small peak'

Reconfiguration of the frill epiossifications of *Kosmoceratops* and *Vagaceratops* does not result in a change in character state, although what was previously considered as eps by (Sampson et al., 2010; Loewen et al., 2013) is here considered as an ep2.

Character 101

"Epiparietal, locus P2 curvature (Sampson, 1995, character 16, modified)"

0: 'straight '

1: 'medially or laterally curved in the plane of the frill'

2: 'recurved onto dorsal surface of frill'

Reconfiguration of the frill epiossifications of *Kosmoceratops* and *Vagaceratops* does not result in a change in character state, although what was previously considered as eps by (Sampson et al., 2010; Loewen et al., 2013) is here considered as an ep2.

Character 102

"Epiparietal locus P3 shape (new)"

0: 'low raised D-shaped process'

1: 'elongate spike'

2: 'strongly recurved triangular or recurved low gnarled triangular process'

3: 'well developed triangular process'

4: 'elongate low process sometimes with a small peak'

This character was then revised for clarity and addition of a new state.

Character 102 (Revised)

"Epiparietal locus P3 shape (new)"

0: 'low D-shaped process'

1: 'anteroposteriorly elongate spike'

2: 'strongly recurved triangular or recurved low gnarled triangular process'

3: 'well developed triangular process'

4: 'elongate base, spindle-shaped low process sometimes with a small peak'

5: 'elongate hook'

Reconfiguration of the frill epiossifications of *Kosmoceratops* changes the character state from (1) to the new state (5). Note that the laterally curving hook-shaped epiossification previously considered as es1 is here coded as an ep3 that is possibly partly borne on the squamosal as an eps (see characters 91 and 92). Reconfiguration of the frill epiossifications of *Vagaceratops* changes the character state from (2) to state (3).

Character 103

"Epiparietal, locus P3 orientation (new)"

0: 'caudally, epiparietal oriented in the plane of the frill'

1: 'directed rostrodorsally'

This character was then revised for the addition of a new state.

Character 103 (Revised)

"Epiparietal, locus P3 orientation (new)"

0: 'caudally, epiparietal oriented in the plane of the frill'

1: 'directed rostrodorsally'

2: 'directed laterally'

Reconfiguration of the frill epiossifications of *Kosmoceratops* changes the character state from (1) to the new state (2). Note that the laterally curving hook-shaped epiossification previously considered as es1 is here coded as an ep3 that is possibly partly borne on the squamosal as an eps (see characters 91 and 92). Reconfiguration of the frill epiossifications of *Vagaceratops* changes the character state from (1) to state (0).

Mojoceratops was originally coded as (0), but in the two specimens that preserve ep3 (holotype TMP 1983.25.1, AMNH 5656) it is clearly oriented laterally to caudolaterally, and is hence recoded as (2). Although fragmentary, part of the parietal of *Agujaceratops* is preserved which probably represents ep3 (UTEP P.37.7.065; Lehman, 1989), and may indicate that it is directed laterally. However, due to the fragmentary nature of this specimen, I have chosen to leave *Agujaceratops* coded as (?).

Chasmosaurus russelli is recoded from (0) to (0&2). Although the drawing in Godfrey and Holmes (1995) shows the ep3 as caudolaterally directed on both sides, in the fossil the right ep3 is laterally directed. This does not seem to be a result of significant distortion. *C. belli* is recoded from (0) to (2). Ep3 is laterally or caudolaterally positioned in YPM 2016, ROM 843, and CMN 2245.

New Characters

The posterior border of the parietal is the single most diagnostic element in chasmosaurines. These new characters help define differences in parietal morphology that are not covered by the character matrix of Sampson et al. (2010) or Mallon et al. (2014).

Character 153 (New)

"Parietal, position of the maximum constriction of the median bar"

0: 'within the anterior 2/3 of the parietal fenestra'

1: 'within the posteriormost 1/3 of the parietal fenestra'

The median bar of the parietal narrows (constricts) to give a "waisted" shape. Specimens vary conspicuously as to the anteroposterior position of the maximum point of constriction. Centrosaurines, *Kosmoceratops*, *Vagaceratops*, and species of *Chasmosaurus* have a maximum constriction point in the posteriormost third of the median bar, often very close to where the median bar meets the posterior bar. By contrast, *Pentaceratops*, *Anchiceratops*, *Arrhinoceratops* and *Torosaurus* exhibit a point of maximum constriction that is roughly at the midpoint of the median bar (as defined by the borders of the parietal fenestrae).

Character 154 (New)

"Epiparietal, locus P1 orientation, angle of the long axis of ep1 relative to the long axis of the parietal (ORDERED)"

0: 0°-30°

1: 30°-60°

2: 60°-90°

3: 90°+

A major difference between specimens is the angle of the long axis of ep1. The character is measured by drawing a line through the lateral and medial edges of the epiparietal and measuring the angle it makes with the long axis of the parietal (measured

along the median bar). This character closely matches the angle formed by the medial meeting of the lateral rami of the posterior bar, but is more easily measurable.

Character 155 (New)

"Parietal, thickness of transverse/posterior bar at thickest point (ORDERED)"

0: narrow and strap-like (1-10 % of maximum parietal width in posterior half)

1: medium thickness (11-15 % of maximum parietal width in posterior half)

2: thick (15-20 % of maximum parietal width in posterior half)

3: very thick (>20% of maximum parietal width in posterior half)

"Maximum parietal width in posterior half " is used as a proxy for size and is chosen over parietal length (as in character 76) as parietal length is very difficult to measure in most specimens as the anterior end is very fragile. This character helps differentiate between taxa that have a uniformly anteroposteriorly thin posterior bar, and those that have a thick posterior bar. Specimens where only one half of the posterior bar is fully preserved have the preserved side measured, then doubled. *Anchiceratops* specimen CMN 8535 was not measured for this character as the lateral width of the parietal is not possible to measure as the parietal-squamosal contact is difficult to discern. *Utahceratops* was coded from the reconstruction in Sampson et al. (2010), which was considered as accurate enough for this measurement.

Character 156 (New)

"Parietal fenestrae: shape (ORDERED character)"

0: angular

1: subangular

2: subrounded

3: rounded

Shape definition based on the same visual criteria as sediment grain roundedness.

APPENDIX E

SUPPLEMENTARY INFORMATION 3 FOR CHAPTER 4:

JUSTIFICATION FOR GENERA

Justification for Placing Taxa into Unique Genera

For taxonomic stability and ease of reference, it was decided to place the new specimens into their own genera as otherwise they would have to be placed within either *Pentaceratops* or *Anchiceratops* (as either new species, or individuals of existing species), either of which would create problems.

An argument could be made that morphologic differences among the new specimens and those previously referred to *Pentaceratops sternbergii* are within that which might be expected of a single species, i.e. that they represent biological variation. However, each morphology is stratigraphically separated over a range of ~1-2 m.y. (with the possible exception of cf. *P. sternbergii*, and aff. *Pentaceratops* n. sp.), demonstrating that they should not be considered as belonging to the same population. Gradual enclosure of the parietal embayment between stratigraphically successive populations further supports their naming as separate taxa. The question is therefore whether the new taxa should be new species within *Pentaceratops*, or whether to erect new genera and species.

Placement of the new taxa as new species within *Pentaceratops* would be similar to the current treatment of stratigraphically separated *Triceratops* species (Scannella et al., 2014). This taxonomic approach would thus illustrate the hypothesis that we are observing evolution within an unbranching lineage, effectively chronospecies within an anagenetic lineage (as similarly suggested for *Triceratops*). However, this is problematic from a practical standpoint. *Triceratops* is a terminal taxon, and as such does not suffer from possible paraphyly emerging as a result of phylogenetic analysis; multiple species

of *Triceratops* all exist within a single clade comprised only of the genus *Triceratops*, and not as stem taxa between separate genera (as is the case with the new taxa). To avoid paraphyly issues, it is current practice among dinosaur taxonomists to maintain monospecific genera. Thus, in order to maintain taxonomic stability, it is therefore preferable to place each morphology into its own genus. This is satisfactory so long as it is remembered that this choice of taxonomy does not necessarily imply vicariance events, and that an anagenetic lineage comprising *Utahceratops*, *Pentaceratops*, *Navajoceratops*, *Terminocavus*, "Taxon C", and *Anchiceratops* is an unfalsified hypothesis.

Reference Cited

Scannella, J. B., D. W. Fowler, M. B. Goodwin, and J. R. Horner. 2014. Evolutionary trends in *Triceratops* from the Hell Creek Formation, Montana. Proceedings of the National Academy of Sciences 111:10245-10250.

APPENDIX F

SUPPLEMENTARY INFORMATION FOR CHAPTER 5 AS PUBLISHED IN THE GEOLOGICAL SOCIETY OF AMERICA SPECIAL PAPER 503

APPENDIX. CATALOGUED MOR SPECIMENS OF *TRICERATOPS* FROM THE HELL CREEK FORMATION

Loc. no.	Spec. no.	Locality	Coll. year	Collector	Unit	Material
HC-135	MOR 004	MORT	1981	M. Hager and crew	Upper unit (upper part)	Articulated skull, distal postorbital horn cores reconstructed
HC-1022	MOR 335	H&M Trike Parietal	1985	J. Horner and R. Makela	Lower unit	Parietal
HC-199	MOR 539	Trumbo Ranch	1987	D. Rasmussen	T.B.D.	Partial disarticulated juvenile skull including postorbital horn cores, right exoccipital
HC-069	MOR 598	Wankel T-Rex	1989	J. Horner	Upper unit	Epinasal
HC-069	MOR 599	Wankel T-Rex	1989	J. Horner	Upper unit	Partial maxilla
HC-196	MOR 622	Engdahl Trike	1989	J. Horner	Upper unit	Partial skull and associated postcranial material; scapula and humerus prepared
HC-085	MOR 652	Maloney Hill N	1990	C. Ancell	Upper unit	Juvenile squamosal
HC-069	MOR 669	Wankel T-Rex	1990	B. Harmon	Upper unit	Partial braincase
HC-069	MOR 670	Wankel T-Rex	1990	B. Harmon	Upper unit	Partial braincase
HC-108	MOR 699	Irv's Triceratops	1991	D. Gabriel	?Lower unit	Skull, lacking nasal horn and associated with postcrania including caudal vertebrae, dorsal vertebrae, pubis, ribs - skull currently on display at Makoshika State Park Visitor Center
HC-172	MOR 799	Bite Trike	1995	K. Olson	T.B.D.	Sacrum
HC-177	MOR 965	Mickey's Trike	1996	B. Harmon and C. Ancell	T.B.D.	Partial skull including nasal horn, sections of parietal and squamosal margin, jugal
HC-192	MOR 966		1996	J. Horner	T.B.D.	Nasal horn
HC-188	MOR 981	TORO I	1991	K. Olson	Lower to lowest middle unit	Articulated skull missing left jugal and left half of frill
HC-191	MOR 987	2/4/Day Site	1997	J. Horner	T.B.D. - 50 ft (15 m) below K-Pg	Partial braincase
HC-193	MOR 989	Pompey	1997	McKinley	T.B.D.	Epinasal, partial rostral
HC-209	MOR 1053	Johnston Lease	1991	P. Leiggi	T.B.D.	Baby postorbital horn core
HC-210	MOR 1059	Howell Lease	1991	Leiggi and Hanson	T.B.D.	Basioccipital and occipital condyle
HC-235	MOR 1098	'Fisk'	1999	B. Harmon	Lower unit	Postorbital horn core
HC-249	MOR 1109	Celestial Clam Bed	1999	B. Harmon and 1999 crew	Lower unit	Fragmentary skeleton including epijugal, vertebra, tooth
HC-250	MOR 1110	SG-5	1999	1999 MOR crew	Upper unit	Disarticulated skull (see Horner and Goodwin, 2006)
HC-256	MOR 1120	Getaway Trike	1999	B. Harmon and crew	Lower unit	Disarticulated skull (see Horner and Goodwin, 2006)
HC-258	MOR 1122	TORO II	2000	B. Harmon, K. Olson, crew	Lower unit	Articulated skull
HC-265	MOR 1129	Coyote Basin	2000	J. Horner	Upper unit	Partial disarticulated skull including postorbital horn core, occipital condyle, and predentary
HC-267	MOR 1133	Larry's BO	2000	L. Boychuk	Lower unit	Basal braincase
HC-283	MOR 1157	#73 Site	2001	M. Goodwin	Lower unit	Braincase
HC-285	MOR 1160	Heaven Site	2001	J. Horner and 2001 crew	Lower unit	Elements of forelimb (associated)
HC-287	MOR 1162	Bandana Site	2001	M. Goodwin and J. Horner	Lower unit	Associated skeletal elements
HC-293	MOR 1167	Celeste's Mag. Micro Site	2001	C. Horner and J. Horner	Lower unit	Juvenile epinasal (see Horner and Goodwin, 2008)
HC-300	MOR 1171	Allard#4	2000	K. Olson	T.B.D.	Braincase
HC-301	MOR 1174	Triceratops Sacrum Site	1995	K. Olson	T.B.D.	Large sacrum, ischia, pubis
HC-308	MOR 1186	Mark's Trike	2002	B. Chinnery and crew	Lower unit	Partial skull - associated postcrania
HC-310	MOR 1188	Triceratopolis	2002	J. Horner	Lower unit	Dorsal vertebrae

APPENDIX. CATALOGUED MOR SPECIMENS OF *TRICERATOPS* FROM THE HELL CREEK FORMATION (*Continued*)

Loc. no.	Spec. no.	Locality	Coll. year	Collector	Unit	Material
HC-317	MOR 1199	Sierra Trike	2003	Sierra College	T.B.D. - ?middle unit	Disarticulated skull - missing epinasal (see Horner and Goodwin, 2006)
HC-376	MOR 1604	Baker Trike	2004	K. Olson	T.B.D. - upper middle/ upper	Articulated skull, syncervical
HC-301	MOR 1612	Triceratops Sacrum Site	2005	K. Olson	T.B.D.	Humerus
HC-385	MOR 1625	Haxby Trike	2004	K. Olson and crew	Upper unit	Partial articulated skull including premax/nasal horn/ rostrum/partial postorbital horn/squamosal/parietal (see Horner and Goodwin, 2008)
HC-389	MOR 1629	Marge's Trike Tibia	1998	M. Baisch and K. Olson	T.B.D.	Tibia
HC-392	MOR 2551	CSTrike2	2005	N. Peterson and crew	T.B.D. - ?upper/middle unit	Partial skull including nasal horn, nasals, postorbital horn, parietal and associated post crania
HC-393	MOR 2552	BOSH	2004	B. Schaff and crew	Lower unit	Partial skull including postorbital horn, partial parietal, squamosal, frill epiossifications
HC-425	MOR 2569	Afternoon Delight	2006	L. Hall and crew	Middle unit (lower part)	Disarticulated skull including parietal, squamosals, postorbital horn core, jugal, maxilla, quadrates (see Goodwin and Horner, 2010)
HC-426	MOR 2570	Mark's Scavenged Trike	2006	M. Goodwin	Middle unit	Nasal horn, epijugal, pieces of maxilla and frill
HC-428	MOR 2572	Mark's Trike Generation	2006	M. Goodwin	T.B.D.	Juvenile squamosal
HC-430	MOR 2574	Quittin' Time	2006	B. Harmon, N. Peterson and crew	Upper unit (lower part)	Bonebed (see Keenan and Scannella, this volume)
HC-431	MOR 2575	Wagon Coulee North	2004	A. Ballarina	?Lower unit	Nasal horn
HC-432	MOR 2576	Snap Creek	2006	J. Horner	Upper unit (upper part)	Nasal horn
HC-435	MOR 2579	"Twitchell North"	2006	B. Harmon	T.B.D.	Juvenile postorbital horn core
HC-275	MOR 2582	Weird Microsite	2006	J. Horner	Lower unit	Frill epiossifications (see Horner and Goodwin, 2008)
HC-109	MOR 2583	Robert's Microsite	1991	R. Ivens	T.B.D.	Frill epiossification
HC-135	MOR 2584	MORT		J. Horner	Upper unit	Epijugal (see Horner and Goodwin, 2008)
HC-135	MOR 2585	MORT	1982	J. Horner	Upper unit	Epijugal
HC-135	MOR 2586	MORT		J. Horner	Upper unit	Epiossification (see Horner and Goodwin, 2008)
HC-438	MOR 2587	6-12-00-CCH Trike	2000	C. Horner	?Middle unit	Right nasal
HC-439	MOR 2588	7-4-00-CCH Microsite	2000	C. Horner	Lower unit	Frill epiossifications
HC-290	MOR 2589	DK Site	2001	2001 MOR crew	Lower unit	Juvenile postorbital horn core
HC-440	MOR 2590	JRH7-2-05-2	2005	J. Horner	Upper unit	Partial disarticulated premaxilla
HC-441	MOR 2593	Thedford Site	2005	N. Peterson and crew	T.B.D.	Quadrate
HC-442	MOR 2594	Bf9	2004	B. Hendricks	T.B.D.	Frill epiossifications
HC-444	MOR 2597	Mark's Trike II	2006	M. Goodwin	Upper unit	Dentaries, postorbital horn core, frill fragment (see Goodwin and Horner, 2010)
HC-430	MOR 2702	BAB	2006	L. Hall and crew	Upper unit (lower part)	Partial skull including nasal horn, postorbital horns, squamosal, section of parietal, maxilla, dentary, partial premaxilla. From Quittin' Time Bonebed (see Keenan and Scannella, this volume)
HC-448	MOR 2704	"Sand Creek, Dawson"	1993	D. Gabriel	T.B.D.	Large partial jugal with epijugal
HC-280	MOR 2728	"F-Rex"	2001	L. Wilson	Lower unit	Partial right nasal

APPENDIX. CATALOGUED MOR SPECIMENS OF *TRICERATOPS* FROM THE HELL CREEK FORMATION (*Continued*)

Loc. no.	Spec. no.	Locality	Coll. year	Collector	Unit	Material
HC-520	MOR 2923	Joe's Half Day Trike	2007	B. Harmon and crew	Upper unit (upper part)	Articulated skull missing squamosals and lower jaw
HC-521	MOR 2924	Lon's Trike	2007	J. Scannella and D. Fowler	Upper unit (lower part)	Disarticulated skull including nasal horn, squamosal, nasal, premaxilla, partial parietal and associated postcrania including humerus and ulna
HC-525	MOR 2927	Trike Basin	2007	J. Horner	Upper unit	Postorbital horn core and squamosal
HC-525	MOR 2928	Trike Basin	2007	J. Horner	Upper unit	Squamosal and dentary
HC-525	MOR 2929	Trike Basin	2007	J. Horner	Upper unit	Juvenile squamosal
HC-528	MOR 2936	Lazy Bones	2006	G. Sorrentino	Upper unit	Partial disarticulated skull including squamosals, nasal horn, maxilla, braincase
HC-529	MOR 2937	Prospero	2007	S. Keenan	Upper unit (upper part)	Partial dentary, frill fragment, and other material
HC-531	MOR 2938	Lauren's Trike	2007	L. Hall, S. Keenan, and crew	Upper unit (upper part)	Partial skull including nasal horn, maxilla, dentary, partial parietal
HC-535	MOR 2941	Nosy Nasal	2007	L. Hall	Upper unit	Nasal horn, ungual
HC-530	MOR 2942	Doldrums	2007	2007 MOR crew	Upper unit	Squamosal
HC-539	MOR 2945	Too Close	2006	B. Harmon	T.B.D.	Dentary
HC-064	MOR 2946	–	–	Unknown Makoshika State Park	Unknown	Partial parietal and squamosal
HC-541	MOR 2950	JDTrike14	2007	J. Scannella and L. Hall	Upper unit (upper part)	Partial skull including braincase, partial squamosal and parietal
HC-544	MOR 2951	DFJuvieTrike 3	2008	D. Fowler, B. Schaff	Upper unit (lower part)	Nearly complete disarticulated skull and associated postcrania including humerus, femur, ilium, vertebrae, ribs
HC-545	MOR 2952	Homer's Nose	2008	H. Hickam	Upper unit	Partial skull including epinasal, postorbital horn core, frill frag
HC-500	MOR 2958	DF Juvie-Horncore	2008	D. Fowler	Upper unit (lower part)	Juvenile postorbital horn core
HC-551	MOR 2959	Great Googoly Moogoly	2006	J. Scannella, B. Harmon, and crew	?Lower unit	Frill fragments including frill epiossifications, occipital condyle, syncervical
HC-1027	MOR 2965	TrkNas	2007	D. Fowler	Upper unit	Epinasal
HC-563	MOR 2969	Jack's 2008 Parietal	2008	J. Horner	T.B.D.	Juvenile parietal
HC-564	MOR 2971	Crazy Trike	2008	B. Schaff	Upper unit (lower part)	Partial skull including premaxilla, nasal horn, rostral, maxilla, frill
HC-565	MOR 2972	Supernasal	2008	D. Fowler and B. Schaff	Upper unit (lower part)	Partial skull including nasal horn, partial squamosal, braincase
HC-566	MOR 2974	Legs	2005	N. Peterson and crew	Upper unit	Partial limb bones (tibia)
HC-567	MOR 2975	More Frill	2009	B. Schaff and crew	Upper unit	Partial skull including postorbital horn core and squamosals
HC-570	MOR 2978	Greene Trike	2008	–	T.B.D.	Articulated skull with syncervical - missing maxillae, premaxillae, and lower jaw
HC-571	MOR 2979	Seth's Trike	2008	D. Fowler and S. Bainbridge	Upper unit	Partial skull including postorbital horns, maxilla, partial premaxilla - missing much of frill and lower jaws
HC-543	MOR 2980	TriSarahTops	2008	J. Scannella and crew	Upper unit	Squamosal
HC-573	MOR 2982	Three Amigos	2008	L. Hall and crew	Middle unit (lower part)	Partial skull including postorbital horn, nasal and nasal horn, dentary, parietal midline, partial squamosal – and associated postcrania including vertebrae and femur
HC-575	MOR 2984	2 Big	2001	L. Boychuk	Lower unit	Squamosal
HC-576	MOR 2985	6 O'Clock Trike	2008	A. Carpana and crew	Lower unit	Squamosal, partial parietal, associated postcrania
HC-579	MOR 2988	Spike the Trike	2008	B. Schaff	Upper unit	Postorbital horn core
HC-622	MOR 2991	Toothburg	2009	P. Ullman	T.B.D.	Includes partial frill, occipital condyle
HC-623	MOR 2992	Halfway Hill	2009	J. Scannella and crew	T.B.D.	Partial squamosal

APPENDIX. CATALOGUED MOR SPECIMENS OF *TRICERATOPS* FROM THE HELL CREEK FORMATION (*Continued*)

Loc. no.	Spec. no.	Locality	Coll. year	Collector	Unit	Material
HC-627	MOR 2999	Situ but Sad	2009	E. Freedman and P. Ullmann	Upper unit (upper part)	Partial skull including parietal, squamosal, braincase and postorbital horns, nasal, maxilla, dentary
HC-628	MOR 3000	Ashes Trike	2009	J. Scannella and crew	Upper unit	Postorbital horn core, parietal, partial squamosal, dentary, scapula
HC-633	MOR 3004	The Horn Resounding	2009	B. Schaff and E. Freedman	Middle unit (lower part)	Skull and associated postcrania
HC-634	MOR 3005	Antsy Trike	2009	P. Ullmann and crew	Middle unit (lower part)	Partial disarticulated skull including parietal and nasal
HC-635	MOR 3006	Warwick's Horn	2009	W. Fowler	Middle unit (lower part)	Postorbital horn core
HC-636	MOR 3008	American Beauty	2009	P. Ullmann	Upper unit (lower part)	Nasal horn
HC-638	MOR 3010	The Golden Goose	2009	J. Scannella and crew	Middle unit (lower part)	Postorbital horn core, nasal horn, dentary
HC-639	MOR 3011	Anky Breaky Heart	2009	H. Woodward and D. Fowler	Middle unit (lower part)	Partial skull including epinasal and parietal
HC-642	MOR 3015	Trash Trike	2009	E. Freedman and crew	Upper unit	Squamosal, partial braincase
HC-643	MOR 3016	Devil's Horns	2009	P. Murphy	Upper unit	Postorbital horn cores and skull frags
HC-668	MOR 3027	Yoshi's Trike	2010	J. Scannella, D. Fowler, E. Freedman	Middle unit (upper part)	Disarticulated skull including nasal horn, squamosal, nasal, premaxilla, partial parietal and associated postcrania
HC-671	MOR 3029	Jared's Trike	2010	D. Fowler and crew	Upper unit (upper part)	Parietal
HC-672	MOR 3030	JDTrike15	2007	J. Scannella and Fowler	Upper unit	Partial postorbital and frill (juvenile)
HC-692	MOR 3041	Joey's Trike	2010	L. Hall and Crew	Upper unit	Partial skull including squamosals and braincase
HC-693	MOR 3042	Ed's Trike	2008	D. Fowler and crew	Upper unit (upper part)	Dentary
HC-694	MOR 3043	GPS Maniac	2009	P. Ullmann	Upper unit	Squamosal
HC-682	MOR 3045	Cliffhanger	2010	M. Pillet, D. Fowler	Middle unit (upper part)	Parietal, squamosal, and other material
HC-696	MOR 3046	Trikey Town 2	2010	J. Scannella and crew	Upper unit	Parietal and dentary
HC-697	MOR 3047	Got the Horn	2010	D. Fowler	Upper unit (lower part)	Postorbital horn core
HC-698	MOR 3048	Wednesday's Trike	2009	J. Scannella and L. Hall	Upper unit	Nasal horn, occipital condyle, other cranial material
HC-699	MOR 3049	Present	2009	P. Ullmann	Upper unit	Nasal horn
HC-700	MOR 3053	PVU Trike	2009	P. Ullmann	Upper unit	Associated material including postorbital horn core
HC-1026	MOR 3055	Brown Nose	2008	L. Hall	Middle unit (lower part)	Nasal horn
HC-702	MOR 3056	JDTrike12	2007	D. Fowler and J. Scannella	Upper unit (upper part)	Juvenile squamosal and postorbital horn core
HC-114	MOR 3057	Brownie Butte Trike	2008	D. Fowler	Upper unit (lower part)	Postorbital horn core
HC-704	MOR 3058	JDExTrike2	2008	J. Scannella and D. Fowler	Middle unit	Partial horn and jugal
HC-1023	MOR 3059	Heck's Horn	2009	C. Heck	Upper unit	Nasal horn
HC-716	MOR 3064	Little Horny Devil	2010	D. Fowler	Middle unit (upper part)	Brow horn, partial squamosal, quadrate, epiossifications, jugals, other cranial
HC-532	MOR 6648	Ducky Tail	2009	A. Carpana and crew	Upper unit (upper part)	Juvenile *Triceratops* parietal and squamosal found among *Edmontosaurus* material
HC-898	MOR 7037	Lost and Found	2008	B. Harmon	Middle unit	Squamosal

Note: All specimens are either *Triceratops* or cf. *Triceratops*. This table does not include specimens that are currently unprepared or housed in off-site storage (as of 2011).
T.B.D.—Precise position relative to unit boundaries to be determined. Specimens have detailed locality data on file at MOR. Loc. no.—locality number; Spec. no.—specimen number; Coll. year—collection year; K-Pg—Cretaceous-Paleogene boundary.

APPENDIX G

SUPPLEMENTARY INFORMATION FOR CHAPTER 6 AS PUBLISHED IN THE PROCEEDINGS OF THE NATIONAL ACADEMY OF SCIENCES

SI Text. Supporting Information for: Evolutionary Trends in *Triceratops* from the Hell Creek Formation, Montana

1) Variation in parietal-squamosal frill
2) Morphology of the rostrum
3) Other triceratopsin taxa
4) *Triceratops* biogeography
5) Stratigraphic placement of upper M3 specimens
6) Calculation of basal skull length
7) Details of cladistic analysis
8) Details of stratocladistic analysis
9) Character list and data matrix
10) References

Institutional Abbreviations

AMNH, American Museum of Natural History, New York, USA; BYU, Brigham Young University Museum of Paleontology, Provo, USA; MOR, Museum of the Rockies, Bozeman, USA; MPM, Milwaukee Public Museum, Milwaukee, USA; MWC, Museum of Western Colorado, Grand Junction, USA; OMNH, Oklahoma Museum of Natural History, Norman, USA; ROM, Royal Ontario Museum, Toronto, CA; RTMP, Royal Tyrrell Museum, Drumheller, Alberta, CA; SMP, State Museum of Pennsylvania, Harrisburg, USA; UCMP, University of California Museum of Paleontology, Berkeley, USA; USNM, National Museum of Natural History, Washington D.C., USA; YPM, Yale Peabody Museum, New Haven, USA.

Variation in Parietal-Squamosal Frill.

Scannella and Horner (2011) suggested that the number of epiossifications present in *Triceratops* may vary stratigraphically. Often, epiossifications are unpreserved or are

detached from the parietal-squamosal frill; which complicates testing of this hypothesis. Data currently available highlights variation in epiossification number and position; as the number and configuration can vary between the squamosals of a single individual [e.g. Museum of the Rockies (MOR) 1120]. Additionally, there may be an ontogenetic component to epiossification number and position in chasmosaurines (see, for example, Scannella and Horner, 2010; 2011; Mallon et al., 2011). Hell Creek Formation (HCF) specimens with the highest numbers of epiparietals (MOR 1122; MOR 3081) and episquamosals (MOR 1120; MOR 1122; MOR 3081) are found lower in the formation.

The development of fenestrae also varies within *Triceratops* (Scannella and Horner, 2010; 2011; but see Farke, 2011; Longrich and Field, 2012; Maiorino et al., 2013). A pronounced transition in thickness on the ventral surface of the parietal surrounding this area (Scannella and Horner, 2010) is noted in *Triceratops* from the upper unit of the HCF (U3) and at least one specimen from the upper part of the middle unit (M3)(MOR 3045), but lower in the formation there appears to be a more gradual transition in the thickness of the parietal (e.g. MOR 335; MOR 1120; MOR 2985). This finding may suggest that the fenestrae developed later, ontogenetically, in *Triceratops* found stratigraphically higher. Alternatively, if *Triceratops* and *Torosaurus* represent distinct but closely related taxa, *Triceratops* found stratigraphically lower may express more basal parietal features including eventual fenestration of the parietal.

The stratigraphically documented cranial morphological trends expressed in *Triceratops* are thus far consistent with the morphology of specimens referred to *Torosaurus latus* (however we note that the majority of specimens exhibiting the

Torosaurus morphology were recovered from the lower half of the formation). Precise locality data for MOR 981 is not available but it was collected in a mudstone located above the basal sandstone. Perhaps the stratigraphically highest known *Torosaurus* from the HCF of Montana, Milwaukee Public Museum (MPM) specimen VP6841 (which, based on study of topographic and geologic maps, appears to have been collected from the upper half of the formation), exhibits an incomplete yet relatively narrow epinasal morphology which is consistent with its stratigraphic position. The observation that a nasal boss morphology appears to occur in relatively mature specimens of *Triceratops* (*Torosaurus* morph; e.g. MOR 1122; MOR 981; Farke, 2007) suggests that development of the boss morphology was ontogenetic, as is seen in some centrosaurine ceratopsids (e.g. Sampson, 1995; Currie et al., 2008). The nasal boss morphology is not exhibited in all *Torosaurus* specimens [MOR 3081, MPM VP 6841,YPM 1830, Yale Peabody Museum (YPM) 1831], and thus the degree to which this feature is developed may vary individually or stratigraphically. UCMP 128561 exhibits a low nasal boss (Cobabe and Fastovsky, 1987; Forster, 1993), however due to the fragmentary nature of the specimen it is unclear if it represents the *Torosaurus* morphology.

Morphology of the Rostrum.

Forster (1996) recognized rostrum morphology as one of the features which distinguishes *T. horridus* from *T. prorsus*. *T. horridus* exhibits a low, elongate rostrum with a sinusoidal dorsal margin whereas in *T. prorsus* the rostrum is shorter and more convex. Longrich and Field (2010) noted that specimens of *T. prorsus* have a more vertically oriented nasal process (= ascending nasal process of the premaxilla sensu

Horner and Goodwin (2008), here referred to as the nasal process of the premaxilla [NPP]) when compared to *T. horridus*. Rostrum morphology appears to be tied to the orientation of the NPP, with a more posteriorly inclined NPP contributing to a low, sinusoidal rostrum in some specimens [e.g. MOR 1120; American Museum of Natural History (AMNH) 5116; National Museum of Natural History (USNM) 1201; YPM 1820].

The angle between the NPP and narial strut appears to increase stratigraphically in the HCF; specimens from the upper M3 and U3 exhibit a larger angle between the NPP and narial strut than specimens found lower in section (Fig. 6.2C). To quantify this shift in morphology, the angle between the NPP and narial strut (Fig. 6.S2) was measured using the Ruler tool in Adobe Photoshop. This angle was measured between the approximate midlines of each process, parallel to the direction representing the primary trend (results presented in Dataset S1; Fig. 6.2). We note that in some more basal taxa (e.g. *Anchiceratops* [Mallon et al., 2011]) the NPP can be oriented nearly perpendicular to the narial strut and as such give the rostrum a more convex appearance in lateral view.

The width of the NPP also affects the rostrum morphology, as a wider NPP reduces the apparent sinuosity of the anterior premaxilla. MOR 3027 and MOR 3045 (both recovered from upper M3) exhibit a more vertically inclined premaxillary articulation with the nasal than specimens found lower in the formation. MOR 3045 (collected ~ 2 m above MOR 3027) exhibits the further derived feature of an anteroposteriorly expanded NPP, contributing to a rostrum which appears even more convex in lateral view.

Rostrum length appears to vary both stratigraphically and ontogenetically. The largest specimens from U3 (e.g. MOR 004, MOR 1625) exhibit more elongate rostra (Fig. 6.2E, Dataset S1); however even these large specimens do not exhibit the strongly posteriorly inclined NPP and sinusoidal dorsal margin of the rostrum exhibited in specimens referred to *T. horridus*. Evolutionary changes in rostrum morphology may reflect the development of an enlarged epinasal.

Other Triceratopsin Taxa.

Longrich (2011) referred Oklahoma Museum of Natural History (OMNH) specimen 10165, a large ceratopsid specimen recovered from Campanian deposits of New Mexico and previously diagnosed as a gigantic specimen of *Pentaceratops sternbergi* (1998), to the new taxon *Titanoceratops ouranos*. Longrich (2011) proposed that *Titanoceratops* represents the oldest member of the Triceratopsini, the clade which includes *Triceratops*, *Torosaurus*, *Nedoceratops*, and *Ojoceratops*. This specimen exhibits several features consistent with its stratigraphic position relative to HCF *Triceratops*. It has a relatively short epinasal, short arched nasals, a posteriorly inclined NPP, and elongate postorbital horn cores. Given the degree of ontogenetic transformation noted in several marginocephalians (e.g. Scannella and Horner, 2010; 2011; Horner and Goodwin, 2006; 2009), it is possible that many of the features considered to distinguish *Titanoceratops* from *Pentaceratops* (including large size, broad epiossifications, extensive cornual sinuses, strongly anteriorly curved postorbital horn cores, elongate premaxilla [Longrich, 2011]) may instead represent ontogenetic or individual variation within the latter taxon (Fowler et al., 2011; which would be consistent with the original

diagnosis by Lehman [1998]). Further assessment of this specimen and its phylogenetic position is beyond the scope of the current study.

Triceratopsin material from the southern region of the western interior of North America includes specimens which have been referred to *Ojoceratops fowleri* and *Torosaurus utahensis* (Gilmore, 1946; Lawson, 1976; Hunt and Lehman, 2008; Longrich, 2011; Sullivan and Lucas, 2010; Sullivan et al., 2005). *Ojoceratops*, from the Ojo Alamo Formation of New Mexico, appears to be closely related to *Triceratops* (Sullivan and Lucas, 2010; Sampson et al., 2010; Mallon, 2011) and has been suggested to be synonymous with the latter taxon (Longrich, 2011). Material referred to *Ojoceratops* thus far consists of isolated or fragmentary elements. Due to the missing morphological information for much of this material, specimens of *O. fowleri* were not included in the current cladistic analysis of HCF *Triceratops*. A nasal horn referred to this taxon [State Museum of Pennsylvania (SMP) VP-1828] exhibits a morphology similar to that observed in several lower unit (L3)/lower M3 *Triceratops*, which is consistent with its stratigraphic position relative to the Hell Creek Formation of Montana. The holotype squamosal (SMP VP-1865) has a greatly reduced anterolateral projection of the squamosal, which has been used to distinguish it from *Torosaurus utahensis*. The degree to which this feature can distinguish *Ojoceratops* from other taxa is unclear; the HCF dataset demonstrates that the morphology of this projection varies within *Torosaurus* and *Triceratops*, and even within a single individual (MOR 2999). Variation in this feature has previously been noted by Hunt and Lehman (2008).

The incomplete or fragmentary nature of specimens which have been referred to *Torosaurus utahensis* has engendered debate regarding what material is referable to this taxon, its stratigraphic and biogeographic range, and which morphologic features, if any, distinguish it from other chasmosaurine taxa (see, for example, Sullivan et al., 2005; Hunt and Lehman, 2008). This material was not included in the current study of HCF specimens.

Tatankaceratops sacrisonorum is represented by a fragmentary partial skull from the upper (~ 20 m below the K/Pg boundary) HCF in South Dakota (Ott and Larson, 2010). The specimen exhibits an enlarged nasal horn and very small postorbital horn cores. As noted by Longrich (2011), this specimen may represent *T. prorsus*, which would be consistent with its stratigraphic position.

Triceratops Biogeography.

Triceratops in the Frenchman Formation (Saskatchewan, Canada) and Laramie Formation (Colorado, USA) appear to exhibit morphologies consistent with those expressed by specimens in the Hell Creek Formation (HCF), Montana. The base of the Frenchman Formation occupies the uppermost C30n magnetozone, with the majority of the unit residing in C29r up to the K-Pg boundary (Lerbekmo, 1999; Lerbekmo and Braman, 2002), whichindicates the Frenchman Formation correlates largely to U3 of the HCF (Lerbekmo, 2009). Thus, we predict that most *Triceratops* skulls from the Frenchman Formation will exhibit *T. prorsus* morphologies. Diagnostic specimens published to date have been referred to *T. prorsus* (Tokaryk, 1986). Conversely, the uppermost Laramie Formation exhibits reversed magnetic polarity, aligning it with

magnetochron C30R (Castle Pines core; Hicks et al., 2003; Raynolds and Johnson, 2003) and making it slightly older than the HCF (Lerbekmos, 2009). Thus, specimens from the Laramie Formation should exhibit cranial morphologies similar to L3 *Triceratops*, and to date this hypothesis remains unfalsified (Carpenter and Young, 2002). The Denver Formation is partly coeval with the HCF of Montana (Hicks et al., 2002) and is predicted to yield a similar stratigraphically segregated *Triceratops* record. Thus far, specimens collected outside of Montana present morphologies which are consistent with their stratigraphic positions relative to the HCF sample. Increased stratigraphic resolution and sampling from the Lance Formation of Wyoming and other coeval formations will permit further testing of biogeographic hypotheses. The historical record remains unresolved and of limited utility.

Stratigraphic Correlations of
Specimens from Upper M3.

MOR 3027, MOR 3045, and UCMP 113697 were all recovered from high in the middle unit of the HCF. The localities which produced MOR 3027 and MOR 3045 (Fig. 6.S2) are within a mile of one another, which facilitates their relative stratigraphic placement. MOR 3027 was collected ~ 5.5 meters below the Apex Sandstone (the base of U3). MOR 3045 was collected from ~ 7.5 meters below this marker bed, thus initially it appeared that MOR 3045 was found stratigraphically lower than MOR 3027. However, the Apex Sandstone is thicker and cuts down further into the underlying strata just above the quarry which produced MOR 3027. There is a prominent organic-rich horizon which can be laterally traced above both quarries. MOR 3027 was found 5.3 m below this

organic-rich bed whereas MOR 3045 was ~ 3.3 meters below. Thus, the quarry which produced MOR 3045 is higher stratigraphically relative to MOR 3027. UCMP 113697 was discovered 21.5 km to the east of these localities. Locally, the Apex Sandstone is ~ 6 meters above the base of the quarry which produced this specimen. An organic-rich horizon which may correlate with the organic-rich bed found above the two MOR localities is ~ 3 meters above the quarry and thus UCMP 113697 appears to have been collected from roughly the same stratigraphic level as MOR 3045.

Estimation of Basal Skull Length.

In this study, basal skull length was considered the distance from the anteriormost point of the rostrum to the posterior surface of the occipital condyle (following previous researchers) (Forster, 1996; Farke, 2007). Skull length measurements for some specimens were taken from reconstructions (Dataset 6.S1). For some largely complete specimens which do not preserve the occipital condyle, or in which it is obscured (e.g. MOR 004), this distance was approximated by measuring the distance from the anteriormost point of the rostrum to the posterior margin of the lateral temporal fenestra (see Dataset 6.S1). For less complete, or disarticulated specimens, basal skull length was estimated using linear regressions of basal skull length against preserved cranial elements. Linear models relating basal skull length to dentary length (measured from the anteriormost point to the posterior surface of the coronoid process), maxilla length (measured along the lateral surface), occipital condyle area (following Anderson, 1999), and jugal length (measured from the base of the orbit to the distal tip) produced R^2 values of 0.995, 0.979, 0.944, and 0.980 respectively (Dataset 6.S1). The use of multiple elements allowed more specimens

to be included in quantitative comparisons. If multiple elements were preserved in a specimen (for example, MOR 2982 has a dentary and jugal), the estimated values for basal skull length produced by the regression analyses were averaged.

Cladistic Analysis.

A cladistic analysis of cranial variation in HCF *Triceratops* initially employed the heuristic search strategy of the program PAUP* 4.0b10 (Swofford, 2003). Nexus files are available on MorphoBank (O'Leary and Kaufman, 2008) as project 1099. Analyses used the random addition sequence with tree-bisection-reconnection (TBR) branch swapping and 1,000 replicates; all most parsimonious trees were saved. Characters were unordered and unweighted. Maxtrees was set to 250,000. Analyses were initially performed using binary coding for morphological characters (see Pleijel, 1995; Frederickson and Tumarkin-Deratzian, 2014). Additional analyses were performed using multistate coding which combined binary characters 10 and 11 (development of the epninasal-nasal protuberance), 25 and 26 (development of the anterolateral projection of the squamosal), and 29 and 30 (number of epiparietals). Support for clades was determined using nonparametric bootstrap resampling (Felsenstein, 1985) in PAUP* 4.0b; 10,000 bootstrap replicates were analyzed with one tree retained per replicate. Application of bootstrap resampling to data in which multistate characters have been distilled to binary characters is problematic (Felsenstein, 1985) but was performed for comparative purposes. In addition, Bremer support indices were calculated using TreeRot.v3 (Sorenson and Franzosa, 2007) and PAUP* 4.0b10 (Swofford, 2003).

This analysis focused on features found to vary within the HCF *Triceratops* dataset. *Eotriceratops* was included in the analysis to test the hypothesis that it represents a taxon distinct from *Triceratops*. As such, characters found to distinguish *Eotriceratops* by Sampson et al. (2010) and characters describing the relative height of the narial process and the morphology of the epijugal (Wu et al., 2007) were examined. Forster (1996) noted five cranial characters which vary within *Triceratops*. Four of these characters were included in this analysis (Forster's character 4, which describes rostrum shape, was modified in this analysis to reflect the influence of NPP orientation [see Longrich and Field, 2012]). Forster's character 1 (describing the postorbital, jugal, squamosal suture pattern) was not found to vary in the HCF data set. All coded specimens either exhibited the 'primitive' state of the jugal contributing to the dorsal margin of the lateral temporal fenestra, or sutural relationships of this region were unpreserved or were obscured by fusion.

Initially, specimens which were collected or stratigraphically relocated during the Hell Creek Project and which were largely complete or exhibited morphologies not otherwise found within their respective stratigraphic units (e.g. MOR 2552, UCMP 128561) were included in the cladistic analysis. Only post-juvenile stage specimens were included in the analyses (see Campione et al., 2013). MOR 981 exhibits the *Torosaurus* morphology, and was collected from a mudstone above the basal sand of the formation however detailed stratigraphic data is unavailable for this specimen.

The initial strict consensus tree produced using binary coding [most parsimonious trees (MPT) 250,000, 55 steps, Consistency Index (CI) 0.7091, Homoplasy Index (HI)

0.4000, Retention Index (RI) .8400] produced a polytomy of all HCF specimens (Fig. 6.S5 A). The holotype of *Eotriceratops* [Royal Tyrrell Museum (RTMP) 2002.57.7] was recovered as being basal to the HCF dataset, consistent with the initial hypothesis proposed by Wu et al. (2007). The 50% majority tree revealed a succession of specimens which was consistent with stratigraphic position aside from some specimens which were missing a large portion of codeable characters (e.g., MOR 2552 and MOR 3010). Specimens exhibiting the *Torosaurus* morphology clustered together as basal to the rest of the HCF dataset as these specimens exhibit several features (including a fenestrated parietal) that are observed in more basal taxa. MOR 3011, which preserves relatively thick sections of parietal-squamosal frill but is too fragmentary to be coded for features of these elements, was not distinguished from the *Torosaurus* group.

Re-running the analysis using multistate rather than binary characters produced a polytomy in the strict consensus tree (MPT 250,000, 54 steps, CI 0.7222, HI 0.3889, RI 0.8469), and the 50% majority-rule tree similarly produced a sequence of specimens consistent with stratigraphic position aside from the most fragmentary specimens (Fig. 6.S5B).

The analysis was next rerun after removing the most incomplete specimens (individuals which did not exhibit at least seven codeable features).This analysis resulted in a strict consensus (MPT 250,000, 55 steps, CI 0.7091, HI 0.4000, RI 0.8161) in which specimens were largely recovered in stratigraphic succession (except for MOR 3011 which, as noted above, grouped with *Torosaurus* specimens). MOR 1120 from L3 was found to be the most basal non-*Torosaurus* HCF specimen and MOR 2982 from the

lower M3 was recovered as the next most basal. Above MOR 2982 is a large polytomy consisting of specimens from the upper half of the formation. The identical topology was recovered when the multistate matrix was analyzed (MPT 250,000, 54 steps, CI 0.7222, HI 0.3889, RI 0.8214; Fig. 6.3), however a bremer decay value of 2 was recovered for the upper M3-U3 polytomy when the binary matrix was used (as opposed to a value of 1 when the multistate matrix was employed).

The analysis was next run after removing specimens which could not be coded for features of the parietal-squamosal frill. A branch and bound search was used with the furthest addition sequence implemented. The strict consensus tree produced using the binary matrix (MPT 218972, 55 steps, CI 0.7091, HI 0.4000, RI 0.8000; Fig. 6.S5 C) recovered a polytomy of *Torosaurus* specimens as basal to other specimens. MOR 1120 and MOR 2982 from the lower half of the formation were recovered together as basal to a large polytomy of specimens from the upper half of the formation. The multistate analysis (MPT 189820, 54 steps, CI 0.7222, HI 0.3889, RI 0.8077; Fig. 6.S5 D) resulted in greater resolution; MOR 1120 was recovered as basal to the stratigraphically higher MOR 2982. MOR 1122 and MOR 981 clustered together. These specimens both exhibit a nasal boss and do not exhibit an episossification or crenulation spanning the parietal-squamosal margin whereas the third *Torosaurus* specimen (MOR 3081) possesses a narrow epinasal and a parietal-squamosal crenulation. As these features appear to exhibit a large degree of variation within *Triceratops* (Scannella and Horner, 2010), intraspecific variation appears more likely than these differences being taxonomic in nature. We note that in this analysis a midline epiparietal (character 32) was coded as absent in MOR

1122 as the element is not present and there does not appear to be a pronounced crenulation on the midline. Scannella and Horner (2011) suggested the presence of a midline epiparietal in this specimen based on vascular patterns observed on the parietal. The 50% majority tree for both analyses (Fig. 6.S5 E,F) found MOR 3045 to be more derived than MOR 3027. UCMP 113697 clusters with MOR 2924 (U3) in the binary analysis, and with MOR 2924 and MOR 2999 in the multistate analysis. This topology suggests that UCMP 113697 is more derived than other specimens from upper M3 however, we note that this result may be influenced by missing data. MOR 2924 (recovered from the sandstone at the base of U3) preserves a broader posterior surface of the epinasal than other specimens from U3, but does not preserve postorbital horn cores. The anteromedial processes of nasals of MOR 2924 are unobservable due to articulation with the premaxillae. The morphology of the anteromedial processes on the nasals of UCMP 113697 are currently obscured due to the mounting of the disarticulated skull elements for display.

When specimens which did not preserve at least 10 codeable features (in the multistate matrix) were removed from the analysis, the strict consensus trees (binary coding: MPT 7036; 54 steps; CI 0.7222; HI 0.3889; RI 0.8000; Fig. 6.S5 G; multistate coding: MPT 7036, 53 steps, CI 0.7358, HI 0.3774, RI 0.8082; Fig. 6.3B) exhibited an identical topology. *Torosaurus* specimens were recovered as basal to MOR 1120 and MOR 1982, and specimens from the upper half of the formation were again recovered in a large polytomy. When MOR 2924 was removed from the analysis, both analyses (binary coding: MPT 282; 53 steps; CI 0.7358; HI 0.3774; RI 0.8028; Fig. 6.S5 H;

multistate coding: MPT 282; 52 steps; CI 0.7500; HI 0.3654; RI 0.8116; Fig. 6.3C) recovered MOR 3045 as basal to U3 specimens and as more derived than UCMP 113697 and MOR 3027, which cluster together.

Stratocladistic Analysis.

Stratocladistics incorporates stratigraphic data into cladistic analyses (see, for example, Fisher, 1994; 2008; Polly, 1997; Pardo et al., 2008; Campione and Reisz, 2010; Rook and Hunter, 2011). A stratocladistic analysis was performed using the program StrataPhy, which produces trees that can indicate possible ancestor-descendant relationships (Marcot and Fox, 2008). The multistate dataset was used for the analysis, with the specimens MOR 981, MOR 1604, and MOR 2978 removed from the analysis due to ambiguity over their precise stratigraphic position. Rather than coding specimens separately, specimens from the lower M3, upper M3, lower U3, and upper U3 were combined into operational units based on stratigraphic position. MOR 3081 and MOR 3005 were considered separately from other specimens from the same stratigraphic zones due to the distinct ontogenetic (Scannella and Horner, 2010; or, alternatively, taxonomic [Farke, 2011; Longrich and Field, 2012; Maiorino et al., 2013]) morphological differences between these specimens. MOR 3005 is a fragmentary specimen, but preserves thin sections of frill and thus may represent the *Torosaurus* morphology. A single stratigraphic character was added [stratighraphic position: (position 0) stratigraphically below the HCF; (position 1) lower L3; (position 2) upper L3; (position 3) lower M3; (position 4) upper M3; (position 5) lower U3; (position 6) upper U3]. *Arrhinoceratops* (ROM 796) was designated the outgroup. MAXTREES was set to

250,000, and all other parameters were StrataPhy's default settings (Marcot and Fox, 2008).

The inital analysis produced 61 trees with nine topologies (total debt = 64) (Fig. 6.S6 A). Aside from one tree which suggests all operational units arose via cladogenesis, specimens from the upper half of the formation were consistently found to represent an anagenetic succession. The position of operational units from the lower half of the formation varied and were not always consistent with stratigraphic position. This result is likely influenced by the fact that specimens from the lower half of M3 do not preserve features of the parietal-squamosal frill that would allow them to be distinguished from the *Torosaurus* morphology. MOR 2982 preserves an anterolateral projection of the squamosal, which is consistent with the morphology expressed in several other HCF specimens including the *Torosaurus* specimen MOR 3081. Incorporation of *Torosaurus* specimens into *Triceratops* operational units (total debt = 67, nine trees, three topologies; Fig. 6.S6 B) produced a single tree suggesting all operational units arose via cladogenesis and two additional topologies which include ancestor-descendant relationships. In four trees, all operational units were recovered within an anagenetic lineage except the lower M3 group. This operational unit was recovered as basal to the upper L3 operational unit, suggesting a cladogenetic event. The remaining four trees exhibit a bifurcation event in L3 giving rise to two lineages.

Given the lack of frill characters for the lower M3 operational unit, the influence of *Torosaurus* specimens on the results was examined by pruning all *Torosaurus* from the analysis. This pruning resulted in reduced total debt (57) and 12 trees (Fig. 6.S6 C).

Four trees indicate that all HCF operational units represent a single anagenetic lineage with specimens exhibiting the *T. horridus* morphology evolving into *T. prorsus* (Fig. 6.4A). Eight trees recovered two lineages suggested to diverge at some point in L3 or prior to the deposition of the HCF. One lineage gives rise to lower M3 specimens and the other to U3 specimens. This result suggests that two anagenetic lineages, one comprised of specimens referable to *T. horridus* and the other giving rise to *T. prorsus*, coexisted in the HCF (for at least some time) (Fig. 6.4B).

Characters Incorporated in Cladistic
Analysis. First Use in a Cladistic Study is Cited.

1) Postorbital horn core length: (code 0) long (postorbital horn core/basal skull length ratio: ≥0.64 ; (code 1) short (postorbital horn core/basal skull length ratio: <.64 (1). [Forster, 1990 character 58 modified; Forster, 1996, character 2 modified]

2) Cross section of postorbital horn core: (code 0) circular to sub-circular; (code 1) narrow. The postorbital horn cores of some specimens of *Triceratops* (e.g. MOR 2702, MOR 2923) exhibit a markedly narrow morphology which does not appear to be a product of taphonomic distortion. MOR 2923 exhibits no evidence of lateral compression and yet the postorbital horn cores of this specimen have a pronounced ventral keel. Specimens for which apparently laterally compressed postorbital horn cores are likely a result of taphonomic processes (e.g. MOR 2982, MOR 3027) have been coded as '?'.

3) Rostrum shape: (code 0) primary axis of nasal process of premaxilla (NPP) is strongly posteriorly inclined; (code 1) NPP vertical or nearly vertical [Forster, 1990; Forster, 1996, character 4 modified; Longrich and Field, 2012; Fig. 6.S2]

4) Frontoparietal fontanelle: (code 0) open fontanelle; (code 1) closed or constricted due to fusion of frontals and parietals. [Forster, 1990, characters 49 and 50 modified; Forster, 1996, character 3 modified]

5) Epijugal: (code 0) comes to a pronounced peak; (code 1) low and blunt (Longrich, 2010, character 102 modified; Sampson et al., 2010 character 50 modified). Epijugal morphology has been used in phylogenetic studies of chasmosaurines (e.g. Sampson et al., 2010; Longrich, 2011) and as a diagnostic feature of some taxa. In most specimens of *Triceratops*, the epijugal is a low, blunt element. Specimens exhibiting the *Torosaurus* morphology exhibit an epijugal which comes to a pronounced peak, similar to the condition noted in more basal taxa such as *Eotriceratops* (Wu et al., 2007). At least one large *Triceratops* with a non-fenestrated parietal (MOR 1625) also exhibits a peaked epijugal.

6) Quadratojugal notch: (code 0) present; (code 1) absent. [sensu Gates and Sampson, 2007, character 71 and McDonald et al., 2010, character 16]. The quadrates of *Triceratops* exhibit a pronounced ridge on the antero-lateral surface. In many specimens this ridge is interrupted by a pronounced notch, however in some specimens this notch is not present.

7) Nasal horn length: (code 0) short (length/width ratio < 1.85); (code 1) long (length/width ratio > 1.85). [Forster, 1990, character 28 modified; Forster, 1996, character 5 modified]

8) Dorsal surface of epinasal: (code 0) narrow to peaked; (code 1) broad. The posterior surface of the epinasal varies from being quite broad to nearly flat in some specimens, to being narrow and coming to a pronounced peak in others. The peaked condition is observed in the holotypes of *Arrhinoceratops* and *Eotriceratops*.

9) Nasal: (code 0) short, arched; (code 1) elongate, straight. A short, arched nasal is observed in the holotype of *T. horridus* (YPM 1820) and several other specimens referred to this taxon. Specimens from U3 of the HCF exhibit a more elongate nasal morphology which lacks pronounced arching of the lateral margin.

10) Anterior nasals and posterior portion of epinasal fused to form a protuberance posterior to epinasal: (code 0) present; (code 1) subtle or absent. Forster (1996) noted a pronounced bump or boss posterior to the nasal horn in UCMP 113697. A similar structure is present in the holotype of *T. 'calicornis'* (USNM 4928) as noted by Ostrom and Wellnhofer (1986). The structure appears to be formed by a combination of the anterior nasals and the posterior portion of the epinasal. Forster (1996) suggested that this feature was due to the incomplete fusion of the epinasal to an underlying boss or horn core; disarticulated nasals reveal no underlying boss (see Horner and Goodwin, 2008) but the anterior nasal can be somewhat thickened relative to the middle segment of this element. Presence of a homologous structure in mature individuals (MOR 1122) suggest

that its presence is not a result of incomplete fusion, though the degree to which this feature varies throughout ontogeny is currently unknown. Development of this feature may be tied to evolutionary elongation of the epinasal.

11) Epinasal-Nasal protuberance: (code 0) reduced or absent (code 1) developed into pronounced boss.

12) Antero-medial process on nasal: (code 0) present, pronounced (code 1) reduced, constricted or absent (Fig. 6.S3). *Triceratops* from the lower half of the HCF appear to exhibit a distinct process on the antero-medial surface of the nasal, medial to the rostroventral process (following the terminology of Fujiwara and Takakuwa [2011]). In specimens from U3 in which this process is visible, it is greatly reduced.

13) Posterior projection on epinasal: (code 0) present; (code 1) absent (Fig. 6.S4). The posterior surface of some epinasals exhibits a small but pronounced posterior projection or shelf. The projection appears to be absent in observed specimens from U3. The projection may contribute to formation of the epinasal-nasal protuberance (see character 9).

14) Nasal process of the premaxilla: (code 0) narrow; (code 1) expanded (Fig. 6.S2). In some specimens of *Triceratops* the NPP is narrow, exhibiting only slight antero-posterior expansion. The premaxilla of the holotype of *Eotriceratops* exhibits an extremely narrow NPP. In many specimens of *Triceratops* from relatively high in the HCF, this process is expanded into a wide, nearly square structure (Dataset 6.S1).

15) Midline peak on nasal process of the premaxilla: (code 0) absent; (code 1) present. The nasal process of MOR 3045 exhibits a pronounced dorsal peak anterior to its posterior margin (see Fig. 6.S2 E). This process appears to be absent or greatly reduced in other specimens, but is clearly present in juvenile specimens from U3 (MOR 1110, MOR 2951). The degree to which this feature varies ontogenetically in specimens from the lower half of the formation is currently unknown.

16) Prominence immediately anterior to or descending from the narial strut, directed into interpremaxillary fenestra: (code 0) absent (code 1) present (See Fig. 6.S7 A).

17) Premaxilla, accessory strut in septal fossa: (code 0) no accessory strut; (code 1) strut present [Sampson et al., 2010; character 12]. Many specimens of *Triceratops* appear to exhibit two prominences or struts directed into the interpremaxillary fenestra (characters 16 and 17; see Fig. 6.S7 A). The degree to which these features are developed varies between specimens.

18) Premaxilla, triangular process recess: (code 0) shallow; (code 1) deep [Dodson et al., 2004; character 12 (modified)]

19) Triangular ('narial' sensu Wu et al., 2007) process of premaxilla: (code 0) dorsal margin (at point of contact with narial strut) positioned roughly at or below the ventral margin of the interpremaxillary fenestra; (code 1) dorsal margin of narial process (at point of contact with narial strut) positioned well above ventral margin of interpremaxillary fenestra (see Wu et al., 2007).

20) Ventromedial foramina of the premaxilla positioned (code 0) close together; (code 1) far apart (more than 1.5 times the width of anterior foramen) [see Fig. S7 B]. The large anterior foramen was highlighted in the description of the holotype of *Eotriceratops* by Wu et al., (2007).

21) Posteroventral surface of the posterior 'prong' of premaxilla (sensu Wu et al., 2007): (code 0) comes to a narrow ridge (code 1) broad posterior surface. The prominent prong of the posteriormost premaxilla exhibits a narrow ridge on its posterior surface in some specimens of *Triceratops*. Specimens from U3, including juveniles (MOR 1110; MOR 2951) appear to exhibit a much broader posterior surface of this element. The degree to which this feature might vary ontogenetically lower in the formation is currently unknown. (See Fig. S7).

22) Posterior prong of premaxilla: (code 0) broad surface for articulation with nasal; (code 1) exhibits a pronounced ridge on the lateral surface and a constricted area for articulation with the nasal (Fig. S6).

23) Episquamosal or squamosal crenulation number (Farke et al., 2011, character 55 modified): (code 0) seven or more; (code 1) six or fewer.

24) Convex margin of squamosal (code 0) absent; (code 1) present (see Longrich and Field, 2012). Longrich and Field (2012) noted that specimens of *T. prorsus* tend to exhibit a strongly convex margin of the squamosal. This study finds the shape of the squamosal to vary within *Triceratops* with some specimens which exhibit *T. horridus*

morphologies (MOR 1120) possessing more convex squamosals than other specimens which exhibit *T. prorsus* morphologies (MOR 2702; Dataset 6.S1). This variation is likely tied to ontogenetic elongation of this element (see Scannella and Horner, 2010). Specimens from higher in the HCF appear to exhibit the convex morphology for a longer period of time, ontogenetically**.** In this study, specimens were coded as possessing a convex squamosal if the ratio of sqamosal length to the distance to the squamosal's lateral margin (measured from and perpendicular to the line representing length) was ≤ 4 (see Dataset 6.S1).

25) Anterolateral projection on squamosal (see Sullivan et al., 2005): (code 0) present; (code 1) greatly reduced or absent

26) Anterolateral projection on squamosal: (code 0) pronounced, forming strongly concave anterior margin of the squamosal; (code 1) reduced or absent (see Sullivan et al., 2005). Sullivan et al. (2005) noted that *Torosaurus latus* specimens exhibit a greatly pronounced projection of the anterolateral surface of the squamosal which causes the otic notch to become constricted. This projection is present to various degrees in many specimens of *Triceratops*, however in some it is greatly reduced (nearly absent).

27) Squamosal bar (code 0) present; (code 1) absent (Forster, 1990, character 90 modified; Sampson et al., 2010, character 64 modified)

28) Ventral surface of parietal in areas surrounding fenestrae/incipient fenestrae: (code 0) smooth transition in thickness; (code 1) thickness transitions in pronounced step from thicker to thinner bone. Scannella and Horner (2010) noted distinct thinning regions on

the ventral surface of the parietal of many *Triceratops* specimens. This region is often rimmed by a pronounced transition in thickness, from thick bone posteriorly to far thinner bone within the depression ("incipient fenestra"; but see Farke, 2011; Longrich and Field, 2012; Tsuihiji, 2010). However, in some specimens of *Triceratops* the transition in thickness in these regions is more gradual and lacks the pronounced step between thicker and thinner bone. MOR 1122, a specimen with fenestrae, exhibits a trace of this step along the edge of a fenestra. The holotype of *'Nedoceratops hatcheri'* (USNM 2412) also appears to exhibit a slight step around its reduced parietal fenestra (Scannella and Horner, 2011). A distinct ventral parietal step appears to be more common in specimens found higher in section.

29) Number of epiparietals or epiparietal crenulations: (code 0) four or fewer; (code 1) five or more [Holmes et al., 2001, character 28 modified; Forster, 1990, character 46 modified]

30) Number of epiparietals or epiparietal crenulations: (code 0) 5 or fewer; (code 1) 6 or more [Holmes et al., 2001 character 28 modified; Forster, 1990, character 46 modified]

31) Parietal fenestrae: (code 0) present; (code 1) absent [Forster, 1990; character 84 modified]

32) Epiossification or crenulation on midline of parietal: (code 0) absent (code 1) present [(Forster, 1996; Sampson et al., 2010, character 95 modified)]. Scannella and Horner (2011) presented evidence suggesting the presence of a midline epiparietal on MOR

1122. For the purposes of the present analysis, epiossification positions were coded based either on presence of the element or a pronounced marginal crenulation indicating position on the parietal-squamosal frill.

33) Epiossification or crenulation spanning parietal-squamosal contact: (code 0) present; (code 1) absent [Farke et al., 2011; character 43 modified)].

Data Matrix.

Specimen codings for this analysis. ROM 796 is the holotype of *Arrhinoceratops brachyops*; RTMP 2002.57.7 is the holotype of *Eotriceratops xerinsularis*.

Matrix (Binary Coding)

ROM796	00010?00000??????00???00000(0 1)0000?
RTMP2002.57.7	0?0?0000?????0000010?????????????0
MOR1122	10010001000????0?1?0??00000(0 1)11001
MOR3081	10??0?00?00????????0??00010010000
MOR1120	1000?0010000?00111?100(0 1)(0 1)001000?10
MOR2552	00?01?????????????????????1?????1
MOR2985	?????????????????????????00110?????
MOR3005	????????0??0?????????0?????0????1
MOR2982	1?0?1?01?01??0?11????0??01???????
MOR3010	1?????01?000??????????????????????
MOR3011	??0???01???000?01????????????????
UCMP113697	0010??11?01??????????1?1011?00110
MOR3027	0?10?0??1??0000101?101?0011000?01
MOR3045	1010?0?1???00111???111100111100110
UCMP128561	??????01????????1????????????????
MOR2574	101???101??1110111????????10???0?
MOR2702	?11??010?10??10?1???11?01111?????
MOR1625	??1?0?10?10????11101??111111?????
MOR2924	??1???111???11???1??11110111??1??
MOR2978	1??1??10110????????????11111??1??
UCMP136092	1?????????????????????11011???1??
MOR2936	?????01?????11??0???11??11???????
MOR2979	11?1?0?????????????11??????????0

MOR2971 ??1???10?10??1?11101?????????????
UCMP137263 10??????1??1???????????????1?????0
MOR004 ??111?10110???????????11?11?00110
MOR2999 10?0?1??1??1??????????1(0 1)(0 1)11100?10
MOR2923 11?1??101?????????????????????0010?
MOR1604 1?1?1011110?????11?????11???????
MOR981 0?0???010?????????????????????010001

Alternative Multistate Characters:

Character 10: Protuberance posterior to epinasal (code 0) very subtle or absent; (code 1) present, prominent (2) enlarged into a pronounced bump or boss (see Forster [1996] and Ostrom and Wellnhofer [1986])

Character 24: Anterolateral projection on squamosal: (code 0) present, projects anteriorly producing strongly concave anterior margin of the squamosal; (code 1) anterior projection present but does not project strongly anteriorly; (code 2) greatly reduced or absent (see Sullivan et al., 2005)

Character 27: Number of epiparietals or parietal crenulations per side of parietal: (code 0) 4 or fewer; (code 1) 5; (code 2) 6 or more (Holmes et al., 2001, character 28 modified; Forster 1996,character 46 modified; Sampson et al., 2010, character 93 modified)

Matrix (Multistate)

ROM 796 00010?0001?????00???0000(0 1)000?
RTMP2002.57.7 0?0?0000????0000010??????????0
MOR1122 10010001010???0?1?0??0000(0 1)2001
MOR3081 10??0?00?1????????0??001001000
MOR1120 1000?001010?00111?100(0 1)(0 1)0100?10
MOR2552 00?01?????????????????1????1
MOR2985 ??????????????????????0110????
MOR3005 ????????0?0?????????0????0???1
MOR2982 1?0?1?01?2??0?11????0??1??????

MOR3010	1?????01?10??????????????????
MOR3011	??0???01??000?01?????????????
UCMP113697	0010??11?2??????????1?111?0110
MOR3027	0?10?0??1?0000101?101?01100?01
MOR3045	1010?0?1??00111???111101110110
UCMP128561	??????01???????1?????????????
MOR2574	101???101?1110111???????10??0?
MOR2702	?11??010?0??10?1???11?0211????
MOR1625	??1?0?10?0????11101??11211????
MOR2924	??1???111??11???1??1111111?1??
MOR2978	1??1??1010?????????????1211?1??
UCMP136092	1?????????????????????1111??1??
MOR2936	?????01????11??0???11??2??????
MOR2979	11?1?0?????????????11????????0
MOR2971	??1???10?0??1?11101??????????
UCMP137263	10??????1?1?????????????1????0
MOR004	??111?1010???????????11?1?0110
MOR2999	10?0?1??1?1???????????1(0 1)(1 2)110?10
MOR2923	11?1??101?????????????????010?
MOR1604	1?1?101110?????11??????2??????
MOR981	0?0???010?????????????????01001

Figure 6.S1. *Triceratops* from upper M3. *(A)* MOR 3027 (cast), a large subadult. *(B)* MOR 3045, subadult recovered from ~ 2 m stratigraphically higher than MOR 3027. These specimens exhibit a combination of primitive and derived features. Both specimens exhibit a more convex rostrum than *Triceratops* found stratigraphically lower. MOR 3045 represents the lowest occurrence of a wide NPP in the HCF dataset. Parietal, squamosal, postorbital, nasal, and epinasal of MOR 3045 mirrored. Orbit is crushed. (Scale bars: 10 cm.)

Figure 6.S2. Variation in the nasal process of the premaxilla. *(A*) RTMP 2002.57.7, the holotype of *Eotriceratops*. *(B)* MOR 1120, collected from L3. *(C)* MOR 3011, collected from the lower part of M3. *(D)* MOR 3027, collected from upper M3. *(E)* MOR 3045, collected from upper M3. This specimen exhibits a pronounced peak on the nasal process (arrow) which is anterior to the posterior margin, a feature which is observed in juveniles from U3. *(F)* MOR 2574, collected from the lower U3. *(G)* MOR 2702, collected from the lower U3 (image mirrored for comparison). Specimens from U3 (F-G) exhibit a wider NPP; MOR 3045 represents the stratigraphically lowest occurrence of a wide NPP. MOR 2574 and MOR 2702 were collected from a multi-individual bone bed and exhibit variation in the morphology of the NPP. A trend towards an increased angle between the NPP and NS is noted in the HCF sample (Dataset 6.S1). NPP, nasal process of the premaxilla. NS, narial strut. (Scale bars: 10cm; *B-G* are to the same scale.)

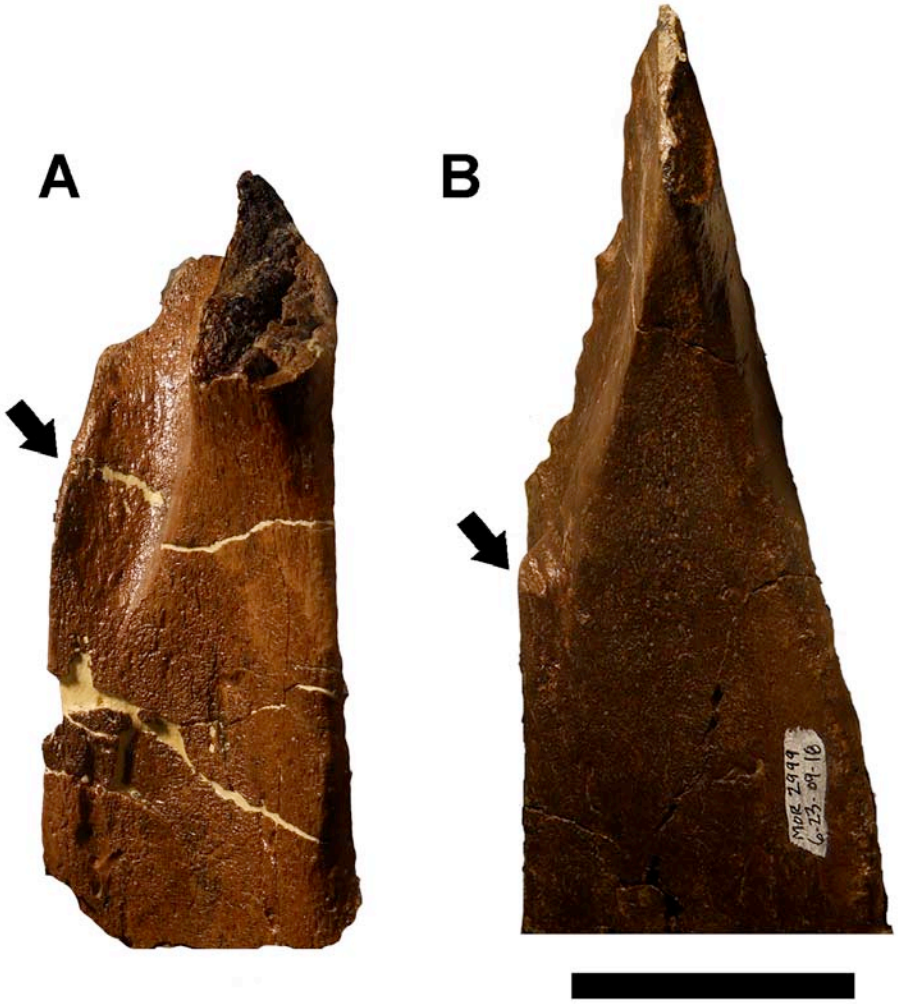

Figure 6.S3. Variation in the anteromedial process of the nasal. *(A)* MOR 3027 (from upper M3) expresses a prominent process on the anteromedial surface of the nasal. *(B)* MOR 2999 (from U3); this process is greatly reduced. (Scale bar: 5 cm.)

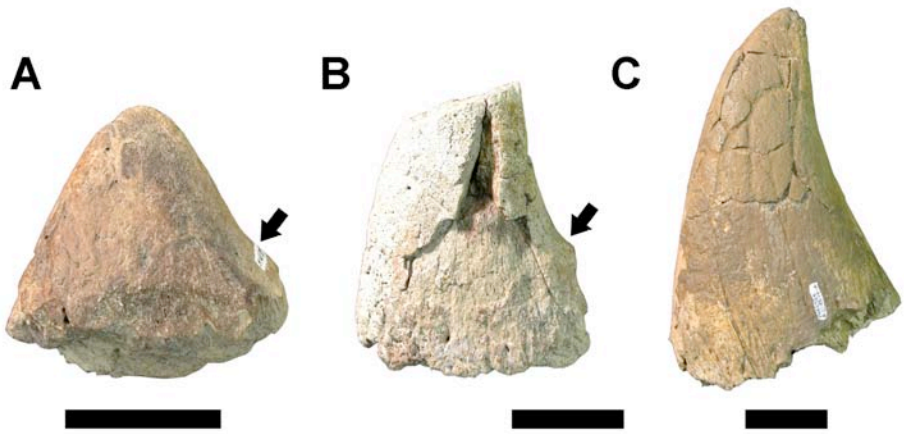

Figure 6.S4. Some specimens exhibit a pronounced shelf or projection on the posterior surface of the epinasal (indicated by arrow; character 13). *(A)* MOR 989, stratigraphic position to be determined. *(B)* MOR 3045 from upper M3. *(C)* MOR 2924 from U3. (Scale bars: 5 cm.)

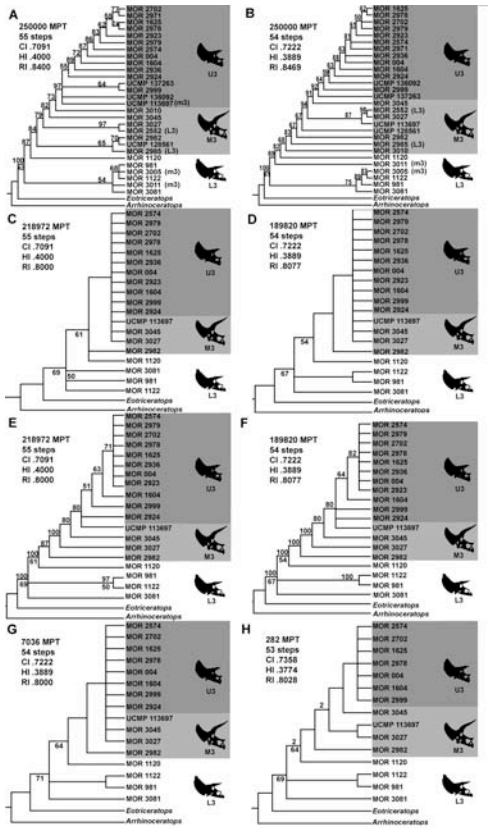

Figure 6.S5. Additional results of cladistic analyses of HCF *Triceratops*. (*A*) 50% majority-rule consensus tree produced by initial analysis using binary coding. Bootstrap support values below nodes. Percent occurrence for nodes are reported above horizontal lines. Specimens group according to relative stratigraphic position, however several fragmentary specimens are recorded in positions inconsistent with stratigraphic position. MOR 981, MOR 1122, MOR 3081, and MOR 3005 exhibit the *Torosaurus* morphology. *(B)* 50 % majority rule tree produced by initial analysis using multistate coding. *(C)* Strict consensus tree produced once specimens which could not be coded for characters of the parietal-squamosal frill are removed (binary coding, branch and bound search). Bremer decay values greater than one reported above nodes. (D) Strict consensus tree produced once specimens which could not be coded for characters of the parietal-squamosal frill are removed (multistate coding, branch-and-bound search). (E) 50% majority-rule consensus tree for analysis in which specimens which specimens which could not be coded for characters of parietal-squamosal frill are removed (binary coding, branch-and-bound search). (F) 50% majority-rule consensus tree for analysis in which specimens which specimens which could not be coded for characters of parietal-squamosal frill are removed (multistate coding, branch-and-bound search). *(G*) Strict consensus tree for analysis including only specimens exhibiting at least 10 cranial characters (in the multistate matrix); binary codings (branch-and-bound search). *(H)* Strict consensus tree for analysis after MOR 2924 is removed from the matrix; binary codings (branch-and-bound search).

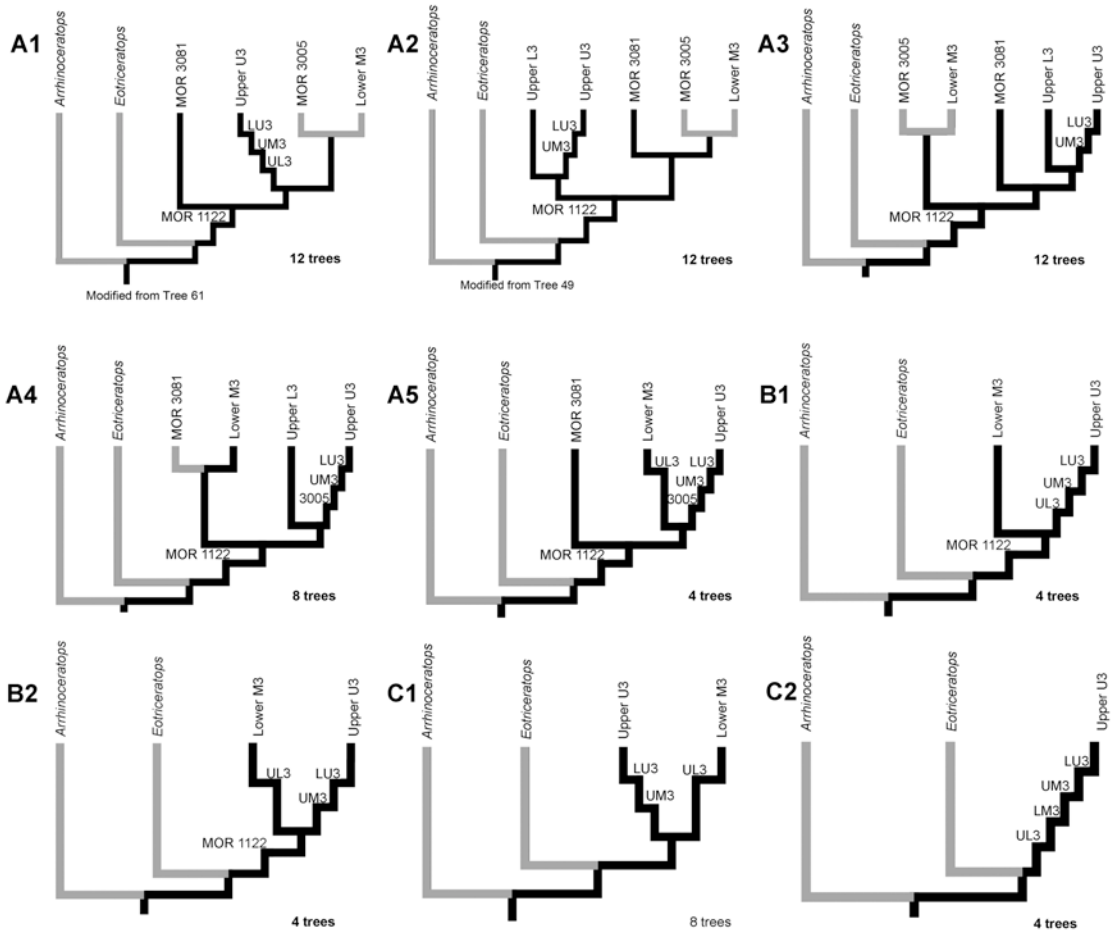

Figure 6.S6. Results of stratocladistic analyses. *(A)* Topologies produced in the initial analysis, in which specimens exhibiting the *Torosaurus* morphology are considered separately from other operational units (61 trees, nine topologies, Debt = 64). Nearly all topologies recover specimens from the upper half of the HCF in an anagenetic sequence, whereas positions for specimens from the lower half of the formation exhibit variation. Nexus file including all tree results are available on Morphobank as project 1099 (O'Leary and Kaufman, 2008). *(B)* Result when specimens exhibiting the *Torosaurus* morphology are incorporated into operational units (nine trees, three topologies, debt = 67). MOR 3081 and MOR 1120 are combined into an upper L3 operational unit; MOR 3005 is incorporated into the lower M3 operational unit. An additional topology suggesting a purely cladogenetic scenario was also recovered. *(C)* Results when *Torosaurus* specimens are pruned from the analysis. Twelve trees are produced and two topologies incorporating anagenesis are recovered (Debt = 57). Gray branches represent operational units which are also recovered as being ancestral in trees presenting the same topology.

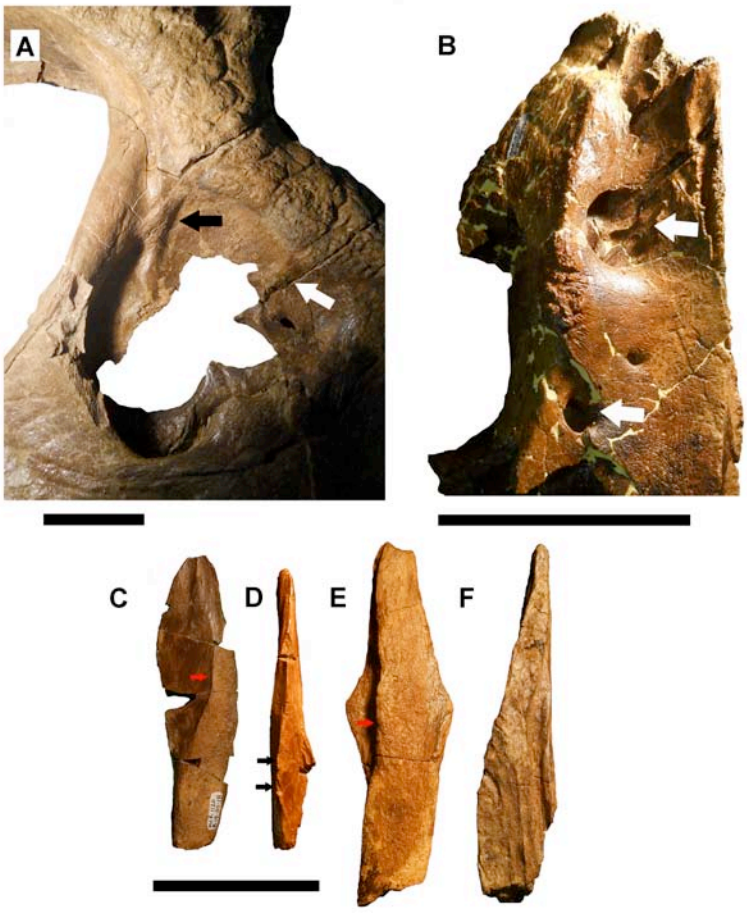

Figure 6.S7. Additional characters of the *Triceratops* premaxilla. *(A)* Rostrum of MOR 1625 (from U3). Black arrow indicates prominence anterior to the narial strut which projects into the interpremaxillary fenestra. White arrow indicates accessory strut in the septal fossa (Sampson et al., 2010, character 12). Scale bar, 5 cm. *(B)* Ventral view of the left premaxilla of MOR 1120. Arrows indicate primary ventro-medial foramina which penetrate the medial shelf. In this specimen these foramina are widely spaced, while in some they are positioned more closely together (≤ 1.5 x width of the anterior foramen). Scale bar, 10 cm. *(C-F)* Posterior prong of the premaxilla (characters 21-22). *(C)* Lateral view of the posterior prong of the left premaxilla of MOR 1120 (from L3). *(D)* Posteroventral surface of prong. *(E)* Lateral view of the posterior prong of the left premaxilla of MOR 2702 (from U3). *(F)* Posteroventral surface of premaxillary prong of MOR 2702. The posterior portion of the prong is narrow and comes to a sharp ridge (indicated by black arrows) in MOR 1120, which contrasts with the condition seen in specimens from U3 in which the posterior surface of the prong is broad. Juvenile specimens from U3 exhibit a broad posterior surface, similar to the condition observed in MOR 2702. Red arrows highlight the lateral surface of the prong; some specimens exhibit a more constricted lateral surface with a pronounced lateral ridge. (Scale bar, 10 cm.)

Dataset 6.S1 (Appendix 1)

Basal Skull Length (BSL) Estimations			
Specimen No.	Unit	Dentary L. (cm)	BSL (cm)
MOR 1199	TBD	27	48.3
MOR 2951	U3	31	58.6
MOR 3027	M3	56.5	110
MOR 1604	TBD	54.8	110
MOR 004	U3	59	122
Estimates :			
UCMP 154452	U3	15.9	24.55162
MOR 2928	U3	40.5	78.4699
MOR 3081	L3	56.5	113.5387
MOR 2982	M3	50.5	100.3879
MOR 3010	M3	est. 50	99.292
MOR 3045	M3	51.5	102.5797
MOR 2702	U3	60	121.21
MOR 2574	U3	51	101.4838
MOR 2597	U3	46.6	91.83988
MOR 2999	U3	49.5	98.1961
MOR 3011	M3	est. 45	88.333
MOR 3046	U3	51	101.4838
MOR 8147	U3	57	114.6346
MOR 8148	U3	58.5	117.9223
MOR 3042	U3	52	103.6756
MOR 2945	TBD	54	108.0592

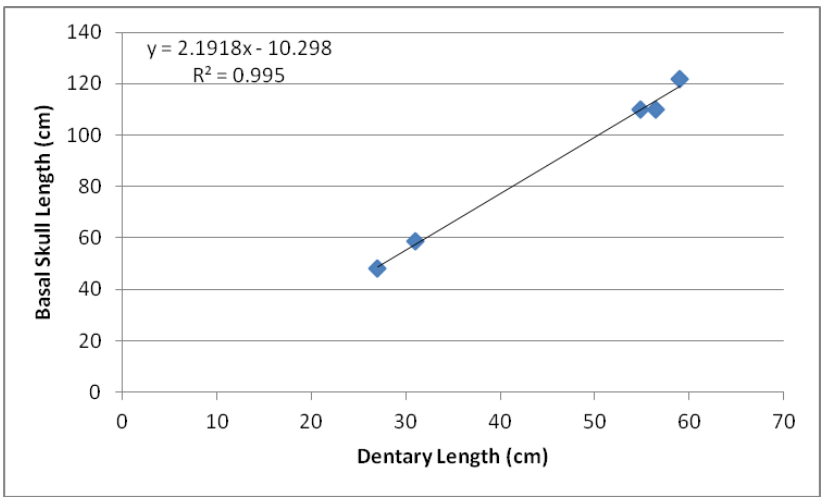

Specimen No.		Jugal L. (cm)	BSL (cm)
MOR 1199	TBD	17.8	48.3
MOR 2951	U3	22.9	58.6
MOR 1110	U3	30	77.6
MOR 3027	M3	38.8	110
MOR 1604	TBD	41	110
MOR 004	U3	42.5	122
MOR 1120	L3	35	98
MOR 1122	L3	48.2	126.4
Estimates:			
MOR 2569	M3	16	41.9811
UCMP 154452	U3	11.5	29.37795
MOR 3064	M3	20.4	54.30418
MOR 2982	M3	35	95.1944
MWC 8574	U3	50.5	138.60525
UCMP 113697	M3	39	106.3972
MOR 3045	M3	36	97.9951
UCMP 136092	U3	41	111.9986
UCMP 137263	U3	35.35	96.174645

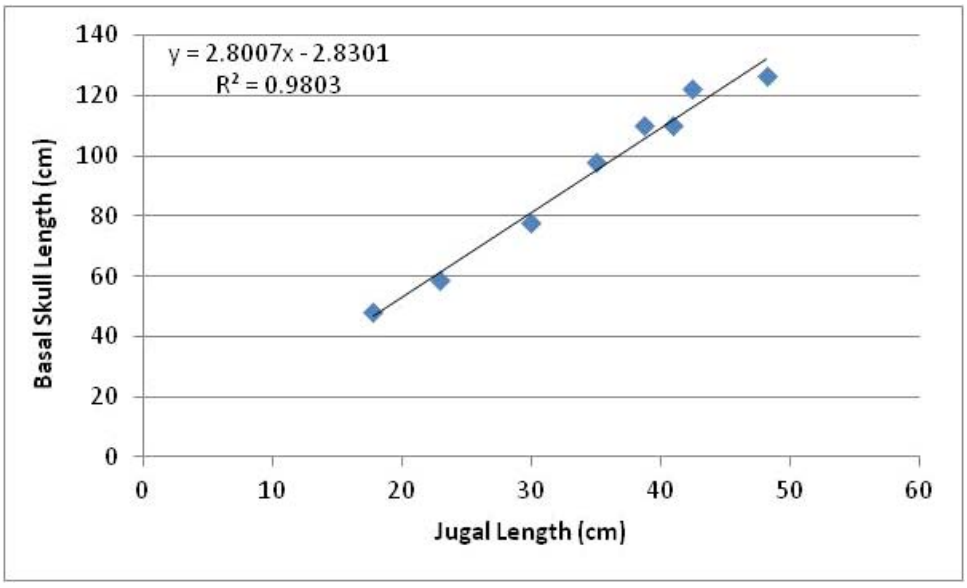

Maxilla Length			
Specimen No.		Maxilla L. (cm)	BSL (cm)
MOR 2951	U3	27 (est. 28)	58.6
MOR 1110	U3	34.5 (est. 35)	77.6
MOR 1199	TBD	21.4 (est. 22)	48.3
MOR 1120	L3	37.8 (est. 41)	98
MOR 3027	M3	50 (est. 52)	110
MOR 1122	L3	58	126.4
MOR 1604	TBD	48	110
Estimates:			
MOR 2999	U3	42	92.9858
UCMP 113697	M3	50	110.5938
RTMP2002.57.7		60	132.6038

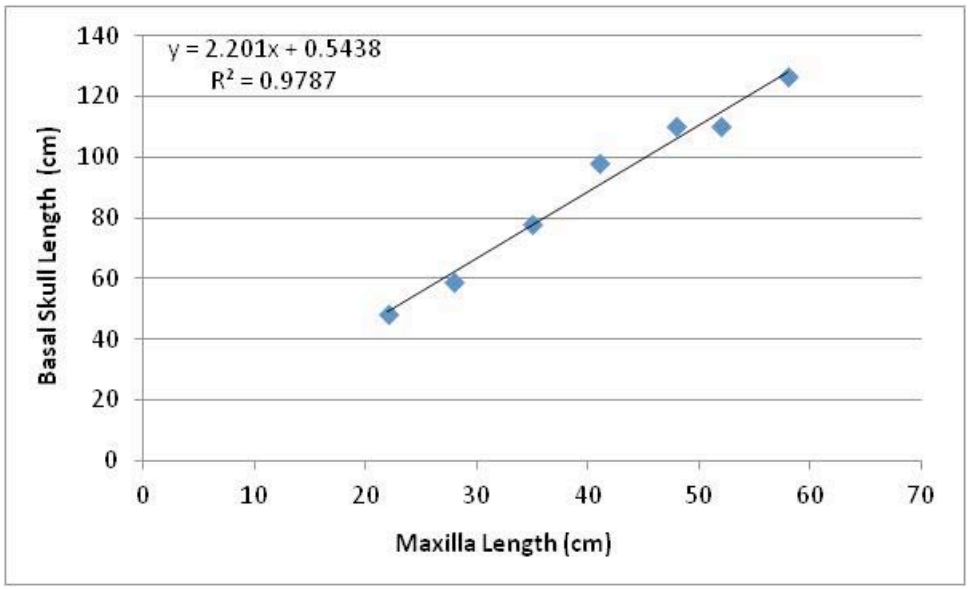

Occiptial Condyle Area					
		O.C. Width (cm)	O.C. Height (cm)	O.C. Area (cm^2)	BSL (cm)
MOR 1199	TBD	4.7	4.9	23.03	48.3
MOR 2951	U3	6.2	6.2	38.44	58.6
MOR 1110	U3	7.4	7.4	54.76	77.6
MOR 1120	L3	8.9	8.5	75.65	98
MOR 3027	M3	11.1	11.3	125.43	110
MOR 1122	L3	11.7	11.8	138.06	126.4
Estimates:					
UCMP 154452	U3	2.9	2.5	7.25	43.31353
MOR 2999	U3	9.1	9.1	82.81	90.83321
MOR 2979	U3	10.8	10.1	109.08	107.3544
MOR 2552	L3	10.7	10.3	110.21	108.0651
MOR 3081	L3	9.5	9.1	86.45	93.12241
MOR 3041	U3	9.4	9.4	88.36	94.3236
MOR 2551	TBD	9.8	9	88.2	94.22298
MOR 2936	U3	9.3	9.2	85.56	92.56268
MOR 1625	U3	11.9	11.2	133.28	122.5738
MOR 2972	U3	9.6	9.8	94.08	97.92091
UCMP 113697	M3	11.5	10.9	125.35	117.5866
MOR 2924	U3	9.3	9.1	84.63	91.97781
MOR 2570	U3	7.8	7.8	60.84	77.01628
MOR 699	TBD	7.3	7.7	56.21	74.10447
MOR 2959	?L3	9.8	9.6	94.08	97.92091

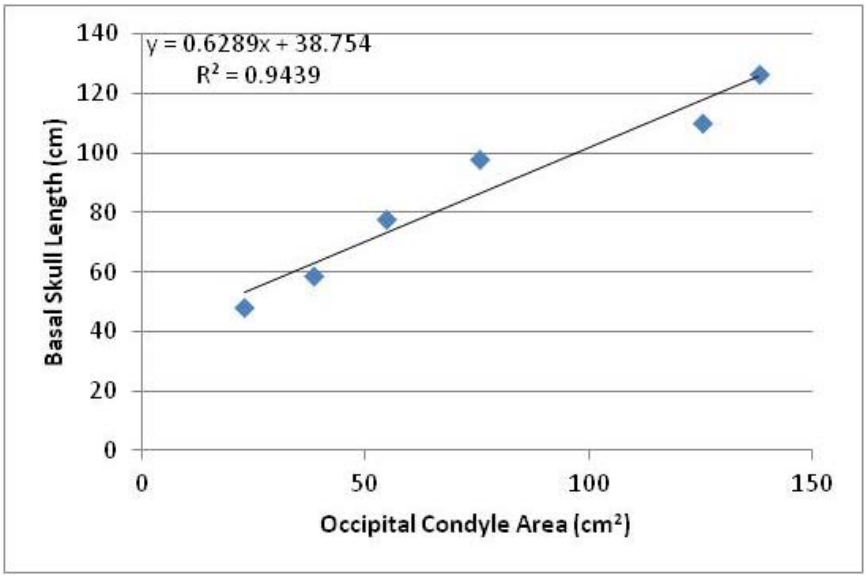

Note: Basal Skull Length measured from anteriormost point of rostrum to posterior surface of occipital condyle (following Forster, 1996). Values for MOR 004, MOR 1604, and MOR 3027 approximated using distance from anterior point of rostrum to posterior margin of lateral temporal fenestra. Rostra of MOR 1110 and MOR 1122 are reconstructed. Measurements taken from skull reconstructions at MOR (MOR 1199, MOR 1110, MOR 2951, MOR 3027) and from articulated specimens (MOR 004, MOR 1604).

	BSL (cm)	Distance from ant. rostrum to posterior margin of lateral temporal fenestra (cm)
MOR 1199	48.3	48.7
MOR 2951	58.6	57.8
MOR 1122	126.4	125.7

Dataset 6.S1 (Appendix 2)

HCF *Triceratops* nasal horns. TBD = to be determined. Red text indicates incomplete specimens. Green text indicates taphonomic distortion. Blue text indicates juvenile specimens. MOR 3011 is either a very large juvenile or a subadult. *RTMP2002.57.7 is the holotype of *Eotriceratops*, collected from the Horseshoe Canyon Formation of Alberta. Specimens highlighted in green were not included in Spearman's rank correlation test. Measurements are in cm.

Specimen no.	Locality Name	HCF Unit	Level	Length	Width	L/W	Mean	Std. Dev.	Std. Error
MOR 1122	TORO II	L3	lower	12	17.4	0.689655			
MOR 3081	JRH-008	L3	upper	13.9	est. 10.4	1.336538	1.088559	0.350696	0.2479795
MOR 1120	Getaway Trike	L3	upper	5.8	6.9	0.84058			
MOR 2982	3 Amigos	M3	lower	10	6.5	1.538462	1.209369	0.342027	0.1710135
MOR 3010	Golden Goose	M3	lower	6.5	8.6	0.755814	1.164553		
MOR 3011	Anky Breaky Heart	M3	lower	6.7	5.1(est. 6.8)	0.98529			
MOR 3055	Brown Nose	M3	lower	14.5	12.6	1.150794			
MOR 2570	Mark's Scavenged Trike	M3	lower	11	7.9	1.392405			
UCMP128561	Dave's Nose	M3	upper	13.6	14.2	0.9577	1.652774	0.613401	0.3541471
MOR 3045	Cliffhanger	M3	upper	12 (est. 16)	8.5	1.882353			
UCMP 113697	Ruben's Triceratops	M3	upper	24	11.33	2.11827			
MOR 2924	Lon's Trike	U3	lower	22.5	10	2.25	2.35038	0.145963	0.059589
MOR 2972	Supernasal	U3	lower	25	11.2	2.232143	2.145602	0.38882	
MOR 3008	American Beauty	U3	lower	26.5	10.1	2.623762	2.308763	0.142503	
MOR 2971	Crazy Trike	U3	lower	26.3	11	2.390909			
MOR 2936	Lazy Bones	U3	lower	19	9	2.111111			
MOR 2702	BAB	U3	lower	30	13	2.307692			
MOR 1625	Haxby Trike	U3	lower	30	13.5	2.222222			
MOR 2574	Quittin' Time	U3	lower	21	9.1	2.307692			
MOR 2965	TrkNas	U3	upper	14	6	2.333333			
MOR 1110	SG5	U3	lower	8.3	5.4	1.537037			
MOR 2951	DFJuvieTrike3	U3	lower	4.5	3.5	1.285714			
MOR 2923	Joe's Half Day Trike	U3	upper	29	13	2.230769	2.355036	0.39088	0.1381969
MOR 2576	Snap Creek	U3	upper	21.3	13.6	1.566176			
MWC 7584		U3	upper	36.6	12.6	2.904762			
MOR 004	MORT	U3	upper	28.5	13	2.192308			
MOR 2952	Homer's Nose	U3	upper	27	11.2	2.410714			
MOR 3048	Wednesday's Trike	U3	upper	19	7.2	2.638889			
MOR 2941	Nosy Nasal	U3	upper	24.8	10	2.48			
MOR 2938	Lauren's Trike	U3	upper	29	12	2.416667			
RTMP2002.57.7	'Dry Island Triceratops'	HCanyonFm		8	11.3	0.707			
MOR 2978	Greene Trike	U3	TBD	25.95	11.3	2.29646			
MOR 3049	Present	U3	TBD	21	10.5	2			
MOR 966		TBD		15.5	11.5	1.347826			
MOR 1604	Baker Trike	TBD		26.5	12	2.208333			
MOR 3058	JDExTrike2	M3		17	11	1.545455			
MOR 965	Mickey's Trike	TBD		24.9	17	1.464706			
MOR 2551	CSTrike2	TBD		22	14.3	1.538462			
MOR 2575		TBD		25	13.5 (est. >17)	<1.470589			
MOR 989	Pompey	TBD		8.1	8	1.0125			
MOR 981	TORO I	TBD		10	13	0.769231			

Dataset 6.S1 (Appendix 3)

Angle between nasal process of the premaxilla (NPP) and narial strut. Measurement taken between approximate midlines of each process, parallel to direction representing primary trend. Blue text indicates juvenile specimens. RTMP2002.57.7 is the holotype of *Eotriceratops*, collected from the Horseshoe Canyon Formation of Alberta.

Specimen no.	Locality Name	HCF Unit	Level	Angle	Mean	Std. Dev	Std. Error
MOR 1122	TORO II	L3	lower	125	124.5	0.707107	0.5
MOR 1122 7-22-00-1	TORO II	L3	lower	124			
MOR 1120	Getaway Trike	L3	upper	126			
MOR 3011	Anky Breaky Heart	M3	lower	127	127	2	1.15470054
MOR 6683	To the Premax	M3	lower	125			
MOR 2982	3 Amigos	M3	lower	129			
MOR 3027	Yoshi's Trike	M3	upper	141	140	2.645751	1.52752523
MOR 3045	Cliffhanger	M3	upper	142			
UCMP 113697	Ruben's Triceratops	M3	upper	137			
MOR 2924	Lon's Trike	U3	lower	144	141.4	5.639149	2.52190404
MOR 2574	Quittin' Time	U3	lower	136	139	6.271629	2.370453
MOR 2702	BAB	U3	lower	135			
MOR 1625	Haxby Trike	U3	lower	144			
MOR 2971	Crazy Trike	U3	lower	148			
MOR 2951	DFJuvieTrike3	U3	lower	135			
MOR 1110	SG5	U3	lower	131			
MOR 004	MORT	U3	upper	136	136		
RTMP 2002.57.7*	'Dry Island Triceratops'	HCanyonFm		114			
MOR 1604	Baker Trike	TBD		137			
MOR 981	TORO I	TBD		104			
MOR 1199	Sierra Trike	TBD		140			
MOR 2590	JRH7-2-05-2 Microsite	TBD		145			

Dataset 6.S1 (Appendix 4)

Nasal process of the premaxilla (NPP). Length measured from dorsalmost point of NPP to ventralmost point of NPP articulation with nasal. Width measured at narrowest point (waist). TBD = to be determined. Red text indicates incomplete specimens. Blue text indicates juvenile specimens. MOR 3011 is either a very large juvenile or a subadult. RTMP2002.57.7 is the holotype of *Eotriceratops*, collected from the Horseshoe Canyon Formation of Alberta. This specimen tapers to a point, width measured at approximate waist though there is some reconstruction in this area. *MOR 3045 exhibits a pronounced midline peak on the NPP; when measured to the base of this peak the length of NPP is 8.2 cm. **Length of the NPP of UCMP 113697 obscured by anterior nasals due to mounting of the skull. Measurements are in cm.

Specimen no.	Locality Name	HCF Unit	Level	Length	Width	L/W	Mean	Std. Dev.	Std. Error
MOR 1122 7-22-00-1	Toro II	L3	lower	14.9	4.9	3.040816			
MOR 1120	Getaway Trike	L3	upper	6.4	3.7	1.72973			
MOR 3011	Anky Breaky Heart	M3	lower	7.6	4.4	1.727273	1.65850816	0.097248	0.068765
MOR 2982	Three Amigos	M3	lower	5.89	3.705	1.589744			
MOR 3027	Yoshi's Trike	M3	upper	7.65	5.5	1.390909	1.42402597	0.046834	0.033117
MOR 3045	Cliffhanger	M3	upper	10.2*	7	1.457143			
MOR 2574	Quittin' Time	U3	lower	8.8	7	1.257143	1.15360747	0.163476	0.094383
MOR 2702	BAB	U3	lower	8.1	6.54	1.238532	1.24254978	0.217482	0.097261
MOR 2936	Lazy Bones	U3	lower	7.2	7.46	0.965147			
MOR 2951	DFJuvieTrike3	U3	lower	5.5	3.5	1.571429			
MOR 1110	SG5	U3	lower	5.69	4.82	1.180498			
RTMP2002.57.7	'Dry Island Triceratops'	HCanyonFm		15.6	est. 6	2.6			
MOR 1199	Sierra Trike	TBD		5.4	2.3	2.347826			
UCMP 113697	Ruben's Triceratops	M3	upper	8.43**	7.25	1.16			
MOR 6653	To the Premax	M3	lower	8.8	4.7	1.87234			

Dataset 6.S1 (Appendix 5)

HCF *Triceratops* nasals. Green text indicates taphonomic distortion. Blue text indicates juvenile specimens. Nasal length (NL) measured from anterior to the epinasal suture to the anteriormost point of the nasal-frontal suture. Basal Skull Length (BSL) measured from anterior of rostrum to posterior of occipital condyle. TBD = to be determined. Measurements are in cm.

Specimen no.	Locality Name	HCF Unit	Level	NL	BSL	NL/BSL	Mean	Std. Dev.	Std. Error
MOR 1122	Toro II	L3	lower	48	126.4	0.379747			
MOR 1120	Getaway Trike	L3	upper	32.3	98	0.329592			
MOR 3006	Antsy Trike	M3	lower	37					
MOR 3027	Yoshi's Trike	M3	upper	43.5	110	0.395455			
MOR 2574	Quittin' Time	U3	lower	39.1	101.48	0.385298	0.415523	0.042746	0.030226
MOR 2924	Lon's Trike U3	U3	lower	41	91.98	0.445749	0.390212	0.045312	0.022656
MOR 1625	Haxby Trike	U3	lower	51	122.57	0.416089	0.415712	0.030228	0.013518
MOR 2951	DFJuvieTrike3	U3	lower	19.9	58.6	0.33959			
MOR 1110	SG5	U3	lower	28.3	77.6	0.364691			
MOR 004	MORT	U3	upper	55.75	122	0.456967	0.435311	0.020568	0.010284
MOR 2999	Situ But Sad	U3	upper	38.8	94	0.412766			
MOR 2923	Joe's Half Day Trike	U3	upper	51.5	115	0.447826			
UCMP 137263	High Ceratopsian	U3	upper	40.75	96.18	0.423685			
MOR 1604	Baker Trike	TBD		46.5	110	0.422727			
MOR 2551	CSTrike2	TBD		54	94.22	0.573127			
MOR 1199	Sierra Trike	TBD		14.8	48.3	0.306418			

Dataset 6.S1 (Appendix 6)

HCF *Triceratops* postorbital horn cores. Red text indicates incomplete specimens. Blue text indicates juvenile specimens. *RTMP2002.57.7 is the holotype of *Eotriceratops*, collected from the Horseshoe Canyon Formation of Alberta. TBD = to be determined; BSL = basal skull length (measured from anterior point of the skull to the posterior surface of the occipital condyle). Measurements are in cm.

Specimen No.	Locality Name	HCF Unit	Level	P.O. Horn L	BSL	P.O./BSL	Mean	Std. Dev.	Std. Error
MOR 1122	Toro II	L3	lower	43 [est 60]	126.4	0.474684			
MOR 1120	Getaway Trike	L3	upper	49	98	0.5	0.574716	0.143592	0.0829031
MOR 2552	BOSH	L3	upper	78 [est 80]	108.07	0.740261			
MOR 3081	JRH-008	L3	upper	32[est 50]	103.33	0.483887			
MOR 2589	DK Site	L3	TBD	19.3					
MOR 1098	Fisk	L3	TBD	10.5					
MOR 2982	3 Amigos	M3	lower	40[est 50]	97.79	0.5113	0.49233	0.026827	0.0189694
MOR 3010	Golden Goose	M3	lower	43[est 47]	99.29	0.473361	0.433194	0.104168	0.0601415
MOR 2569	Afternoon Delight	M3	lower	13	41.28	0.314922			
MOR 3006	Warwick's Horn	M3	lower	43[est 51]					
MOR 3064	Little Horny Devil	M3	upper	25	54.3	0.460405	0.716357	0.121877	0.070366
MOR 3027	Yoshi's Trike	M3	upper	90	110	0.818182	0.652369	0.162113	0.0810564
UCMP 113697	Ruben's Triceratops	M3	upper	83.6	111.53	0.749574			
MOR 3045	Cliffhanger	M3	upper	58.3	100.29	0.581314			
MOR 2979	Seth's Trike	U3	lower	48.95	107.35	0.455985	0.451291	0.044987	0.0224933
MOR 2702	BAB	U3	lower	40.3[est 55]	121.21	0.453758	0.437942	0.157017	0.0593469
MOR 2574	Quittin' Time	U3	lower	51	101.48	0.502562			
UCMP 136092	Russell Basin Triceratops	U3	lower	44	112	0.392857			
MOR 2972	Supernasal	U3	lower	26.7	97.92	0.272672			
MOR 1110	SG5	U3	lower	50	77.6	0.64433			
UCMP 154452		U3	lower	4.15	32.41	0.128047			
MOR 2951	DFJuvieTrike3	U3	lower	28.6	58.6	0.488055			
MOR 2958	DFJuvieHornCore	U3	lower	42					
MOR 3047	Got the Horn	U3	lower	37.2					
MOR 3000	Ashes Trike	U3	lower	30					
MOR 2927	Trike Basin	U3	upper	30					
MOR 2923	Joe's Half Day Trike	U3	upper	55	115	0.478261	0.512576	0.043524	0.0194644
MOR 2597	Mark's Trike II	U3	upper	53.5	91.84	0.582535			
MOR 3041	Joey's Trike	U3	upper	42[est. 47]	94.32	0.498304			
MOR 2999	Situ But Sad	U3	upper	45	94	0.478723			
UCMP 137263	High Ceratopsian	U3	upper	50.5	96.18	0.525057			
MOR 2952	Homer's Nose	U3	upper	57[est 60]					
MOR 3053	PVU Trike	U3	TBD	53.5					
MOR 2988	Spike the Trike	U3	TBD	56					
MOR 539	Trumbo Ranch	TBD		18.35					
MOR 2579	Twitchell North	TBD		20.5					
MOR 1199	Sierra Trike	TBD		17	48.3	0.351967			
MOR 1604	Baker Trike	TBD		60.5	110	0.55			
MOR 2551	CSTrike 2	TBD		40.7[est. 50]	94.22	0.530673			
MOR 981	Toro I	TBD		83.5	129.5	0.644788			
RTMP2002.57.7	'Dry Island *Triceratops*'	HCanyonFm		74[est. 85]	132.6	0.641026			

Dataset 6.S1 (Appendix 7)

HCF *Triceratops* rostra. Blue text indicates juvenile specimens. Rostrum length measured from the anteriormost point of the rostrum to the narial strut. BSL = basal skull length. Measurements for MWC 8574 and RTMP 2002.57.7 taken from photographs. Measurements are in cm.

Specimen no.	Locality Name	HCF Unit	Level	RL	BSL	RL/BSL	Mean	Std. Dev.	Std. Error
MOR 1120	Getaway Trike	L3	upper	28	98	0.285714			
MOR 3045	Cliffhanger	M3	upper	23	100.29	0.229335	0.239667	0.014612	0.0103325
MOR 3027	Yoshi's Trike	M3	upper	27.5	110	0.25			
MOR 1625	Haxby Trike	U3	lower	34	127.06	0.26759	0.244654	0.032436	0.0229358
MOR 2574	Quittin' Time	U3	lower	22.5	101.48	0.221719	0.245583	0.022992	0.013274
MOR 2951	DFJuvieTrike3	U3	lower	14.5	58.6	0.24744			
MOR 004	MORT	U3	upper	33	122	0.270492	0.260778	0.013737	0.0097138
MWC 8574		U3	upper	est. 34.8	138.61	0.251064			
RTMP 2002.57.7*	'Dry Island Triceratops'	HCanyonFm		47	132.604	0.354439			
MOR 1604	Baker Trike	TBD		24	110	0.218182			
MOR 1199	Sierra Trike	TBD		10.3	48.3	0.213251			
MOR 981	Toro I	TBD		47	129.5	0.362934			

Dataset 6.S1 (Appendix 8)

Squamosal Convexity. Squamosal length measured from parietal/squamosal contact to anterolateral projection. Distance to lateral margin of squamosal measured perpendicular to squamosal length measurement, from lateral margin to intersection with squamosal length measurement. In this study, specimens were coded as possessing a convex squamosal if SQL/DtLM was ≤4.

		Unit	SQ Length (cm)	Distance to lateral margin (cm)	SQ L/DtLM
UCMP 154452		U3	11	2.2	5
MOR 1199		TBD	33.5	5.8	5.77586207
MOR 2951		U3	39	10	3.9
MOR 1110	right:	U3	54	14	3.85714286
	left:		61.5	14.5	4.24137931
MOR 1120	left:	L3	78.5	21	3.73809524
	right:		82	19	4.31578947
MOR 3045		M3	76.5	17.8	4.29775281
MOR 3027		M3	84.5	19.8	4.26767677
UCMP 113697		M3	85.5	24.5	3.48979592
MOR 2924		U3	75.6	19.3	3.91709845
MOR 2999	right:	U3	72.5	17.6	4.11931818
	left:		75.5	19	3.97368421
MOR 1625		U3	87.2	22	3.96363636
UCMP 136092		U3	88	22	4
MOR 004		U3	est. 93	24	3.875
MOR 2985		L3	93	21	4.380952
MOR 2702		U3	100	19.5	5.12820513
MOR 3081		L3	108	12.5	8.64
MOR 1122	right:	L3	120	14	8.57142857

Supporting Material References

Anderson J. 1999. Occipital condyle in the ceratopsian dinosaur *Triceratops,* with comments on body size variation. Contributions from the Museum of Paleontology University of Michigan 30(8): 215-231.

Campione N.E., and R.R. Reisz. 2010. *Varanops brevirostris* (Eupelycosauria: Varanopidae) from the Lower Permian of Texas, with discussion of varanopid morphology and interrelationships. Journal of Vertebrate Paleontology 30(3):724-746.

Campione, N.E., K.S. Brink, E.A. Freedman, T. McGarrity, and D.C. Evans. 2013. '*Glishades ericksoni*', an indeterminate juvenile hadrosaurid from the Two Medicine Formation of Montana: implications for hadrosauroid diversity in the latest Cretaceous (Campanian-Maastrichtian) of western North America. Paleobiodiversity and Paleoenvironments 93: 65-75.

Carpenter K., and D.B. Young. 2002. Late Cretaceous dinosaurs from the Denver Basin, Colorado. Rocky Mountain Geology 37(2): 237-254.

Cobabe E.A., and D.E.Fastovsky. 1987. *Ugrosaurus olsoni*, a new ceratopsian (Reptilia: Ornithischia) from the Hell Creek Formation of eastern Montana. Journal of Paleontology 61(1): 148–154.

Currie, P. J., W. Langston Jr, and D. H. Tanke. 2008. A new species of Pachyrhinosaurus (Dinosauria, Ceratopsidae) from the Upper Cretaceous of Alberta, Canada. A New Horned Dinosaur from an Upper Cretaceous Bone Bed in Alberta. Edited by PJ Currie, W. Langston, Jr., and DH Tanke. NRC Research Press, Ottawa 1–108.

Dodson, P., C. A. Forster, and S. D. Sampson. 2004. Ceratopsidae; pp. 494-513 in D. B. Weishampel, P. Dodson, and H. Osmólska (eds.), The Dinosauria. Univ. California Press, Berkeley.

Farke, A. A. 2007. Cranial osteology and phylogenetic relationships of the chasmosaurine ceratopsid *Torosaurus latus*; pp. 235-257 in K. Carpenter (ed.), Horns and Beaks: Ceratopsian and Ornithopod Dinosaurs. Indiana University Press, Bloomington and Indianapolis.

Farke A.A. 2011. Anatomy and taxonomic status of the chasmosaurine ceratopsid *Nedoceratops hatcheri* from the Upper Cretaceous Lance Formation of Wyoming, U.S.A. PLoS One 6(1): e16196.doi:10.1371/journal.pone.0016196.

Farke, A. A., M.J. Ryan, P.M. Barrett, D.H., Tanke, D. R. Braman, M.A. Loewen, and M.R. Graham. 2011. A new centrosaurine from the Late Cretaceous of Alberta, Canada, and the evolution of parietal ornamentation in horned dinosaurs. Acta Palaeontologica Polonica *56*(4): 691-702.

Felsenstein J. 1985. Confidence limits on phylogenies: an approach using the bootstrap. Evolution 39(4): 783-791.

Fisher D.C. 1994. Stratocladistics: morphological and temporal patterns and their relation to phylogenetic process pp. 133-171 in Interpreting the hierarchy of nature: from systematic patterns to evolutionary process theories, L. Grande, and O. Rieppel (eds.) Academic Press, San Diego, California.

Fisher D.C. 2008. Stratocladistics: integrating temporal data and character data in phylogenetic inference. Annual Revieve of Ecology, Evolution, and Systematics (39): 365-385.

Forster, C.A. 1990. The cranial morphology and systematics of *Triceratops* with a preliminary analysis of ceratopsid phylogeny. PhD dissertation. University of Pennsylvania. Philadelphia. PA.

Forster C.A. 1993. Taxonomic validity of the ceratopsid dinosaur *Ugrosaurus olsoni* (Cobabe and Fastovsky). Journal of Paleontology 67(2): 316–318.

Forster C.A. 1996. Species resolution in *Triceratops*: cladistic and morphometric approaches. Journal of Vertebrate Paleontology 16(2): 259-270.

Fowler D.W., J.B. Scannella, and J.R. Horner. 2011. Reassessing ceratopsid diversity using unified frames of reference. Journal of Vertebrate Paleontology 31(5): 111A.

Frederickson J.A., and A.R. Tumarkin-Deratzian. 2014. Craniofacial ontogeny in *Centrosaurus apertus*. PeerJ 2:e252; DOI 10.7717/peerj.252

Fujiwara S., and Y. Takakuwa. 2011. A sub-adult growth stage indicated in the degree of suture co-ossification in *Triceratops*. Bulletin of Gunma Museum of Natural History 15: 1-17.

Gates T.A., and S.D. Sampson. 2007. A new species of *Gryposaurus* (Dinosauria: Hadrosauridae) from the Late Campanian Kaiparowits Formation, southern Utah, USA. Zoological Journal of the Linnean Society 151: 351-376.

Gilmore, C.W. 1946. Reptilian fauna of the North Horn Formation of central Utah. United States Geological Survey Professional Paper 210C: 29-51.

Hicks J.F., K.R. Johnson, J.D. Obradovich, L. Tauxe, and D. Clark. 2002. Magnetostratigraphy and geochronology of the Hell Creek and basal Fort Union Formations of southwestern North Dakota and a recalibration of the age of the Cretaceous-Tertiary boundary, pp. 35-55 in The Hell Creek Formation and the Cretaceous -Tertiary boundary in the northern Great Plains: an integrated continental record of the end of the Cretaceous, J.H. Hartman, K.R. Johnson, and D.J. Nichols (eds.) Geological Society of America Special Paper 361, Boulder, Colorado.

Hicks J.F., K.R. Johnson, J.D. Obradovich, D.P. Miggins, and L. Tauxe. 2003. Magnetostratigraphy of Upper Cretaceous (Maastrichtian) to lower Eocene strata of the Denver Basin, Colorado. Rocky Mountain Geology 38: 1-27.

Holmes R.B., C. Forster, M. Ryan, K.M. Shepherd. 2001. A new species of *Chasmosaurus* (Dinosauria:Ceratopsia) from the Dinosaur Park Formation of Southern Alberta. Canadian Journal of Earth Sciences 38: 1423-1438.

Horner J.R. and, M.B. Goodwin. 2006. Major cranial changes during *Triceratops* ontogeny. Proceedings of the Royal Society B 273: 2757-2761.

Horner J.R. and, M.B. Goodwin. 2008. Ontogeny of cranial epi-ossifications in *Triceratops*. Journal of Vertebrate Paleontology 28(1): 134–144..

Horner J.R., and M.B. Goodwin. 2009. Extreme cranial ontogeny in the upper Cretaceous dinosaur *Pachycephalosaurus*. PLoS ONE 4(10): e7626. doi.10.1371/journal.pone.0007626.

Hunt RK, Lehman, TM (2008) Attributes of the ceratopsian dinosaur *Torosaurus* and new material from the Javelina Formation (Maastrichtian) of Texas. *J Paleo* 82(6): 1127-1138.

Lawson, D.A. 1976. *Tyrannosaurus* and *Torosaurus*, Maestrichtian dinosaurs from Trans-Pecos, Texas. Journal of Paleontology 50(1): 158-164.

Lehman T.M. 1998. A gigantic skull and skeleton of the horned dinosaur *Pentaceratops sternbergi* from New Mexico. Journal of Paleontology 72(5): 894-906.

Lerbekmo J.F. 1999. Magnetostratigraphy of the Canadian continental drilling program Cretaceous-Tertiary (K-T) boundary project core holes, western Canada. Canadian Journal of Earth Sciences 36: 705-715.

Lerbekmo J.F. 2009. Glacioeustatic sea level fall marking the base of supercycle TA-1 at 66.5 Ma recored by the kaolinization of the Whitemud Formation and the Colgate

Member of the Fox Hills Formation. Marine and Petroleum Geology 26: 1299-1303.

Lerbekmo J.F., and D.R. Braman. 2002. Magnetostratigraphic and biostratigraphic correlation of late Campanian and Maastrichtian marine and continental strata from the Red Deer Valley to the Cypress Hills, Alberta, Canada. Canadian Journal of Earth Sciences 39: 539-557.

Longrich N. R. 2010. *Mojoceratops perifania*, a new chasmosaurine ceratopsid from the Late Campanian of Western Canada. Journal of Paleontology 84(4): 681-694.

Longrich N. R. 2011. *Titanoceratops ouranos*, a giant horned dinosaur from the late Campanian of New Mexico. Cretaceous Research 32:264-276.

Longrich N. R., and D.J. Field. 2012. *Torosaurus* Is Not *Triceratops*: Ontogeny in Chasmosaurine Ceratopsids as a Case Study in Dinosaur Taxonomy. PLoS ONE 7(2): e32623.doi:10.1371/journal.pone. 0032623

Maiorino L., A. A. Farke, T. Kotsakis, and P. Piras. 2013. Is *Torosaurus Triceratops*? Geometric morphometric evidence of Late Maastrichtian ceratopsid dinosaurs. PLoS ONE 8(11): e81608: doi:10.1371/journal.pone.0081608

Mallon J. C., R. Holmes, D.A. Eberth, M. J. Ryan, J. S. Anderson. 2011. Variation in the skull of *Anchiceratops* (Dinosauria,Ceratopsidae) from the Horseshoe Canyon Formation (Upper Cretaceous) of Alberta. Journal of Vertebrate Paleontology 31(5): 1047–1071.

Marcot J. D., and D. L. Fox. 2008. StrataPhy: a new computer program for stratocladistic analysis. Palaeontologica Electronica 11:5A.

McDonald A. T., D. G. Wolfe, and J. I. Kirkland. 2010. A new basal hadrosauroid (Dinosauria: Ornithopoda) from the Turonian of New Mexico. Journal of Vertebrate Paleontology 3(3): 799–812.

O'Leary M. A., and S. G. Kaufman. 2008. MorphoBank 2.5: Web application for morphological phylogenetics and taxonomy, http://www.morphobank.org.

Ostrom J. H., and P. Wellnhofer. 1986. The Munich specimen of *Triceratops* with a revision of the genus. *Zitteliana* 14: 111-158.

Ott C. J., and P. L. Larson. 2010. A new, small ceratopsian dinosaur from the latest Cretaceous Hell Creek Formation, northwest South Dakota, United States: a preliminary description pp. 203-218 in New Perspectives on Horned Dinosaurs: The Royal Tyrell Museum Ceratopsian Symposium, M. J. Ryan, B. J. Chinnery-

Allgeier, and D. A. Eberth (eds.) Indiana University Press, Bloomington and Indianapolis.

Pardo J. D., A. K. Huttenlocker, and J. D. Marcot. 2008. Stratocladistics and evaluation of evolutionary modes in the fossil record: an example from the ammonite genus *Semiformiceras*. Palaeontology. 51(4): 767-773.

Pleijel F. 1995. On character coding for phylogeny reconstruction. Cladistics. 11:309-315.

Polly P. D. 1997. Ancestry and species definition in paleontology: stratocladistic analysis of Paleocene-Eocene Viverravidae (Mammalia, Carnivora) from Wyoming. Contributions from the Museum of Paleontology University of Michigan 30(1): 1-53.

Raynolds R. G., and K. R. Johnson. 2003. Synopsis of the stratigraphy and paleontology of the uppermost Cretaceous and lower Tertiary strata in the Denver Basin, Colorado. Rocky Mountain Geology 38**:** 171-181.

Rook D. L., and J. P. Hunter. 2011. Phylogeny of the Taeniodonta: evidence from dental characters and stratigraphy. Journal of Vertebrate Paleontology 31(2): 422-427.

Sampson S. D. 1995. Two new horned dinosaurs from the Upper Cretaceous Two Medicine Formation of Montana; with a phylogenetic analysis of the Centrosauriane (Ornithischia: Ceratopsidae). Journal of Vertebrate Paleontology 15(4): 743-760.

Sampson S. D., M. A. Loewen, A. A. Farke, E. M. Roberts, C. A. Forster, J. A. Smith, and A. L. Titus. 2010. New horned dinosaurs from Utah provide evidence for intracontinental dinosaur endemism. *PLoS ONE* 5(9): e12292. doi:10.1371/journal.pone.0012292.

Scannella J. B., and J.R. Horner. 2010. *Torosaurus* Marsh, 1891, is *Triceratops* Marsh, 1889 (Ceratopsidae: Chasmosaurinae): synonymy through ontogeny. Journal of Vertebrate Paleontology 30(4): 1157-1168.

Scannella J. B., and J. R. Horner. 2011. '*Nedoceratops*': An example of a transitional morphology. *PLoS ONE* 6(12): e28705. doi:10.1371/journal.pone.0028705

Sorenson, M. D., and E. A. Franzosa. 2007. TreeRot, version 3. Boston University, Boston, MA.

Sullivan, R. M., and S. G. Lucas. 2010. A new chasmosaurine (Ceratopsidae, Dinosauria) from the Upper Cretaceous Ojo Alamo Formation (Naashoibito Member), San

Juan Basin, New Mexico, pp. 169-180 in New Perspectives on Horned Dinosaurs: The Royal Tyrell Museum Ceratopsian Symposium, M. J. Ryan, B. J. Chinnery-Allgeier, and D. A. Eberth (eds.) Indiana University Press, Indiana University Press.

Sullivan, R. M., A. C. Boere, and S. G. Lucas. 2005. Redescription of the ceratopsid dinosaur *Torosaurus utahensis* (Gilmore, 1946) and a revision of the genus. Journal of Paleontology 79(3):564–582.

Swofford D. L. 2003. PAUP*. Phylogenetic Analysis Using Parsimony (*and Other Methods). Version 4. Sinauer Associates, Sunderland, Massachusetts.

Tokaryk T. T. 1986. Ceratopsian dinosaurs from the Frenchman Formation (Upper Cretaceous) of Saskatchewan. Canadian Field-Naturalist 100: 192-196.

Tsuihiji T. 2010. Reconstructions of the axial muscle insertions in the occipital region of dinosaurs: evaluations of past hypotheses on marginocephalia and tyrannosauridae using the Extant Phylogenetic Bracket approach. The Anatomical Record 293:1360–1386.

Wu X., D. B. Brinkman, D. A. Eberth, and D. R. Braman. 2007. A new ceratopsid dinosaur (Ornithischia) from the uppermost Horseshoe Canyon Formation (upper Maastrichtian), Alberta, Canada. Canadian Journal of Earth Sciences 44: 1243–1265.

REFERENCES CITED

Achenbach, J. Unveiled: The Surprisingly Small Precursor of T. Rex. Washington Post 18th September 2009. http://www.washingtonpost.com/wp-dyn/content/article/2009/09/17/AR2009091702573.html?hpid=topnews&sid=ST2009091800725. Retrieved 2011 March 8.

Adams, D. C., and E. Otárola-Castillo. 2013. geomorph: an R package for the collection and analysis of geometric morphometric shape data. Methods in Ecology and Evolution 4:393-399.

Aitken, J. F., and S. S. Flint. 1994. High-frequency sequences and the nature of incised-valley fills in fluvial systems of the Breathitt Group (Pennsylvanian), Appalachian foreland basin, eastern Kentucky. 353–368.

Alexander, E. C., G. M. Mickelson, and M. A. Lanphere. 1978. Mmhb-1: a new 40Ar/39Ar dating standard. Short Papers of the Fourth International Conference, Geochronology, Cosmochronology, and Isotope Geology: US Geological Survey Open-File Report 78–701.

Anderson, J. 1999. Occipital condyle in the ceratopsian dinosaur Triceratops, with comments on body size variation. Contributions from the Museum of Paleontology University of Michigan 30(8):215-231.

Anderson, J. S., and H.-D. Sues eds. 2007. Major Transitions in Vertebrate Evolution. Indiana University Press, 432 pp.

Antia, J., and C. R. Fielding. 2011. Sequence stratigraphy of a condensed low-accommodation succession: Lower Upper Cretaceous Dakota Sandstone, Henry Mountains, southeastern Utah. AAPG Bulletin 95:413–447.

Arbour, V. M., M. E. Burns, and R. L. Sissons. 2009. A redescription of the ankylosaurid dinosaur Dyoplosaurus acutosquameus Parks, 1924 (Ornithischia: Ankylosauria) and a revision of the genus. Journal of Vertebrate Paleontology 29:1117–1135.

Archibald, J. D. 1982. A study of Mammalia and geology across the Cretaceous-Tertiary boundary in Garfield County, Montana. University of California Publications in the Geological Sciences 122:1–286.

Archibald, J. D. 2011. Extinction and Radiation: How the Fall of Dinosaurs Led to the Rise of Mammals, 1st ed. The Johns Hopkins University Press, 120 pp.

Archibald, J. D., R. F. Butler, E. H. Lindsay, W. A. Clemens, and L. Dingus. 1982. Upper Cretaceous–Paleocene biostratigraphy and magnetostratigraphy, Hell Creek and Tullock Formations, northeastern Montana. Geology 10:153–159.

Arens, N. C., and A. H. Jahren. 2002. Chemostratigraphic correlation of four fossil-bearing sections in southwestern North Dakota. Geological Society of America Special Papers 361:75–93.

Arens, N. C., A. H. Jahren, and D. C. Kendrick. 2014. Carbon isotope stratigraphy and correlation of plant megafossil localities in the Hell Creek Formation of eastern Montana, USA. Geological Society of America Special Papers 503:149–171.

Atchley, S. C., L. C. Nordt, and S. I. Dworkin. 2004. Eustatic Control on Alluvial Sequence Stratigraphy: A Possible Example from the Cretaceous-Tertiary Transition of the Tornillo Basin, Big Bend National Park, West Texas, U.S.A. Journal of Sedimentary Research 74:391–404.

Aze, T., T. H. Ezard, A. Purvis, H. K. Coxall, D. R. Stewart, B. S. Wade, and P. N. Pearson. 2011. A phylogeny of Cenozoic macroperforate planktonic foraminifera from fossil data. Biological Reviews 86:900–927.

Baadsgaard, H., J. F. Lerbekmo, J. R. Wijbrans, C. C. Swisher III, and M. Fanning. 1993. Multimethod radiometric age for a bentonite near the top of the Baculites reesidei Zone of southwestern Saskatchewan (Campanian–Maastrichtian stage boundary?). Canadian Journal of Earth Sciences 30:769–775.

Baksi, A. K., D. A. Archibald, and E. Farrar. 1996. Intercalibration of 40Ar39Ar dating standards. Chemical Geology 129:307–324.

Baltz, E. H., S. R. Ash, and R. Y. Anderson. 1966. History of nomenclature and stratigraphy of rocks adjacent to the Cretaceous-Tertiary boundary, western San Juan Basin, New Mexico. US Government Printing Office.

Barnosky, A. D. 2001. Distinguishing the effects of the Red Queen and Court Jester on Miocene mammal evolution in the northern Rocky Mountains. Journal of Vertebrate Paleontology 21:172–185.

Barrell, J. 1917. Rhythms and the measurements of geologic time. Bulletin of the Geological Society of America 28:745–904.

Bauer, C. M. 1916. Contributions to the Geology and Paleontology of San Juan County, New Mexico: Part 1. Stratigraphy of a Part of the Chaco River Valley. U.S. Geological Survey Professional Paper.

Bauer, C. M., and J. B. Reeside. 1921. Contributions to Economic Geology, 1920, Part II, Mineral Fuels--Coal in the Middle and Eastern Parts of San Juan County, New Mexico. United States Geological Survey, pp.

Beaumont, E. C., and G. K. Hoffman. 1992. Interrelationships between the upper coal member of the Menefee Formation, the La Ventana Tongue, and the Lewis Shale in the southeastern San Juan Basin, New Mexico. New Mexico: New Mexico Geological Society 43rd Guidebook 207–216.

Beckinsale, R. D., and N. H. Gale. 1969. A reappraisal of the decay constants and branching ratio of 40K. Earth and Planetary Science Letters 6:289–294.

Befus, K. S., R. E. Hanson, T. M. Lehman, and W. R. Griffin. 2008. Cretaceous basaltic phreatomagmatic volcanism in west Texas: maar complex at Pena Mountain, Big Bend National park. Journal of Volcanology and Geothermal Research 173:245–264.

Behringer, D. H. 2008. Geometry, genesis and sequence stratigraphic framework of the Colgate Sandstone Member of the Fox Hills, Garfield County, MT. M.S., Montana State University, Bozeman, Montana, 134 pp.

Bell, P. R. 2011. Cranial Osteology and Ontogeny of Saurolophus angustirostris from the Late Cretaceous of Mongolia with Comments on Saurolophus osborni from Canada. Acta Palaeontologica Polonica 56:703–722.

Belt, E. S., J. F. Hicks, and D. A. Murphy. 1997. A pre-Lancian regional unconformity and its relationship to Hell Creek paleogeography in south-eastern Montana. Rocky Mountain Geology 31:1–26.

Benammi, M., C. M. Ramos, and E. C. Garcia. 2006. Preliminary Magnetostratigraphic Study of the Upper Cretaceous Dinosaur Site from La Barranca Los Bonites, Tiquicheo (Michoacan State, Southern Mexico). Geophysical Research Abstracts 8:10656.

Benson, R. B. J. 2008. New information on *Stokesosaurus*, a tyrannosauroid (Dinosauria: Theropoda) from North America and the United Kingdom. Journal of Vertebrate Paleontology 28:732-750.

Benson, R. B. J., P. M. Barrett, T. H. Rich, and P. Vickers-Rich. 2010. A Southern Tyrant Reptile. Science 327:1613.

Benton, M. J. 2009. The Red Queen and the Court Jester: Species Diversity and the Role of Biotic and Abiotic Factors Through Time. Science 323:728–732.

Benton M.J., and P.N. Pearson. 2001. Speciation in the fossil record. Trends in Ecology and Evolution 16(7): 405-411.

Bercovici, A., V. Vajda, D. Pearson, U. Villanueva-Amadoz, and D. Kline. 2012. Palynostratigraphy of John's Nose, a new Cretaceous–Paleogene boundary section in southwestern North Dakota, USA. Palynology 36:36–47.

Bertog, J. 2011. Stratigraphy of the Lower Pierre Shale (Campanian): Implications for the Tectonic and Eustatic Controls on Facies Distributions. Journal of Geological Research 2010.

Binda, P. L., E. V. Nambudiri, S. K. Srivastava, M. Schmitz, A. Longinelli, and P. Iacumin. 1991. Stratigraphy, paleontology, and aspects of diagenesis of the Whitemud Formation (Maastrichtian) of Alberta and Saskatchewan. AAPG Sixth International Williston Basic Symposium October 7, 8, and 9, 1991:179-192.

Bird, P. 1988. Formation of the Rocky Mountains, Western United States: A Continuum Computer Model. Science 239:1501–1507.

Blair, W. F. 1955. Mating Call and Stage of Speciation in the Microhyla olivacea-M. carolinensis Complex. Evolution 9:469.

Boake, C. R. B., M. P. DeAngelis, and D. K. Andreadis. 1997. Is sexual selection and species recognition a continuum? Mating behavior of the stalk-eyed fly Drosophila heteroneura. Proceedings of the National Academy of Sciences 94:12442–12445.

Boggs, S. 2001. Principles of Sedimentology and Stratigraphy. Prentice Hall, Upper Saddle River, N.J., 568 pp.

Bouligand, C., J. Dyment, Y. Gallet, and G. Hulot. 2006. Geomagnetic field variations between chrons 33r and 19r (83–41 Ma) from sea-surface magnetic anomaly profiles. Earth and Planetary Science Letters 250:541–560.

Bown, T. M., and M. J. Kraus. 1987. Integration of channel and floodplain suites; I, Developmental sequence and lateral relations of alluvial Paleosols. Journal of Sedimentary Research 57:587–601.

Boyd, D. W., and J. A. Lillegraven. 2011. Persistence of the Western Interior Seaway Historical background and significance of ichnogenus Rhizocorallium in Paleocene strata, south-central Wyoming. Rocky Mountain Geology 46:43–69.

Boyle, A. Tiny T. rex? Big surprise! MSNBC News. http://cosmiclog.msnbc.msn.com/archive/2009/09/17/2072603.aspx. Retrieved 2011 March 8.

Braman, D. R. 2001. Terrestrial palynomorphs of the upper santonian-? Lowest campanian milk river formation, Southern Alberta, Canada. Palynology 25:57–107.

Braman, D. R., and A. R. Sweet. 1999. Terrestrial palynomorph biostratigraphy of the Cypress Hills, Wood Mountain, and Turtle Mountain areas (Upper Cretaceous-Paleocene) of western Canada. Canadian Journal of Earth Sciences 36:725–741.

Braman, D. R., and A. R. Sweet. 2012. Biostratigraphically useful Late Cretaceous–Paleocene terrestrial palynomorphs from the Canadian Western Interior sedimentary basin. Palynology 36:8–35.

Braman, D. R., A. R. Sweet, and J. F. Lerbekmo. 1999. Upper Cretaceous - lower Tertiary lithostratigraphic relationships of three cores from Alberta, Saskatchewan, and Manitoba, Canada. Canadian Journal of Earth Sciences 36:669–683.

Breyer, J. A., A. B. Busbey III, R. E. Hanson, K. E. Befus, W. R. Griffin, U. S. Hargrove, and S. C. Bergman. 2007. Evidence for Late Cretaceous Volcanism in Trans-Pecos Texas. The Journal of Geology 115:243–251.

Brink, K. S., D. K. Zelenitsky, D. C. Evans, J. R. Horner, and F. Therrien. 2014. Cranial morphology and variation in Hypacrosaurus stebingeri; pp. 245–266 in Hadrosaurs. Indiana University Press.

Brinkman, D. B. 2003. A review of nonmarine turtles from the Late Cretaceous of Alberta. Canadian Journal of Earth Sciences 40:557–571.

Brinkman, D. B., and A. G. Neuman. 2002. Teleost centra from uppermost Judith River Group (Dinosaur Park Formation, Campanian) of Alberta. Canadian Journal of Paleontology 76:138-155.

Brinkman, D. B., M. J. Ryan, and D. A. Eberth. 1998. The paleogeographic and stratigraphic distribution of ceratopsids (Ornithischia) in the upper Judith River Group of Western Canada. Palaios 13:160–169.

Brochu, C. A. 1996. Closure of neurocentral sutures during crocodilian ontogeny: implications for maturity assessment in fossil archosaurs. Journal of Vertebrate Paleontology 16:49-62.

Brochu, C. A. 2003. Osteology of *Tyrannosaurus rex*: Insights from a nearly complete skeleton and high-resolution computed tomographic analysis of the skull. Journal of Vertebrate Paleontology Memoir 7:1-138.

Brookins, D. G., and J. K. Rigby. 1987. Geochronologic and geochemical study of volcanic ashes from the Kirtland Shale (Cretaceous), San Juan Basin, New Mexico. Geological Society of America Special Papers 209:105–110.

Brown, B. 1907. The Hell Creek beds of the Upper Cretaceous of Montana□: their relation to contiguous deposits, with faunal and floral lists, and a discussion of their correlation. Bulletin of the American Museum of Natural History 823–845.

Brown, B. 1910. The Cretaceous Ojo Alamo Beds of New Mexico: With Description of the New Dinosaur Genus Kritosaurus. Bulletin of the American Museum of Natural History 267–274.

Brown, B. 1913a. A new trachodont dinosaur, Hypacrosaurus, from the Edmonton Cretaceous of Alberta. Bulletin of the American Museum of Natural History 32:395–406.

Brown, B. 1913b. The Skeleton of Saurolophus: A Crested Duck-billed Dinosaur from the Edmonton Cretaceous. Bulletin of the American Museum of Natural History 32:387–393.

Brown, B. 1914a. Anchiceratops, a New Genus of Horned Dinosaurs from the Edmonton Cretaceous of Alberta. With Discussion of the Origin of the Ceratopsian Crest and the Brain Casts of Anchiceratops and Trachodon. Bulletin of the American Museum of Natural History 33:539–548.

Brown, B. 1914b. Corythosaurus Casuarius, a New Crested Dinosaur from the Belly River Cretaceous: With Provisional Classification of the Family Trachodontidae. Bulletin of the American Museum of Natural History.

Brown, B. 1914c. Leptoceratops, a new genus of Ceratopsia from the Edmonton Cretaceous of Alberta. Bulletin of the American Museum of Natural History 33:567–580.

Brown, B. 1916. A new crested trachodont dinosaur Prosaurolophus maximus. Bulletin of the American Museum of Natural History 35:701–708.

Brown, B. 1917. A complete skeleton of the horned dinosaur Monoclonius, and a description of a second skeleton showing skin impressions. Bulletin of the American Museum of Natural History 37: 281–306.

Brown, B. 1933. A new longhorned Belly River ceratopsian. American Museum Novitates 669:1-3.

Brown, B., and E. Schlaikjer. 1940. The structure and relationships of *Protoceratops*. Annals of the New York Academy of Sciences 40:133-266.

Brown, B., and E. M. Schlaikjer. 1942. The skeleton of Leptoceratops with the description of a new species. American Museum Novitates 1169:1–15.

Brown, C. M., A. P. Russell, and M. J. Ryan. 2009. Pattern and transition of surficial bone texture of the Centrosaurine frill and their ontogenetic and taxonomic implications. Journal of Vertebrate Paleontology 29:132-141.

Brown, C. M., and D. M. Henderson. 2015. A New Horned Dinosaur Reveals Convergent Evolution in Cranial Ornamentation in Ceratopsidae. Current Biology 25:1641–1648.

Brown, C. M., A. P. Russell, and M. J. Ryan. 2009. Pattern and transition of surficial bone texture of the centrosaurine frill and their ontogenetic and taxonomic implications. Journal of Vertebrate Paleontology 29:132-141.

Brown, R. W. 1948. The Cretaceous-Eocene boundary in Montana and North Dakota. Washington Academy of Sciences Proceedings 28:421–422.

Brown, R. W. 1962. Paleocene Flora of the Rocky Mountains and Great Plains. United State Geological Survey Professional Paper 375. 119 pp.

Brownfield, M. E., and E. A. Johnson. 2008. The Yampa Bed-A Regionally Extensive Tonstein in the Williams Fork Formation, Northwestern Piceance Creek and Southern Sand Wash Basins, Colorado. Geological Survey (US), pp.

Brusatte, S. L., T. D. Carr, G. M. Erickson, G. S. Bever, and M. A. Norell. 2010. A long-snouted, multihorned tyrannosaurid from the Late Cretaceous of Mongolia. Proceedings of the National Academy of Science 106:17261-17266.

Buatois, L. A., and M. G. Mángano. 2004. Animal-substrate interactions in freshwater environments: applications of ichnology in facies and sequence stratigraphic analysis of fluvio-lacustrine successions. Geological Society, London, Special Publications 228:311–333.

Burgess, P. M. 2008. Phanerozoic evolution of the sedimentary cover of the North American craton. Sedimentary Basins of the World 5:31–63.

Butler, R. D. 1980. Stratigraphy, sedimentology, and depositional environments of the Hell Creek Formation (Late Cretaceous) and adjacent strata, Glendive area, Montana. Ph.D, University of North Dakota, Grand Forks, North Dakota, 398 pp.

Butler, R. F., and E. H. Lindsay. 1985. Mineralogy of Magnetic Minerals and Revised Magnetic Polarity Stratigraphy of Continental Sediments, San Juan Basin, New Mexico. The Journal of Geology 93:535–554.

Bybee, P. J., A. H. Lee, and E. Lamm. 2006. Sizing the Jurassic theropod dinosaur *Allosaurus*: assessing growth strategy and evolution of ontogenetic scaling of limbs. Journal of Morphology 267:347-359.

Calvert, W. R., C. F. Bowen, F. A. Herald, J. H. Hance, E. Stebinger, and A. L. Beekly. 1912. Geology of certain lignite fields in eastern Montana. U.S. Geological Survey Bulletin 471:187–201.

Campbell, J. A. 2015. A reassessment of the horned dinosaur *Judiceratops tigris* (Ornithischia: Ceratopsidae) from the Upper Cretaceous (Campanian) of Montana, USA. Canadian Journal of Earth Sciences 52:85-95.

Campbell, J. A., M. J. Ryan, R. B. Holmes, and C. J. Schröder-Adams. 2016. A Re-Evaluation of the Chasmosaurine Ceratopsid Genus Chasmosaurus (Dinosauria: Ornithischia) from the Upper Cretaceous (Campanian) Dinosaur Park Formation of Western Canada. PLoS ONE 11:e0145805.

Campbell, J. A., M. J. Ryan, C. J. Schröder-Adams, and R. B. Holmes. 2015: Evolutionary trends in *Vagaceratops* (Ornithischia: Ceratopsidae) and the status of *Kosmoceratops* in the Upper Cretaceous (Campanian) Dinosaur Park Formation of Alberta. Society of Vertebrate Paleontology Annual Meeting, Dallas, Texas, 2015.

Campbell, J., M. J. Ryan, C. Schröder-Adams, R. B. Holmes, and D. C. Evans. 2013: A specimen-based phylogenetic analysis of the chasmosaurine ceratopsid *Chasmosaurus* (Ornithischia) form the Upper Cretaceous (Campanian) Dinosaur Park Formation of western Canada suggests the validity of only one species. Society of Vertebrate Paleontology 73rd Annual Meeting, Abstracts of Papers, Los Angeles, 2013.

Campione, N. E., and D. C. Evans. 2011. Cranial Growth and Variation in Edmontosaurs (Dinosauria: Hadrosauridae): Implications for Latest Cretaceous Megaherbivore Diversity in North America. PLoS ONE 6:e25186.

Campione N.E., and R.R. Reisz. 2010. *Varanops brevirostris* (Eupelycosauria: Varanopidae) from the Lower Permian of Texas, with discussion of varanopid morphology and interrelationships. Journal of Vertebrate Paleontology 30(3):724-746.

Campione, N. E., K. S. Brink, E. A. Freedman, C. T. McGarrity, and D. C. Evans. 2013. '*Glishades ericksoni*', an indeterminate juvenile hadrosaurid from the Two Medicine Formation of Montana: implications for hadrosauroid diversity in the latest Cretaceous (Campanian-Maastrichtian) of western North America. Palaeobiodiversity and Palaeoenvironments 93:65-75.

Cantrell, A. K., T. L. Suazo, S. G. Lucas, and R. M. Sullivan. 2013. Preliminary Report Of A Nearly Complete Juvenile Pentaceratops From The Upper Cretaceous Kirtland Formation (Hunter Wash Member), San Juan Basin, New Mexico. New Mexico Geological Society 17.

Carpenter, K., and D.B. Young. 2002. Late Cretaceous dinosaurs from the Denver Basin, Colorado. Rocky Mountain Geology 37(2): 237–254.

Carpenter, K., C. Miles, and K. Cloward. 2005. New small theropod from the Upper Jurassic Morrison Formation of Wyoming; pp. 23-48 in K. Carpenter (ed.), The Carnivorous Dinosaurs. Indiana University Press, Bloomington.

Carr, I. D., R. L. Gawthorpe, C. A. Jackson, I. R. Sharp, and A. Sadek. 2003. Sedimentology and sequence stratigraphy of early syn-rift tidal sediments: the Nukhul Formation, Suez Rift, Egypt. Journal of Sedimentary Research 73:407–420.

Carr, T. D. 1999. Craniofacial ontogeny in Tyrannosauridae (Dinosauria, Coelurosauria). Journal of Vertebrate Paleontology 19:497-520.

Carr, T. D., and T. E. Williamson. 2004. Diversity of Late Maastrichtian Tyrannosauridae (Dinosauria: Theropoda) from western North America. Zoological Journal of the Linnean Society-London 142:419-523.

Carr, T. D., T. E. Williamson, and D. E. Schwimmer. 2005. A new genus and species of tyrannosaurid from the Late Cretaceous (Middle Campanian) Demopolis Formation of Alabama. Journal of Vertebrate Paleontology 25:119-143.

Case, T. J. 1978. Speculation on the growth rate and reproduction of some dinosaurs. Paleobiology 4:320-328.

Castellano, S., and P. Cermelli. 2006. Reconciling sexual selection to species recognition: A process-based model of mating decision. Journal of Theoretical Biology 242:529–538.

Catuneanu, O. 2006. Principles of Sequence Stratigraphy. Elsevier Science, Amsterdam, 375 pp.

Catuneanu, O., and A. R. Sweet. 1999. Maastrichtian-Paleocene foreland-basin stratigraphies, western Canada: a reciprocal sequence architecture. Canadian Journal of Earth Sciences 36:685–703.

Catuneanu, O., M. A. Khalifa, and H. A. Wanas. 2006. Sequence stratigraphy of the Lower Cenomanian Bahariya Formation, Bahariya Oasis, Western Desert, Egypt. Sedimentary Geology 190:121–137.

Catuneanu, O., V. Abreu, J. P. Bhattacharya, M. D. Blum, R. W. Dalrymple, P. G. Eriksson, C. R. Fielding, W. L. Fisher, W. E. Galloway, M. R. Gibling, K. A. Giles, J. M. Holbrook, R. Jordan, C. G. S. C. Kendall, B. Macurda, O. J. Martinsen, A. D. Miall, J. E. Neal, D. Nummedal, L. Pomar, H. W. Posamentier, B. R. Pratt, J. F. Sarg, K. W. Shanley, R. J. Steel, A. Strasser, M. E. Tucker, and C. Winker. 2009. Towards the standardization of sequence stratigraphy. Earth-Science Reviews 92:1–33.

Cebula, G. T., M. J. Kunk, H. H. Mehnert, C. W. Naeser, J. D. Obradovich, and J. F. Sutter. 1986. The Fish Canyon Tuff, a potential standard for the 40Ar-39Ar and fission-track dating methods. Terra Cognita 6:139–140.

Chen, D., C. W. Langenberg, and A. P. Beaton. 2005. Horseshoe Canyon-Bearpaw Transition and Correlation of Associated Coal Zones across the Alberta Plains. Alberta Energy and Utilities Board: Alberta Geological Survey, Edmonton, Alberta, 22 pp.

Chinnery, B. 2004. Description of Prenoceratops pieganensis gen. et sp. nov. (Dinosauria: Neoceratopsia) from the Two Medicine Formation of Montana. Journal of Vertebrate Paleontology 24:572–590.

Chinnery, B. J., and D. B. Weishampel. 1998. Montanoceratops cerorhynchus (Dinosauria: Ceratopsia) and relationships among basal neoceratopsians. Journal of Vertebrate Paleontology 18:569–585.

Chinnery, B. J., and J. R. Horner. 2007. A new neoceratopsian dinosaur linking North American and Asian taxa. Journal of Vertebrate Paleontology 27:625–641.

Christensen, A. E. 2005. Sequence Stratigraphy, Sedimentology and Provenance of the Drip Tank Member, Straight Cliffs Formation, Kaiparowits Plateau, Southwestern Utah. .

Christensen, W. K. 1996. A review of the Upper Campanian and Maastrichtian belemnite biostratigraphy of Europe. Cretaceous Research 17:751–766.

Cifelli, R. L., J. J. Eberle, D. L. Lofgren, J. A. Lillegraven, and W. A. Clemens. 2004. Mammalian biochronology of the latest Cretaceous; pp. 21–42 in M. O. Woodburne (ed.), Late Cretaceous and Cenozoic Mammals of North America. Columbia University Press, New York.

Clark, J. 2009. Becoming *T. rex*. Science 326:373-374.

Clemens, W. A. 1963. Fossil mammals of the type Lance Formation Wyoming Part I: Introduction and Multituberculata. University of California Publications in the Geological Sciences 48:1–105.

Clemens, W. A. 1994. Continental vertebrates from the Late Cretaceous of the North Slope, Alaska. 1992 Proceedings International Conference on Arctic Margins: Outer Continental Shelf Study, Mineral Management Service 94–0040.

Clemens, W. A., and J. D. Archibald. 1980. Evolution of terrestrial faunas during the Cretaceous-Tertiary transition. Société Géologique de France, Mémoires 139:67–74.

Cleveland, D. M., S. C. Atchley, and L. C. Nordt. 2007. Continental Sequence Stratigraphy of the Upper Triassic (Norian–Rhaetian) Chinle Strata, Northern New Mexico, U.S.A.: Allocyclic and Autocyclic Origins of Paleosol-Bearing Alluvial Successions. Journal of Sedimentary Research 77:909–924.

Cobabe, E.A., and D.E. Fastovsky. 1987. *Ugrosaurus olsoni*, a new ceratopsian (Reptilia: Ornithischia) from the Hell Creek Formation of eastern Montana: Journal of Paleontology 61 (1):148–154.

Cobban, W. A. 1950. Telegraph Creek Formation of Sweetgrass Arch, north-central Montana. American Association of Petroleum Geologists Bulletin 34.

Cobban, W. A. 1955. Cretaceous Rocks of Northwestern Montana. Billings Geological Society: Guidebook: Sixth Annual Field Conference 107–119.

Cobban, W. A. 1969. The Late Cretaceous ammonites Scaphites leei Reeside and Scaphites hippocrepis (DeKay) in the western interior of the United States. United States Geological Survey, Professional Paper.

Cobban, W. A. 1993. Diversity and distribution of Late Cretaceous ammonites, Western Interior, United States. Evolution of the Western Interior Basin: Geological Association of Canada Special Paper 39:435–451.

Cobban, W. A., and J. B. Reeside. 1952. Correlation of the Cretaceous formations of the Western Interior of the United States. Geological Society of America Bulletin 63:1011–1044.

Cobban, W. A., E. A. Merewether, T. D. Fouch, and J. D. Obradovich. 1994. Some Cretaceous shorelines in the western interior of the United States. In Caputo, M. V., Peterson, J. A., and Frenczyk, K. J., eds., Mesozoic Systems of the Rocky Mountain Region, USA: Rocky Mountain Section, Society of Economic Paleontologists and Mineralogists, Society for Sedimentary Geology:393-414.

Cobban, W. A., I. Walaszczyk, J. D. Obradovich, and K. C. McKinney. 2006. USGS Zonal Table for the Upper Cretaceous Middle Cenomanian-Maastrichtian of the Western Interior of the United States Based on Ammonites, Inoceramids, and Radiometric Ages. United States Geological Survey.

Cochran, J. K., N. H. Landman, K. K. Turekian, A. Michard, and D. P. Schrag. 2003. Paleoceanography of the late cretaceous (Maastrichtian) Western Interior Seaway of North America: evidence from Sr and O isotopes. Palaeogeography, Palaeoclimatology, Palaeoecology 191:45–64.

Collier, A. J., and M. M. Knechtel. 1939. Coal resources of McCone County, Montana. U.S. Geological Survey Bulletin 905:1–80.

Cook, O. F. 1906. Factors of species-formation. Science 23:506–507.

Coney, P. J., and S. J. Reynolds. 1977. Cordilleran Benioff zones. Nature 270:403–406.

Connor, C. W. 1992. The Lance Formation; Petrography and Stratigraphy, Powder River Basin and Nearby Basins, Wyoming and Montana. United States Geological Survey Bulletin 1917-I:17 pp.

Conrad, J. E., E. H. Mackee, and B. D. Turrin. 1992. Age of Tephra Beds at the Ocean Point Dinosaur Locality, North Slope, Alaska, Based on K-Ar and 40Ar/39Ar Analyses. U.S. Geological Survey Bulletin, pp.

Cross, W. 1909. The Laramie Formation and the Shoshone Group. Washington Academy of Sciences, Proceedings 11:27–45.

Cross, A. T., and M. S. Yi. 1997. Palynology and a review of vertebrate faunas of the Late Cretaceous-Paleocene North Horn Formation, Price Canyon, Wasatch Plateau and environs, Utah, USA. Dinofest International, Academy of Natural Sciences, Philadelphia 417–455.

Csiki, Z., M. Vremir, S. L. Brusatte, and M. A. Norell. 2010. An aberrant island-dwelling theropod dinosaur from the Late Cretaceous of Romania. Proceedings of the National Academy of Science 107:15357-15361.

Cullins, H. L. 1971. Geologic Map of the Rangely Quadrangle, Rio Blanco County, Colorado. United States Geological Survey, pp.

Currie, P. J. 2003a. Allometric growth in tyrannosaurids (Dinosauria: Theropoda) from the Upper Cretaceous of North America and Asia. Canadian Journal of Earth Sciences 40:651-665.

Currie, P. J. 2003b. Cranial anatomy of tyrannosaurid dinosaurs from the Late Cretaceous of Alberta, Canada. Acta Palaeontolgica Polonica 48:191-226.

Currie, P. J., and Z. Dong. 2001. New information on *Shanshanosaurus huoyanshanensis*, a juvenile tyrannosaurid (Theropoda, Dinosauria) from the Late Cretaceous of China. Canadian Journal of Earth Sciences 38:1729-1737.

Currie, P. J., and D. A. Eberth. 1993. Palaeontology, sedimentology, and palaeoecology of the Iren Dabasu Formation (Upper Cretaceous), Inner Mongolia, People's Republic of China. Cretaceous Research 14:127-144.

Currie, P. J., and D. A. Russell. 2005. The geographic and stratigraphic distribution of articulated and associated dinosaur remains; pp. 537–569 in P. J. Currie and E. B. Koppelhus (eds.), Dinosaur Provincial Park. Indiana University Press, Bloomington, Indiana.

Currie, P. J., W. Langston Jr, and D. H. Tanke. 2008. A new species of Pachyrhinosaurus (Dinosauria, Ceratopsidae) from the Upper Cretaceous of Alberta, Canada; pp. 1–108 in P. J. Currie and W. Langston Jr (eds.), A New Horned Dinosaur from an Upper Cretaceous Bone Bed in Alberta. NRC Research Press, Ottawa, Ontario, Canada.

Daeschler, E. B., N. H. Shubin, and F. A. Jenkins. 2006. A Devonian tetrapod-like fish and the evolution of the tetrapod body plan. Nature 440:757-763.

Dalrymple, G. B., and W. A. Duffield. 1988. High precision 40Ar/39Ar dating of Oligocene rhyolites from the Mogollon-Datil Volcanic Field using a continuous laser system. Geophysical Research Letters 15:463–466.

Darwin, C. 1859. The Origin of Species by Means of Natural Selection. John Murray, London.

Darwin, C. 1871. The Descent of Man and Selection in Relation to Sex. John Murray, London.

Davies, J. H. F. L., J.-F. Wotzlaw, A. P. Wolfe, and L. M. Heaman. 2014. Assessing the age of the Late Cretaceous Danek Bonebed with U–Pb geochronology. Canadian Journal of Earth Sciences 51:982–986.

Davies, K. L. 1983. Hadrosaurian dinosaurs of Big Bend National Park, Brewster County, Texas. M.A., The University of Texas at Austin, 235 pp.

Dawkins, R. 1986. The Blind Watchmaker: Why the Evidence of Evolution Reveals a Universe without Design. WW Norton & Company, 227 pp.

Dawson, F. M., W. D. Kalkreuth, and A. R. Sweet. 1994a. Stratigraphy and Coal Resource Potential of the Upper Cretaceous to Tertiary Strata of Northwestern Alberta. Geological Survey of Canada, pp.

Dawson, F. M., C. G. Evans, R. Marsh, and R. Richardson. 1994b. Uppermost Cretaceous and Tertiary strata of the Western Canada sedimentary basin. Geological Atlas of the Western Canadian Sedimentary Basin. G. Mossop and I. Shetsen (comps.). Canadian Society of Petroleum Geologists and Alberta Research Council 387–406.

DeCelles, P. G. 2004. Late Jurassic to Eocene evolution of the Cordilleran thrust belt and foreland basin system, western U.S.A. American Journal of Science 304:105–168.

DeCelles, P. G., and K. A. Giles. 1996. Foreland basin systems. Basin Research 8:105–123.

Decker, P. L. 2007. Brookian Sequence Stratigraphic Correlations, Umiat Field to Milne Point Field, West-Central North Slope, Alaska. Division of Geological & Geophysical Surveys, 19 pp.

Deibert, J. E., and B. H. Breithaupt. 2006. Ferdinand v. Hayden's 1868 "huge bird" tracks in the upper Cretaceous Almond Formation: field evidence for the first dinosaur fossil discovered in Wyoming. Late Cretaceous Vertebrates from the Western Interior: Bulletin 35 35:69.

Denson, N. M. 1950. The Lignite Deposits of the Cheyenne River and Standing Rock Indian Reservations, Corson, Dewey, and Ziebach Counties, South Dakota and Sioux County, North Dakota. U.S. Geological Survey Circular 78:1–22.

Dickinson, W. R., and W. S. Snyder. 1978. Plate tectonics of the Laramide orogeny. Geological Society of America Memoir 151:355–366.

Dickinson, W. R., M. A. Klute, M. J. Hayes, S. U. Janecke, E. R. Lundin, M. A. McKittrick, and M. D. Olivares. 1988. Paleogeographic and paleotectonic setting of Laramide sedimentary basins in the central Rocky Mountain region. Geological Society of America Bulletin 100:1023–1039.

Diem, S., and J. D. Archibald. 2005. Range extension of southern chasmosaurine Ceratopsian dinosaurs into northwestern Colorado. Journal of Paleontology 79:251–258.

Difley, R. 2007. Biostratigraphy of the North Horn Formation at North Horn Mountain, Emery County, Utah. Central Utah: Diverse Geology of a Dynamic Landscape 439–454.

Difley, R., and A. A. Ekdale. 1999. Biostratigraphic aspects of the Cretaceous-Tertiary (KT) boundary interval at North Horn Mountain, Emery County, Utah. Vertebrate Paleontology in Utah. Utah Geological Survey Miscellaneous Publication. Utah Geological Survey, Salt Lake City 389–398.

Difley, R. L., and A. A. Ekdale. 2002. Footprints of Utah's Last Dinosaurs: Track Beds in the Upper Cretaceous (Maastrichtian) North Horn Formation of the Wasatch Plateau, Central Utah. PALAIOS 17:327–346.

Dilkes, D. W. 2001. An ontogenetic perspective on locomotion in the Late Cretaceous dinosaur Maiasaura peeblesorum (Ornithischia: Hadrosauridae). Canadian Journal of Earth Sciences 38:1205-1227.

Dingus, L., and M.A. Norell 2010. Barnum Brown: The Man Who Discovered *Tyrannosaurus rex*. University of California Press, Berkeley, California, 368 pp.

Dobbin, C. E., and J. B. Reeside. 1929. The Contact of the Fox Hills and Lance Formations. US Government Printing Office, pp.

Dobzhansky, T. 1940. Speciation as a stage in evolutionary divergence. American Naturalist 74:312–321.

Dodson, P. 1975. Taxonomic implications of relative growth in Lambeosaurine hadrosaurs. Systematic Zoology 24:37-54.

Dodson, P. 1976. Quantitative aspects of relative growth and sexual dimorphism in *Protoceratops*.

Dodson, P. 1986. Avaceratops lammersi: A New Ceratopsid from the Judith River Formation of Montana. Proceedings of the Academy of Natural Sciences of Philadelphia 138:305–317.

Dodson, P. 1996. The Horned Dinosaurs. Princeton University Press, Princeton, New Jersey, 346 pp.

Dodson, P. 1997. Neoceratopsia; pp. 473-478 in P. J. Currie and K. Padian (eds.), Encyclopedia of Dinosaurs. Academic Press, San Diego.

Dodson, P., and P. J. Currie. 1988. The smallest ceratopsid skull - Judith River Formation of Alberta. Canadian Journal of Earth Sciences 25:926-930.

Dodson, P., and P. J. Currie. 1990. Neoceratopsia; pp. 593-618 in in D. B. Weishampel, P. Dodson, and H. Osmolska (eds.), The Dinosauria. Univ. Calif. Press, Berkeley, CA.

Dodson, P., C. A. Forster, and S. D. Sampson. 2004. Ceratopsidae; pp. 494-513 in D. B. Weishampel, P. Dodson, and H. Osmolska (eds.), The Dinosauria. University of California Press, Berkeley.

Doelling, H. H. 1997. Interim geologic map of the Smoky Mountain 30'x 60'Quadrangle. Utah Geological Survey Open-File Report 359.

Dong, Z. 1977. On the dinosaurian remains from Turpan, Xinjiang. Vertebrata PalAsiatic 15:59-66.

Duffield, W. A., and G. B. Dalrymple. 1990. The Taylor Creek Rhyolite of New Mexico: a rapidly emplaced field of lava domes and flows. Bulletin of Volcanology 52:475–487.

Eaton, J. G. 1991. Biostratigraphic framework for the Upper Cretaceous rocks of the Kaiparowits Plateau, southern Utah. Geological Society of America Special Papers 260:47–64.

Eaton, J. G. 2002. Multituberculate Mammals from the Wahweap (Campanian, Aquilan) and Kaiparowits (Campanian, Judithian) Formations, within and near Grand Staircase-Escalante National Monument, Southern Utah. Utah Geological Survey Miscellaneous Publication 02-4, 66 pp.

Eaton, J. G. 2006. Santonian (late Cretaceous) mammals from the John Henry Member of the Straight Cliffs Formation, Grand Staircase-Escalante National Monument, Utah. Journal of Vertebrate Paleontology 26:446–460.

Eaton, J. G., and R. L. Cifelli. 1988. Preliminary report on Late Cretaceous mammals of the Kaiparowits Plateau, southern Utah. Rocky Mountain Geology 26:45–55.

Eaton, J. G., S. Diem, J. D. Archibald, C. Schierup, and H. Munk. 1999. Vertebrate paleontology of the Upper Cretaceous rocks of the Markagunt Plateau, southwestern Utah. Vertebrate Paleontology in Utah 99:323–334.

Eaton, J. G., J. Laurin, J. I. Kirkland, N. E. Tibert, R. M. Leckie, B. B. Sageman, P. M. Goldstrand, D. W. Moore, A. W. Straub, W. A. Cobban, and others. 2001. Cretaceous and Early Tertiary Geology of Cedar and Parowan Canyons, Western Markagunt Plateau, Utah Utah Geological Association Field Trip Road Log September, 2001. The Geologic Transition, High Plateaus to Great Basin - A Symposium and Field Guide.

Eberth, D. A. 1990. Stratigraphy and sedimentology of vertebrate microfossil sites in the uppermost Judith River Formation (Campanian), Dinosaur Provincial Park, Alberta, Canada. Palaeogeography, Palaeoclimatology, Palaeoecology 78:1–36.

Eberth, D. A. 1996. Origin and significance of mud-filled incised valleys (Upper Cretaceous) in southern Alberta, Canada. Sedimentology 43:459–477.

Eberth, D. A. 2005. The Geology; pp. 54–82 in Dinosaur Provincial Park: A spectacular ancient ecosystem revealed. Indiana University Press.

Eberth, D. A. 2010. A revised regional stratigraphy and stratigraphic architecture for the Horseshoe Canyon Formation: outcrop and subsurface. Field Trip 14, May 17–18, 2010.

Eberth, D. A. 2011. A Revised Chronostratigraphy for the Oldman, Dinosaur Park and Bearpaw formations at Dinosaur Provincial Park, Alberta, Canada. Speaker Series, Royal Tyrrell Museum, Drumheller, Alberta.

Eberth, D. A., and P. R. Bell. 2014. Stratigraphy of the Danek Bonebed (Upper Cretaceous Horseshoe Canyon Formation, central Alberta) and correlations with strata in the Drumheller and Grande Prairie regions. Canadian Journal of Earth Sciences 51:975–981.

Eberth, D. A., and D. R. Braman. 2012. A revised stratigraphy and depositional history for the Horseshoe Canyon Formation (Upper Cretaceous), southern Alberta plains. Canadian Journal of Earth Sciences 49:1053–1086.

Eberth, D. A., and A. L. Deino. 1992. A geochronology of the non-marine Judith River Formation of southern Alberta. SEPM Theme Meeting, Mesozoic of the Western Interior 24–25.

Eberth, D. A., and A. Deino. 2005. New 40Ar/39Ar ages from three bentonites in the Bearpaw, Horseshoe Canyon, and Scollard formations (Upper Cretaceous-

Paleocene) of southern Alberta, Canada. Dinosaur Park Symposium: Short Papers, Abstracts, and Program. Royal Tyrrell Museum of Paleontology, Drumheller, Alberta 23–24.

Eberth, D. A., and A. P. Hamblin. 1993. Tectonic, stratigraphic, and sedimentologic significance of a regional discontinuity in the upper Judith River Group (Belly River wedge) of southern Alberta, Saskatchewan, and northern Montana. Canadian Journal of Earth Sciences 30:174–200.

Eberth, D. A., D. Brinkman, and S. M. Kwasniowski. 1994. Sequence Stratigraphy, Depositional Environments and Paleoecology of the Judith River Group (Upper Cretaceous), Southern Alberta. Society of Petroleum Geologists Field guide PR-3, Calgary, Alberta, 69 pp.

Eberth, D. A., R. G. Thomas, and A. Deino. 1992. Preliminary K-Ar dates from bentonites in the Judith River and Bearpaw Formations (Upper Cretaceous) of Dinosaur Provincial park, southern Alberta, Canada. Aspects of Nonmarine Cretaceous Geology. China Ocean Press, Beijing 296–304.

Eberth, D. A., C. R. D. de Jesús, R. A. R. de la Rosa, J. F. Lerbekmo, D. B. Brinkman, and S. D. Sampson. 2004. Cerro del Pueblo Fm (Difunta Group, Upper Cretaceous), Parras Basin, southern Coahuila, Mexico: reference sections, age, and correlation. Revista Mexicana de Ciencias Geológicas 21:335–352.

Eberth, D. A., D. C. Evans, D. B. Brinkman, F. Therrien, D. H. Tanke, and L. S. Russell. 2013. Dinosaur biostratigraphy of the Edmonton Group (Upper Cretaceous), Alberta, Canada: evidence for climate influence. Canadian Journal of Earth Sciences 50:701–726.

Eberth, D. A., D. B. Brinkman, P.-J. Chen, F.-T. Yuan, S.-Z. Wu, G. Li, and X.-S. Cheng. 2001. Sequence stratigraphy, paleoclimate patterns, and vertebrate fossil preservation in Jurassic–Cretaceous strata of the Junggar Basin, Xinjiang Autonomous Region, People's Republic of China. Canadian Journal of Earth Sciences 38:1627–1644.

Eldredge, N., and S. J. Gould. 1972. Punctuated equilibria: an alternative to phyletic gradualism; pp. 82-115 in T. J. M. Schopf (ed.), Models in Paleobiology. Freeman, Cooper and Co., San Francisco.

Endt, P. M. 1990. Energy levels of A= 21–44 nuclei (VII). Nuclear Physics A 521:1–400.

Endt, P. M., and C. Van der Leun. 1973. Energy levels of A= 21-44 nuclei (V). Nuclear Physics A 214:1–625.

English, J. M., and S. T. Johnston. 2004. The Laramide Orogeny: What Were the Driving Forces? International Geology Review 46:833–838.

Erickson, G. M., P. J. Makovicky, P. J. Currie, M. A. Norell, S. A. Yerby, and C. A. Brochu. 2004. Gigantism and comparative life-history parameters of tyrannosaurid dinosaurs. Nature 430:772-775.

Evans, D. C., and R. R. Reisz. 2007. Anatomy and relationships of Lambeosaurus magnicristatus, a crested hadrosaurid dinosaur (Ornithischia) from the Dinosaur Park Formation, Alberta. Journal of Vertebrate Paleontology 27:373–393.

Evans, D. C., and M. J. Ryan. 2015. Cranial Anatomy of Wendiceratops pinhornensis gen. et sp. nov., a Centrosaurine Ceratopsid (Dinosauria: Ornithischia) from the Oldman Formation (Campanian), Alberta, Canada, and the Evolution of Ceratopsid Nasal Ornamentation. PLOS ONE 10:e0130007.

Evans, D. C., C. A. Forster, and R. R. Reisz. 2005. The type specimen of Tetragonosaurus erectofrons (Ornithischia: Hadrosauridae) and the identification of juvenile Lambeosaurines; pp. 349–366 in P. J. Currie and E. B. Koppelhus (eds.), Dinosaur Provincial Park: A Spectacular Ancient Ecosystem Revealed. Indianapolis, Indiana University Press, Bloomington, Indianapolis.

Evans, D. C., R. R. Reisz, and K. Dupuis. 2007. A juvenile Parasaurolophus (Ornithischia: Hadrosauridae) Braincase from Dinosaur Provincial Park, Alberta, with comments on crest ontogeny in the genus. Journal of Vertebrate Paleontology 27:642–650.

Evans, D. C., R. Bavington, and N. E. Campione. 2009. An unusual hadrosaurid braincase from the Dinosaur Park Formation and the biostratigraphy of Parasaurolophus (Ornithischia: Lambeosaurinae) from southern Alberta. Canadian Journal of Earth Sciences 46:791–800.

Evans, D., P. Currie, D. Eberth, and M. Ryan. 2006. High-resolution lambeosaurine dinosaur biostratigraphy, Dinosaur Park Formation: Sexual dimorphism reconsidered. Journal of Vertebrate Paleontology 26 Supplement: 59A.

Evans, D. C., L. M. Witmer, and J. R. Horner. 2011: A new low-crested lambeosaurine hadrosaurid from the Dinosaur Park Formation of Sandy Point, eastern Alberta. International Hadrosaur Symposium abstracts volume, 2011.

Evans, D. C., R. K. Schott, D. W. Larson, C. M. Brown, and M. J. Ryan. 2013. The oldest North American pachycephalosaurid and the hidden diversity of small-bodied ornithischian dinosaurs. Nature Communications 4:1828.

Everhart, M. J. 2011. Rediscovery of the *Hesperornis regalis* Marsh 1871 holotype locality indicates an earlier stratigraphic occurrence. Transactions of the Kansas Academy of Science 114:59-68.

Fanti, F., and O. Catuneanu. 2009. Stratigraphy of the Upper Cretaceous Wapiti Formation, west-central Alberta, Canada. Canadian Journal of Earth Sciences 46:263–286.

Fanti, F., and O. Catuneanu. 2010. Fluvial Sequence Stratigraphy: The Wapiti Formation, West-Central Alberta, Canada. Journal of Sedimentary Research 80:320–338.

Fanti, F., P. J. Currie, and M. E. Burns. 2015. Taphonomy, age, and paleoecological implication of a new Pachyrhinosaurus (Dinosauria: Ceratopsidae) bonebed from the Upper Cretaceous (Campanian) Wapiti Formation of Alberta, Canada. Canadian Journal of Earth Sciences 52:250–260.

Farke, A. A., 1997. The distribution and taxonomy of Triceratops p. 47-79 in Wolberg, D.L., E. Stump, and G.D. Rosenberg (eds.), Dinofest International Proceedings Volume. Philadelphia Academy of Natural Sciences, Philadelphia, Pennsylvania.

Farke, A. A. 2004. Ceratopsid dinosaurs from the Upper Cretaceous Almond Formation of southwestern Wyoming. Rocky Mountain Geology 39:1–5.

Farke, A. A. 2006. Morphology and ontogeny of the cornual sinuses in chasmosaurine dinosaurs (Ornithischia: Ceratopsidae). Journal of Paleontology 80:780-785.

Farke, A. A., 2007. Cranial osteology and phylogenetic relationships of the chasmosaurine ceratopsid Torosaurus latus,p. 235-257 in Carpenter, K., (ed.), Horns and Beaks: Ceratopsian and Ornithopod Dinosaurs. Indiana University Press, Bloomington, Indiana.

Farke, A. A. 2010. Evolution, homology, and function of the supracranial sinuses in ceratopsian dinosaurs. Journal of Vertebrate Paleontology 30 (5):1486–1500.

Farke, A. A. 2011. Anatomy and taxonomic status of the chasmosaurine ceratopsid *Nedoceratops hatcheri* from the Upper Cretaceous Lance Formation of Wyoming, U.S.A. PLoS ONE 6:e16196 p. 1-9. doi:10.1371/journal.pone.0016196.

Farke, A. A., D. J. Chok, A. Herrero, B. Scolieri, and S. Werning. 2013. Ontogeny in the tube-crested dinosaur Parasaurolophus (Hadrosauridae) and heterochrony in hadrosaurids. PeerJ.

Farke, A. A., M. J. Ryan, P. M. Barrett, D. H. Tanke, D. R. Braman, M. A. Loewen, and M. R. Graham. 2011. A New Centrosaurine from the Late Cretaceous of Alberta,

Canada, and the Evolution of Parietal Ornamentation in Horned Dinosaurs. Acta Palaeontologica Polonica 56:691–702.

Fassett, J. E. 1973. The saga of the Ojo Alamo Sandstone; or the rock-stratigrapher and the paleontologist should be friends. Cretaceous and Tertiary Rocks of the Southern Colorado Plateau 123–130.

Fassett, J. E. 2009. New geochronologic and stratigraphic evidence confirms the Paleocene age of the dinosaur-bearing Ojo Alamo Sandstone and Animas Formation in the San Juan Basin, New Mexico and Colorado. Palaeontologia Electronica 12:1-150.

Fassett, J. E., and J. S. Hinds. 1971. Geology and fuel resources of the Fruitland Formation and Kirtland shale of the San Juan Basin, New Mexico and Colorado. U.S. Geological Survey Professional Paper 676.

Fassett, J. E., and M. B. Steiner. 1997. Precise age of C33N-C32R magnetic-polarity reversal, San Juan Basin, New Mexico and Colorado. New Mexico Geological Society Guidebook 48:239–247.

Fastovsky, D. E. 1987. Paleoenvironments of Vertebrate-Bearing Strata during the Cretaceous-Paleogene Transition, Eastern Montana and Western North Dakota. PALAIOS 2:282.

Fastovsky, D. E., and K. McSweeney. 1987. Paleosols spanning the Cretaceous-Paleogene transition, eastern Montana and western North Dakota. Geological Society of America Bulletin 99:66–77.

Fastovsky, D. E., and P. M. Sheehan. 2005. The Extinction of the Dinosaurs in North America. GSA Today 15(3):4-10.

Fastovsky, D. E., and A. Bercovici. 2015. The Hell Creek Formation and its contribution to the Cretaceous–Paleogene extinction: A short primer. Cretaceous Research 57:368-390.

Fastovsky, D. E., D. B. Weishampel, M. Watabe, R. Barsbold, K. H. Tsogtbaatar, and P. Narmandakh. 2011. A nest of *Protoceratops andrewsi* (Dinosauria, Ornithischia). Journal of Paleontology 85:1035-1041.

Feder, J. L., J. B. Roethele, K. Filchak, J. Niedbalski, and J. Romero-Severson. 2003. Evidence for Inversion Polymorphism Related to Sympatric Host Race Formation in the Apple Maggot Fly, Rhagoletis pomonella. Genetics 163:939–953.

Felsenstein J. 1985. Confidence limits on phylogenies: an approach using the bootstrap. Evolution 39(4): 783-791.

Fiorillo, A. R. 1991. Taphonomy and depositional setting of Careless Creek Quarry (Judith River Formation), Wheatland County, Montana, U.S.A. Palaeogeography, Palaeoclimatology, Palaeoecology 81:281–311.

Fiorillo, A. R., and R. S. Tykoski. 2012. A New Maastrichtian Species of the Centrosaurine Ceratopsid Pachyrhinosaurus from the North Slope of Alaska. Acta Palaeontologica Polonica 57:561–573.

Fiorillo, A. R., and R. S. Tykoski. 2014. A Diminutive New Tyrannosaur from the Top of the World. PLOS ONE 9:e91287.

Fiorillo, A. R., P. J. McCarthy, P. P. Flaig, E. Brandlen, D. W. Norton, P. Zippi, L. Jacobs, and R. A. Gangloff. 2010. Paleontology and Paleoenvironmental Interpretation of the Kikak-Tegoseak Quarry (Prince Creek Formation: Late Cretaceous), Northern Alaska: a Multi-Disciplinary Study of a High-Latitude Ceratopsian Dinosaur Bonebed; pp. 456–477 in New Perspectives on Horned Dinosaurs. The Royal Tyrrell Museum Ceratopsian Symposium. Indiana University Press.

Fisher D. C. 1994. Stratocladistics: morphological and temporal patterns and their relation to phylogenetic process pp. 133-171 in Interpreting the hierarchy of nature: from systematic patterns to evolutionary process theories, L. Grande, and O. Rieppel (eds.) Academic Press, San Diego, California.

Flight, J. N. 2004. Sequence stratigraphic analysis of the Fox Hills and Hell Creek Fms (Maastrichtian), Eastern Montana and its relationship to dinosaur paleontology. MS, Montana State University, Bozeman, Montana, 164 pp.

Flores, R. M., M. D. Myers, D. W. Houseknecht, G. D. Stricker, D. W. Brizzolara, T. J. Ryherd, and K. I. Takahashi. 2007. Stratigraphy and Facies of Cretaceous Schrader Bluff and Prince Creek Formations in Colville River Bluffs, North Slope, Alaska. Geological Survey (U.S.), pp.

Foreman, B. Z., R. R. Rogers, A. L. Deino, K. R. Wirth, and J. T. Thole. 2008. Geochemical characterization of bentonite beds in the Two Medicine Formation (Campanian, Montana), including a new< sup> 40</sup> Ar/< sup> 39</sup> Ar age. Cretaceous Research 29:373–385.

Forster, C.A. 1990. The cranial morphology and systematics of *Triceratops* with a preliminary analysis of ceratopsid phylogeny. PhD dissertation. University of Pennsylvania. Philadelphia. PA.

Forster, C. A. 1993. Taxonomic validity of the ceratopsid dinosaur Ugrosaurus olsoni (Cobabe and Fastovsky). Journal of Paleontology 67(2):316–318.

Forster, C. A. 1996a. New information on the skull of Triceratops. Journal of Vertebrate Paleontology 16(2): 246–258.

Forster, C. A. 1996b. Species resolution in Triceratops: Cladistic and morphometric approaches. Journal of Vertebrate Paleontology 16(2): 259–270.

Forster, C. A., and A. A. Farke. 2005. Dinosaur disputes, What good was all that headgear: for defense. Natural History May 2005:48–49.

Forster, C. A., P. C. Sereno, T. W. Evans, and T. Rowe. 1993. A complete skull of Chasmosaurus mariscalensis (Dinosauria: Ceratopsidae) from the Aguja Formation (late Campanian) of West Texas. Journal of Vertebrate Paleontology 13:161–170.

Fouch, T. D., T. F. Lawton, D. J. Nichols, W. B. Cashion, and W. A. Cobban. 1983. Patterns and Timing of Synorogenic Sedimentation in Upper Cretaceous Rocks of Central and Northeast Utah. Mesozoic Paleogeography of the West-Central United States: Rocky Mountain Symposium 2 305–336.

Fowler, D. 2006. Terrestrial Late Cretaceous stratigraphy of North America and the utility of ceratopsids in biostratigraphy. Society of Vertebrate Paleontology Annual Meeting 26:63A.

Fowler, D. W. 2009. A sequence stratigraphic subdivision of the Hell Creek Formation: Beginnings of a high-resolution regional chronostratigraphic framework for the terminal Cretaceous, p. 136 in Storrs, G.W. (ed.) 9th North American Paleontological Convention Abstracts. University of Cincinnati, Cincinnati Museum Center Scientific Contributions 3, Cincinnati, Ohio.

Fowler, D. 2010. Anagenesis and long-term morphologic trends in Chasmosaurinae (Dinosauria: Ceratopsidae) revealed by a new high-resolution chronostratigraphic framework, ontogenetic analysis, and description of two new taxa. Journal of Vertebrate Paleontology 30:91A.

Fowler, D. W., and L. E. Hall. 2011. Scratch-digging sauropods, revisited. Historical Biology 23:27–40.

Fowler, D. W., J. B. Scannella, and J. R. Horner. 2011: Reassessing ceratopsid diversity using unified frames of reference. Journal of Vertebrate Paleontology 31(5):111A.

Fowler, D. W., H. N. Woodward, E. A. Freedman, P. L. Larson, and J. R. Horner. 2011. Reanalysis of *Raptorex kriegsteini*: A Juvenile Tyrannosaurid Dinosaur from Mongolia. PLoS ONE 6:e21376.

Fox, R. C. 1978. Upper Cretaceous terrestrial vertebrate stratigraphy of the Gobi Desert (Mongolian People's Republic) and western North America. Geological Association of Canada Special Paper 18:571–594.

Francillon-Vieillot, H., V. de Buffrenil, J. Castanet, J. Geraudie, F. J. Meunier, J. Y. Sire, L. Zylberberg, and A. de Ricqlès. 1990. Microstructure and mineralization of vertebrate skeletal tissues.; pp. 471-548 in J. G. Carter (ed.), Skeletal Biomineralization: Patterns, Processes and Evolutionary Trends, Volume 1. Van Nostrand Reinhold, New York.

Franczyk, K. J., J. K. Pitman, and D. J. Nichols. 1990. Sedimentology, Mineralogy, Palynology, and Depositional History of Some Uppermost Cretaceous and Lowermost Tertiary Rocks along the Utah Book and Roan Cliffs East of the Green River. pp.

Fraser, F. J., F. H. McLearn, L. S. Russell, P. S. Warren, and R. T. D. Wickenden. 1935. Geology of Southern Saskatchewan. Geological Survey of Canada Memoir 176:137 pp.

Frederickson J.A., and A.R. Tumarkin-Deratzian. 2014. Craniofacial ontogeny in *Centrosaurus apertus*. PeerJ 2:e252; DOI 10.7717/peerj.252

Frederiksen, N. O. 1991. Pollen Zonation and Correlation of Maastrichtian Marine Beds and Associated Strata, Ocean Point Dinosaur Locality, North Slope of Alaska. US Department of the Interior, US Geological Survey, pp.

Frederiksen, N. O., D. J. McIntyre, and T. P. Sheehan. 2002. Palynological dating of some Upper Cretaceous to Eocene outcrop and well samples from the region extending from the easternmost part of NPRA in Alaska to the western part of ANWR. North Slope of Alaska: US Geological Survey, Open-File Report 02–405.

Freedman Fowler, E. A., and J. R. Horner. 2015. A New Brachylophosaurin Hadrosaur (Dinosauria: Ornithischia) with an Intermediate Nasal Crest from the Campanian Judith River Formation of Northcentral Montana. PLOS ONE 10:e0141304.

Frye, C. I. 1967. The Hell Creek Formation in North Dakota. Ph.D, University of North Dakota, Grand Forks, North Dakota, 411 pp.

Frye, C. I. 1969. Stratigraphy of the Hell Creek Formation in North Dakota. North Dakota Geological Survey Bulletin 54:1–65.

Fujiwara S., and Y. Takakuwa. 2011. A sub-adult growth stage indicated in the degree of suture co-ossification in *Triceratops*. Bulletin of Gunma Museum of Natural History 15: 1-17.

Gaffney, E. S., H. Tong, and P. A. Meylan. 2006. Evolution of the side-necked turtles: the families bothremydidae, euraxemydidae, and araripemydidae. Bulletin of the American Museum of Natural History 1–698.

Gangloff, R. A., and A. R. Fiorillo. 2010. Taphonomy and Paleoecology of a Bonebed from the Prince Creek Formation, North Slope, Alaska. PALAIOS 25:299–317.

Gangloff, R. A., A. R. Fiorillo, and D. W. Norton. 2005. The first pachycephalosaurine (dinosauria) from the paleo-arctic of alaska and its paleogeographic implications. Journal of Paleontology 79:997–1001.

Gates, T. A. 2007. Taxonomy, Biogeography, and Paleoecology of North American Hadrosaurid (Ornithopoda) Dinosaurs. University of Utah, 290 pp.

Gates, T. A., and S. D. Sampson. 2007. A new species of Gryposaurus (Dinosauria: Hadrosauridae) from the late Campanian Kaiparowits Formation, southern Utah, USA. Zoological Journal of the Linnean Society 151:351–376.

Gates, T. A., A. Prieto-Márquez, and L. E. Zanno. 2012. Mountain Building Triggered Late Cretaceous North American Megaherbivore Dinosaur Radiation. PLoS ONE 7:e42135.

Gates, T. A., J. R. Horner, R. R. Hanna, and C. R. Nelson. 2011. New unadorned hadrosaurine hadrosaurid (Dinosauria, Ornithopoda) from the Campanian of North America. Journal of Vertebrate Paleontology 31:798–811.

Gates, T. A., S. D. Sampson, C. R. D. D. Jesús, L. E. Zanno, D. Eberth, R. Hernandez-Rivera, M. C. A. Martínez, and J. I. Kirkland. 2007. Velafrons coahuilensis, a new lambeosaurine hadrosaurid (Dinosauria: Ornithopoda) from the late Campanian Cerro del Pueblo Formation, Coahuila, Mexico. Journal of Vertebrate Paleontology 27:917–930.

Gates, T. A., S. D. Sampson, L. E. Zanno, E. M. Roberts, J. G. Eaton, R. L. Nydam, J. H. Hutchison, J. A. Smith, M. A. Loewen, and M. A. Getty. 2010. Biogeography of terrestrial and freshwater vertebrates from the late Cretaceous (Campanian) Western Interior of North America. Palaeogeography, Palaeoclimatology, Palaeoecology 291:371–387.

Gates, T. A., E. K. Lund, C. A. Boyd, D. D. DeBlieux, A. L. Titus, D. C. Evans, M. A. Getty, J. I. Kirkland, J. G. Eaton, A. L. Titus, and others. 2013. Ornithopod dinosaurs from the Grand Staircase-Escalante National Monument region, Utah and their role in paleobiogeographic and macroevolutionary studies. Advances in Late Cretaceous Western Interior Basin Paleontology and Geology; pp. 463–481 in At the top of the Grand Staircase: The Late Cretaceous of southern Utah. Indiana University Press.

Gee, J. S., and D. V. Kent. 2007. Source of Oceanic Magnetic Anomalies and the Geomagnetic Polarity Timescale; pp. 455–507 in Treatise on Geophysics. Elsevier.

Gibling, M. R., C. R. Fielding, and R. Sinha. 2011. Alluvial valleys and alluvial sequences: towards a geomorphic assessment. From River to Rock Record: The Preservation of Fluvial Sediments and Their Subsequent Interpretation. SK Davidson, S. Leleu, and CP North (eds.). Society for Sedimentary Geology, Special Publication 97:423–447.

Gill, J. R., and W. A. Cobban. 1973. Stratigraphy and Geologic History of the Montana Group and Equivalent Rocks, Montana, Wyoming, and North and South Dakota. U.S. Geological Survey Professional Paper 776. 37 pp.

Gill, J. R., and W. J. Hail Jr. 1975. Stratigraphic Sections across Upper Cretaceous Mancos Shale-Mesaverde Group Boundary, Eastern Utah and Western Colorado. U.S. Geological Survey Oil and Gas Investigation Chart 68. 1 pp.

Gill, J. R., W. A. Cobban, and L. G. Schultz. 1972. Correlation, Ammonite Zonation, and a Reference Section for the Montana Group, Central Montana. Montana Geological Society, Twenty-First Annual Geological Conference: Crazy Mountains Basin 21:91–97.

Gillespie, J. M., and J. E. Fox. 1991. Tectonically Influenced Sedimentation in the Lance Formation, Eastern Wind River Basin, Wyoming. The Mountain Geologist 28:53–66.

Gilmore, C. W. 1919. Reptilian faunas of the Torrejon, Puerco, and underlying Upper Cretaceous formations of San Juans County, New Mexico. United States Geological Survey Professional Paper 119:1-71.

Gilmore, C. W. 1922. A New Sauropod Dinosaur from the Ojo Alamo Formation of New Mexico (with Two Plates). Smithsonian Miscellaneous Collections 72:1–9.

Gilmore, C. W. 1924. On the skull and skeleton of Hypacrosaurus, a helmet-crested dinosaur from the Edmonton Cretaceous of Alberta. Canada Geological Survey Bulletin 38:49–89.

Gilmore, C. W. 1930. On dinosaurian reptiles from the Two Medicine Formation of Montana. Proceedings of the United States National Museum 77:1–39.

Gilmore, C. W. 1939. Ceratopsian dinosaurs from the Two Medicine Formation, Upper Cretaceous of Montana. Proceedings of the United States National Museum 87:1–18.

Gilmore, C. W. 1946a. A new carnivorous dinosaur from the Lance Formation of Montana. Smithsonian Miscellaneous Collections 106:1–19.

Gilmore, C. W. 1946b. Reptilian fauna of the North Horn Formation of central Utah. U.S. Geological Survey Professional Paper 210-C 1–52.

Gingerich P.D. 1985. Species in the fossil record: concepts, trends, and transitions. Paleobiology 11(1):27-41.

Godefroit, P., F. Escuillié, Y. L. Bolotsky, and P. Lauters. 2012. A new basal hadrosauroid dinosaur from the Upper Cretaceus of Kazakhstan; pp. 335–338 in P. Godefroit (ed.), Bernissart Dinosaurs and Early Cretaceous Terrestrial Ecosystems. Indiana University Press, Bloomington, Indiana.

Godfrey, S. J., and R. Holmes. 1995. Cranial morphology and systematics of Chasmosaurus (Dinosauria: Ceratopsidae) from the Upper Cretaceous of western Canada. Journal of Vertebrate Paleontology 15:726–742.

Goodwin, M. A. 2005. Dinosaur disputes, What good was all that headgear: for decoration. Natural History May 2005:48–49.

Goodwin, M. B., and A. L. Deino. 1989. The first radiometric ages from the Judith River Formation (Upper Cretaceous), Hill County, Montana. Canadian Journal of Earth Sciences 26:1384–1391.

Goodwin, M. B., and J. R. Horner. 2010. Historical collecting bias and the fossil record of Triceratops in Montana, p. 551-564 in Ryan, M.J., Chinnery-Allgeier, B.J., and Eberth, D.A. (eds.), New Perspectives on Horned Dinosaurs: The Royal Tyrrell Museum Ceratopsian Symposium. Indiana University Press, Bloomington, Indiana.

Goodwin, M. B., W. A. Clemens, J. R. Horner, and K. Padian. 2006. The smallest known *Triceratops* skull: new observations on ceratopsid cranial anatomy and ontogeny. Journal of Vertebrate Paleontology 26:103-112.

Gradstein, F., and J. Ogg. 2004. Geologic Time Scale 2004 – why, how, and where next! Lethaia 37:175–181.

Gradstein, F. M., J. G. Ogg, and A. G. Smith. 2004. A Geologic Time Scale 2004. Cambridge University Press, 589 pp.

Gradstein, F. M., J. G. Ogg, M. Schmitz, and G. Ogg. 2012. The Geologic Time Scale 2012 2-Volume Set, 1st ed. Elsevier, 1176 pp.

Gradstein, F. M., F. P. Agterberg, J. G. Ogg, J. Hardenbol, P. van Veen, J. Thierry, and Z. Huang. 1994. A Mesozoic time scale. Journal of Geophysical Research: Solid Earth 99:24051–24074.

Hajek, E. A., P. L. Heller, and B. A. Sheets. 2010. Significance of channel-belt clustering in alluvial basins. Geology 38:535–538.

Hajek, E. A., P. L. Heller, and E. L. Schur. 2012. Field test of autogenic control on alluvial stratigraphy (Ferris Formation, Upper Cretaceous–Paleogene, Wyoming). Geological Society of America Bulletin 124:1898–1912.

Hall, L., and S. Keenan 2010, Taphonomy of a new specimen of Tyrannosaurus rex from the Hell Creek Formation, Montana. Journal of Vertebrate Paleontology: SVP Program and Abstracts Book, v. 30:100A-101A.

Hamblin, A. P. 1998. Edmonton Group/St. Mary River Formation: summary of literature and concepts. Geological Survey of Canada Open File Report 3578. 36 pp.

Hamblin, A. P. 2010. Scollard/Willow Creek/Coalspur Formations: Summary of Literature and Concepts. Natural Resources Canada, 25 pp.

Hamblin, A. P., and B. W. Abrahamson. 1996. Stratigraphic Architecture of "Basal Belly River" Cycles, Foremost Formation, Belly River Group, Subsurface of Southern Alberta and Southwestern Saskatchewan. Bulletin of Canadian Petroleum Geology 44:654–673.

Happ J.W., and C.M. Morrow. 1996. Separation of *Triceratops* (Dinosauria: Ceratopsidae) into two allopatric species by cranial morphology. Journal of Vertebrate Paleontology 16:40A.

Haq, B. U., J. Hardenbol, and P. R. Vail. 1987. Chronology of fluctuating sea levels since the Triassic. Science 235:1156–1167.

Haq, B. U., J. Hardenbol, and P. R. Vail. 1988. Mesozoic and Cenozoic Chronostratigraphy and Cycles of Sea-Level Change. Society of Economic Paleontologists and Mineralogists Special Publication No. 42:71-108.

Hares, C. J. 1928. Geology and lignite resources of the Marmarth field, southwestern North Dakota. U.S. Geological Survey Bulletin 775:1–110.

Harrell, T. L. J., and J. e. Martin. 2015. A mosasaur from the Maastrichtian Fox Hills Formation of the northern Western Interior Seaway of the United States and the synonymy of Mosasaurus maximus with Mosasaurus hoffmanni (Reptilia: Mosasauridae). Netherlands Journal of Geosciences 94:23–37.

Hartman, J. H., and J. I. Kirkland. 2002. Brackish and marine mollusks of the Hell Creek Formation of North Dakota: Evidence for a persisting Cretaceous seaway. Geological Society of America Special Papers 361:271–296.

Hartman, J. H., R. D. Butler, M. W. Weiler, and K. K. Schumaker. 2014. Context, naming, and formal designation of the Cretaceous Hell Creek Formation lectostratotype, Garfield County, Montana. In Wilson, G. P., Clemens, W. A., Horner, J. R., and Hartman, J. H., eds., Through the End of the Cretaceous in the Type Locality of the Hell Creek Formation in Montana and Adjacent Areas. Geological Society of America Special Papers 503:89–121.

Hatcher, J. B. 1893. The Ceratops Beds of Converse County, Wyoming. American Journal of Science 45:135–144.

Hatcher, J. B., O. C. Marsh, and R. S. Lull. 1907. The Ceratopsia. United States Geological Monograph 49:1-300.

Hausdorf, B. 2011. Progress Toward a General Species Concept. Evolution 65:923–931.

Heckert, A. B., C. Lewis, S. Lucas, and T. Williamson. 2007. New Mixed Marine-Nonmarine Microvertebrate Fauna From The Upper Cretaceous (Late Santonian-Early Campanian) Menefee Formation, Northwestern New Mexico. Abstracts with Programs - Geological Society of America 39:73.

Herne, M. C., J. P. Nair, and S. W. Salisbury. 2010. Comment on "A Southern Tyrant Reptile". Science 329:1013.

Hettinger, R. D., and M. A. Kirschbaum. 2002. Stratigraphy of the Upper Cretaceous Mancos Shale (upper part) and Mesaverde Group in the southern part of the Uinta and Piceance basins, Utah and Colorado. U.S. Geological Survey 1–21.

Hicks, J. F., J. D. Obradovich, and L. Tauxe. 1995. A New Calibration Point for the Late Cretaceous Time Scale: The (40)Ar/(39)Ar Isotopic Age of the C33r/C33n Geomagnetic Reversal from the Judith River Formation (Upper Creataceous), Elk Basin, Wyoming, USA. Journal of Geology 103:243–256.

Hicks, J. F., D. Fastovsky, D. J. Nichols, and M. Watabe. 2001. Magnetostratigraphic correlation of Late Cretaceous dinosaur-bearing localities in the Nemegt and Ulan Nuur basins, Gobi Desert, Mongolia. Abstracts with Programs - Geological Society of America 33:323.

Hicks, J. F., K. R. Johnson, J. D. Obradovich, L. Tauxe, and D. Clark. 2002. Magnetostratigraphy and geochronology of the Hell Creek and basal Fort Union Formations of southwestern North Dakota and a recalibration of the age of the Cretaceous-Tertiary boundary. pp. 35-55 in The Hell Creek Formation and the Cretaceous -Tertiary boundary in the northern Great Plains: an integrated continental record of the end of the Cretaceous, J.H. Hartman, K.R. Johnson, and D.J. Nichols (eds.) Geological Society of America Special Paper 361, Boulder, Colorado.

Hicks, J. F., K. R. Johnson, J. D. Obradovich, D. P. Miggins, and L. Tauxe. 2003. Magnetostratigraphy of upper Cretaceous (Maastrichtian) to lower Eocene strata of the Denver Basin, Colorado. Rocky Mountain Geology 38:1–27.

Hicks, J. F., M. Watabe, D. E. Fastovsky, K. R. Johnson, and D. J. Nichols. 1999. Magnetostratigraphic correlation of Late Cretaceous dinosaur-bearing localities, Nemegt Basin, Gobi Desert, Mongolia. Abstracts with Programs - Geological Society of America 31:234.

Hofmann, M. H., A. Wroblewski, and R. Boyd. 2011. Mechanisms Controlling the Clustering of Fluvial Channels and the Compensational Stacking of Cluster Belts. Journal of Sedimentary Research 81:670–685.

Hoganson, J. W., and E. C. Murphy. 2002. Marine Breien Member (Maastrichtian) of the Hell Creek Formation in North Dakota: Stratigraphy, vertebrate fossil record, and age. Geological Society of America Special Papers 361:247–269.

Holbrook, J. M. 1996. Complex fluvial response to low gradients at maximum regression; a genetic link between smooth sequence-boundary morphology and architecture of overlying sheet sandstone. Journal of Sedimentary Research 66:713–722.

Holbrook, J. M. 2010. Valleys that never were: time surfaces versus stratigraphic surfaces—discussion. Journal of Sedimentary Research 80:2–3.

Holbrook, J. M., and J. P. Bhattacharya. 2012. Reappraisal of the sequence boundary in time and space: Case and considerations for an SU (subaerial unconformity) that is not a sediment bypass surface, a time barrier, or an unconformity. Earth-Science Reviews 113:271–302.

Holmes, R. B., C. A. Forster, M. Ryan, and K. M. Shepherd. 2001. A new species of Chasmosaurus (Dinosauria: Ceratopsia) from the Dinosaur Park Formation of southern Alberta. Canadian Journal of Earth Sciences 38:1423–1438.

Holroyd, P. A., and J. H. Hutchison. 2002. Patterns of geographic variation in latest Cretaceous vertebrates: Evidence from the turtle component. Geological Society of America Special Papers 361:177–190.

Holroyd, P. A., G. P. Wilson, and J. H. Hutchison. 2014. Temporal changes within the latest Cretaceous and early Paleogene turtle faunas of northeastern Montana. Geological Society of America Special Papers 503:299–312.

Holtz Jr., T. R. 2001. The phylogeny and taxonomy of the Tyrannosauridae; pp. 64-83 in D. H. Tanke and K. Carpenter (eds.), Mesozoic Vertebrate Life. Indiana University Press, Bloomington.

Holtz Jr., T. R. 2004. Tyrannosauroidea; pp. 111-136 in D. Weishampel, P. Dodson, and H. Osmolska (eds.), The Dinosauria. University of California Press, Berkeley.

Hone, D. W. E., and D. Naish. 2013. The "species recognition hypothesis" does not explain the presence and evolution of exaggerated structures in non-avialan dinosaurs. Journal of Zoology 290:172-180.

Hone, D. W. E., D. Naish, and I. C. Cuthill. 2012. Does mutual sexual selection explain the evolution of head crests in pterosaurs and dinosaurs? Lethaia 45:139–156.

Hone, D. W., K. Wang, C. Sullivan, X. Zhao, S. Chen, D. Li, S. Ji, Q. Ji, and X. Xu. 2011. A new tyrannosaurine theropod, *Zhuchengtyrannus magnus* is named based on a maxilla and dentary. Cretaceous Research doi: 10.1016/j.cretres.2011.03.005.

Horner, J. R. 1979. Upper Cretaceous Dinosaurs from the Bearpaw Shale (Marine) of South-Central Montana with a Checklist of Upper Cretaceous Dinosaur Remains from Marine Sediments in North America. Journal of Paleontology 53:566–577.

Horner, J. R. 1983. Cranial osteology and morphology of the type specimen of *Maiasaura peeblesorum* (Ornithischia: Hadrosauridae), with discussion of its phylogenetic position. Journal of Vertebrate Paleontology 3:29-38.

Horner, J. R. 1984. Three ecologically distinct vertebrate faunal communities from the Late Cretaceous Two Medicine Formation of Montana, with discussion of evolutionary pressures induced by interior seaway fluctuations. Field Conference Guidebook 299–304.

Horner, J. R. 1992. Cranial Morphology of Prosaurolophus (Ornithischia: Hadrosauridae): With Descriptions of Two New Hadrosaurid Species and an Evaluation of Hadrosaurid Phylogenetic Relationships. Museum of the Rockies Occasional Paper 119.

Horner, J. R., and P. J. Currie. 1994. Embryonic and neonatal morphology and ontogeny of a new species of Hypacrosaurus (Ornithischia, Lambeosauridae) from Montana and Alberta; pp. 312–336 in K. Carpenter, K. F. Hirsch, and J. R. Horner (eds.), Dinosaur Eggs and Babies. Cambridge University Press, New York.

Horner, J. R., and M. B. Goodwin. 2006. Major cranial changes during Triceratops ontogeny. Proceedings of the Royal Society B: Biological Sciences 273:2757–2761.

Horner, J. R., and M. B. Goodwin. 2008. Ontogeny of cranial epi-ossifications in *Triceratops*. Journal of Vertebrate Paleontology 28:134-144.

Horner J.R., and M.B. Goodwin. 2009. Extreme cranial ontogeny in the upper Cretaceous dinosaur *Pachycephalosaurus*. PLoS ONE 4(10): e7626.

Horner, J. R., and E.-T. Lamm. 2011. Ontogeny of the parietal frill of *Triceratops*: a preliminary histological analysis. Comptes Rendus Palevol 10:439-452.

Horner, J. R., and R. Makela. 1979. Nest of juveniles provides evidence of family structure among dinosaurs. Nature 282:296–298.

Horner, J. R., and K. Padian. 2004. Age and growth dynamics of *Tyrannosaurus rex*. Proceedings of the Royal Society of London Series B 271:1875-1880.

Horner, J. R., M. B. Goodwin, and N. Myhrvold. 2011. Dinosaur Census Reveals Abundant Tyrannosaurus and Rare Ontogenetic Stages in the Upper Cretaceous Hell Creek Formation (Maastrichtian), Montana, USA. PLoS ONE 6:e16574.

Horner, J. R., A. d. Ricqlès, and K. Padian. 2000. Long bone histology of the hadrosaurid dinosaur *Maiasaura peeblesorum*: growth dynamics and physiology based on an

ontogenetic series of skeletal elements. Journal of Vertebrate Paleontology 20:115-129.

Horner, J. R., D. J. Varricchio, and M. B. Goodwin. 1992. Marine transgressions and the evolution of Cretaceous dinosaurs. Nature 358:59–61.

Horner, J. R., J. G. Schmitt, F. Jackson, and R. Hanna. 2001. Bones and rocks of the Upper Cretaceous Two Medicine-Judith River clastic wedge complex, Montana. Field Trip Guidebook, Society of Vertebrate Paleontology 61st Annual Meeting: Mesozoic and Cenozoic Paleontology in the Western Plains and Rocky Mountains. Museum of the Rockies Occasional Paper 3:3–14.

Hull, P. M., and R. D. Norris. 2009. Evidence for abrupt speciation in a classic case of gradual evolution. Proceedings of the National Academy of Sciences 106:21224-21229.

Hunt, A. P. 1986. "Bisti member" of the Kirtland Shale, San Juan Basin, New Mexico: implications for basin development. Geological Society of America, Abstracts with Programs 24:26–27.

Hunt, A. P., and S. G. Lucas. 1992. Stratigraphy, paleontology and age of the Fruitland and Kirtland formations (Upper Cretaceous), San Juan Basin, New Mexico. New Mexico Geological Society Guidebook 43:217–239.

Hunt, A. P., and S. G. Lucas. 1993. Cretaceous Vertebrates of New Mexico. New Mexico Museum of Natural History and Science Bulletin 2:77–91.

Hunt, A. P., and S. G. Lucas. 2003. Origin and stratigraphy of historic dinosaur quarries in the Upper Cretaceous Fruitland Formation of the Fossil Forest research Natural Area, northwestern New Mexico. New Mexico Geological Society Guidebook 54:383–388.

Hunt, R. K., and T. M. Lehman. 2008. Attributes of the ceratopsian dinosaur Torosaurus, and new material from the Javelina Formation (Maastrichtian) of Texas. Journal of Paleontology 82:1127–1138.

Hunter, J. P., R. E. Heinrich, and D. B. Weishampel. 2010. Mammals from the St. Mary River Formation (Upper Cretaceous), Montana. Journal of Vertebrate Paleontology 30:885–898.

Hurum, J. H., and K. Sabath. 2003. Giant theropod dinosaurs from Asia and North America: skulls of *Tarbosaurus bataar* and *Tyrannosaurus rex* compared. Acta Palaeontolgica Polonica 48:161-190.

Hutt, S., D. W. Naish, D. M. Martill, M. J. Barker, and P. Newberry. 2001. A preliminary account of a new tyrannosauroid theropod from the Wessex Formation (Early Cretaceous) of southern England. Cretaceous Research 22:227-242.

Hutton, J. M. 1986. Age determination of living Nile crocodiles from the cortical stratification of bone. Copeia 2:332-341.

Ifrim, C., W. Stinnesbeck, and J. F. Ventura. 2013. An endemic cephalopod assemblage from the lower Campanian (Late Cretaceous) Parras Shale, western Coahuila, Mexico. Journal of Paleontology 87:881–901.

Ifrim, C., W. Stinnesbeck, R. R. Garza, and J. F. Ventura. 2010. Hemipelagic cephalopods from the Maastrichtian (Late Cretaceous) Parras Basin at La Parra, Coahuila, Mexico, and their implications for the correlation of the lower Difunta Group. Journal of South American Earth Sciences 29:597–618.

Imhof, M., and L. B. Albright. 2003. Preliminary Magnetostratigraphic Analysis Of The Upper Cretaceous Kaiparowits Formation, Southern Utah. Journal of Vertebrate Paleontology 23:65A–65A.

Irion, G., J. Müller, J. O. Morais, G. Keim, J. N. de Mello, and W. J. Junk. 2009. The impact of Quaternary sea level changes on the evolution of the Amazonian lowland. Hydrological Processes 23:3168–3172.

Irish, E. J. W. 1970. The Edmonton Group of South-Central Alberta. Bulletin of Canadian Petroleum Geology 18:125–155.

Izett, G. A., and J. D. Obradovich. 1994. 40Ar/39Ar age constraints for the Jaramillo Normal Subchron. Journal of Geophysical Research 99:2925–2934.

Izett, G. A., W. A. Cobban, J. D. Obradovich, and G. B. Dalrymple. 1998. 40Ar/39Ar age of the Manson impact structure, Iowa, and correlative impact ejecta in the Crow Creek Member of the Pierre Shale (Upper Cretaceous), South Dakota and Nebraska. Geological Society of America Bulletin 110:361–376.

Jeletzky, J. A., and W. A. Clemens. 1965. Comments on Cretaceous Eutheria, Lance Scaphites, and Inoceramus? ex gr. tegulatus. Journal of Paleontology 39:952–959.

Jensen, F. S., and H. D. Varnes. 1964. Geology of the Fort Peck Area, Garfield, McCone and Valley Counties, Montana. USGS Professional Paper 414-F, 49 pp.

Jerzykiewicz, T., and D. K. Norris. 1994. Stratigraphy, structure and syntectonic sedimentation of the Campanian “Belly River” clastic wedge in the southern Canadian Cordillera. Cretaceous Research 15:367–399.

Jinnah, Z. A. 2011. Tectonic and sedimentary controls, age and correlation of the Upper Cretaceous Wahweap Formation, southern Utah, USA. Faculty of Science, University of the Witwatersrand pp.

Jinnah, Z. A. 2013. Tectonic and Sedimentary Controls, Age, and Correlation of the Upper Cretaceous Wahweap Formation, Southern Utah; pp. 57–73 in At the Top of the Grand Staircase: The Late Cretaceous of Southern Utah. Indiana University Press.

Jinnah, Z. A., and E. M. Roberts. 2011. Facies Associations, Paleoenvironment, and Base-Level Changes in the Upper Cretaceous Wahweap Formation, Utah, U.S.A. Journal of Sedimentary Research 81:266–283.

Jinnah, Z. A., E. M. Roberts, A. L. Deino, J. S. Larsen, P. K. Link, and C. M. Fanning. 2009. New 40Ar-39Ar and detrital zircon U-Pb ages for the Upper Cretaceous Wahweap and Kaiparowits formations on the Kaiparowits Plateau, Utah: implications for regional correlation, provenance, and biostratigraphy. Cretaceous Research 30:287–299.

Johnson, K. R. 1989. A high resolution megafloral biostratigraphy spanning the Cretaceous-Tertiary boundary in the Northern Great Plains. Ph.D, Yale University, New Haven, Connecticut, 581 pp.

Johnson, K. R. 2002. Megaflora of the Hell Creek and lower Fort Union Formations in the western Dakotas: Vegetational response to climate change, the Cretaceous-Tertiary boundary event, and rapid marine transgression. Geological Society of America Special Papers 361:329–391.

Johnson, K. R., and L. J. Hickey. 1990. Megafloral change across the Cretaceous/Tertiary boundary in the northern Great Plains and Rocky Mountains, U.S.A. Geological Society of America Special Papers 247:433–444.

Johnson, K. R., D. J. Nichols, and J. H. Hartman. 2002. Hell Creek Formation: A 2001 synthesis. Geological Society of America Special Papers 361:503–510.

Johnson, N. A. 2008. Direct Selection for Reproductive Isolation: The Wallace Effect and Reinforcement; pp. 114–124 in C. H. Smith and G. Beccaloni (eds.), Natural selection and beyond: the intellectual legacy of Alfred Russel Wallace. Oxford University Press, Oxford, UK.

Jordan, T. E. 1995. Retroarc Foreland and Related Basins; pp. 331–362 in C. J. Busby and R. V. Ingersoll (eds.), Tectonics of Sedimentary Basins. Blackwell, London.

Jourdan, F., C. Verati, and G. Féraud. 2006. Intercalibration of the Hb3gr 40 Ar/39 Ar dating standard. Chemical Geology 231:177–189.

Kamola, D. L., and J. C. Van Wagoner. 1995. Stratigraphy and Facies Architecture of Parasequences with Examples from the Spring Canyon Member, Blackhawk Formation, Utah. American Association of Petroleum Geologists, Memoir 64:27–54.

Kauffman, E. G. 1984. Paleobiogeography and evolutionary response dynamic in the Cretaceous Western Interior Seaway of North America. Geological Association of Canada, Special Paper 27:273–306.

Kauffman, E. G., and W. G. E. Caldwell. 1993. The Western Interior Basin in space and time. Geological Association of Canada, Special Paper 39:1–30.

Kauffman, E. G., B. B. Sageman, J. I. Kirkland, W. P. Elder, P. J. Harries, and T. Villamil. 1993. Molluscan biostratigraphy of the Cretaceous western interior basin, North America. Evolution of the Western Interior Basin: Geological Association of Canada Special Paper 39:397–434.

Keenan, S.W., and J.B. Scannella. 2014. Paleobiological implications of a Triceratops bonebed from the Hell Creek Formation, Garfield County, northeastern Montana, in Wilson, G.P., W.A. Clemens, J.R. Horner, and J.H. Hartman, (eds.) Through the End of the Cretaceous in the Type Locality of the Hell Creek Formation in Montana and Adjacent Areas: Geological Society of America Special Paper 503, doi:10.1130/2014.2503(14).

Kennedy, W. J., N. H. Landman, W. K. Christensen, W. A. Cobban, and J. M. Hancock. 1998. Marine connections in North America during the late Maastrichtian: palaeogeographic and palaeobiogeographic significance ofJeletzkytes nebrascensisZone cephalopod fauna from the Elk Butte Member of the Pierre Shale, SE South Dakota and NE Nebraska. Cretaceous Research 19:745–775.

Kirkland, J. I. 2001. The quest for new dinosaurs at Grand Staircase–Escalante National Monument: Utah Geological Survey Notes, v. 33. Utah Geological Survey Survey Notes 33:4.

Kirkland, J. I., and D. D. DeBlieux. 2007. New horned dinosaurs from the Wahweap Formation. Utah Geological Survey Survey Notes 39:4–5.

Kirkland, J. I., and D. D. DeBlieux. 2010. New basal centrosaurine ceratopsian skulls from the Wahweap Formation (Middle Campanian), Grand Staircase-Escalante National Monument, southern Utah; pp. 117–140 in New Perspectives on Horned

Dinosaurs: The Royal Tyrrell Museum Ceratopsian Symposium. Indiana University Press Bloomington.

Kirkland, J. I., R. Hernández-Rivera, M. C. Aguillón Martínez, C. R. Delgado de Jesús, R. Gómez-Nuñez, and I. Vallejo. 2000. The Late Cretaceous Difunta Group of the Parras Basin, Coahuila, Mexico, and its vertebrate fauna. Society of Vertebrate Paleontology Annual Meeting 133–172.

Kirkland, J. I., R. Hernández-Rivera, T. Gates, G. S. Paul, S. J. Nesbitt, C. I. Serrano-Brañas, and J. P. Garcia-de la Garza. 2006. Large hadrosaurine dinosaurs from the latest Campanian of Coahuila, Mexico. New Mexico Museum of Natural History and Science Bulletin 35:299–315.

Kirschbaum, M. A., and R. D. Hettinger. 2004. Facies Analysis and Sequence Stratigraphic Framework of Upper Campanian Strata (Neslen and Mount Garfield Formations, Bluecastle Tongue of the Castlegate Sandstone, and Mancos Shale), Eastern Book Cliffs, Colorado and Utah. pp.

Klein, N., and P. M. Sander. 2008. Ontogenetic stages in the long bone histology of sauropod dinosaurs. Paleobiology 34:248-264.

Knell, R. J., and S. Sampson. 2011a. Bizarre structures in dinosaurs: species recognition or sexual selection? A response to Padian and Horner. Journal of Zoology 283:18–22.

Knell, R. J., and S. Sampson. 2011b. Bizarre structures in dinosaurs: species recognition or sexual selection? A response to Padian and Horner. Journal of Zoology 283:18–22.

Knell, R. J., D. Naish, J. L. Tomkins, and D. W. E. Hone. 2013a. Sexual selection in prehistoric animals: detection and implications. Trends in Ecology & Evolution 28:38–47.

Knell, R. J., D. Naish, J. L. Tomkins, and D. W. E. Hone. 2013b. Is sexual selection defined by dimorphism alone? A reply to Padian and Horner. Trends in Ecology & Evolution 28:250–251.

Knoll, F., K. Padian, and A. d. Ricqlès. 2010. Ontogenetic change and adult body size of the early ornithischian dinosaur *Lesothosaurus diagnosticus*: implications for basal ornithischian taxonomy. Gondwana Research 17:171-179.

Koppelhus, E. B., and D. R. Braman. 2010. Upper Cretaceous palynostratigraphy of the Dry Island area. Canadian Journal of Earth Sciences 47:1145–1158.

Kosuth, P., J. Callède, A. Laraque, N. Filizola, J. L. Guyot, P. Seyler, J. M. Fritsch, and V. Guimarães. 2009. Sea-tide effects on flows in the lower reaches of the Amazon River. Hydrological Processes 23:3141.

Kraus, M. J. 1987. Integration of channel and floodplain suites; II, Vertical relations of alluvial Paleosols. Journal of Sedimentary Research 57:602–612.

Kraus, M. J. 1999. Paleosols in clastic sedimentary rocks: their geologic applications. Earth-Science Reviews 47:41–70.

Kraus, M. J. 2002. Basin-Scale Changes in Floodplain Paleosols: Implications for Interpreting Alluvial Architecture. Journal of Sedimentary Research 72:500–509.

Krystinik, L. F., and B. B. DeJarnett. 1995. Lateral Variability of Sequence Stratigraphic Framework in the Campanian and Lower Maastrichtian of the Western Interior Seaway. Sequence stratigraphy of foreland basin deposits: Outcrop and subsurface examples from the Cretaceous of North America. American Association of Petroleum Geologists, Memoir 64:11–25.

Kuiper, K. F., A. Deino, F. J. Hilgen, W. Krijgsman, P. R. Renne, and J. R. Wijbrans. 2008. Synchronizing Rock Clocks of Earth History. Science 320:500–504.

Kwon, J., K. Min, P. J. Bickel, and P. R. Renne. 2002. Statistical Methods for Jointly Estimating the Decay Constant of 40K and the Age of a Dating Standard. Mathematical Geology 34:457–474.

Laird, W. M., and R. H. Mitchell. 1942. Geology of the southern part of Morton County, North Dakota. North Dakota Geological Survey Bulletin 14:1–42.

Lambe, L. M. 1902. New genera and species from the Belly River series (Mid-Cretaceous). Contributions to Canadian Palaeontology 3:25–81.

Lambe, L. M. 1904. On the Squamoso-parietal Crest of the Horned Dinosaurs Centrosaurus Apertus and Monoclonius Canadensis from the Cretaceous of Alberta. The Ottawa Naturalist 18:81–84.

Lambe, L. M. 1913. A New Genus and Species of Ceratopsia from Belly River Formation of Alberta. The Ottawa Naturalist 27:109–116.

Lambe, L. M. 1914a. On the fore-limb of a carnivorous dinosaur from the Belly River Formation of Alberta, and a new genus of Ceratopsia from the same horizon, with remarks on the integument of some Cretaceous herbivorous dinosaurs. The Ottawa Naturalist 27:130-135.

Lambe, L. M. 1914b. On Gryposaurus notabilis, a new genus and species of trachodont dinosaur from the Belly River Formation of Alberta, with a description of the skull of Chasmosaurus belli. The Ottawa Naturalist 27:145–155.

Lambe, L. M. 1915. On *Eoceratops canadensis*, gen. nov., with remarks on the other genera of Cretaceous horned dinosaurs. Geological Survery of Canada Museum Bulletin 12:1-49.

Lambe, L. M. 1917. A new genus and species of crestless hadrosaur from the Edmonton Formation of Alberta. The Ottawa Naturalist 31:65–73.

Landman, N. H., and W. A. Cobban. 2003. Ammonites from the upper part of the Pierre Shale and Fox Hills Formation of Colorado. American Museum Novitates 1–45.

Landman, N. H., and K. M. Waagé. 1993. Scaphitid ammonites of the Upper Cretaceous (Maastrichtian) Fox Hills Formation in South Dakota and Wyoming. Bulletin of the American Museum of Natural History 215:1–257.

Landman, N. H., R. O. Johnson, and L. E. Edwards. 2004. Cephalopods from the Cretaceous/Tertiary boundary interval on the Atlantic Coastal Plain, with a description of the highest ammonite zones in North America. Part 2. Northeastern Monmouth County, New Jersey. Bulletin of the American Museum of Natural History 1–107.

Langston, W. 1959. Anchiceratops from the Oldman Formation of Alberta. Natural History Papers 3:11.

Langston, W. 1975. The Ceratopsian Dinosaurs and Associated Lower Vertebrates from the St. Mary River Formation (Maestrichtian) at Scabby Butte, Southern Alberta. Canadian Journal of Earth Sciences 12:1576–1608.

Langston, W. 1976. A Late Cretaceous vertebrate fauna from the St. Mary River Formation in Western Canada. Essays on Palaeontology in Honour of Loris Shano Russell. Edited by CS Churcher. Royal Ontario Museum, Life Sciences Miscellaneous Publications 114–133.

Lanphere, M. A., G. B. Dalrymple, R. J. Fleck, and M. S. Pringle. 1990. Intercalibration of mineral standards for K-Ar and 40Ar/39Ar age measurements. EOS, Transactions of the American Geophysical Union 71:1–658.

Larson, D. W. 2008. Diversity and variation of theropod dinosaur teeth from the uppermost Santonian Milk River Formation (Upper Cretaceous), Alberta: a quantitative method supporting identification of the oldest dinosaur tooth assemblage in Canada. Canadian Journal of Earth Sciences 45:1455–1468.

Lawson, D. A. 1976. Tyrannosaurus and Torosaurus, Maastrichtian dinosaurs from Trans-Pecos, Texas. Journal of Paleontology 50:158–164.

Lawton, T. F. 2008. Chapter 12 Laramide Sedimentary Basins; pp. 429–450 in A. D. Miall (ed.), Sedimentary Basins of the World. vol. 5. Elsevier.

Lawton, T. F., and A. E. Christensen. 2005. Sequence Boundaries in Terrestrial Foreland-Basin Strata: Do They Lie Above or Below the Amalgamated Fluvial Facies Tract? American Association of Petroleum Geologists Annual Meeting Abstracts.

Lawton, T. F., S. L. Pollock, and R. A. J. Robinson. 2003. Integrating sandstone petrology and nonmarine sequence stratigraphy: application to the Late Cretaceous fluvial systems of Southwestern Utah, USA. Journal of Sedimentary Research 73:389–406.

Leahy, G. D., and J. F. Lerbekmo. 1995. Macrofossil magnetobiostratigraphy for the upper Santonian-lower Campanian interval in the Western Interior of North America: comparisons with European stage boundaries and planktonic foraminiferal zonal boundaries. Canadian Journal of Earth Sciences 32:247–260.

LeCain, R., W. C. Clyde, G. P. Wilson, and J. Riedel. 2014. Magnetostratigraphy of the Hell Creek and lower Fort Union Formations in northeastern Montana. Geological Society of America Special Papers 503:137–147.

Legarreta, L., and M. A. Uliana. 1998. Anatomy of hinterland depositional sequences: Upper Cretaceous fluvial strata, Neuquen basin, west-central Argentina; pp. 83–92 in K. W. Shanley and P. McCabe (eds.), Relative role of eustasy, climate and tectonism in continental rocks. SEPM Special Publication vol. 59.

Legarreta, L., M. A. Uliana, C. A. Larotonda, and G. R. Meconi. 1993. Approaches to nonmarine sequence stratigraphy – theoretical models and examples from Argentine basins. Proceedings of Institut Francais Du Petrole, Conference on Exploration and Production: Subsurface Reservoir Characterization from Surface Observations, April 12-17, 1992 125–143.

Lehman, T. M. 1981. The Alamo Wash local fauna: a new look at the old Ojo Alamo fauna. Advances in San Juan Basin Paleontology. New Mexico University Press, Albuquerque, New Mexico 189–221.

Lehman, T. M. 1987. Late Maastrichtian paleoenvironments and dinosaur biogeography in the western interior of North America. Palaeogeography, Palaeoclimatology, Palaeoecology 60:189–217.

Lehman, T. M. 1989. Chasmosaurus mariscalensis, sp. nov., a new ceratopsian dinosaur from Texas. Journal of Vertebrate Paleontology 9:137–162.

Lehman, T. M. 1990a. The ceratopsian subfamily Chasmosaurinae: sexual dimorphism and systematics; pp. 211-229 in K. Carpenter and P. J. Currie (eds.), Dinosaur Systematics Approaches and Perspectives. Cambridge University Press, Cambridge.

Lehman, T. M. 1990b. Paleosols and the Cretaceous/Tertiary transition in the Big Bend region of Texas. Geology 18:362–364.

Lehman, T. M. 1993. New data on the ceratopsian dinosaur Pentaceratops sternbergii Osborn from New Mexico. Journal of Paleontology 67:279–288.

Lehman, T. M. 1997. Late Campanian dinosaur biogeography in the western interior of North America. Dinofest International:223–240.

Lehman, T. M. 1998. A gigantic skull and skeleton of the horned dinosaur *Pentaceratops sternbergi* from New Mexico. Journal of Paleontology 72:894-906.

Lehman, T. M. 2001. Late Cretaceous Dinosaur Provinciality; pp. 310–328 in D. H. Tanke and K. Carpenter (eds.), Mesozoic Vertebrate Life. Indiana University Press, Bloomington, Indiana.

Lehman, T. M. 2007. Growth and population age structure in the horned dinosaur *Chasmosaurus*; pp. 259-317 in K. Carpenter (ed.), Horns and Beaks: Ceratopsian and Ornithopod Dinosaurs. Indiana University Press, Bloomington.

Lehman, T. M., and A. B. Busbey III. 2007. Big Bend Field Trip Guidebook. Society of Vertebrate Paleontology, 67th Annual Meeting Field Trip Guidebook:1-69.

Lehman, T. M., and A. B. Coulson. 2002. A juvenile specimen of the sauropod dinosaur Alamosaurus sanjuanensis from the Upper Cretaceous of Big Bend National Park, Texas. Journal of Paleontology 76:156–172.

Lehman, T. M., and S. L. Tomlinson. 2004. Terlinguachelys fischbecki, a new genus and species of sea turtle (Chelonioidea: Protostegidae) from the Upper Cretaceous of Texas. Journal of Paleontology 78:1163–1178.

Lehman, T. M., F. W. Mcdowell, and J. N. Connelly. 2006. First isotopic (U-Pb) age for the Late Cretaceous Alamosaurus vertebrate fauna of West Texas, and its significance as a link between two faunal provinces. Journal of Vertebrate Paleontology 26:922–928.

Lerbekmo, J. F. 1985. Magnetostratigraphic and Biostratigraphic Correlations of Maastrichtian to Early Paleocene Strata Between South-Central Alberta and Southwestern Saskatchewan. Bulletin of Canadian Petroleum Geology 33:213–226.

Lerbekmo, J. F. 1987. Magnetostratigraphic Restrictions on the Age of the Frenchman Formation and the Magnitude of the Sub-Frenchman Disconformity in Southwest Saskatchewan. Bulletin of Canadian Petroleum Geology 35:454–459.

Lerbekmo, J. F. 1989. The stratigraphic position of the 33-33r (Campanian) polarity chron boundary in southeastern Alberta. Bulletin of Canadian Petroleum Geology 37:43–47.

Lerbekmo, J. F. 1999. Magnetostratigraphy of the Canadian Continental Drilling Program Cretaceous-Tertiary (KT) Boundary Project core holes, western Canada. Canadian Journal of Earth Sciences 36:705–715.

Lerbekmo, J. F. 2002. The Dorothy bentonite: an extraordinary case of secondary thickening in a late Campanian volcanic ash fall in central Alberta. Canadian Journal of Earth Sciences 39:1745–1754.

Lerbekmo, J. F. 2005. Paleomagnetostratigraphy; pp. 83–87 in Dinosaur Provincial Park. Indiana University Press.

Lerbekmo, J. F. 2009. Glacioeustatic sea level fall marking the base of supercycle TA-1 at 66.5 Ma recorded by the kaolinization of the Whitemud Formation and the Colgate Member of the Fox Hills Formation. Marine and Petroleum Geology 26:1299–1303.

Lerbekmo, J. F. 2014. The Chicxulub-Shiva extraterrestrial one-two killer punches to Earth 65 million years ago. Marine and Petroleum Geology 49:203–207.

Lerbekmo, J. F., and D. R. Braman. 2002. Magnetostratigraphic and biostratigraphic correlation of late Campanian and Maastrichtian marine and continental strata from the Red Deer Valley to the Cypress Hills, Alberta, Canada. Canadian Journal of Earth Sciences 39:539–557.

Lerbekmo, J. F., and D. R. Braman. 2005. Magnetostratigraphic and Palynostratigraphic Correlation of Late Campanian to Early Maastrichtian strata of the Bearpaw and Horseshoe Canyon formations between the CPOG Strathmore Corehole and the Red Deer Valley Section, Alberta, Canada. Bulletin of Canadian Petroleum Geology 53:154–164.

Lerbekmo, J. F., and K. C. Coulter. 1985. Late Cretaceous to early Tertiary magnetostratigraphy of a continental sequence: Red Deer Valley, Alberta, Canada. Canadian Journal of Earth Sciences 22:567–583.

Lerbekmo, J. F., and M. E. Evans. 2012. Cryptochrons and tiny wiggles: New magnetostratigraphic evidence from chrons 32 and 33 in Western Canada. Physics of the Earth and Planetary Interiors 202:8–13.

Lerbekmo, J. F., and N. Lehtola. 2011. Magnetostratigraphy of the Bearpaw and Blood Reserve formations on the St. Mary River: Evidence for the effect of the Sweetgrass Arch. Bulletin of Canadian Petroleum Geology 59:1–6.

Lerbekmo, J. F., A. R. Sweet, and M. J. Duke. 1996. A normal polarity subchron that embraces the K/T boundary: A measure of sedimentary continuity across the boundary and synchroneity of boundary events. Geological Society of America Special Papers 307:465–476.

Lerbekmo, J. F., D. R. Braman, O. Catuneanu, and N. C. Humphrey. 2003. Magnetostratigraphic and Palynostratigraphic Correlation of Late Campanian Strata of the Bearpaw and Horseshoe Canyon Formations of the RCA Castor Corehole to the Red Deer Valley, Alberta. Bulletin of Canadian Petroleum Geology 51:70–77.

Lewis, C., A. Heckert, S. Lucas, and T. Williamson. 2007. A diverse new microvertebrate fauna from the Upper Cretaceous (late Santonian-early Campanian) Menefee Formation of New Mexico. 27:105A–105A.

Li, P.-X., D.-Y. Su, Y.-G. Li, and J.-X. Yu. 1994. Age assignment of the *Lycoptera*-bearing bed. Acta Geologica Sinica-English Edition 7:329-349.

Lillegraven, J. A., and M. C. McKenna. 1986. Fossil mammals from the “Mesaverde” Formation (late Cretaceous, Judithian) of the Bighorn and Wind River basins, Wyoming : with definitions of late Cretaceous North American land-mammal “ages”. American Museum novitates ; no. 2840. American Museum Novitates 2840:1–68.

Lillegraven, J. A., and L. M. Ostresh. 1990. Late Cretaceous (earliest Campanian/Maastrichtian) evolution of western shorelines of the North American Western Interior Seaway in relation to known mammalian faunas. Geological Society of America Special Papers 243:1–30.

Lindsay, E. H., R. F. Butler, and N. M. Johnson. 1981. Magnetic polarity zonation and biostratigraphy of Late Cretaceous and Paleocene continental deposits, San Juan Basin, New Mexico. American Journal of Science 281:390–435.

Livaccari, R. F., K. Burke, and A. M. C. Şengör. 1981. Was the Laramide orogeny related to subduction of an oceanic plateau? Nature 289:276–278.

Loewen, M. A., R. B. Irmis, J. J. W. Sertich, P. J. Currie, and S. D. Sampson. 2013a. Tyrant Dinosaur Evolution Tracks the Rise and Fall of Late Cretaceous Oceans. PLOS ONE 8:e79420.

Loewen, M. A., A. A. Farke, S. D. Sampson, M. A. Getty, E. K. Lund, and P. M. O'Connor. 2013b. Ceratopsid dinosaurs from the Grand Staircase of southern Utah. At the Top of the Grand Staircase: The Late Cretaceous of Southern Utah. Indiana University Press, Bloomington 488–503.

Loewen, M. A., S. D. Sampson, E. K. Lund, A. A. Farke, M. C. Aguillón-Martínez, C. A. de Leon, R. A. Rodríguez-de la Rosa, M. A. Getty, and D. A. Eberth. 2010. Horned dinosaurs (Ornithischia: Ceratopsidae) from the Upper Cretaceous (Campanian) Cerro del Pueblo Formation, Coahuila, Mexico; pp. 99–116 in M. J. Ryan, B. J. Chinnery-Allgeier, and D. A. Eberth (eds.), New Perspectives on Horned Dinosaurs: The Royal Tyrrell Museum Ceratopsian Symposium. Indiana University Press, Bloomington.

Lofgren, D. L. 1995. The Bug Creek Problem and the Cretaceous-Tertiary Transition at McGuire Creek, Montana. University of California Publications in Geological Sciences 140:1-185.

Lohmann, G. P., and B. A. Malmgren. 1983. Equatorward migration of *Globorotalia truncatulinoides* ecophenotypes through the late Pleistocene; gradual evolution or ocean change? Paleobiology 9:414-421.

Longrich, N. R. 2010. Mojoceratops perifania, A New Chasmosaurine Ceratopsid from the Late Campanian of Western Canada. Journal of Paleontology 84:681–694.

Longrich, N. R. 2011. *Titanoceratops ouranos*, a giant horned dinosaur from the Late Campanian of New Mexico. Cretaceous Research 32:264-276.

Longrich, N. R. 2013. *Judiceratops tigris*, a new horned dinosaur from the middle Campanian Judith River Formation of Montana. Bulletin of the Peabody Museum of Natural History 54:51-65.

Longrich, N. R. 2014. The horned dinosaurs Pentaceratops and Kosmoceratops from the upper Campanian of Alberta and implications for dinosaur biogeography. Cretaceous Research 51:292–308.

Longrich, N. R. 2015. Systematics of Chasmosaurus - new information from the Peabody Museum skull, and the use of phylogenetic analysis for dinosaur alpha taxonomy. F1000Research.

Longrich, N. R., and P. J. Currie. 2009. Albertonykus borealis, a new alvarezsaur (Dinosauria: Theropoda) from the Early Maastrichtian of Alberta, Canada: implications for the systematics and ecology of the Alvarezsauridae. Cretaceous Research 30:239–252.

Longrich, N. R., and D. J. Field. 2012. *Torosaurus* is not *Triceratops*: ontogeny in chasmosaurine ceratopsids as a case study in dinosaur taxonomy. PLoS ONE 7:e32623 p. 1-10. doi:10.1371/journal.pone.0032623.

Longrich, N. R., J. Sankey, and D. Tanke. 2010. Texacephale langstoni, a new genus of pachycephalosaurid (Dinosauria: Ornithischia) from the upper Campanian Aguja Formation, southern Texas, USA. Cretaceous Research 31:274–284.

Longrich, N. R., T. Tokaryk, and D. J. Field. 2011. Mass extinction of birds at the Cretaceous–Paleogene (K–Pg) boundary. Proceedings of the National Academy of Sciences 108:15253–15257.

Lorenz, J. C., and W. Gavin. 1984. Geology of the Two Medicine Formation and the sedimentology of a dinosaur nesting ground. Montana Geological Society 1984 Field Conference Guidebook 1984:175–186.

Love, J. D., and A. C. Christiansen. 1985. Geologic map of Wyoming.

Lucas, S. G., and R. M. Sullivan. 2000. The sauropod dinosaur Alamosaurus from the Upper Cretaceous of the San Juan Basin, New Mexico. New Mexico Museum of Natural History and Science Bulletin 17:147–156.

Lucas, S. G., A. P. Hunt, and R. M. Sullivan. 2006a. Stratigraphy and age of the Upper Cretaceous Fruitland Formation, west-central San Juan Basin, New Mexico. New Mexico Museum of Natural History and Science Bulletin 35:1–6.

Lucas, S. G., R. M. Sullivan, and A. P. Hunt. 2006b. Re-evaluation of Pentaceratops and Chasmosaurus (Ornithischia: Ceratopsidae) in the Upper Cretaceous of the Western Interior. New Mexico Museum of Natural History and Science Bulletin 35:367–370.

Lucas, S. G., R. M. Sullivan, and J. A. Spielmann. 2012. Cretaceous vertebrate biochronology, North American Western Interior. Journal of Stratigraphy 36:436–461.

Lucas, S. G., J. A. Spielmann, J. I. Kirkland, J. R. Foster, and R. M. Sullivan. 2006c. A juvenile hadrosaurine from the middle Campanian (Late Cretaceous) interval of the Mancos Shale, western Colorado. Late Cretaceous Vertebrates from the Western Interior: New Mexico Museum of Natural History and Science Bulletin 35:281–292.

Lucas, S. G., R. M. Sullivan, S. M. Cather, S. E. Jasinski, D. W. Fowler, A. B. Heckert, J. A. Spielmann, and A. P. Hunt. 2009. No definitive evidence of Paleocene dinosaurs in the San Juan Basin. Paleontologia Electronica 12:1–10.

Lull, R.S. 1915. The mammals and horned dinosaurs of the Lance formation of Niobrara County, Wyoming. American Journal of Science 4:319–348.

Lull, R. S. 1933. A revision of the Ceratopsia or horned dinosaurs. Memoirs of the Peabody Museum of Natural History 3:175.

Lull, R. S., and N. E. Wright. 1942. Hadrosaurian Dinosaurs of North America. Geological Society of America Special Papers 40:1–272.

Lund, S. P., J. H. Hartman, and S. K. Banerjee. 2002. Magnetostratigraphy of interfingering upper Cretaceous–Paleocene marine and continental strata of the Williston Basin, North Dakota and Montana. Geological Society of America Special Papers 361:57–74.

Ma, F. 1987. Review of *Lycoptera davidi*. Vertebrata PalAsiatic 25:8-19.

Machalski, A., J. W. M. Jagt, N. H. Landman, and N. Motchurova-Dekova. 2007. The highest records of North American scaphitid ammonites in the European Maastrichtian (Upper Cretaceous) and their stratigraphic implications. Acta Geologica Polonica 57:169–185.

Macleod N. 1991. Punctuated anagenesis and the importance of stratigraphy to paleobiology. Paleobiology 17(2):167-188.

Maddison, W.P., and D.R. Maddison. 2011. Mesquite: a modular system for evolutionary analysis. Version 2.75. http://mesquiteproject.org/

Maddison, W. P., and D. R. Maddison. 2015. Mesquite: a modular system for evolutionary analysis. Version 3.02;http://mesquiteproject.org.

Madsen, J. H. 1974. A new theropod dinosaur from the Upper Jurassic of Utah. Journal of Paleontology 48:27-31.

Maidment, S. C. R., and P. M. Barrett. 2011. A new specimen of Chasmosaurus belli (Ornithischia: Ceratopsidae), a revision of the genus, and the utility of postcrania in the taxonomy and systematics of ceratopsid dinosaurs. Zootaxa 2963:1–47.

Main, R. P., A. R. De, J. R. Horner, and K. Padian. 2005. The evolution and function of thyreophoran dinosaur scutes: implication for plate function in stegosaurs. Paleobiology 294–314.

Maiorino, L., A. A. Farke, T. Kotsakis, and P. Piras. 2013. Is *Torosaurus Triceratops*? Geometric morphometric evidence of Late Maastrichtian ceratopsid dinosaurs. PLoS ONE 8:e81608. doi:10.1371/journal.pone.0081608.

Mair, W. 2010. Reinforcing Reinforcement. PLoS Biology 8:e1000340.

Maleev, E. A. 1955. Giant carnivorous dinosaurs of Mongolia. Doklady Akademii Nauka SSSR+ 104:634-637.

Mallon, J. C., D. C. Evans, M. J. Ryan, and J. S. Anderson. 2012. Megaherbivorous dinosaur turnover in the Dinosaur Park Formation (upper Campanian) of Alberta, Canada. Palaeogeography, Palaeoclimatology, Palaeoecology 350–352:124–138.

Mallon, J. C., R. B. Holmes, D. A. Eberth, M. J. Ryan, and J. S. Anderson. 2011. Variation in the skull of Anchiceratops (Dinosauria, Ceratopsidae) from the Horseshoe Canyon Formation (Upper Cretaceous) of Alberta. Journal of Vertebrate Paleontology 31:1047–1071.

Mallon, J. C., R. Holmes, J. S. Anderson, A. A. Farke, D. C. Evans, and H.-D. Sues. 2014. New information on the rare horned dinosaur Arrhinoceratops brachyops (Ornithischia: Ceratopsidae) from the Upper Cretaceous of Alberta, Canada. Canadian Journal of Earth Sciences 51:618–634.

Malmgren, B. A., W. A. Berggren, and G. P. Lohmann. 1984. Species Formation Through Punctuated Gradualism in Planktonic Foraminifera. Science 225:317-319.

Marcot, J.D., and D.L. Fox. 2008. StrataPhy: a new computer program for stratocladistic analysis. Palaeontologica Electronica 11:5A.

Margottini, L. 2011. Is it time to declutter the dinosaur roster? Science 332:782.

Marriott, S. B. 1999. The use of Models in the Interpretation of the Effects of Base-Level Change on Alluvial Architecture; pp. 269–281 in N. D. Smith and J. Rogers (eds.), Fluvial Sedimentology VI. Blackwell Publishing Ltd.

Marsh, O. C. 1888. A new family of horned dinosaurs from the Cretaceous. American Journal of Science 3:477-478.

Marsh, O. C. 1889. Notice of gigantic horned Dinosauria from the Cretaceous. American Journal of Science 38:173–175.

Marsh O. C. 1890. Description of new dinosaurian reptiles. American Journal of Science 3:81-86.

Marsh, O. C. 1890. Additional characters of the Ceratopsidae with notice of new Cretaceous dinosaurs. American Journal of Science 3:418-426.

Marsh, O. C. 1892. Notice of new reptiles from the Laramie Formation. American Journal of Science s3-43:449–453.

Marshall, J. A. R. 2011. Group selection and kin selection: formally equivalent approaches. Trends in Ecology & Evolution 26:325–332.

Marshall, J. L., M. L. Arnold, and D. J. Howard. 2002. Reinforcement: the road not taken. Trends in Ecology & Evolution 17:558–563.

Martin, A. J. 2000. Flaser and wavy bedding in ephemeral streams: a modern and an ancient example. Sedimentary Geology 136:1–5.

Martins, A. B., M. A. de Aguiar, and Y. Bar-Yam. 2013. Evolution and stability of ring species. Proceedings of the National Academy of Sciences.

Maryanska, T., and H. Osmolska. 1979. Aspects of hadrosaurian cranial anatomy. Lethaia 12:265-273.

Mason, I. P., M. T. Heizler, and T. E. Williamson. 2013. 40 Ar/39 Ar Sanidine Chronostratigraphy Of K-Pg Boundary Sediments Of The San Juan Basin, Nm. New Mexico Geological Society 2013 Spring Meeting 42.

Mateer, N. J. 1980. The reptilian megafauna from the Kirtland Shale (Late Cretaceous) of the San Juan Basin, New Mexico; pp. 49-75 in S. G. Lucas, J. K. Rigby Jr., and B. S. Kues (eds.), Advances in San Juan Basin Paleontology. University of New Mexico Press, Albuquerque.

Matute, D. R. 2010. Reinforcement can overcome gene flow during speciation in Drosophila. Current Biology: CB 20:2229–2233.

Mayr, E. 1959. Darwin and the evolutionary theory in biology, p. 1-10 in Meggers J., ed., Evolution and Anthropology: A Centennial Appraisal: Anthropological Society of Washington, Washington, D.C.

McCarthy, P. J., and A. G. Plint. 1998. Recognition of interfluve sequence boundaries: Integrating paleopedology and sequence stratigraphy. Geology 26:387–390.

McDonald A. T., D. G. Wolfe, and J. I. Kirkland. 2010. A new basal hadrosauroid (Dinosauria: Ornithopoda) from the Turonian of New Mexico. Journal of Vertebrate Paleontology 3(3): 799–812.

McDougall, I., and T. M. Harrison. 1999. Geochronology and Thermochronology by the 40Ar/39Ar Method, 2nd ed. Oxford University Press, 288 pp.

McKenna, M. C., and J. D. Love. 1970. Local stratigraphic and tectonic significance of Leptoceratops, a Cretaceous dinosaur in the Pinyon Conglomerate, northwestern Wyoming. United States Geological Survey, Professional Paper 700:55–61.

Meek, F. B., and F. V. Hayden. 1861. Descriptions of New Lower Silurian,(Primordial), Jurassic, Cretaceous and Tertiary Fossils: Collected in Nebraska, by the Exploring Expeditions Under the Command of Capt. Wm. F. Raynolds,... Proceedings of the Academy of Natural Sciences of Philadelphia 415–447.

Mendelson, T. C., and K. L. Shaw. 2012. The (mis)concept of species recognition. Trends in Ecology & Evolution 27:421–427.

Meyers, S. R., S. E. Siewert, B. S. Singer, B. B. Sageman, D. J. Condon, J. D. Obradovich, B. R. Jicha, and D. A. Sawyer. 2012. Intercalibration of radioisotopic and astrochronologic time scales for the Cenomanian-Turonian boundary interval, Western Interior Basin, USA. Geology 40:7–10.

Miall, A. D. 1985. Architectural-element analysis: a new method of facies analysis applied to fluvial deposits.

Miall, A. D. 1991. Stratigraphic Sequences and Their Chronostratigraphic Correlation. Journal of Sedimentary Petrology 61:497-505.

Miall, A. D. 1996. The Geology of Fluvial Deposits. Springer Verlag Berlín, 582 pp.

Miall, A. D. 2002. Architecture and sequence stratigraphy of Pleistocene fluvial systems in the Malay Basin, based on seismic time-slice analysis. American Association of Petroleum Geologists Bulletin 86:1201–1206.

Miall, A. D. 2010. The Geology of Stratigraphic Sequences. Springer Science & Business Media, 522 pp.

Miall, A. D., O. Catuneanu, B. K. Vakarelov, and R. Post. 2008. The Western Interior Basin; pp. 329–362 in Andrew D. Miall (ed.), Sedimentary Basins of the World. vol. 5. Elsevier.

Miller, K. G., G. S. Mountain, J. D. Wright, and J. V. Browning. 2011. A 180-Million-Year Record of Sea Level and Ice Volume Variations from Continental Margin and Deep-Sea Isotopic Records. Oceanography 24:651–655.

Min, K., R. Mundil, P. R. Renne, and K. R. Ludwig. 2000. A test for systematic errors in 40 Ar/39 Ar geochronology through comparison with U/Pb analysis of a 1.1-Ga rhyolite. Geochimica et Cosmochimica Acta 64:73–98.

Mitchell, J. H. 2002. Sedimentary record of Late Cretaceous through Paleocene evolution of the Bighorn Basin, Wyoming. M.S., University of Montana, Missoula. 107 pp.

Mitchum Jr., R. M., and J. C. Van Wagoner. 1991. High-frequency sequences and their stacking patterns: sequence-stratigraphic evidence of high-frequency eustatic cycles. Sedimentary Geology 70:131–160.

Mitchum Jr, R. M., P. R. Vail, and S. Thompson III. 1977. Seismic Stratigraphy and Global Changes of Sea Level: Part 2. The Depositional Sequence as a Basic Unit for Stratigraphic Analysis: Section 2. Application of Seismic Reflection Configuration to Stratigraphic Interpretation. Seismic Stratigraphy - Applications to hydrocarbon exploration. American Association of Petroleum Geologists, Tulsa, Oklahoma.165:53–62.

Molenaar, C. M., W. A. Cobban, E. A. Merewether, C. L. Pillmore, D. G. Wolfe, and J. M. Holbrook. 2002. Regional Stratigraphic Cross Sections of Cretaceous Rocks from East-Central Arizona to the Oklahoma Panhandle. U.S. Geological Survey, pp.

Molina, E., L. Alegret, I. Arenillas, J. A. Arz, N. Gallala, J. Hardenbol, K. von Salis, E. Steurbaut, N. Vandenberghe, and D. Zaghbib-Turki. 2006. The Global Boundary Stratotype Section and Point for the base of the Danian Stage (Paleocene, Paleogene,“ Tertiary”, Cenozoic) at El Kef, Tunisia-Original definition and revision. Episodes 29:263–273.

Montgomery, P., E. A. Hailwood, A. S. Gale, and J. A. Burnett. 1998. The magnetostratigraphy of Coniacian-Late Campanian chalk sequences in southern England. Earth and Planetary Science Letters 156:209–224.

Moore, J. R., G. P. Wilson, M. Sharma, H. R. Hallock, D. R. Braman, and P. R. Renne. 2014. Assessing the relationships of the Hell Creek–Fort Union contact, Cretaceous-Paleogene boundary, and Chicxulub impact ejecta horizon at the Hell Creek Formation lectostratotype, Montana, USA. Geological Society of America Special Papers 503:123–135.

Mori, H., P. S. Druckenmiller, and G. M. Erickson. 2015. A new Arctic hadrosaurid from the Prince Creek Formation (lower Maastrichtian) of northern Alaska. Acta Palaeontologica Polonica.

Mull, C. G., D. W. Houseknecht, and K. J. Bird. 2003. Revised Cretaceous and Tertiary Stratigraphic Nomenclature in the Colville Basin, Northern Alaska. US Department of the Interior, US Geological Survey, pp.

Mullen, W. Fossil identified as mini-T.rex. Chicago Tribune, 18th September 2009. http://articles.chicagotribune.com/2009-09-18/news/0909170802_1_fossil-bones-tyrannosaurus-rex-chicago-paleontologist-paul-sereno. Retrieved 2011 March 8.

Murphy, D. A. 1986. Sedimentation of the upper Hell Creek Formation (Upper Cretaceous), Carter County, Montana. M.S., San Diego State University, San Diego, California, 104 pp.

Murphy, E. C., J. W. Hoganson, and K. R. Johnson. 2002. Lithostratigraphy of the Hell Creek Formation in North Dakota. Geological Society of America Special Papers 361:9–34.

Nambudiri, E. M. V., and P. L. Binda. 1991. Paleobotany, palynology and depositional environment of the Maastrichtian Whitemud Formation in Alberta and Saskatchewan, Canada. Cretaceous Research 12:579–596.

Newbrey, M. G., A. M. Murray, D. B. Brinkman, M. V. H. Wilson, and A. G. Neuman. 2010. A new articulated freshwater fish (Clupeomorpha, Ellimmichthyiformes) from the Horseshoe Canyon Formation, Maastrichtian, of Alberta, Canada. Canadian Journal of Earth Sciences 47:1183-1196.

Newman, K. R. 1987. Biostratigraphic correlation of Cretaceous-Tertiary boundary rocks, Colorado to San Juan Basin, New Mexico; pp. 151-163 in J. E. Fassett and J. K. Rigby Jr. (eds.), Cretaceous–Tertiary Boundary in the San Juan and Raton Basins, New Mexico and Colorado. Geological Society of America Special Paper.

Nicholls, E. L., and A. P. Russell. 1990. Paleobiogeography of the Cretaceous Western Interior Seaway of North America: the vertebrate evidence. Palaeogeography, Palaeoclimatology, Palaeoecology 79:149–169.

Nichols, D. J. 1995. Palynostratigraphy in Relation to Sequence Stratigraphy, Straight Cliffs Formation (Upper Cretaceous), Kaiparowits Plateau, Utah. U.S. G.P.O., pp.

Nichols, D. J. 1997. Palynology and ages of some Upper Cretaceous formations in the Markagunt and northwestern Kaiparowits Plateaus, southwestern Utah. US Geological Survey Bulletin.

Nichols, D. J. 2002. Palynology and palynostratigraphy of the Hell Creek Formation in North Dakota: A microfossil record of plants at the end of Cretaceous time. Geol. Soc. Am. Spec. Pap 361:393–456.

Nordt, L., S. Atchley, and S. Dworkin. 2003. Terrestrial evidence for two greenhouse events in the latest Cretaceous. GSA Today 13:4–9.

Obradovich, J. D. 1993. A Cretaceous time scale. Evolution of the Western Interior Basin 39:379–396.

Obradovich, J. D. 2002. Geochronology of Laramide synorogenic strata in the Denver Basin, Colorado. Rocky Mountain Geology 37:165–171.

Obradovich, J. D., and W. A. Cobban. 1975. A Time-Scale For The Late Cretaceous Of The Western Interior Of North America. Geological Association of Canada Special Paper 13:31–54.

O'Connor, P. M., E. M. Roberts, L. Tapanila, A. L. Deino, T. Hieronymous, and Z. A. Jinnah. 2009. Reconnaissance paleontology in the Straight Cliffs and Wahweap formations (Turonian– Campanian), Grand Staircase–Escalante National Monument, Utah. Advances in Western Interior Late Cretaceous Paleontology and Geology, St. George, Utah, Abstracts with Program.

Ogg, J. G. 2012. Geomagnetic Polarity Time Scale; pp. 85–113 in The geologic time scale. vol. 1. Elsevier.

Ogg, J. G., and A. G. Smith. 2004. The geomagnetic polarity time scale; pp. 63–86 in F. M. Gradstein, J. G. Ogg, and A. G. Smith (eds.), A Geologic Time Scale. Cambridge University Press, Cambridge, UK.

Ogg, J. G., L. A. Hinnov, and C. Huang. 2012. Cretaceous; pp. 793–853 in F. M. Gradstein, J. G. Ogg, M. D. Schmitz, and G. M. Ogg (eds.), The Geologic Time Scale 2012. Elsevier, Amsterdam.

Ogg, J. G., F. P. Agterberg, and F. M. Gradstein. 2004. The Cretaceous Period; pp. 344–383 in A Geologic Time Scale.

O'Leary M. A., and S. G. Kaufman. 2008. MorphoBank 2.5: Web application for morphological phylogenetics and taxonomy, http://www.morphobank.org.

Olsen, T., R. Steel, K. Hogseth, T. Skar, and S. L. Roe. 1995. Sequential architecture in a fluvial succession; sequence stratigraphy in the Upper Cretaceous Mesaverde Group, Prince Canyon, Utah. Journal of Sedimentary Research 65:265–280.

Osborn, H.F. 1905. Tyrannosaurus and other Cretaceous carnivorous dinosaurs. Bulletin of the American Museum of Natural History 22: 475–479.

Osborn, H. F. 1923. A new genus and species of Ceratopsia from New Mexico, Pentaceratops sternbergii. American Museum Novitates 93:3.

Ostrom, J. H. 1961. A New Species of Hadrosaurian Dinosaur from the Cretaceous of New Mexico. Journal of Paleontology 35:575–577.

Ostrom J.H., and P. Wellnhofer. 1986. The Munich specimen of *Triceratops* with a revision of the genus. Zitteliana 14:111-158.

Ostrom, J.H., and P. Wellnhofer. 1990. Triceratops: An example of flawed systematics, p. 245-254 in Carpenter, K., and Currie, P.J., eds., Dinosaur Systematics: Approaches and Perspectives. Cambridge University Press, New York, New York.

O'Sullivan, R. B., and H. M. Beikman. 1963. Geology, structure, and uranium deposits of the Shiprock Quadrangle, New Mexico and Arizona, Report 345.

O'Sullivan, R. B., G. R. Scott, and J. S. Heller. 1979. Preliminary geologic map of the Bisti Trading Post Quadrangle, San Juan County, New Mexico, Report 1075.

Ott, C. J. 2006. Cranial anatomy and biogeography of the first Leptoceratops gracilis (Dinosauria: Ornithischia) specimens from the Hell Creek Formation, southeast Montana; pp. 213–233 in Horns and Beaks. Ceratopsian and Ornithopod Dinosaurs. Indiana University Press.

Ott C. J., and P. L. Larson. 2010. A new, small ceratopsian dinosaur from the latest Cretaceous Hell Creek Formation, northwest South Dakota, United States: a preliminary description pp. 203-218 in New Perspectives on Horned Dinosaurs: The Royal Tyrell Museum Ceratopsian Symposium, M. J. Ryan, B. J. Chinnery-Allgeier, and D. A. Eberth (eds.) Indiana University Press, Bloomington and Indianapolis.

Owen, R. 1842. Report on British Fossil Reptiles. Part II. Reports of the British Association for the Advancement of Science 11:60-204.

Padian, K., and J. R. Horner. 2011a. The definition of sexual selection and its implications for dinosaurian biology. Journal of Zoology 283:23–27.

Padian, K., and J. R. Horner. 2011b. The evolution of "bizarre structures" in dinosaurs: biomechanics, sexual selection, social selection or species recognition? Journal of Zoology 283:3–17.

Padian, K., and J. R. Horner. 2013. Misconceptions of sexual selection and species recognition: a response to Knell et al. and to Mendelson and Shaw. Trends in Ecology & Evolution 28:249–250.

Padian, K., and C. L. May. 1993. The earliest dinosaurs. New Mexico Museum of Natural History and Science Bulletin 3:379-381.

Padian, K., J. R. Horner, and A. d. Ricqlès. 2004. Growth in small dinosaurs and pterosaurs: the evolution of archosaurian growth strategies. Journal of Vertebrate Paleontology 24:555-571.

Padian, K., A. d. Ricqlès, and J. R. Horner. 2001. Dinosaurian growth rates and bird origins. Nature 412:405-408.

Pardo J. D., A. K. Huttenlocker, and J. D. Marcot. 2008. Stratocladistics and evaluation of evolutionary modes in the fossil record: an example from the ammonite genus *Semiformiceras*. Palaeontology. 51(4):767-773.

Parks, W. A. 1919. Preliminary description of a new species of trachodont dinosaur of the genus Kritosaurus, Kritosaurus incurvimanus. Transactions of the Royal Society of Canada, Series 3:51–59.

Parks, W. A. 1920. The osteology of the trachodont dinosaur Kritosaurus incurvimanus. University of Toronto Studies 5–74.

Parks, W. A. 1922. Parasaurolophus Walkeri: A New Genus and Species Of Crested Trachodont Dinosaur. University of Toronto Studies 5–32.

Parks, W. A. 1925. Arrhinoceratops brachyops, a new genus and species of Ceratopsia from the Edmonton Formation of Alberta. University of Toronto Studies 5–15.

Paterson, H. E. 1985. The recognition concept of species. Species and Speciation 4:21–29.

Payenberg, T. H., D. R. Braman, D. W. Davis, and A. D. Miall. 2002. Litho-and chronostratigraphic relationships of the Santonian Campanian Milk River

Formation in southern Alberta and Eagle Formation in Montana utilising stratigraphy, U Pb geochronology, and palynology. Canadian Journal of Earth Sciences 39:1553–1577.

Peale, A. C. 1909. On the application of the term Laramie. American Journal of Science 45–58.

Pearson, D.A., T., Schaefer, K.R., Johnson, D.J., Nichols, and J.P., Hunter. 2002. Vertebrate biostratigraphy of the Hell Creek Formation in southwestern North Dakota and northwestern South Dakota, p. 145-167 in Hartman, J.H., K.R., Johnson, and D.J., Nichols (eds.) The Hell Creek Formation and the Cretaceous-Tertiary Boundary in the Northern Great Plains: An Integrated Continental Record of the End of the Cretaceous. Geological Society of America Special Paper 361.

Pearson, P. N., and T. H. G. Ezard. 2014. Evolution and speciation in the Eocene planktonic foraminifer Turborotalia. Paleobiology 40:130-143.

Penkalski, P., and P. Dodson. 1999. The morphology and systematics of Avaceratops, a primitive horned dinosaur from the Judith River Formation (Late Campanian) of Montana, with the description of a second skull. Journal of Vertebrate Paleontology 19:692–711.

Peterson, F. 1969. Four New Members of the Upper Cretaceous Straight Cliffs Formation in the Southeastern Kaiparowits Region, Kane County, Utah. United States Geological Survey, pp.

Pleijel F. 1995. On character coding for phylogeny reconstruction. Cladistics. 11:309-315.

Plint, A. G., P. J. McCarthy, and U. F. Faccini. 2001. Nonmarine sequence stratigraphy: Updip expression of sequence boundaries and systems tracts in a high-resolution framework, Cenomanian Dunvegan Formation, Alberta foreland basin, Canada. AAPG Bulletin 85:1967–2001.

Polly P. D. 1997. Ancestry and species definition in paleontology: stratocladistic analysis of Paleocene-Eocene Viverravidae (Mammalia, Carnivora) from Wyoming. Contributions from the Museum of Paleontology University of Michigan 30(1):1-53.

Posamentier, H. W., and P. R. Vail. 1988. Eustatic controls on clastic deposition II—sequence and systems tract models. SEPM Special Publication 42:125–154.

Posamentier, H. W., and G. P. Allen. 1999. Siliciclastic Sequence Stratigraphy: Concepts and Applications. SEPM (Society for Sedimentary Geology), 210 pp.

Powell, J. S. 1973. Paleontology and sedimentation models of the Kimbeto Member of the Ojo Alamo Sandstone. Cretaceous and Tertiary Rocks of the Southern Colorado Plateau 111–122.

Prieto-Marquez, A. 2008. Phylogeny and historical biogeography of hadrosaurid dinosaurs. Florida State University, 861 pp.

Prieto-Marquez, A. 2010. The braincase and skull roof of Gryposaurus notabilis (Dinosauria, Hadrosauridae), with a taxonomic revision of the genus. Journal of Vertebrate Paleontology 30:838–854.

Prieto-Márquez, A. 2012. The skull and appendicular skeleton of Gryposaurus latidens, a saurolophine hadrosaurid (Dinosauria: Ornithopoda) from the early Campanian (Cretaceous) of Montana, USA. Canadian Journal of Earth Sciences 49:510–532.

Prieto-Márquez, A. 2013. Skeletal morphology of Kritosaurus navajovius (Dinosauria: Hadrosauridae) from the Late Cretaceous of the North American south-west, with an evaluation of the phylogenetic systematics and biogeography of Kritosaurini. Journal of Systematic Palaeontology 12:133–175.

Prieto-Márquez, A., and J. Wagner. 2013. Saurolophus morrisi, a new species of hadrosaurid dinosaur from the Late Cretaceous of the Pacific coast of North America. Acta Palaeontologica Polonica.

R Core Team. 2013. R: A language and environment for statistical computing. R Foundation for Statistical Computing, Vienna, Austria. URL http://www.R-project.org/.

R_Core_Team. 2014. R: A language and environment for statistical computing. R Foundation for Statistical Computing, Vienna, Austria. ISBN 3-900051-07-0, URL http://www.R-project.org/.

Rambaut, A. 2014. FigTree, Tree Figure Drawing Tool, Version 1.4.2; http://mesquiteproject.org.

Ramírez-Velasco, A. A., M. Benammi, A. Prieto-Márquez, J. A. Ortega, and R. Hernández-Rivera. 2012. Huehuecanauhtlus tiquichensis, a new hadrosauroid dinosaur (Ornithischia: Ornithopoda) from the Santonian (Late Cretaceous) of Michoacán, Mexico. Canadian Journal of Earth Sciences 49:379–395.

Rand, A. S., and E. E. Williams. 1970. An estimation of redundancy and information content of anole dewlaps. The American Naturalist 104:99–103.

Rasband, W. S. 1997-2014. ImageJ. U. S. National Institutes of Health, Bethesda, Maryland, USA; http://imagej.nih.gov/ij/.

Rauhut, O. W. M. 2003. A tyrannosauroid dinosaur from the Upper Jurassic of Portugal. Palaeontology 46:903-910.

Raynolds, R. G. 2002. Upper Cretaceous and Tertiary stratigraphy of the Denver Basin, Colorado. Rocky Mountain Geology 37:111–134.

Raynolds, R. G., and K. R. Johnson. 2003. Synopsis of the stratigraphy and paleontology of the uppermost Cretaceous and lower Tertiary strata in the Denver Basin, Colorado. Rocky Mountain Geology 38:171–181.

Reeside, J. B. 1924. Upper Cretaceous and Tertiary Formations of the Western Part of San Juan Basin, Colorado, and New Mexico. United States Geological Survey, pp.

Reeside, J. B. 1927. The cephalopods of the Eagle Sandstone and related formations in the Western Interior of the United States. United States Geological Survey, Professional Paper 151.

Reisz, R. R., D. Scott, H.-D. Sues, D. C. Evans, and M. A. Raath. 2005. Embryos of an early Jurassic prosauropod dinosaur and their evolutionary significance. Science 309:761-764.

Renne, P. R., R. Mundil, G. Balco, K. Min, and K. R. Ludwig. 2010. Joint determination of 40K decay constants and 40Ar□/40K for the Fish Canyon sanidine standard, and improved accuracy for 40Ar/39Ar geochronology. Geochimica et Cosmochimica Acta 74:5349–5367.

Renne, P. R., G. Balco, K. R. Ludwig, R. Mundil, and K. Min. 2011. Response to the comment by WH Schwarz et al. on "Joint determination of 40 K decay constants and 40 Ar□/40 K for the Fish Canyon sanidine standard, and improved accuracy for 40 Ar/39 Ar geochronology" by PR Renne et al.(2010). Geochimica et Cosmochimica Acta 75:5097–5100.

Renne, P. R., C. C. Swisher, A. L. Deino, D. B. Karner, T. L. Owens, and D. J. DePaolo. 1998. Intercalibration of standards, absolute ages and uncertainties in 40Ar/39Ar dating. Chemical Geology 145:117–152.

Renne, P. R., A. L. Deino, R. C. Walter, B. D. Turrin, C. C. Swisher, T. A. Becker, G. H. Curtis, W. D. Sharp, and A.-R. Jaouni. 1994. Intercalibration of astronomical and radioisotopic time. Geology 22:783–786.

Rensch B. 1947. Neure Probleme der Abstammungslehre. Die transspezifische evolution. Ferdinand Enke, Stuttgart.

Rensch, B. 1959. Evolution Above the Species Level. English translation Edition, Columbia Biological Series. Columbia University Press, New York, 419 pp.

Ricqlès, A. d., K. Padian, and J. R. Horner. 2003. On the bone histology of some Triassic pseudosuchian archosaurs and related taxa. Annales de Paléontologie 89:67-101.

Rivera, T. A., M. Storey, C. Zeeden, F. J. Hilgen, and K. Kuiper. 2011. A refined astronomically calibrated 40 Ar/39 Ar age for Fish Canyon sanidine. Earth and Planetary Science Letters 311:420–426.

Roberts, E. M. 2007. Facies architecture and depositional environments of the Upper Cretaceous Kaiparowits Formation, southern Utah. Sedimentary Geology 197:207–233.

Roberts, E. M., A. L. Deino, and M. A. Chan. 2005. 40Ar/39Ar age of the Kaiparowits Formation, southern Utah, and correlation of contemporaneous Campanian strata and vertebrate faunas along the margin of the Western Interior Basin. Cretaceous Research 26:307–318.

Roberts, E. M., S. D. Sampson, A. L. Deino, S. A. Bowring, and R. Buchwaldt. 2013. The Kaiparowits Formation: a remarkable record of Late Cretaceous terrestrial environments, ecosystems and evolution in Western North America; pp. 85–106 in A. L. Titus and M. A. Loewen (eds.), At the Top of the Grand Staircase: the Late Cretaceous of Southern Utah. Indiana University Press, Bloomington.

Roberts, L. N. R., and M. A. Kirschbaum. 1995. Paleogeography and the Late Cretaceous of the Western Interior of Middle North America; Coal Distribution and Sediment Accumulation. United States Geological Survey.

Roca, X., and G. C. Nadon. 2007. Tectonic Control on the Sequence Stratigraphy of Nonmarine Retroarc Foreland Basin Fills: Insights from the Upper Jurassic of Central Utah, U.S.A. Journal of Sedimentary Research 77:239–255.

Roehler, H. W. 1990. Stratigraphy of the Mesaverde Group in the Central and Eastern Greater Green River Basin, Wyoming, Colorado, and Utah. United States Geological Survey, Professional Paper 1508.

Rogers, R. R. 1993. Marine facies of the Judith River Formation (Campanian) in the type area, north-central Montana. Montana Geological Society: 1993 Field Conference Guidebook: Old Timers' Rendezvous Edition: Energy and Mineral Resources of Central Montana 61–69.

Rogers, R. R. 1994. Nature and origin of through-going discontinuities in nonmarine foreland basin strata, Upper Cretaceous, Montana: Implications for sequence analysis. Geology 22:1119–1122.

Rogers, R. R. 1995. Sequence stratigraphy and vertebrate taphonomy of the Upper Cretaceous Two Medicine and Judith River Formations, Montana. Ph.D, University of Chicago, Chicago, Illinois, 400 pp.

Rogers, R. R. 1998. Sequence analysis of the Upper Cretaceous Two Medicine and Judith River formations, Montana; nonmarine response to the Claggett and Bearpaw marine cycles. Journal of Sedimentary Research 68:615–631.

Rogers, R. R., and C. C. Swisher. 1996. The Claggett and Bearpaw transgressions revisited; new 40Ar/39Ar data and a review of possible drivers. Geological Society of America 28:62.

Rogers, R. R., and M. E. Brady. 2010. Origins of microfossil bonebeds: insights from the Upper Cretaceous Judith River Formation of north-central Montana. Paleobiology 36:80–112.

Rogers, R. R., C. C. Swisher III, and J. R. Horner. 1993. 40Ar/39Ar age and correlation of the nonmarine Two Medicine Formation (Upper Cretaceous), northwestern Montana, U.S.A. Canadian Journal of Earth Sciences 30:1066–1075.

Rook D. L., and J. P. Hunter. 2011. Phylogeny of the Taeniodonta: evidence from dental characters and stratigraphy. Journal of Vertebrate Paleontology 31(2):422-427.

Rowe, T., E. H. Colbert, and J. D. Nations. 1981. The occurrence of Pentaceratops with a description of its frill; pp. 29–48 in S. G. Lucas, J. K. Rigby, and B. S. Kues (eds.), Advances in San Juan Basin Paleontology. University of New Mexico Press, Albuquerque.

Rowe, T., R. L. Cifelli, T. M. Lehman, and A. Weil. 1992. The Campanian Terlingua local fauna, with a summary of other vertebrates from the Aguja Formation, Trans-Pecos Texas. Journal of Vertebrate Paleontology 12:472–493.

Rozhdestvensky, A. K. 1965. Growth changes in Asian dinosaurs and some problems of their taxonomy. Paleontologischeskii Zhurnal 3:95-109.

Russell, D. A. 1970. Tyrannosaurs from the Late Cretaceous of western Canada. National Museums of Canada Publications in Paleontology 1:1-34.

Russell, L. S. 1964. Cretaceous non-marine faunas of northwestern North America. Life Sciences Contributions, Royal Ontario Museum 61:1–21.

Russell, L. S. 1975. Mammalian faunal succession in the Cretaceous System of western North America. Geological Association of Canada Special Paper 13:137–161.

Russell, L. S. 1983. Evidence for an unconformity at the Scollard–Battle contact, Upper Cretaceous strata, Alberta. Canadian Journal of Earth Sciences 20:1219–1231.

Russell, L. S., and R. W. Landes. 1940. Geology of the southern Alberta plains. Geological Survey of Canada, Memoir 221.

Ryan, M. J. 2003. Taxonomy, systematics and evolution of centrosaurine ceratopsids of the Campanian Western Interior Basin of North America. Ph.D, University of Calgary, Calgary, 578 pp.

Ryan, M. J. 2007. A new basal centrosaurine ceratopsid from the Oldman Formation, southeastern Alberta. Journal of Paleontology 81:376–396.

Ryan, M. J., and D. C. Evans. 2005. Ornithischian dinosaurs; pp. 312–348 in Dinosaur Provincial Park: A spectacular ancient ecosystem revealed. Indiana University Press.

Ryan, M. J., and A. S. Rand. 1993. Sexual Selection and Signal Evolution: The Ghost of Biases past. Philosophical Transactions of the Royal Society of London. Series B: Biological Sciences 340:187–195.

Ryan, M. J., and A. P. Russell. 2005. A new centrosaurine ceratopsid from the Oldman Formation of Alberta and its implications for centrosaurine taxonomy and systematics. Canadian Journal of Earth Sciences 42:1369–1387.

Ryan, M. J., R. Holmes, and A. P. Russell. 2007. A revision of the late campanian centrosaurine ceratopsid genus Styracosaurus from the Western Interior of North America. Journal of Vertebrate Paleontology 27:944–962.

Ryan, M. J., A. P. Russell, and S. Hartman. 2010a. A new chasmosaurine ceratopsid from the Judith River Formation, Montana; pp. 181–188 in New Perspectives on Horned Dinosaurs. The Royal Tyrrell Museum Ceratopsian Symposium. Indiana University Press.

Ryan, M. J., D. C. Evans, and K. M. Shepherd. 2012a. A new ceratopsid from the Foremost Formation (middle Campanian) of Alberta. Canadian Journal of Earth Sciences 49:1251–1262.

Ryan, M. J., D. C. Evans, P. J. Currie, and M. A. Loewen. 2014. A new chasmosaurine from northern Laramidia expands frill disparity in ceratopsid dinosaurs. Naturwissenschaften 101:505-512.

Ryan, M. J., A. P. Russell, D. A. Eberth, and P. J. Currie. 2001. The taphonomy of a Centrosaurus (Ornithischia: Ceratopsidae) bone bed from the Dinosaur Park Formation (Upper Campanian), Alberta, Canada, with comments on cranial ontogeny. Palaios 16:482-506.

Ryan, M. J., D. A. Eberth, D. B. Brinkman, P. J. Currie, and D. H. Tanke. 2010b. A new Pachyrhinosaurus-like ceratopsid from the upper Dinosaur Park Formation (late Campanian) of southern Alberta, Canada; pp. 141–155 in New Perspectives on Horned Dinosaurs. The Royal Tyrrell Museum Ceratopsian Symposium. Indiana University Press.

Ryan, M. J., D. C. Evans, P. J. Currie, C. M. Brown, and D. Brinkman. 2012b. New leptoceratopsids from the Upper Cretaceous of Alberta, Canada. Cretaceous Research 35:69–80.

Ryan, M. J., D. Tanke, D. Brinkman, D. Eberth, and P. Currie. 2006. A New Pachyrhinosaurus-Like Ceratopsian From The Upper Dinosaur Park Formation (Late Campanian) Of Southern Alberta, Canada. 117A.

Sageman, B. B., B. S. Singer, S. R. Meyers, S. E. Siewert, I. Walaszczyk, D. J. Condon, B. R. Jicha, J. D. Obradovich, and D. A. Sawyer. 2014. Integrating 40Ar/39Ar, U-Pb, and astronomical clocks in the Cretaceous Niobrara Formation, Western Interior Basin, USA. Geological Society of America Bulletin 126:956–973.

Sahni, A. 1972. The vertebrate fauna of the Judith River Formation, Montana. Bulletin of the American Museum of Natural History 147:325–412.

Sampson, S. D. 1995. Two new horned dinosaurs from the upper Cretaceous Two Medicine Formation of Montana; with a phylogenetic analysis of the Centrosaurinae (Ornithischia: Ceratopsidae). Journal of Vertebrate Paleontology 15:743–760.

Samspon, S. D., and E. C. Alexander Jr. 1987. Calibration of the interlaboratory 40Ar/39Ar dating standard, MMhb-1. Chemical Geology: Isotope Geoscience Section 66:27–34.

Sampson, S. D., and M. A. Loewen. 2005. Tyrannosaurus rex from the Upper Cretaceous (Maastrichtian) North Horn Formation of Utah: biogeographic and paleoecologic implications. Journal of Vertebrate Paleontology 25:469–472.

Sampson, S. D., and M. Loewen. 2010. Unraveling a radiation: a review of the diversity, stratigraphic distribution, biogeography, and evolution of horned dinosaurs. (Ornithischia: Ceratopsidae); pp. 405–427 in M. J. Ryan, B. J. Chinnery, and D. A. Eberth (eds.), New Perspectives on Horned Dinosaurs. The Royal Tyrrell Museum Ceratopsian Symposium. Indiana University Press, Bloomington, Indiana.

Sampson, S. D., M. J. Ryan, and D. H. Tanke. 1997. Craniofacial ontogeny in centrosaurine dinosaurs (Ornithischia: Ceratopsidae): taxonomic and behavioral implications. Zoological Journal of the Linnean Society 121:293-337.

Sampson, S. D., M. A. Loewen, E. M. Roberts, and M. A. Getty. 2013. A new macrovertebrate assemblage from the Late Cretaceous (Campanian) of Southern Utah; pp. 599-620 in A. L. Titus and M. A. Loewen (eds.), At the Top of the Grand Staircase: the Late Cretaceous of Southern Utah. Indiana University Press, Bloomington.

Sampson, S. D., E. K. Lund, M. A. Loewen, A. A. Farke, and K. E. Clayton. 2013. A remarkable short-snouted horned dinosaur from the Late Cretaceous (late Campanian) of southern Laramidia. Proceedings of the Royal Society of London B: Biological Sciences 280:20131186.

Sampson, S. D., M. A. Loewen, A. A. Farke, E. M. Roberts, C. A. Forster, J. A. Smith, and A. L. Titus. 2010. New Horned Dinosaurs from Utah Provide Evidence for Intracontinental Dinosaur Endemism. PLoS ONE 5:e12292.

Sander, P. M., and N. Klein. 2005. Developmental plasticity in the life history of a prosauropod dinosaur. Science 310:1800-1802.

Sankey, J. T. 2001. Late Campanian southern dinosaurs, Aguja Formation, Big Bend, Texas. Journal of Paleontology 75:208–215.

Sankey, J. T. 2006. Turtles of the upper Aguja Formation (late Campanian), Big Bend National Park, Texas. New Mexico Museum of Natural History and Science Bulletin 35:235–243.

Sankey, J. T. 2010. Faunal composition and significance of high-diversity, mixed bonebeds containing Agujaceratops mariscalensis and other dinosaurs, Aguja Formation (Upper Cretaceous), Big Bend, Texas. New Perspectives on Horned Dinosaurs. The Royal Tyrrell Museum Ceratopsian Symposium 520–37.

Sankey, J. T., and W. A. Gose. 2001. Late Cretaceous mammals and magnetostratigraphy, Big Bend, Texas. Occasional Papers of the Museum of Natural Science, Louisiana State University 77:1–16.

Sarna-Wojcicki, A. M., and M. S. Pringle Jr. 1992. Laser-fusion 40 Ar/39 Ar ages of the Tuff of Taylor Canyon and Bishop Tuff, E. California-W. Nevada. Eos Trans. AGU 73:43.

Scannella, J. 2010. Triceratops: A model organism for deciphering dinosaur heterochrony. Journal of Vertebrate Paleontology, SVP Program and Abstracts Book 30:158A.

Scannella, J. B., and D. W. Fowler. 2009. Anagenesis in Triceratops: evidence from a newly resolved stratigraphic framework for the Hell Creek Formation. p. 148-149 in Storrs, G.W. (ed.), 9th North American Paleontological Convention Abstracts. University of Cincinnati, Cincinnati Museum Center Scientific Contributions 3, Cincinnati, Ohio.

Scannella, J. B., and D. W. Fowler. 2014. A stratigraphic survey of Triceratops localities in the Hell Creek Formation, northeastern Montana (2006–2010). pp. 313-332 in Through the End of the Cretaceous in the Type Locality of the Hell Creek Formation in Montana and Adjacent Areas, G.P. Wilson, W.A. Clemens, J.R. Horner, and J.H. Hartman (eds.) Geological Society of America Special Paper, Boulder, Colorado.

Scannella, J. B., and J. R. Horner. 2010. Torosaurus Marsh, 1891, is Triceratops Marsh, 1889 (Ceratopsidae: Chasmosaurinae): synonymy through ontogeny. Journal of Vertebrate Paleontology 30:1157–1168.

Scannella, J. B., and J. R. Horner. 2011. *'Nedoceratops'*: an example of a transitional morphology. PLoS ONE 6:e28705 p. 1-9. doi:10.1371/journal.pone.0028705.

Scannella, J. B., D. W. Fowler, M. B. Goodwin, and J. R. Horner. 2014. Evolutionary trends in Triceratops from the Hell Creek Formation, Montana. Proceedings of the National Academy of Sciences 111:10245–10250.

Schiebout, J. A., C. A. Rigsby, S. D. Rapp, J. A. Hartnell, and B. R. Standhardt. 1987. Stratigraphy of the Cretaceous-Tertiary and Paleocene-Eocene transition rocks of Big Bend National Park, Texas. The Journal of Geology 95:359–375.

Schmitz, M. D. 2012a. Radiogenic isotope geochronology; pp. 115–125 in The Geological Time Scale. Elsevier.

Schmitz, M. D. 2012b. Radiometric Ages used in GTS2012; pp. 1045–1082 in The Geological Time Scale. Elsevier.

Schmitz, M. D., and S. A. Bowring. 2001. U-Pb zircon and titanite systematics of the Fish Canyon Tuff: an assessment of high-precision U-Pb geochronology and its application to young volcanic rocks. Geochimica et Cosmochimica Acta 65:2571–2587.

Schoene, B., J. L. Crowley, D. J. Condon, M. D. Schmitz, and S. A. Bowring. 2006. Reassessing the uranium decay constants for geochronology using ID-TIMS U–Pb data. Geochimica et Cosmochimica Acta 70:426–445.

Schoene, B., K. M. Samperton, M. P. Eddy, G. Keller, T. Adatte, S. A. Bowring, S. F. R. Khadri, and B. Gertsch. 2015. U-Pb geochronology of the Deccan Traps and relation to the end-Cretaceous mass extinction. Science 347:182–184.

Schumm, S. A. 1993. River response to baselevel change: implications for sequence stratigraphy. Journal of Geology 279–294.

Schwarz, W. H., K. Kossert, M. Trieloff, and J. Hopp. 2011. Comment on the "Joint determination of 40K decay constants and 40Ar□/40K for the Fish Canyon sanidine standard, and improved accuracy for 40Ar/39Ar geochronology" by Paul R. Renne et al. (2010). Geochimica et Cosmochimica Acta 75:5094–5096.

Scott, G. R., R. B. O'Sullivan, and J. S. Heller. 1979. Preliminary geologic map of the Burnham Trading Post Quadrangle, San Juan County, New Mexico, Report 1076.

Seager, O. A., W. N. Ballard, D. L. Blackstone, W. A. Cobban, and G. R. Downs. 1942. Discussion; Stratigraphy of North Dakota. AAPG Bulletin 26:1414–1423.

Sealey, P., J. A. Smith, and T. E. Williamson. 2005: An unusual *Pentaceratops* from New Mexico. Society of Vertebrate Paleontology Annual Meeting, Mesa, Arizona, 2005.

Seeley, H. G. 1887. On the classification of the fossil animals commonly called Dinosauria. Proceedings of the Royal Society of London 43:165-171.

Sereno, P. C. 1998. A rationale for phylogenetic definitions, with application to the higher-level taxonomy of Dinosauria. Neues Jahrbuch für Geologie und Paläontologie - Abhandlungen 210:41-83.

Sereno, P. C., L. Tan, S. L. Brusatte, H. J. Kriegstein, X. Zhao, and K. Cloward. 2009. Tyrannosaurid skeletal design first evolved at small body size. Science 326:418-422.

Servedio, M. R. 2004. The What and Why of Research on Reinforcement. PLoS Biol 2:e420.

Shanley, K. W., and P. J. McCabe. 1994. Perspectives on the Sequence Stratigraphy of Continental Strata. AAPG Bulletin 78:544–568.

Shanley, K. W., and P. J. McCabe. 2009. Alluvial Architecture in a Sequence Stratigraphic Framework: A Case History from the Upper Cretaceous of Southern Utah, USA; pp. 21–55 in S. S. Flint and I. D. Bryant (eds.), The Geological Modelling of Hydrocarbon Reservoirs and Outcrop Analogues. Blackwell Publishing Ltd.

Shelton, J. A. 2007. Application of sequence stratigraphy to the nonmarine Upper Cretaceous Two Medicine Formation, Willow Creek anticline, northwestern Montana. M.S., Montana State University, Bozeman, Montana, 238 pp.

Simpson, G. G. 1940. Types in modern taxonomy. American Journal of Science 238:413-431.

Simpson, G. G. 1944. Tempo and mode in evolution. Columbia University Press, New York.

Simpson, G. G. 1951. The species concept. Evolution 5: 285-298.

Simpson, G. G. 1953. The major features of evolution. New York, Columbia University Press, New York.

Simpson, G. G. 1961. Principles of Animal Taxonomy, Columbia Biological Series. Columbia University Press, New York, 247 pp.

Singer, B. S., B. R. Jicha, R. S. Coe, and N. Mochizuki. 2012. An Earthtime Chronology for the Matuyama-Brunhes Geomagnetic Field Reversal. AGU Fall Meeting Abstracts 21.

Soegaard, K., H. Ye, N. Halik, A. T. Daniels, J. Arney, and S. Garrick. 2003. Stratigraphic evolution of latest Cretaceous to early Tertiary Difunta foreland basin in northeast Mexico: Influence of salt withdrawal on tectonically induced subsidence by the Sierra Madre Oriental fold and thrust belt. AAPG Memoir 79:364–394.

Sorenson M.D., and E.A. Franzosa. 2007. TreeRot, version 3. Boston University, Boston, MA.

Spear, B., and M. A. Kirschbaum. 2012. Re-evaluation of depositional environments of the Neslen Formation from subsurface and surface data, Book Cliffs, Utah. 2012 AAPG Rocky Mountain Section Meeting.

Speiker, E. M. 1946. Late Mesozoic and early Cenozoic history of central Utah. United States Geological Survey Prof. Paper 205:117–161.

Sprain, C. J., P. R. Renne, G. P. Wilson, and W. A. Clemens. 2014. High-resolution chronostratigraphy of the terrestrial Cretaceous-Paleogene transition and recovery interval in the Hell Creek region, Montana. Geological Society of America Bulletin 127:393–409.

Stanton, T. W. 1909. The age and stratigraphic relations of the "Ceratops beds" of Wyoming and Montana. Proceedings of the Washington Academy of Sciences 11:239–293.

Stanton, T. W. 1910. Fox Hills sandstone and Lance Formation (" Ceratops beds") in South Dakota, North Dakota, and eastern Wyoming. American Journal of Science 172–188.

Stanton, T. W. 1914. Boundary between Cretaceous and Tertiary in North America as indicated by stratigraphy and invertebrate faunas. Geological Society of America Bulletin 25:341–354.

Steiger, R., and E. Jäger. 1977. Subcommission on geochronology: convention on the use of decay constants in geo-and cosmochronology. Earth and Planetary Science Letters 36:359–362.

Sternberg, C. M. 1929. A new species of horned dinosaur from the Upper Cretaceous of Alberta. Bulletin of the National Museum of Canada 54:34–37.

Sternberg, C. M. 1935. Hooded Hadrosaurs of the Belly River Series of the Upper Cretaceous: Canada Department of Mines Bulletin. Bulletin of the National Museum of Canada 52:1–37.

Sternberg, C. M. 1940. Ceratopsidae from Alberta. Journal of Paleontology 14:468–480.

Sternberg, C. M. 1950a. Pachyrhinosaurus canadensis, representing a new family of the Ceratopsia, from southern Alberta. National Museum of Canada Bulletin 118:109–120.

Sternberg, C. M. 1950b. Steveville - west of the fourth meridian, Alberta. Geological Survey of Canada Topographic Map A.

Sternberg, C. M. 1951. Complete Skelton of Leptoceratops Gracilis Brown from the Upper Edmonton Member on Red Deer River, Alberta. Bulletin of the National Museum of Canada 225–255.

Sternberg, C. M. 1953. A new hadrosaur from the Oldman Formation of Alberta: discussion of nomenclature. Bulletin of the National Museum of Canada 1–12.

Straight, W. H., and D. A. Eberth. 2002. Testing the Utility of Vertebrate Remains in Recognizing Patterns in Fluvial Deposits: An Example from the Lower Horseshoe Canyon Formation, Alberta. PALAIOS 17:472–490.

Strong, N., and C. Paola. 2008. Valleys that never were: time surfaces versus stratigraphic surfaces. Journal of Sedimentary Research 78:579–593.

Stuart, Y. E., and J. B. Losos. 2013. Ecological character displacement: glass half full or half empty? Trends in Ecology & Evolution.

Sues, H.-D., and D. W. Larson. 2008. Diversity and variation of theropod dinosaur teeth from the uppermost Santonian Milk River Formation (Upper Cretaceous), Alberta: a quantitative method supporting identification of the oldest dinosaur tooth assemblage in Canada. Canadian Journal of Earth Sciences 45:1455–1468.

Sullivan, R. M. 2006. Ah-shi-sle-pah Wilderness Study Area (San Juan Basin, New Mexico): a paleontological (and historical) treasure and resource. New Mexico Museum of Natural History and Science Bulletin 34:169–174.

Sullivan, R. M., and T. E. Williamson. 1999. A new skull of Parasaurolophus (Dinosauria: Hadrosauridae) and a revision of the genus. New Mexico Museum of Natural History and Science. New Mexico Museum of Natural History and Science Bulletin 15:52.

Sullivan, R. M., and G. E. Bennett. 2000. A juvenile Parasaurolophus (Ornithischia: Hadrosauridae) from the Upper Cretaceous Fruitland Formation of New Mexico. New Mexico Museum of Natural History and Science Bulletin 17:215–220.

Sullivan, R. M., and S. G. Lucas. 2003. The Kirtlandian, a new land-vertebrate “age” for the Late Cretaceous of western North America. New Mexico Geological Society Guidebook 54:369–377.

Sullivan, R. M., and S. G. Lucas. 2006a. The Kirtlandian land-vertebrate “age”–faunal composition, temporal position and biostratigraphic correlation in the nonmarine Upper Cretaceous of western North America. New Mexico Museum of Natural History and Science Bulletin 35:7–29.

Sullivan, R. M., and S. G. Lucas. 2006b. The pachycephalosaurid dinosaur *Stegoceras validum* from the Upper Cretaceous Fruitland Formation, San Juan Basin, New Mexico. New Mexico Museum of Natural History and Science Bulletin 35:329-330.

Sullivan, R. M., and S. G. Lucas. 2010. A New Chasmosaurine (Ceratopsidae, Dinosauria) from the Upper Cretaceous Ojo Alamo Formation (Naashoibito Member), San Juan Basin, New Mexico; pp. 169–180 in M. J. Ryan, B. J. Chinnery, and D. A. Eberth (eds.), New Perspectives on Horned Dinosaurs. The Royal Tyrrell Museum Ceratopsian Symposium. Indiana University Press, Bloomington, Indiana.

Sullivan, R. M., and S. G. Lucas. 2011. Charles Hazelius Sternberg and his San Juan Basin Cretaceous dinosaur collections: correspondence and photographs (1920-1925). New Mexico Museum of Natural History and Science Bulletin 53:429-471.

Sullivan, R. M., A. C. Boere, and S. G. Lucas. 2005a. Redescription of the ceratopsid dinosaur Torosaurus utahensis (Gilmore, 1946) and a revision of the genus. Journal of Paleontology 79:564–582.

Sullivan, R. M., S. G. Lucas, and D. R. Braman. 2005b. Dinosaurs, pollen, and the Cretaceous-Tertiary boundary in the San Juan Basin, New Mexico. New Mexico Geological Society Guidebook 56:395–407.

Sullivan, R. M., S. E. Jasinkski, M. Guenther, and S. G. Lucas. 2011. The first lambeosaurin (Dinosauria, Hadrosauridae, Lambeosaurinae) from the Upper Cretaceous Ojo Alamo Formation (Naashoibito Member), San Juan Basin, New Mexico. New Mexico Museum of Natural History and Science Bulletin 53:405–417.

Swisher, C.C., L., Dingus. and R.F., Butler. 1993. 40Ar/39Ar dating and magnetostratigraphic correlation of the terrestrial Cretaceous-Paleogene boundary and Puercan mammal age, Hell Creek-Tullock Formations, eastern Montana. Canadian Journal of Earth Sciences 30(9):1981–1996.

Swisher, C. C., Y. Wang, X. Wang, X. Xu, and Y. Wang. 1999. Cretaceous age for the feathered dinosaurs of Liaoning, China. Nature 400:58–61.

Swisher, C. C., X. Wang, Z. Zhou, Y. Wang, F. Jin, J. Zhang, X. Xu, F. Zhang, and Y. Wang. 2002. Further support for a Cretaceous age for the feathered-dinosaur beds of Liaoning,China:New 40Ar/39Ar dating of the Yixian and Tuchengzi Formations. Chinese Science Bulletin 47:136–139.

Swofford, D. L. 2002. PAUP*. Phylogenetic Analysis Using Parsimony (*and Other Methods). Version 4.0b10. Sinauer Associates, http://paup.csit.fsu.edu/, Sunderland, Massachusetts.

Swofford D. L. 2003. PAUP*. Phylogenetic Analysis Using Parsimony (*and Other Methods). Version 4. Sinauer Associates, http://paup.csit.fsu.edu/, Sunderland, Massachusetts.

Talling, P. J., D. W. Burbank, T. F. Lawton, R. S. Hobbs, and S. P. Lund. 1994. Magnetostratigraphic Chronology of Cretaceous-to-Eocene Thrust Belt Evolution, Central Utah, USA. The Journal of Geology 102:181–196.

Tamm, V. 1993. Depositional environments of the Lower Hell Creek Formation (Maastrichtian), Eastern Montana. M.S., University of Rhode Island, Kingston, 122 pp.

Tandon, S. K., and M. R. Gibling. 1994. Calcrete and coal in late Carboniferous cyclothems of Nova Scotia, Canada: Climate and sea-level changes linked. Geology 22:755–758.

Tanke, D. H. 2004. The 2003 Royal Tyrrell Museum of Palaeontology Expedition to the Grande Prairie Region (Northwestern Alberta, Canada). Alberta Palaeontological Society Bulletin 19:3–31.

Tanke, D. H. 2005. Identifying lost quarries; pp. 34-53 in P. J. Currie and E. B. Koppelhaus (eds.), Dinosaur Provincial Park. Indiana University Press, Bloomington.

Tanke, D. H. 2006. Sixty years of pachyrhinosaur (Dinosauria: Ceratopsidae) discoveries in North America. Alberta Paleontological Society, 10th Annual Symposium, Abstract Volume. Alberta Paleontological Society, Calgary, Alta 33–35.

Tanke, D. H. 2010. Ceratopsian discoveries and work in Alberta, Canada: A historical review and census. in Ryan, M.J., B.J., Chinnery-Allgeier, and D.A., Eberth, (eds.), New Perspectives on Horned Dinosaurs: The Royal Tyrrell Museum Ceratopsian Symposium. Indiana University Press, Bloomington, Indiana, supplemental CD-ROM, 488 pp.

Tanke, D. H., and B. M. Rothschild. 2002. Dinosores: an annotated bibliography of dinosaur paleopathology and related topics - 1838-2001. New Mexico Museum of Natural History and Science Bulletin 20:1-97.

Thom, W. T., and C. E. Dobbin. 1924. Stratigraphy of Cretaceous-Eocene transition beds in eastern Montana and the Dakotas. Geological Society of America Bulletin 35:481–505.

Thomas, R. G., D. G. Smith, J. M. Wood, J. Visser, E. A. Calverley-Range, and E. H. Koster. 1987. Inclined heterolithic stratification—terminology, description, interpretation and significance. Sedimentary Geology 53:123–179.

Thomas, R. G., D. A. Eberth, A. L. Deino, and D. Robinson. 1990. Composition, radioisotopic ages, and potential significance of an altered volcanic ash (bentonite) from the Upper Cretaceous Judith River Formation, Dinosaur Provincial Park, southern Alberta, Canada. Cretaceous Research 11:125–162.

Thomson, T. J., R. B. Irmis, and M. A. Loewen. 2013. First occurrence of a tyrannosaurid dinosaur from the Mesaverde Group (Neslen Formation) of Utah: Implications for upper Campanian Laramidian biogeography. Cretaceous Research 43:70–79.

Tibbetts, E. A., and J. Dale. 2007. Individual recognition: it is good to be different. Trends in Ecology & Evolution 22:529–537.

Tokaryk T. T. 1986. Ceratopsian dinosaurs from the Frenchman Formation (Upper Cretaceous) of Saskatchewan. Canadian Field-Naturalist 100(2):192-196.

Trexler, D. 2001. Two Medicine Formation, Montana: geology and fauna; pp. 298–309 in Mesozoic Vertebrate Life. Indiana University Press.

Trueman, C. N., and M. J. Benton. 1997. A geochemical method to trace the taphonomic history of reworked bones in sedimentary settings. Geology 25:263-266.

Trueman, C. N., A. K. Behrensmeyer, R. Potts, and N. Tuross. 2006. High-resolution records of location and stratigraphic provenance from the rare earth element composition of fossil bones. Geochimica et Cosmochimica Acta 70:4343-4355.

Tsai, C.-H., and R. E. Fordyce. 2015. Ancestor-descendant relationships in evolution: origin of the extant pygmy right whale, *Caperea marginata*. Biology Letters 11:1-4.

Tsuihiji T. 2010. Reconstructions of the axial muscle insertions in the occipital region of dinosaurs: evaluations of past hypotheses on marginocephalia and tyrannosauridae using the Extant Phylogenetic Bracket approach. The Anatomical Record 293:1360–1386.

Tsuihiji, T., M. Watabe, K. Tsogtbaatar, R. Barsbold, S. Suzuki, A. H. Lee, R. C. Ridgely, Y. Kawahara, and L. M. Witmer. 2011. Cranial osteology of a juvenile

specimen of *Tarbosaurus bataar* from the Nemegt Formation (Upper Cretaceous) of Bugin Tsav, Mongolia. Journal of Vertebrate Paleontology 31:497-517.

Tsujita, C. J. 1995. Origin of Concretion-Hosted Shell Clusters in the Late Cretaceous Bearpaw Formation, Southern Alberta, Canada. PALAIOS 10:408–423.

Tucker, A. D. 1997. Validation of skeletochronology to determine age of freshwater crocodiles (*Crocodylus johnstoni*). Australian Journal of Marine and Freshwater Research 48:343-351.

Turner, B.W. 2010. Testing the Local Diachroneity of the Terrestrial Lithostratigraphic KPg Boundary, Northern Montana [M.S. thesis]: Montana State University, Bozeman, Montana, 187 pp.

Tyson, H. 1981. The structure and relationships of the horned dinosaur Arrhinoceratops Parks(Ornithischia: Ceratopsidae). Canadian Journal of Earth Sciences 18:1241–1247.

Upchurch, P., P. M. Barrett, and P. Dodson. 2004. Sauropoda; pp. 259–322 in The Dinosauria II. University of California Press.

Vail, P. R., R. M. Mitchum Jr., and S. Thompson. 1977. Seismic stratigraphy and global changes of sea level, part 3: relative changes of sea level from coastal onlap; pp. 63–81 in Seismic Stratigraphy - Applications to hydrocarbon exploration. American Association of Petroleum Geologists, Tulsa, Oklahoma.

van Valen, L. 1973. A new evolutionary law. Evolutionary Theory 1:1–30.

Varricchio, D. J., C. Koeberl, R. F. Raven, W. S. Wolbach, W. C. Elsik, and D. P. Miggins. 2010. Tracing the Manson impact event across the Western Interior Cretaceous Seaway. Geological Society of America Special Papers 465:269–299.

Veatch, A. C. 1907. Origin and definition of the geologic term Laramie. American Journal of Science 4:18–22.

Villeneuve, M. 2004. Radiogenic Isotope Geochronology; pp. in A Geologic Time Scale 2004. Cambridge University Press.

Vrba, E. S. 1980. Evolution, species and fossils: how does life evolve. South African Journal of Science 76:61–84.

Vrba, E. S. 1985. Environment and evolution: alternative causes of the temporal distribution of evolutionary events. South African Journal of Science 81:229–236.

Vrba, E. S. 1993. Turnover-pulses, the Red Queen, and related topics. American Journal of Science 293:418–452.

Waagé, K. M. 1968. The Type Fox Hills Formation, Cretaceous (Maestrichtian), South Dakota. Peabody Museum of Natural History, Yale University Bulletin, pp.

Waagé, K. M. 1975. Deciphering the basic sedimentary structure of the Cretaceous System in the Western Interior. Geological Association of Canada, Special Paper 13:55–81.

Wagner, J. R. 2001. The hadrosaurian dinosaurs (ornithiscia: hadrosauria) of Big Bend National Park, Brewster County, Texas, with implications for late Cretaceous paleozoogeography. Thesis, Texas Tech University pp.

Wagner P. J., and D. H. Erwin. 1995. Phylogenetic patterns as tests of speciation models. pp. 87-122 in *New Approaches to Speciation in the Fossil Record*, D.H. Erwin, and R.H. Anstey (eds.) Columbia University Press, New York.

Wagner, J. R., and T. M. Lehman. 2009. An enigmatic new lambeosaurine hadrosaur (Reptilia: Dinosauria) from the Upper Shale member of the Campanian Aguja Formation of Trans-Pecos Texas. Journal of Vertebrate Paleontology 29:605–611.

Wagoner, J. C. V., R. M. Mitchum, K. M. Campion, and V. D. Rahmanian. 1990. Siliciclastic Sequence Stratigraphy in Well Logs, Cores, and Outcrops: Concepts for High-Resolution Correlation of Time and Facies. American Association of Petroleum Geologists, Methods in Exploration 174:55.

Wall, W. P., and P. M. Galton. 1979. Notes on pachycephalosaurid dinosaurs (Reptilia: Ornithischia) from North America, with comments on their status as ornithopods. Canadian Journal of Earth Sciences 16:1176–1186.

Wang, S. C., and P. Dodson. 2006. Estimating the diversity of dinosaurs. Proceedings of the National Academy of Sciences 103:13601–13605.

Wang, Y., K. M. Straub, and E. A. Hajek. 2011. Scale-dependent compensational stacking: An estimate of autogenic time scales in channelized sedimentary deposits. Geology 39:811–814.

Wedel, M. J. 2003. The evolution of vertebral pneumaticity in sauropod dinosaurs. Journal of Vertebrate Paleontology 23:344-357.

Weide, D. L., G. B. Schneider, J. W. Mytton, and G. R. Scott. 1979. Geologic map of the Pueblo Bonito Quadrangle, San Juan County, New Mexico, Report 1119.

Weimer, R. J. 1960. Upper Cretaceous stratigraphy, Rocky Mountain area. AAPG Bulletin 44:1–20.

Weishampel, D. B., and J. A. Jensen. 1979. Parasaurolophus (Reptilia: Hadrosauridae) from Utah. Journal of Paleontology 53:1422–1427.

Weishampel, D. B., D. E. Fastovsky, M. Watabe, D. Varricchio, F. Jackson, K. Tsogtbaatar, and R. Barsbold. 2008. New oviraptorid embryos from Bugin-Tsav, Nemegt Formation (Upper Cretaceous), Mongolia, with insights into their habitat and growth. Journal of Vertebrate Paleontology 28:1110-1119.

West-Eberhard, M. J. 1983. Sexual selection, social competition, and speciation. Quarterly Review of Biology 155–183.

Wheeler, K. L. 1983. Maestrichtian shoreline sedimentation in northeastern Montana. University of Iowa, 310 pp.

Whitlock, J. A., J. A. Wilson, and M. C. Lamanna. 2010. Description of a nearly complete juvenile skull of *Diplodocus* (Sauropoda: Diplodocoidea) from the Late Jurassic of North America. Journal of Vertebrate Paleontology 30:442-457.

Wick, S. L., and T. M. Lehman. 2013. A new ceratopsian dinosaur from the Javelina Formation (Maastrichtian) of West Texas and implications for chasmosaurine phylogeny. Naturwissenschaften 100:667–682.

Wiley, E. O. 1981. Phylogenetics. The Theory and Practice of Phylogenetic Systematics. Wiley- Interscience, New York, 439 pp.

Williamson, T. E. 1996. ?Brachychampsa sealeyi, sp nov., (Crocodylia, Alligatoroidea) from the Upper Cretaceous (lower Campanian) Menefee Formation, northwestern New Mexico. Journal of Vertebrate Paleontology 16:421–431.

Williamson, T. E. 1997. A new Late Cretaceous (early Campanian) vertebrate fauna from the Allison Member, Menefee Formation, San Juan Basin, New Mexico. New Mexico Museum of Natural History and Science Bulletin 11:51–59.

Williamson, T. E. 2000. Review of Hadrosauridae (Dinosauria, Ornithischia) from the San Juan Basin, New Mexico. Dinosaurs of New Mexico. SG Lucas and AB Heckert (eds.). New Mexico Museum of Natural History and Science, Bulletin 17:191–213.

Williamson, T. E., and A. Weil. 2008. Stratigraphic distribution of sauropods in the Upper Cretaceous of the San Juan Basin, New Mexico, with comments on North

America's Cretaceous "sauropod hiatus." Journal of Vertebrate Paleontology 28:1218–1223.

Willmarth, M. G. 1938. Lexicon of geologic names of the United States (including Alaska). Part 1, A-L. US Geological Survey Bulletin 896: 1244 pp.

Wilson, G. P. 2004. A quantitative assessment of mammalian change leading up to and across the Cretaceous-Tertiary boundary in northeastern Montana. Ph.D, University of California, Berkeley, Berkeley, 432 pp.

Wilson, G. P. 2005. Mammalian Faunal Dynamics During the Last 1.8 Million Years of the Cretaceous in Garfield County, Montana. Journal of Mammalian Evolution 12:53–76.

Wilson, G. P. 2014. Mammalian extinction, survival, and recovery dynamics across the Cretaceous-Paleogene boundary in northeastern Montana, USA. Geological Society of America Special Papers 503:365–392.

Wiman, C. 1930. Uber Ceratopsia aus der oberen Kreide in New Mexico. Nova Acta Regiae Societatis Scientarum Upsaliensis 4-7:1-19.

Wiman, C. 1931. Parasaurolophus tubicen n. sp. aus der Kreide in New Mexico. Nova Acta Regiae Scientiarum Upsaliensis 7:3–11.

Wolberg, D. L., J. P. Hall, and D. Bellis. 1988. First record of dinosaur footprints from the Fruitland Formation, San Juan County, New Mexico. New Mexico Bureau of Mines and Mineral Resources, Bulletin 122:33–34.Breyer, J. A., A. B. Busbey III, R. E. Hanson, K. E. Befus, W. R. Griffin, U. S. Hargrove, and S. C. Bergman. 2007. Evidence for Late Cretaceous Volcanism in Trans-Pecos Texas. The Journal of Geology 115:243-251.

Wolfe, D. G., and J. I. Kirkland. 1998. Zuniceratops christopheri n. gen. & n. sp., a ceratopsian dinosaur from the Moreno Hill Formation (Cretaceous, Turonian) of west-central New Mexico. Lower and Middle Cretaceous Terrestrial Ecosystems. New Mexico Museum of Natural History and Science Bulletin 14:303–317.

Woodward, H. N., E. A. Freedman Fowler, J. O. Farlow, and J. R. Horner. 2015. *Maiasaura*, a model organism for extinct vertebrate population biology: a statistically robust assessment of growth dynamics and survivorship. Paleobiology 41:503-527.

Wright, V. P., and S. B. Marriott. 1993. The sequence stratigraphy of fluvial depositional systems: the role of floodplain sediment storage. Sedimentary Geology 86:203–210.

Wroblewski, A. F.-J. 2006. Relative influences of tectonism, climate, and sea level on valley incision and sedimentary fill: new insights from Upper Cretaceous and Paleocene examples. SEPM Special Publication 85:309–326.

Wu, X., D. B. Brinkman, D. A. Eberth, and D. R. Braman. 2007. A new ceratopsid dinosaur (Ornithischia) from the uppermost Horseshoe Canyon Formation (upper Maastrichtian), Alberta, Canada. Canadian Journal of Earth Sciences 44:1243–1265.

Xing, H., X. Zhao, K. Wang, D. Li, S. Chen, J. C. Mallon, Y. Zhang, and X. Xu. 2014. Comparative Osteology and Phylogenetic Relationship of Edmontosaurus and Shantungosaurus (Dinosauria: Hadrosauridae) from the Upper Cretaceous of North America and East Asia. Acta Geologica Sinica - English Edition 88:1623–1652.

Xu, X., K. Wang, X. Zhao, and D. Li. 2010. First ceratopsid dinosaur from China and its biogeographical implications. Chinese Science Bulletin 55:1631-1635.

Xu, X., C. A. Forster, M. A. Norell, G. M. Erickson, D. A. Eberth, C. Jia, and Q. Zhao. 2006. A basal tyrannosauroid dinosaur from the Late Jurassic of China. Nature 439:715-718.

Xu, X., M. A. Norell, X. Kuang, X. Wang, Q. Zhao, and C. Jia. 2004. Basal tyrannosauroids from China and evidence for protofeathers in tyrannosauroids. Nature 431:680-684.

Yi, M.-S., and A. T. Cross. 1997. Palynostratigraphy of Upper Cretaceous-Lower Tertiary strata, Price Canyon, Utah. Review of Palaeobotany and Palynology 97:53–66.

Zanno, L. E., D. J. Varricchio, P. M. O'Connor, A. L. Titus, and M. J. Knell. 2011. A new troodontid theropod, Talos sampsoni gen. et sp. nov., from the Upper Cretaceous Western Interior Basin of North America. PLOS ONE 6:e24487.

Zaragüeta, B. 2004. Basal clupeomorphs and ellimmichthyiform phylogeny; pp. 391-404 in G. Arratia and A. Tintori (eds.), Mesozoic Fishes 3 - Systematics, Paleoenvironments, and Biodiversity. Verlag Dr. Friedrich Pfeil, Munich.

Zerfass, H., E. L. Lavina, C. L. Schultz, A. J. V. Garcia, U. F. Faccini, and F. Chemale Jr. 2003. Sequence stratigraphy of continental Triassic strata of southernmost Brazil: a contribution to Southwestern Gondwana palaeogeography and palaeoclimate. Sedimentary Geology 161:85–105.

Zhang, J.-Y. 2002. A new species of *Lycoptera* from Liaoning, China. Vertebrata PalAsiatic 40:257-266.